ISOLATION AND IDENTIFICATION OF CYCLIC POLYKETIDES FROM *ENDIANDRA KINGIANA* GAMBLE (LAURACEAE), AS BCL-XL/BAK AND MCL-1/BID DUAL INHIBITORS, AND APPROACHES TOWARD THE SYNTHESIS OF KINGIANINS

MOHAMAD NURUL AZMI BIN MOHAMAD TAIB

FACULTY OF SCIENCE
UNIVERSITY OF MALAYA
KUALA LUMPUR, MALAYSIA

AND

ECOLE POLYTECHNIQUE
PALAISEAU, FRANCE

2015

ISOLATION AND IDENTIFICATION OF CYCLIC POLYKETIDES FROM *ENDIANDRA KINGIANA* GAMBLE (LAURACEAE), AS BCL-XL/BAK AND MCL-1/BID DUAL INHIBITORS, AND APPROACHES TOWARD THE SYNTHESIS OF KINGIANINS

MOHAMAD NURUL AZMI BIN MOHAMAD TAIB

THESIS SUBMITTED IN FULFILMENT
OF THE REQUIREMENTS FOR
THE DEGREE OF DOCTOR OF PHILOSOPHY

FACULTY OF SCIENCE
UNIVERSITY OF MALAYA
KUALA LUMPUR, MALAYSIA

AND

ECOLE POLYTECHNIQUE
PALAISEAU, FRANCE

2015

UNIVERSITY OF MALAYA

ORIGINAL LITERARY WORK DECLARATION

Name of Candidate: **Mohamad Nurul Azmi MOHAMAD TAIB**

Registration/Matric No: **SHC110066**

Name of Degree: **Doctor of philosophy (PhD.)**

Title of Project Paper/Research Report/Dissertation/Thesis ("this Work"):

Isolation and identification of cyclic polyketides from *Endiandra kingiana* Gamble (Lauraceae), as Bcl-xL/Bak and Mcl-1/Bid dual inhibitors, and approaches toward the synthesis of kingianins.

Field of Study: **Chemistry**

I do solemnly and sincerely declare that:

(1) I am the sole author/writer of this Work;
(2) This Work is original;
(3) Any use of any work in which copyright exists was done by way of fair dealing and for permitted purposes and any excerpt or extract from, or reference to or reproduction of any copyright work has been disclosed expressly and sufficiently and the title of the Work and its authorship have been acknowledged in this Work;
(4) I do not have any actual knowledge nor do I ought reasonably to know that the making of this work constitutes an infringement of any copyright work;
(5) I hereby assign all and every rights in the copyright to this Work to the University of Malaya ("UM"), who henceforth shall be owner of the copyright in this Work and that any reproduction or use in any form or by any means whatsoever is prohibited without the written consent of UM having been first had and obtained;
(6) I am fully aware that if in the course of making this Work I have infringed any copyright whether intentionally or otherwise, I may be subject to legal action or any other action as may be determined by UM.

Candidate's Signature Date:

Subscribed and solemnly declared before,

Witness's Signature Date:

Name:

Designation:

ABSTRACT

The preliminary screening showed that the bark of ***Endiandra kingiana*** Gamble exhibited potency as a modulating agent between Bcl-xL and Bak, which prompted its chemical investigation. Two groups of compounds were isolated and characterized; the endiandric acid series and the kingianin series. Eight new endiandric acid analogues (kingianic acids A-H [**120**-**127**]) and three new kingianin analogues (kingianin O-Q [**128**-**130**]) were isolated and structurally elucidated. The isolated compounds were evaluated for two bioassays; Bcl-xL/Bak and Mcl-1/Bid of binding affinities and cytotoxic effects against various human tumour cells. The second part describes the progression towards the total synthesis of kingianin analogues. The pentacyclic kingianin skeleton was formed by Diels-Alder reaction between two monomers having a bicyclo[4.2.0]octadiene backbone formed by a stereospecific electrocyclization of polyenes. The research was focusing on construction of bicyclo[4.2.0]octadiene monomer using [2+2] ketene cycloaddition approach at the early stage of the synthesis. One of the main advantages of such a strategy is the rapid assembly of the carbon skeleton of kingianins, thus maximizing the chances for good overall yields of the final products. So far, an efficient synthesis of the bicyclo[4.2.0]octene backbone was successfully achieved. Five approaches to synthesize this backbone starting from [2+2] cycloaddition of the cyclohexadienes to functionalized ketenes followed by functionalization of substituent at C-7 and C-8 positions with the correct relative configuration were described. From these approaches, compounds **280** and **311** were identified as the key intermediates. This key step of the synthesis provided an access to the kingianins skeleton.

ABSTRAK

Pemeriksaan awal menunjukkan bahawa kulit pokok ***Endiandra kingiana*** Gamble mempunyai potensi sebagai ejen modulasi antara protein Bcl-xL dan Bak, yang mendorong kepada penyiasatan sebatian kimianya. Dua kumpulan sebatian telah diasingkan dan dikenalpasti iaitu; siri asid endiandrik dan siri kingianin. Lapan analog asid endiandrik baharu (asid kingianik A-H [**120-127**]) dan tiga analog kingianin baharu (kingianin O-Q [**128-130**]) telah diasingkan dan dikenalpasti. Sebatian tulen yang diasingkan telah dinilai terhadap dua bioassei; kebolehan untuk mengikat antara protein Bcl-xL/Bak dan Mcl-1/Bid dan kesan sitotoksik terhadap sel tumor manusia. Bahagian kedua menerangkan perkembangan sintesis analog kingianin. Rangka pentasiklik kingianin adalah terbentuk daripada tindak balas Diels-Alder antara dua monomer yang mempunyai struktur bisiklo[4.2.0]oktadiena yang dibentuk daripada elektrosiklik poliena. Kajian ini memberi tumpuan kepada pembinaan bisiklo[4.2.0]oktadiena monomer dengan menggunakan pendekatan sikloadisi [2+2] ketena pada peringkat awal sintesis. Salah satu kelebihan utama strategi ini adalah pembentukan pantas rangka karbon kingianin, sekaligus meningkatkan peluang pembentukan hasil yang maksimum. Setakat ini, sintesis bisiklo[4.2.0]oktana telah berjaya dicapai. Sebanyak lima pendekatan telah dilakukan bermula dari sikloadisi [2+2] antara sikloheksadiena dengan ketena diikuti dengan fungsionalisasi kumpulan berfungsi dikedudukan C-7 dan C-8 dengan konfigurasi yang betul. Daripada pendekatan ini, sebatian **280** dan **311** telah dikenalpasti sebagai sebatian perantara yang terbaik bagi menghasilkan analog kingianin.

.

RÉSUMÉ

Un criblage biologique préliminaire a montré que l'extrait des écorces ***d'Endiandrakingiana***possédait une forte affinité pour la protéine anti-apoptotique Bcl-xL, motivant ainsi la réalisationd'une étude chimique complète. Deux groupes de composés ont été isolés et caractérisés: d'une part, huit nouveaux dérivés de l'acide endiandrique (les acides kingianiques A à H [**120**−**127**]) et d'autre part, trois nouvelleskingianines (les kingianines O à Q [**128**−**130**]). Le potentiel inhibiteur des nouvelles molécules vis-à-vis des interactionsBcl-xL/Bak et Mcl-1/Bida ensuite été évalué, ainsi que leurs propriétés cytotoxiques sur diverses lignées cellulaires tumorales humaines. La seconde partie du manuscrit présente une approche vers la synthèse totale des kingianines et de composés analogues.Le squelette pentacyclique des produits naturels résulte formellement d'une réaction de Diels-Alder entre deux unités bicyclo[4.2.0]octadiène, elles-mêmes issues d'une cascade d'électrocyclisation de tétraènes entièrement conjugués. Une stratégie de construction directe de motifs bicyclo[4.2.0]octadiènespar une cycloaddition [2+2] entre des cycloalcènes et des cétènes convenablement choisisdoit assurer l'obtention des molécules cibles avec de bons rendements globaux. Au total, cinq approches ont été implémentées. Elles débutent par la cycloaddition [2+2] entre des cyclohexadiènes et des cétènes fonctionnalisés et se poursuivent par la fonctionnalisation des positions C7 et C8 en contrôlant la configuration relative de ces centres. Les résultats obtenus ont conduit à identifier les composés **280** et **311** comme des intermédiaires clefs à même d'être convertis en dienes ou en diénophiles, pouvant alors être engagés dans des cycloadditions de Diels-Alder pour accéder à la structure pentacyclique des kingianines.

ACKNOWLEDGEMENTS

In the name of Allah, most Gracious, most Merciful. I would like to convey my gratitude to my supervisors, Prof. Dr. Khalijah Awang (UM), late Assoc. Prof. Dr. Khalit Mohamad (UM), Dr Yvan Six (EP) and Dr. Marc Litaudon (ICSN) for their kind supervision, concern, understanding and support throughout the development of this research project in University of Malaya, Malaysia and Ecole Polytechnique, France. Honestly, I am a natural product background with very little background in organic synthesis. Looking back, I was very fortunate that Dr. Yvan even let me joint his laboratory in the first place eventhough my knowledge in synthetic chemistry is very limited. He spends an enormous amount of time working with me during winter (end Feb 2013) on laboratory techniques and teaches me how to be an experimentalist. Learning synthesis from him first-hand in the early years was certainly one of the most fun and valuable experience. Prof. Khalijah and Dr. Marc were good mentors I spend a lot of time with them to understand the NMR of cyclic polyketides and the possible application as a dual inhibitors of Bcl-xL and Mcl-1. Their availability, dynamism, enthusiasm and encouragement have been of great value for me. Our extensive discussions around my work have been very helpful during this research project.

This work was accomplished in Phytochemistry Laboratory (PhytoLab) at University of Malaya, DCSO Laboratory at Ecole Polytechnique and Institut de Chimie des Substances Naturelles (ICSN), CNRS. My PhD program was under the Cotutelle Program between University of Malaya, Malaysia and Ecole Polytechnique, France (MOA signed 2011), and within the framework of the LIA (Associated International Laboratory) International French Malaysian Natural Product Laboratory (IFM-NatProLab). During this research program, 18 month was spent in University of Malaya, Malaysia and the other 18 month at Ecole Polytechnique and Institut de Chimie des Substances Naturelles (ICSN), France.

I would like to express my sincere appreciation to the member of jury; Prof. Dr. Hasnah Mohd Sirat (UTM), Prof. Dr. Benoit Crousse (Uni. Paris-Sud), Prof. Dr. Sylvie Michel (Uni. Rene Descartes), Assoc. Prof. Dr. Rozana (UM) and Dr. Fabien L. Gagosz (EP) for accepting to participate in my PhD defense. I would like to take this occasion to thank Prof. Dr. Samir Z. Zard, Director of the Laboratory of Organic Synthesis (LSO) for believing in me and for giving the opportunity to work at LSO during my PhD. I was grateful to the Bright Spark Unit (Prof. Dr. Sharifuddin Md Zin and Mdm. Munirah), Institute of Graduate Studies (Prof. Dr. Norhanom, Prof. Dr. Fauza, Prof. Dr. Kamila and Prof. Dr. Mohamed Kheireddine**)** and the French Embassy for the PhD scholarship. Many thanks to Mr. Mahamad Apandi, Mr. Hud Hanapi, Mr. Mohd Hadi, Ms. Audrey Lemarechal, Mr. Emmanuel Fullenwarth, and Mdm. Brigitte Oisline for helping me for administration matter, and Dr. Mathieu Guerin, Dr. Maxime Feraille, Mr. Xavier Flamand (Officers at French Embassy in Malaysia) for their advice and support during my preparation to France and my stay in France. Special thanks also to Mr. Shahir Shaari (PPL JPA in France), Arif France, Masaf France and Malaysian Embassy in Paris for assistance and support.

I wish to forward my greatest appreciation to the late Prof. Datuk Dr. A. Hamid A. Hadi (UM), late Associate Professor Dr. Mat Ropi Mukhtar (UM), Prof. Emeritus Dr. Thierry Sevenet (ICSN), Dr. Francoise Gueritte (ICSN), Dr. Fanny Roussi (ICSN), Dr. Odile Thoison (ICSN), Dr. Marie-Thérèse Martin (ICSN), Dr. Beatrice Quiclet-Sire (EP), and Ms Lelia Lebon (EP) for their valuable advice and support in making this research a reality. My appreciation also extends to Dr. Leong K. H (UM), Dr. Vincent Dumontet (ICSN), Dr. Charlotte Geny (ICSN) and Dr. Camille Remeur (ICSN) for their help on biological activity testing. I also thank Mr. Din, Mr. Rafly and Mr. T. Leong Eng for the collection and identification of plant material. Great appreciation is also given to Dr. Marie-Thérèse Martin (ICSN) and Mr. Nordin M. (UM) for NMR advice,

and Dr. Michel Levart (EP), Ms. Cecile Apel (ICSN) and Ms. Nina Corlay (ICSN) for recoding my HRESIMS. We thank the University of Malaya (PV050/2012A, SF018-2013, RP001-2012A, and RP001-2012B), the Agence National de la Recherche (ANR), contract number ANR-2010-JCJC-702-1 and ANR-10-LABEX-25-01 for financial support.

Last but not least, I wish to extend my thanks to my friends in Phytochemistry Laboratory (PhytoLab, UM), Campus Gif (ICSN, CNRS) and DCSO (EP) with whom I shared all these wonderful moments over the years; Dr. Kee (MY), Dr. Yasodha (MY), Dr. Mario (AR), Dr. Valentin (RU), Dr. Jiri (CZ), Dr. Azlan (MY), Dr. Kartini (MY), Dr. Mehdi (FR), Dr. Melanie (FR), Dr. Jeremy (FR), Dr. Jane (UG), Dr. Pierre-Marie (FR), Mr. Fadzli, Mr. Chong, Mrs. Norsita, Mr. Omer, Mr. Ahmad Kaleem, Mrs. Chan, Ms. Aimi, Ms. Devi, Mrs. Azeana, Mrs. Nurul Nazneem, Mrs. Faizah, Mrs. Nadia, Ms. Maryam, Mr. Aqmal, Mr. Hafiz, Mr. Azrul, Ms. Julia, Ms. Haslinda, Mr. Mehran, Mr. Wei, Mr. Liang, Mr. Ling, Mr. Laurent, Mr. Shiguang, Mr. Fabien, Mr. Songzhe, Mr. Pierre, Mr. Guilhem, Ms. Lucile, Ms. Helene, Mr. Louis-felix and others for their kindness, support and friendship. Thank you to one of my best friends, Mr. Pavels Ostrovskis (late) for your motivation in helping me to solve the internet problem and wifi setting on my laptop, and to discuss about chemistry and other issues.

Finally, I would like to express my special appreciation to my beloved wife; Munirah Suhaimi, my beautiful daughters; Nur Izzah Insyirah, Nur Alia Humairah, Nur Amira Safiya, my father; Mohamad Taib Baba; my mother; Che Feradah Abd. Wahab, my father in-law; Suhaimi Aman, my mother in-law; Noraini Idris, brothers and sisters whose support and affection helped me complete my PhD studies both in Malaysia and France. Without their prayers and relenting support, I could not be here.

TABLE OF CONTENTS

CHAPTER 7: METHODOLOGY AND EXPERIMENTAL

LIST OF SCHEMES

LIST OF FIGURES

LIST OF TABLES

LIST OF ABBREVIATIONS AND SYMBOLS

ABBREVIATIONS

A

ACN	Acetonitrile
AcCoA	Acetyl Co-enzyme A
AcOH	Acetic acid
ACP	Acyl carrier protein
AIBN	Azobisisobutyronitrile
$AgNO_3$	Silver nitrate
ANOVA	Analysis of variance
ASTM	American society for testing and material
AT	Acyl transferase
A-549	Human non-small cell lung cancer

B

Bak	Bcl-2 homologous antagonist/killer
Bax	Bcl-2-associated X protein
Bcl-2	B-cell lymphoma 2
Bcl-xL	B-cell lymphoma – extra large
BH3	Bcl-2 homology domain 3
Bid	BH3-interacting domain death agonist
Bim	Bcl-2-like protein 11
bp.	Boiling point
br s	Broadened singlet
br d	Broadened doublet

C

Calcd.	Calculated
CBr_4	Tetrabromomethane
CC	Column chromatography
CCl_4	Carbon tetrachloride
$CDCl_3$	Deuterated chloroform
CH	Methine
CH_2	Methylene

CH_3	Methyl group
CH_3CHO	Acetaldehyde
CH_2Cl_2	Methylene chloride / Dichloromethane
$CHCl_3$	Chloroform
c-maf	V-maf avian musculoaponeurotic fibrosarcoma oncogene homolog
CNRS	Centre National de la Recherche Scientifique
COOH	Carboxyl group
COSY	H-H correlation spectroscopy
CO_2	Carbon dioxide
CuCl	Copper (I) chloride
CuI	Copper (I) iodide
$CuSO_4$	Copper (II) sulfate

D

DBU	1,8-Diazabicyclo[5.4.0]undec-7-ene
DCM	Methylene chloride / Dichloromethane
DEPT	Distortionless enhancement by polarization transfer
d	Doublet
dd	Doublet of doublets
ddd	Doublet of doublet of doublets
dddd	Doublet of doublet of doublet of doublets
ddt	Doublet of doublet of triplets
DH	Dehydratase
DIBAL-H	Diisobutyl ammonium hydride
DMAP	Dimethylmino pyridine
DMF	Dimethylformamide
DMP	Dess-Martin periodinane
DMSO	Dimethyl sulfoxide
DNA	Deoxyribonucleic acid
dq	Doublet of quartets
dt	Doublet of triplets

E

E1	Elimination reaction
EDC.HCl	1-Ethyl-3-(3-dimethylaminopropyl)carbodiimide
EDTA	Ethylenediaminetetraacetic acid
ER	Enoyl reductase
ESIMS	Electron spray ionization mass spectroscopy
EtOAc	Ethyl acetate
EtOH	Ethanol
$EtNH_2$	Ethylamine
Et_3N	Triethylamine

F

FA	Formic acid
FAS	Fatty acid synthase
F-Bak	BH3 domain of BAK protein
F-Bid	BH3 domain of BID protein

H

H^+	Hydrogen ion
H_2	Hydrogen gas
HCl	Hydrochloric acid
HMBC	Heteronuclear multiple bond coherence
HOAc	Acetic acid
HOBt	Hydroxybenzotriazole
HPLC	High-performance liquid chromatography
HRMS	High-resolution mass spectrometry
HRESIMS	High-resolution electrospray ionisation mass spectrometry
$HSnBu_3$	Tributyltin hydride
Hsp90	Heat shock protein 90
HSQC	Heteronuclear single quantum coherence
HT-29	Human colorectal adenocarcinoma cell line
HWE	Horner–Wadsworth–Emmons reaction
H_2O	Water
H_2O_2	Hydrogen peroxide
H_2SO_4	Sulfuric acid

I

IBX	2-Iodoxybenzoic acid
ICSN	Institut de Chimie des Substances Naturelles
IC_{50}	Concentration required to inhibit of 50% activity
iNOS	Nitric oxide synthase
iPr_3P	Triisopropylphosphine
IR	Infrared

J

JEOL	Japan Electronic Optics Laboratory Co. Ltd., Tokyo, Japan

K

KOH	Potassium hydroxide
KR	Keto-reductase
KS	Ketosynthase

L

LCMS-IT-TOF	Liquid chromatography mass spectrometer ion-trap and time-of-flight
$LiAlH_4$	Lithium ammonium hydride
LiBr	Lithium bromide
LiCl	Lithium chloride
Li_2CO_3	Lithium carbonate

M

m	Multiplet
MAC	***Mycobacterium avium*** complex
MCAT	Malonyl-co-enzyme A
MCl-1	Myeloid cell leukemia 1
m-CPBA	***meta***-Chloroperoxybenzoic acid
MeCN	Acetonitrile
MeOH	Methanol
Me_3SiOTf	Trimethylsilyl trifluoromethanesulfonate
$MgSO_4$	Magnesium sulfate
MIC	Minimum inhibitory concentration

MOM	Mitochondrial outer membrane
MOMP	Mitochondrial outer membrane permeabilization
mRNA	Messenger RNA
MRSA 108	Methicillin-resistant ***Staphylococcus aureus***
MS	Mass spectrometry
MsCl	Methanesulfonyl chloride
MT	Methyltrasferase
MTS	(3-(4,5-dimethylthiazol-2-yl)-5-(3-carboxymethoxyphenyl)-2-(4-sulfophenyl)-2H-tetrazolium)

N

N_2	Nitrogen gas
$NaBH_4$	Sodium borohydride
NBS	N-Bromosuccinimide
NaCl	Sodium chloride
Na_2CO_3	Sodium carbonate
NaH	Sodium hydride
$NaHCO_3$	Sodium hydrogen carbonate
Na_2HPO_4	Disodium phosphate (DSP)
NaHMDS	Sodium bis(trimethylsilyl)amide
NaOAc	Sodium acetate
NaOCl	Sodium hypochlorite
NaOH	Sodium hydroxide
Na_2SO_3	Sodium Sulfit
Na_2SO_4	Sodium Sulfat
nBu$_4$NBF$_4$	Tetrabutylammonium tetrafluoroborate
NCI-H460	Human lung cancer cell NCI-H460
n.d	Not determined
NFAT	Nuclear factor of activated T-cells
NF54	***Plasmodium falciparum*** strain NF54
NH_3	Ammonia
NH_4Cl	Ammonium chloride
NMR	Nuclear magnetic resonance
NO	Nitric oxide
NOE	Nuclear overhauser effect

NOESY	Nuclear overhauser effect spectroscopy
NSP	Neurotoxic shellfish poisoning
N.T	Not tested

O

$^1O_2$	Singlet oxygen
O_2	Oxygen gas
OCH_3	Methoxyl group
OH	Hydroxyl group
ORTEP	Oak ridge thermal ellipsoid plot

P

PBr_3	Phosphorus tribromide
PC3	Human prostate cancer cell lines
Pd/C	Palladium on carbon
$PdCl_2(dppf)$	[1,1′-Bis(diphenylphosphino)ferrocene]dichloropalladium(II), complex with dichloromethane
$Pd_2(dba)_3$	Tris(dibenzylideneacetone)dipalladium(0)
$Pd_2(PPh_3)_4$	Tetrakis(triphenylphosphine)palladium(0)
$Pd(OAc)_2$	Palladium (II) acetate
$PhCH_3$	Toluene
$(PhSe)_2$	Diphenyl diselenide
Pet. Ether	Petroleum ether 40-60
PKS	Polyketide synthase
PKSs	Polyketide synthases
P_2O_5	Phosphorus pentoxide
$POCl_3$	Phosphoryl trichloride
PPh_3	Triphenylphosphine
PTAB	Phenyl trimethyl ammonium perbromide
PUMA	p53 upregulated modulator of apoptosis
P-388	Murine lymphocytic leukemia cell P-388
$(Ph_3PCH_2I)^+ I^-$	(Iodomethyl)triphenylphosphonium iodide

Q

q	quartet

R

RCDA	Radical cation Diels-Alder
rel	Relative
R_f	Retention factor
$[Rh(Cod)Cl]_2$	Chloro(1,5-cyclooctadiene)rhodium (I) dimer
rt	Room temperature

S

s	Singlet
SAR	Structure-activity relationship
$SbC_6.N(\textbf{\textit{p}}\text{-}BrPh)_3$	Ledwith-Weitz salt
SEM	Standard error of the mean
SET	Single electron transfer
SiO_2	Silica dioxide
SMAC	Second mitochondria-derived activator of caspases
SMI	Small molecule inhibitors
$SOCl_2$	Thionyl chloride
SO_2Cl_2	Sulfuryl chloride

T

t	triplet
TBAB	Tetrabutyl ammonium bromide
TBAF	Tetrabutyl ammonium floride
TBDPS	***tert***-Butyldiphenylsilyl
TBDPSCl	***tert***-Butyldiphenylchlorosilane
TBSCl	***tert***-Butyldimethylsilyl chloride
t-BuOK	Potassium ***tert***-butoxide
td	Triplet of doublets
TE	thionyl esterase
TEA	Triethylamine
TFA	Trifluoroacetic acid
THF	Tetrahydrofuran
TFP	Tetrafluoropropanol
TMEDA	Tetramethylethylenediamine
TMS	Tetramethylsilane

TMSOtf	Trimethylsilyl trifluoromethanesulfonate
TPP	Tetraphenylporphyrin

U

UV	Ultraviolet

Z

Zn	Zinc
Zn-Cu	Zinc-copper couple

SYMBOLS

α	Alfa
Amp	Ampere
β	Beta
cm	Centimeter
cm^{-1}	Per centimeter
δ	Chemical shift
δ_C	Chemical shift carbon
δ_H	Chemical shift proton
g	Gram
$gmol^{-1}$	Gram per mol
h	Hour
Hz	Hertz
J	Coupling constant (Hz)
Kg/m^3	Kilogram per cubic meter
L	Liter
λ_{max}	Lambda (maximum wavelength)
M	Mole/L
m	Meter
m/z	Mass / Charge
mBar	Milli Bar
mg	Miligram
MHz	Mega Hertz
min	Minute
µL	Micro liter

µM	Micro molar
mL	Milli liter
mL/min	Milli liter per minute
mM	Milli molar
mmol	Milli mol
N	Normality
nM	Nanomolar
nm	Nanometer
ppm	Part permillion
Volt	Voltan
v/v	volume / volume

LIST OF APPENDICES

CHAPTER 1

INTRODUCTION

1.1 General

Since the dawn of civilization, natural products (secondary metabolite) have been the source of medication to treat various medical ailments (Appendino et al., 2010; Dias, 2012; Cragg & Newman, 2005; Newman et al., 2003; Harvey, 2008; Butler, 2004; Mishra & Tiwari, 2011). The earliest records of natural products application were depicted on clay tablets in cuneiform from Mesopotamia (2600 B.C.) which documented the usage of oils from *Cupressus sempervirens* and *Commiphora* species to treat coughs, colds and inflammation (Cragg & Newman, 2005). The Ebers Papyrus (2900 B.C.) is an Egyptian pharmaceutical record, which documents over 700 plant-based drugs ranging from gargles, pills, infusions, to ointments. The Chinese Materia Medica (1100 B.C., contains 52 prescriptions), Shennong Herbal (~100 B.C., 365 drugs) and the Tang Herbal (659 A.D., 850 drugs) are documented records of the uses of natural products (Cragg & Newman, 2005).

The Greek physician, Dioscorides, (100 A.D.), recorded the collection, storage and the uses of medicinal herbs, whilst the Greek philosopher and natural scientist, Theophrastus (~300 B.C.) dealt with medicinal herbs. During the Dark and Middle Ages, the monasteries in England, Ireland, France and Germany preserved this Western knowledge whilst the Arabs preserved the Greco-Roman knowledge and expanded the uses of their own resources, together with Chinese and Indian herbs unfamiliar to the Greco-Roman world (Cragg & Newman, 2005). It was the Arabs who were the first to privately own pharmacies (8^{th} century) with Avicenna, a Persian pharmacist, physician, philosopher and poet, contributing much to the sciences of pharmacy and medicine through works such as the *Canon Medicinae* (Cragg & Newman, 2005).

"When you have no idea where to begin in a drug discovery program, Nature is a good starting point."

L. H. Caporale (Rouhi, 2003).

Today, scientists including phytochemists and pharmacologists continue to study the chemical components of plants hoping to find new compounds with biological activities which can be used as lead compounds and further develop them into therapeutic agents (Figure 1.1). Among the plant derived therapeutic agents are vinblastine (**1**) and vincristine (**2**), the natural alkaloids isolated from *Catharantus roseus* (L) G. Don (Apocynaceae) (Figure 1.1). These major drugs are used to treat Hodgkin's lymphoma and acute childhood leukemia (Barnett et al., 1978). Paclitaxel (**3**) which is found naturally in the bark of *Taxus brevifolia* Nutt. (Taxaceae), has a unique mode of anticancer action (Wani et al., 1971). In vitro, paclitaxel (**3**) enhances the polymerization of the tubulin to stable microtubules and also interacts directly with microtubules, stabilizing them against depolymerization and is active against breast, brain, tongue, endometrial and ovarian cancers (Manfredi et al., 1984; Cragg & Suffness, 1988; Kingston, 1991). The alkaloid colchicine (**4**) was isolated from *Colchicum autumnale* L. (Liliaceae). It has long been and is still used medicinally, currently to treat gout and familial Mediterranean fever (Figure 1.1). This compound is a mitotic inhibitor, which inhibits the polymerization of tubulin (Brossi, 1984; Altmann & Gertsch, 2007).

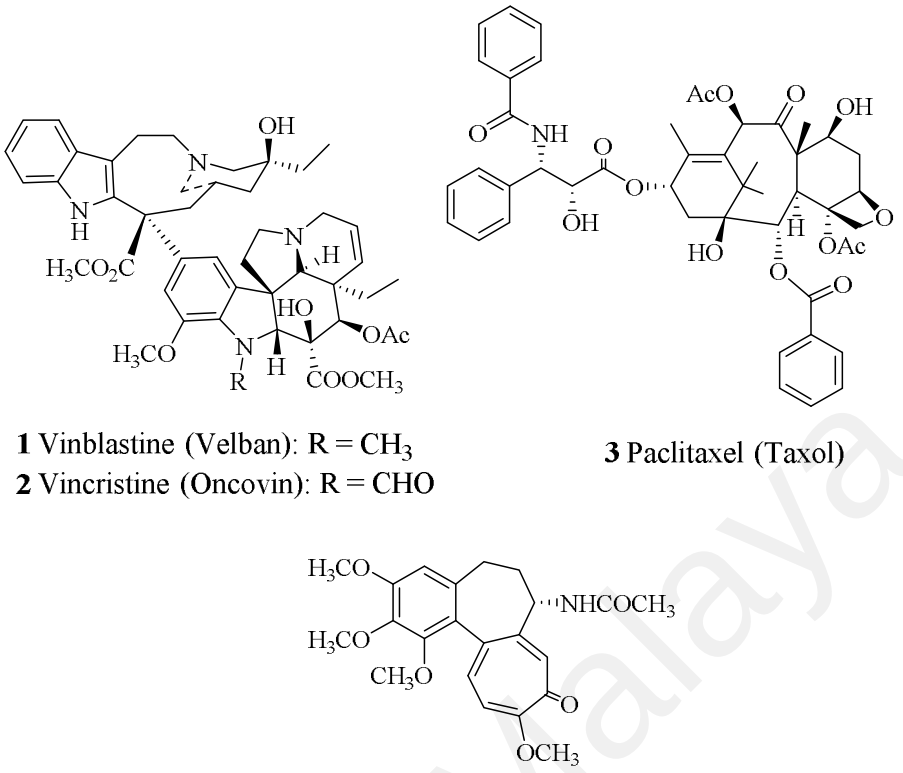

1 Vinblastine (Velban): R = CH_3
2 Vincristine (Oncovin): R = CHO

3 Paclitaxel (Taxol)

4 Colchicine

Figure 1.1: Lead compounds for therapeutic agents

At present, attention to targeted therapy has dramatically increased especially in cancer treatments. The term "targeted cancer therapy" refers to a new generation of drugs designed to interfere with a specific molecular target that is believed to play a critical role in tumor growth or progression and is not expressed significantly in normal cells. There has been a rapid increase in the identification of targets that have potential therapeutic application (Chon & Hu, 2006). In this context, pro and antiapoptotic proteins play central roles in cell death regulation and are capable of regulating diverse cell death mechanisms that encompass apoptosis, necrosis and autophagy (Yip & Reed, 2008; Lessene et al., 2008; Cotter, 2009; Elmore, 2007).

The antiapoptotic protein Bcl-xL, has become an attractive molecular target in cancer treatment and this target was almost unknown before 1993 (Wang, 2008). However, the number of publications related to this protein has increased dramatically over the past

few years, indicating a promising new laboratory approach (Dharap et al., 2006). The substances that can down-regulate Bcl-2 and/or Bcl-xL expression or activity may be useful for cancer chemotherapy (Leo et al., 2008). The discovery of potent inhibitors of Bcl-xL has resulted from NMR studies and parallel synthesis (Petros et al., 2005), or has been based on computational structure based modelling (Enyedy et al., 2001) or multiple high-throughput screening platforms (Qian et al., 2004).

Recent studies have shown that most cancers depend on more than one antiapoptotic Bcl-2 member for survival. Among these proteins, Mcl-1 is overexpressed in many cancers, contributes to tumor progression, and has emerged as one of the major resistance factors in cancer cells (Lessene et al., 2008; Jeng & Cheng, 2013). Thus, the effective treatment suggested by Placzek's team, require inhibition of multiple antiapoptotic Bcl-2 proteins (Placzek et al., 2010). Placzek and co-workers investigated the mRNA expression levels of all six antiapoptotic Bcl-2 subfamily members in 68 human cancer cell lines (Placzek et al., 2010). The study revealed that Mcl-1 represents the anti-apoptotic Bcl-2 subfamily member with the highest mRNA levels in the lung, prostate, breast, ovarian, renal, and glioma cell lines (Placzek et al., 2010). In this context, Mcl-1 and Bcl-xL are crucial regulators of apoptosis; therefore dual inhibitors of both proteins could serve as promising new anticancer drugs.

In recent years, various screenings have been undertaken to find natural molecules that could be used either as tools to understand the roles of the Bcl-2 family proteins or to develop the next generation of anticancer drugs (Lessene et al., 2008) (Figure 1.2). The natural product (-)-gossypol (**5**), derived from cotton plant, showed the antiproliferative properties (Dodou et al., 2005; Li et al., 2008). Further studies have revealed that these enantiomers bind Bcl-3 (K_i = 320 nM), Bcl-xL (K_i = 480 nM) and Mcl-1 (K_i = 180 nM) (Tang et al., 2008). Others include natural products such as chelerythrine (**6**) (Wan et al., 2008), incednine (**7**) (Futamura et al., 2008) and

meiogynine A (**8**) (Litaudon at al., 2009; Fotsop et al., 2010; Dardenne et al., 2013; Desrat et al., 2014) (Figure 1.2). Chelerythrine (**6**) was identified as an inhibitor of the antiapoptotic protein Bcl-xL, after a systematic *in vitro* evaluation on 107,423 extracts derived from natural products (Chan et al., 2003). This compound was a benzophenanthridine alkaloid and showed the Bcl-xL-Bak BH3 peptide binding with IC_{50} of 1.5 µM (Chan et al., 2003). The ability of chelerythrine (**6**) to displace the Bak BH3 peptide in the FP assay suggests that it may be able to displace BH3-containing proteins from Bcl-xL (Chan et al., 2003) (Figure 1.2). Meanwhile, meiogynine A (**8**) was a dimeric sesquiterpenoid isolated from *Meiogyne cylindrocarpa* (Litaudon et al., 2009). This compound possessed an unprecedented substituted *cis*-decalin carbon skeleton and showed the Bcl-xl/Bak binding affinity with a K_i of 10.3 ± 3.1 µM (Litaudon et al., 2009) (Figure 1.2).

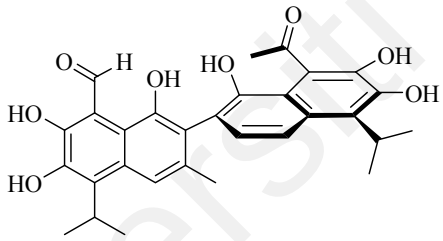

(-)-Gossypol (**5**)

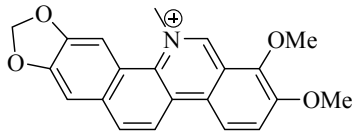

Chelerythrine (**6**)

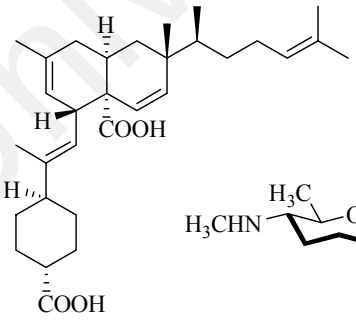

Meiogynine A (**8**)

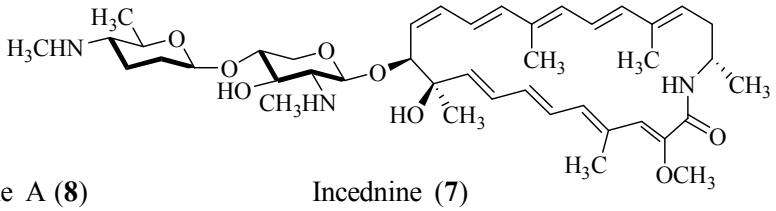

Incednine (**7**)

Figure 1.2: Natural inhibitors of the anti-apoptotic protein

In the context of a Malaysian-French collaborative program, 1476 extracts (prepared from approximately 700 Malaysian plants) were screened for Bcl-xL binding affinity. This preliminary study showed that the bark of *Endiandra kingiana* Gamble (Lauraceae) exhibited potency as a modulating agent between Bcl-xL and Bak (Leverrier et al., 2010, 2011), which prompted its chemical investigation by the author.

1.2 Lauraceae: general appearance and morphology

In Malaysia, the Lauraceae family is known as *Medang* or *Tejur*. The Lauraceae or Laurel family comprises a group of flowering plants included on the order Laurales. The family contains about 68 genera and over 2980 species worldwide, mostly from tropical regions, especially Southeast Asia and tropical America (The Plant List, 2013). The tree of Lauraceae are usually evergreen, shrubs and without buttresses (Keng, 1978; Foxworthy, 1927; Desch, 1957; Corner, 1988; Rohwer, 1993).

In the highlands, Lauraceae like fagaceae, become more abundant upon reaching the top layer of the forest, which lies at 1200 – 1600 m. For example, Oak-Laurel Forest is a feature of the mountains of tropical Asia from Himalayas to New Guinea. The bark is usually smooth, rarely fissured, scaly or dippled, often covered with large lenticels, grey-brown to reddish-brown. The inner bark is usually very thick, granular, mottled or laminated, often with strong aromatic smell, yellow, orange-brown, pinkish or reddish. Sapwood is pale yellow to pale brown with satiny luster when freshly cut. Terminal buds are naked or covered with bud scales which sometimes appear like small leaves.

The leaves of species belonging to this family appear in a simple way. They are spiral, alternate, opposite, subopposite, or whorled (*Actinodaphne*), entire and leathery. The secondary veins pinnate have only one pair as in *Cinnamomum*. The colours of the new leaves vary from nearly white to pink, purple or brown (Keng, 1978; Foxworthy, 1927; Desch, 1957; Corner, 1988; Rohwer, 1993; The Plant List, 2013).

The flowers of Lauraceae are usually small, regular, greenish, white or yellow, fragrant or with rancid smell, bisexual or unisexual, perianth free or united with six sepals in two rows. The flowers are pollinated chiefly by flies and beetles which are attracted by smell emitted from the flowers. The fruit of this family are small to large (one seed berry), sometimes enveloped by the accrescent perianth tube or persisting and clasping the base of fruit. In some genera perianth lobes are dropping, but the tubes develop into a shallow or deep cut at base of fruit. The fruits stalks enlarge and become highly coloured in some species of *Dehaasia* and *Alseodaphne*. The seeds of Lauraceae are without albumen, with thin testa. Cotyledons large, flat, convex, pressed against each other (Keng, 1978; Foxworthy, 1927; Desch, 1957; Corner, 1988; Rohwer, 1993; The Plant List, 2013).

Wood of Lauraceae is soft to moderately hard, light to moderately heavy to varying from 350-880 kg/m^3 dry air. Grain straight or slightly interlocked, texture moderately fine and even. Sapwood usually is a distinctly lighter shade than the heartwood. The heartwood is yellow-white (*Beilschmiedia*), yellow-brown or red-brown in most species *Cinnamomum*, *Cryptocarya* and *Endiandra*, olive green in species of *Litsea*, *Actinodaphne*, *Alseodaphne*, *Nataphoebe*, *phoebe*, and dark olive green-brown in *Dehaasia* (The Plant List, 2013). The family of Lauraceae provides many useful economic products. Most of the economically important species, other than sources of excellent wood function as spices or flavoring agent. For example avocado (*Persea*) is a well known important tropical fruit.

1.3 Lauraceae: classification of tribes

Classification of Lauraceae can be illustrated in the list below. The classification included 68 genera, mainly found in Southeast Asia and Latin America (The Plant List, 2013; Kerrigan el al., 2011).

Kingdom : Plantae.

Division : Magnoliophyta.

Class : Magnoliopsida.

Order : Laurales.

Family : Lauraceae.

Genus :

Actinodaphne	*Aiouea*	*Alseodaphne*	*Aniba*
Apollonias	*Aspidostemon*	***Beilschmiedia***	*Camphora*
Caryodaphnopsis	*Cassytha*	*Chlorocardium*	*Cinnadenia*
Cinnamomum	*Cryptocarya*	*Dehaasia*	*Dicypellium*
Dodecadenia	***Endiandra***	*Endlicheria*	*Eusideroxylon*
Gamanthera	*Hufelandia*	*Hypodaphnis*	*Iteadaphne*
Kubitzkia	*Laurus*	*Licaria*	*Lindera*
Litsea	*Machilus*	*Malapoenna*	*Mespilodaphne*
Mezilaurus	*Misanteca*	*Mocinnodaphne*	*Mutisiopersea*
Nectandra	*Neocinnamomum*	*Neolitsea*	*Notaphoebe*
Nothaphoebe	*Ocotea*	*Oreodaphne*	*Paraia*
Parasassafras	*Parthenoxylon*	*Persea*	*Phoebe*
Phyllostemonodaphne	*Pleurothyrium*	*Polyadenia*	*Potameia*
Potoxylon	*Povedadaphne*	*Ravensara*	*Rhodostemonodaphne*
Sassafras	*Schauera*	*Sextonia*	*Sinopora*
Sinosassafras	*Syndiclis*	*Systemonodaphne*	*Tetranthera*
Umbellularia	*Urbanodendron*	*Williamodendron*	*Yasunia*

1.4 The genus: *Endiandra*

Endiandra is a genus of evergreen trees which belongs to the Laurel family, Lauraceae. The genus includes more than 125 species distributed in Southeast Asia, Pacific region and Australia (The Plant List, 2013). Meanwhile, ten species are found in Malaysia namely; *E. holttumii*, *E. kingiana*, *E. macrophylla*, *E. maingayi*, *E. praeclara*, *E. rubescens*, *E. wrayi*, *E. sp.1* and *E. sp. 2* (Ng, 1989; Burkill, 1966). The leaves are alternate, pinnatinerved, with areolate venation (except in *E. introsa*). Inflorescences in axillary and substerminal panicles. Flowers in axillary panicles are usually shorter than the leaves. Flowers are bisexual, mostly 3-merous (4-merous in *E. globosa*). Perianth segments 6 or 8, not persistent in fruit. Stamens usually 3 (4–6 in *E. globosa*), anthers 2-locular, dehiscence usually extrorse (introrse in *E. introrsa*); associated glands present or occasionally absent, staminodes usually 3 (sometimes 2–0 in *E. globosa*). Ovaries are often superior, producing fruits in the form of drupe which are free on the receptacles. The seeds are dispersed by animals and birds (Ng, 1989; Burkill, 1966).

1.5 *Endiandra kingiana* Gamble

Endiandra kingiana (Figure 1.3) is a large sub-canopy tree growing up to 33 m tall, 210 cm girth, and bole with buttresses. Bark is ochre grey and smooth. Inner bark is reddish and sapwood is pale yellow. Leaves stalk up to 2 cm long, stout, hairy to glabrous, blade thickly leathery and elliptic to oblong. Inflorescences in are 5 cm long pubescent panicles. The flowers are perianth waxy yellow, 3 mm diameter and placed in panicles. Fruits are oblong shape (3 x 1.5 cm), shiny green to drying brown. The species can be found in Dipterocarp forest up to 100 m altitude in Pahang, Perak, Kelantan, Negeri Sembilan, Johor and Borneo (Ng, 1989; Burkill, 1966; Maberley, 2008).

Figure 1.3: *Endiandra kingiana* Gamble

(Herbarium of the Department of Chemistry, University of Malaya, Kuala Lumpur)

1.6 Problem statement

In Lauraceae species only two genus; *Endiandra* and *Beilschmiedia* were reported to contain polyketides in the form of endiandric acids and kingianins (Lenta et al., 2015). The chemical investigation of endemic *Endiandra kingiana* led to the isolation of the series of polyketides named kingianins A-N (**45**-**58**). Among them, kingianin G (**51**) was found to be the most potent inhibitor of Bcl-xL/Bak interaction with $Ki \approx 2.0$ µM (Leverrier et al., 2011).

Based on these finding, the methanol extract of *Endiandra kingiana* was subjected to affinity displacement assays and it also showed a moderate potency as a modulating agent with both antiapoptotic proteins, Bcl-xL/Bak (30% at 10 µg/ml) and Mcl-1/Bid (22% at 10 µg/ml). These preliminary results motivated its chemical investigation and its application as dual inhibitors of both anti-apoptotic proteins (Bcl-xL/Bak and Mcl-1/Bid). The cytotoxic activity of isolated compounds was performed to understand the correlation between targeted and cytotoxic therapies.

The isolation and identification of natural products not only provides a foundation for new biological active compound and drug candidates, but also a feedstock of complex and unique molecular structures to inspire and challenge synthetic chemists. Therefore, an approach to the synthesis of kingianins which involved the construction of bicyclo[4.2.0]octadiene backbone was designed.

1.7 The objectives of studies

The objectives of the study are as follows:

1. To isolate and identify the cyclic polyketides from *Endiandra kingiana* Gamble. using spectroscopic methods such as NMR, UV, IR and HRMS

2. To investigate the biological activities of the compounds isolated from *Endiandra kingiana* in particular their Bcl-xL/Bak and Mcl-1/Bid binding affinities, and their cytotoxic activity on various cancer cell lines.
3. To synthesize the pentacyclic polyketide skeleton of kingianins via conventional organic synthetic methods (non-biomimetic synthesis).

1.8 Scope of research

In this study, the methanol extract from *Endiandra kingiana* will be subjected to chromatographic separation and spectroscopic analysis for isolation and identification of cyclic polyketides. The isolated compounds will be tested on binding affinities towards Bcl-xL/Bak and Mcl-1/Bid and cytotoxic effects against various human tumour cell lines. The SAR analysis will be performed to provide further insight and understanding on the structural features that could influence the activity of a compound belonging to a cyclic polyketide type.

For the synthesis of kingianins, a new strategy with a more original and diversity-oriented approach (non-biomimetic synthesis) was designed. The synthesis will begin with the construction of bicyclo[4.2.0]octadiene backbone.

1.9 Significance of research

This study highlights some of the major questions in polyketides natural product research, including the biogenesis of compounds, structural identifications and binding affinities towards Bcl-xL/Bak and Mcl-1/Bid (on antiapoptotic proteins). Two groups of compounds were isolated and characterized; the endiandric acid series and the kingianin series. Among them, the kingianin series has a promising approach in the development of anticancer agents.

For the synthesis part, the finding emphasized a new and more direct synthetic approach to synthesize the bicyclo[4.2.0]octadiene sub-units of kingianins. It involved a [2+2] cycloaddition of cyclohexadiene substrates to functionalized ketenes which occurred by simultaneous C-C bond formation. These approaches will prove applicable to step-economical syntheses of kingianins, thus maximizing the chances for an overall good yield of the final products.

1.10 Thesis content

Results are presented in three chapters: i) Phytochemical studies of *Endiandra kingiana* Gamble (Chapter 3); ii) Bcl-xL/Bak and Mcl-1/Bid binding affinities and cytotoxic activity of cyclic polyketides (Chapter 4); and iii) Approaches to the synthesis of kingianins (Chapter 5). Each of these chapters contains a presentation of the results and their full discussion. Meanwhile, Chapter 2 consists of literature review on polyketides, biogenesis of cyclic polyketides and examples of cyclic polyketides isolated from *Endiandra* and *Beilschmiedia* species. Experimental procedures, general conclusion and corresponding list of references are covered in this manuscript.

CHAPTER 2

GENERAL AND CHEMICAL ASPECTS

2.1 Introduction

The secondary metabolites are organic compounds that are not directly involved in the normal growth, development, or reproduction of an organism. The absence of secondary metabolites do not result in immediate death, but rather in long-term impairment of the organism's survivability, fecundity, or aesthetics, or perhaps results in no significant change at all. Secondary metabolites are often restricted to a narrow set of species within a phylogenetic group. Secondary metabolites often play an important role in plant defense against herbivory and other interspecies defenses. Humans use secondary metabolites as medicine, flavorings, and recreational drugs (Dickschat, 2011; Crozier et al., 2006; Wink, 2010; Bourgaud et al., 2001; Sanchez et al., 2011; Zhong, 2011; Hanson, 2003). The structures of secondary metabolites may seem to be bewilderingly diverse. However, the majority of these compounds belong to one of a number of families, each of which has particular structural characteristics arising from their biosynthesis (Hanson, 2003). The secondary metabolites can be classified into six types;

- Polyketides and fatty acids
- Terpenoids and steroids
- Phenylpropanoids
- Alkaloids
- Specialized amino acids and peptides
- Specialized carbohydrate

Endiandra species are especially known to be a rich producer of polyketides. So, the following paragraph shall discuss briefly the polyketides and their chemical aspects.

2.2 Polyketides

Polyketides are the compounds which possess a chain of alternating ketone and methylene groups (>CH_2). Each methylene group in a polyketide is flanked by two carbonyl groups (>C=O). The biosynthesis of polyketides begins with the condensation of the starter unit i.e typically acetyl-CoA (**9**) / propionyl-CoA (**10**) and with an extender unit (commonly malonyl-CoA (**11**) or methylmalonyl-CoA (**12**)), followed by decarboxylative condensation unit (Claisen condensation) (Figure 2.1). The polyketide chains produced by minimal polyketide synthases (PKSs), are often derivatized and modified into bioactive natural products (refer Schemes 2.2 and 2.3) (Hanson, 2003; Stanforth, 2006; Staunton & Weissmn, 2001; Scott et al., 2007).

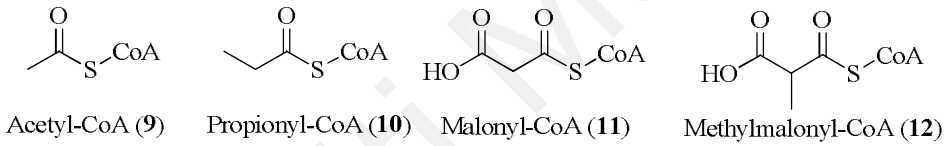

Figure 2.1: Polyketides synthase extender unit

The polyketides are a large family of natural products found in bacteria, fungi and plants. In addition to exhibiting a staggering range of functional and structural diversity, they boast a wealth of medicinally important activities, including antibiotic, anticancer, antifungal, antiparasitic and immunosuppressive properties. The polyketides are broadly divided into eight following major groups based on carbon skeleton characteristics (Scheme 2.1) (Hertweck, 2009):-

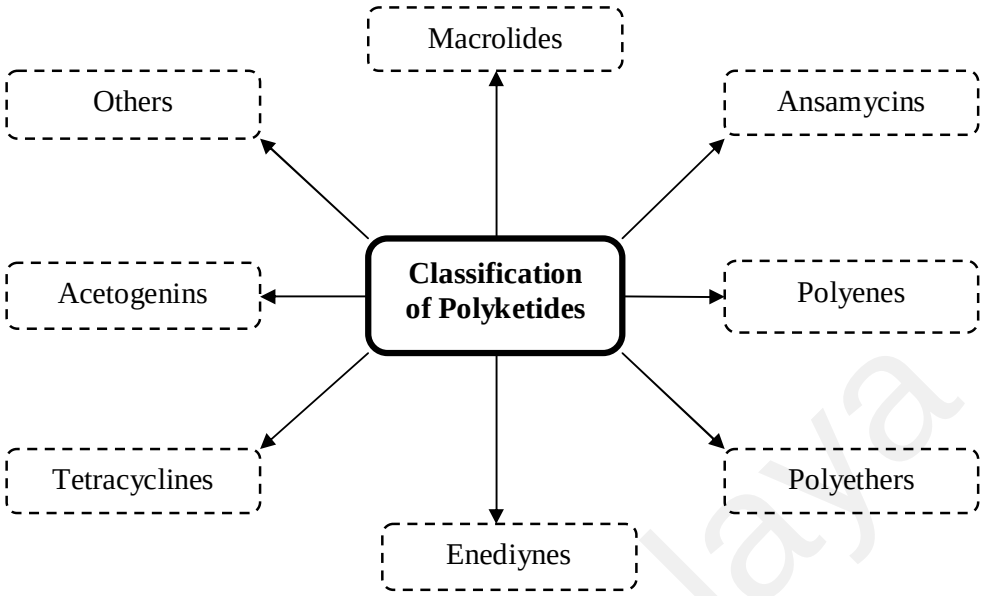

Scheme 2.1: Classification of polyketides

2.2.1 Macrolides

A group of naturally occurring chemical compounds that contain a large macrocyclic lactone ring with one or more deoxy sugars, usually cladinose and desosamine, may be attached (Figure 2.2). The lactone rings are usually 14-, 15-, or 16-membered. Erythromycin A (**14**) and avermectins (**15**) are examples of drugs that are structurally related to the macrolides and generally used as antibiotic and antihelminthic (Mcguire et al., 1952; Lund, 1953; Pitterna et al., 2009; Omura & Shiomi, 2007).

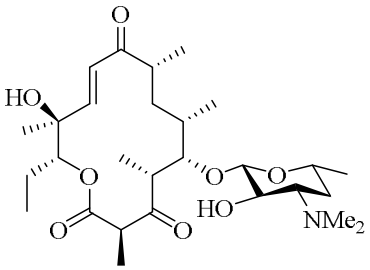

Pikromycin (13)
first isolated macrolide

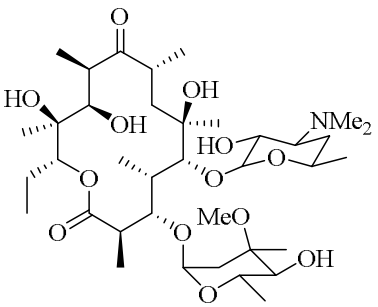

Erythromycin A (14)
macrolide antibiotic

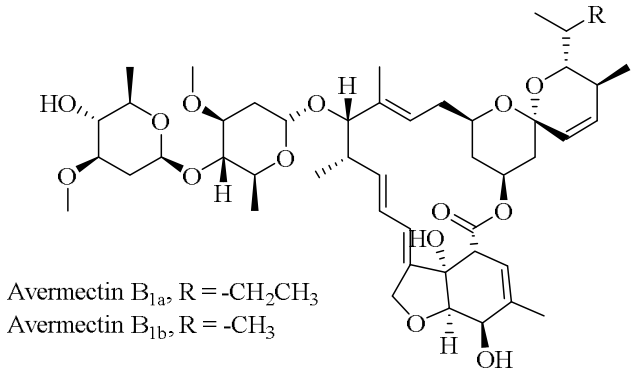

Avermectins (15)
macrolide antihelminthic

Figure 2.2: Example of macrolides

2.2.2 Ansamycins

These types of compounds comprise an aromatic moiety bridged by an aliphatic chain. The main structural differences within the ansamycins series concern aromatic moiety, which can be either a benzene, a naphthalene, a naphthoquinone or a benzoquinone ring system (Figure 2.3). For example, rifamycin S (**16**) is particularly effective against mycobacteria and is often used to treat tuberculosis, leprosy and *Mycobacterium avium* complex (MAC) infections (Wehrli & Staehelin, 1971; Aristoff et al., 2010; Selva & Lancini, 2010). Geldanamycin (**17**) and macbecin (**18**) are used in anticancer treatment, where these drugs inhibit the functions of Hsp90 (Heat Shock Protein 90) (Bedin et al., 2004; Miyata, 2005; Bohen, 1998). Hsp90 client proteins play important roles in the regulation of the cell cycle, cell growth, cell survival, apoptosis, angiogenesis and oncogenesis.

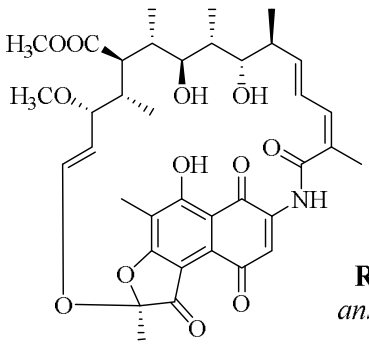

Rifamycin S (16)
ansamycin antibiotic

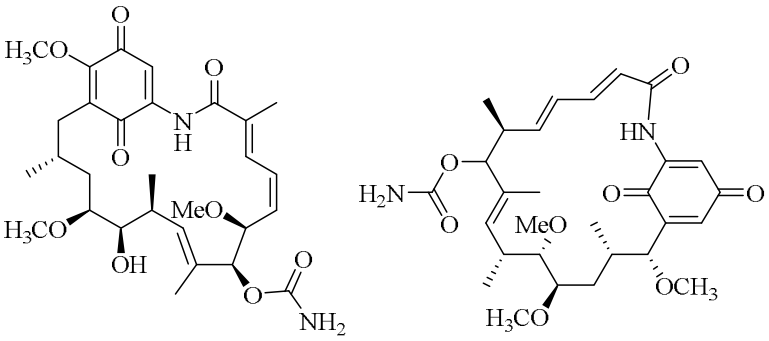

Geldanamycin (17)
ansamycin antitumor

Macbecin (18)
ansamycin antitumor

Figure 2.3: Example of ansamycins

2.2.3 Polyenes

Polyenes are poly-unsaturated organic compounds that contain one or more sequences of alternating double and single carbon-carbon bonds (Figure 2.4). In some cases, the late-stage pericyclic process may happen, which involves the cyclization of conjugated polyene (e.g. endiandric acids). Rapamycin (**19**) was originally developed as an antifungal agent (Vézina et al., 1975). However, it was discovered to have potent immunosuppressive, antiproliferative properties and useful in the treatment of certain cancer (Law, 2005; Bundscherer, 2008). Meanwhile, natamycin (**20**) was classified as a polyene antifungal and used to treat fungal keratitis, an infection of the eye (Thomas, 2003; Pradhan et al., 2011). Endiandric acid H (**21**) was used to treat asthma and was patented by Eder et al. (2004, 2006).

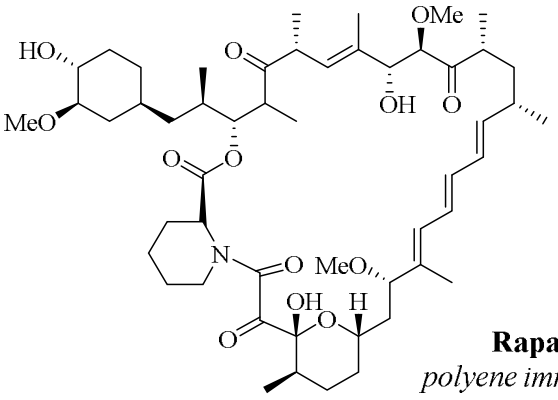

Rapamycin (19)
polyene immunosuppressant

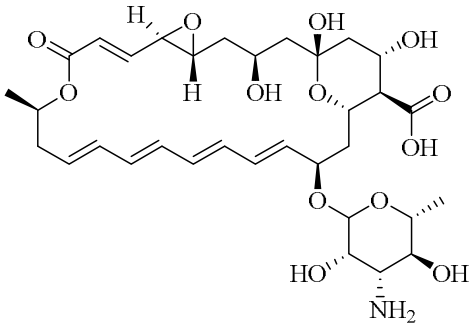

Natamycin (20)
polyene antifungal

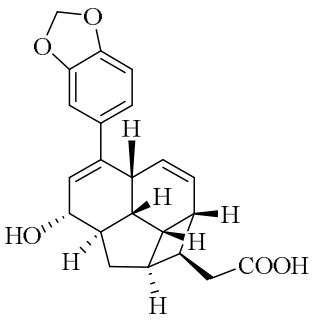

Endiandric acid H (21)
late-stage electrocyclization of polyene antiasthamatic

Figure 2.4: Example of polyenes

2.2.4 Polyethers

Polyethers generally refer to compounds which contain ether functional groups in their main skeleton (Figure 2.5). For example, monensin A (**22**) was a broad-spectrum anticoccicidial antibiotic which exhibits antifungal and antiviral activity (Mollenhauer et al., 1990; Huczyński et al., 2008). On the other hand, brevetoxin-1 (**23**) was a neurotoxin that binds to voltage-gated sodium channels in nerve cells, leading to the disruption of normal neurological process and thus, causing the illness clinically described as neurotoxic shellfish poisoning (Watkins et al., 2008; Nicolaou et al., 1998).

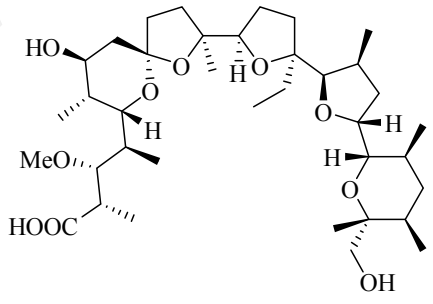

Monensin A (22)
polyether antibiotic

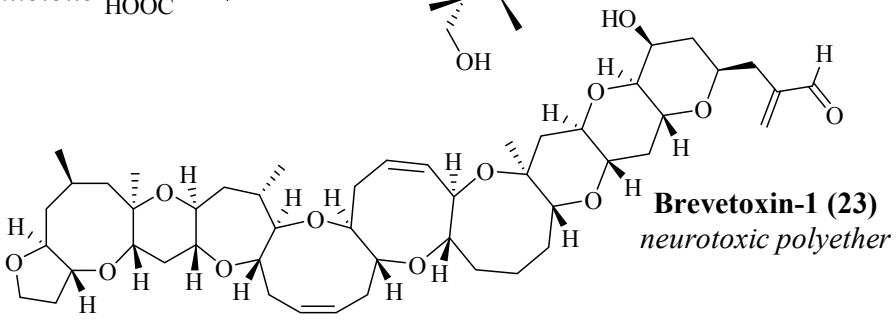

Brevetoxin-1 (23)
neurotoxic polyether

Figure 2.5: Example of polyethers

2.2.5 Enediynes

The enediyne family compounds are characterized by the enediyne core, a unit consisting of two acetylenic groups conjugated to a double bond or incipient double bond within a nine-membered ring or and ten-membered ring (Figure 2.6). The pharmacological properties of neocarzinostatin (**24**) and dynemicin A (**25**) have not been fully explored but current literatures has suggested that they may be potential anticancer agents (Hall et al., 1983; Kobayashi et al., 2006, Nicolaou et al., 1991, Konishi et al., 1990; Kamei et al., 1991, Myers et al., 1995).

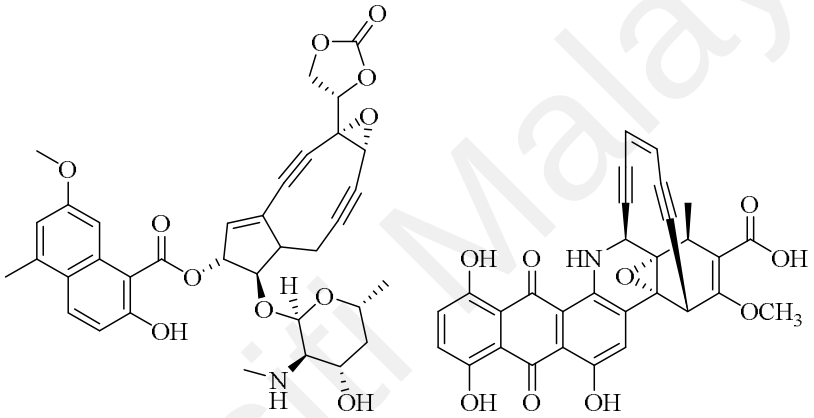

Figure 2.6: Example of enediynes

2.2.6 Tetracyclines

Tetracyclines are broad-spectrum polyketide antibiotic produced by the *Streptomyces* genus of *Actinobacteria*, famously used against many bacterial infections (Ian Chopra et al., 2001). The term 'tetracycline' is used to relate substances that contain the same four-ring system (Figure 2.7). They are defined as 'a subclass of polyketide having an octahydrotetracene-2-carboxamide skeleton'. Tetracycline (**26**), minocycline (**27**) and oxytetracycline (**28**) are frequently used as antibiotic (Ian Chopra et al., 2001; Strauss et al., 2007; Olszewska, 2006). Minocycline (**27**) was synthesized semi-synthetically by

Lederle Laboratories, marketed by them under the brand name Minocin® and frequently used for the treatment of acne vulgaris (Redin, 1966).

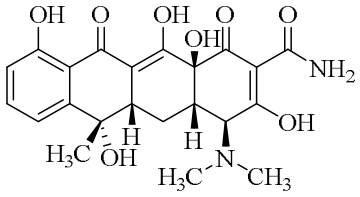

Tetracycline (26)
antibiotic

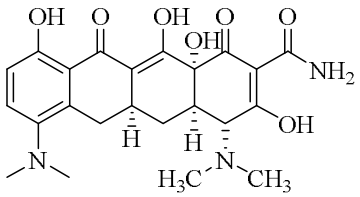

Minocycline (27)
antibiotic

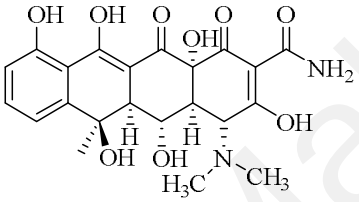

Oxytetracycline (28)
antibiotic

Figure 2.7: Example of tetracyclines

2.2.7 Acetogenins

Acetogenins are characterized by linear 32- or 34-carbon chains containing oxygenated functional groups including hydroxyls, ketones, epoxides, tetrahydrofurans and tetrahydropyrans (Figure 2.8). They are often terminated with a lactone or a butenolide (Li et al., 2008; Rupprecht et al., 1990). Bullatacin (**29**) and uvaricin (**30**) were the examples of compounds with potent anticancer activity (Hui et al., 1989; Chih et al., 2001; Naito et al., 1995; Tempesta et al., 1982). Their toxicity probably arises from their strong inhibition of mitochondrial electron transport with a specific action at complex 1 (NADH ubiquinone oxidoreductase) (Degli et al., 1994; Zafra-Polo et al., 1996).

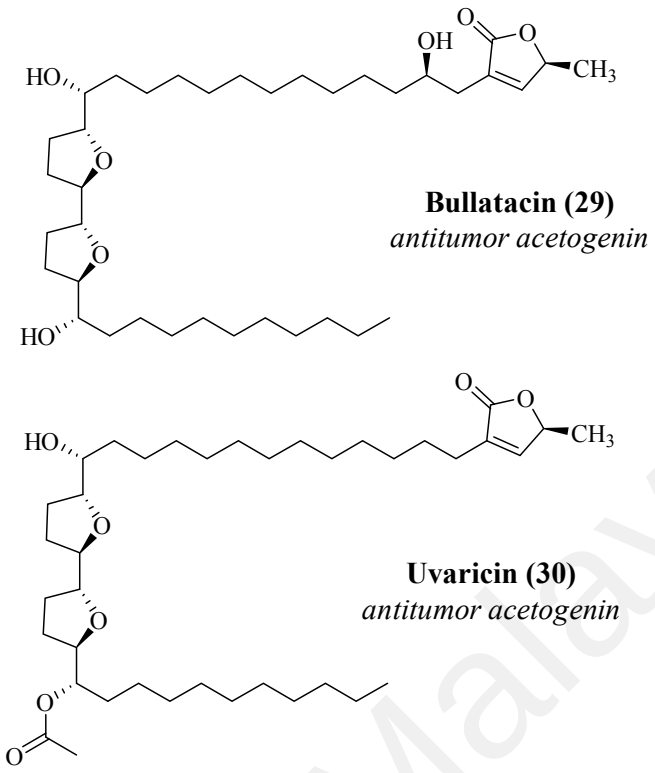

Figure 2.8: Example of acetogenins

2.2.8 Others

Compounds that do not have the same skeleton as above are categorized in this group (Figure 2.9). For example, actinorhodin (**31**) is a polyketide antibiotic produced by *Streptomyces coelicolor* and aflatoxin B1 (**32**) is toxic and considered carcinogenic (Magnolo et al., 1991; Brian et al., 1996; Boonen et al., 2012). Meanwhile, lovastatin (**33**) and radicicol (**34**) are used as anticholesterol and anticancer, respectively (Alberts, 1988; Wang et al., 2008; Winssinger & Barluenga, 2007).

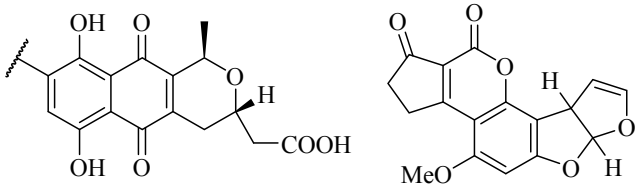

Actinorhodin (31)
aromatic antibiotic

Aflatoxin B1 (32)
mycotoxin carcinogen

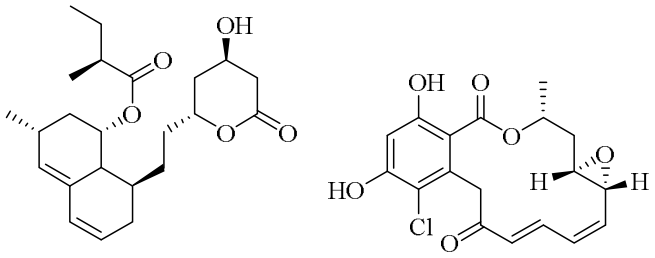

Lovastatin (33)
anticholesterol

Radicicol (34)
anticancer

Figure 2.9: Example of other polyketides

2.3 Polyketide biosynthesis

In 1950s, scientists realized that the polyketide biosynthetic pathway was similar to the biosynthesis of fatty acids (Scott et al., 2007). Polyketide biosynthesis takes place in the polyketide synthase (PKS), and for each turn of the cycle the fatty acid chain length is extended by two carbons (Ben et al., 2007; Weissman, 2009; Kwan & Schulz, 2011). The thionyl bonds are used to attach the growing fatty acid, incoming monomers and intermediates to the enzyme complexes. The fatty acid chain is attached initially to a ketosynthase (KS), and the process is initiated when an unbound KS enzyme attacks acetyl co-enzyme A (AcCoA). Once initiated, a free acyl carrier protein (ACP) acquires a malonyl group from malonyl-co-enzyme A (MCAT) obtained from the organism's primary metabolism, a process mediated by acyl transferase (AT) (Ben et al., 2007; Weissman, 2009; Kwan & Schulz, 2011; Cummings et al., 2014).

Claisen condensation takes place with the loss of CO_2, and by exchanging the growing fatty acid onto the ACP. The β-ketothioester is then carried through a reductive pathway until the β-ketone is fully reduced to the saturated methylene. The cycle is continued until the fatty acid chain has reached a specific length, then the thionyl esterase (TE) ejects the molecule as a long-chain fatty acid (Scheme 2.2). After the condensation process, further reductive manipulations may take place as the ketide is passed around the enzyme complex or megasynthase via the ACP. First, the keto-

reductase (KR) reduces the *β*-ketone to an alcohol, which then eliminates water as a result of the dehydratase (DH) to give an olefin, and the enoyl reductase (ER) then reduces it further to the saturated thioester (Ben et al., 2007; Weissman, 2009; Kwan & Schulz, 2011; Cummings et al., 2014).

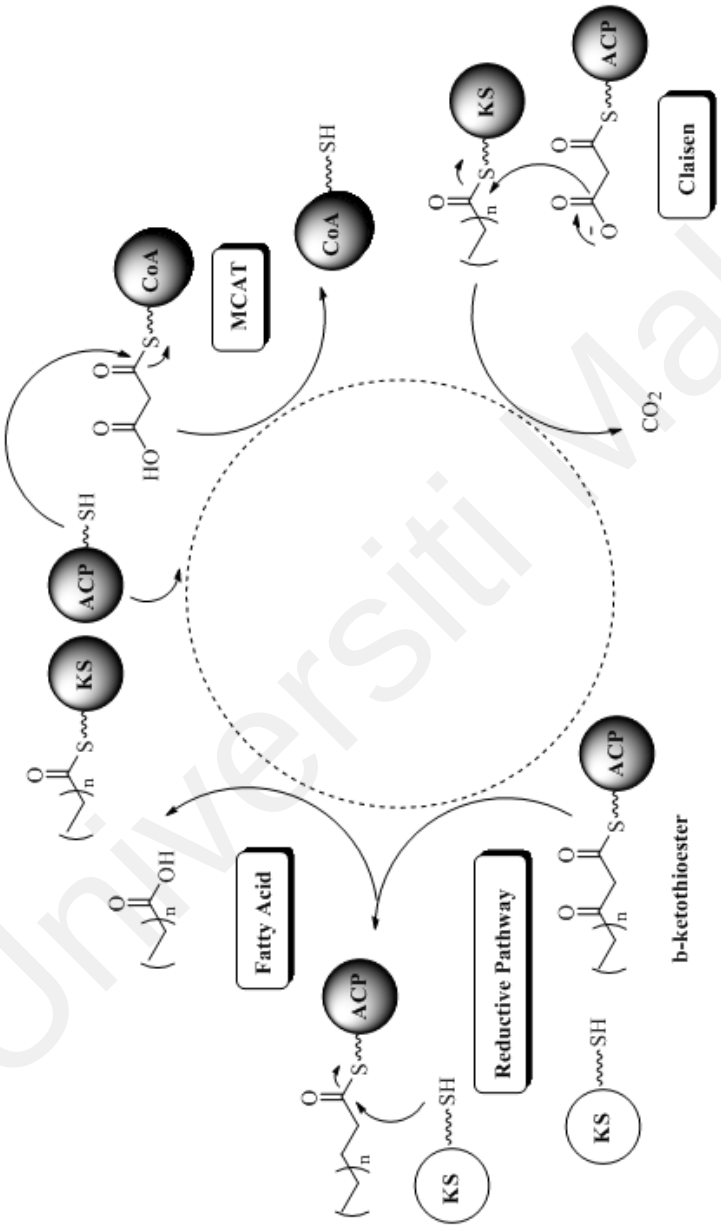

Scheme 2.2: General polyketide biosynthesis

Rather than following the full reductive pathway to give saturated products, polyketide synthesis can omit certain transformations to leave a more oxidized skeleton (Scheme 2.3). For example, the cycle can be terminated after the ketoreductase step giving a *β*-hydroxy ketone. The thionyl esterase (TE) has an important role to facilitate lactonization to give macrolides. Further to this, polyketide synthesis has access to a variety of starting materials and aromatizing enzymes that produce polyaromatic structures. Often the initial products are the basic compound skeleton; further functionalization can be achieved through oxidation and glycosylation. These can be explained on classes of polyketide synthases (PKSs) (Ben et al., 2007; Weissman, 2009; Kwan & Schulz, 2011; Cummings et al., 2014).

Different families of PKSs generate very distinct classes of polyketides. There are three classes of PKSs (the collective term for the group of enzymes) according to their sequences, primary structures and catalytic mechanism, aptly named type I, II, and III (Shen, 2003; Ben et al., 2007; Weissman, 2009; Kwan & Schulz, 2011; Cummings et al., 2014). Type I PKS is similar to type I fatty acid synthase (FAS). It is a giant assembly of multifunctional enzymes that are organized into modules, each consisting of a series of catalytic domains. Ketosynthase (KS), acyl transferase and acyl carrier protein (ACP) are three essential domains for chain elongation. Other domains such as ketoreductase, dehydratase, enoyl reductase and methyltrasferase (MT) may be present to form different polyketide structure. Macrolides, polyethers, polyenes and eyediynes are synthesized through type 1 PKS. Type II PKS are a large multienzyme complex of small, discrete enzymes with particular functions. The pivotal component that is responsible for the condensing activity resembles *β*-ketoacyl synthase II of type II FAS found in bacteria and plants. This class of PKSs is responsible for biosynthesis of aromatic polyketides (i.e tetracyclines, polycyclic polyketide). Type III PKSs, also known as chalcone synthase-like PKSs are self-contained enzymes that form

homodimers. Their single active site in each monomer catalyzes the priming, extension, and cyclization reaction interactively to form a wide array of polyketide products (often monocylic or bicyclic) such as chalcones, pyrones, acridones, phloroglucinols, stilbenes and resorcinolic lipids (Ben et al., 2007; Weissman, 2009; Kwan & Schulz, 2011; Cummings et al., 2014).

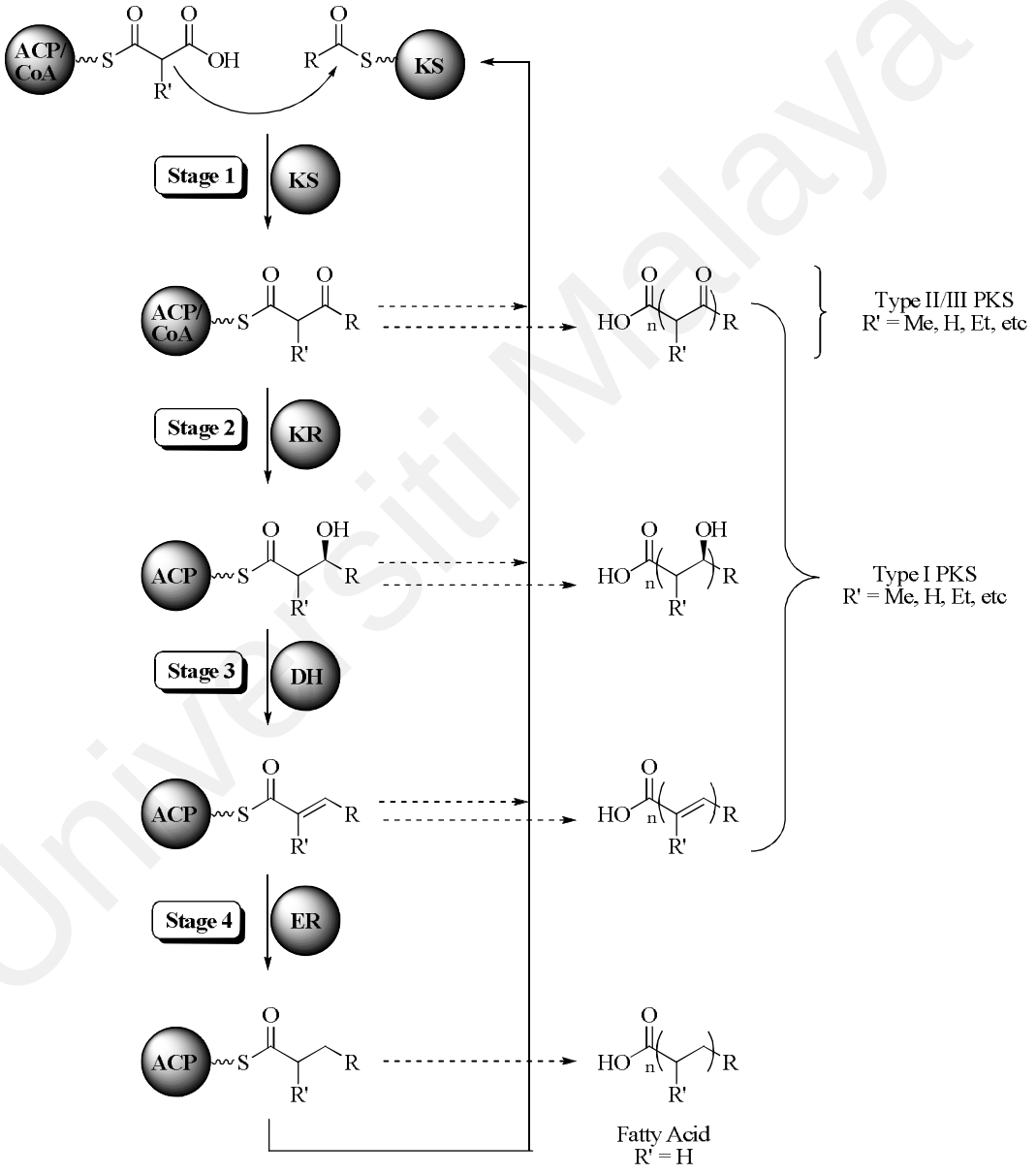

Scheme 2.3: Stepwise illustration of polyketide biosynthesis

Scheme 2.3 and Table 2.1 summarize the polyketide biosynthesis and its break downs into sub-stages. Stages 1 and 2 are classified as lower order, and common to all polyketides. They involve the formation of the carbon chain, which eventually lead to fragments ripe for conversion into more complex structures through complexity generation reactions. Stages 3 or 4 are later stages and often provide the complex polyketide natural products. The next subchapter will explain the electrocyclization process towards polyketide compounds. This process usually happens during stage 3 or 4 in polyketide biosynthesis route (Burnley et al., 2011).

Table 2.1 Polyketide biosynthesis broken down into sub-stages

Stage	**Description**
Stage 1	Formation of the carbon chain / Claisen condensation of a monomer from the primary metabolism on to the growing fatty acid chain.
Stage 2	Post-condensation transformation. i.e Reduction of the *β*-ketothioester by the ketoreductase to the corresponding *β*-hydroxythioester.
Stage 3	Complexity generation (dehydration, aromatization, cyclization, electrocyclization, oxidation). Dehydration by the dehydratase yielding the unsaturated thioester.
Stage 4	The reductase reduced the olefinic bond to give the fully saturated fatty acid backbone.

2.4 Electrocyclization towards polyketide natural products

Electrocyclization reactions are pericyclic process that involves the cyclization of conjugated polyenes (stage 3, Table 2.1). The formation of polyenes begins with the action of the dehydratase DH. The dehydratase DH catalyzes the transformation of the *β*-hydroxythioester into the *(E)-α,β*-unsaturated species which consists of histidine and

asparagine residues in the active site. The histidine acts as a base removing the enolic proton, and the asparagine provides a proton to release water and the unsaturated polyketide (i.e polyenes). In some cases, the electrocyclization process can be generated with surprising spontaneity, and it appears that molecular complexity might emerge with minimal (if any) enzymatic assistance through self-construction mechanism (Burnley et al., 2011). There are two types of electrocyclization reaction namely; 6π and 8π-6π electrocyclizations. The 8π-6π electrocyclization of polyenes will form the basis of discussion for the rest of this chapter, focusing on the biogenetic hypothesis of endiandric acids and kingianins.

2.4.1 8π – 6π electrocyclizations

The 8*π*–6*π* electrocyclic cascade (*Black's cascade*) is probably the most elegant and classical display of the power of electrocyclization reactions in nature (Burnley et al., 2011; Gravel & Poupon, 2008). This tandem reaction sequence, which involves a cascade of thermally induced 8*π*, then 6*π* electrocyclizations, has proven its worth in biomimetic synthesis. The most well-known example of this excellent and amazing transformation was demonstrated by Prof. Black in isolation of endiandric acids A-C (**35**-**37**) (Bandaranayake et al., 1980, 1981, 1982), followed by Nicolaou et al. (1982, 1984) in their elegant syntheses of endiandric acids A-G (**35**-**41**). In this sub-chapter, we will discuss the 8*π*–6*π* electrocyclization process on endiandric acids and kingianins. These types of compounds were regularly found in *Endiandra* and *Beilschmiedia* species.

2.4.1.1 Endiandric acids

Endiandric acids A-C (**35-37**) were isolated from the leaves of the Australian plant *Endiandra introrsa* (Lauraceae) and their structures were established by spectroscopic and X-ray analyses (Bandaranayake et al., 1980, 1981, 1982). This type of polycyclic compounds, which generally possess eight asymmetric centers, exists as racemic mixture rather than enantiomeric form, a rather unusual observation for naturally occurring compounds. This observation led Black and his collaborators to propose a brilliant and provocative hypothesis for the "biogenesis" of these compounds in nature from achiral precursors by a series of non-enzymatic electrocyclization (Bandaranayake et al., 1980; Banfield et al., 1982, 1983). The Black hypothesis suggests a cascade of reactions, shown in Scheme 2.4, by which endiandric acids A-G (**35-37**) are formed in nature. Thus, endiandric acid E (**38**), F (**39**) and D (**40**) were proposed as intermediate precursors to the tetracyclic acids A (**35**), B (**36**), and C (**37**), respectively; the conversation being facilitated by an intramolecular Diels-Alder reaction.

It is specifically proposed that these polycyclics are formed from phenyl polyenes **42**, which contain a central conjugated tetraene unit. All-*cis*-isomer **42a** or the *trans,cis,cis,trans*-isomer **42b** had undergone 8π-6π electrocyclizations to form **38** and **39**. It is followed by an intramolecular π4s + π2s cycloaddition (intramolecular Diels-Alder) to lead to the *α,β*–unsaturated acids **35** and **36**. Meanwhile, the polyenes **42a** and **42b** could act as precursors of cyclo-octatriene (**44**), a ring-invertomer of **43**. The conformer (**44**) should then undergo the same electrocyclization process to afford compounds **40** and **41**, which on intramolecular Diels-Alder cyclization would yield the cage-like structure (**37**) with a free phenylbutadiene unit. Based on this biomimetic hypothesis, Nicolaou and his team reported a total synthesis of endiandric acid A and its analogues (Nicolaou et al., 1982; 1984).

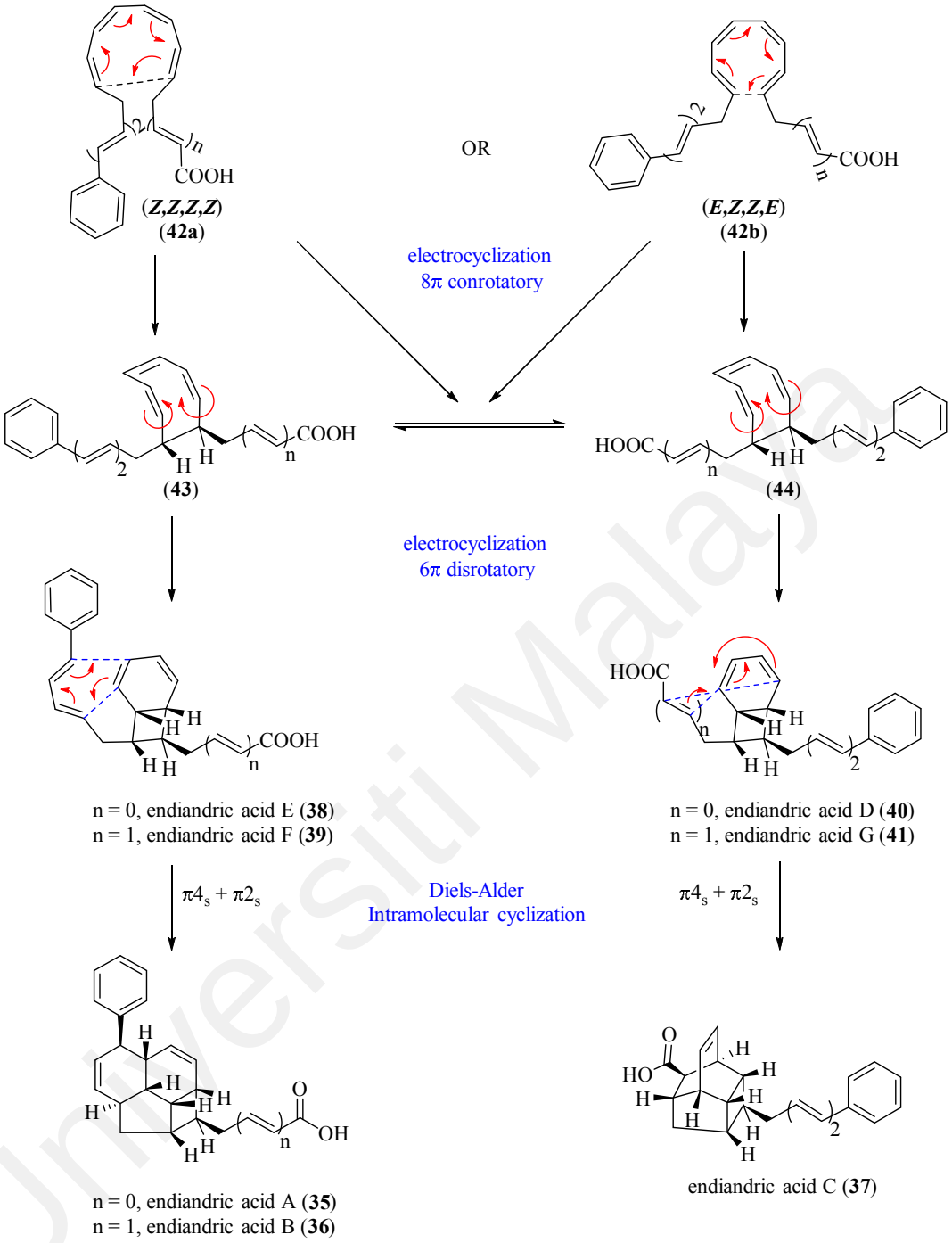

Scheme 2.4: Biosynthesis of endiandric acids analogues

2.4.1.2 Kingianins

The kingianins are unique natural products which have an unprecedented pentacyclic framework, isolated from the bark of *Endiandra kingiana* (Lauraceae) by Litaudon group. The first reported kingianin, kingianin A (**45**), formulates as dimer of bicyclo[4.2.0]octadiene and Litaudon group proposed a biosynthesis involving spontaneous Diels-Alder dimerization (Scheme 2.5) (Leverrier et al., 2010, 2011).

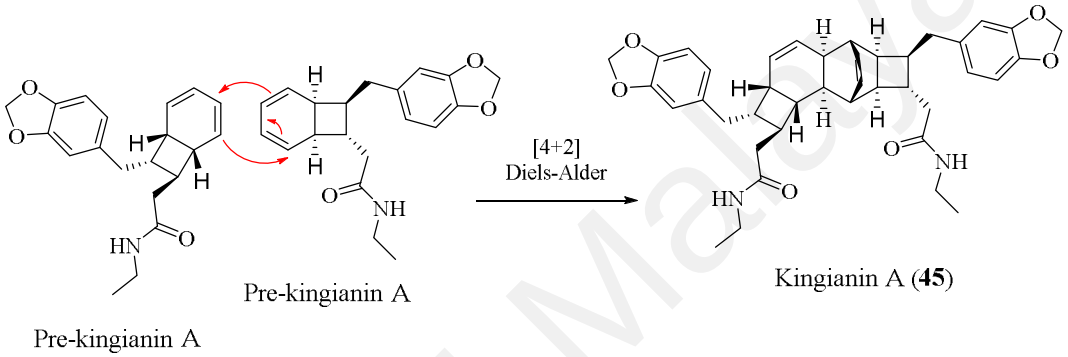

Scheme 2.5: Diels-Alder biosynthetic pathway to (±)-kingianin A (**45**)

The monomer of kingianin A (**59**) most likely formed via a tandem 8π-6π thermal electrocyclization sequence from the tetraene **60** (Scheme 2.6); a sequence closely resembling the endiandric acid electrocyclisation cascade. Sharma et al. (2011) reported the biomimetic synthesis of the monomer **59** based on the electrocyclization strategy described above. An elegant synthesis of monomer **59** was achieved, but all attempts to induce thermal dimerization failed (Sharma et al., 2011). Furthermore, an enzymatic construction of the pentacyclic ring system in the later stages of their biosynthesis is unlikely because the kingianin metabolites are all isolated as racemic mixture.

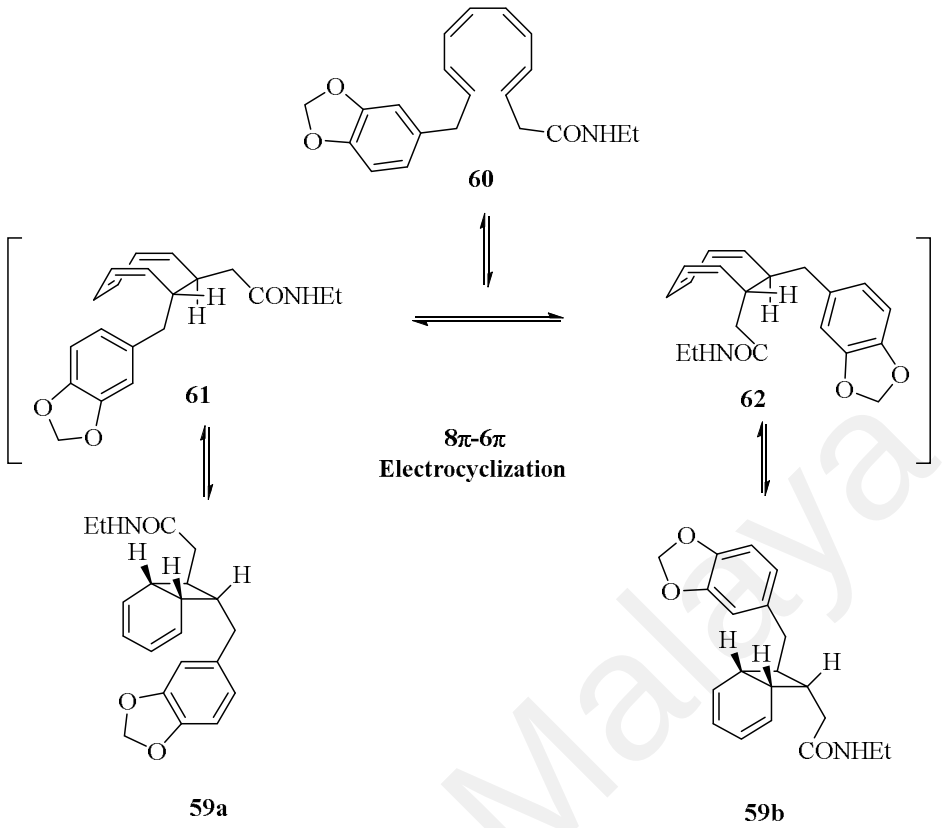

Scheme 2.6: Biogenetic hypothesis of kingianin A monomer (Sharma et. al., 2011)

Recent publications reported that a radical cation Diels-Alder (RCDA) dimerization could explain the formation of the kingianins in nature. The first total synthesis of kingianin A (**45**) was reported by Lim and Parker (2013). Their synthetic approach centered on a novel intramolecular radical cation activated Diels-Alder (RCDA) cycloaddition of a tethered bicyclo[4.2.0]octadienyl monomer (**63**) (Scheme 2.7). At the same time, Drew et al. (2013) reported total syntheses of the kingianin A (**45**), D (**48**) and F (**50**) employing the same approach (Scheme 2.8). Both groups employed the Ledwith-Weits salt to initiate the electron transfer reaction (Drew et al., 2013; Lim & Parker; 2014). The details about this will be explained in Chapter 5.

.

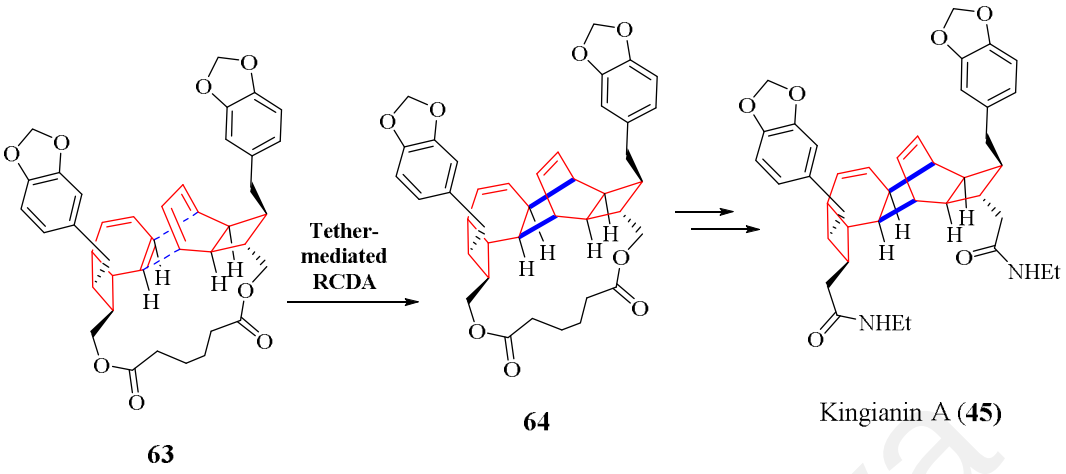

Scheme 2.7: Total synthesis of kingianin A (**45**) by Lim and Parker (2013)

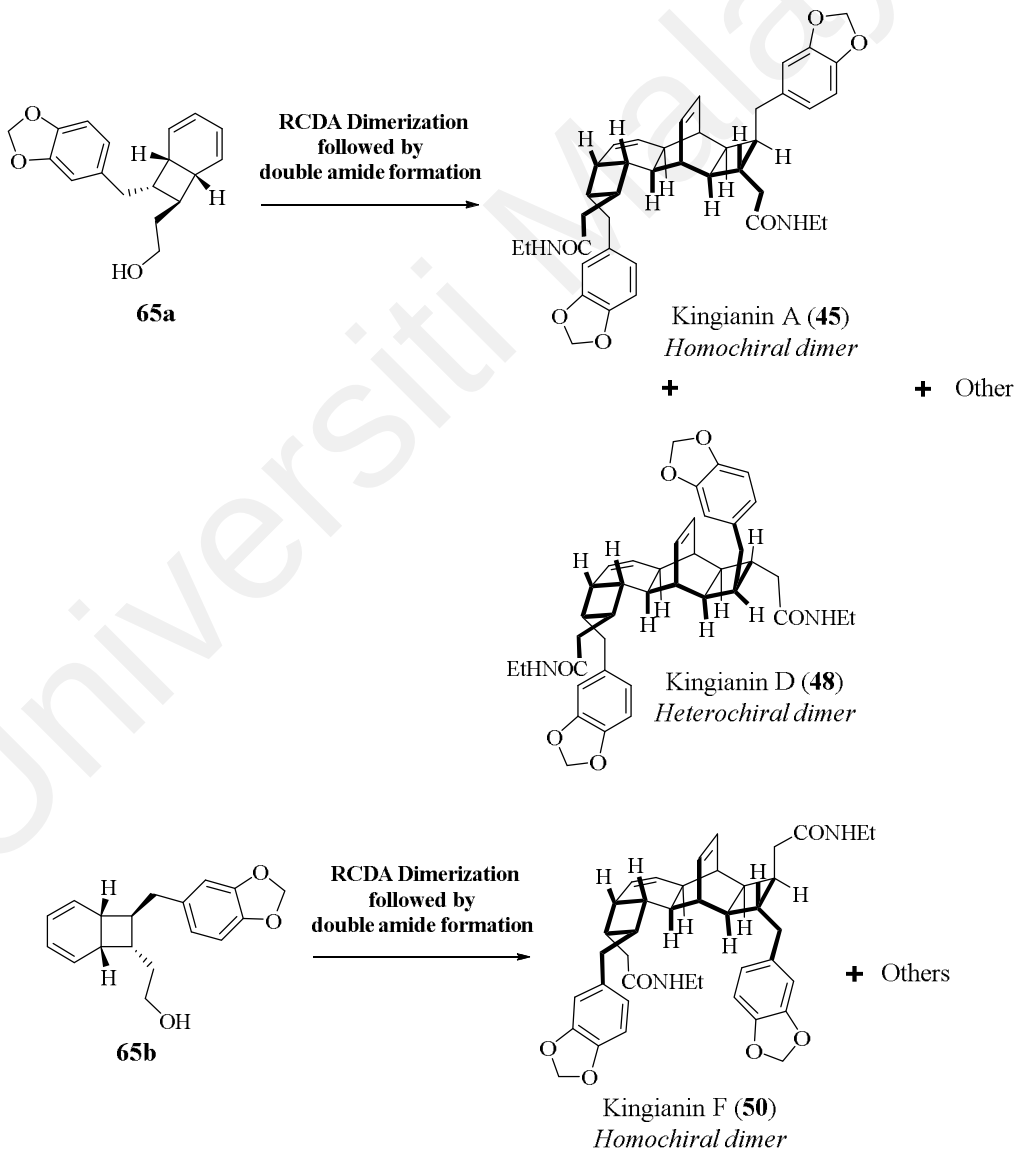

Scheme 2.8: Total synthesis of kingianin A (**45**) by Drew et al. (2013)

Based on these observation and hypothesis above, the biogenesis of kingianins involves a series of electrocyclization from an achiral precursor (Scheme 2.9). The polyketide **66** might lead to a phenyl propylene unit with a central conjugated tetraene. The 8π conrotatory electrocyclization of the all-*cis* tetraene **66a** or the *trans,cis,cis,trans* isomer **66b**, followed by a 6π disrotatory electrocyclization would lead to bicyclo **69** and **70**. Finally, an intermolecular Diels-Alder (4π*s* + 2π*s*) cycloaddition would provide kingianins.

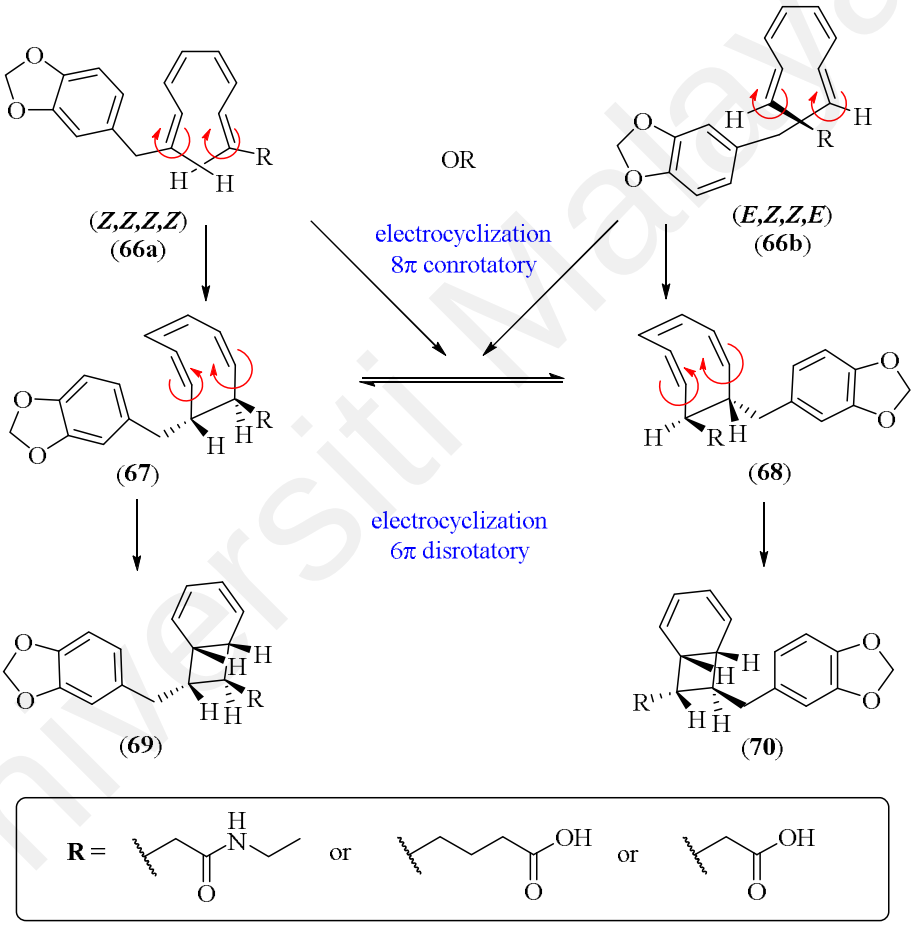

Scheme 2.9: Biogenetic hypothesis of monomers of kingianins

The kingianin skeleton could arise from non-spontaneous Diels-Alder reaction between two bicyclo[4.2.0]octa-2,4-diene. The cyclization could explain the racemic mixtures of kingianin compounds (Figure 2.10).

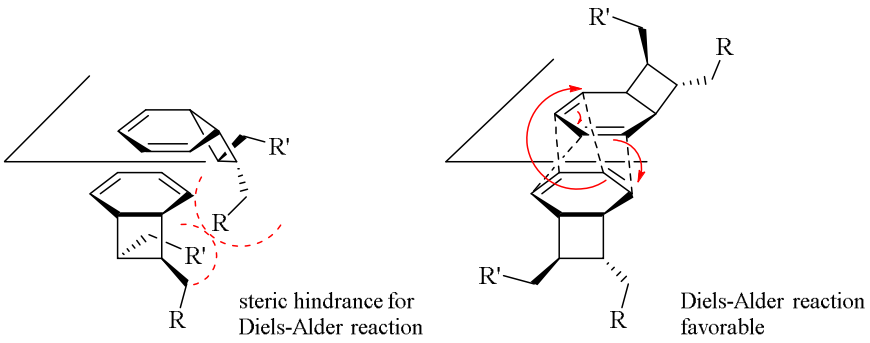

Figure 2.10: Possible steric hindrance in the intermolecular cyclization

The relative configuration of the pentacyclic carbon skeleton is identical for all kingianins, but the substituents located on the cyclobutane of each monomer are systematically in an *anti* configuration. The all *cis* configuration at the ring conjugations is due to a series of electrocyclisations involved in their biogenesis. The *anti* configuration of the cyclobutane rings may be explained by the last step of their biogenesis. The two monomers are indeed in parallel plane during the Diels-Alder reaction. An *anti* orientation of the two cyclobutanes with respect to the reaction plane could be more sterically favorable (Figure 2.10 and Scheme 2.10).

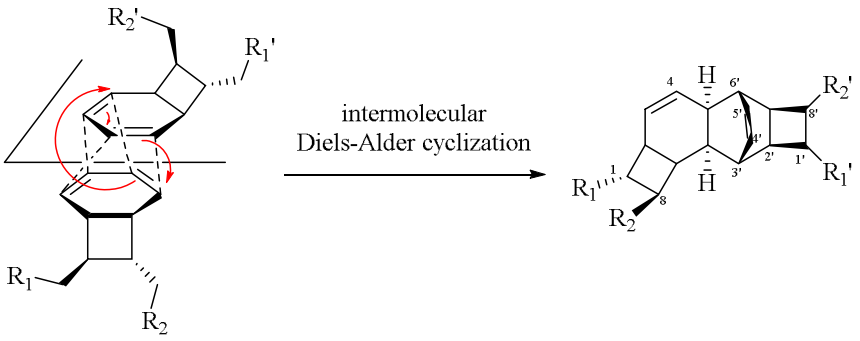

	R1	R2	R1' (*a*)	R2' (*β*)
54	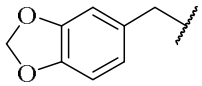	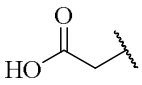	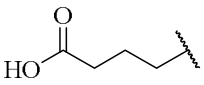	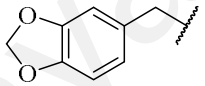
55	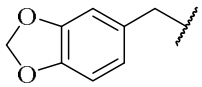	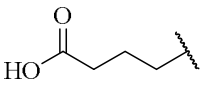	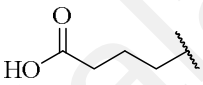	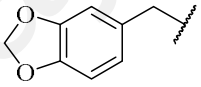
56	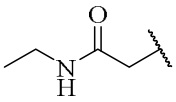	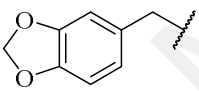	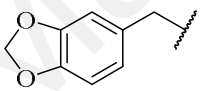	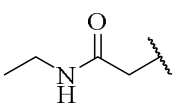
58	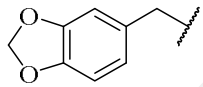	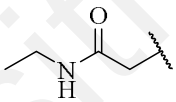	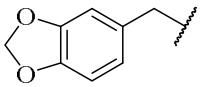	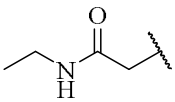
45	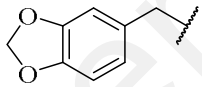	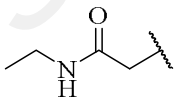	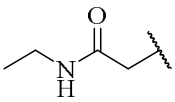	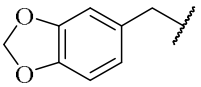
47	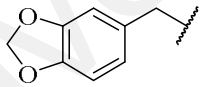	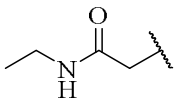	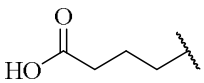	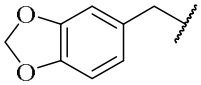
48	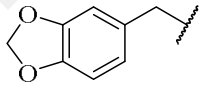	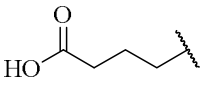	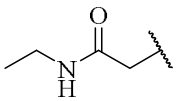	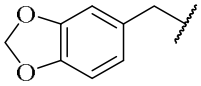
49	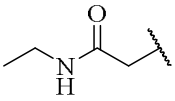	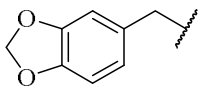	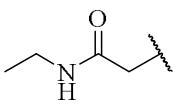	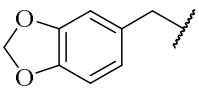

Scheme 2.10: Biogenesis hypothesis of kingianins: Diels-Alder reaction

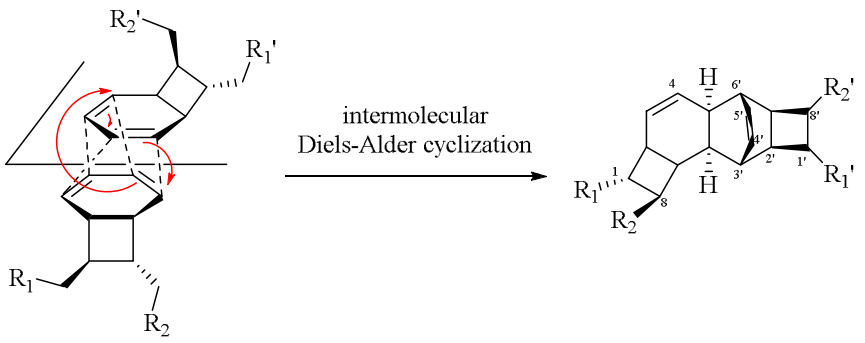

	R1	R2	R1' (α)	R2' (β)
50	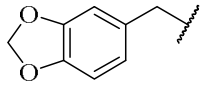	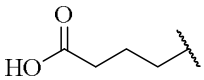	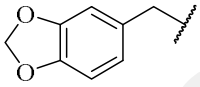	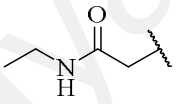
51	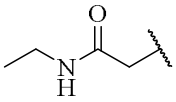	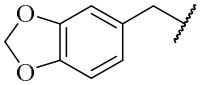	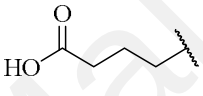	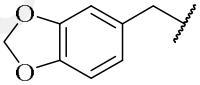
52	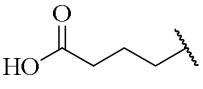	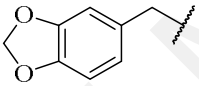	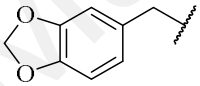	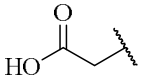
53	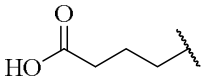	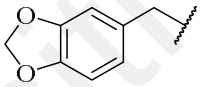	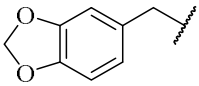	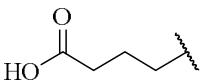

	R1	R2	R1' (β)	R2' (α)
46	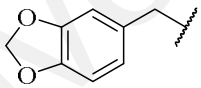	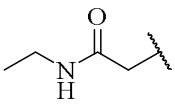	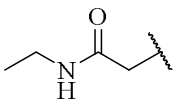	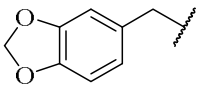
57	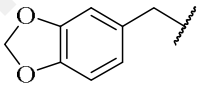	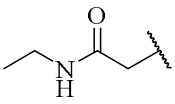	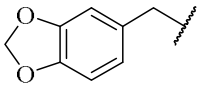	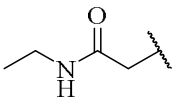

Scheme 2.10: Biogenesis hypothesis of kingianins: Diels-Alder reaction (Cont.)

2.5 Polyketides from *Endiandra* and *Beilschmiedia* species

In Lauraceae species only two genus; *Endiandra* and *Beilschmiedia* were reported to contain polyketides in the form of endiandric acids and kingianins. *Endiandra* species are medium-sized evergreen trees, distributed throughout the Peninsular Malaysia and Borneo (Ng, 1989; Burkill, 1966). This genus contains a specific type of polyketide namely endiandric acids (derived from late-stage electrocyclization of polyenes). There are about 125 *Endiandra* species found throughout the tropical regions, but to our knowledge only three species; *E. introrsa* (Bandaranayake et al., 1980, 1981, 1982), *E. anthropophagorum* (Rohan et al., 2007, 2009) and *E. kingiana* (Leverrier et al., 2010, 2011), have been studied for their phytochemicals. Meanwhile, another plant from the genus *Beilschmiedia* also possesses this unique tetracyclic carbon skeleton. In the past three years, no extensive works on *Endiandra* and *Beilschmiedia* plants have been performed by scientists as these plants are rare.

The first polyketides related to a Lauraceae species are endiandric acids A-C (**35**-**37**) isolated from *E. Introrsa* (Bandaranayake et al., 1980, 1981, 1982). After 13 years, the same compounds were also isolated from *B. oligandra* by Banfield et al. (1994). In addition, the first biological activity on endiandric acid compound was reported by Eder's group in 2004 (Eder et al., 2004). They isolated endiandric acid H (**21**) from *B. fulva* and patented it for the treatment of allergic disorders, asthmatic disorder, inflammatory concomitant symptoms of asthma and diseases which can be treated by inhibiting c-maf and NFAT (Eder et al., 2004). Until now, reports have shown that the endiandric acids possess various biological activities, such as antibacterial (Chouna et al., 2009, 2010; Talontsi et al., 2013), antiplasmodial (Talontsi et al., 2013), antitubercular (Yang et al., 2009), iNOS inhibitory activity (Huang et al., 2011) and cytotoxic properties (Talontsi et al., 2013; Huang et al., 2011).

In 2009, eight endiandric acid derivatives, beilschmiedic acids A-G (**71-77**) and beilschmiedin (**78**) were isolated from the bark of *B. anacardioides* (Chouna et al., 2009, 2010, 2011). Compounds **71-73** were tested in vitro for their antibacterial activity against five strains of microbes. Based on these results, compound **73** demonstrated the best potency against *Bacillus subtilis*, *Micrococcus luteus* and *Streptococcus faecalis* (MICs > 23µM) compared to reference antibiotic Ampicillin (Chouna et al., 2009). This cyclic polyketide indicated that it possessed antibacterial property with the gram positive bacteria and might be a possible candidate for antibacterial drugs.

B. erythrophloia studied by Chen's group have led to the isolation of nine endiandric acid analogues, beilcyclone A (**79**), endiandric acid I-J (**80-81**) erythrophloins A-F (**82-87**) (Yang et al., 2008, 2009). Erythrophloin C (**84**) exhibited antitubercular activity against *Mycobacterium tuberculosis* H37Rv, showing MIC values 50 µg/mL. This compound was also reported to inhibit the growth of P-388 murine lymphocytic leukemia cells (Yang et al., 2009). Meanwhile, Huang et al. (2011) also screened for anti-inflammatory activity using an inducible nitric oxide synthase (iNOS) assays, a methanolic extract of root of *B. tsangii*. The latter showed potent inhibition of NO production, with no cytotoxicity against RAW 264.7 cells. Bioassay-guided fractionation of the extract led to the isolation of nine new endiandric acid analogues (Huang et al., 2011, 2012) named tsangibeilin A-D (**88-89** and **95-96**), endiandramides A (**90**) and B (**94**), and endiandric acids K-M (**91-93**). Compounds **90** and **94** exhibited potent iNOS inhibitory activity, with IC_{50} values of 9.59 and 16.40 µM, respectively (Huang et al., 2011).

Williams and co-worker published a series of endiandric acid analogues named beilschmiedic acids H-O (**97-104**), together with known compounds, beilschmiedic acids A and C (**71** and **73**), were isolated from a Gabonese *B.* species (Williams et al., 2012). All compounds were screened for cytotoxic and antibacterial activities against

NCI-H460 human lung cancer cells and a clinical isolate of methicillin-resistant *Staphylococcus aureus* (MRSA 108). Based on this screening, only compound **71** showed potent activity in the NCI-H460 human cancer cell line assay with an IC_{50} values 6.1 µM, and was found to exhibit good antibacterial activity against *S. Aureus* (IC_{50} = 10.0 µM) (Williams et al., 2012). Talonsti et al. (2013) reported the isolation of four beilschmiedic acids; cryptobeilic acids A-D (**105-108**) and tsangibeilin B (**89**) from the bark of *E. cryptocaryoides*. These compounds showed moderate antiplasmodial activity against the chloroquino-resistant *Plasmodium falciparum* strain NF54, and antibacterial activities against *Escherichia coli*, *Acinetobacter calcoaceticus* and *Pseudomonas stutzeri* (Talonsti et al., 2013).

Recently, a rapid NMR-based screening on EtOAc extracts of *Endiandra* and *Beilschmiedia* species had led to the isolation of eleven tetracyclic endiandric acids named ferrugineic acid A-K (**109-119**). These polyketides were isolated from *B. ferruginea* by Apel et al. (2014) and assayed for Bcl-xL and Mcl-1 binding affinities. In 2011, a novel polyketide series possessing a [4.2.0] bicyclic main skeleton named kingianins A-N (**45-58**) were reported by Leverrier et al. (2010, 2011). These compounds were isolated from *E. kingiana* and extensively studied for Bcl-xL binding affinity. The other polyketides found in *Endiandra* and *Beilschmiedia* species, and their references are listed in Table 2.2 and Figure 2.11 (from 1981 – 2015).

Table 2.2: List of polyketides isolated from *Endiandra* and *Beilschmiedia* species

Name of Polyketides	Name of Plants	Biological activity	References
Endiandric acid A (**35**)	*E. Introrsa,* *B. oligandra*	-	Bandaranayake et al., 1980; Banfield et al., 1994.
Endiandric acid B (**36**)	*E. Introrsa,* *B. erythrophloia*	-	Bandaranayake et al., 1982; Yang et al., 2009.
Endiandric acid C (**37**)	*E. Introrsa*	-	Banfield et al., 1983.
Endiandric acid H (**21**)	*B. fulva*	Antiallergic Antiasthmatic Antiinflammatory	Eder et al., 2004, 2006.
Beilschmiedic acid A (**71**)	*B. anacardioides,* *B. sp (*Gabonese species)	Antibacterial Cytotoxicity	Chouna et al., 2009, 2011; Williams et al., 2012.
Beilschmiedic acid B (**72**)	*B. anacardioides*	Antibacterial	Chouna et al., 2009.
Beilschmiedic acid C (**73**)	*B. anacardioides,* *B. sp (*Gabonese species)	Antibacterial Cytotoxicity	Chouna et al., 2009, 2011; Williams et al., 2012.

Table 2.2, continued

Name of polyketides	Name of Plants	Biological activity	References
Beilschmiedic acid D (**74**)	*B. anacardioides*	-	Chouna et al., 2009.
Beilschmiedic acid E (**75**)		-	
Beilschmiedic acid F (**76**)		-	Chouna et al., 2011.
Beilschmiedic acid G (**77**)		-	
Beilschmiedin (**78**)		-	Chouna et al., 2009.
Beilcyclone A (**79**)	*B. erythrophloia*	Antitubercular	Yang et al., 2009.
Endiandric acid I (**80**)		-	Yang et al., 2008.
Endiandric acid J (**81**)		-	
Erythrophloin A (**82**)		Antitubercular	Yang et al., 2009.
Erythrophloin B (**83**)			
Erythrophloin C (**84**)			
Erythrophloin D (**85**)			
Erythrophloin E (**86**)			
Erythrophloin F (**87**)			
Tsangibeilin A (**88**)	*B. tsangii*	Antiinflammatory	Huang et al., 2011.
Tsangibeilin B (**89**)	*B. cryptocaryoides, B. tsangii*	Antiinflammatory Antibacterial Antiplasmodial Cytotoxicity	Talontsi et al., 2012; Huang et al., 2011.

Table 2.2, continued

Name of polyketides	Name of Plants	Biological activity	References
Endiandramide A (**90**)	*B. tsangii*	Antiinflammatory	Huang et al., 2011.
Endiandric acid K (**91**)			
Endiandric acid L (**92**)			
Endiandric acid M (**93**)			Huang et al., 2012.
Endiandramide B (**94**)			Huang et al., 2011.
Tsangibeilin C (**95**)			Huang et al., 2012.
Tsangibeilin D (**96**)			
Beilschmiedic acid H (**97**)	*B. sp* (Gabonese species)	Cytotoxicity	Williams et al., 2012.
Beilschmiedic acid I (**98**)		-	
Beilschmiedic acid J (**99**)		-	
Beilschmiedic acid K (**100**)		Cytotoxicity Antibacterial	
Beilschmiedic acid L (**101**)			
Beilschmiedic acid M (**102**)			
Beilschmiedic acid N (**103**)			
Beilschmiedic acid O (**104**)			
Cryptobeilic acid A (**105**)	*B. cryptocaryoides*	Cytotoxicity Antibacterial Antiplasmodial	Talontsi et al., 2013.
Cryptobeilic acid B (**106**)			
Cryptobeilic acid C (**107**)			
Cryptobeilic acid D (**108**)			

Table 2.2, continued

Name of polyketides	Name of Plants	Biological activity	References
Ferrugineic acid A (**109**)	*B. ferruginea*	Bcl-xL/Bak and Mcl-1/Bid binding Affinities	Apel et al., 2014.
Ferrugineic acid B (**110**)			
Ferrugineic acid C (**111**)			
Ferrugineic acid D (**112**)			
Ferrugineic acid E (**113**)			
Ferrugineic acid F (**114**)			
Ferrugineic acid G (**115**)			
Ferrugineic acid H (**116**)			
Ferrugineic acid I (**117**)			
Ferrugineic acid J (**118**)			
Ferrugineic acid K (**119**)			
Kingianin A (**45**)	*E. kingiana*	Bcl-xL/Bak binding affinity	Leverrier et al., 2010, 2011.
Kingianin B (**46**)			Leverrier et al., 2011.
Kingianin C (**47**)			
Kingianin D (**48**)			
Kingianin E (**49**)			
Kingianin F (**50**)			
Kingianin G (**51**)			
Kingianin H (**52**)			
Kingianin I (**53**)			

Table 2.2, continued

Name of polyketides	Name of Plants	Biological activity	References
Kingianin J (**54**)	*E. kingiana*	Bcl-xL/Bak binding affinity	Leverrier et al., 2011
Kingianin K (**55**)			
Kingianin L (**56**)			
Kingianin M (**57**)			
Kingianin N (**58**)			

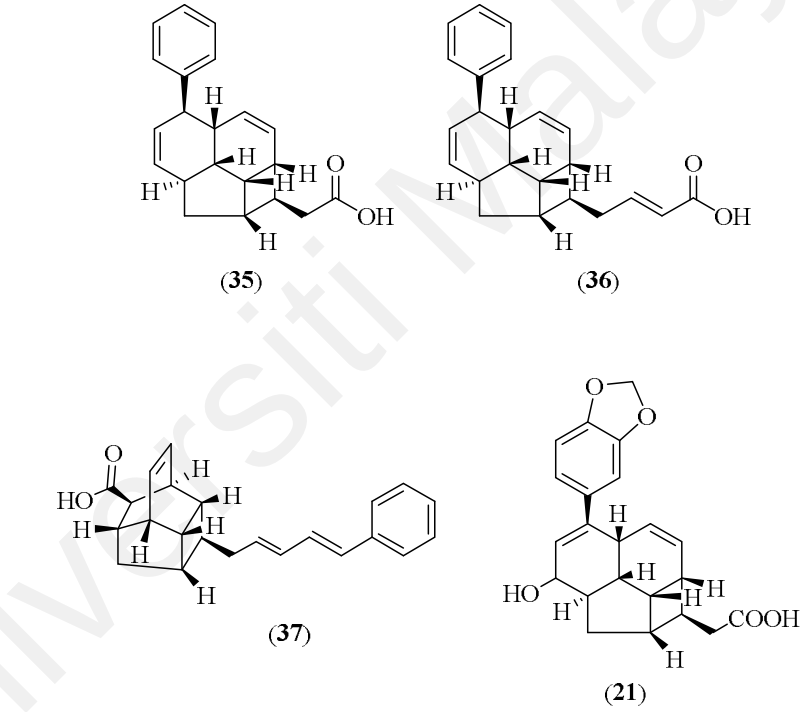

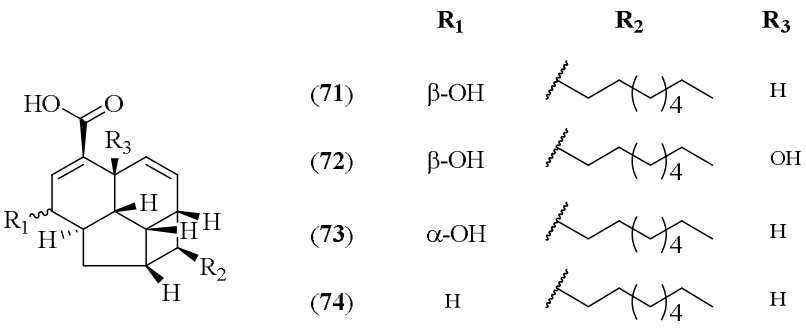

Figure 2.11: Polyketides isolated from *Endiandra* and *Beilschmiedia* species

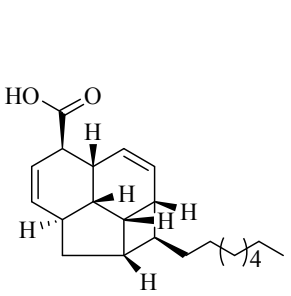

(**75**)

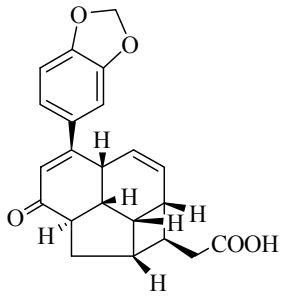

(**76**)

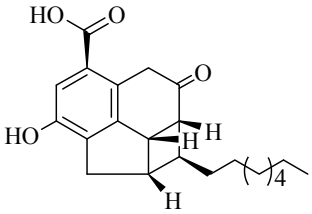

(**77**)

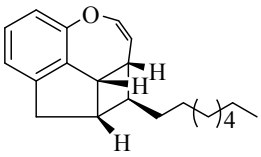

(**78**)

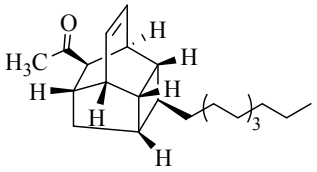

(**79**)

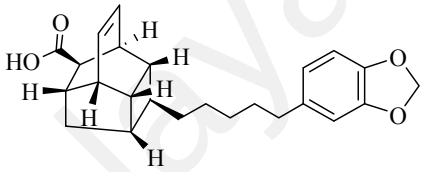

(**80**)

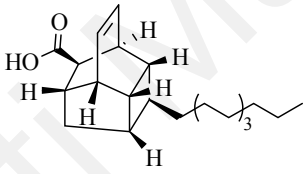

(**81**)

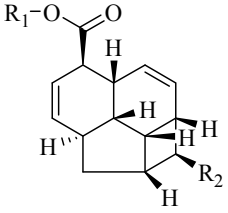

	R_1	R_2
(**82**)	CH_3	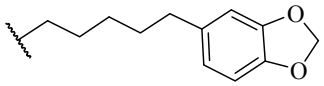
(**83**)	CH_3	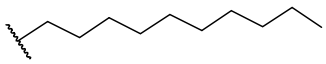
(**84**)	CH_3	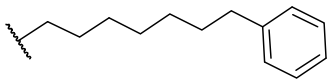
(**85**)	CH_3	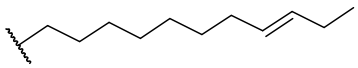
(**86**)	H	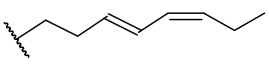
(**87**)	H	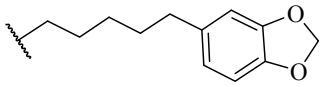

Figure 2.11: continued

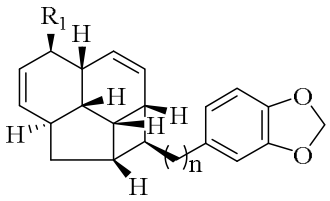

	R_1	n
(**88**)	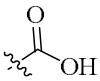	3
(**89**)	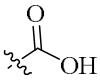	1
(**90**)	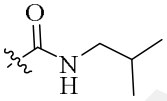	1

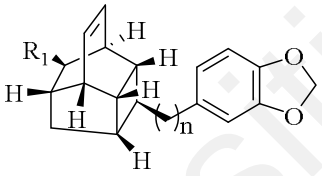

	R_1	n
(**91**)	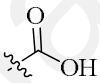	3
(**92**)	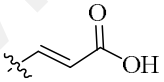	5
(**93**)	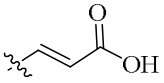	1
(**94**)	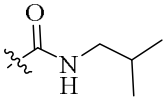	3

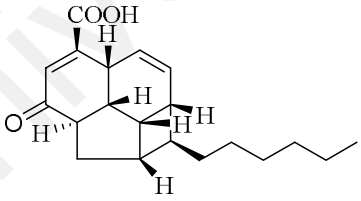

(**95**)

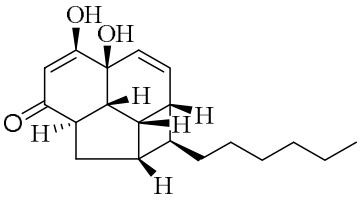

(**96**)

Figure 2.11: continued

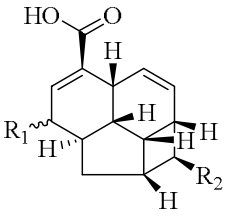

	R_1	R_2
(**97**)	α-OH	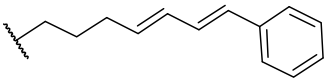
(**98**)	β-OH	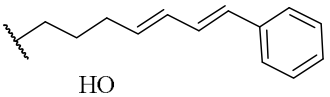
(**99**)	H	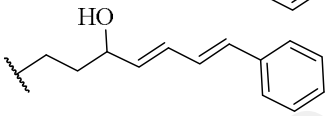
(**100**)	α-OH	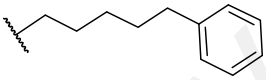
(**101**)	α-OH	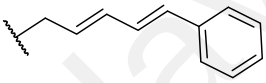
(**102**)	α-OH	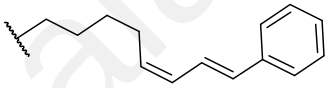
(**103**)	α-OH	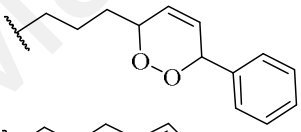
(**104**)	α-OH	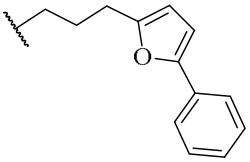

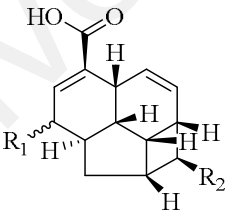

	R_1	R_2
(**105**)	β-OH	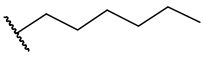
(**106**)	α-OH	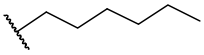
(**107**)	=O	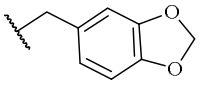

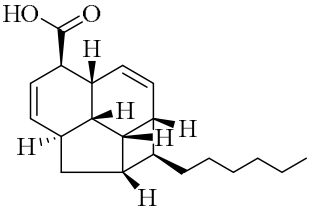

(**108**)

Figure 2.11: continued

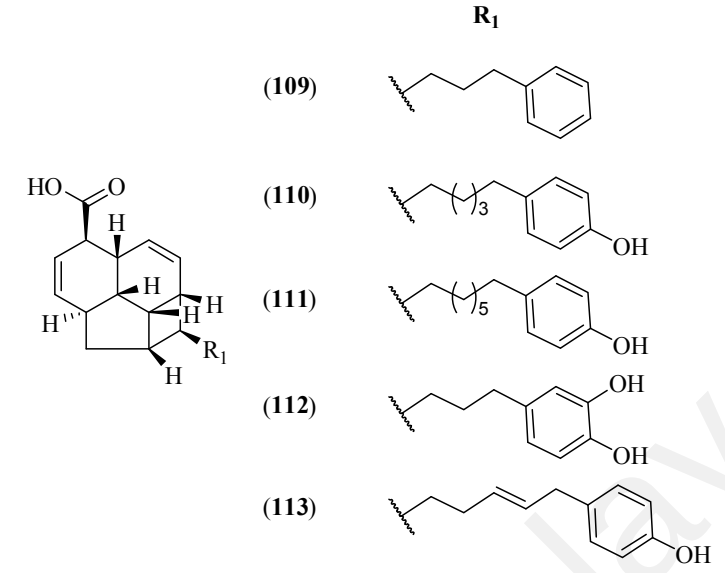

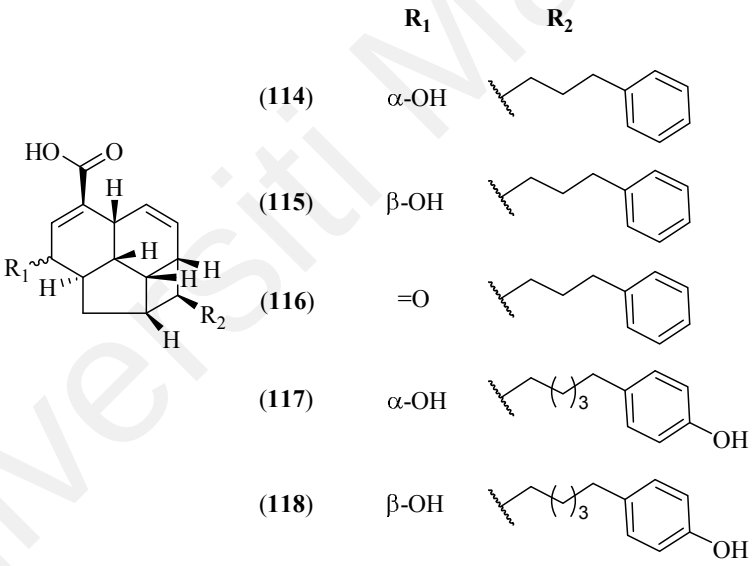

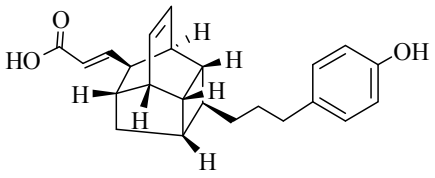

(**119**)

Figure 2.11: continued

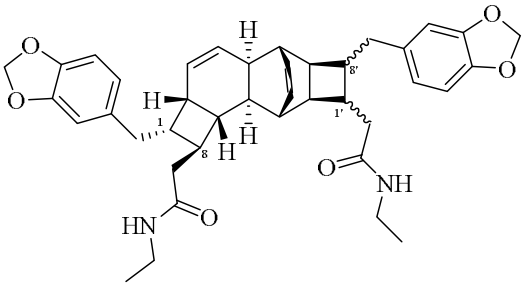

45 : H-1' β, H-8' α
46 : H-1' α, H-8' β

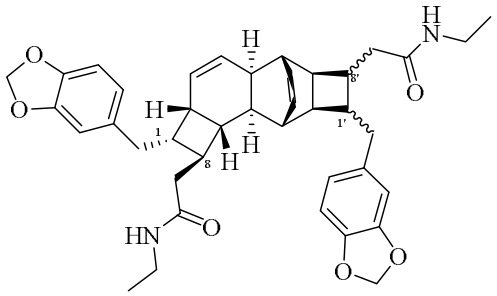

47 : H-1' β, H-8' α
48 : H-1' α, H-8' β

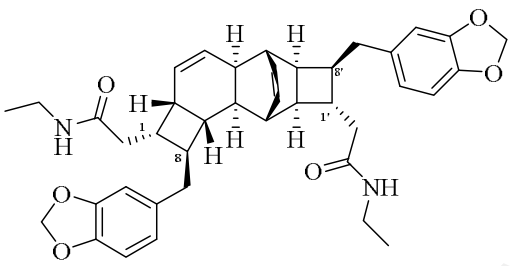

(**49**)

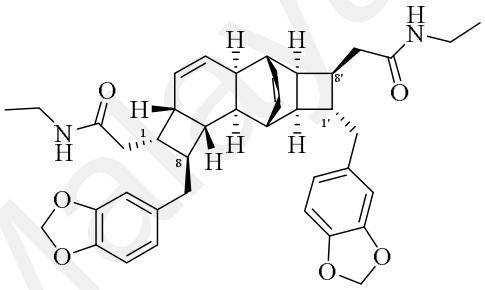

(**50**)

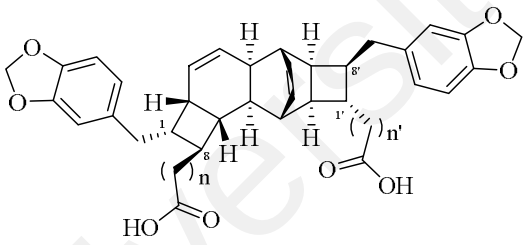

51 : n = 1, n' = 3
52 : n, n' = 3

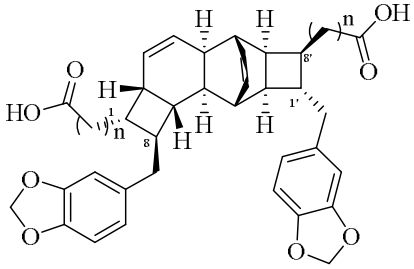

53 : n = 3, n' = 1
54 : n, n' = 3

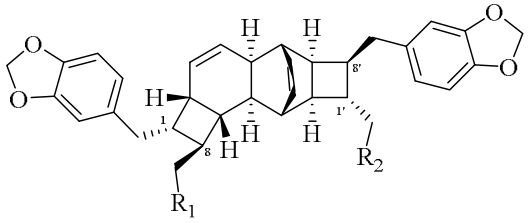

55 : R_1 = CONHEt, R_2 = CH_2CH_2COOH
56 : R_1 = CH_2CH_2COOH, R_2 = CONHEt

Figure 2.11: continued

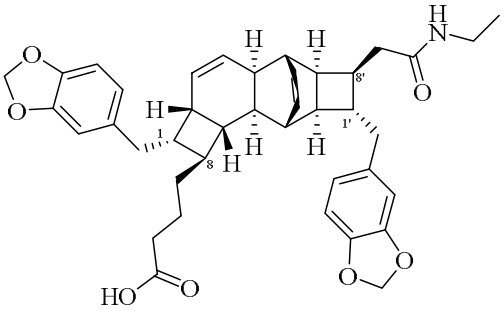

(**57**)

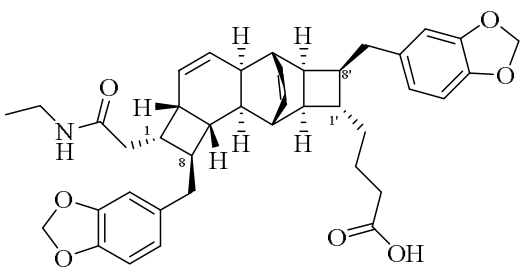

(**58**)

Figure 2.11: continued

CHAPTER 3

PHYTOCHEMICAL STUDIES OF *ENDIANDRA KINGIANA* GAMBLE

3.1 Phytochemistry of *Endiandra kingiana* Gamble

The bark of ***Endiandra kingiana*** (KL5243) collected from Kuala Lipis Reserved Forest, Pahang, East-coast of Peninsular Malaysia was investigated for its chemical constituents using the conventional and modern methods such as column chromatography (CC), high-performance liquid chromatography (HPLC) for their isolation and purification. Spectroscopic techniques such as 1D and 2D NMR, IR, UV and HRESIMS were utilized for structure elucidation. The following sub-chapters discuss briefly the structural elucidation of all the isolated compounds. Two groups of compounds were isolated and characterized from this extract; the endiandric acid series and the kingianin series. In the endiandric acid series, eight new tetracyclic endiandric acid analogues were isolated; kingianic acids A-H (**120**-**127**), together with the known endiandric acid M (**93**) and tsangibeilin B (**89**). Nine compounds were isolated from the kingianin series whereby, three of the compounds are new; kingianin O-Q (**128**-**130**) while the remaining kingianin A (**45**), kingianin F (**50**), kingianin K (**55**), kingianin L (**56**), kingianin M (**57**) and kingianin N (**58**) were known.

.

3.1.1 Endiandric acid series

Endiandric acids have a unique tetracyclic carbon skeleton and are exclusively produced by the ***Endiandra*** and ***Beilschmiedia*** species. These cyclic polyketides, possessing 8 chiral centers and usually isolated as racemic mixtures [α_D] = 0°, can be divided into three main skeletal types; type A, type B and type B′ (Figure 3.1).

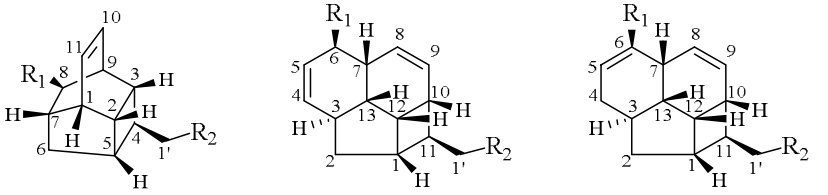

Figure 3.1: Endiandric acids main skeleton

The framework of the endiandric acids (types A, B and type B′), comprising two cyclohexanes, one cyclopentane and one cyclobutane rings, are generally substituted with a phenyl ring and a carboxylic acid chain. The presence of the phenyl group is suggested by absorption bands at λ_{max} 233 and 286 nm in UV spectrum and is confirmed by analysis of the spectroscopic data (Silvertein et al., 1991; Pavia et al., 2009). The carboxylic acid moiety presence is proven by the absorption band at ν_{max} 1700 cm^{-1} in the IR spectrum and further corroborated by the signal at around δ_C 178 in the ^{13}C NMR spectrum (Pretsch et al., 2009; Silverstein et al., 1997; Pavia et al., 2009; Crews et al., 1998). Types A and B are characterized by a common endiandric acid carbon skeleton which differ from each other by the substituents at the western (R_1) and eastern (R_2) parts located at C-4 and C-8 for type A, and C-6 and C-11 for types B and B′.

The main structural feature for the endiandric acids type A is a ‘cage-like’ tetracyclic frame connected by an alkene-bridge (C-10 and C-11). In general, the ^1H NMR spectra will display a triplet with a coupling constant of 4.0 Hz at about δ_H 6.20 corresponding to the two olefinic protons of the bridge; H-10 and H-11 (Huang et al., 2011; Pavia et al., 2009). The ^{13}C NMR spectra will exhibit signals at δ_C 131.0 and 132 corresponding to the olefinic carbons C-10 and C-11, respectively. The main structural feature for endiandric acids type B, is also a tetracyclic system, however not ‘cage-like’. The type B endiandric acids have four ***cis*** olefinic protons giving rise to signals between δ_H 5.40 – 5.45 for H-8, H-9 and H-5, and at δ_H 6.20 ppm for H-4 (Huang et al., 2011; Pavia et

al., 2009). In some cases, the displacement of the double bond from H-C(4)-H-C(5) to H-C(5)-H-C(6) may happen (type B′) (Apel et al., 2014). The 2D NMR correlations are important in elucidating the structure of the endiandric acids. The COSY experiment was used to establish the connectivity of the main tetracyclic skeleton, while the HMBC experiment aided in confirming the position of the phenyl and carboxylic acid moieties at the western (R_1) and eastern (R_2) parts.

The following paragraphs discuss briefly the structural elucidation of endiandric acids. All compounds were optically inactive, thus suggesting that they were racemic mixtures and their spectroscopic data were very similar. In this research, five new endiandric acids type A namely; kingianic acids A-E (**120**-**124**) and three new endiandric acids types B and B′ (i.e kingianic acids F-H (**125**-**127**), together with the known endiandric acid M (**93**) and tsangibeilin B (**89**) were successfully isolated.

Compound A: Kingianic acid A (**120**)

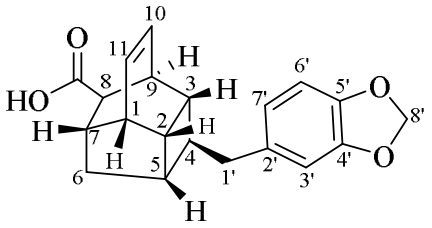

Kingianic acid A (**120**) was classified as an endiandric acid type A ('cage-like' structure). It was isolated as an optically inactive colourless oil [α_D] = 0°. The HRESIMS spectrum of **120** showed a pseudomolecular ion peak $[M-H]^-$ at ***m/z*** 323.1279 (calcd. for $C_{20}H_{19}O_4$; 323.1284), consistent with a molecular formula of $C_{20}H_{20}O_4$, with 11 degrees of unsaturation. Its UV spectrum showed absorption bands at λ_{max} 233 and 286 nm, suggesting the presence of a benzenoid moiety, while its IR spectrum indicated the presence of OH (3431 cm^{-1}), carbonyl (1701 cm^{-1}) and methylenedioxy (1040 and 936 cm^{-1}) groups (Silverstein et al., 1991; 1997; Pavia et al., 2009; Pretsch et al., 2009).

The ^{1}H NMR spectrum of **120** revealed two ***cis***-form mutually coupled vinyl H-atoms at δ_H 6.22 (br t, ***J*** = 5.2 Hz, H-10 and H-11). These signals were the characteristic features for an endiandric acid type A. Meanwhile, the aromatic proton H-3′ which resonated as a ***meta***-coupled doublet at δ_H 6.66 (d, ***J*** = 1.2 Hz) along with an ***ortho-meta***-coupled doublets at δ_H 6.72 (d, ***J*** = 8.0 Hz, H-6′) and 6.60 (dd, ***J*** = 8.0, 1.2 Hz, H-7′) suggested the presence of a 1,3,4-trisubstututed aromatic ring. In addition, a downfield singlet at δ_H 5.92 corresponding to H_2-8′ methylene protons confirmed the presence of the methylenedioxy group. The ^{13}C NMR and DEPT spectra exhibited 20 signals; 13 methines, 3 methylenes, and 4 quaternary carbons. Resonances of the methines at C-1 (δ_C 41.8), C-2 (δ_C 39.7), C-3 (δ_C 38.8), C-4 (δ_C 40.6), C-5 (δ_C 39.8), C-7 (δ_C 38.3), C-8 (δ_C 48.8) and C-9 (δ_C 34.8), including the two olefinic carbons at

C-10 (δ_C 131.3), C-11 (δ_C 132.0), and a methylene at C-6 (δ_C 38.5) were characteristic of the 'cage-like' endiandric acid structure (Table 3.1).

Table 3.1: ^{1}H (600 MHz) and ^{13}C (150 MHz) NMR data of compound **120** in $CDCl_3$

Position	**120**	
	δ_H (***J*** in Hz)	δ_C
*1	2.71 ddd (7.2, 5.2, 2.0)	41.8
2	2.42 dt (8.5, 5.2)	39.7
3	1.73 m	38.8
4	2.00 dd (7.8, 7.8)	40.6
5	2.34 dd (7.8, 7.8)	39.8
6α	1.55 d (13.0)	38.5
6β	1.90 ddd (13.0, 7.8, 5.3)	
7	2.57 dd (5.3, 5.3)	38.3
8	2.86 d (3.8)	48.8
9	2.98 ddd (7.5, 5.2, 2.2)	34.8
10	6.22 br, t (5.2)	131.3
11	6.22 br, t (5.2)	132.0
*1′	2.72 m	41.7
	2.78 m	
2′	-	134.7
3′	6.66 d (1.2)	109.1
4′	-	147.5
5′	-	145.7
6′	6.72 d (8.0)	108.1
7′	6.60 dd (8.0, 1.2)	121.5
8′	5.92 s	100.8
C=O	-	179.3

*Overlapping signals

Through the ^{1}H-^{1}H COSY and ^{1}H-^{13}C HSQC data, the connectivities within the tetracyclic core were determined. Correlations of the H-atom signals between H-1/H-2, H-2/H-5, H-5/H-6, H-6/H-7, H-7/H-1 and H-8/H-9, H-9/H-3, H-3/H-2, H-2/H1, H-1/H-7, H7/H8 established the presence of the cyclopentane ring and a cyclohexane ring; C-1-C-2-C-5-C-6-C-7 and C-8-C-9-C-3-C-2-C-1-C-7, respectively. The presence of the other six-membered ring (C-10-C-11-C-1-C-2-C-3-C-9) was deduced from correlations between H-10/H-11, H-11/H-1, H-1/H-2, H-2/H-3, H-3/H-9 and H-9/H-10 as observed in the COSY spectrum. Finally, the COSY correlations

between H-2/H-3, H-3/H-4, H-4/H-5 and H-5/H-2 confirmed the existence of the cyclobutane ring C-2-C-3-C-4-C-5. The HMBC experiment enabled the establishment of the connectivities of the substituents of the western and the eastern parts. The long-range correlations between H-7 and H-8 to the carboxylic acid carbon; COOH (δ_C 179.3) indicated the presence of a carboxylic acid moiety attached to C-8 of the tetracyclic skeleton. The following heteronuclear correlations, H-3′, H-7′/C-1′, H-1′/C-2′ and H-1′/C-4 confirmed the linkage of the methylenedioxyphenyl moiety to the tetracyclic core through C-1′ (Figure 3.2).

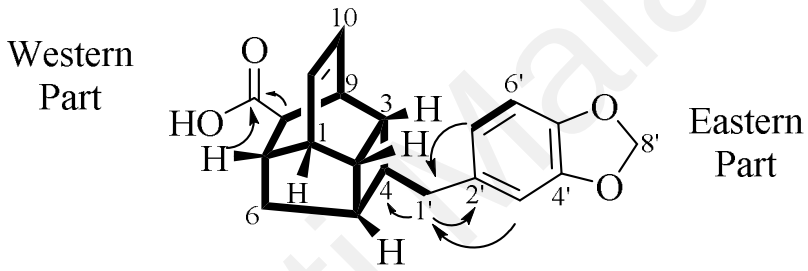

Figure 3.2: Key ^{1}H-^{1}H COSY (bold) and HMBC (^{1}H→^{13}C) correlations of **120**

The relative configuration of **120** was deduced from the NOESY analysis (Figure 3.3) in combination with biogenetic consideration (Bandaranayake et al., 1980) and comparison with literature (Huang et al., 2011). Based on the NOESY spectrum, assuming that H-8 is α-oriented, the stereochemistry of H-9 and H-4 were deduced as α from the correlations of H-9/H-8 and H-8/H-4. In return, H-4 correlated with H-6α. Then H-6β showed correlation with H-5 and H-7, while the latter also showed correlation with H-1, therefore suggesting that H-1, H-5 and H-7 were all β-oriented. Finally, correlations of H-1/H-2 and H-2/H-3 implied that both H-2 and H-3 were placed in β-position. Thus, the relative configuration was assigned as ***rel-***(1***RS***, 2***RS***, 3***RS***, 4***SR***, 5***SR***, 7***SR***, 8***RS***, 9***SR***).

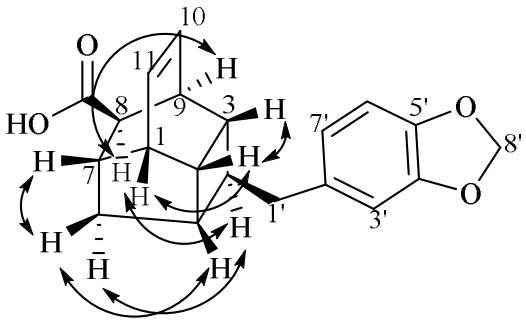

Figure 3.3: Key NOESY ($^1H \leftrightarrow ^1H$) correlations of compound **120**

Thorough analysis of compound **120** led to the conclusion that compound A is a new endiandric acid type A named; kingianic acid A. This compound was the major compound (0.0053% yield) for the endiandric acid type A skeleton.

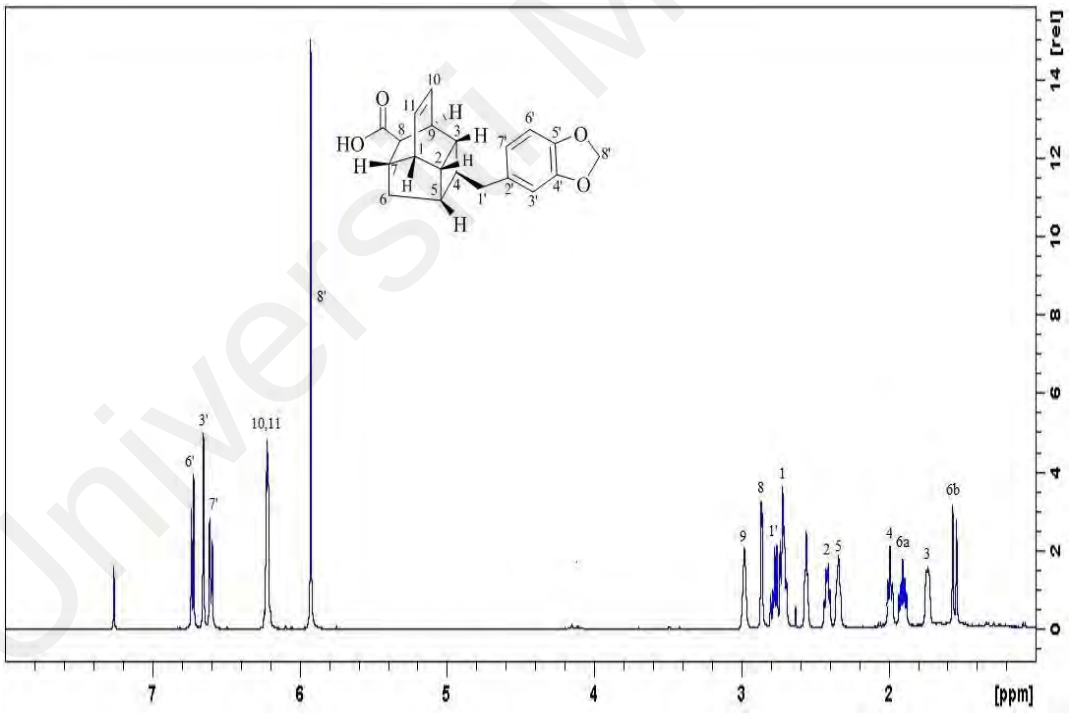

Figure 3.4: ^1H NMR spectrum for compound **120**

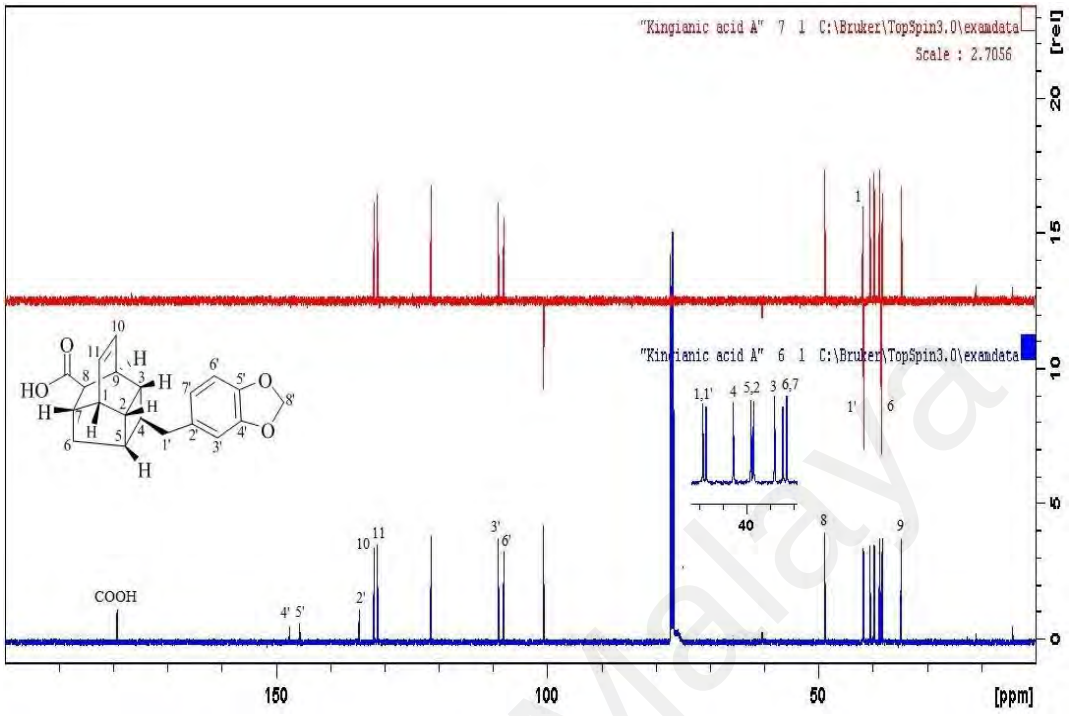

Figure 3.5: ^{13}C NMR and DEPT-135 spectrum for compound **120**

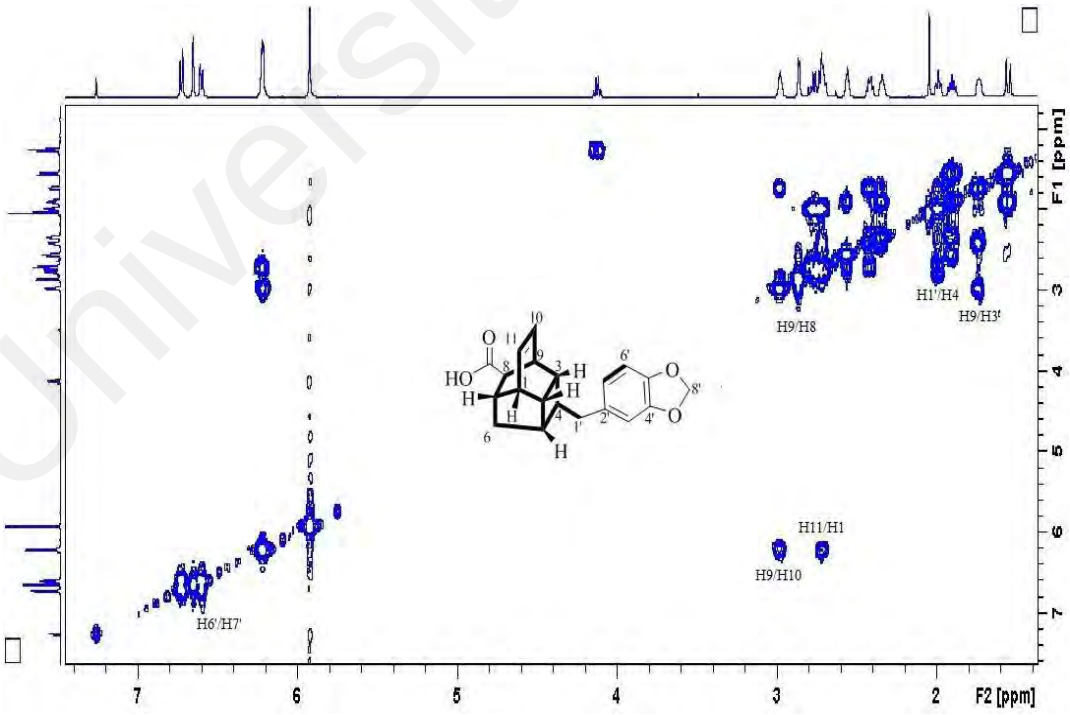

Figure 3.6: COSY-2D NMR spectrum for compound **120**

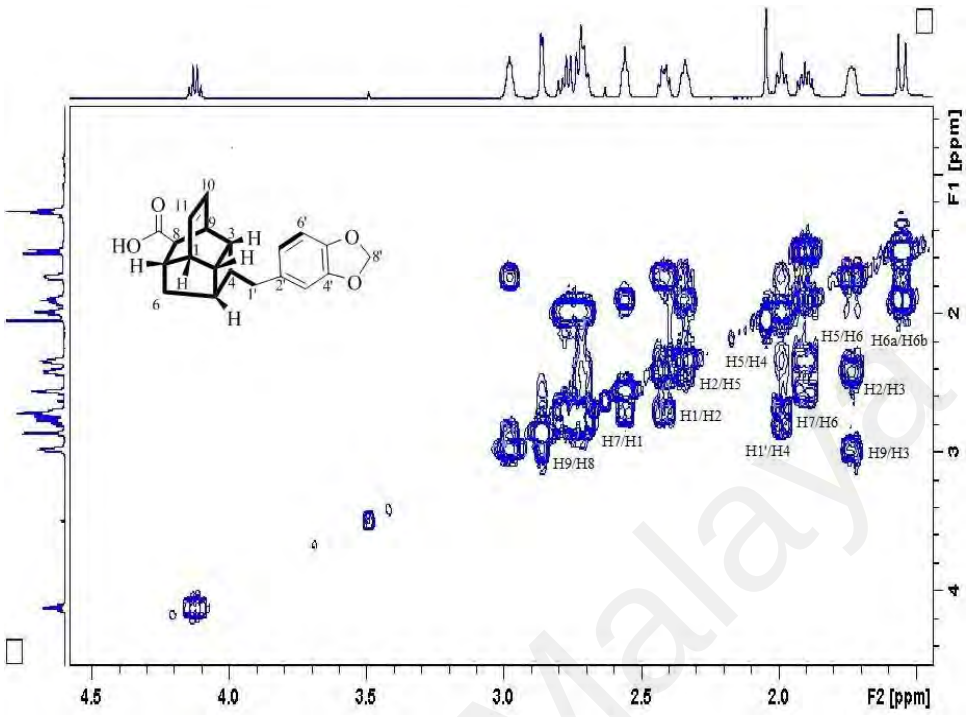

Figure 3.7: COSY-2D NMR (expanded) spectrum for compound **120**

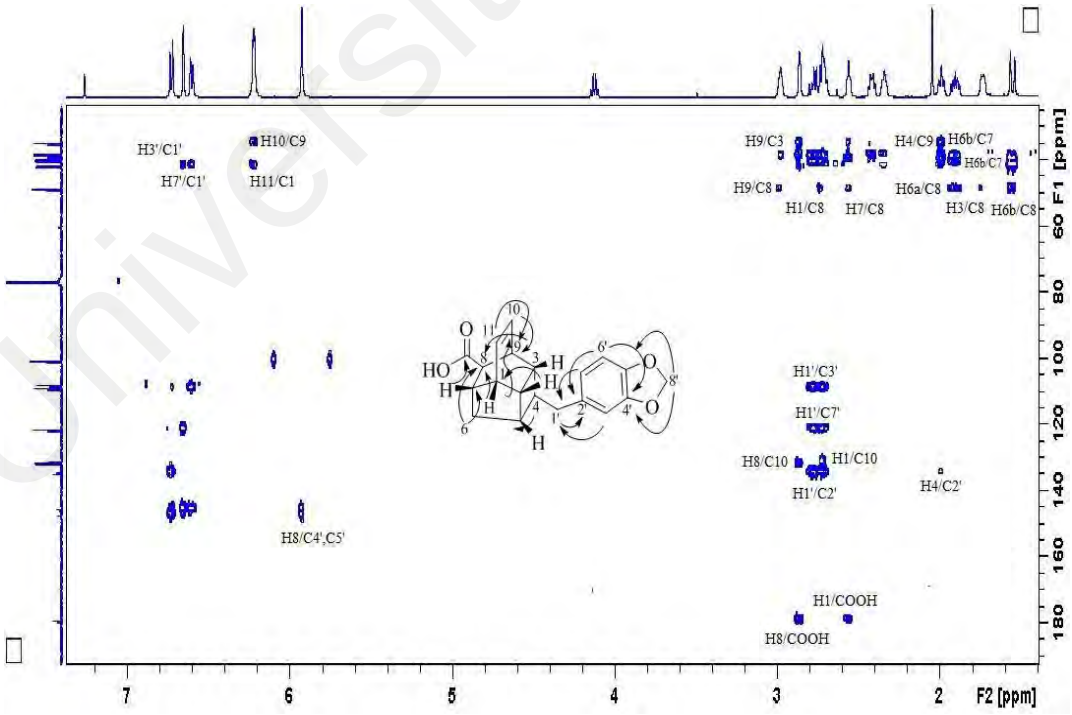

Figure 3.8: HMBC-2D NMR spectrum for compound **120**

Compound B: Kingianic acid B (**121**)

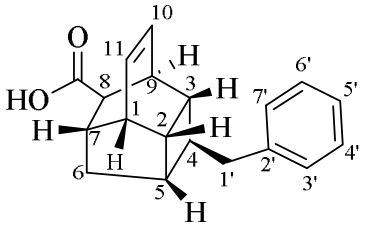

Kingianic acid B (**121**) was isolated as optically inactive yellowish oil. The HRESIMS of **121** showed a pseudomolecular ion peak $[M-H]^-$ at ***m/z*** 279.1398 (calcd for $C_{19}H_{19}O_2$; 279.1385) which indicated the molecular formula of $C_{19}H_{20}O_2$, and was consistent with 10 degrees of unsaturation. The UV, IR, ^1H and ^{13}C NMR data (Table 3.2) were similar to those of compound **120**.

The NMR data of compound **121** closely resembled those of **120** with the exception of the methylenedioxyphenyl substituent at C-4 in **120** being replaced by a monosubstituted phenyl moiety in **121** [δ_H 7.15 (d, ***J*** **=** 7.1 Hz, H-3′ and H-7′); 7.28 (t, ***J*** **=** 7.6 Hz, H-4′ and H-6′) and 7.19 (t, ***J*** **=** 7.3 Hz, H-5′)]. Two ***cis***-form vinyl protons resonated at δ_H 6.22 (ddd, ***J*** = 5.3, 3.6, 2.0 Hz, H-10 and H-11) indicating a type A skeleton and two methylene protons; H-1′α and H-1′β, gave rise to multiplet between δ_H 2.83-2.86. The ^{13}C NMR and DEPT spectra exhibited 11 signals; a methylene at δ_C 38.4 (C-6) and 10 methines inclusive of signals of two olefinic carbons at δ_C 131.3 (C-10) and δ_C 132.0 (C-11), which confirmed the 'cage-like' tetracyclic structure corresponding to the type A endiandric acid moiety. The ^{13}C NMR spectrum (Table 3.2) of **121** showed the characteristic signals of a monosubstituted phenyl moiety between δ_C 125 – 129. Furthermore, the peak at δ_C 140.9 might be attributed to the quaternary carbon at C-2′. The absorption band at ν_{max} 1721 cm^{-1} in the IR spectrum and the resonance at δ_C 179.4 in the ^{13}C NMR spectrum revealed the presence of carboxylic acid moiety (Pretsch et al., 2009; Silverstein et al., 1997; Crews et al., 1998). The correlations between H-7 and H-8 to carboxylic acid carbon; COOH (δ_C 179.4)

observed from the HMBC spectrum, indicated the presence of a carboxylic acid moiety attached to C-8 of the tetracyclic skeleton. Meanwhile, the heteronuclear correlations between H-3′ and H-7′ with C-1′, and that of H-1′ with C-2′ confirmed the connectivity of the phenyl moiety to the tetracyclic core through C-1′ (Table 3.2).

The NOESY spectrum showed similar profile to that of **120**; the H-9 was α-oriented, which was confirmed from the H-10/H-9 NOE correlation. NOEs for H-9/H-4 and H-8 indicated that H-4 and H-8 were on the same side of the molecular plane as H-9, therefore assuming an α-orientation. On the other hand, the following NOE cross peaks, H-3/H-2, H-2/H-1 and H-5, H-5/H-6β, and H-6β/H-7 implied that H-1, H-2, H-3, H-5, and H-7 were β-oriented. Thus, the relative configurations of H-1, H-2, H-3, H-4, H-5, H-7, H-8, and H-9 were assigned as ***rel***-(1***RS***, 2***RS***, 3***RS***, 4***SR***, 5***SR***, 7***SR***, 8***RS***, 9***SR***) identical to the relative configuration of **120** (Figure 3.9).

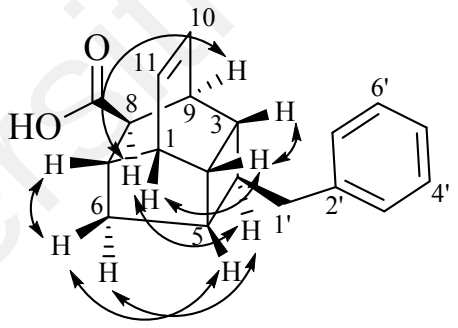

Figure 3.9: Key NOESY (^{1}H↔^{1}H) correlations of compound **121**

The complete ^{1}H and ^{13}C assignments were achieved through a combination of the COSY, HSQC, HMBC, and NOESY experiments. Analysis of compound **121** led to the conclusion that compound B was a new endiandric acid type A named; kingianic acid B.

Table 3.2. ^{1}H (600 MHz) and ^{13}C (150 MHz) NMR data of compound **121** in $CDCl_3$

Position	**121**	
	δ_H (***J*** in Hz)	δ_c
*1	2.72 ddd (10.4, 5.2, 2.0)	41.8
2	2.44 dt (10.4, 4.9)	39.7
3	1.76 m	38.9
4	2.07 dd (7.8, 7.8)	40.2
5	2.37 dd (7.8, 7.8)	39.9
6α	1.54 d (12.8)	38.4
6β	1.90 ddd (12.8, 7.8, 5.6)	
7	2.56 dd (5.6, 5.6)	38.3
8	2.87 d (5.2)	48.8
9	2.98 ddd (7.5, 5.2, 2.0)	34.8
10	6.22 ddd (5.3, 3.6, 2.0)	131.3
11	6.22 ddd (5.3, 3.6, 2.0)	132.0
*1′	2.83 m	41.9
	2.86 m	
2′	-	140.9
3′	7.15 d (7.1)	128.7
4′	7.28 t (7.6)	128.3
5′	7.19 t (7.3)	125.8
6′	7.28 t (7.6)	128.4
7′	7.15 d (7.1)	128.6
C=O	-	179.4

*Overlapping signals

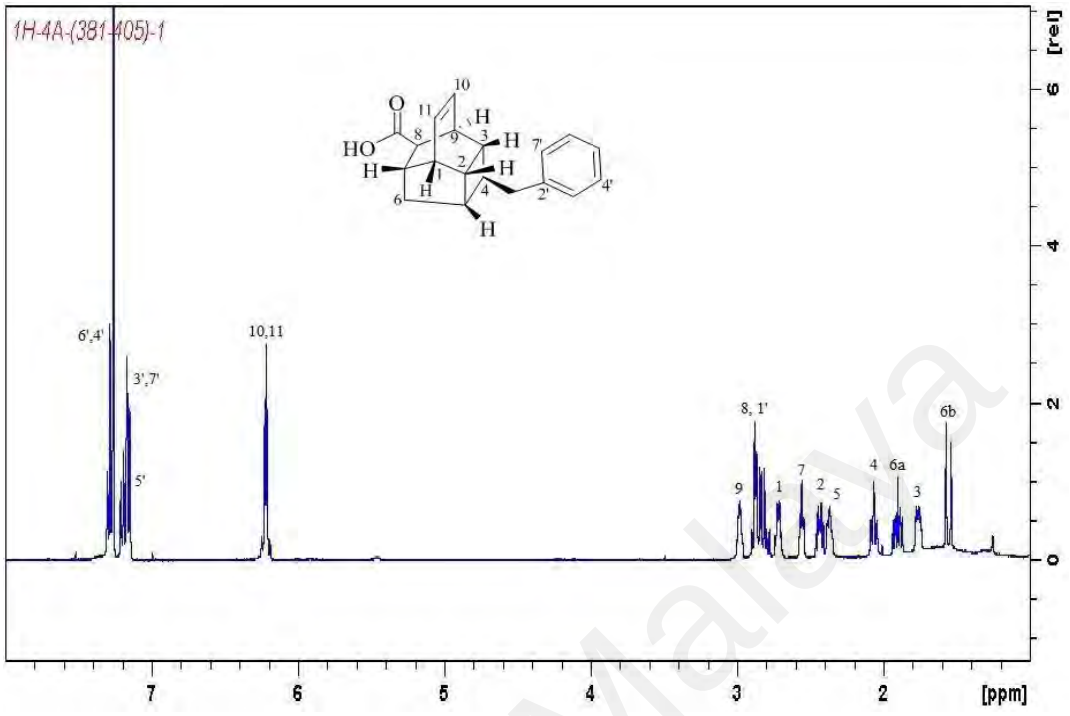

Figure 3.10: ^{1}H NMR spectrum for compound **121**

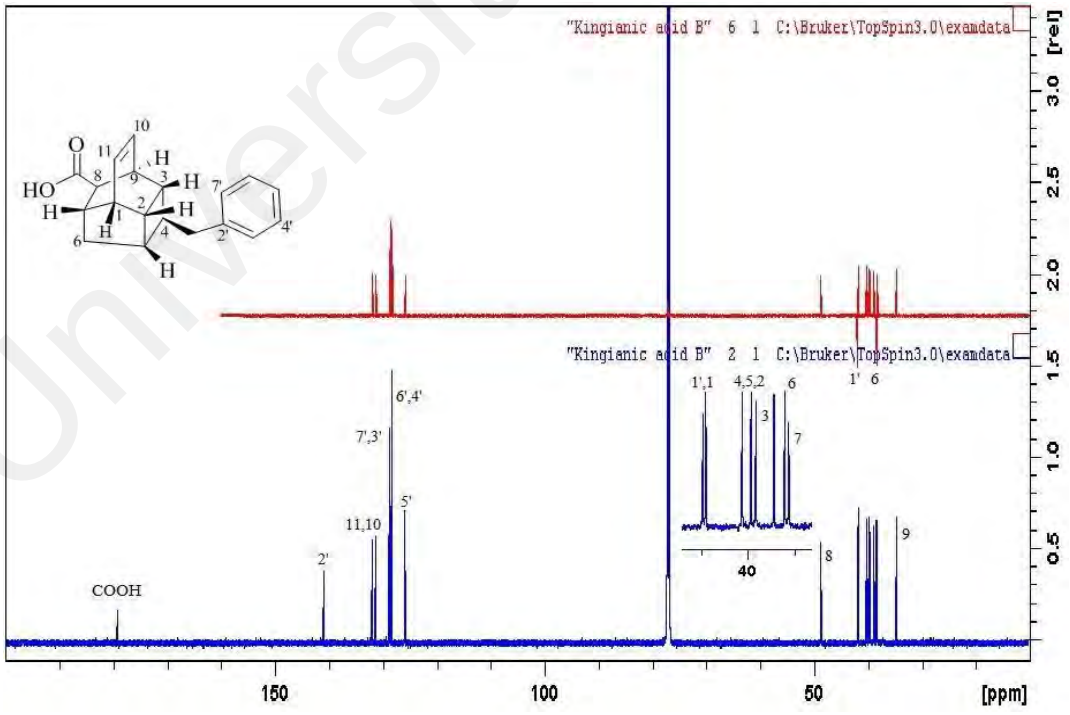

Figure 3.11: ^{13}C NMR and DEPT-135 spectrum for compound **121**

Compound C: Kingianic acid C (**122**)

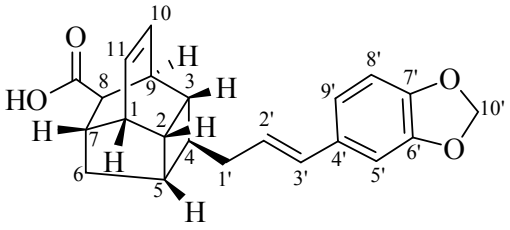

Kingianic acid C (**122**) was isolated as a yellowish oil with $[\alpha_D] = 0°$. The molecular formula of **122** ($C_{22}H_{22}O_4$) was established by the $[M-H]^-$ ion peak at ***m/z*** 349.1439 (calcd. for $C_{22}H_{21}O_4$; 349.1440) in the HRESIMS, corresponding to 12 degrees of unsaturation. UV absorptions showed the presence of a benzenoid moiety at λ_{max} 212 and 290 nm, while the IR spectrum indicated the presence of OH (3437 cm^{-1}), carbonyl (1697 cm^{-1}), and methylenedioxy (1037 and 923 cm^{-1}) groups (Silverstein et al., 1991, 1997; Pavia et al., 2009; Pretsch et al., 2009).

The ^{1}H NMR spectrum of **122** exhibited two ***cis***-form olefinic protons appearing as a triplet at δ_H 6.24 (***J*** = 3.7, H-10, H-11). These signals were the characteristic feature for an endiandric acid type A. For the eastern side chain moiety of **122**, the remaining signals were a methylene (δ_H 2.35 m, H-1′) and two olefinic protons which resonated as a doublet of triplet for H-2′ (δ_H 6.02 dt, ***J*** = 15.7, 6.9 Hz) and a doublet for H-3′ (δ_H 6.29, d, ***J*** = 15.7 Hz). The geometry of the C-2′, C-3′ double bond was assigned as ***trans*** on the basis of their coupling constant value of 15.7 Hz (Pavia et al., 2009). The aromatic proton H-5′, which resonated as a doublet at δ_H 6.90 (d, ***J*** = 1.4 Hz, H-5') and the two ***ortho***-***meta***-coupled doublets at δ_H 6.73 (d, ***J*** = 8.0 Hz, H-8′) and δ_H 6.76 (dd, ***J*** = 8.0, 1.4 Hz, H-9′), suggested the presence of a 1,3,4-tribustituted aromatic ring. In addition, a downfield singlet corresponding to two methylene protons at δ_H 5.94 (H-10′) confirmed the presence of the methylenedioxy group. The ^{13}C NMR and DEPT spectra exhibited 22 signals; three methylenes, 15 methines, and four quaternary carbons inclusive of a carboxylic acid group at δ_C 178.3. The two ***cis***-olefinic carbons at δ_C

131.9 (C-10) and 132.3 (C-11) along with the methylene carbon at δ_C 38.4 (C-6) were characteristic of the tetracyclic endiandric acid skeleton. The resonances of the six aromatic carbons at δ_C 131.4 (C-4′), 108.4 (C-5′), 148.0 (C-6′), 146.7 (C-7′), 108.2 (C-8′) and 120.3 (C-9′), and of a methylenedioxy group at δ_C 101.0 (C-10′) in ^{13}C NMR spectra were indicative of the presence of the methylenedioxyphenyl group (Table 3.3). In the HMBC spectra of **122**, the correlations of H-8 and H-7 with COOH confirmed the connectivity of the carboxylic acid functionality to C-8 (δ_C 48.6). Besides the characteristic tetracyclic moiety, analysis of the COSY and HMBC correlations indicated that the methylenedioxyphenyl moiety was attached to C-3′ in compound **122** (Figure 3.12).

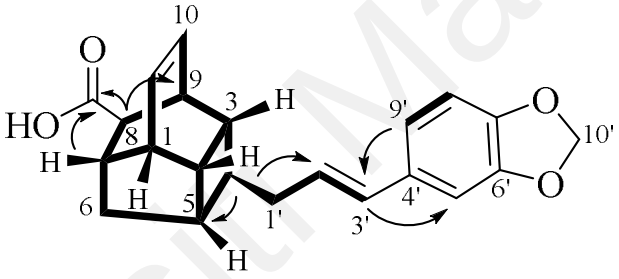

Figure 3.12: Key ^{1}H-^{1}H COSY (bold) and HMBC (^{1}H→^{13}C) correlations of **122**

The NOESY correlation between H-8/H-4 and H9/H8 indicated that these protons were *α*-orientation, and the substituents at C-4 were assumed to be *β*-position on the tetracyclic framework. In contrast, the correlations between H-3/H-2, H-2/H-1, H-5/H-6*β*, and H-6*β*/H-7 suggested the protons H-1, H-2, H-3, H-5, and H-7 are *β*-oriented (Figure 3.13). Thus, the relative configuration of **122** was determined to be ***rel***-(1***RS***, 2***RS***, 3***RS***, 4***SR***, 5***SR***, 7***SR***, 8***RS***, 9***SR***), which was the same as for compound **120**.

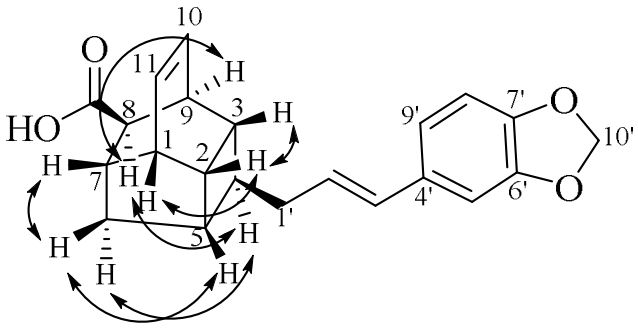

Figure 3.13: Key NOESY ($^1H \leftrightarrow {}^1H$) correlations of compound **122**

The complete assignments of the ^1H and ^{13}C NMR spectra were achieved with the aid of the 2D-NMR experiment and with this; compound **122** was named as kingianic acid C, a new type A tetracyclic polyketide.

Table 3.3: ^1H (600 MHz) and ^{13}C (150 MHz) NMR data of compound **122** in $CDCl_3$

Position	**122**	
	δ_H (***J*** in Hz)	δ_C
1	2.72 ddd (9.9, 6.3, 3.7)	41.8
*2	2.41 m	39.9
3	1.74 m	38.9
4	1.85 br, t (7.5)	39.0
5	2.38 m	39.8
6α	1.58 d (12.8)	38.4
6β	1.93 ddd (12.8, 7.5, 5.0)	
7	2.57 dd (5.0, 5.0)	38.3
8	2.89 d (3.7)	48.6
9	3.05 ddd (8.8, 5.3, 3.7)	34.8
10	6.24 t (3.7)	131.9
11	6.24 t (3.7)	132.3
*1′	2.35 m	39.3
2′	6.02 dt (15.7, 6.9)	126.9
3′	6.29 d (15.7)	130.5
4′	-	131.4
5′	6.90 d (1.4)	108.4
6′	-	148.0
7′	-	146.7
8′	6.73 d (8.0)	108.2
9′	6.76 dd (8.0, 1.4)	120.3
10′	5.94 s	101.0
C=O	-	178.3

*Overlapping signals

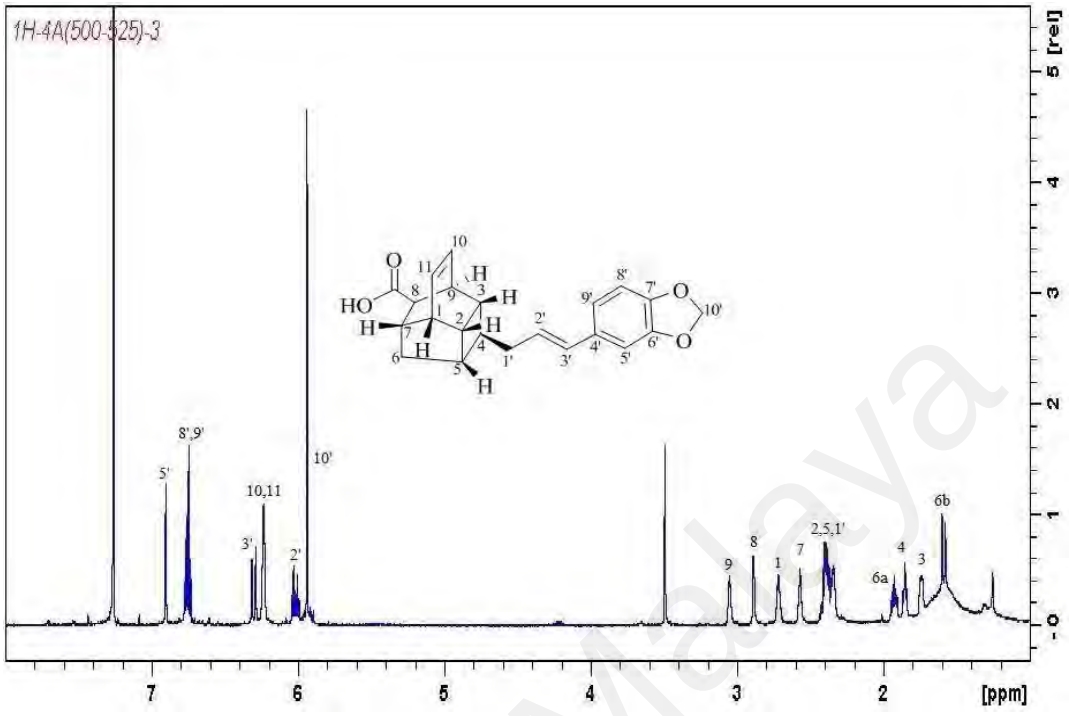

Figure 3.14: ^{1}H NMR spectrum for compound **122**

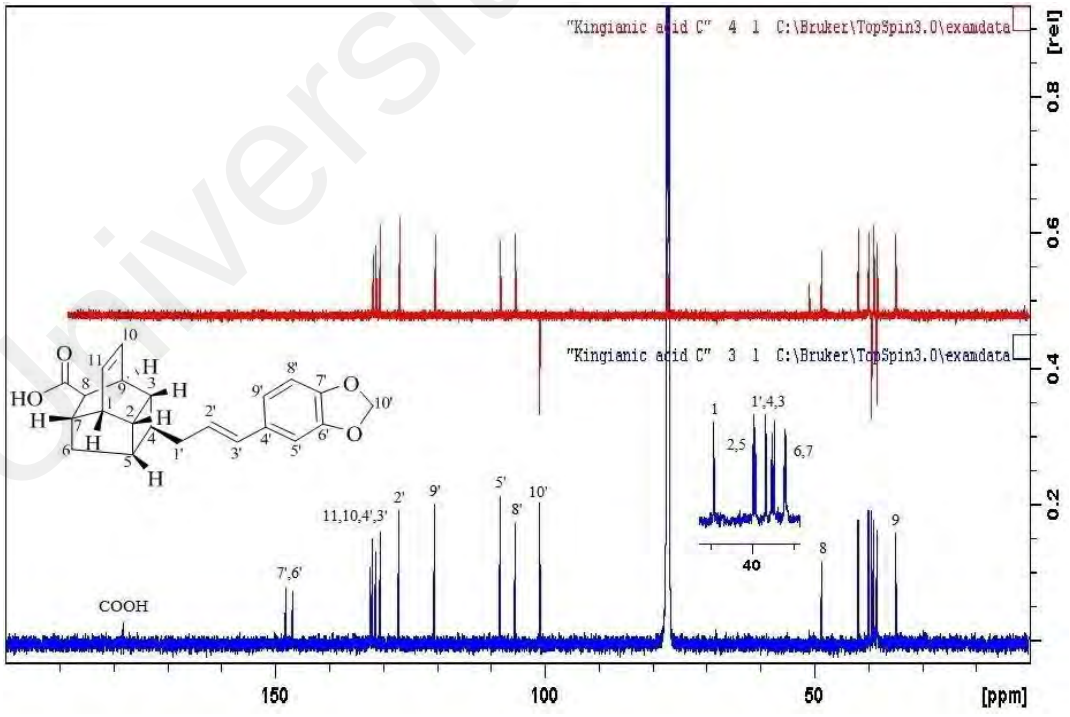

Figure 3.15: ^{13}C NMR and DEPT-135 spectrum for compound **122**

Compound D: Kingianic acid D (**123**)

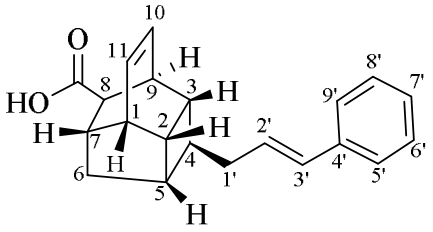

Kingianic acid D (**123**) was isolated as optically inactive yellowish oil [α_D] = 0°. The molecular formula of **123** ($C_{21}H_{22}O_2$) was established by the pseudomolecular ion peak $[M-H]^-$ at ***m/z*** 305.1539 (calcd. for $C_{21}H_{21}O_2$; 305.1542) in the HRESIMS suggesting eleven double bond equivalents. Its IR spectrum revealed absorption bands for hydroxyl and carbonyl groups at 3340 and 1693 $cm^{-1,}$ respectively (Pretsch et al., 2009; Silverstein et al., 1997).

The ^{1}H NMR spectrum of **123** exhibited two ***cis***-form olefinic protons, each appearing as a doublet of doublets at δ_H 6.23 (***J*** = 4.8, 2.9 Hz, H-10) and δ_H 6.24 (***J*** = 4.8, 2.9 Hz, H-11) which are characteristic features of an endiandric acid type A. The methylene protons at δ_H 2.43 (m, H-1′), the olefinic protons which resonated as a doublet of triplet at δ_H 6.19 (***J*** = 15.8, 6.9 Hz H-2′) and a doublet at δ_H 6.19 (***J*** = 15.8 Hz, H-3′) and the five aromatic protons resonating between δ_H 7.20 – 7.35 ppm (H-5′ – H-9′) corresponded to side chain moiety of **123**. The olefinic carbons C2′ and C3′ resonated at δ_H 6.19 and 6.38 was assigned as ***trans*** on the basis of their coupling constant, ***J*** = 15.8 (Pavia et al., 2009). The ^{1}H and ^{13}C NMR data (Table 3.4) of compound **123** displayed two methylenes, 13 methines and four olefinic carbons. The hall marks of the 'cage-like' endiandric acid type A; two ***cis***-olefinic carbons and the methylene carbon gave signals at δ_C 131.4 (C-10), 131.9 (C-11) and 38.4 (C-6), respectively. The resonances of the six aromatic carbons were apparent at δ_C 126.0 (C-5′, C-9′), 128.5 (C-6′, C-8′) and 127.0 (C-7′), and one quaternary carbon at δ_C 137.7 (C-4′) in ^{13}C NMR spectra suggested the presence of the monosubstituted aromatic ring.

In fact, a monosubstituted phenyl group in **123** replaced the methylenedioxyphenyl group in **122**. The presence of a carboxylic acid group was inferred by the strong absorption band at ν_{max} 3440 and 1693 cm^{-1} in the IR spectrum of **123**, and confirmed by the signal at δ_C 177.5 in its ^{13}C NMR spectra (Pretsch et al., 2009; Crews et al., 1998). The carboxylic acid group is connected to C-8 as in **120** as evidenced by the HMBC correlations between H-8 and H-7 to the carbonyl group of the COOH moiety (δ_C 177.5). HMBC correlations; H-3′/C-5′ and H-9′/C-3′ proved that the position of the monosubstituted phenyl moiety is at C-3′ (Figure 3.16).

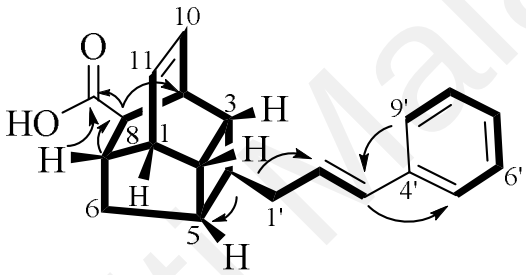

Figure 3.16: Key ^1H-^1H COSY (bold) and HMBC ($^1H \rightarrow ^{13}C$) correlations of **123**

The NOESY spectrum showed similar profile as in the previous compounds **120**-**122**. H-9 was arbitrarily assigned as *α*-oriented. The correlations of H-9/H-8, H-8/H-4 and H-4/H-6*α* indicated that H-8, H-6*α* and H-4 were *α*-oriented and thus suggesting that the substituent at C-4 implied *β*-oriented on the tetracyclic framework. The correlations between H-6*β*/H-7, H-6*β*/H-5, H-5/H-2 and H-2/H-3 suggested that H-2, H-3, H-5 and H-7 assume a *β*-orientation (Figure 3.17). Thus, the relative configuration of **123** was determined as ***rel-***(1***RS***, 2***RS***, 3***RS***, 4***SR***, 5***SR***, 7***SR***, 8***RS***, 9***SR***), which was the same as compound **122**.

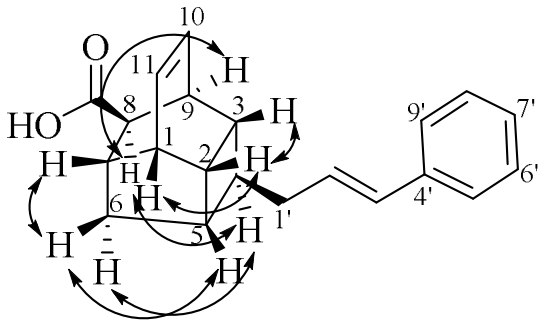

Figure 3.17: Key NOESY ($^1H \leftrightarrow {}^1H$) correlations of compound **123**

Thorough analysis of compound **123** led to the conclusion that it is a new endiandric acid type A named kingianic acid D.

Table 3.4: ^1H (600 MHz) and ^{13}C (150 MHz) NMR data of compound **123** in $CDCl_3$

Position	**123**	
	δ_H (***J*** in Hz)	δ_C
1	2.73 ddd (9.4, 6.3, 4.8)	41.9
*2	2.40 m	39.8
3	1.76 m	39.0
4	1.88 dd (7.4, 7.4)	38.9
5	2.36 dd (7.4, 7.4)	39.9
6α	1.61 d (12.7)	38.4
6β	1.93 ddd (12.7, 7.4, 4.8)	
7	2.58 m	38.3
8	2.90 m	48.6
9	3.06 ddd (7.7, 4.8, 3.1)	34.8
10	6.23 dd (4.8, 2.9)	131.4
11	6.24 dd (4.8, 2.9)	131.9
*1′	2.43 m	39.4
2′	6.19 dt (15.8, 6.9)	128.7
3′	6.38 d (15.8)	131.0
4′	-	137.7
5′	7.35 d (7.2)	126.0
6′	7.30 t (7.6)	128.5
7′	7.20 t (7.3)	127.0
8′	7.30 t (7.6)	128.5
9′	7.35 d (7.2)	126.0
C=O	-	177.5

*Overlapping signals

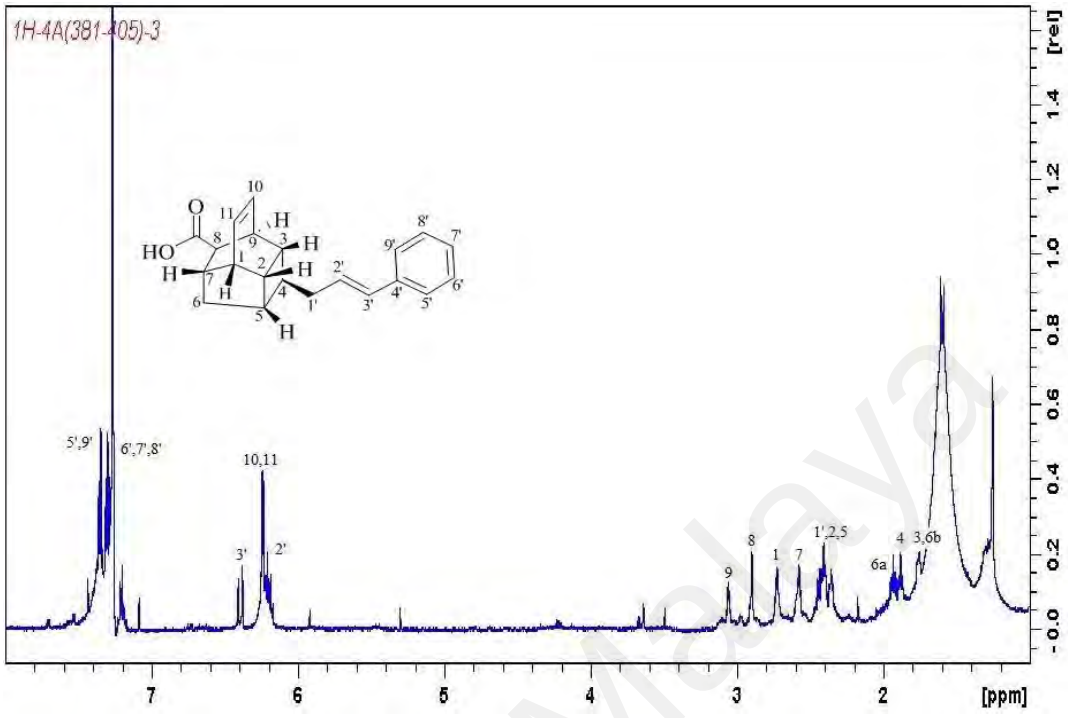

Figure 3.18: ^{1}H NMR spectrum for compound **123**

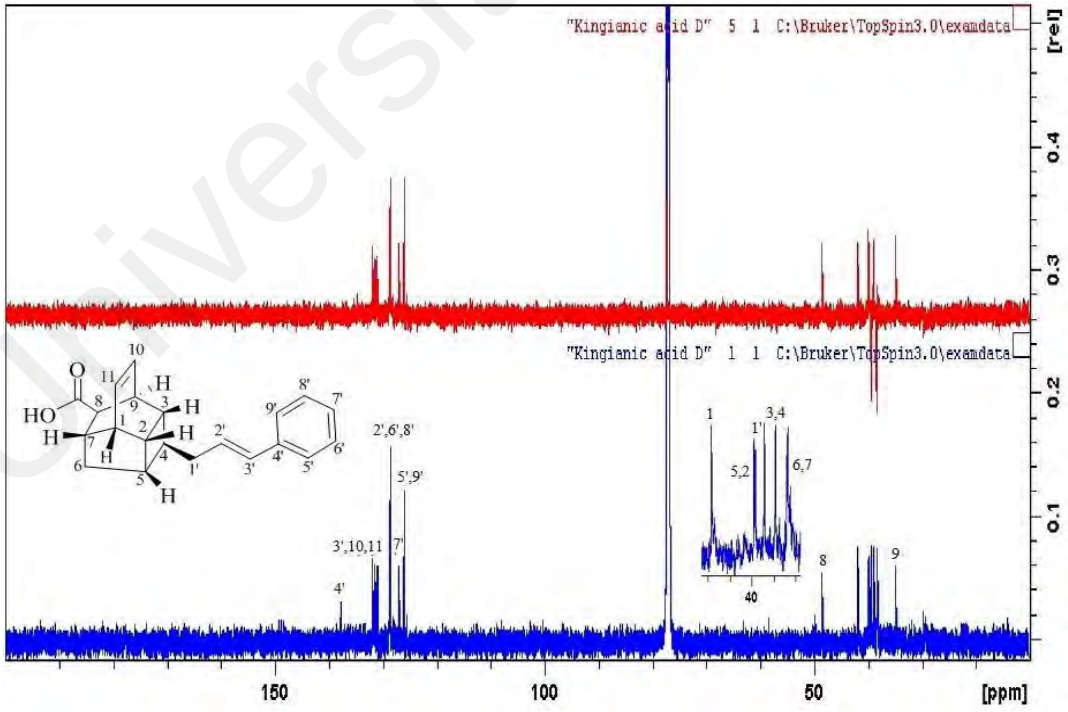

Figure 3.19: ^{13}C NMR and DEPT-135 spectrum for compound **123**

Compound E: Kingianic acid E (**124**)

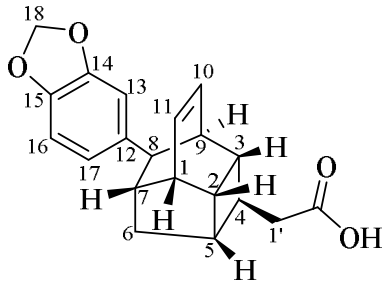

Kingianic acid E (**124**) was isolated as a yellowish oil with $[\alpha_D] = 0°$. HRESIMS of **124** gave an $[M-H]^-$ ion at ***m/z*** 323.1298 (calcd. for $C_{20}H_{19}O_4$ 323.1284), consistent with a molecular formula of $C_{20}H_{20}O_4$ with 11 degrees of unsaturation. Its UV spectrum showed absorption bands at λ_{max} 234 and 286 nm, suggesting the presence of a benzenoid moiety, while its IR spectrum indicated the presence of OH (3444 cm^{-1}), carbonyl (1665 cm^{-1}) and methylenedioxy (1039 and 938 cm^{-1}) groups (Silverstein et al., 1991, 1997; Pavia et al., 2009; Pretsch et al., 2009).

The tetracyclic endiandric acid type A nature of **124** was deduced from the presence of two ***cis***-form olefinic protons appearing at δ_H 5.93 (br t, ***J*** = 7.1 Hz, H-10) and δ_H 6.29 (br t, ***J*** = 7.1 Hz, H-10) (Pavia et al., 2009). The H-13 aromatic proton which resonated as a singlet at δ_H 6.61 (s, H-13) and the two ***ortho***-***meta***-coupled doublets at δ_H 6.67 (d, ***J*** = 8.0 Hz, H-16) and 6.54 (dd, ***J*** = 8.0, 1.3 Hz, H-17) suggested the presence of a 1,3,4-***tri***substituted aromatic ring. In addition, a downfield singlet corresponding to two protons at δ_H 5.89 (H-18) confirmed the presence of the methylenedioxy group. The structure of **124** was found to consist of 13 methines carbons, inclusive of two olefinic carbons [C-10 (δ_C 132.3) and C-11 (δ_C 130.5)], three methylenes, and four quaternary carbons inclusive of the carboxylic acid carbon at δ_C 176.9. The resonances of the six aromatic carbons at δ_C 140.2 (C-12), 109.5 (C-13), 146.9 (C-14), 145.2 (C-15), 107.4 (C-16) and 121.6 (C-17), and of a methylenedioxy group at δ_C 100.7 (C-18) in ^{13}C NMR spectra suggested the presence of the

methylenedioxyphenyl group (Table 3.5). The position of this moiety was determined via HMBC correlations.

A close examination of the NMR spectra of compound **124** indicated that **124** possessed the same tetracyclic moiety (endiandric acid type A) as **120**, but with different substituents at the C-4 and C-8 parts. The two substituents consisted of an acetic acid group [δ_H 2.64 (***m***, H_2-1′); δ_C 176.9 (COOH)] and a methylenedioxyphenyl moiety. The COSY correlation between H-4 and H_2-1′ and the HMBC correlations of H-4 (δ_H 2.44) with C-1′ (δ_C 40.4) confirmed the connectivity of the acetic acid moiety to the tetracyclic core through C-1′. Meanwhile, the position of the methylenedioxyphenyl moiety at C-8 was determined from HMBC correlations of H-8/C-12, C-9 and of H-13, H-17/C-8.

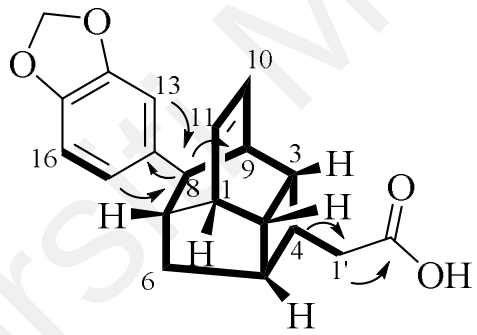

Figure 3.20: Key ^{1}H-^{1}H COSY (bold) and HMBC (^{1}H→^{13}C) correlations of **124**

Based on the NOESY spectrum, the *β*-orientation of acetic acid and 3,4-methylenedioxyphenyl moieties were deduced from the correlations between H6α/H-8, H6α/H-4, H-8/H-9 and H-8/H-4. The correlations between H-3/H-2, H-2/H-1, H-5/H-6*β*, and H6*β*/H-7 suggested that these protons were *β*-oriented. Thus, the relative configuration was assigned as ***rel***-(1***RS***, 2***RS***, 3***RS***, 4***SR***, 5***SR***, 7***SR***, 8***RS***, 9***SR***), the same as **120**. Thorough analysis of the 1D and 2D NMR spectroscopic data, led to the deduction that compound **124** is kingianic acid E, a new endiandric acid type A.

Table 3.5: ^{1}H (600 MHz) and ^{13}C (150 MHz) NMR data of compound **124** in $CDCl_3$

Position	**124**	
	δ_H (***J*** in Hz)	δ_C
1	2.76 ddd (7.1, 5.0, 5.0)	42.4
*2	2.46 m	39.9
#3	2.64 m	40.3
*4	2.44 m	35.3
5	2.37 dd (7.2, 7.2)	40.2
6α	1.74 d (12.6)	39.3
6β	1.94 ddd (12.6, 7.2, 5.0)	
7	2.31 dd (5.0, 5.0)	43.1
8	3.25 d (3.5)	47.9
9	2.72 m	39.6
10	5.93 br t (7.1)	132.3
11	6.29 br t (7.1)	130.5
12	-	140.2
13	6.61 d (1.3)	109.5
14	-	146.9
15	-	145.2
16	6.67 d (8.0)	107.4
17	6.54 dd (8.0, 1.3)	121.6
18	5.89 s	100.7
#1′	2.64 m	40.4
C=O	-	176.9

*,#Overlapping signals

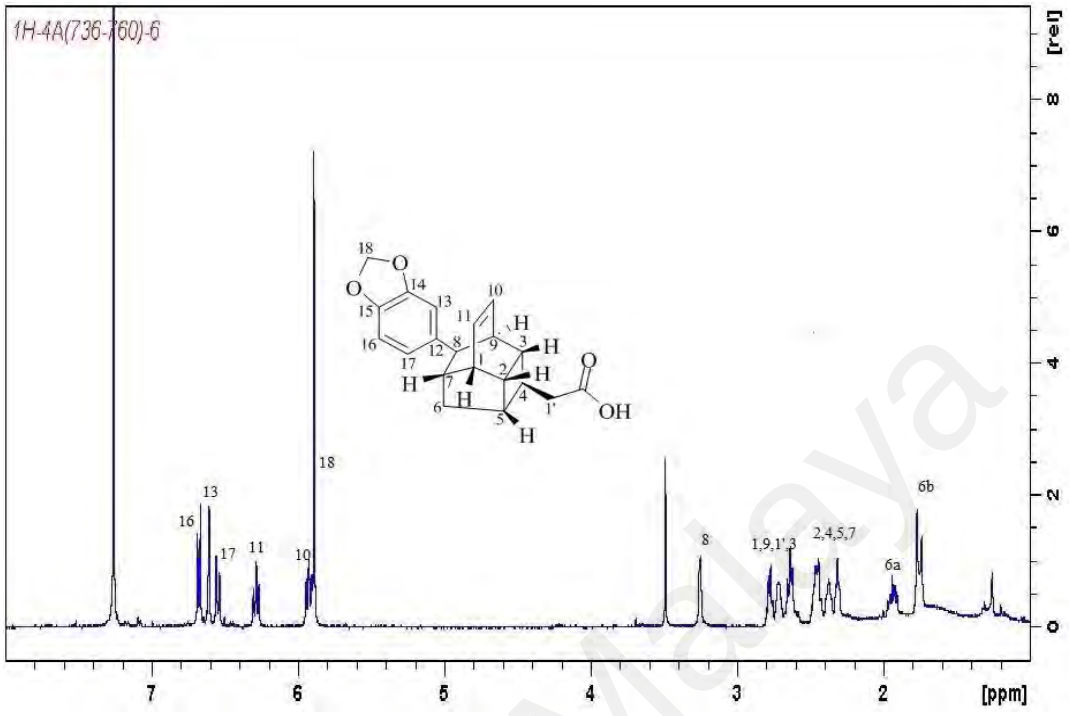

Figure 3.21: ^{1}H NMR spectrum for compound **124**

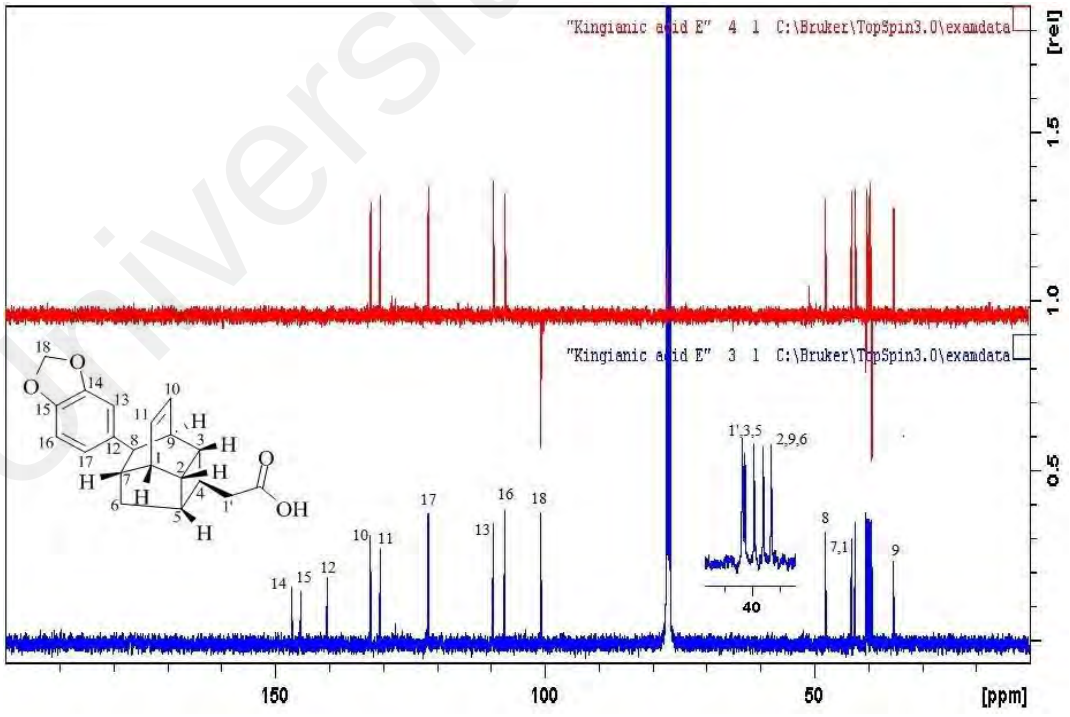

Figure 3.22: ^{13}C NMR and DEPT-135 spectrum for compound **124**

Compound F: Endiandric acid M (**93**)

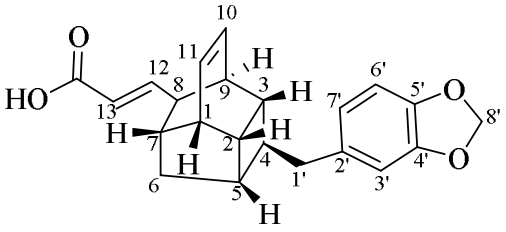

Compound F was isolated as a yellowish oil with a molecular formula of $C_{22}H_{22}O_4$ corresponding to 12 degrees of unsaturation as deduced from its HRESIMS similar to **122**. Its UV spectrum revealed a typical benzenoid absorption band at 232 and 288 nm (Silverstein et al., 1991; Pavia et al., 2009). The IR spectrum of compound F showed absorption bands indicative of a carboxylic acid functionality at 3462 (OH acid) and 1692 (C=O acid) and 1040, 937 cm^{-1} (methylenedioxyl, O-CH_2-O) (Pretsch et al., 2009; Silverstein et al., 1997).

Analysis of the NMR data of compound F revealed the characteristics of an endiandric acid type A. The ^{13}C NMR and DEPT data of compound F displayed three methylenes, fifteen methines; including four olefinic carbons at δ_C 132.5 (C-10), 130.7 (C-11), 156.7 (C-12) and 118.8 (C-13) and four quaternary carbons. The spectroscopic data of compound F was similar to those of **120**, but the HMBC correlations showed the presence of an *α,β*-unsaturated carboxylic acid [δ_H 6.85 (dd, ***J*** = 15.7, 8.3 Hz, H-12); 5.68 (d, ***J*** = 15.7 Hz, H-13); δ_C 171.2 (COOH)] at C-8 (Table 3.6). The geometry of the $\Delta^{12,13}$ double bond was assigned as ***trans*** on the basis of the coupling constant ***J*** = 15.7 Hz (Huang et al., 2011; Silverstein et al., 1991). The HMBC correlations between H-12 with C-7, C-9 and the carboxylic acid; COOH along with the COSY correlation between H-12 and H-8 proved that the *α,β*-unsaturated carboxylic acid chain was located at C-8. The aromatic protons at δ_H 6.66 (d, ***J*** = 1.3 Hz, H-3′) and δ_H 6.72 (d, ***J*** = 7.9 Hz, H-6′) and 6.61 (d, ***J*** = 7.9, 1.3 Hz, H-7′) suggested the presence of a 1,3,4-trisubstituted aromatic ring. In addition, the proton signal at δ_H 5.93 (s, H-8′)

confirmed the presence of the methylenedioxy group which was connected to the tetracyclic core through C-1′ which was verified from the H-1′/C-3′, C-7′ HMBC correlations (Figure 3.23).

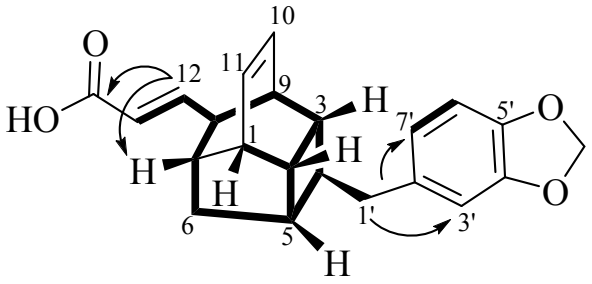

Figure 3.23: Key COSY (bold) and HMBC ($^{1}H \rightarrow ^{13}C$) correlations of compound F (**93**)

The NOESY spectrum showed the same profile as previous compounds. The correlations between H-6α/H-4, H-6α/H-8, H-9/H-8 indicated a β-orientation for the phenyl group at C-4 and the α,β-unsaturated carboxylic acid at C-8. Thus, the relative configuration was assigned as ***rel-***(1***RS***, 2***RS***, 3***RS***, 4***SR***, 5***SR***, 7***SR***, 8***RS***, 9***SR***), the same as that of kingianic acids A-E (**120**-**124**). In summary, compound F was established as endiandric acid M (**93**), a known endiandric acid after comparing the spectroscopic data with literature values (Huang et al., 2012), which was previously isolated from ***Beilschmiedia tsangii*** by Huang et al. (2012).

Table 3.6: ^{1}H (600 MHz) and ^{13}C (150 MHz) NMR data of compound F in $CDCl_3$

Position	**Compound F ($CDCl_3$)**	
	δ_H (***J*** in Hz)	δ_C
*1	2.69 m	42.2
2	2.44 dt (8.9, 5.1)	39.9
3	1.73 m	39.7
4	1.92 t (5.1)	41.7
5	2.35 t (7.0)	39.5
6α	1.57 d (12.7)	38.8
6β	1.86 ddd (12.7, 7.0, 5.8)	
7	2.10 t (8.3)	40.0
8	2.78 d (8.3)	47.3
9	2.53 m	37.2
10	6.16 t (7.1)	132.5
11	6.24 t (7.1)	130.7
12	6.85 dd (15.7, 8.3)	156.7
13	5.68 d (15.7)	118.8
*1′	2.71 m	41.8
	2.76 m	
2′	-	134.9
3′	6.66 d (1.3)	109.1
4′	-	147.5
5′	-	145.6
6′	6.72 d (7.9)	108.1
7′	6.61 dd (7.9, 1.3)	121.5
8′	5.93 s	100.6
C=O	-	171.2

*Overlapping signals

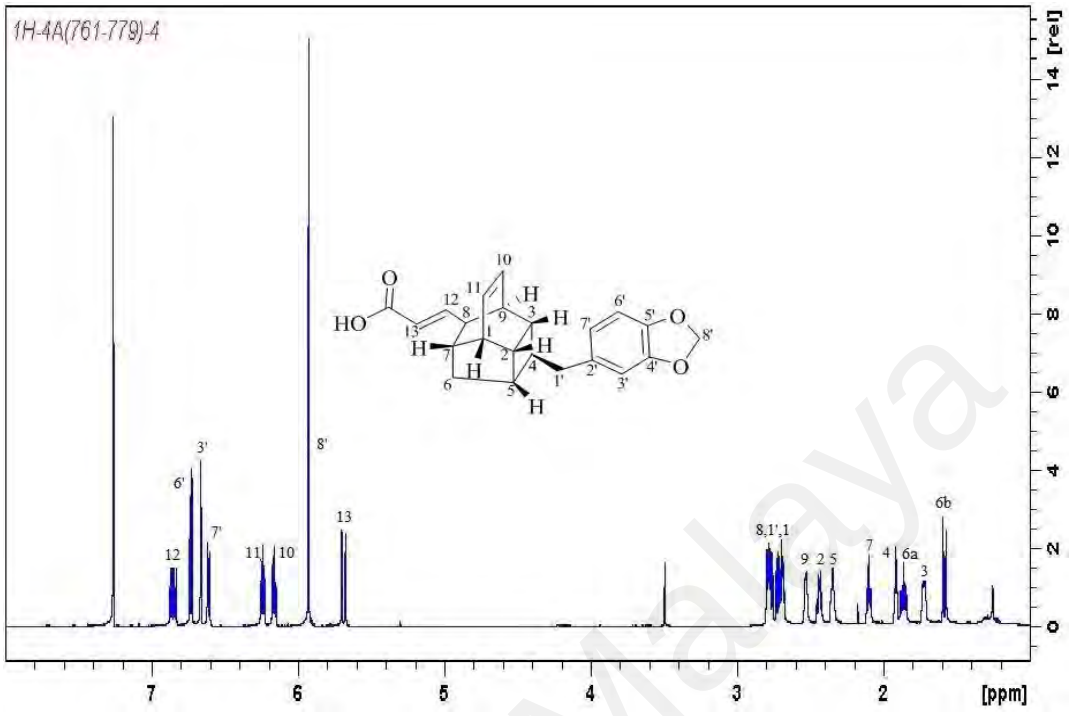

Figure 3.24: ^{1}H NMR spectrum for compound **93**

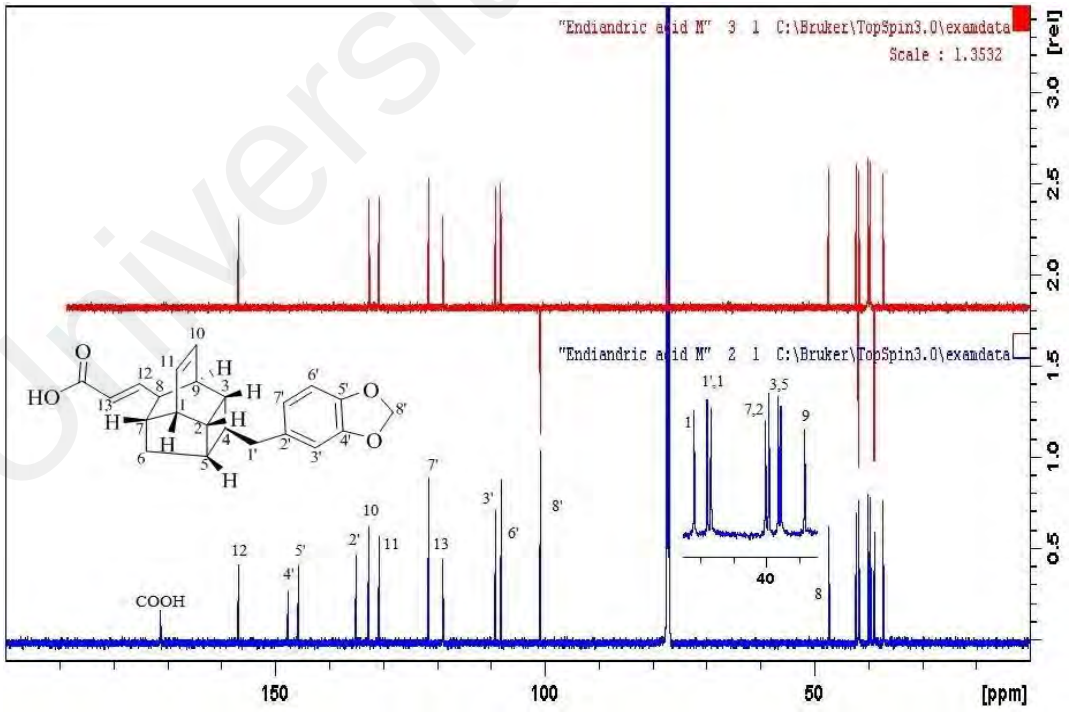

Figure 3.25: ^{13}C NMR and DEPT-135 spectrum for compound **93**

Compound G: Kingianic acid F (**125**)

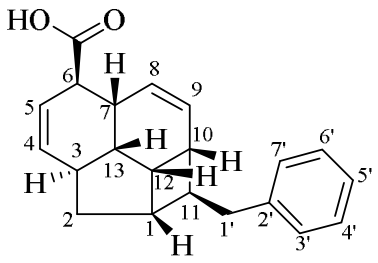

Compound G has the molecular formula $C_{21}H_{22}O_2$ as determined by HRESIMS analysis; 305.1557 $[M–H]^-$ (calcd for $C_{21}H_{21}O_2$; 305.1542), of which 10 degrees of unsaturation could be deduced. This compound was isolated as optically inactive yellowish oil. The UV spectrum of **125** showed characteristic absorption bands at ν_{max} 232 and 288 nm suggesting the presence of a benzenoid moiety (Silverstein et al., 1991; Pavia et al., 2009). Its IR spectrum showed absorption bands at 3432 cm^{-1} for an OH group and 1696 cm^{-1} for carboxylic acid carbonyl functionality (Pretsch et al., 2009; Silverstein et al., 1997).

The ^1H NMR data showed signals at δ_H 7.15 (d, ***J*** = 6.8 Hz, H-3′ and H-7′), 7.20 (t, ***J*** = 7.0 Hz, H-5′) and 7.24 (t, ***J*** = 6.8 Hz, H-4′ and H-6′), suggesting the presence of a mono-substituted benzene ring. The two sets of olefinic proton signals at δ_H 5.40 (br s, H-8), 5.42 (br s, H-9), 5.72 (dt, ***J*** = 9.6, 2.5 Hz, H-5) and 6.19 (dt, ***J*** = 9.6, 2.5 Hz, H-4) were characteristic features of an endiandric acid type B. The ^{13}C NMR and DEPT spectra exhibited 21 signals among which two were methylenes, 16 methines, and three quaternary carbons inclusive of a carboxylic acid carbon resonating at δ_C 179.4. The methylene at δ_C 34.7 (C-2) and the four olefinic carbons at δ_C 134.4 (C-4), 123.9 (C-5), 129.8 (C-8) and 129.1 (C-9) were characteristics of the tetracyclic skeleton of endiandric acid type B which has different skeletal features with compounds **120**-**124**. The resonances of the six aromatic carbons appeared at δ_C 128.6 (C-3′, C-7′), 128.4

(C-4′, C-6′), 125.8 (C-5′), and 140.7 (C-2′) in ^{13}C NMR spectrum were indicative of the presence of monosubstituted aromatic ring (Table 3.7).

The tetracyclic skeleton which consists of 13 carbons and 14 protons may be divided into three fragments; A, B and C. Signals for contiguous protons and carbons were evident from the COSY and HSQC spectra; fragment **A**; (H-9, H-8, H-7 [δ_H 2.84 (m)], H-13 [δ_H 1.73 (ddd**,** ***J*** = 10.7, 7.5, 3.6 Hz)], H-12 [δ_H 2.84 (dd**,** ***J*** = 13.2, 7.5 Hz)], H-1 [δ_H 2.39 (td**,** ***J*** = 6.3, 1.6 Hz)], H-11 [δ_H 1.82 (ddd**,** ***J*** = 13.2, 8.1, 5.5 Hz)], H-10 [δ_H 2.45 (m)]), fragment **B**; (H-6 [δ_H 3.00 (m)], H-5, H-4) and fragment **C**; (H-13, H-3 [δ_H 2.55 (m)], H-2 [δ_H 1.30 (dt**,** ***J*** = 12.0, 5.5 Hz), 1.53 (dd**,** ***J*** = 12.0, 6.3 Hz)]) (Table 3.7). They were further connected through the ^{2}***J*** and ^{3}***J*** correlations based on the HMBC spectrum. Cross peaks between H-2 with C-1, C-3, C-4 and C-11, H-8 with C-6, C-7, C-13 and C-10, and H-6 with C-5 were used to connect the three fragments, **A** to **C**, thus aiding in establishing the tetracyclic structural unit, which composed of one cyclobutane, one cyclopentane, and two cyclohexane rings for **125** (Figure 3.26).

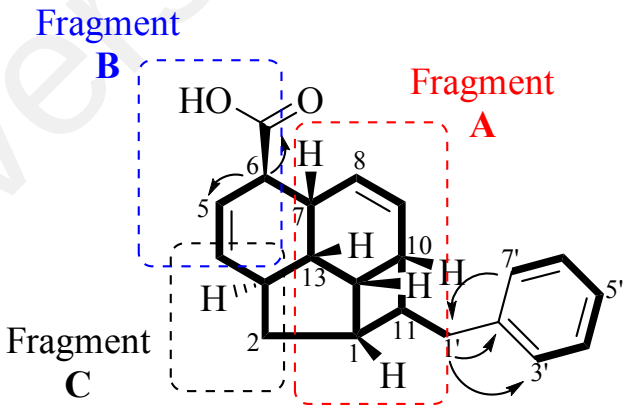

Figure 3.26: Key ^{1}H-^{1}H COSY (bold) and HMBC (^{1}H→^{13}C) correlations of **125**

The position of a carboxylic acid; COOH group was established from the HMBC correlation between H-6 with the carbonyl carbon at δ_C 179.4, thus confirming the connectivity of the carboxyl group to C-6. Finally, the COSY correlation between H-11

and H_2-1′ and the HMBC correlation of H-1′/C-2′, C-3′, and of H-7′/C-1′ indicated that the core structure and the benzyl moiety were connected at C-11 (Figure 3.26).

Table 3.7: ^{1}H (600 MHz) and ^{13}C (150 MHz) NMR data of compound **125** in $CDCl_3$

Position	**125**	
	δ_H (***J*** in Hz)	δ_C
1	2.39 td (6.3, 1.6)	34.5
2α	1.30 dt (12.0, 5.5)	34.7
2β	1.53 dd (12.0, 6.3)	
3	2.55 m	36.9
4	6.19 dt (9.6, 2.5)	134.4
5	5.72 dt (9.6, 2.5)	123.9
6	3.00 m	49.0
*7	2.84 m	32.8
8	5.40 br s	129.8
9	5.42 br s	129.1
10	2.45 m	41.0
11	1.82 ddd (13.2, 8.1, 5.5)	46.9
12	2.70 dd (13.2, 7.5)	32.9
13	1.73 ddd (10.7, 7.5, 3.6)	42.0
*1′	2.81 m	42.9
2′	-	140.7
3′	7.15 d (6.8)	128.6
4′	7.24 t (6.8)	128.4
5′	7.20 t (7.0)	125.8
6′	7.24 t (6.8)	128.4
7′	7.15 d (6.8)	128.6
C=O	-	179.4

*Overlapping signals

The relative configuration of **125** was ascertained by the careful inspection of the NOESY spectrum. H-7 was arbitrarily assigned as *β*-oriented. NOESY correlations between H-7/H-13, H-13/H-12, H-12/H-1, H-1/H-10, H-1/H-2*β* indicated that H-13, H-12, H-10, H-1, H-2*β* are *β*-oriented spatially. The other proton H-3 correlated with H-2*α*, and H-3 also sees H-11, therefore both H-3 and H-11 are *α*–oriented spatially (Figure 3.27). These spatial assignments are the same as the ones in ferrugenic acid A (**109**) due to biogenetic reasoning (Apel et al., 2014). Thus, the relative configuration of

125, named kingianic acid F or 11{1'-[phenyl]}tetracyclo[5.4.2.$0^{3,13}$.$0^{10,12}$]trideca-4,8-dien-6-carboxylic acid, was assigned as ***rel-***(1***RS***, 2***RS***, 3***RS***, 4***SR***, 5***SR***, 7***SR***, 8***RS***, 9***SR***).

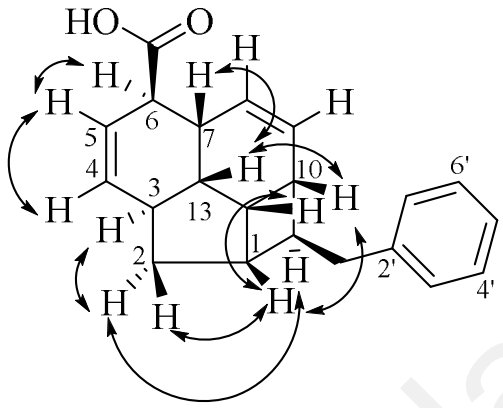

Figure 3.27: Key NOESY ($^1H \leftrightarrow {}^1H$) correlations of compound **125**

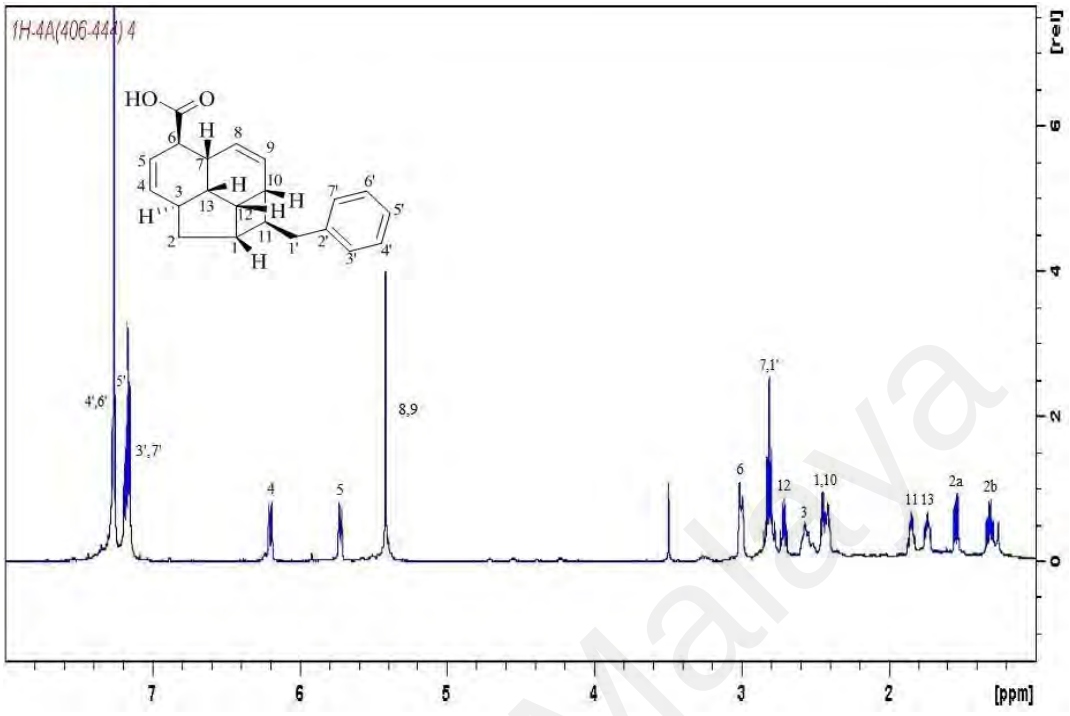

Figure 3.28: ^{1}H NMR spectrum for compound **125**

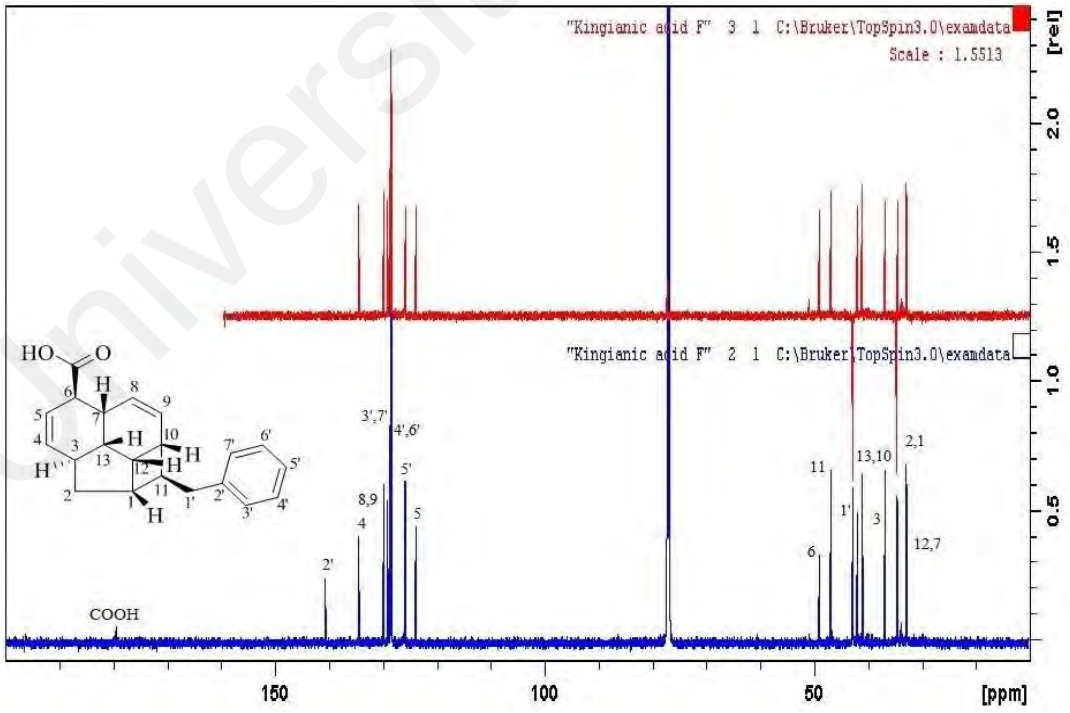

Figure 3.29: ^{13}C NMR and DEPT-135 spectrum for compound **125**

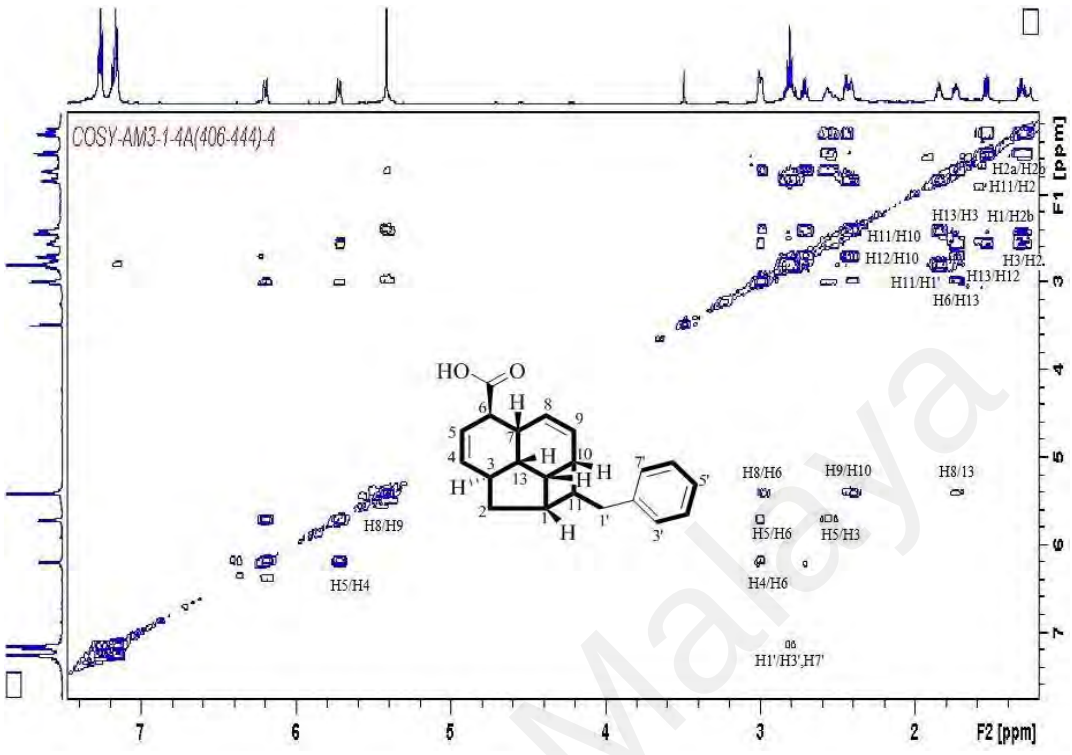

Figure 3.30: COSY-2D NMR spectrum for compound **125**

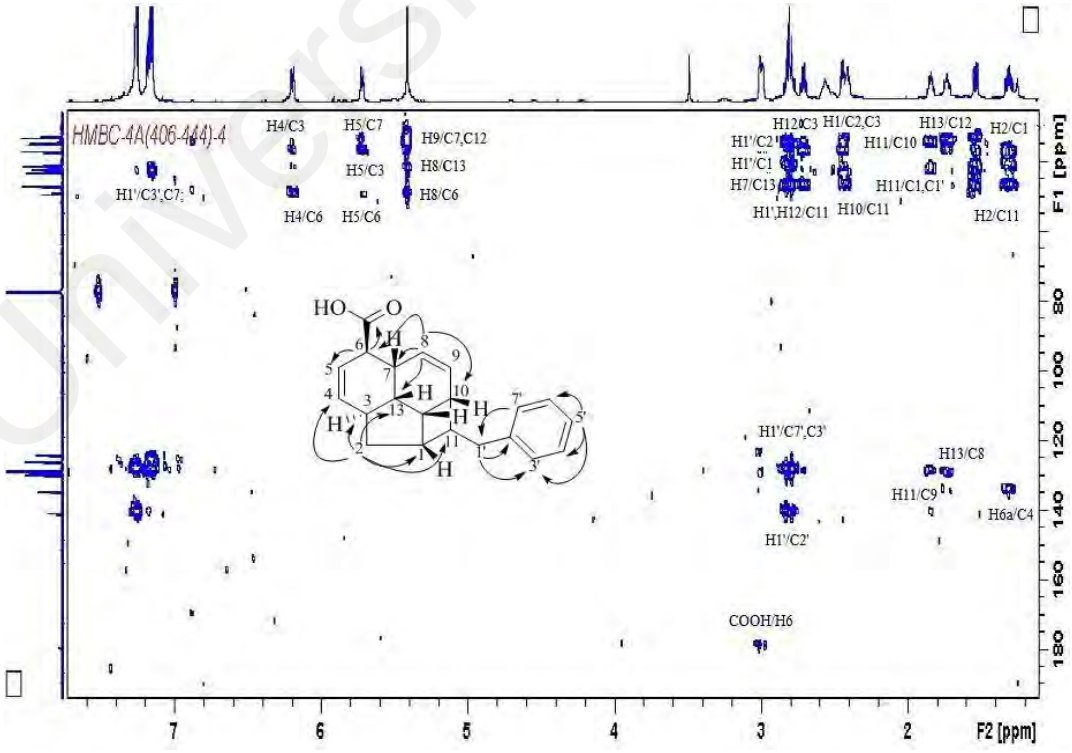

Figure 3.31: HMBC-2D NMR spectrum for compound **125**

Compound H: Tsangibeilin B (**89**)

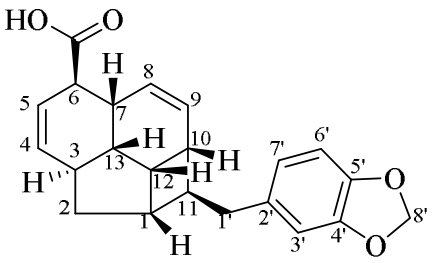

Compound H was isolated as an optically inactive white solid. The HRESIMS gave a pseudomolecular ion peak $[M–H]^-$ at ***m/z*** 349.1433 (calcd. for $C_{22}H_{21}O_4$; 349.1440), consistent with molecular formula $C_{22}H_{22}O_4$ which indicated 12 degrees of unsaturation. The ^{13}C NMR and DEPT-135 spectra exhibited 22 carbons thus supporting the proposed molecular formula. The UV spectrum of compound **89** showed characteristic absorption bands at ν_{max} 234 and 286 nm suggesting the presence of a benzenoid moiety (Silverstein et al., 1991; Pavia et al., 2009). Its IR spectrum showed absorption bands at 3430 cm^{-1} for an OH group, 1685 cm^{-1} for a carboxylic acid carbonyl, and 1039, 935 cm^{-1} for methylenedioxyl functionalities (Silverstein et al., 1997; Pretsch et al., 2009).

Similar to **125**, the characteristic features of endiandric acid type B with ***cis*** double bonds at position C-4, C-5, C-8 and C-9 were evident from the ^1H and ^{13}C NMR data; δ_H 6.19 (br d, ***J*** = 9.5 Hz, H-4; δ_C 134.4, C-4), δ_H 5.72 (dt, ***J*** = 9.5, 2.4 Hz, H-5; δ_C 123.9, C-5), δ_H 5.43 (m, H-8; δ_C 129.1, C-8) and δ_H 5.45 (m, H-9; δ_C 129.8, C-9). In general, compound H was almost the same as in kingianic acid F (**125**) except for the substitution at the C-11. The monosubstituted benzene ring in **125** was replaced with a methylenedioxyphenyl group at δ_H 6.65 (d, ***J*** = 1.5 Hz, H-3′); 6.71 (d, ***J*** = 8.0 Hz, H-6′), and 6.61 (dd, ***J*** = 8.0, 1.5 Hz, H-7′) ppm. The ^{13}C NMR spectrum of compound H showed the signal of an unconjugated carboxylic acid group, COOH at δ_C 179.0 (COOH). It also contained 13 skeletal signals of the endiandric acid type B moiety, including the presence of 12 methine and one methylene carbons (Table 3.8). The

position of the carboxylic acid; COOH group was revealed from the HMBC correlation between H-6 to the carbonyl carbon at δ_C 179.0 which established the connectivity of carboxyl group at C-6. Finally, the COSY correlation between H-11 and H_2-1′ and HMBC correlation of H-1′/C-2′, C-3′, and H-7′/C-1′ indicated that the core structure and the methylenedioxyphenyl moiety were connected by the remaining one methylene group; C-1′ (δ_C 42.6) (Figure 3.32).

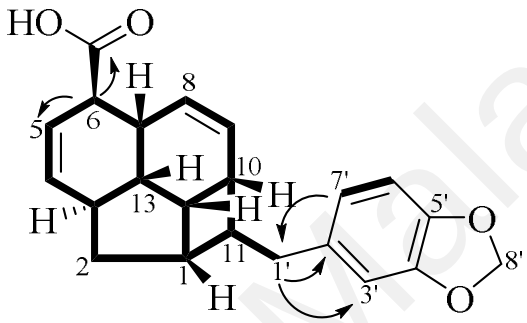

Figure 3.32: Key COSY (bold) and HMBC ($^1H \rightarrow ^{13}C$) correlations of compound H (**89**)

The relative configuration of the stereogenic centers was established from the biogenetic consideration in combination with the NOESY analysis (Figure. 3.33). According to the NOESY spectrum, H-7 was arbitrarily assigned as β-oriented. NOE correlations between H-7/H-13 and H-13/H-10 indicated that H-10 and H-13 were on the same side of the molecular plane, thus assuming β–orientation. On the other hand, the NOE cross peaks of H-12/H-10, H-1/H-12 and H-1/H-2β indicated a β-orientation for H-1, H-2β and H-12. The α–orientation of H-11 was deduced from the correlation of H-2α/H-11. Thus, the relative configuration of compound H was assigned as ***rel***-(1***SR***, 3***RS***, 6***RS***, 7***RS***, 10***RS***, 11***SR***, 12***SR***, 13***SR***) the same as that of kingianic acid F (**125**). In summary, compound H was established as tsangibeilin B (**89**) upon comparison of its spectroscopic data with the literature data (Huang et al., 2011).

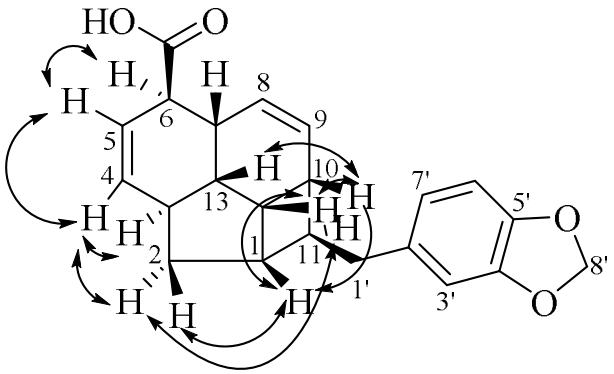

Figure 3.33: Key NOESY (^{1}H↔^{1}H) correlations of compound H (**89**)

The structure and relative configuration of tsangibeilin B (**89**) were confirmed by single-crystal X-ray analysis (Figure 3.34).

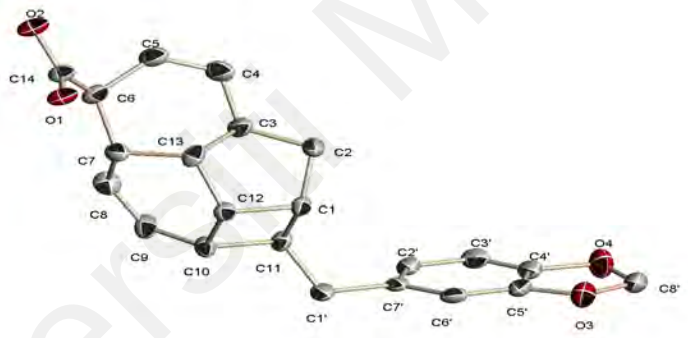

Figure 3.34: ORTEP Diagram of compound **89**. Arbitrary atom numbering

Table 3.8: ^{1}H (600 MHz) and ^{13}C (150 MHz) NMR data of compound H in $CDCl_3$

Position	**Compound H**		**Tsangibeilin B (Huang et al., 2011)**	
	δ_H (***J*** in Hz)	δ_C	δ_H (***J*** in Hz)	δ_C
1	2.38 m	34.4	2.39 m	34.4
2α	1.31 td (12.6, 5.5)	34.8	1.31 td (12.1, 6.0)	34.7
2β	1.55 dd (12.6, 4.8)		1.54 dd (12.1, 5.4)	
3	2.56 m	36.9	2.56 m	36.8
4	6.19 br d (9.5)	134.4	6.20 dt (9.6, 2.2)	134.3
5	5.72 dt (9.5, 2.4)	123.9	5.72 dt (9.6, 2.8)	123.9
6	3.01 m	49.0	3.01 m	49.2
7	2.99 m	32.7	2.99 m	32.8
8	5.43 m	129.1	5.42 br d (10.6)	129.8
9	5.45 m	129.8	5.46 br dd (10.6, 2.8)	129.0
10	2.41 m	41.0	2.41 m	40.9
11	1.78 m	47.1	1.78 m	47.1
12	2.70 m	32.9	2.70 br d (7.6)	32.9
13	1.74 m	42.0	1.72 m	41.9
1’	2.72 m	42.6	2.71 br d (8.2)	42.5
			2.73 br d (17.0, 8.2)	
2′	-	134.5	-	134.5
3′	6.65 d (1.5)	109.0	6.65 d (1.6)	108.9
4′	-	147.5	-	147.4
5′	-	145.6	-	145.6
6′	6.71 d (8.0)	108.0	6.71 d (8.0)	108.0
7′	6.61 dd (8.0, 1.5)	121.4	6.61 dd (8.0, 1.6)	121.3
8′	5.91 s	100.7	5.91 s	100.7
C=O	-	179.0	-	180.5

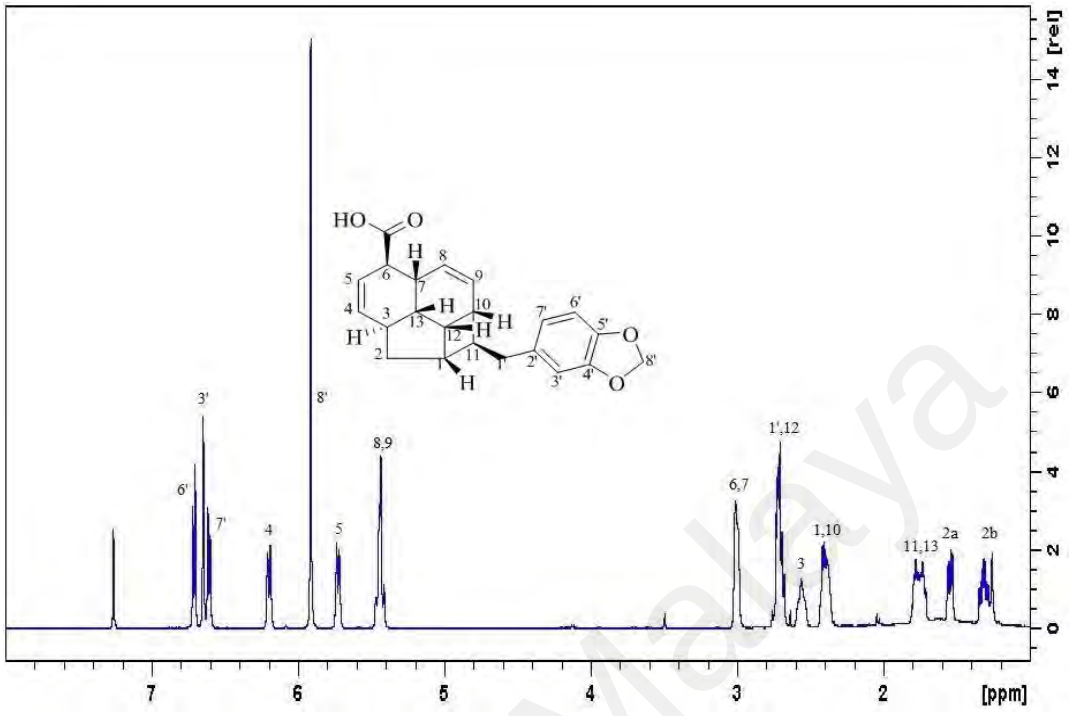

Figure 3.35: ^{1}H NMR spectrum for compound **89**

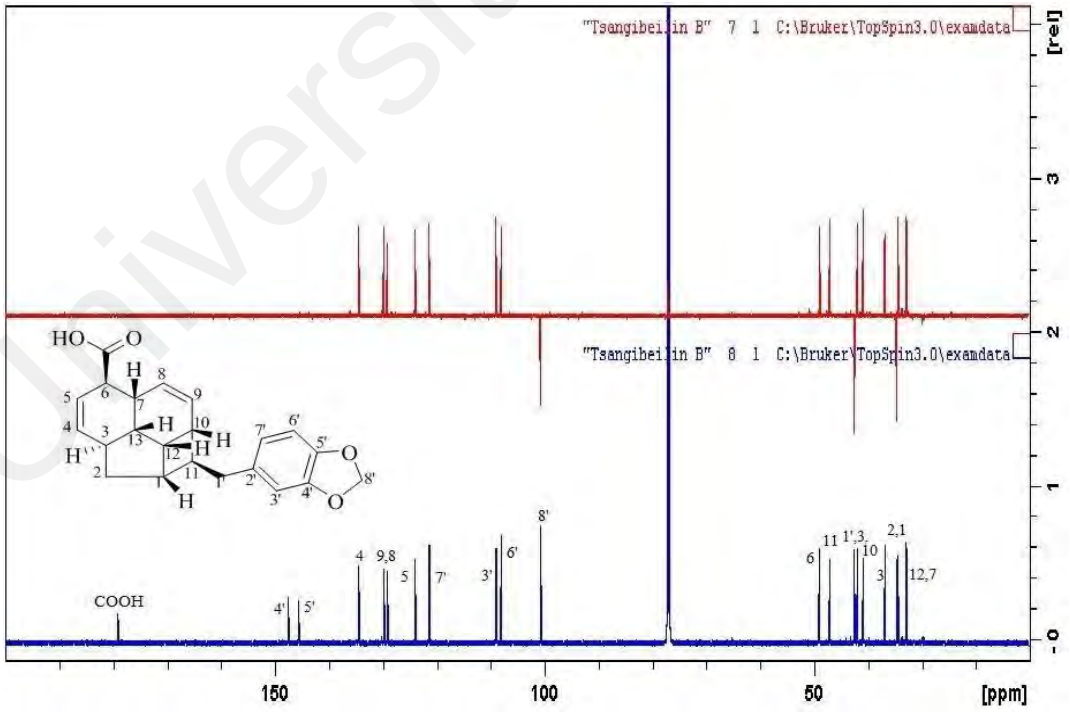

Figure 3.36: ^{13}C NMR and DEPT-135 spectrum for compound **89**

Compound I: Kingianic acid G (**126**)

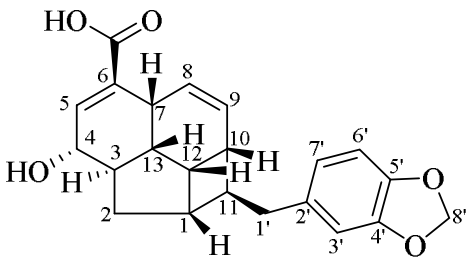

Kingianic acid G (**126**) was obtained as yellowish oil. The negative-mode HRESIMS exhibited a quasimolecular ion peak at ***m/z*** 365.1401 $[M-H]^-$ (calcd. for $C_{22}H_{21}O_5$; 365.1389), which suggested the molecular formula of $C_{22}H_{22}O_5$, thus implying 12 degrees of unsaturation. The UV absorption bands at λ_{max} 234 and 286 nm confirmed the presence of a benzenoid nucleus (Silverstein et al., 1991; Pavia et al., 2009). The absorption bands at ν_{max} 3300, 1687, 1632, 1040 and 937 cm^{-1} in the IR spectrum revealed the presence of OH, C=O, C=C and O-CH_2-O groups (Silverstein et al., 1997; Pretsch et al., 2009), respectively.

The ^1H and ^{13}C NMR data of **126** were similar to those of **125** and **89** suggesting that both share a common tetracyclic endiandric acid type B skeleton, however one olefinic proton in the ^1H NMR spectrum is missing. In the ^{13}C NMR spectrum, instead of having four sp^2 olefinic methine carbons as in **125** and **89**, only three sp^2 olefinic methines were apparent and a quaternary sp^2 carbon was present in place of the missing sp^2 methine carbon. These observations suggest that kingianic acid G (**126**) has its double bond position altered from C-4-C-5 in **125** and **89** to C-5-C-6. In addition, an OH group indicated by the signal at 4.23 (dt, ***J*** = 9.8, 1.8 Hz, H-4) and three ***cis***-form protons resonating at δ_H 7.03 (br s, H-5), 5.43 (dt, ***J*** = 10.5, 3.6 Hz, H-8) and 5.53 (dt, ***J*** = 10.5, 3.6 Hz, H-9). Other feature of the main skeleton is the same as **125** and **89**. The aromatic proton H-3′, which resonated as a doublet at δ_H 6.64 (d, ***J*** = 2.0 Hz, H-3′) and the two ***ortho-meta***-coupled doublets at δ_H 6.71 (d, ***J*** = 7.9 Hz, H-6′) and 6.59 (dd, ***J*** =

7.9, 2.0 Hz, H-7′) suggested the presence of a 1,3,4-trisubstituted aromatic ring. In addition, a downfield singlet corresponding to two methylene protons at δ_H 5.91 (s, H-8′) confirmed the presence of the methylenedioxy group (Table 3.9).

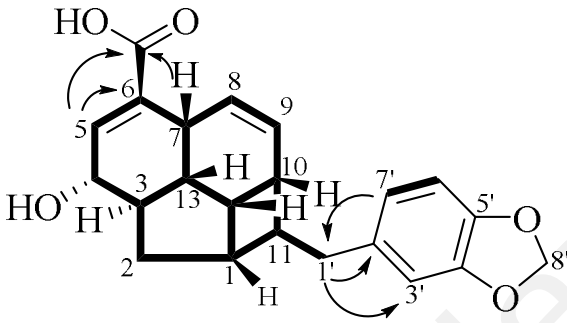

Figure 3.37: Key ^{1}H-^{1}H COSY (bold) and HMBC (^{1}H→^{13}C) correlations of **126**

The COSY and HMBC data made it possible to establish the connectivities at the C-6 and C-11 parts. The correlation between H-5 (δ_H 7.03) and H-7 (δ_H 3.23) to the carboxylic acid; COOH (δ_C 170.3) indicated the presence of a carboxylic acid moiety which was attached to C-6 of the tetracyclic skeleton. The correlations between H-1′ with C-2′ (δ_C 134.6) and C-3′ (δ_C 108.9), and that of H-7′ to C1′ (δ_C 40.9) prove the position of the methylenedioxyphenyl moiety was at C-1′. Meanwhile, the position of the hydroxyl group at C-4 was deduced from the COSY correlations between H-3/H-4 and H-4/H-5, and HMBC correlations between H-2 (δ_H 1.29), H-3 and H-13 to C-4 (Figure 3.37).

The relative configuration of the stereogenic centers was established by biogenetic consideration (Bandaranayake et al., 1980), analysis of the NOESY spectrum and comparison with NMR data reported in the literature (Williams et al., 2012). The NOESY correlations between H-12/H-10, H-12/H-1, H-10/H-13, H-13/H-7 and H-13/H-4 confirmed that protons H-1, H-4, H-7, H-10, H-12 and H-13 were all cofacial, arbitrarily assigned as ***ß***-oriented. Since the cross peaks between H-4 at δ_H 4.23 and

H-2α and H-2β, at δ_H 1.29 and 1.79 respectively, were equally intense, the relative configuration at C-4 could not be deduced from the NOESY spectrum.

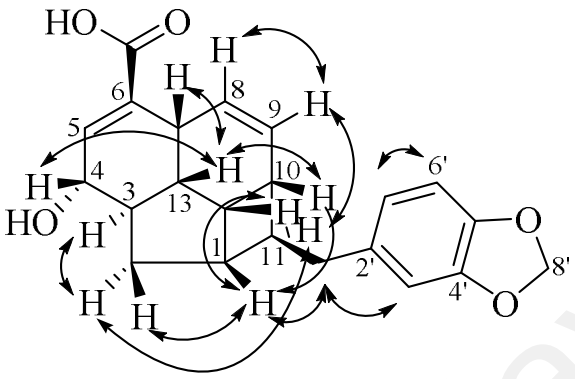

Figure 3.38: Key NOESY ($^1H \leftrightarrow {}^1H$) correlations of compound **126**

However, comparison of the NMR data of kingianic acid G (**126**) with the data reported in the literature for beilschmiedic acids H (**97**) and I (**98**) allowed the assignment of the configuration of the 4-OH group (Williams et al., 2012). Indeed, since compound **126** possessed similar ^{13}C chemical shifts to beilschmiedic acid H (**97**) for carbons C-3, C-4 and C-5 [δ_C 44.1, 73.6 and 145.6, respectively for **126**; δ_C 45.1, 74.5 and 145.8, respectively for beilschmiedic acid H (**97**)], it can be deduced that the hydroxyl group was **-**oriented, as was in the case for beilschmiedic acid H (**97**) (Williams et al., 2012). In the case of beilschmiedic acid I (**98**), having a ***ß***-oriented hydroxyl group at C-4, the chemical shifts of C-3, C-4 and C-5 are more shielded; δ_C 43.1, 65.9 and 141.5, respectively. Thus, kingianic acid G (**126**) was proposed to have the same relative configuration as beilschmiedic acid H (**97**) (Williams et al., 2012).

Table 3.9: ^{1}H (600 MHz) and ^{13}C (150 MHz) NMR data of compound **126** in $CDCl_3$

Position	**126**	
	δ_H (***J*** in Hz)	δ_C
*1	2.48 dd (12.7, 5.5)	40.9
2α	1.29 td (12.7, 6.3)	35.0
2β	1.79 m	
3	2.08 m	44.1
4	4.23 dt (9.8, 1.8)	73.6
5	7.03 br s	145.6
6	-	134.3
7	3.23 br s	33.2
8	5.43 dt (10.5, 3.6)	127.7
9	5.53 dt (10.5, 3.6)	126.2
*10	2.42 m	33.7
11	1.76 m	46.8
12	2.80 dd (12.7, 8.2)	33.6
13	1.86 ddd (13.6, 8.2, 4.2)	40.8
1′	2.71 d (8.0)	42.5
2′	-	134.6
3′	6.64 d (2.0)	108.9
4′	-	147.5
5′	-	145.6
6′	6.71 d (7.9)	108.1
7′	6.59 dd (7.9, 2.0)	121.3
8′	5.91 s	100.7
C=O	-	170.3

*Overlapping signals

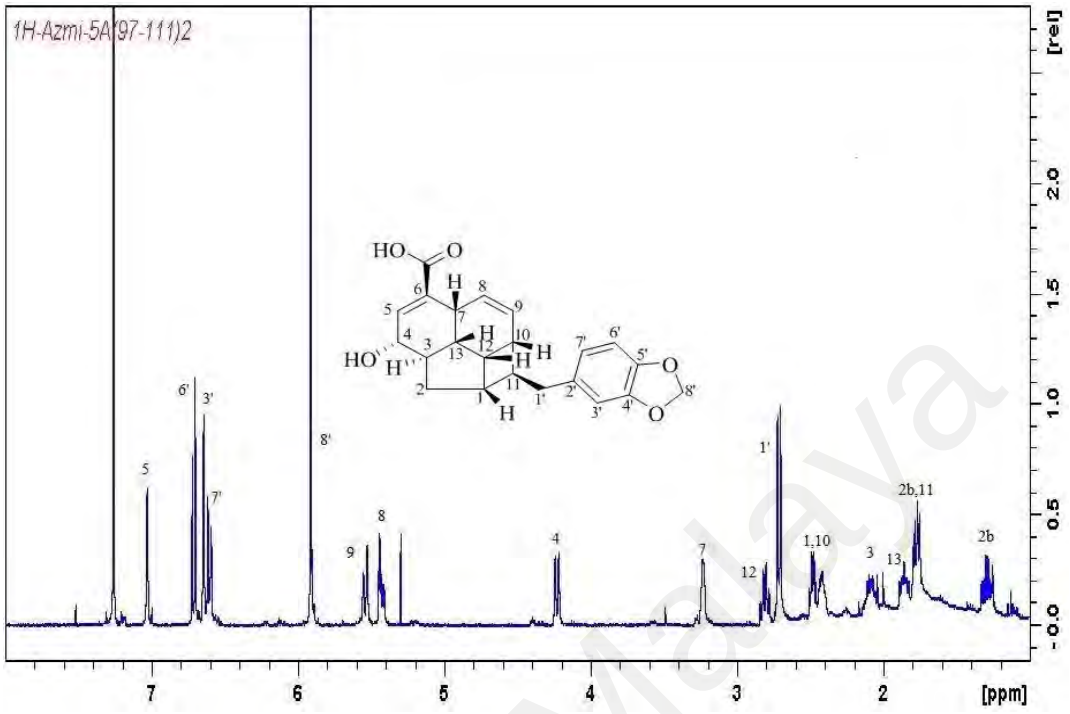

Figure 3.39: ^{1}H NMR spectrum for compound **126**

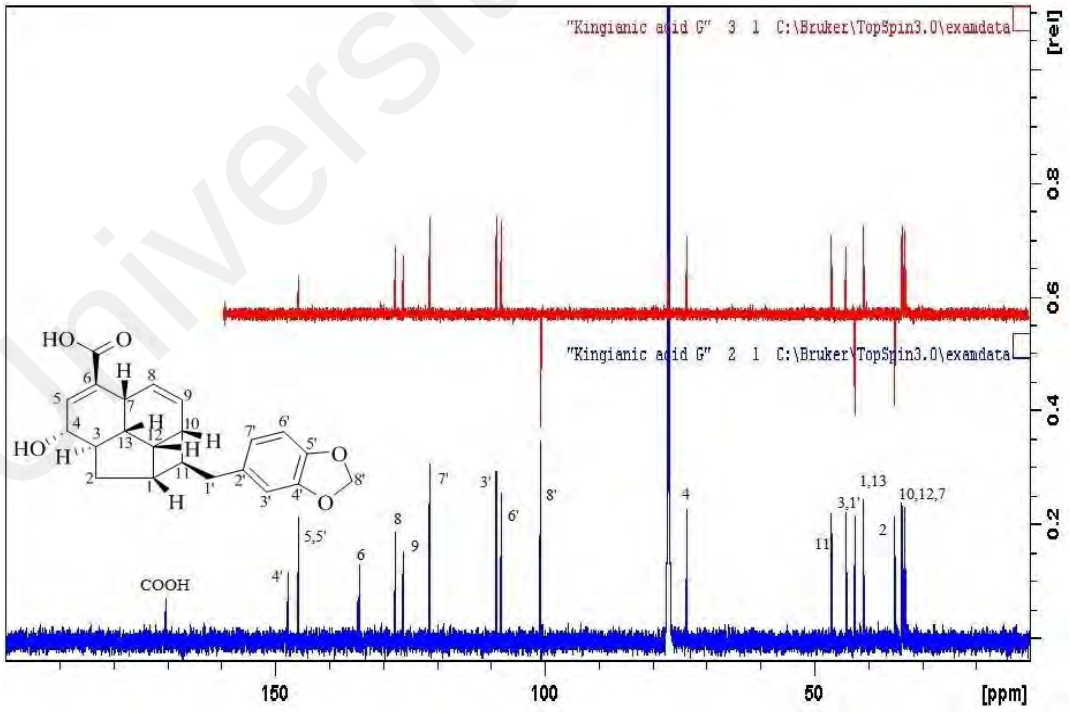

Figure 3.40: ^{13}C NMR and DEPT-135 spectrum for compound **126**.

Compound J: Kingianic acid H (**127**)

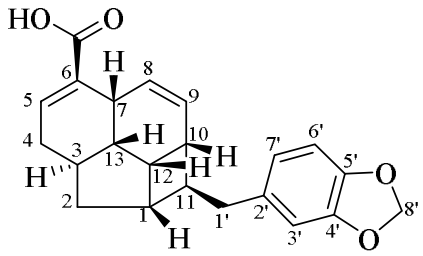

Compound **127** was obtained as an amorphous solid. The HRESIMS spectrum of **127** showed a pseudomolecular ion peak $[M-H]^-$ at ***m/z*** 349.1431 (calcd. for $C_{22}H_{21}O_4$; 349.1440), consistent with a molecular formula of $C_{22}H_{22}O_4$, with 12 degrees of unsaturation. The UV absorption typical of a benzenoid nucleus was observed at λ_{max} 234 and 286 (Silverstein et al., 1991; Pavia et al., 2009). The IR spectrum showed strong absorption bands at ν_{max} 1685 cm^{-1} for C=O, 1630 cm^{-1} for C=C, and the methylenedioxy bands at 1039 and 935 cm^{-1} (Silverstein et al., 1997; Pretsch et al., 2009). The ^{1}H NMR data showed the downfield singlet at δ_H 5.91 along with the ABX spin system at δ_H 6.60 (dd, ***J*** = 7.9, 1.7 Hz, H-7′), 6.65 (d, ***J*** = 1.7 Hz, H-3′) and 6.71 (d, ***J*** = 7.9 Hz, H-6′) in the ^{1}H NMR spectrum, suggested the presence of a methylenedioxyphenyl moiety. Three ***cis***-form protons resonating at δ_H 7.23 (br s, H-5), 5.39 (d, ***J*** = 10.0 Hz, H-8) and 5.54 (d, ***J*** = 10.0 Hz, H-9) were characteristic features of an endiandric acid type B′, similar to **126**.

The ^{13}C NMR spectrum of **127** contained 22 carbons signals, which were sorted by the DEPT-135 and HSQC experiments into 5 quaternary, 13 methines and 4 methylene carbons. Resonances of the methine carbons at δ_C 40.9 (C-1), 35.6 (C-3), 144.6 (C-5), 33.3 (C-7), 127.1 (C-8), 127.0 (C-9), 33.2 (C-10), 46.9 (C-11), 34.0 (C-12) and 42.2 (C-13), and the methylene groups at δ_C 37.0 (C-2) and 32.2 (C-4) were indicative of a tetracyclic endiandric acid type B skeleton as seen in cryptobeilic acids A-D (**105**-**108**) (Talontsi et al., 2013). The spectroscopic data of **127** was closely related to those of **89**,

suggesting that they were positional isomers. The ^{13}C NMR spectrum also showed signals of a conjugated carbonyl group at δ_C 178.0 (COOH) and olefinic carbons at δ_C 144.6 (C-5), 127.1 (C-8), 127.0 (C-9) and an olefinic quaternary carbon at δ_C 134.6 (C-6), suggesting the displacement of the double bond from C-4-C-5 in **89** to C-5-C-6 in **127** (Endiandric acid type B′). The presence of the olefinic methines in **127** was confirmed in the ^{1}H NMR spectrum (Table 3.10), by the presence of a broad singlet at δ_H 7.23 (H-5) and a pair of doublets at δ_H 5.39 (d, ***J*** = 10.0 Hz, H-8) and 5.54 (d, ***J*** = 10.0 Hz, H-9).

The HMBC correlations (Figure 3.40) of H-5 with C-6 (δ_C 134.6) and COOH (δ_C 178.0), and between H-8 and C-6 established the position of the carboxylic group at C-6. The attachment of the methylenedioxybenzyl moiety at H-11 was confirmed by the correlations between H-11 and C-2′, and that of H-1′ with C-10 and C-1 (Figure 3.41).

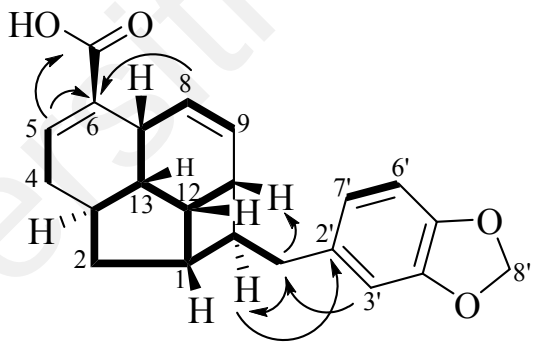

Figure 3.41: Key ^{1}H-^{1}H COSY (bold) and HMBC (^{1}H→^{13}C) correlations of **127**

Table 3.10: ^{1}H (600 MHz) and ^{13}C (150 MHz) NMR data of compound **127** in $CDCl_3$

Position	**127**	
	δ_H (***J*** in Hz)	δ_C
*1	2.42 m	40.9
2	1.20 m	37.0
	1.53 dd (12.3, 3.9)	
3	2.04 m	35.6
*4	2.08 m	32.2
	2.47 m	
5	7.23 br s	144.6
6	-	134.6
7	3.26 br s	33.3
8	5.39 d (10.0)	127.1
9	5.54 d (10.0)	127.0
*10	2.40 m	33.2
11	1.74 dd (7.5, 7.5)	46.9
12	2.77 dd (12.5, 8.2)	34.0
13	1.68 m	42.2
1′	2.70 d (7.0)	42.6
2′	-	134.6
3′	6.65 d (1.7)	109.0
4′	-	147.4
5′	-	145.6
6′	6.71 d (7.9)	108.0
7′	6.60 dd (7.9, 1.7)	121.3
8′	5.91 s	100.7
C=O	-	178.0

*Overlapping signals

The relative configuration of the asymmetric carbons was established by the NOESY analysis (Figure 3.42) and further confirmed by the X-ray crystallographic analysis (Figure 3.43). The NOESY spectrum showed similar profile to that of **126**. Assuming the H-7 is *β*–oriented, thus the correlations between H-7/H-13, H-13/H-10, H-10/H-12, H-12/H-1 and H-1/H2*β* suggested that H-1, H-2*β*, H-10, H-12, and H-13 are also *β*-oriented. In contrast, the *α*-orientation of H-3 and H-11 were deduced from the correlations of H-4*α*/H-3 and H-2*α*/H-11. Therefore, the relative configuration of H-1, H-3, H-6, H-7, H-10, H-11, H-12, and H-13 was assigned as ***rel***-(1***SR***, 3***RS***, 7***RS***, 10***RS***, 11***SR***, 12***SR***, 13***SR***), same as that of beilschmiedic acid H (**97**) (Williams et al., 2012).

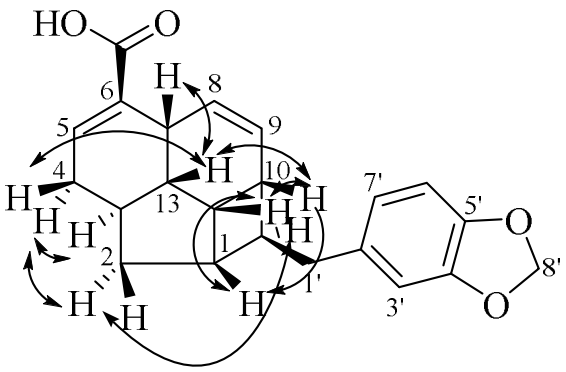

Figure 3.42: Key NOESY ($^1H \leftrightarrow {}^1H$) correlations of compound **127**

A colourless crystal was obtained from MeOH, crystallized in the monoclinic crystal system with P21/***c*** space group. X-ray analysis confirmed the relative configuration of **127**.

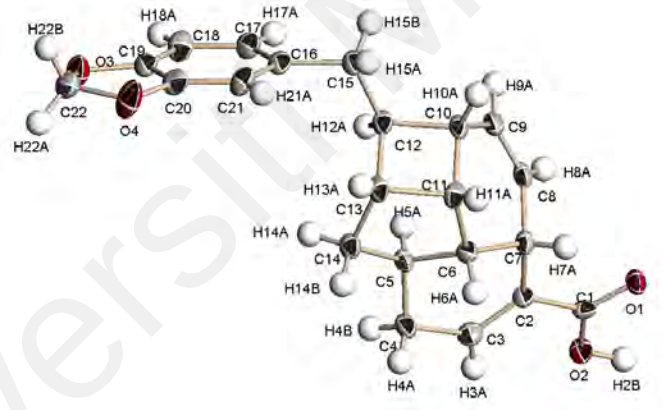

Figure 3.43: ORTEP Diagram of compound **127**. Arbitrary atom numbering

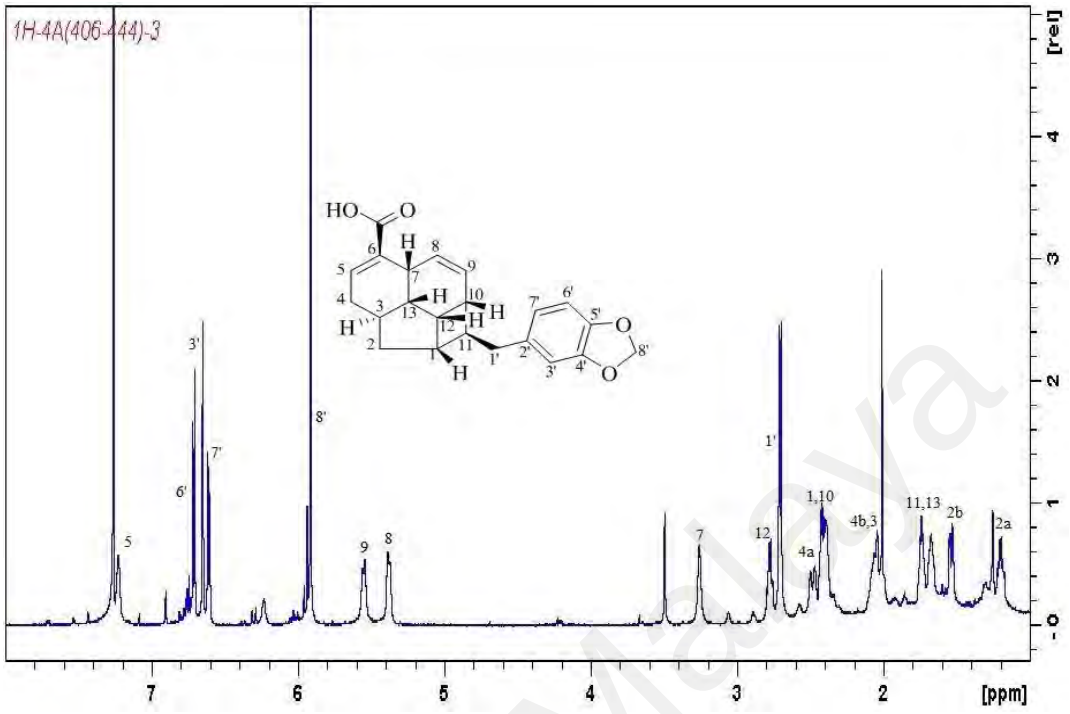

Figure 3.44: ^{1}H NMR spectrum for compound **127**

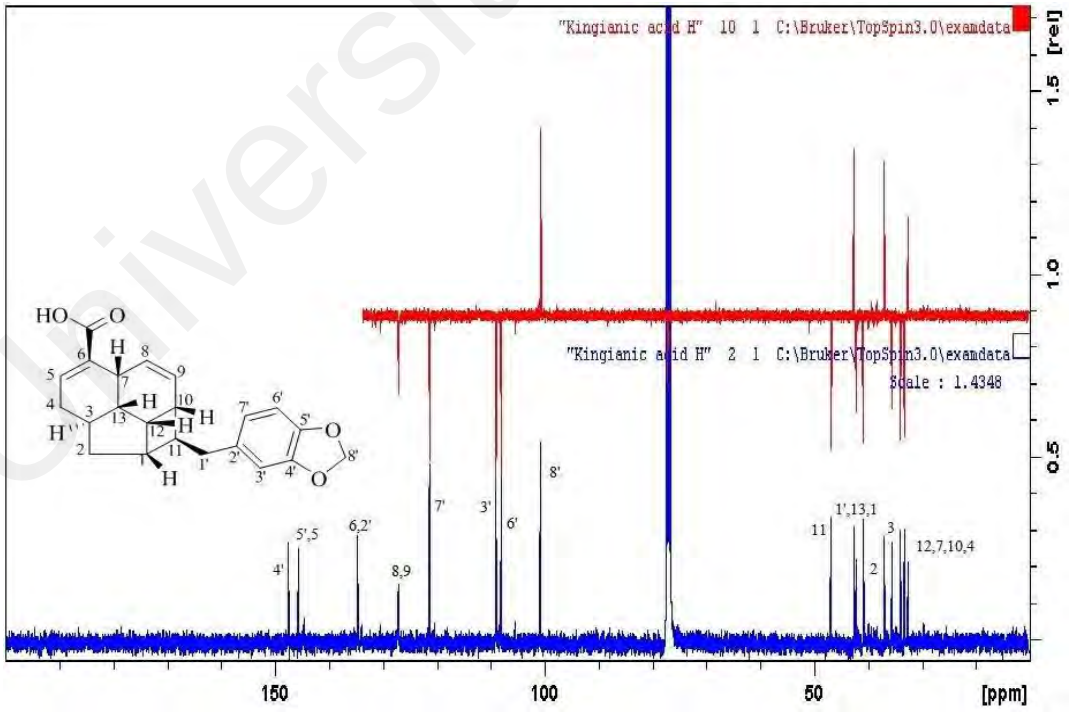

Figure 3.45: ^{13}C NMR and DEPT-135 spectrum for compound **127**

3.1.2 Kingianin Series

Kingianins were isolated as optically inactive white powder or amorphous solid and their spectroscopic data were similar to one another. Their common characteristic feature is a pentacyclic carbon skeleton (bicyclo[4.2.0] backbone). However, they differ from each other by the position of the four substituents attached at C-1, C-8, C-1′ and C-8′. Two of the substituents were methylenedioxyphenyl groups, which were inferred from the absorption bands at λ_{max} 289 and 240 nm in UV spectrum and were confirmed by analysis of their NMR spectroscopic data (Silverstein et al., 1991; Pavia et al., 2009).

In general, the main skeleton of kingianins comprised 16 carbons of a pentacyclic moiety, including four ***cis***-form olefinic carbons. The characteristic four ***cis***-form olefinic protons were evident between δ_H 5.55 - 5.65 and 6.10 - 6.25 in the ^{1}H NMR spectrum (Leverrier et al., 2010, 2011; Pavia et al., 2009). The structure can be divided onto two fragments of contiguous protons at the **western part** (H-1, H-2, H-3, H-4, H-5, H-6, H-7 and H-8), and at the **eastern part** (H-1′, H-2′, H-3′, H-4′, H-5′, H-6′, H-7′ and H-8′). Their connectivities were further confirmed by ^{1}H-^{1}H COSY, HSQC and HMBC.

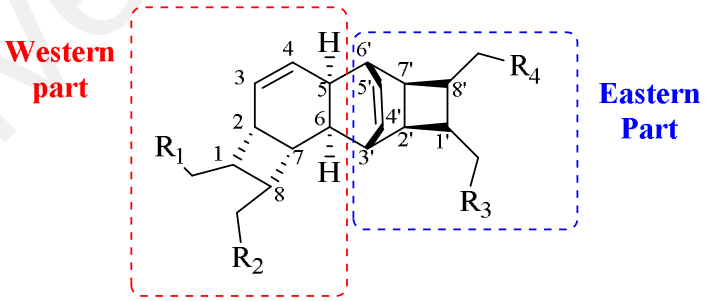

Figure 3.46: Kingianin pentacyclic skeleton

Two substituents are methylenedioxyphenyl groups and the remaining substituents are ***N***-ethylacetamide, butyric acid and acetic acid chains. The ^{1}H NMR spectra showed signals of two sets of three ***ortho*-*meta***-coupled phenyl protons between δ_H 6.55 – 6.70, associated with two singlet around δ_H 5.89 ppm for two methylenedioxy, suggesting the presence of two 1,3,4-trisubstituted aromatic ring (methylenedioxyphenyl groups). The connectivities between the four substituents and the pentacyclic skeleton were verified via the HMBC and COSY correlations.

In this study, three new kingianins named; kingianin O-Q (**128**-**130**), together with the known kingianins A (**45**), F (**50**), K (**55**), L (**56**), M (**57**) and N (**58**) were isolated and characterized. The total assignment of the 1D NMR data and 2D NMR correlations of the kingianins series are presented in the following paragraphs. The structure of the pentacyclic framework will only be described for compound O (**128**), as it is identical with the rest of the kingianin series, but the planar and spatial positions of the four substituents will be discussed for every compound.

Compound K: Kingianin O (**128**)

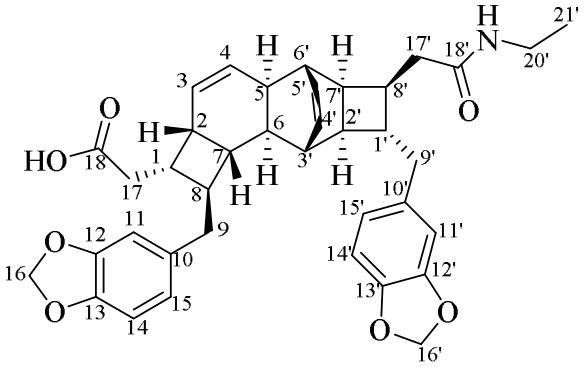

Compound **128** was obtained as a white powder. Its HRESIMS indicated a pseudomolecular ion peak $[M+H]^+$ at ***m/z*** 624.2954; suggesting a molecular formula of $C_{38}H_{41}NO_7$ (calcd. for $C_{38}H_{42}NO_7$; 624.2961); from which 19 degrees of unsaturation was deduced. The IR spectrum of **128** showed the absorption bands at ν_{max} 3295, 1718, 1624, and 1542 cm^{-1} corresponding to the N-H amide elongation, C=O stretching of an acid, C=O stretching of an amide and N-H amide deformation, respectively thus indicating the presence of a carboxylic acid group and an amide group.

The ^1H NMR spectrum of **128** showed In addition, a set of multiplets was found between δ_H 1.25 and 2.60 corresponding to twelve protons of the pentacyclic skeleton which is the characteristic feature of the kingianin series. Correlations observed from the ^1H-^1H COSY and HSQC spectra revealed two sets of eight contiguous structural sequence involving (H-1 [δ_H 2.18 (m)], H-2 [δ_H 2.46 (m)], H-3, H-4, H-5 [δ_H 2.06 (m)], H-6 [δ_H 1.26 (d, ***J*** = 9.5 Hz), H-7 [δ_H 1.86 (m)], H-8 [δ_H 1.70 (m)]), and (H-1′ [δ_H 1.84 (m)], H-2′ [δ_H 2.09 (m)], H-3′ [δ_H 2.08 (m)], H-4′, H-5′, H-6′ [δ_H 2.50 (m)], H-7′ [δ_H 2.49 (m)] and H-8′ [δ_H 2.46 (m)]). The HMBC correlations from H-6/C-2, C-8, C-4′ and C-6′, H6′/C-2′, H-4/C-2, H-7/C-3 and C-3′, H-5/C-3′, H6′/C-2′ and H-1′/C-7′ established the pentacyclic main skeletal structure of **128** consisting of two four-membered rings and three six-membered rings. In addition, four ***cis***-form vinyl proton signals at δ_H 5.48

(dd, ***J*** = 9.5, 9.7 Hz, H-3), 5.60 (dd, ***J*** = 9.5, 9.7 Hz, H-4), 6.00 (dd, ***J*** = 7.6, 7.1 Hz, H-4′), and 6.10 (t, ***J*** = 7.1 Hz, H-5′). These signals were characteristic features of the pentacyclic skeleton of the kingianin series.

Meanwhile, the presence of two 1,3,4-trisubstituented benzene moieties was suggested by a doublet at δ_H 6.60 (d, ***J*** = 1.1 Hz, H-11, H-11′) and the two ***ortho-meta***-coupled doublets at δ_H 6.69 (d, ***J*** = 8.1 Hz, H-14, H-14′) and 6.53 (dd, ***J*** = 8.1, 1.1 Hz, H-15, H-15′). In addition, the two singlets corresponding to two protons each at δ_H 5.93 and 5.94 (H_2-16 and H_2-16′, respectively) confirmed the presence of the methylenedioxy group. An ***N***-ethylacetamide group presence was implied from the observation of a doublet of quartets representing two protons at δ_H 3.22 (***J*** = 5.7, 7.1 Hz, H-20′), a triplet corresponding to a methyl group at δ_H 1.10 (***J*** = 7.1 Hz, H-21′) and another triplet at δ_H 5.36 belonging to NH-19′ (***J*** = 5.7 Hz). The COSY spectrum showed correlations corresponding to the NH-19′-H_2-20′-H_3-21′ spin system; H-19′/ H_2-20′, H_2-20′/ H_2-21′ (Table 3.11).

The ^{13}C NMR and DEPT spectra displayed 38 carbon resonances; one methyl, 7 methylenes, of which two were methylenedioxyls, 22 methines, and 8 quaternary carbons including two carbonyl groups which resonated at δ_C 178.0 (C-18, acetic acid moiety) and δ_C 172.6 (C-18′, ***N***-ethylacetamide moiety). Resonances of the sixteen carbons of the pentacyclic of kingianins appeared as twelve sp^3 methine carbons at δ_C 38.5 (C-1), 32.7 (C-2), 37.9 (C-5), 37.9 (C-6), 41.8 (C-7), 47.2 (C-8), 43.7 (C-1′), 44.3 (C-2′), 42.8 (C-3′), 38.4 (C-6′), 39.1 (C-7′) and 38.8 (C-8′) and the four sp^2 methine carbons at δ_C 124.9 (C-3), 132.2 (C-4), 132.7 (C-4′) and 134.3 (C-5′) as observed in DEPT spectrum (Table 3.11). The pentacyclic rings were fused at the C-2-C-7, C-5-C-6, C-6′-C-3′ and C-2′-C-7′ junctions. These were evidenced by the ^{1}H-^{1}H COSY correlations between the protons of the respective carbons. Finally, the connectivities between the four substituents and the pentacyclic skeleton were established by the

HMBC and COSY correlations (Figure 3.47). The connectivity of the ***N***-ethylacetamide group to the core skeleton was confirmed by the correlations between H-8′ and H_2-17′ in the COSY spectrum, and between H-8′ and C-17′ in the HMBC spectrum indicating that this group is attached to C-8′. In addition, the COSY spectrum showed cross peaks between the methylene protons (H_2-17) with H-1, therefore indicating that the acetic acid is linked to the pentacyclic core at C-1. Finally, the location of the two methylenedioxybenzyl groups at C-8 and C-1′ respectively were deduced from the correlation between H-8/H_2-9 and H-1′/H_2-9′, and the HMBC cross peaks observed between C-9/C-9′ with H-11/H-11′ and H-15/H-15′ (Figure 3.47).

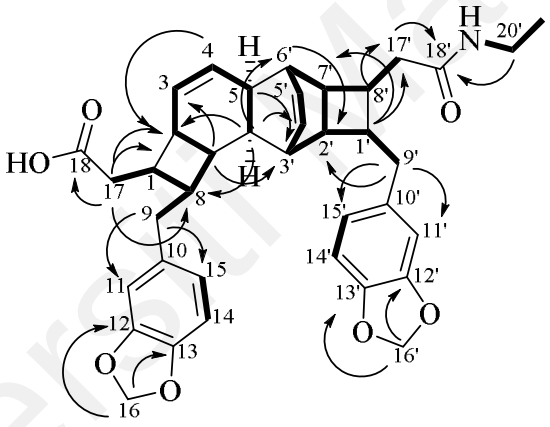

Figure 3.47: Key ^{1}H-^{1}H COSY (bold) and HMBC (^{1}H→^{13}C) correlations of **128**

Based on biogenetic reasoning, the relative configuration of the pentacyclic framework of kingianin is assumed to be the same as kingianin F (**50**) isolated from the same plant. The relative configuration of all of the stereocenters in **128** could be deduced from the NOESY experiment (Figure 3.48). The cross peaks between H-6, H-5, H-3′, and H-7′, which in turn correlated with H-2′, indicated that the junctions 5-6 and 2′-7′ were ***cis*** and that H-5, H-6, H-2′, and H-7′ were arbitrarily assigned as *α*–oriented. This necessarily implied the *β*–position for the bridge formed by the C-4′-C-5′, and for the cyclobutane formed by C-1′-C-2′-C-7′-C-8′. Other NOESY correlations between

H-4′, H-2, and H-7 indicated that H-2 and H-7 were ***cis*** and *β*–oriented. Thus, the second cyclobutane ring C-1-C-2-C-7-C-8 is spatially oriented in an *α* position. The configuration at C-1, C-8, C-1′ and C-8′ where the four substituents are attached could be deduced from the NOESY experiment (Figure 3.48). The cross peaks between H-6/H-8 and H-2′/H-8′ indicated that the benzyl group at C-8 and the amide group at C-8′ were in the *β*–position. Meanwhile, the NOESY correlations between H-7/H-1 and H-4′/H-1′ suggested that the acetic acid group at C-1 and benzyl group at C-1′ were in the *α*–position. Consequently, the phenyl substituent at C-1′ was ***anti*** to the butyric acid chain on the cyclobutane ring C-1′-C-2′-C-7′-C-8′. This was supported by the correlation between H_2-9′ and H-2′, which was *α*-oriented. Finally, the NOESY correlations between H_2-9 and H-7 implied the two substituents at C-1 and C-8 were in an ***anti*** position on the second cyclobutane C-1-C-2-C-7-C-8 (Figure 3.48).

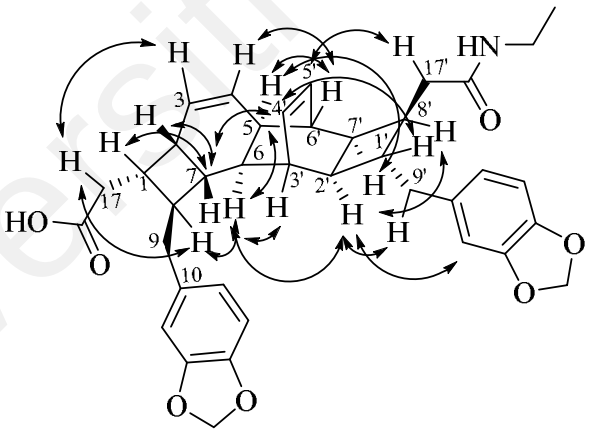

Figure 3.48: Key NOESY ($^1H \leftrightarrow {}^1H$) correlations of compound **128**

Therefore, the relative configuration of **128** was determined as ***rel***-(***1SR, 2SR, 5SR, 6RS, 7RS, 8SR, 1′SR, 2′RS, 3′RS, 6′SR, 7′SR, 8′SR***), the same as in kingianin F (**50**) (Leverrier et al., 2011). All physicochemical data were in full agreement with the proposed structure of **128** as shown, which was named kingianin O.

Table 3.11: ^{1}H (600 MHz) and ^{13}C (150 MHz) NMR data of compound **128** in $CDCl_3$

128					
Part A_1			**Part A_2**		
Position	δ_H (***J*** in Hz)	δ_C	Position	δ_H (***J*** in Hz)	δ_C
1	2.18 m	38.5	1′	1.84 m	43.7
2	2.46 m	32.7	2′	2.09 m	44.3
3	5.48 dd (9.7, 9.5)	124.9	3′	2.08 m	42.8
4	5.60 dd (9.7, 9.5)	132.2	4′	6.00 dd (7.6, 7.1)	132.7
5	2.06 m	37.9	5′	6.10 t (7.1)	134.3
6	1.26 d (9.5)	37.9	6′	2.50 m	38.4
7	1.86 m	41.8	7′	2.49 m	39.1
8	1.70 m	47.2	8′	2.46 m	38.8
9	2.55 m	40.4	9′	2.57 m	41.9
10	-	134.5	10′	-	134.9
11	6.60 d (1.1)	109.0	11′	6.61 d (1.1)	109.3
12	-	147.4	12′	-	147.5
13	-	145.5	13′	-	145.7
14	6.69 d (8.1)	108.1	14′	6.72 d (8.1)	108.1
15	6.53 dd (8.1, 1.1)	121.3	15′	6.56 dd (8.1, 1.1)	121.6
16	5.93 s	100.7	16′	5.94 s	100.7
17	1.82 m	37.5	17′	1.90 m	36.9
	2.05 m			2.12 m	
18	-	178.0	18′	-	172.6
			19′	5.36 t (5.7)	-
			20′	3.22 dq (7.1, 5.7)	34.3
			21′	1.10 t (7.1)	14.9

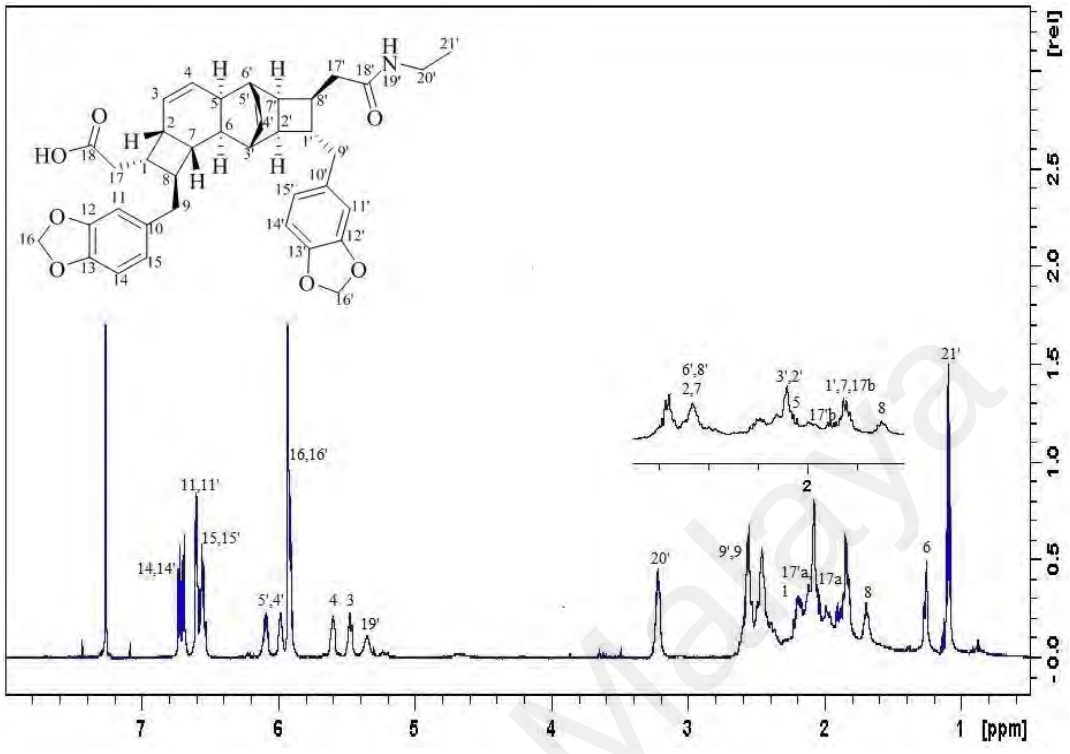

Figure 3.49: ^{1}H NMR spectrum for compound **128**

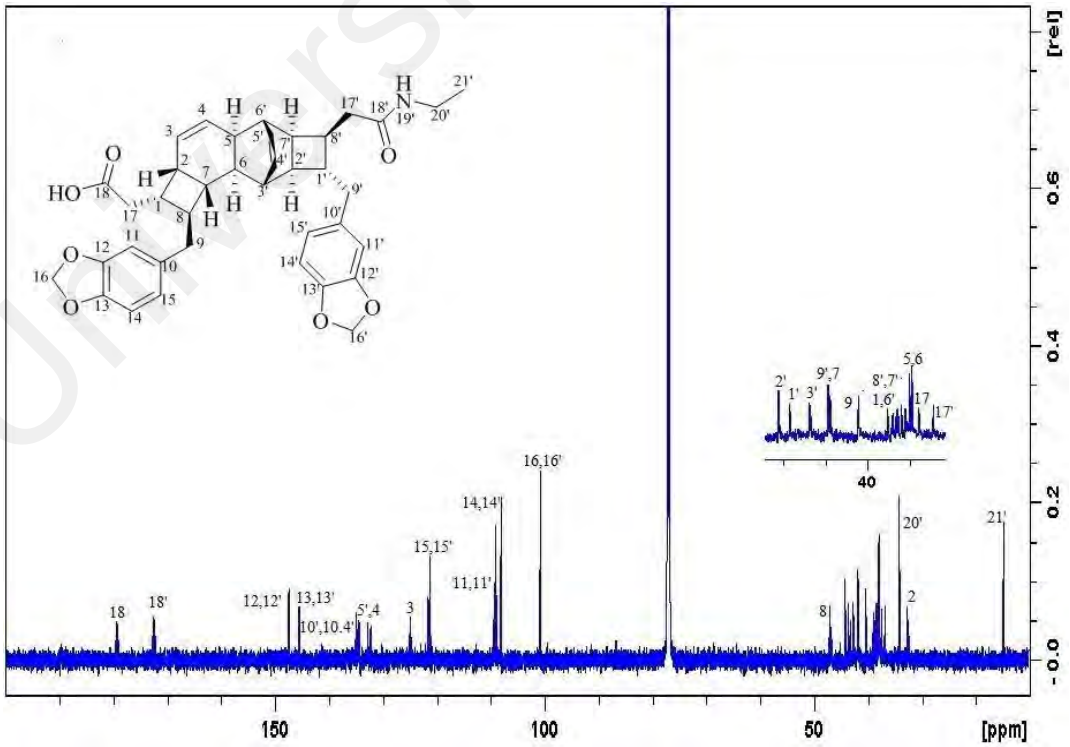

Figure 3.50: ^{13}C NMR and DEPT-135 spectrum for compound **128**

Compound L: Kingianin P (**129**)

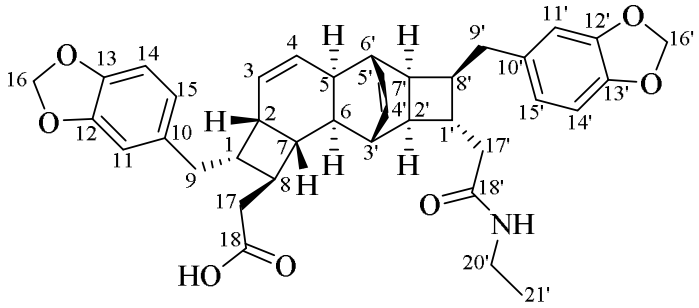

Compound **129** was obtained as a white powder. Its HRESIMS showed a pseudomolecular ion peak $[M+H]^+$ at m/z 624.2928, corresponding to the molecular formula of $C_{38}H_{42}NO_7$ (calcd. for $C_{38}H_{42}NO_7$; 624.2961). The IR spectrum of **129** exhibited absorption bands at ν_{max} 3297, 1725, 1630, and 1541 cm^{-1} corresponding to the N-H amide elongation, C=O stretching of an acid, C=O stretching of an amide and N-H amide deformation, indicating the presence of a carboxylic acid group and an amide group, respectively.

The ^1H and ^{13}C NMR data for **129** was reminiscent to those of **128** (Table 3.12), with the same pentacyclic skeleton but differing in the position of the acetic acid, the ***N***-ethylacetamide and the two methylenedioxybenzyl moieties (Table 3.12). The ^1H NMR spectrum of **129** showed signals for ***cis*** olefinic protons at δ_H 5.58 (dd, ***J*** = 9.3, 9.5 Hz, H-3), 5.68 (dd, ***J*** = 9.3, 9.5 Hz, H-4), 6.12 (dd, ***J*** = 7.5, 7.0 Hz, H-4′) and 6.24 (t, ***J*** = 7.0 Hz, H-5′). These signals were the characteristic features for kingianin. The aromatic protons H-11 and H-11′ which resonated as doublets at δ_H 6.69 (d, ***J*** = 1.2 Hz) and the four ***ortho*-*meta***-coupled doublets at δ_H 6.79 (dd, ***J*** = 8.1 Hz, H-14 and H-14′), 6.56 (dd, ***J*** = 8.1, 1.2 Hz, H-15) and 6.58 (dd, ***J*** = 8.1, 1.2 Hz, H-15′) suggested the presence of a 1,3,4-trisubstituted aromatic ring. In addition, the two singlets corresponding to the four protons at δ_H 5.90 (s, H-16) and 5.91 (s, H-16′) confirmed the presence of the methylenedioxy group. The multiplets were found between δ_H 1.70 –

2.55 integrating to fourteen protons corresponded to the fourteen methine groups (H-1 to H-8, and H-1′ to H-8′) of the pentacyclic skeleton of **129**. The signal corresponding to the acetyl group appeared at δ_H 2.15 - 2.26 (H_2-17). Finally, the ***N***-ethylacetamide group was suggested by the presence of one triplet at δ_H 5.20, a doublet of quartets at δ_H 3.21 and a triplet of a methyl group at δ_H 1.10 ppm corresponding to NH-19′, H_2-20′ and H_3-21′, respectively (Table 3.12).

The ^{13}C NMR and DEPT-135 spectra displayed 38 carbon signals, which were sorted into 7 methylenes, one methyl, 8 quaternary including the carbonyl groups at δ_C 178.2 (C-18) and 171.6 (C-18') ppm respectively, and 22 methine carbons. Among the methine carbons, sixteen methine of them resonated between δ_C 35.0 - 44.2 ppm while those of the four ***cis*** olefinic carbons resonated at δ_C 125.0 (C-3), 132.2 (C-4), 132.5 (C-4′) and 134.8 (C-5′) all of which corresponded to the pentacyclic skeleton of **129**. The presence of two methylenedioxyphenyl groups were inferred from the resonances of the twelve aromatic carbons at δ_C 135.2 (C-10 and C10′), 108.3 (C-11 and C-11′), 147.6 (C-12 and C-12′), 145.5 (C-13 and C-13′), 108.9 (C-14 and C-14′), 121.0 (C-15 and C-15′), and the methylenedioxy groups at δ_C 100.7 (C-16 and C-16′) in ^{13}C NMR spectra (Table 3.12).

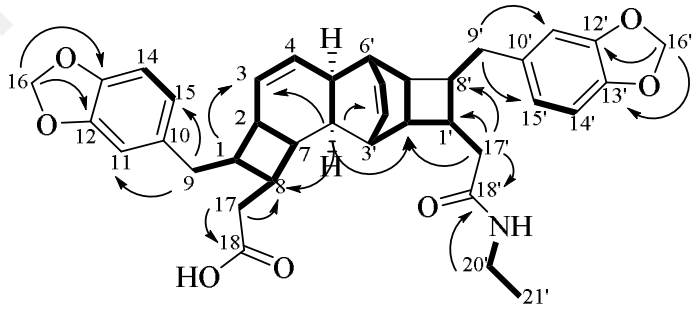

Figure 3.51: Key ^{1}H-^{1}H COSY (bold) and HMBC (^{1}H→^{13}C) correlations of **129**

The ^{1}H-^{1}H COSY spectrum of **129** revealed the following cross peaks; H-1/H_2-9 and H-8′/H_2-9′, allowing the placement of the two methylenedioxybenzyl groups at C-1 and C-8′. In addition, the HMBC correlations between H_2-9 with C-11 (δ_C 108.3) and C-15 (δ_C 121.0), and that of H_2-9′ with C-11′ (δ_C 108.3) and C-15′ (δ_C 121.0), further verified the connectivities of the methylenedioxyphenyl groups at C-1 and C-8′, respectively. Meanwhile, the presence of the H-8-H_2-17 spin system as evidenced from the COSY correlations, and the HMBC correlations between H_2-17 with C-8 and C-18 carbonyl carbon (δ_C 178.2), confirmed that the acetic acid chain is attached to C-8. The ***N***-ethylacetamide group is located at C-1′, as suggested from the COSY correlations between H-1′ and H_2-17′, and the HMBC correlations between H_2-17′ with C-1′, C-2′, C-8′ and the C-18′ carbonyl carbon (δ_C 171.6) (Figure 3.51).

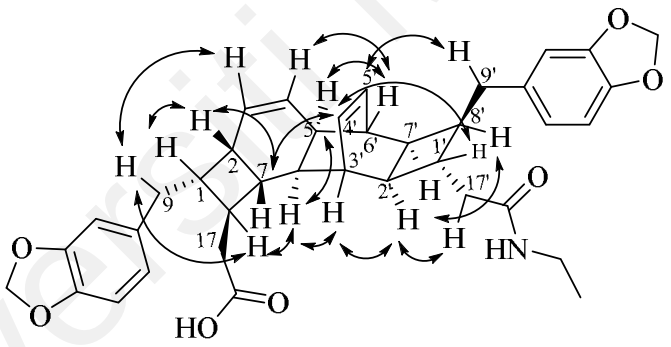

Figure 3.52: Key NOESY (^{1}H↔^{1}H) correlations of compound **129**

The configuration at C-1, C-8, C-1′ and C-8′ were determined from the NOESY experiment. The correlations between H-2′/H-8′ and H-4′/H-1′ in NOESY spectra indicated that the benzyl moiety at C-8′ was in the *β*–position and the amide chain at C-1′ in the *α*–position on the cyclobutane. Meanwhile, the correlations between H-2/H-1 and H-6/H-8, indicated the *α*–orientation of the benzyl group at C-1, and the *β*-orientation of the acid chain at C-8 (Figure 3.52). Therefore, the relative configuration of **129** was thus assigned as ***rel***-(***1SR, 2SR, 5SR, 6RS, 7RS, 8SR, 1′RS, 2′RS, 3′RS, 6′SR,***

7′SR, 8′RS), similar to that of kingianin A (**45**) (Leverrier et al., 2010, 2011). Hence, the structure of **129** was elucidated as shown, and was named kingianin P.

Table 3.12: ^{1}H (600 MHz) and ^{13}C (150 MHz) NMR data of compound **129** in $CDCl_3$

129					
Part A_1			**Part A_2**		
Position	δ_H (***J*** in Hz)	δ_C	Position	δ_H (***J*** in Hz)	δ_C
1	2.04 m	43.7	1′	2.13 m	38.1
2	2.49 m	33.3	2′	2.26 m	44.2
3	5.58 dd (9.5, 9.3)	125.0	3′	2.44 m	42.7
4	5.68 dd (9.5, 9.3)	132.3	4′	6.12 dd (7.5, 7.0)	132.5
5	2.24 m	37.9	5′	6.24 t (7.0)	134.8
6	1.70 d (10.2)	37.9	6′	2.52 m	38.4
7	1.95 m	42.6	7′	2.52 m	39.7
8	2.02 m	42.3	8′	2.31 m	43.6
9	2.47 m	36.0	9′	2.54 m	35.1
	2.60 m			2.64 m	
10	-	135.2	10′	-	135.2
11	6.69 d (1.2)	108.3	11′	6.69 d (1.2)	108.3
12	-	147.6	12′	-	147.6
13	-	145.5	13′	-	145.5
14	6.79 d (8.1)	108.9	14′	6.79 d (8.1)	108.9
15	6.56 dd (8.1, 1.2)	121.0	15′	6.58 dd (8.1, 1.2)	121.0
16	5.90 s	100.7	16′	5.91 s	100.7
17	2.15 m	39.7	17′	2.01 m	41.8
	2.26 m				
18	-	178.2	18′	-	171.6
			19′	5.20 t (5.6)	-
			20′	3.21 dq (7.2, 5.6)	34.3
			21′	1.10 t (7.2)	14.8

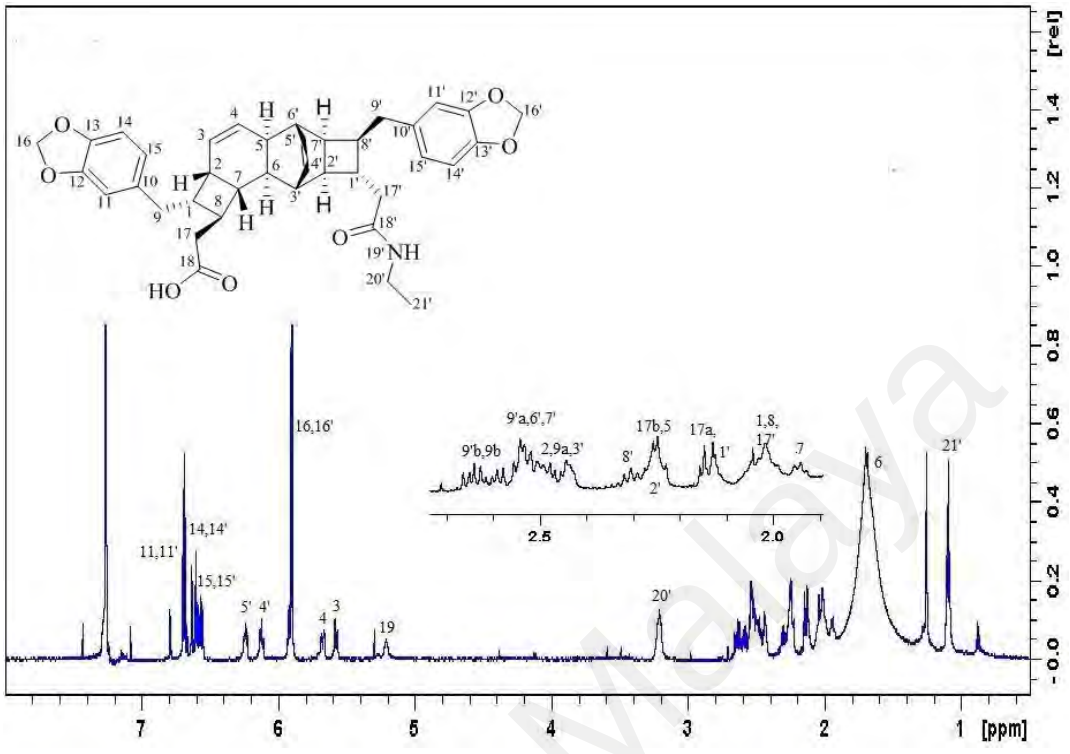

Figure 3.53: ^{1}H NMR spectrum for compound **129**

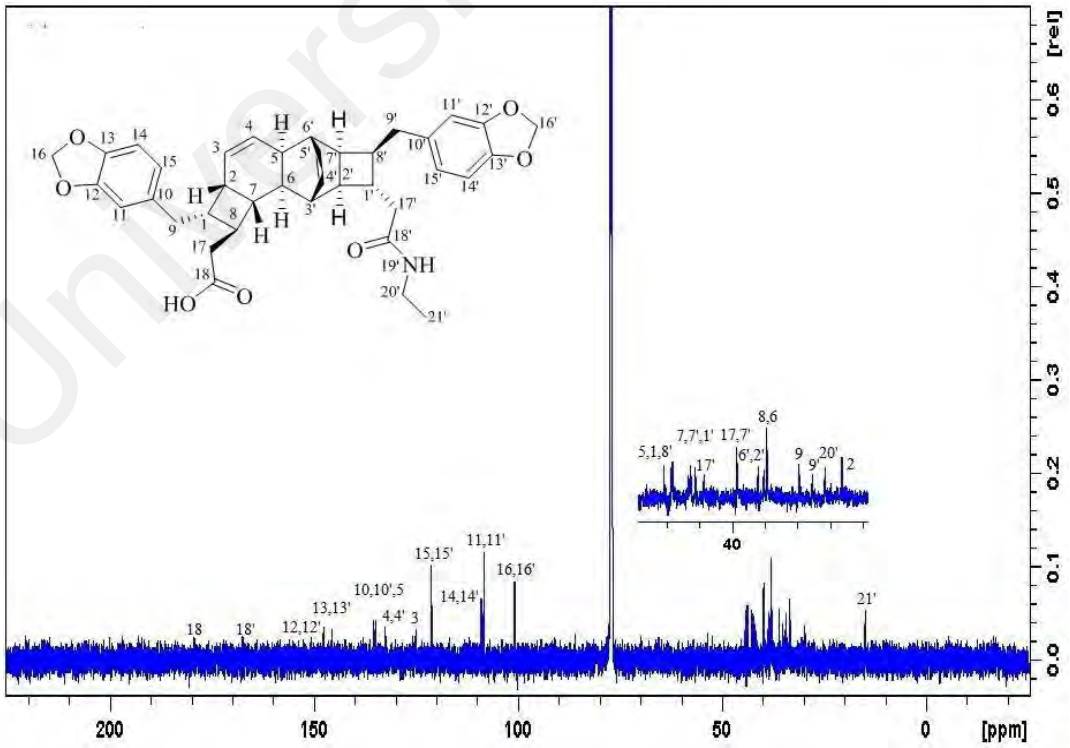

Figure 3.54: ^{13}C NMR and DEPT-135 spectrum for compound **129**

Compound M: Kingianin Q (**130**)

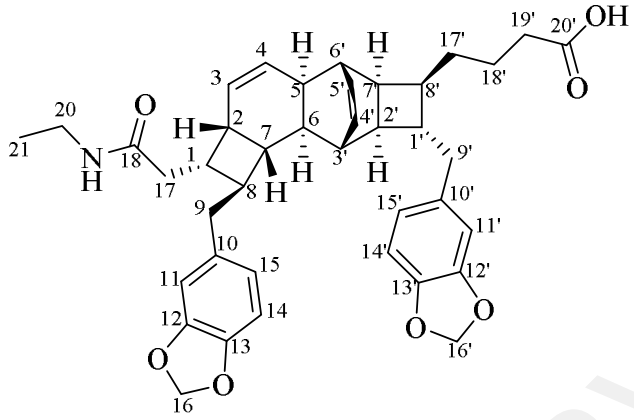

Compound **130** was obtained as a white powder. Its HRESIMS indicated a pseudomolecular ion peak $[M–H]^-$ at ***m/z*** 650.3047; suggesting a molecular formula of $C_{40}H_{44}NO_7$ (calcd. for $C_{40}H_{44}NO_7$; 650.3118); from which 19 degrees of unsaturation was deduced. The IR spectrum of **3** showed the absorption bands at ν_{max} 3296, 1718, 1625, and 1540 cm^{-1} corresponding to the N-H amide elongation, C=O stretching of an acid, C=O stretching of an amide and N-H amide deformation, indicating the presence of a carboxylic acid group and an amide group, respectively.

Based on the ^1H and ^{13}C NMR data, compound **130** possessed the same pentacyclic carbon skeleton as **128**, but differing in the position and type of substituents attached at C-1 and C-8' (Table 3.13). The ^1H NMR spectrum of **130** revealed four ***cis***-form vinyl protons resonating at δ_H 5.49 (dd, ***J*** = 9.8, 10.0 Hz, H-3), 5.58 (dd, ***J*** = 9.8, 10.0 Hz, H-4), 5.99 (dd, ***J*** = 7.7, 7.3 Hz, H-4′), and 6.10 (t, ***J*** = 7.3 Hz, H-5′). These signals were the characteristic feature for kingianin. Meanwhile, the presence of two 1,3,4-trisubstituted benzene moieties were suggested by a doublets at δ_H 6.59 (d, ***J*** = 1.2 Hz, H-11) and the two ***ortho*-*meta***-coupled doublets at δ_H 6.69 (d, ***J*** = 7.8 Hz, H-14) and 6.53 (dd, ***J*** = 7.8, 1.1 Hz, H-15) observed in the ^1H NMR spectrum with the chemical shifts for H-11′, H-14′, and H-15′ being almost identical with the former three. In addition, the two singlets corresponding to two protons each at δ_H 5.93 and 5.94 (H_2-16

and H_2-16′, respectively) confirmed the presence of the methylenedioxy group. An ***N***-ethylacetamide group was suggested from the presence of a doublet of quartets corresponding to two protons resonating at δ_H 3.23 (***J*** = 5.6, 7.1 Hz, H-20), a triplet corresponding to a methyl group at δ_H 1.11 (***J*** = 7.1 Hz, H-21) and another triplet at δ_H 5.29 (***J*** = 5.6 Hz, NH-19). Meanwhile, the presence of the butanoic acid group was inferred from the presence of the methylene protons at δ_H 2.22, 1.42-1.48 and 1.03-1.25 (H_2-19′, H_2-18′ and H_2-17′, respectively). The ^{13}C (Table 3.13) and DEPT 135 NMR spectra exhibited 40 signals comprising one methyl, 9 methylene, 22 methine, and 8 quaternary carbons including two carbonyl groups, which resonated at δ_C 172.6 (C-18) and 178.1 (C-20′). Resonances of the methine carbons at δ_C 38.4 (C-1), 32.3 (C-2), 38.0 (C-5), 38.1 (C-6), 41.7 (C-7), 47.3 (C-8), 43.8 (C-1′), 44.3 (C-2′), 42.9 (C-3′), 38.6 (C-6′), 39.1 (C-7′) and 42.2 (C-8′) as observed in DEPT spectrum, were characteristic for the pentacyclic kingianin skeleton. The ^{13}C NMR spectrum also showed signals of the olefinic carbons at δ_C 125.3 (C-3), 131.9 (C-4), 132.8 (C-4′) and 134.5 (C-5′).

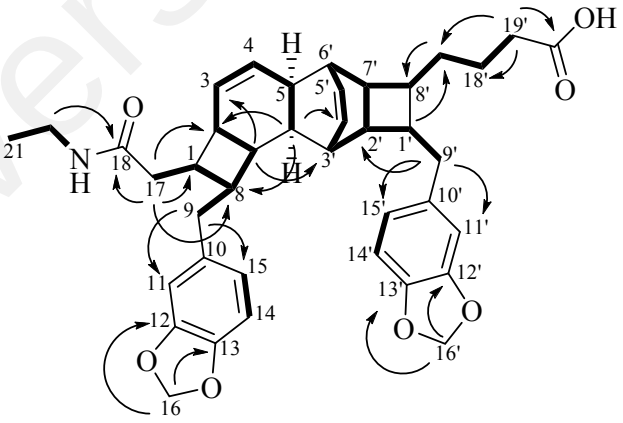

Figure 3.55: Key ^1H-^1H COSY (bold) and HMBC ($^1H \rightarrow ^{13}C$) correlations of **130**.

The HMBC and COSY data made the establishment of the connectivity of the four substituents; ***N***-ethylacetamide, butanoic acid and two methylenedioxybenzyl moieties possible (Figure 3.55). The correlations of H_2-17/C-1, H_2-17/C-18 and H_2-20/C-18

confirmed the presence of the ***N***-ethylacetamide substituent, which is attached to the skeleton at C-1. Meanwhile, the H-8′-H_2-17′-H_2-18′-H_2-19′ spin systems inferred from the COSY spectrum, and the HMBC correlations between H_2-17′ with C-8′, and H_2-19′ with C-18′ and the C-20′ carbonyl carbon (δ_C 178.1), confirmed the connectivity of the butanoic acid chain to C-8′. In the HMBC spectrum, the cross peaks observed between C-9 (C-9′) with H-11 and H-15 (H-11′ and H-15′) and COSY correlations between H_2-9 and H-8, and H_2-9′ and H-1′, confirmed that the two methylenedioxybenzyl moieties were located at positions C-8 and C-1′, respectively (Figure 3.55).

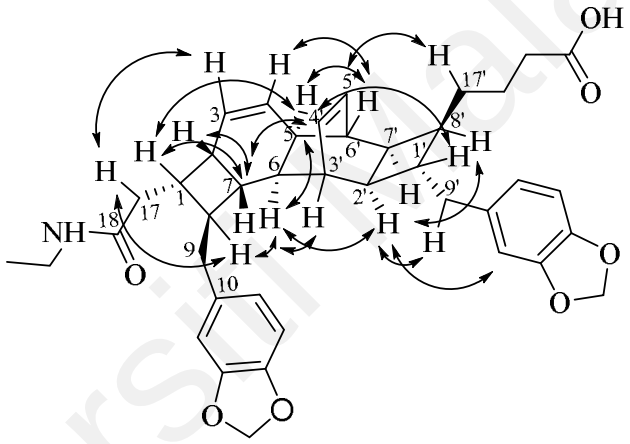

Figure 3.56: Key NOESY ($^1H \leftrightarrow {}^1H$) correlations of compound **130**.

Finally, the relative configuration of all of the stereocenters in **130**, deduced from the NOESY experiment (Figure 3.56), and is similar to compound **128**. The cross peaks between H-4′/H-1′, and H-2′/H-8′ indicated that H-1′ is *β*–oriented while H-8′ is *α*–oriented. The NOESY correlations between H-7/H-1 and H-6/H-8, indicated an *α*–orientation of the amide chain at C-1, and *β*-orientation of the benzyl moiety at C-8. Therefore, the relative configuration of **130** is determined as ***rel***-(***1SR, 2SR, 5SR, 6RS, 7RS, 8SR, 1′SR, 2′RS, 3′RS, 6′SR, 7′SR, 8′SR***), same as that of kingianin F (**50**) (Leverrier et al., 2011). Thus, the structure of **130** was elucidated as shown, and was named kingianin Q.

Table 3.13: ^{1}H (600 MHz) and ^{13}C (150 MHz) NMR data of compound **130** in $CDCl_3$

130					
	Part A_1			**Part A_2**	
Position	δ_H (***J*** in Hz)	δ_C	Position	δ_H (***J*** in Hz)	δ_C
1	2.10 m	38.4	1′	1.84 m	43.8
2	2.38 m	32.3	2′	2.07 m	44.3
3	5.49 dd (10.0, 9.8)	125.3	3′	2.08 m	42.9
4	5.58 dd (10.0, 9.8)	131.9	4′	5.99 dd (7.7, 7.3)	132.8
5	2.09 m	38.0	5′	6.10 t (7.3)	134.5
6	1.23 m	38.1	6′	2.49 m	38.6
7	1.78 m	41.7	7′	2.45 m	39.1
8	1.65 m	47.3	8′	2.00 m	42.2
9	2.56 m	41.0	9′	2.58 m	41.9
10	-	134.7	10′	-	134.9
11	6.59 d (1.1)	109.0	11′	6.61 d (1.1)	109.3
12	-	147.4	12′	-	147.4
13	-	145.5	13′	-	145.5
14	6.69 d (7.8)	108.0	14′	6.73 d (7.8)	108.0
15	6.53 dd (7.8, 1.1)	121.0	15′	6.56 dd (7.8, 1.1)	121.3
16	5.93 s	100.7	16′	5.94 s	100.7
17	1.90 m	37.0	17′	1.03 m	29.7
	2.19 m			1.25 m	
18	-	172.6	18′	1.42 m	23.3
				1.48 m	
19	5.29 t (5.6)	-	19′	2.22 m	34.3
20	3.23 dq (7.1, 5.6)	34.3	20′	-	178.1
21	1.11 t (7.1)	14.9			

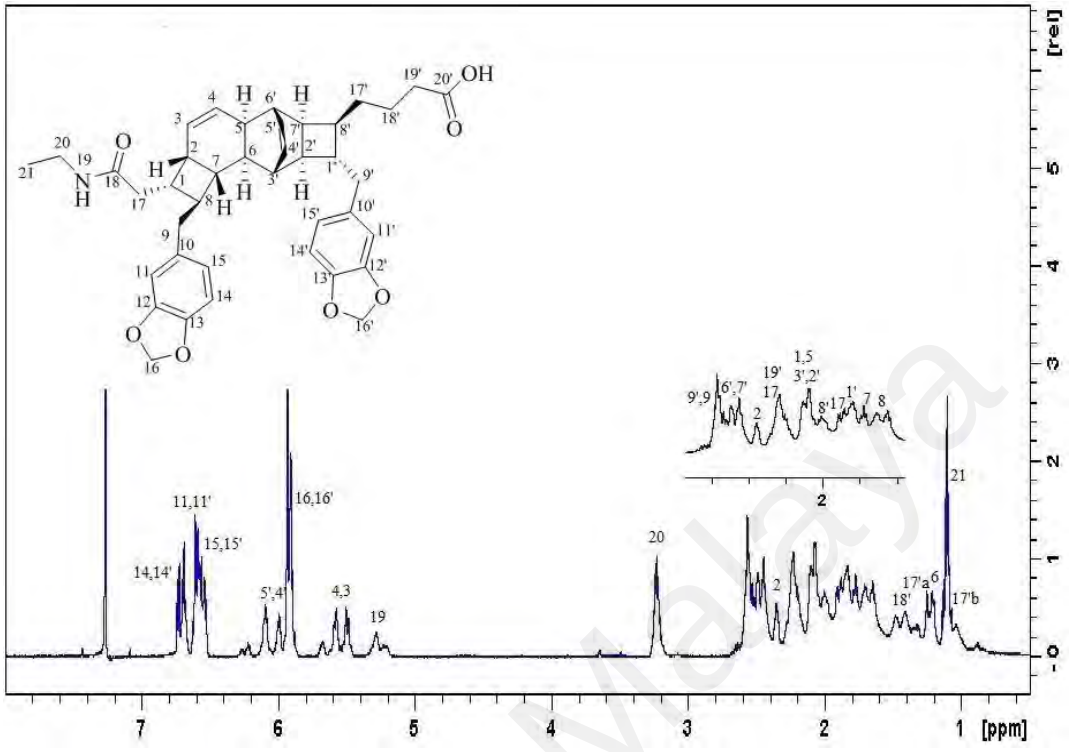

Figure 3.57: ^{1}H NMR spectrum for compound **130**

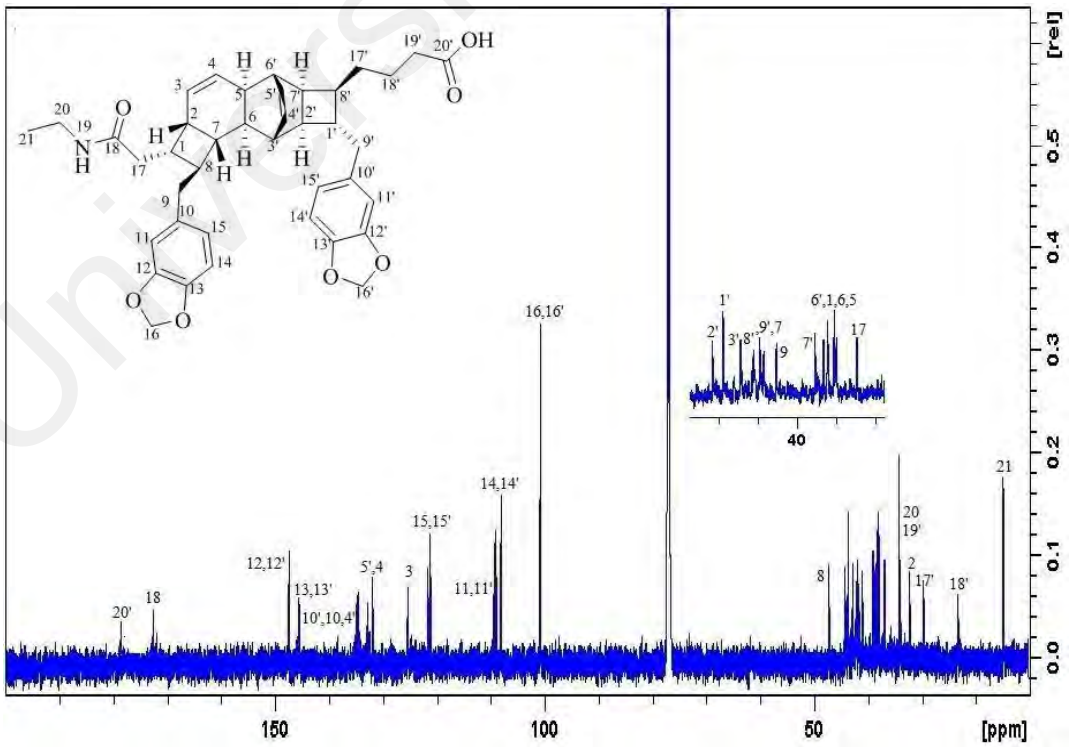

Figure 3.58: ^{13}C NMR and DEPT-135 spectrum for compound **130**

Compound N: Kingianin A (**45**)

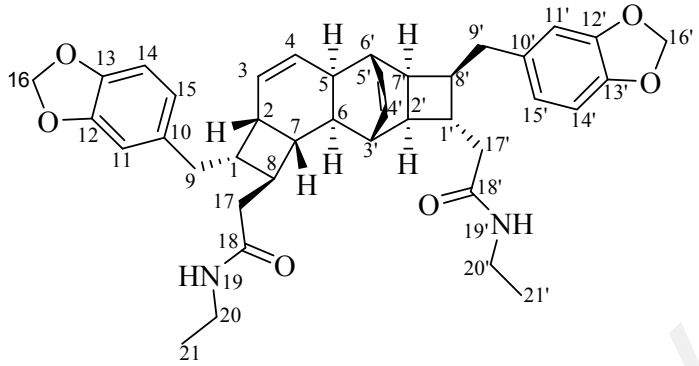

Compound N was obtained as a white powder. Its HRESIMS indicated a pseudomolecular ion peak $[M+H]^+$ at ***m/z*** 651.3431 suggesting a molecular formula of $C_{40}H_{47}N_2O_6$ (calcd. for $C_{40}H_{47}N_2O_6$; 651.3434), for which 19 degrees of unsaturation was deduced. The IR spectrum of compound N showed absorption bands at ν_{max} 3295, 1628 and 1540 cm^{-1} for N-H, C=O elongations and N-H amide deformation, respectively (Pretsch et al., 2009; Silverstein et al., 1997), indicating the presence of an amide group.

The characteristic four ***cis***-form olefinic protons resonated at δ_H 5.58 (d, ***J*** = 9.5 Hz, H-3), 5.68 (d, ***J*** = 9.5 Hz, H-4), 6.12 (dd, ***J*** = 7.1, 7.4 Hz, H-4′) and 6.24 (dd, ***J*** = 7.1, 7.4 Hz, H-5′) (Pavia et al., 2009). In addition, the multiplet was found between δ_H 1.70 – 2.55 integrating to twelve protons corresponded to the twelve methine groups; H-1 to H-8 and H-1′ to H-8′, which were the characteristic features for the pentacyclic kingianin (Table 3.14). The three aromatic protons which resonated as a doublet at δ_H 6.61 (***J*** = 1.2 Hz, H-11), a doublet at δ_H 6.68 (***J*** = 8.2 Hz, H-14) and a doublet of doublets at δ_H 6.56 (***J*** = 8.2, 1.2 Hz, H-15) suggested the presence of a 1,3,4-trisubstituted aromatic ring, with the chemical shifts for H-11′, H-14′ and H-15′ being almost identical to the former three. In addition, the proton signals at δ_H 5.89 and 5.91 (H-16 and H-16′) confirmed the presence of two methylenedioxyphenyl substituents.

The two ***N***-ethylacetamide groups were suggested by the presence of a doublet of quartets corresponding to four protons at δ_H 3.22 (***J*** = 5.6, 7.2 Hz, H_2-20 and H_2-20′), a triplet representing six protons at δ_H 1.10 (***J*** = 5.6 Hz, H_3-21 and H_3-21′), together with two triplets at δ_H 5.16 (***J*** = 7.2 Hz) and 5.20 (***J*** = 7.2 Hz), corresponding to NH-19′ and NH-19 respectively. The ^{13}C and DEPT-135 NMR spectra exhibited 40 signals comprising 2 methyls, 8 methylenes, 22 methines and 8 quaternary carbons (Table 3.14). There were 16 skeletal signals of a pentacyclic kingianin moiety between δ_C 33.2 - 43.7, including the presence of the four ***cis*** olefinic carbons at δ_C 124.9, 132.3, 132.4 and 134.8 corresponding to C-3, C-4, C-4′ and C-5′, respectively. The spectroscopic data of **45** was closely resembled to those of **129**, indicating that this compound possessed the same carbon skeleton except for the substituent at C-8, indicating that the acid moiety in **129** was replaced by an ***N***-ethylacetamide moiety in compound N. The connectivity of the two methylenedioxyphenyl and the two ***N***-ethylacetamide groups were determined based on ^1H-^1H COSY and ^1H-^{13}C HMBC correlations (Figure 3.59).

The HMBC cross peaks of H-8/H_2-17, H_2-17/C-18, H-1′/H_2-17′, H_2-17′/C-18′, and H_2-20/C-18 (H_2-20′/C-18′) confirmed the connectivity of the two ***N***-ethylacetamide substituents at C-8 and C-1′. Meanwhile, the ^1H-^1H COSY spectrum of compound N revealed the H-1/H_2-9 and H-8′/H_2-9′ cross peaks, allowing the placement of the two methylenedioxyphenyl groups at C-1 and C-8′. In addition, the HMBC correlations between H_2-9 and C-11 (δ_C 108.8) and C-15 (δ_C 121.0) and between H_2-9′ to C-11′ (δ_C 108.7) and C-15′ (δ_C 121.0), further confirmed the connectivities of the methylenedioxybenzyl groups at C-1 and C-8′, respectively.

Their spatial arrangements were determined from the NOESY experiment and those of the pentacyclic main skeleton showed similar profile to compound **129**. The correlations between H-4′/H-1′, H-2′/H-8′, H-2′/H-17′ and H-5′/H_2-9′ indicated that the ***N***-ethylacetamide group was β–oriented at C-1′ while the phenyl group was α–oriented

at C-8′. Meanwhile, the correlations between H-1/H-2 and H-6/H-8, suggested that the spatial arrangement of carbon C-1 and C-8 of compound N were identical to those of **129**, namely the *α*–orientation for the phenyl group at C-1, and the *β*–orientation for the ***N***-ethylacetamide group at C-8. Thus, the relative configuration of compound N was determined as ***rel***-(***1SR, 2SR, 5RS, 6RS, 7RS, 8SR, 1′SR, 2′RS, 3′RS, 6′SR, 7′SR, 8′RS***).

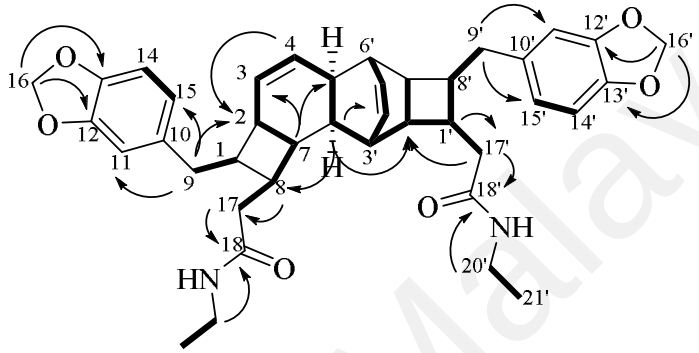

Figure 3.59: Key COSY (bold) and HMBC ($^{1}H \rightarrow {}^{13}C$) correlations of compound N

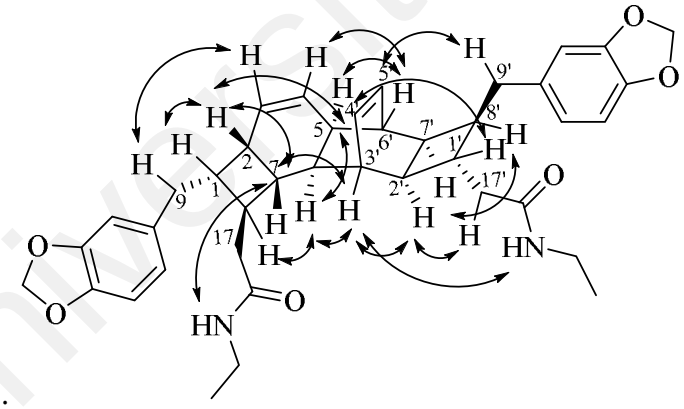

Figure 3.60: Key NOESY ($^{1}H \leftrightarrow {}^{1}H$) correlations of compound N

From the above observation and upon comparison of the spectral data obtained with those in the literature, compound N was found to be kingianin A (**45**) (Leverrier et al., 2010). This compound was the first major compound (0.00075% yield) for the kingianin series.

Table 3.14: ^{1}H (600 MHz) and ^{13}C (150 MHz) NMR data of compound N in $CDCl_3$

Position	Compound N		Kingianin A (Leverrier et al., 2010)	
	δ_H (***J*** in Hz)	δ_C	δ_H (***J*** in Hz)	δ_C
1	2.05 m	43.7	2.03 m	43.9
2	2.48 m	33.2	2.46 m	33.4
3	5.56 d (10.5)	124.9	5.54 br d (10.4)	125.1
4	5.56 d (10.5)	132.3	5.64 br d (10.4)	132.4
5	2.26 m	38.1	2.22 m	38.3
6	1.70 d (9.0)	38.1	1.68 br d (9.0)	38.1
7	1.92 m	42.4	1.89 m	42.6
8	2.00 m	42.4	2.00 m	42.6
9	2.50 m, 2.64 m	35.2	2.44 m, 2.55 m	36.0
10	-	135.3	-	135.5
11	6.61 d (1.2)	108.8	6.61 d (1.2)	109.0
12	-	147.5	-	147.7
13	-	145.4	-	145.6
14	6.68 d (8.2)	108.1	6.67 d (7.9)	108.3
15	6.56 dd (8.2, 1.2)	121.0	6.54 dd (7.9, 1.2)	121.2
16	5.89 s	100.7	5.88 s	100.9
17	2.04 m	41.8	2.00 m	42.0
18	-	171.9	-	172.1
19	5.20 t (5.6)	-	5.28 t (5.7)	
20	3.22 dq (7.2, 5.6)	34.3	3.19 dq (7.2, 5.7)	34.5
21	1.10 t (7.2)	14.9	1.07 t (7.2)	15.1
1′	2.09 m	38.9	2.07 m	39.0
2′	2.26 m	42.2	2.24 m	44.5
3′	2.42 m	42.8	2.39 m	43.0
4′	6.12 dd (7.4, 7.1)	132.4	6.09 dd (7.6, 7.1)	132.6
5′	6.23 dd (7.4, 7.1)	134.8	6.20 t (7.1)	135.0
6′	2.53 m	38.4	2.50 m	38.6
7′	2.49 m	39.7	2.47 m	39.9
8′	2.28 m	43.7	2.26 m	43.9
9′	2.45 m, 2.58 m	35.8	2.47 m, 2.61 m	35.4
10′	-	135.5	-	135.7
11′	6.63 d (1.2)	108.7	6.58 br s	109.0
12′	-	147.5	-	147.7
13′	-	145.4	-	145.6
14′	6.68 d (8.2)	108.1	6.66 d (7.9)	108.3
15′	6.61 dd (8.2, 1.2)	121.0	6.55 br d (7.9)	121.2
16′	5.91 s	100.7	5.86 s	100.9
17′	2.03 m	43.0	1.93 m, 2.05 m	43.2
18′	-	171.9	-	172.1
19′	5.16 t (5.6)	-	5.23 t (5.7)	
20′	3.22 dq (7.2, 5.6)	34.2	3.19 dq (7.2, 5.7)	34.4
21′	1.10 t (7.2)	14.9	1.07 t (7.2)	15.1

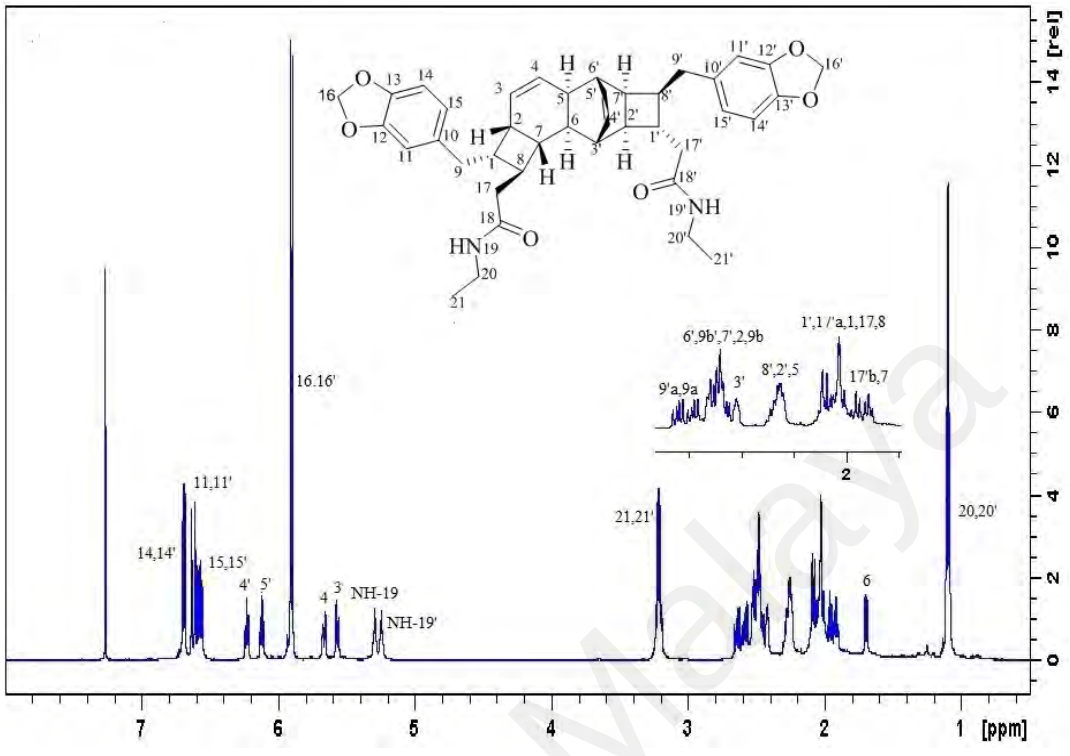

Figure 3.61: ^{1}H NMR spectrum for compound **45**

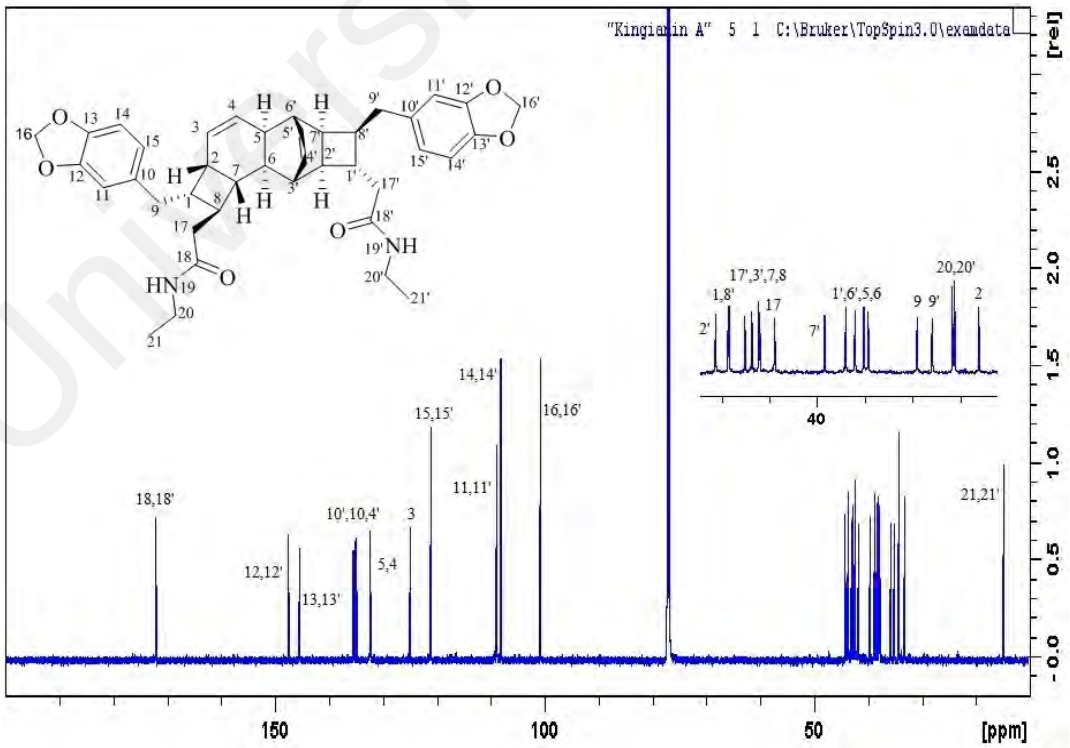

Figure 3.62: ^{13}C NMR spectrum for compound **45**

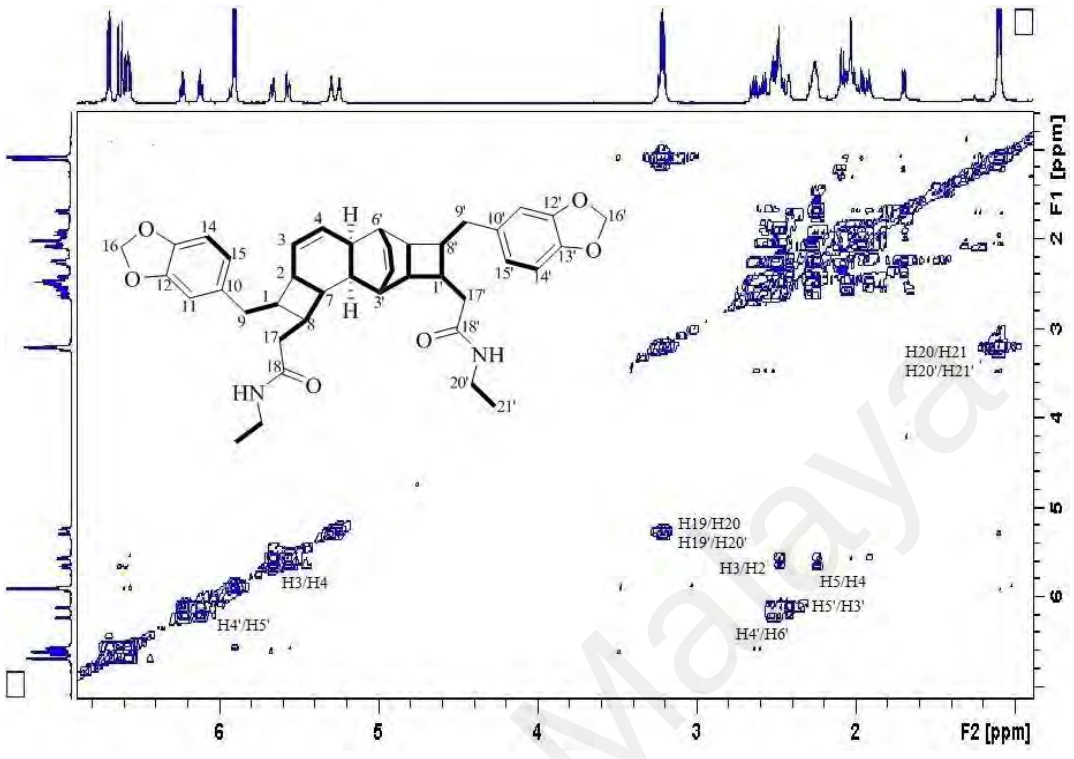

Figure 3.63: COSY-2D NMR spectrum for compound **45**

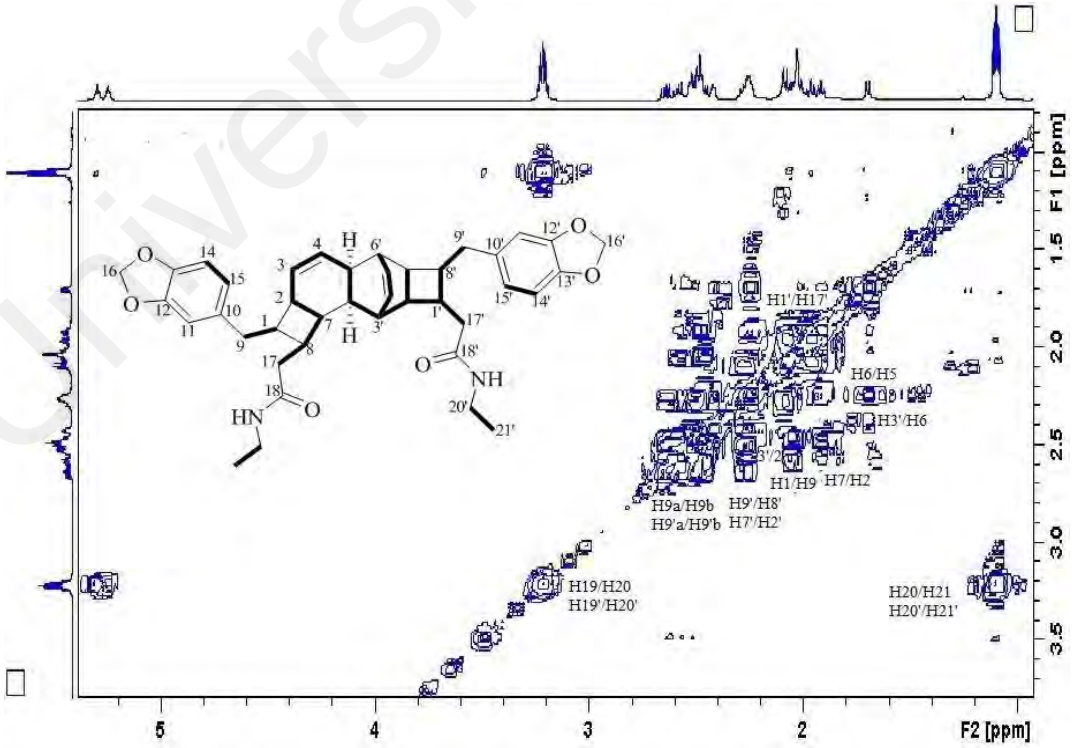

Figure 3.64: COSY-2D NMR (expended) spectrum for compound **45**

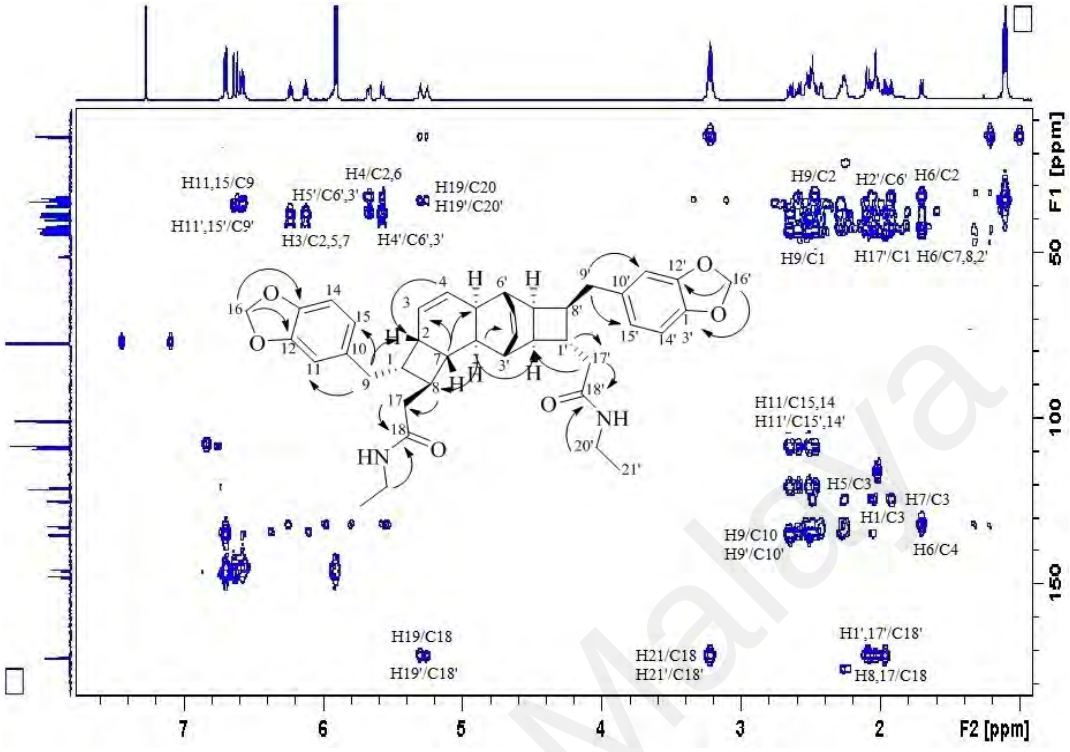

Figure 3.65: HMBC-2D NMR spectrum for compound **45**

Compound O: Kingianin F (**50**)

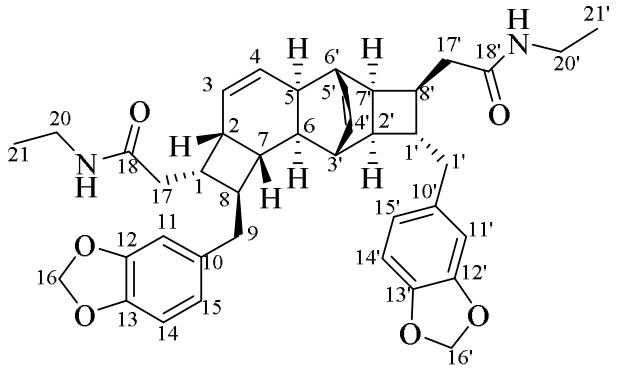

Compound O was isolated as an optically in active white powder. A molecular formula of $C_{40}H_{46}N_2O_6$ was assigned on the basis of ^{13}C NMR and HRESIMS data indicated a pseudomolecular ion peak $[M+H]^+$ at ***m/z*** 651.3423 suggesting a molecular formula $C_{40}H_{47}N_2O_6$ (calcd. for $C_{40}H_{47}N_2O_6$; 651.3434), for which 19 degrees of unsaturation was deduced. The UV and IR data were similar to those of kingianin A (**45**) (Leverrier et al., 2010; 2011).

The ^1H NMR spectrum of compound O, revealed four ***cis*** olefinic protons at δ_H 5.62 (d, ***J*** = 10.5 Hz, H-4), 5.78 (d, ***J*** = 10.5 Hz, H-3), 5.87 (t, ***J*** = 7.2 Hz, H-4′) and 6.11 (t, ***J*** = 7.2 Hz, H-5′). In addition, the multiplet signals between δ_H 1.35 – 2.80 integrating to twelve protons corresponded to twelve methine groups, which represented the 16 skeletal signals of a pentacyclic kingianin moiety. This compound also contained four substituents; two methylenedioxyphenyl and two ***N***-ethylacetamide groups, similar to those of compounds **45** and **47** (Table 3.15). The positions of these substituents were determined based on the 2D NMR correlations. The ^{13}C and DEPT NMR spectra exhibited 40 signals consistent with two methyls, 8 methylenes, 22 methines and 8 quaternary carbons, including two carbonyl groups resonated at δ_C 173.0 and 173.2 (C-18 and C-18′). The four ***cis*** olefinic methines which resonated at δ_C 126.9, 133.1, 133.7 and 136.0, corresponded to C-3, C-4, C-4′ and C-5′, respectively. In general, the

structure of compound O was similar to that of **47**, except for the position of the methylenedioxyphenyl and ***N***-ethylacetamide groups at the C-1 and C-8.

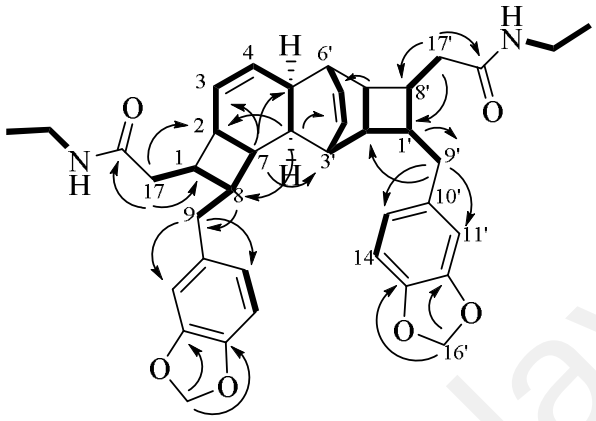

Figure 3.66: Key COSY (bold) and HMBC ($^{1}H \rightarrow {}^{13}C$) correlations of compound O.

In the COSY spectrum, the following correlations, H-1/H_2-17, H-8/H_2-9, H-1′/H_2-9′ and H-8′/H_2-17′ suggested that the two phenyl groups were located at C-8 and C-1′, while the two amide groups at C-1 and C-8′. The connectivities of the two methylenedioxyphenyl groups were inferred from the HMBC correlations between H-8/C-9, H_2-9/C-11 and C-15, H-1′/C-9′ and H_2-9′/C-2′, C-11′ and C-15′. Meanwhile, the HMBC correlations between H_2-17/C-1, C-2 and C-18, and that of H_2-17′/C-8′, C-1′ and C-18′ confirmed the connectivity of the two ***N***-ethylacetamide groups to C-1 and C-8′, respectively (Figure 3.66). The spatial arrangement was established by the NOESY experiment and the arrangement of the pentacyclic skeleton showed similar profile to that of compounds **45** and **47**. The cross peaks between H-2/H-1 and H-6/H-8, suggested that the ***N***-ethylacetamide group was in the α–position at C-1, and the phenyl group in the β–position at C-8. The cross peaks between H-4′/H-1′ and H-2′/H-8′, indicated an α–position for the phenyl group at C-1′ and a β–position for the ***N***-ethylacetamide group at C-8′ (Figure 3.67). The relative configuration of compound

O could therefore be determined as ***rel***-(***1SR, 2SR, 5SR, 6RS, 7RS, 8SR, 1′SR, 2′RS, 3′RS, 6′SR, 7′SR, 8′SR***).

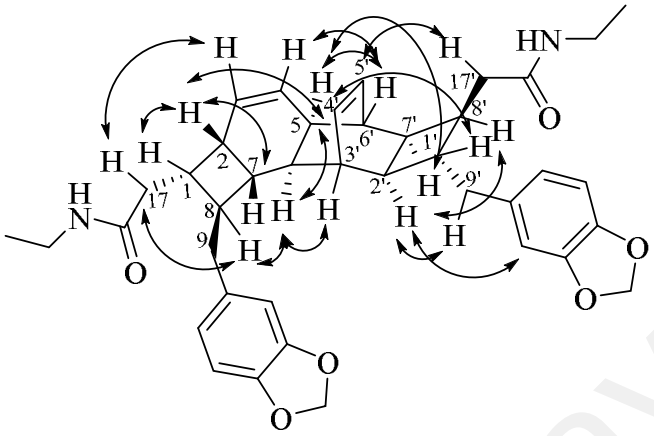

Figure 3.67: Key NOESY ($^1H \leftrightarrow {}^1H$) correlations of compound O.

Extensive analysis of the observed data and comparison with the literature, led to the deduction that compound O was kingianin F (**50**) (Leverrier et al., 2011).

Table 3.15: ^{1}H (600 MHz) and ^{13}C (150 MHz) NMR data of compound O in Pyrdine-D_5

Position	Compound O		Kingianin F (Leverrier et al., 2011)	
	δ_H (***J*** in Hz)	δ_C	δ_H (***J*** in Hz)	δ_C
1	2.51 m	40.2	2.54 m	39.8
2	2.57 m	34.3	2.61 m	33.9
3	5.78 d (10.5)	126.9	5.82 d (10.5)	126.4
4	5.62 d (10.5)	133.1	5.66 d (10.5)	132.7
5	2.08 m	39.4	2.12 m	38.9
6	1.35 d (8.8)	39.3	1.39 d d (8.8)	38.9
7	1.77 t (8.8)	42.8	1.81 t (8.8)	42.3
8	1.87 m	48.4	1.91 m	48.0
9	2.67 m, 2.57 m	41.4	2.72 m, 2.62 m	41.0
10	-	135.9	-	135.6
11	6.81 d (1.1)	110.8	6.85 d (1.3)	110.4
12	-	149.0	-	148.5
13	-	147.0	-	146.6
14	6.88 d (7.7)	109.3	6.91 d (7.9)	108.9
15	6.66 dd (7.7, 1.1)	122.9	6.70 dd (7.9, 1.3)	122.7
16	5.92 s	102.1	5.98 s	101.7
17	2.36 m, 2.23 m	38.7	2.40 m, 2.27 m	38.3
18	-	173.0	-	172.5
19	8.21 t (5.2)	-	8.21 t (5.3)	
20	3.41 dq (7.2, 5.2)	35.3	3.45 dq (7.2, 5.3)	34.8
21	1.10 t (7.2)	16.1	1.14 t (7.2)	15.7
1′	2.06 m	45.1	2.11 m	44.7
2′	2.16 m	45.4	2.22 m	45.0
3′	2.11 m	44.2	2.16 m	43.7
4′	5.87 t (7.2)	133.7	5.91 t (7.2)	133.3
5′	6.11 t (7.2)	136.0	6.15 t (7.2)	135.4
6′	2.59 m	39.8	2.62 m	39.4
7′	2.42 m	40.6	2.47 m	40.2
8′	2.79 m	40.2	2.83 m	39.7
9′	2.81 m, 2.61 m	43.1	2.86 m, 2.66 m	42.6
10′	-	136.1	-	136.2
11′	6.87 d (1.1)	110.5	6.91 d (1.3)	110.0
12′	-	149.0	-	148.5
13′	-	147.1	-	146.6
14′	6.93 d (7.7)	109.4	6.96 d (7.9)	109.0
15′	6.75 dd (7.7, 1.1)	123.2	6.79 dd (7.9 1.3)	122.7
16′	5.94 s	102.1	5.95 s	101.7
17′	2.46 m, 2.30 m	38.0	2.50 m, 2.34 m	37.5
18′	-	173.2	-	172.8
19′	8.21 t (5.2)	-	8.21 t (5.3)	
20′	3.41 dq (7.2, 5.2)	35.3	3.45 dq (7.2, 5.3)	34.7
21′	1.10 t (7.2)	16.2	1.14 t (7.2)	15.7

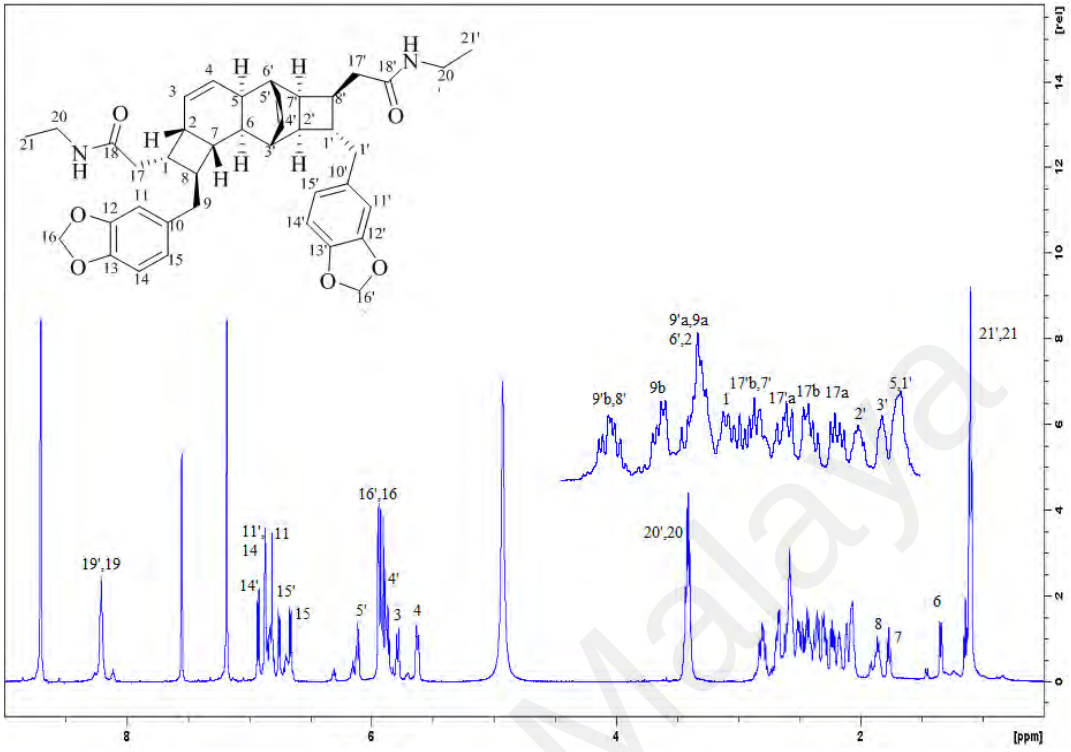

Figure 3.68: ^{1}H NMR spectrum for compound **50**

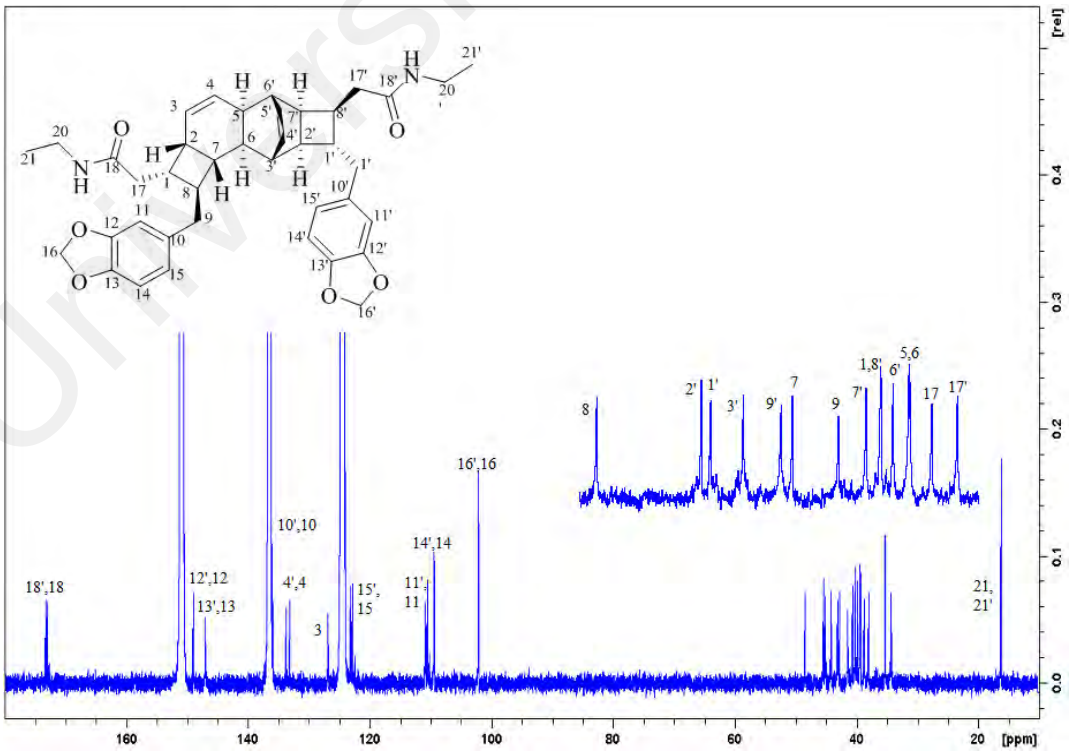

Figure 3.69: ^{13}C NMR spectrum for compound **50**

Compound P: Kingianin K (**55**)

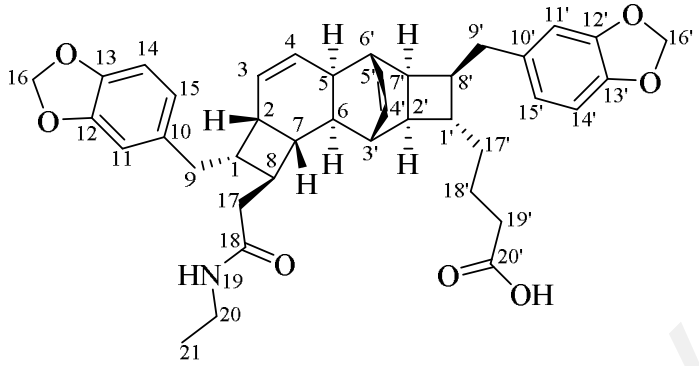

Compound P was isolated as an optically inactive white powder. Its HRESIMS showed a pseudomolecular ion peak, $[M+H]^+$ at ***m/z*** 652.3284, corresponding to $C_{40}H_{46}NO_7$ (calcd. for $C_{40}H_{46}NO_7$; 652.3274) containing 19 degrees of unsaturation. Comparison of the molecular formula proposed for **129**, and that of compound P, revealed that compound P possessed two additional CH_2 groups. Its IR spectra revealed an absorption band at ν_{max} 1736 cm^{-1} for carboxyl of carboxylic acid functionality and at ν_{max} 3336 and 1645 cm^{-1} for an amide group (Pretsch et al., 2009; Silverstein et al., 1997).

The ^1H NMR spectrum of **55** revealed four ***cis***-form vinyl protons resonating at δ_H 5.56 (d, ***J*** = 10.2 Hz, H-3), 5.66 (d, ***J*** = 10.2 Hz, H-4), 6.06 (dd, ***J*** = 7.1, 7.3 Hz, H-4′), and 6.22 (dd, ***J*** = 7.1, 7.3 Hz, H-5′). These signals were the characteristic features for kingianin. Meanwhile, the aromatic protons at δ_H 6.60 (d, ***J*** = 1.1 Hz, H-11′), 6.64 (d, ***J*** = 1.1 Hz, H-11), 6.68 (d, ***J*** = 7.8 Hz, H-14′), 6.70 (d, ***J*** = 7.8 Hz, H-14), 6.55 (dd, ***J*** = 7.8, 1.1 Hz, H-15′) and 6.58 (dd, ***J*** = 7.8, 1.1 Hz, H-15) suggested the presence of two 1,3,4-trisubstituted aromatic rings. In addition, the two downfield singlets corresponding to four protons at δ_H 5.90 (H-16′) and 5.91 (H-16) confirmed the presence of the two methylenedioxy group. The ***N***-ethylacetamide group was suggested from the presence of a doublet of quartets corresponding to two protons resonating at δ_H

3.23 (***J*** = 5.5, 7.0 Hz, H-20), a triplet corresponding to the methyl group at δ_H 1.11 (***J*** = 7.0 Hz, H-21) and a triplet at δ_H 5.21 (***J*** = 5.5 Hz, NH-19). Meanwhile, the presence of butanoic acid group was suggested from the presence of the methylenes at δ_H, 1.18-1.41 and 2.20, corresponding to H_2-17′, H_2-18′ and H_2-19′, respectively (Table 3.16).

The ^{13}C and DEPT-135 NMR spectra exhibited 40 signals comprising one methyl, 9 methylenes, 22 methines, and 8 quaternary carbons (Table 3.16). Resonances of the methine carbons between δ_C 33.3 – 44.3 as observed in the DEPT spectrum were characteristics of the pentacyclic kingianin skeleton. This pentacyclic skeleton comprised two cyclobutanes and three cyclohexanes, and was connected to each other to form the kingianin framework. The ^{13}C NMR spectrum also showed signals of four ***cis*** olefinic methine carbons at δ_C 125.3 (C-3), 131.9 (C-4), 132.8 (C-4′) and 134.5 (C-5′). The presence of the two methylenedioxyphenyl groups were suggested by the resonances of the twelve aromatic carbons at δ_C 135.2 (C-10), 135.8 (C10′), 108.9 (C-11 and C-11′), 147.4 (C-12), 147.5 (C-12′), 145.4 (C-13), 145.5 (C-13′), 108.1 (C-14′), 108.2 (C-14′), 121.1 (C-15 and C-15′), and of the two methylenedioxy groups at δ_C 100.7 (C-16 and C-16′) in ^{13}C NMR spectra. In addition, the presence of the acid and the ***N***-ethylacetamide groups were supported by their ^{13}C NMR spectra showing two signals at δ_C 176.7 and 172.0 ppm, respectively (Table 3.16) (Crews et al., 1998; Pavia et al., 2009).

The COSY spectrum of compound P reveled a H-1′-H_2-17′-H_2-18′-H_2-19′ spin system, with the carbon of the latter being correlated to the C-20′ carbonyl carbon (δ_C 176.7) in the HMBC spectrum. This suggested the presence of a butanoic acid group attach to C-1′ (δ_C 41.7). An ***N***-ethylacetamide group was observed from a triplet at δ_H 5.21 ppm (NH-19) in the ^{1}H NMR spectrum and from the cross peaks in the COSY spectrum between H_2-20 at δ_H 3.23 ppm and H_3-21 at δ_H 1.11 ppm and NH-19. The cross peaks between H-8 and H_2-17, which in turn is correlated to the C-18 carbonyl

carbon at δ_C 172.0, confirmed the position of the ***N***-ethylacetamide group at the C-8. In addition, the correlations between H-1 and H_2-9, and between H-8′ to H_2-9′ in COSY spectrum, allowed the assignment of the two methylenedioxybenzyl groups at position C-1 and C-8′ (Figure 3.70).

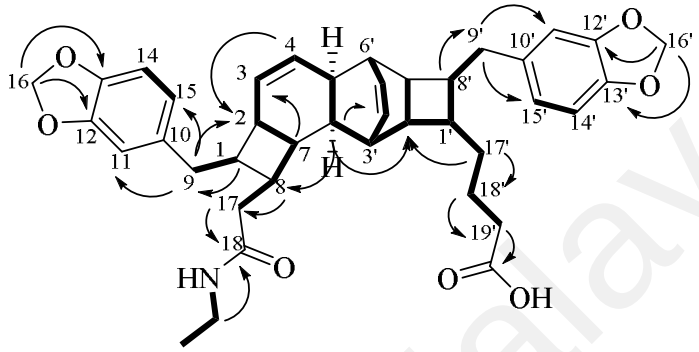

Figure 3.70: Key COSY (bold) and HMBC ($^1H \rightarrow ^{13}C$) correlations of compound P.

The configuration of compound P was identical to **45**. H-5 and H-6 were arbitrarily assigned as *α*-oriented. The NOESY correlations between H-2′/H-8′ and H-1′/H-4′ indicated a *β*–orientation for the phenyl group at C-8′ and an *α*–orientation for the butanoic acid chain at C-1′. The correlation between H-2/H-1 and H-6/H-8 suggested that the phenyl group was *α*–oriented at C-1 and the ***N***-ethylacetamide group was *β*–oriented at C-8. The configuration of phenyl and ***N***-ethylacetamide at the western part was identical to that of **45** (Figure 3.71). Thus, the relative configuration of compound P was determined as ***rel***-(***1SR, 2SR, 5SR, 6RS, 7RS, 8SR, 1′SR, 2′RS, 3′RS, 6′SR, 7′SR, 8′SR***).

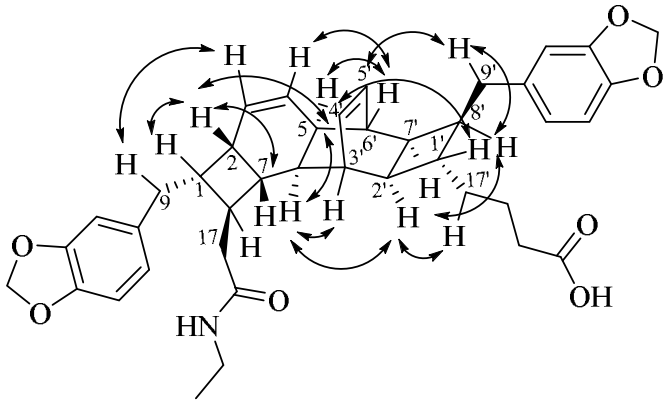

Figure 3.71: Key NOESY ($^1H \leftrightarrow {}^1H$) correlations of compound P.

Comparison of the observed data with those in the literature confirmed that compound P was kingianin K (**55**) (Leverrier et al., 2011).

Table 3.16 ^{1}H (600 MHz) and ^{13}C (150 MHz) NMR data of compound P in $CDCl_3$

Position	Compound P		Kingianin K (Leverrier et al., 2011)	
	δ_H (***J*** in Hz)	δ_C	δ_H (***J*** in Hz)	δ_C
1	2.00 m	43.7	2.03 m	43.9
2	2.44 m	33.3	2.47 m	33.5
3	5.56 d (10.2)	124.8	5.55 br d (10.4)	125.0
4	5.66 d (10.2)	132.2	5.65 br d (10.4)	132.6
5	2.23 m	38.1	2.22 m	38.3
6	1.70 m	38.2	1.68 br d (9.0)	38.4
7	1.93 m	42.3	1.92 m	42.5
8	2.02 m	42.6	1.98 m	42.8
9	2.46 m, 2.59 m	35.9	2.44 m, 2.57 m	36.1
10	-	135.3	-	135.5
11	6.64 d (1.1)	108.9	6.62 d (1.2)	109.1
12	-	147.4	-	147.7
13	-	145.4	-	145.6
14	6.70 d (7.8)	108.2	6.67 d (7.9)	108.3
15	6.58 dd (7.8, 1.1)	121.1	6.57 dd (7.9, 1.2)	121.3
16	5.91 s	100.7	5.88 s	100.9
17	2.01 m	41.6	2.01 m	41.8
18	-	172.0	-	172.3
19	5.21 t (5.5)	-	5.22 t (5.7)	
20	3.23 dq (7.0, 5.5)	33.7	3.20 dq (7.2, 5.7)	34.6
21	1.11 t (7.0)	14.9	1.08 t (7.2)	15.1
1′	1.67 m	41.7	1.65 m	41.9
2′	2.06 m	44.3	2.08 m	44.5
3′	2.34 m	43.3	2.31 m	43.5
4′	6.06 dd (7.3, 7.1)	132.4	6.04 dd (7.6, 7.1)	132.4
5′	6.22 dd (7.3, 7.1)	135.0	6.20 t (7.1)	135.2
6′	2.52 m	38.6	2.49 m	38.8
7′	2.46 m	39.4	2.45 m	39.6
8′	2.11 m	43.9	2.18 m	44.1
9′	2.48 m, 2.64 m	35.5	2.46 m, 2.61 m	35.7
10′	-	135.8	-	136.0
11′	6.60 d (1.1)	108.9	6.58 br s	109.1
12′	-	147.5	-	147.7
13′	-	145.5	-	145.7
14′	6.68 d (7.8)	108.1	6.67 d (7.9)	108.3
15′	6.55 dd (7.8, 1.1)	121.1	6.53 br d (7.9)	121.3
16′	5.90 s	100.7	5.88 s	100.9
17′	1.18 m, 1.23 m	36.0	1.16 m, 1.23 m	36.2
18′	1.31 m, 1.41 m	22.6	1.33 m, 1.42 m	22.8
19′	2.20 m	34.4	2.19 m	34.1
20′	-	176.7	-	178.2

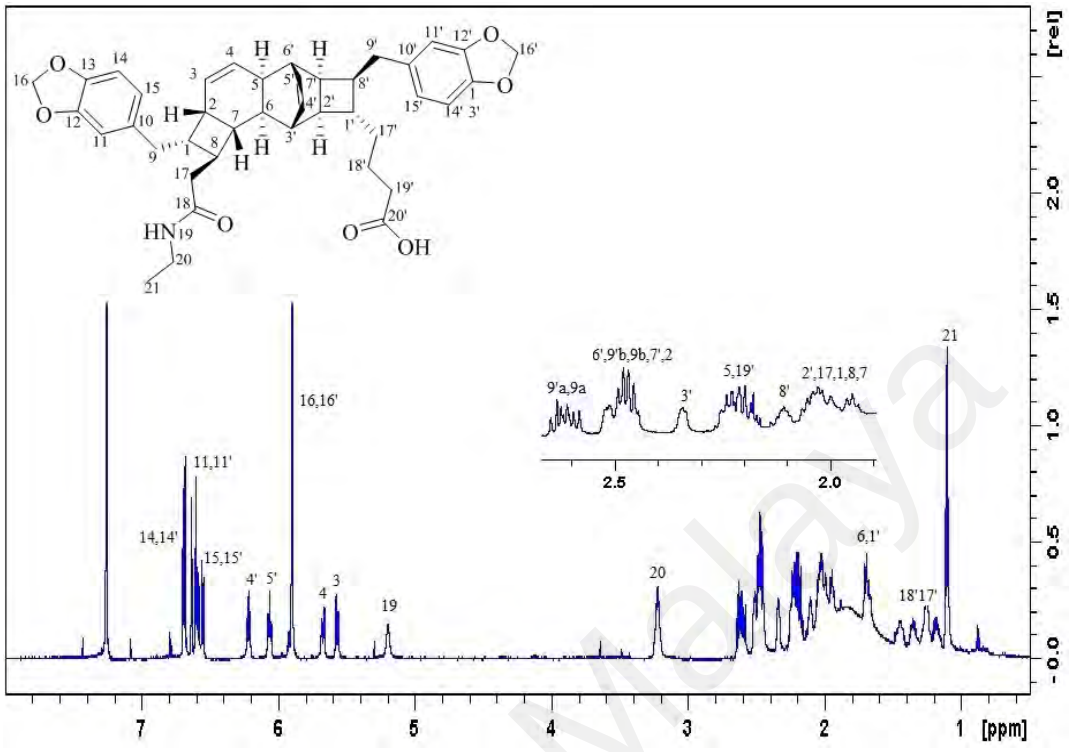

Figure 3.72: ^{1}H NMR spectrum for compound **55**

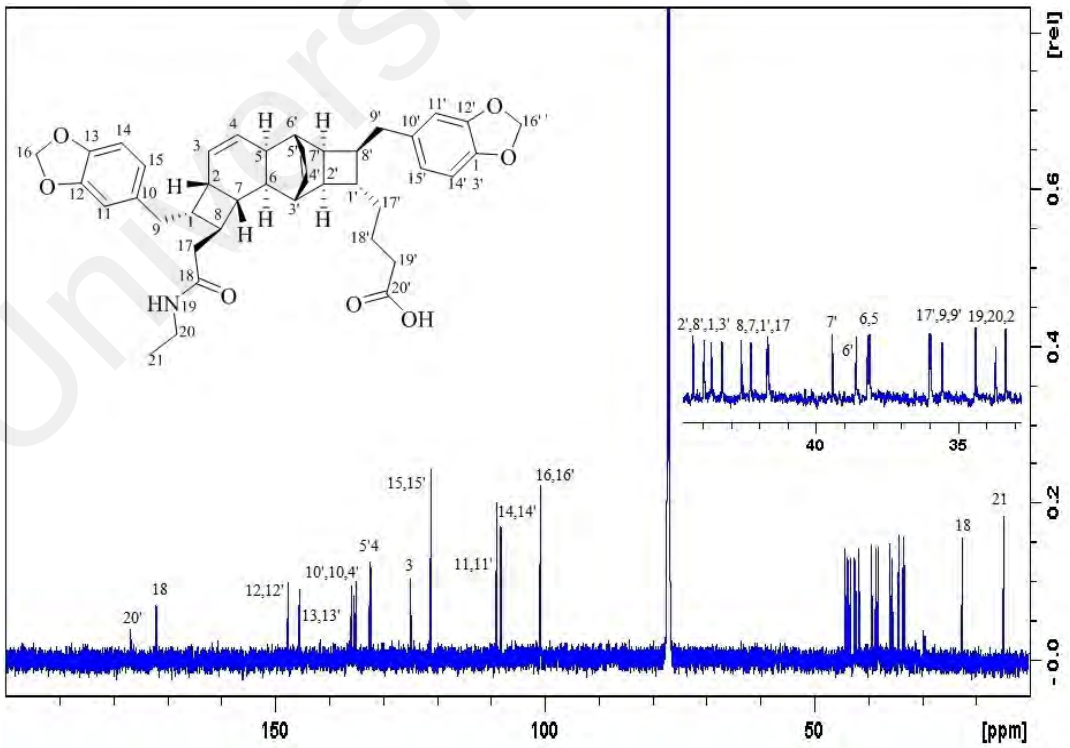

Figure 3.73: ^{13}C NMR spectrum for compound **55**

Compound Q: Kingianin L (**56**)

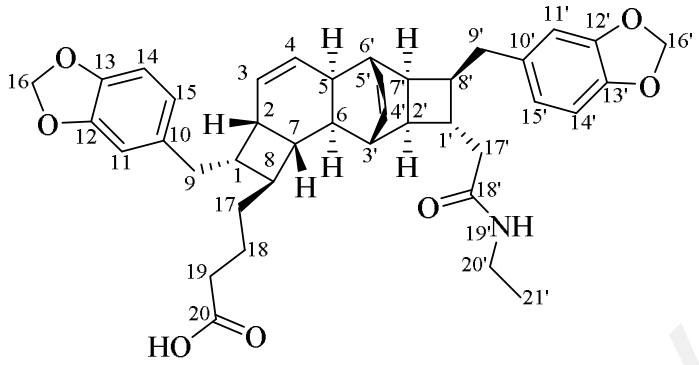

Compound Q was obtained as a white amorphous powder. Its HRESIMS showed a pseudomolecular ion peak, $[M+H]^+$ at m/z 652.3278, corresponding to a molecular formula of $C_{40}H_{46}NO_7$ (Calcd. for $C_{40}H_{46}NO_7$; 652.3274) containing 19 degrees of unsaturation. The UV, IR and NMR spectrum of compound Q were similar to those of **55**, but differed in the location of the ***N***-ethylacetamide and butyric acid groups.

In ^{1}H NMR spectrum, the characteristic four ***cis*** olefinic protons which appeared at δ_H 5.56 (dd, ***J*** = 10.1, 10.3 Hz, H-3), 5.56 (dd, ***J*** = 10.1, 10.3 Hz, H-4), 6.12 (dd, ***J*** = 7.2, 7.5 Hz, H-4′) and 6.23 (dd, ***J*** = 7.2, 7.5 Hz, H-5′) in compound Q were almost the same as in **55**. The signals for the two methylenedioxyphenyl moieties resonated between δ_H 5.89 – 5.91 and 6.55 – 6.70. In addition, the ***N***-ethylacetamide group was suggested from the presence of a doublet of quartets corresponding to two protons resonating at δ_H 3.23 (***J*** = 5.6, 7.1 Hz, H-20′), a triplet of a methyl group at δ_H 1.10 (***J*** = 7.1 Hz, H-21′) and a triplet at δ_H 5.20 (***J*** = 5.6 Hz, NH-19′). Meanwhile, the presence of the butanoic acid group was inferred from the presence of the methylene protons at δ_H 1.28-1.31, 1.51-1.54 and 2.25, corresponding to H_2-17, H_2-18 and H_2-19, respectively (Table 3.17).

The ^{13}C and DEPT-135 spectrum of compound R displayed 40 carbon signals, which were sorted into 22 methines which were inclusive of the four ***cis*** olefinic carbons at δ_C 125.6 (C-3), 131.9 (C-4), 132.4 (C-4′) and 134.8 (C-5′), 9 methylenes, one methyl and 8 quaternary carbons which included those of the carbonyl carbons at δ_C 172.0 (C-20) and

176.4 (C-18′), consistent with an amide and a carboxylic acid functionality (Table 3.17) (Crews et al., 1998; Pavia et al., 2009). In addition, the presence of the two methylenedioxyphenyl groups were suggested by the resonances of twelve aromatic carbons between δ_C 108.0 – 148.0 corresponding to C-10 – C-15 and C-10′ – C-15′, and of the two methylenedioxy group at δ_C 100.7 (C-16 and C-16′) in ^{13}C NMR spectra. In the ^{13}C NMR spectrum of compound Q, carbons C-8 and C-1′ resonate at δ_C 45.1 and 39.0, respectively, instead of δ_C 42.6 and 41.7 as for **55**.

Moreover, the COSY spectrum of compound Q revealed a spin system of H-8-H_2-17-H_2-18-H_2-19, which in turn was correlated to C-20 at δ_C 176.4 ppm in the HMBC spectrum. This indicated that the butanoic acid chain was attached to the central core at C-8. The amide group was therefore located at C-1′. This was further supported by the H-1′/H_2-17′ COSY correlations, and by the HMBC correlations between the H_2-17′ and H_2-20′ to C-18′ (δ_C 172.0). The butanoic acid and ***N***-ethylacetamide groups were attached to the pentacyclic frame at C-8 (δ_C 45.1) and C-1′ (δ_C 39.0), respectively. In addition, the correlations between H-1 and H_2-9, and between H-8′ to H_2-9′ in COSY spectrum and HMBC correlations between H-1/C-9 and H-8′/C-9′, allowed the assignment of the two methylenedioxybenzyl groups at position C-1 and C-8′ (Figure 3.74).

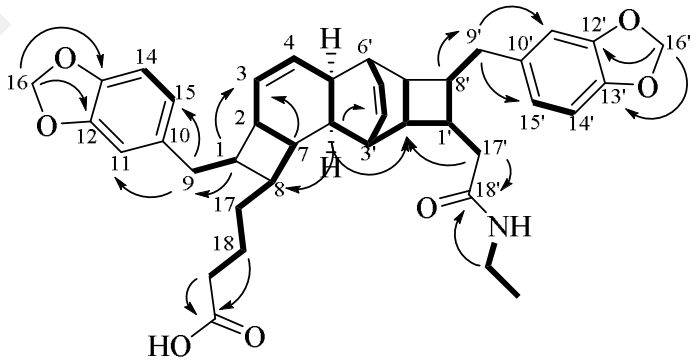

Figure 3.74: Key COSY (bold) and HMBC (^{1}H→^{13}C) correlations of compound Q.

The NOESY spectrum showed similar profile especially for those of the pentacyclic main skeleton to that of **55**. H-6 was arbitrarily assigned as α-oriented. The cross peak between H-2/H-1, H-6/H-8, and H-1/H_2-17 suggested that the phenyl group was α–oriented at C-1 and the butanoic acid chain was β–oriented at C-8. Meanwhile, the correlation between H-2′/H-8′ and H-4′/H-1′ indicated a β–orientation for the phenyl group at C-8′ and an α–orientation for the ***N***-ethylacetamide group at C-1′. The configurations of four substituents are in an ***anti*** position on the cyclobutane frames (Figure 3.75). Thus, the relative configuration of compound Q was determined as ***rel***-(***1SR, 2SR, 5RS, 6RS, 7RS, 8SR, 1′SR, 2′RS, 3′RS, 6′SR, 7′SR, 8′SR***).

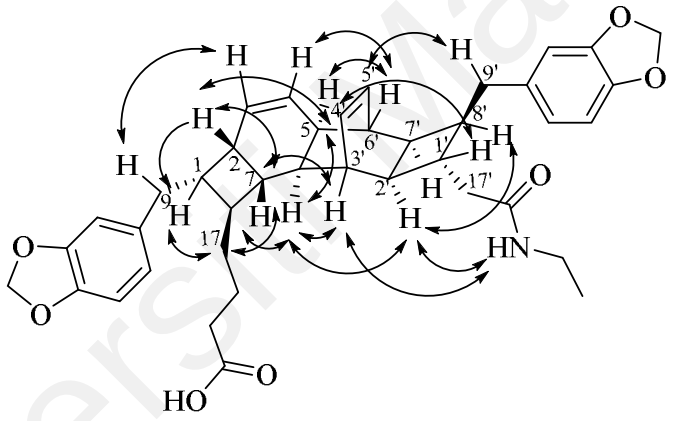

Figure 3.75: Key NOESY ($^1H \leftrightarrow {}^1H$) correlations of compound Q

Based on the spectroscopic data, compound Q was established as kingianin L (**56**), a known compound upon comparison of its spectroscopic data with those of the literature values of compound previously isolated from ***Endiandra kingiana*** by Leverrier et al. (2011).

Table 3.17: ^{1}H (600 MHz) and ^{13}C (150 MHz) NMR data of compound Q in $CDCl_3$

Position	Compound Q		Kingianin L (Leverrier et al., 2011)	
	δ_H (***J*** in Hz)	δ_C	δ_H (***J*** in Hz)	δ_C
1	2.01 m	43.4	1.99 m	43.6
2	2.43 m	32.6	2.43 m	32.9
3	5.56 dd (10.1, 10.3)	125.6	5.55 br d (10.4)	125.8
4	5.64 dd (10.1, 10.3)	131.9	5.63 br d (10.4)	132.1
5	2.23 m	38.2	2.21 m	38.5
6	1.67 d (8.8)	39.0	1.65 br d (9.0)	39.2
7	1.82 t (7.9)	42.4	1.80 m	42.7
8	1.59 m	45.1	1.57 m	45.3
9	2.46 m, 2.58 m	36.3	2.44 m, 2.56 m	36.5
10	-	135.4	-	135.6
11	6.63 d (1.2)	108.8	6.61 d (1.2)	109.0
12	-	147.5	-	147.7
13	-	145.4	-	145.6
14	6.67 d (7.8)	108.0	6.68 d (7.9)	108.3
15	6.57 dd (1.2, 7.8)	121.1	6.55 dd (7.9, 1.2)	121.3
16	5.89 s	100.7	5.89 s	100.9
17	1.28 m, 1.31 m	34.5	1.25 m, 1.30 m	34.7
18	1.51 m, 1.54 m	22.9	1.49 m	23.1
19	2.25 m	34.0	2.24 m	34.4
20	-	176.4	-	177.8
1’	2.08 m	39.0	2.07 m	39.2
2’	2.31 m	44.2	2.29 m	44.4
3’	2.43 m	42.9	2.41 m	43.1
4’	6.12 dd (7.2, 7.5)	132.4	6.10 dd (7.1, 7.6)	132.6
5’	6.23 dd (7.2, 7.5)	134.8	6.20 t (7.1)	135.0
6’	2.50 m	38.5	2.51 m	38.7
7’	2.50 m	39.7	2.49 m	39.9
8’	2.29 m	43.8	2.27 m	44.0
9’	2.50 m, 2.64 m	35.2	2.50 m, 2.62 m	35.4
10’	-	135.5	-	135.6
11’	6.61 d (1.0)	108.8	6.59 br s	109.0
12’	-	147.5	-	147.7
13’	-	145.4	-	145.6
14’	6.69 d (7.8)	108.1	6.66 d (7.9)	108.2
15’	6.56 dd (7.8, 1.0)	121.0	6.55 br d (7.9)	121.2
16’	5.91 s	100.7	5.87 s	100.9
17’	1.95 m, 2.08 m	43.0	1.93 m, 2.05 m	43.2
18’	-	172.0	-	172.4
19’	5.20 t (5.6)	-	5.20 t (5.7)	-
20’	3.23 dq (5.6, 7.1)	34.5	3.20 dq (7.2, 5.7)	34.5
21’	1.10 t (7.1)	15.1	1.08 t (7.2)	15.1

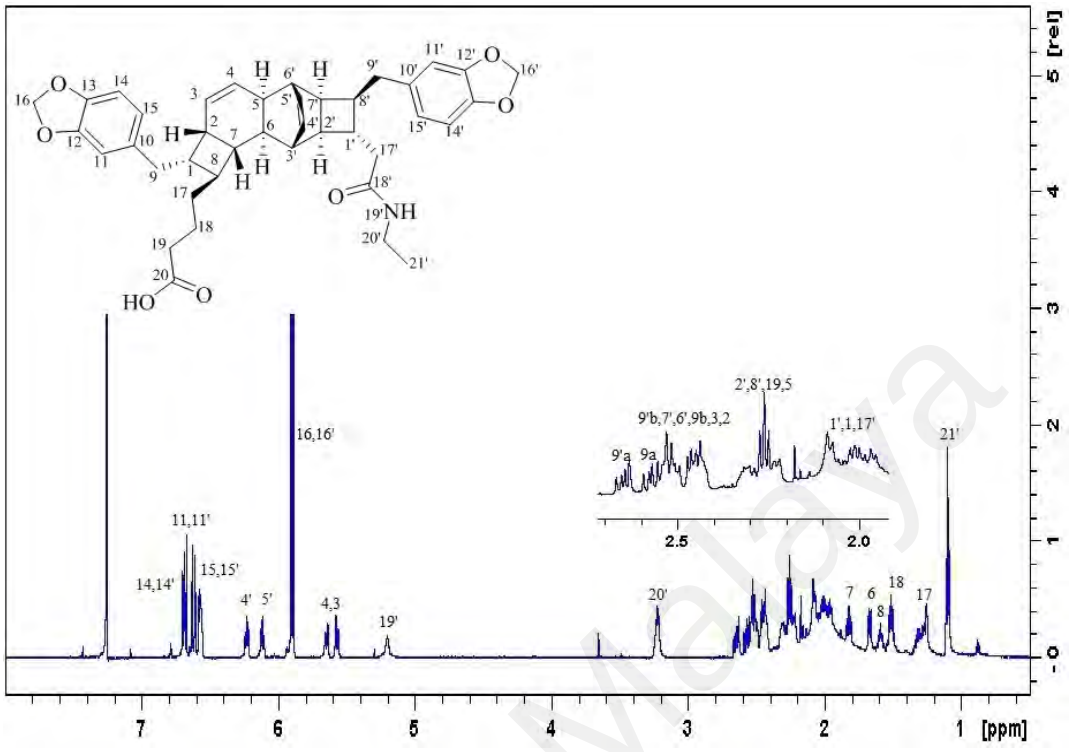

Figure 3.76: ^{1}H NMR spectrum for compound **56**

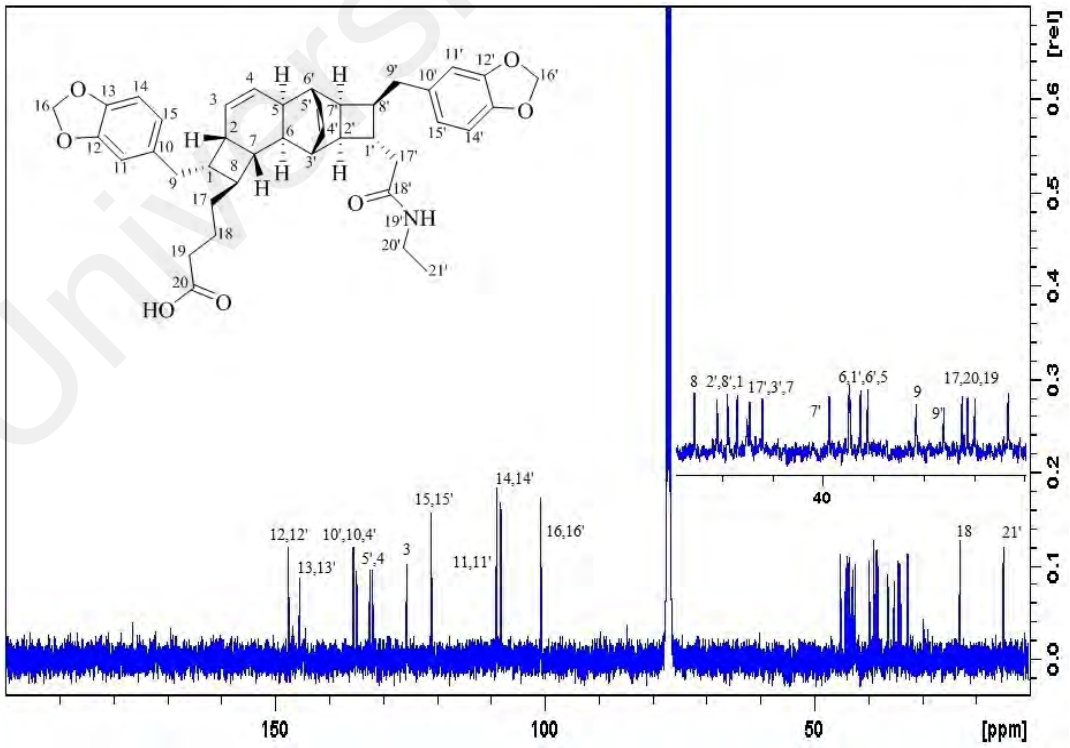

Figure 3.77: ^{13}C NMR spectrum for compound **56**

Compound R: Kingianin M (**57**)

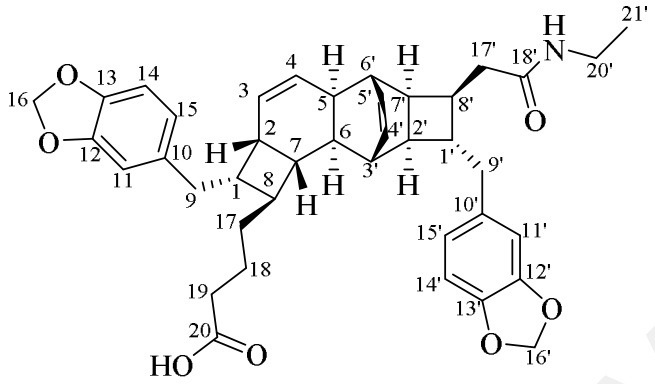

Compound R was isolated as an optically inactive white powder. The HRESIMS gave a pseudomolecular ion peak $[M+H]^+$ at ***m/z*** 652.3229 (calcd. for $C_{40}H_{46}NO_7$; 652.3274), consistent with a molecular formula of $C_{40}H_{46}NO_7$, the same as for **55** and **56**. The UV absorption of the benzenoid nucleus at 287 and 235 nm and the absorption bands around ν_{max} 3296, 1724, 1628 and 1500 cm^{-1} for N-H amide stretching, C=O acid and amide elongations, and N-H amide deformation in the IR spectrum (Silverstein et al., 1991, 1997; Pavia et al., 2009; Pretsch et al., 2009).

The ^1H NMR spectrum of compound R revealed four ***cis***-form vinyl protons resonating at δ_H 5.55 (dd, ***J*** = 10.1, 10.4 Hz, H-3), 5.67 (dd, ***J*** = 10.1, 10.4 Hz, H-4), 6.04 (dd, ***J*** = 7.1, 7.3 Hz, H-4′), and 6.14 (dd, ***J*** = 7.1, 7.3 Hz, H-5′). These signals were the characteristic features for kingianin. In addition, the signals for the two methylenedioxy groups, which resonated at δ_H 5.92 (s, H-16 and H-16′) and the 1,3,4-trisubstituted benzene ring systems at δ_H 6.65 (d, ***J*** = 1.3 Hz, H-11), 6.66 (d, ***J*** = 1.3 Hz, H-11′), 6.69 (d, ***J*** = 7.8 Hz, H-14 and H-14′), 6.58 (dd, ***J*** = 7.8, 1.3 Hz, H-15) and 6.59 (dd, ***J*** = 7.8, 1.3 Hz, H-15′) suggested the presence of the two methylenedioxyphenyl moieties (Leverrier et al., 2011). This compound was also characterized by the presence of the ***N***-ethylacetamide and butyric acid chains (Table 3.18).

The ^{13}C NMR and DEPT-135 spectra exhibited 40 signals for one methyl, 9 methylenes, 22 methines, including the four ***cis*** olefin carbons which resonated at δ_C 125.6 (C-3), 131.9 (C-4), 132.8 (C-4′) and 134.6 (C-5′), and 8 quaternary carbons (Table 3.18). Compound R was an isomer of compounds **55** and **56**. The ^{13}C NMR spectra exhibited signals for two quaternary carbons around δ_C 172.5 and 177.0, consistent with an amide and a carboxylic acid functionality (Pretsch et al., 2009; Crews et al., 1998). The presence of the two methylenedioxyphenyl groups were suggested by the resonances of the twelve aromatic carbons at δ_C 134.9 (C-10), 135.3 (C10′), 108.8 (C-11), 109.0 (C-11′), 147.3 (C-12), 147.4 (C-12′), 145.3 (C-13), 145.6 (C-13′), 108.0 (C-14 and C-14′) and 121.0 (C-15) 121.3 (C-15′), and those of the two methylenedioxy groups at δ_C 100.7 (C-16 and C-16′) in ^{13}C NMR spectra (Table 3.18). As a conclusion, this compound consists of four substituents; two methylenedioxybenzyl groups, one butyric acid chain and one ***N***-ethylacetamide group. The positions of these substituents were determined based on the 2D NMR correlations.

The COSY spectrum of compound R revealed correlations between H-1/H_2-9 and H-1′/H_2-9′ indicating that the two methylenedioxybenzyl groups were located at C-1 and C-1′. In addition, the HMBC correlations between H_2-9 and C-1, C-15 and C-2, and that of H_2-9′ with C-1′, C-15′ and C-11′ confirmed the connectivities of two methylenedioxybenzyl groups at C-1 and C-1′, respectively. Meanwhile, the COSY correlations of H-8-H_2-17-H_2-18-H_2-19, and the HMBC correlations between H_2-18 and H_2-19 with the C-20 carbonyl carbon (δ_C 177.0) confirmed that the butanoic acid chain was attached to C-8. Therefore, the ***N***-ethylacetamide group was located at C-8′. This was inferred from the COSY correlations between H-8′ and H_2-17′ and the HMBC correlations between the H_2-17′ and H_2-20′ with the C-18′ carbonyl carbon at δ_C 172.5 (Figure 3.78).

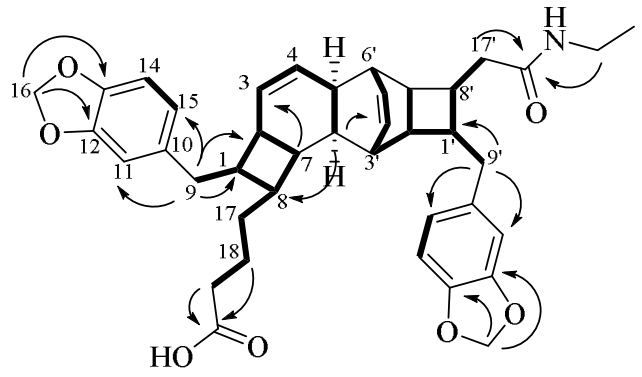

Figure 3.78: COSY (bold) and HMBC ($^{1}H \rightarrow ^{13}C$) correlations of compound R.

The relative configuration of compound R was assigned as ***rel***-(***1SR, 2SR, 5RS, 6RS, 7RS, 8SR, 1′SR, 2′RS, 3′RS, 6′SR, 7′SR, 8′SR***) via its NOESY experiment (Figure 3.79). The spatial arrangements of the pentacyclic main skeleton are similar to **55** and **56**. The correlations between H-2′/H-8′ and H-4′/H-1′ indicated the *β*–orientation of the ***N***-ethylacetamide group at C-8′ and the *α*–orientation of the phenyl group at C-1′. Meanwhile, the correlations between, H-6/H-8, H-8/H_2-9, H-7/H-1 and H-1/H_2-17 indicated the *β*–orientation of the acid chain at C-8, and the *α*–orientation of the methylenedioxyphenyl group at C-1.

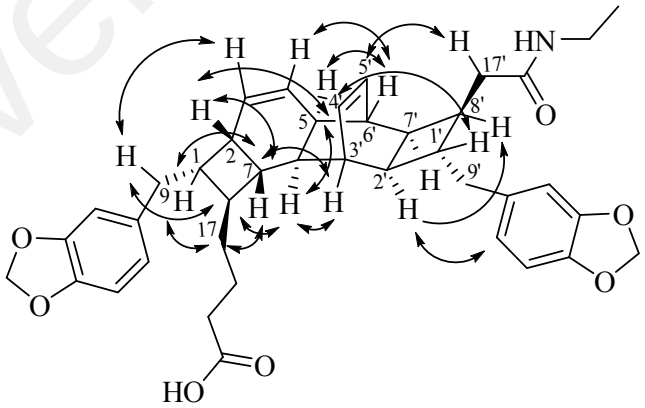

Figure 3.79: Key NOESY ($^{1}H \leftrightarrow ^{1}H$) correlations of compound R.

Based on these data and upon comparison with the literature values, compound R was identified as kingianin M (**57**), a known pentacyclic polyketide.

Table 3.18: ^{1}H (600 MHz) and ^{13}C (150 MHz) NMR data of compound R in $CDCl_3$

Position	Compound R		Kingianin M (Leverrier et al., 2011)	
	δ_H (***J*** in Hz)	δ_C	δ_H (***J*** in Hz)	δ_C
1	2.01 m	43.5	1.96 m	43.7
2	2.43 m	32.6	2.39 m	32.9
3	5.55 dd (10.1, 10.4)	125.5	5.53 br d (10.4)	125.7
4	5.67 dd (10.1, 10.4)	131.9	5.56 br d (10.4)	132.3
5	2.25 m	38.1	2.23 m	38.7
6	1.63 m	38.8	1.61 br d (9.0)	39.1
7	1.75 m	42.4	1.73 m	42.6
8	1.58 m	45.1	1.56 m	45.5
9	2.45 m, 2.59 m	36.3	2.42 m, 2.55 m	36.6
10	-	134.9	-	135.6
11	6.65 d (1.3)	108.8	6.61 d (1.2)	109.0
12	-	147.3	-	147.7
13	-	145.3	-	145.7
14	6.69 d (7.8)	108.0	6.65 d (7.9)	108.3
15	6.58 dd (7.8, 1.3)	121.0	6.54 dd (7.9, 1.2)	121.2
16	5.92 s	100.7	5.87 s	100.9
17	1.27 m, 1.37 m	34.7	1.24 m, 1.36 m	34.9
18	1.50 m	23.0	1.47 m	23.3
19	2.27 m	34.0	2.23 m	34.6
20	-	177.0	-	177.8
1′	1.92 m	43.6	1.87 m	43.8
2′	2.29 m	44.5	2.24 m	44.7
3′	2.21 m	43.0	2.16 m	43.3
4′	6.04 dd (7.3, 7.1)	132.8	5.99 dd (7.6, 7.1)	133.0
5′	6.14 dd (7.3, 7.1)	134.6	6.10 t (7.1)	134.8
6′	2.57 m	38.4	2.54 m	38.3
7′	2.55 m	39.0	2.53 m	39.3
8′	2.48 m	38.7	2.46 m	38.9
9′	2.60 m	41.9	2.56 m	42.1
10′	-	135.3	-	135.1
11′	6.66 d (1.3)	109.0	6.58 br s	109.2
12′	-	147.4	-	147.6
13′	-	145.6	-	145.6
14′	6.69 d (7.8)	108.0	6.68 d (7.9)	108.3
15′	6.59 dd (7.8, 1.3)	121.3	6.54 br d (7.9)	121.5
16′	5.92 s	100.7	5.87 s	100.9
17′	1.87 m	37.0	1.86 m, 2.21 m	37.2
18′	-	172.5	-	172.7
19′	5.25 t (5.9)	-	5.20 t (5.7)	-
20′	3.25 dq (5.9, 7.3)	34.3	3.21 dq (7.2, 5.7)	34.5
21′	1.11 t (7.3)	14.7	1.09 t (7.2)	15.2

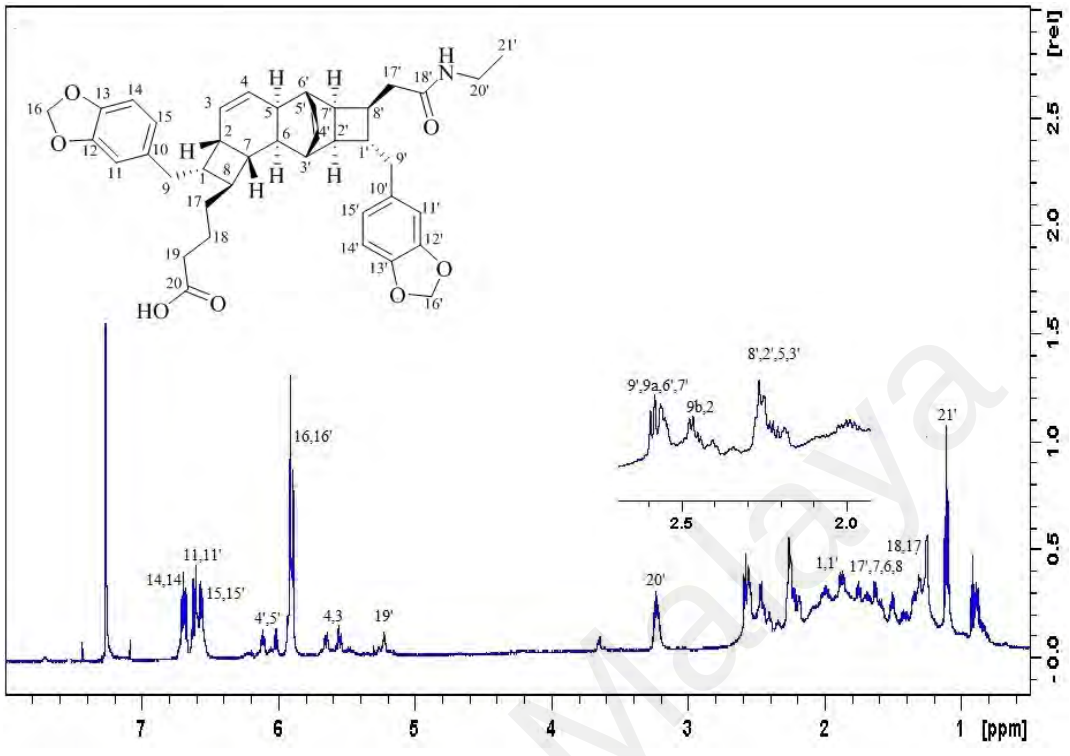

Figure 3.80: ^{1}H NMR spectrum for compound **57**

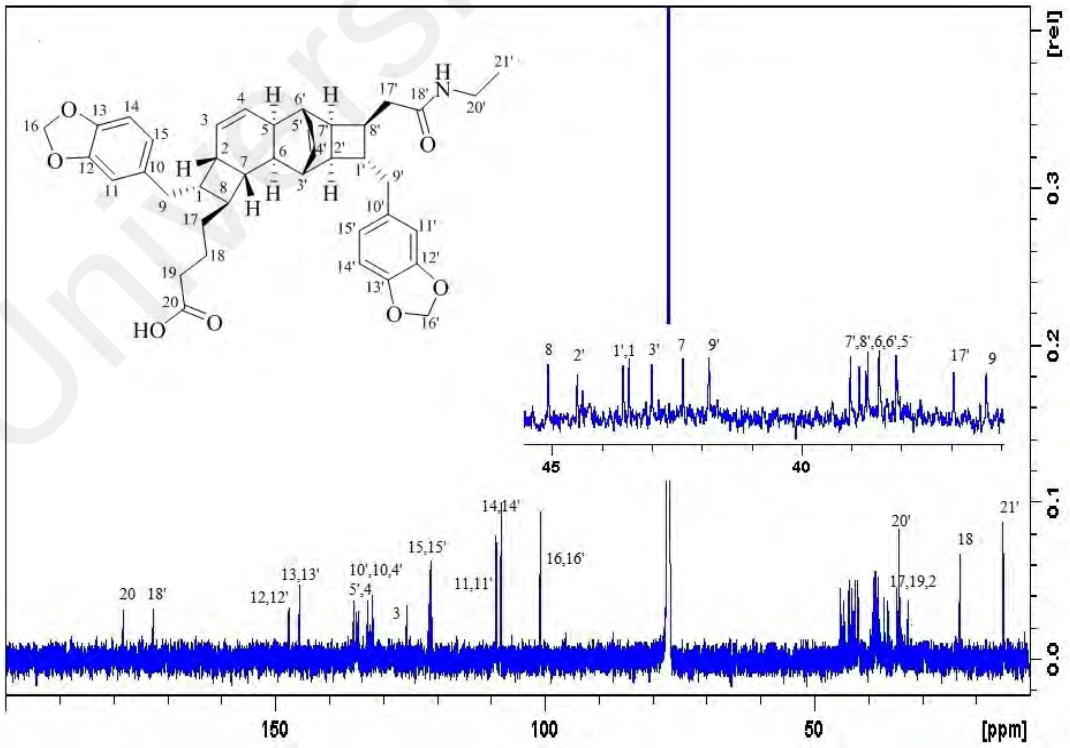

Figure 3.81: ^{13}C NMR spectrum for compound **57**

Compound S: Kingianin N (**58**)

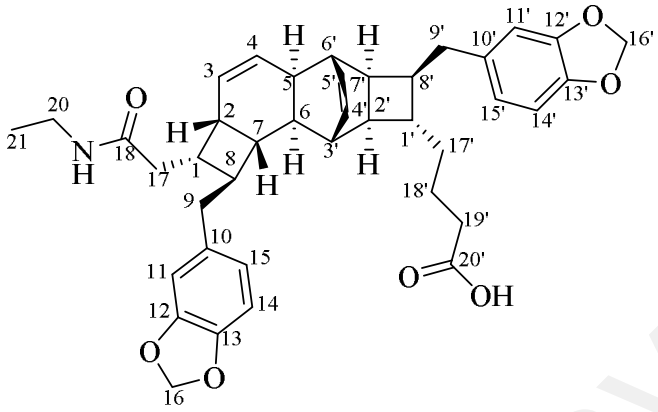

Compound S was obtained as white amorphous powder. The molecular formula was established by the $[M+H]^+$ ion peak at ***m/z*** 652.3286, corresponding to $C_{40}H_{46}NO_7$ (Calcd. for $C_{40}H_{46}NO_7$; 652.3282) in its HRESI mass spectra. The IR spectra revealed absorption bands at ν_{max} 3298, 1720, 1625 and 1541 cm^{-1} for the carboxylic acid and ***N***-ethylacetamide functionalities, similar to compounds **55-57** (Pretsch et al., 2009; Silverstein et al., 1997).

The characteristic four ***cis*** olefinic protons appeared at δ_H 5.48 (dd, ***J*** = 9.8, 10.2 Hz, H-3), 5.60 (dd, ***J*** = 9.8, 10.2 Hz, H-4), 6.06 (dd, ***J*** = 7.2, 7.5 Hz, H-4′) and 6.20 (dd, ***J*** = 7.2, 7.5 Hz, H-5′) in ^{1}H NMR spectrum. The signals for the two methylenedioxyphenyl moieties resonated as doublets at δ_H 6.63 (***J*** = 1.3 Hz, H-11) and 6.60 (***J*** = 1.3 Hz, H-11′), four ***ortho-meta***-coupled doublets at δ_H 6.68 (d, ***J*** = 8.0 Hz, H-14), 6.56 (dd, ***J*** = 8.0, 1.3 Hz, H-15), 6.71 (d, ***J*** = 8.0 Hz, H-14′) and 6.54 (dd, ***J*** = 8.0, 1.3 Hz, H-15′), and two singlets corresponding to two protons at δ_H 5.91 (H_2-16 and H_2-16′, respectively). An ***N***-ethylacetamide group was suggested from the presence of a doublet of quartets corresponding to two protons resonating at δ_H 3.23 (***J*** = 5.7, 7.3 Hz, H-20), a triplet of a methyl group at δ_H 1.10 (***J*** = 7.3 Hz, H-21) and a triplet at δ_H 5.27 (***J*** = 5.7 Hz, NH-19). Meanwhile, the presence of the butanoic acid group was suggested from the methylene

protons at δ_H 1.20-1.28, 1.38-1.47 and 2.26 ppm, corresponding to H_2-17′, H_2-18′ and H_2-19′, respectively (Table 3.19).

The ^{13}C NMR spectrum of compound S was similar to that of **57** and also contained the 16 skeletal signals of a pentacyclic carbon skeleton. The resonances of the methine carbons at C-1 (δ_C 38.5), C-2 (δ_C 32.8), C-5 (δ_C 38.0), C-6 (δ_C 38.3), C-7 (δ_C 42.0), C-8 (δ_C 47.3), C-1′ (δ_C 41.7), C-2′ (δ_C 44.3), C-3′ (δ_C 43.2), C-6′ (δ_C 38.6), C-7′ (δ_C 39.4) and C-8′ (δ_C 43.8), including the four olefinic carbons at C-3 (δ_C 124.8), C-4 (δ_C 132.2), C-4′ (δ_C 132.4) and C-5′ (δ_C 135.0) observed in the DEPT spectrum, confirmed the characteristic pentacyclic structure of kingianin. The presence of the two methylenedioxyphenyl fragments were confirmed by the ^{13}C NMR spectrum which showed characteristic signals of two 1,3,4-trisubstituted benzene rings between δ_C 108.0 – 148.0 and the two methylenedioxy groups at δ_C 100.7 (C-16 and C-16′). The presences of a butyric acid chain and an ***N***-ethylacetamide group were supported by their ^{13}C NMR spectra exhibiting two signals for the quaternary carbons at δ_C 178.0 (C-20′) and 172.2 (C-18), respectively (Table 3.19) (Crews et al., 1998; Pavia et al., 2009).

The COSY spectrum of compound S revealed cross peaks between H-8 and H_2-9, and between H-8′ and H_2-9′, allowing the placement of the two methylenedioxybenzyl groups at C-8 and C-8′. Meanwhile, the position of the ***N***-ethylacetamide group at C-1 was suggested by the HMBC correlations between H_2-17 with C-1, C-2 and C-18. Based on that evidence, the butanoic acid chain was therefore located at C-1′. This was supported by the correlations between H-1′/H_2-17′/H_2-18′/H_2-19′ observed in the COSY spectrum (Figure 3.82).

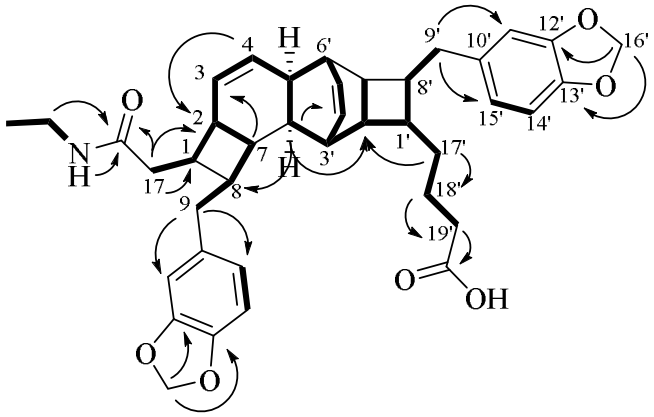

Figure 3.82: Key COSY (bold) and HMBC ($^{1}H \rightarrow {}^{13}C$) correlations of compound S.

The NOESY spectrum showed similar profile as in the previous compounds. The correlations between H-2′/H-8′, H-3′/H-8, H-2/H-1 and H-4′/H-1′ indicated the *β*–orientation of the two methylenedioxybenzyl groups at C-8 and C-8′, and the *α*–orientation of the ***N***-ethylacetamide and butanoic acid chains at C-1 and C-1′, respectively. These four substituents are in the ***anti*** position on the cyclobutane rings. Thus, the relative configuration of compound S was determined as ***rel***-(***1SR, 2SR, 5SR, 6RS, 7RS, 8SR, 1′SR, 2′RS, 3′RS, 6′SR, 7′SR, 8′RS***). Thus upon comparison of the obtained data with those of the literature values, compound S was identical to kingianin N (**58**) (Leverrier et al., 2011).

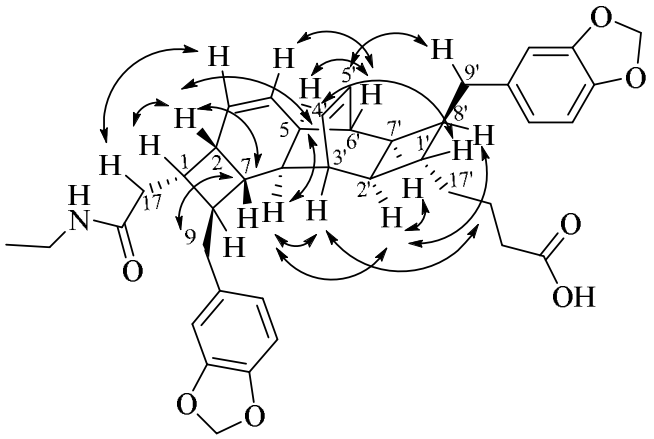

Figure 3.83: Key NOESY ($^{1}H \leftrightarrow {}^{1}H$) correlations of compound S.

Table 3.19: ^{1}H (600 MHz) and ^{13}C (150 MHz) NMR data of compound S in $CDCl_3$

Position	Compound S		Kingianin N (Leverrier et al., 2011)	
	δ_H (***J*** in Hz)	δ_C	δ_H (***J*** in Hz)	δ_C
1	2.21 m	38.5	2.20 m	38.9
2	2.52 m	32.8	2.49 m	33.0
3	5.48 dd (9.8, 10.2)	124.8	5.47 br d (10.4)	125.1
4	5.60 dd (9.8, 10.2)	132.2	5.59 br d (10.4)	132.6
5	2.09 m	38.0	2.07 m	38.3
6	1.30 d (8.7)	38.3	1.29 br d (9.0)	38.5
7	1.90 m	42.0	1.89 m	42.2
8	1.71 m	47.3	1.69 m	47.5
9	2.58 m	40.5	2.56 m	40.7
10	-	137.4	-	137.7
11	6.63 d (1.3)	109.3	6.60 d (1.2)	109.6
12	-	147.4	-	147.7
13	-	145.3	-	145.8
14	6.68 d (8.0)	108.0	6.69 d (7.9)	108.3
15	6.56 dd (8.0, 1.3)	121.6	6.56 dd (7.9, 1.2)	121.9
16	5.91 s	100.7	5.88 s	100.9
17	1.84 m, 2.06 m	37.6	1.83 m, 2.05 m	37.9
18	-	172.2	-	172.4
19	5.27 t (5.7)	-	5.25 t (5.7)	-
20	3.23 dq (7.3, 5.7)	34.3	3.21 dq (7.2, 5.7)	34.5
21	1.10 t (7.3)	14.9	1.08 t (5.7)	15.1
1′	1.66 m	41.7	1.64 m	41.9
2′	1.93 m	44.3	1.91 m	44.5
3′	2.25 m	43.2	2.24 m	43.4
4′	6.06 dd (7.2, 7.5)	132.4	6.03 dd (7.6, 7.1)	132.4
5′	6.20 dd (7.2, 7.5)	135.0	6.17 t (7.1)	135.5
6′	2.44 m	38.6	2.44 m	38.7
7′	2.39 br t (7.3)	39.4	2.37 m	39.6
8′	2.17 m	43.8	2.15 m	44.1
9′	2.45 m, 2.62 m	35.5	2.43 m, 2.59 m	35.7
10′	-	135.8	-	136.0
11′	6.60 d (1.3)	108.8	6.57 br s	109.0
12′	-	147.4	-	147.7
13′	-	145.6	-	145.6
14′	6.71 d (8.0)	108.1	6.66 d (7.9)	108.3
15′	6.54 dd (8.0, 1.3)	121.0	6.52 br d (7.9)	121.2
16′	5.91 s	100.7	5.88 s	100.9
17′	1.20 m, 1.28 m	36.0	1.16 m, 1.25 m	36.2
18′	1.38 m, 1.47 m	22.6	1.34 m, 1.45 m	22.7
19′	2.26 m	34.2	2.22 m	34.1
20′	-	178.0	-	178.2

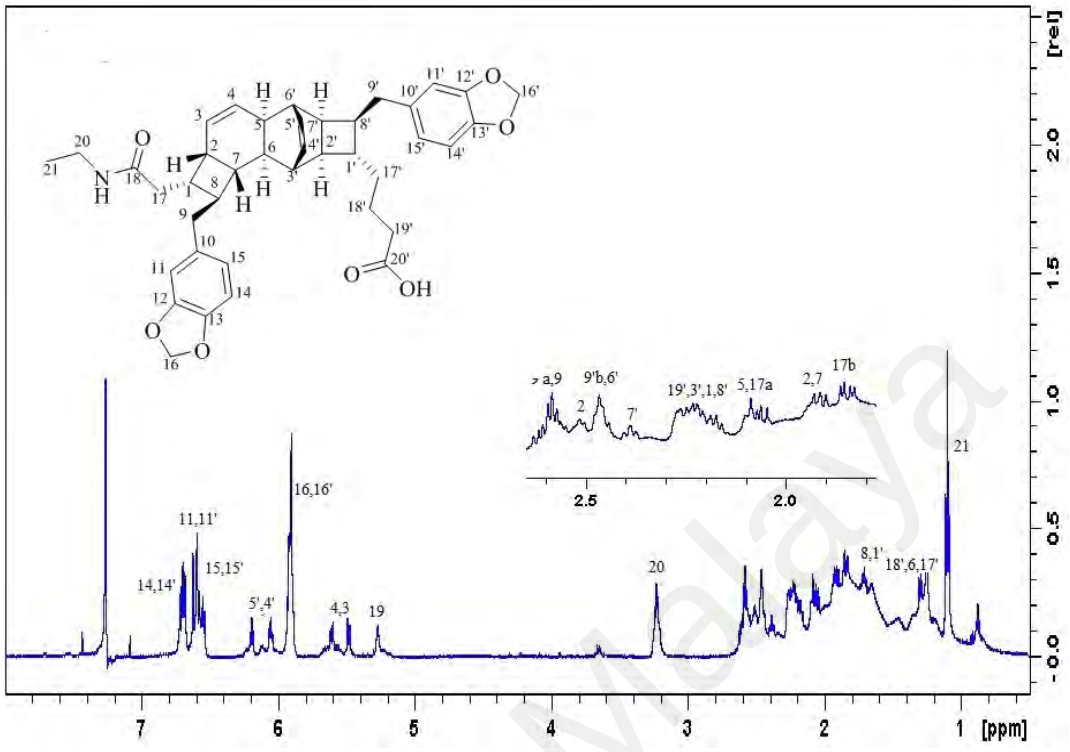

Figure 3.84: ^{1}H NMR spectrum for compound **58**

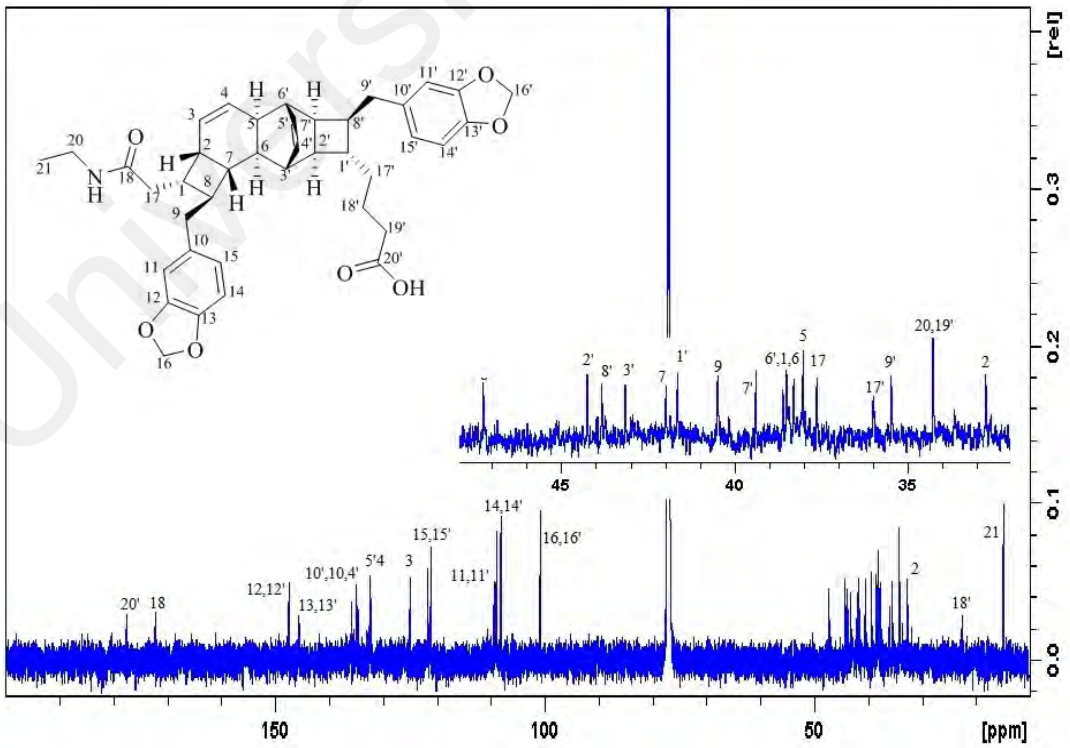

Figure 3.85: ^{13}C NMR spectrum for compound **58**

3.2 Conclusion

The phytochemical study of methanol extract of ***Endiandria kingiana***, led to the isolation and characterization of 19 cyclic polyketides. These compounds were divided into two major classes; endiandric acids and kingianins. Ten tetracyclic endiandric acids were isolated named; kingianic acids A-H (**120**-**127**), together with known endiandric acid M (**93**) and tsangibeilin B (**89**). Among them, three were new (kingianin O-Q [**128**-**130**]) while the remaining have already been reported by Leverrier et al. (2011).

In Lauraceae family, endiandric acids and kingianins are frequently isolated as racemic mixture from genus ***Endiandra*** and ***Beilschmiedia.*** Beside these two polyketides, five flavonoids were reported from ***B. zenkeri*** (Lenta et al., 2009) and ***B. miersii*** (Harborne & Méndez, 1969), while lignans and triterpenoids were isolated from ***B. tsangii*** (Chen et al., 2006, 2007). In addition, several alkaloids were also isolated from ***B. madang***, ***B. elliptica***, ***B. obscura***, ***B. alloiophylla***, ***B. kunstleri*** and ***B. brevipes*** (Kitagawa et al., 1993; Clezy et al., 1966; Lenta et al., 2011, Mollataghi et al., 2011, 2012; Pudjiastuti et al., 2010). The abundance of these endiandric acids and kingianins in different ***Endiandra*** and ***Beilschmiedia*** species is highly variable. It has been hypothesized that these cyclic polyketides are the primary metabolites from these two plant species and may be useful as chemotaxonomic markers within the Lauraceae family. Their structures can be differentiated by the modification status of the phenyl or alkyl side chain on tetracyclic core at C-11 (endiandric acid type A) or C-13 (endiandric acid type B/B'). In the endiandric acids, the substituents at western and eastern parts are carboxylic acid and aromatic moieties, respectively, similar to the species collected in Asia and Africa but not in Australia. Meanwhile, the kingianins with pentacyclic carbon skeleton (bicyclo [4.2.0] backbone) skeleton and fourteen stereocenters are reported herein for the first time form the ***Endiandra*** species. Some of these compounds were

subjected to Bcl-xL and Mcl-1 binding affinities, cytotoxic activity on various cancer cell lines, anti-inflammatory, anti-bacterial, anti-plasmodial and neuroprotective assays.

The biogenetic hypothesis of kingianin series are based on electrocyclization reaction from conjugated polyenes. It justified the racemic character and the relative configuration of kingianins in particular the ***anti*** position (2 substituents positioned on the same side of the cyclobutane). This probable biogenesis led to consideration of a reversed biomimetic synthetic scheme in order to achieve their total synthesis. Preliminary work was undertaken to develop a strategy synthesis of the monomer and this work was carried out under the supervision of Dr. Yvan Six (Ecole Polytechnique).

CHAPTER 4

BCL-XL/BAK AND MCL-1/BID BINDING AFFINITIES AND CYTOTOXIC ACTIVITY OF CYCLIC POLYKETIDES

4.1 Introduction

Natural products have always been used as sources of lead molecules for the development of the most effective drugs currently available for the treatment of variety of human diseases (Cragg & Newman, 2005; Newman et al., 2003; Harvey, 2008). Today, over 100 natural product derivatives are currently undergoing clinical trials and at least 100 similar projects are in preclinical development (Butler, 2004). The projects based on natural products are predominantly being studied for use in the therapeutic areas of infectious diseases and cancer. They are also able to interact with many specific targets within the cell, and indeed for many years have been central in the drug discovery programs (Mishra & Tiwari et al., 2011). In this study, the isolated compounds were evaluated for two bioassays: Bcl-xL and Mcl-1 of binding affinities and cytotoxic effects against various human tumour cells.

4.2 Evaluation of Bcl-xL/Bak and Mcl-1/Bid binding affinities

Bcl-xL (B-cell lymphoma – extra large), Mcl-1 (myeloid cell leukemia 1) and Bcl-2 (B-cell lymphoma 2) are antiapoptotic proteins, which play a major role in cell death in many eukaryotic systems (Yip & Reed, 2008; Lessene et al., 2008; Cotter, 2009; Elmore, 2007; Wang, 2008; Dharap et al., 2006). These proteins are members of the "Bcl-2" family. The over expression of these proteins and the damage of Bcl-2 gene have given rise to a number of cancers including melanoma, breast, prostate, chronic lymphocytic leukemia and lung cancer, as well as a possible cause of schizophrenia and autoimmunity. It has also lead to the resistance of tumor cells toward the apoptosis

process (Jeng & Cheng, 2013; Youle & Strasser et al., 2008; Lessene at al., 2013; Strasser et al., 2011). Consequently, antiapoptotic Bcl-2 proteins, such as Bcl-xL and Mcl-1 have become attractive molecular targets for cancer treatment or prevention drug discovery (Fesik, 2005; Glaser et al., 2012; Wells & McClendon, 2007; Mullard, 2012; Beroukhim et al., 2010; Czabotar et al., 2013).

Many apoptotic signals culminate in permeabilizing the mitochondrial outer membrane (MOM), resulting in the release of apoptogenic factors such as cytochrome ***c*** and SMAC to activate caspases. Bax and Bak are essential effectors responsible for mitochondrial outer membrane permeabilization (MOMP), while Bcl-2, Bcl-xL and Mcl-1 preserve mitochondrial integrity (Figure 4.1). The third Bcl-2 subfamily, "BH3-only" proteins (BH3s), promote apoptosis by either activating Bax and Bak (activator BH3s) or inactivating Bcl-2, Bcl-xL and Mcl-1 (in activator BH3s) (Youle & Strasser, 2008; Kim et al., 2009).

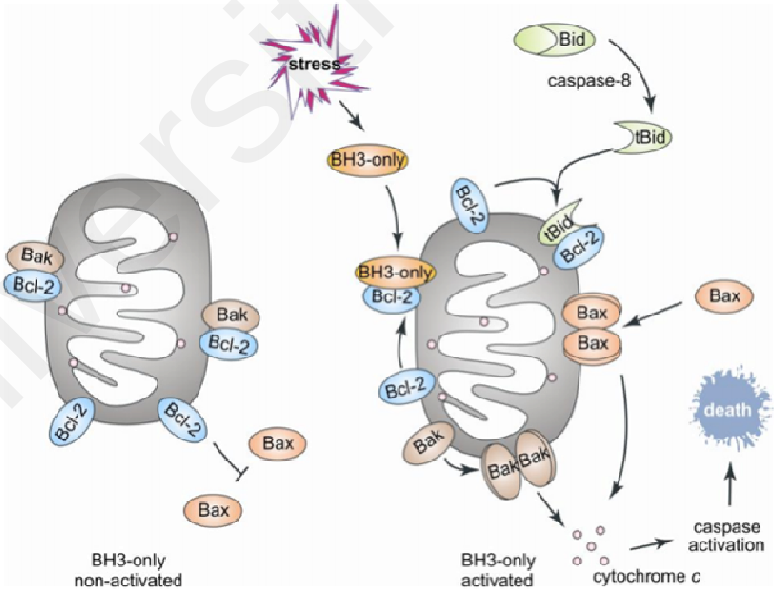

Figure 4.1: Apoptosis in mitochondria membrane (Rautureau et al., 2010)

In normal cells, Bax and Bak are generally monomeric and inactive either through auto inhibition or because they are held in check by anti-apoptotic Bcl-2 proteins. In

response to apoptotic signals, activator BH3s, including truncated Bid (a BH3-interacting domain death agonist), Bim and PUMA, bind Bax and Bak to induce structural reorganization and oligomerization of Bax and Bak at the MOM for MOMP (Czabotar et al., 2013; Kim et al., 2009; Davids & Letai, 2012).

Antiapoptotic "Bcl-2" proteins prevent apoptosis by sequestering either activator BH3s or monomeric Bax and Bak, thus preventing the oligomerization and activation of Bax and Bak (Davids & Letai, 2012). In both scenarios, the protein-protein interactions are mediated by the hydrophobic groove of anti-apoptotic Bcl-2 members and by the BH3 domain of proapoptotic Bcl-2 members. The ability of anti-apoptotic Bcl-2 proteins to sequester proapoptotic Bcl-2 members can be further modulated by 'inactivator' BH3s through high-affinity competitive binding (Davids & Letai, 2012).

Cancer cells often over-express the antiapoptotic "Bcl-2" proteins through mutations such as chromosomal translocation involving Bcl-2 or amplification of Bcl-xL and Mcl-1 (Davids & Letai, 2012; Walensky, 2012). The hydrophobic binding groove of anti-apoptotic "Bcl-2" proteins is critical for their prosurvival function; targeted inhibition of this groove can induce apoptosis in cancer cells by liberating the trapped activator BH3s or multi domain Bax and Bak (Davids & Letai, 2012; Walensky, 2012).

To date, only a few compounds targeting these proteins have progressed to clinical studies owing to the challenges associated with targeting protein-protein interactions (Davids & Letai, 2012). The first inhibitor of antiapoptotic "Bcl-2" proteins is ABT-737 (**131**), developed by Abbott Laboratories in mid-2000s (Davids & Letai, 2012; Walensky, 2012). This compound is part of BH3 mimetic small molecule inhibitors (SMI), which target these "Bcl-2" proteins except proteins A1 and Mcl-1 (Lessene et al, 2008; Ren et al., 2010; Azmi & Mohammad, 2009; Vogler et al., 2008; Rooswinkel et al., 2012). This compound showed efficacy for treating lymphoma and blood cancer (Tahir et al., 2007; Hann et al., 2008; Anderson et al., 2014). Meanwhile, its analogues

ABT-263 (Navitoclax®) **132** showed function like Bad mimetics that bind Bcl-2, Bcl-xL, and Bcl-w (Walensky, 2012; Park et al., 2008; Tse et al., 2008). This compound was evaluated in clinic for lymphoid malignancies, especially in Bcl2-addicted chronic lymphocytic leukemia (Anderson et al., 2014; Roberts et al., 2012; Ackler et al., 2008; Wilson et al., 2010). ABT-199 (**133**) was designed as BH3-mimetic drug to block the function of the Bcl-2 proteins, on patients with chronic lymphocytic leukemia (Davids & Letai, 2013; Touzeau et al., 2014; Souers et al., 2013). This analogue was developed because inhibition of Bcl-xL by ABT-263 (**132**) caused dose-dependent thrombocytopenia due to the dependence of platelets on Bcl-xL for survival (Souers et al., 2013).

The major gateway to apoptosis is guarded by Bcl-2 and its prosurvival relatives, such as Bcl-xL and Mcl-1, which are strongly implicated in tumor development and the resistance to diverse cytotoxic therapies. In this study, the goal is to investigate the Bcl-xL and Mcl-1 binding affinities of selected compounds isolated from ***Endiandra kingiana***. This is based on the preliminary study on this extract that showed the potent inhibition and high potency as a modulating agent between Bcl-xL and Bak (Leverrier et al., 2011). The idea of targeting Bcl-2 family proteins for cancer therapy is explained in Figure 4.3.

Cancers commonly express elevated levels of antiapoptotic "Bcl-2" proteins to prevent the activation of Bax and Bak by activator BH3-only molecules (BH3s, for example Bim or PUMA, orange circles, Figure 4.3). Natural compounds can displace bound activator BH3s or monomeric Bax and Bak from Bcl-xL to induce the homo-oligomerization of Bax and Bak, leading to MOMP and apoptosis (Figure 4.3). (**a**) In cancer cells that overexpress multiple antiapoptotic Bcl-2 members (Bcl-xL, Bcl2 and Mcl-1), these "Bcl-2" proteins are not fully engaged by proapoptotic Bcl-2 members (activator BH3s, Bax and Bak). Consequently, Bax and Bak will remain monomeric,

and cells will survive. (**b**) Targeting cancer-specific survival or death pathways to induce activator BH3s will saturate the binding pockets of antiapoptotic Bcl-2 members, allowing the natural compound to function as a single-agent inducer of apoptosis while sparing normal cells.

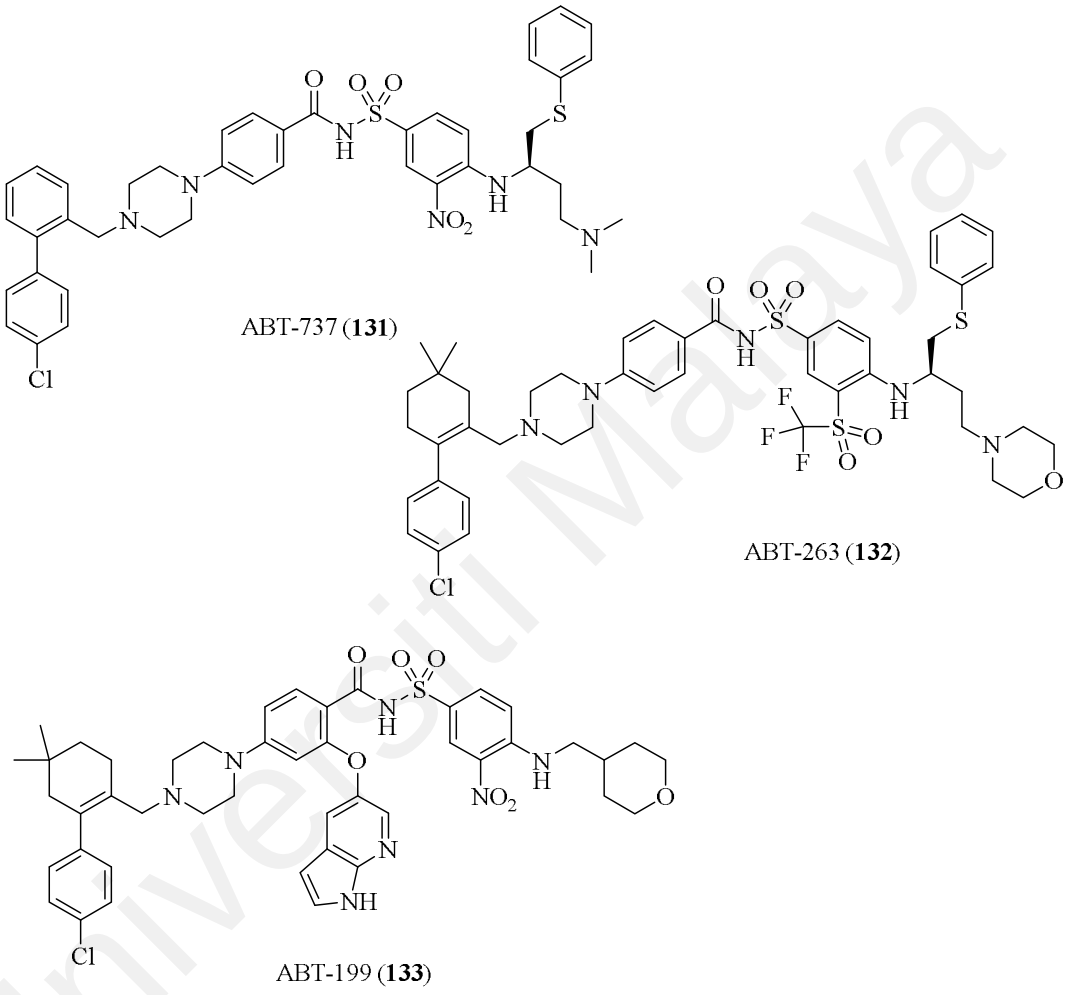

Figure 4.2: Example of antiapoptotic inhibitors

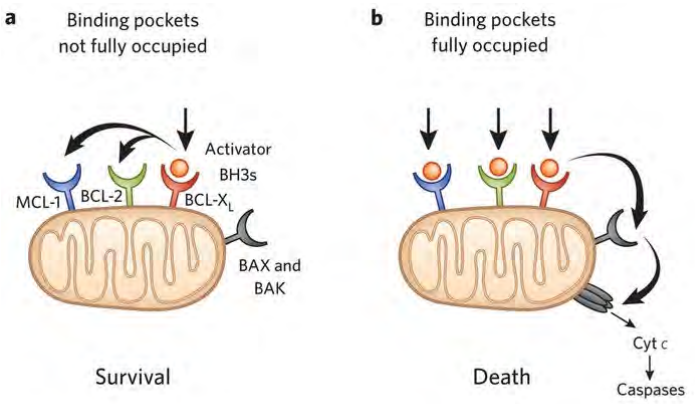

Figure 4.3: Targeting Bcl-2 family proteins for cancer therapy (Jeng & Cheng, 2013)

The aim of this study was to investigate the Bcl-xL and Mcl-1 binding affinities of endiandric acids analogues and new kingianins, and to fulfill a SAR analysis on these types of compounds. The knowledge acquired from this investigation hopes to provide further insights and understanding on the structural features that could influence the activity of a compound belonging to a cyclic polyketide type.

4.2.1 Evaluation of endiandric acid analogues on Bcl-xL/Bak and Mcl-1/Bid binding affinities

In this assay, compounds **89**, **93**, **120**, **122**, **124-126** were screened against the antiapoptotic proteins Bcl-xL and Mcl-1 using fluorescence polarization methods according to Qian et al. (2004). These assays are based on the interaction of fluorescein-labeled peptides [the BH3 domain of BAK protein (F-Bak) or BID protein (F-Bid) to Bcl-xL and Mcl-1, respectively]. The results are given as the percentage (%) of binding at 20 and 100 µM, and biological data were compared with the result obtained for ferrugineic acids (Apel et al., 2014) to perform the SAR analysis. The results are summarized in Table 4.1. Based on these results, all tested compounds showed no binding activity on Bcl-xL, and only moderate binding affinity for Mcl-1 (25-30%

inhibition at 20 μM and ≥ 75% at 100 μM) were obtained with compounds **89**, **122** and **125**. Compounds **121**, **123** and **127** were not evaluated due to the lack of amount.

Table 4.1: Bcl-xL and Mcl-1 binding affinities of endiandric acid analogues

	Compounds	**Bcl-xL/Bak binding affinity (%)**		**Mcl-1/Bid binding affinity (%)**	
		20 μM	100 μM	20 μM	100 μM
GROUP 1	Kingianic acid A (**120**)	3 ± 2	21 ± 2	3 ± 2	36 ± 2
	Kingianic acid C (**122**)	9 ± 2	25 ± 2	30 ± 2	75 ± 1
	Kingianic acid E (**124**)	2 ± 1	1 ± 1	3 ± 1	8 ± 6
	Endiandric acid M (**93**)	0	10 ± 1	4 ± 1	39 ± 1
	Ferrugineic acid K (**119**) [a]	NT	22 ± 3	NT	81 ± 3
GROUP 2	Kingianic acid F (**125**)	4 ± 2	22 ± 3	28 ± 4	80 ± 1
	Tsangibeilin B (**89**)	6 ± 2	26 ± 3	25 ± 2	81 ± 3
	Ferrugineic acid A (**109**) [a]	NT	22 ± 2	NT	0
	Ferrugineic acid B (**110**) [a]	NT	60 ± 6	NT	85 ±2
	Ferrugineic acid C (**111**) [a]	NT	93 ± 3	NT	82 ± 2
	Ferrugineic acid D (**112**) [a]	NT	39 ± 3	NT	82 ± 2
	Ferrugineic acid E (**113**) [a]	NT	20 ± 1	NT	82 ± 2
GROUP 3	Kingianic acid G (**126**)	5 ± 1	19 ± 2	8 ± 1	47 ± 3
	Ferrugineic acid F (**114**) [a]	NT	7 ± 1	NT	14 ± 3
	Ferrugineic acid G (**115**) [a]	NT	17 ± 1	NT	0
	Ferrugineic acid I (**117**) [a]	NT	35 ± 1	NT	3 ± 1
	Ferrugineic acid J (**118**) [a]	NT	58 ± 7	NT	7 ± 2
	ABT-737 (Ki)	NT	57 ± 10 nM	NT	47 ± 22 nM

NT: not tested
[a] Data for comparison and SAR study (Apel et al., 2014)

The structure-activity relationships (SAR) analyses were performed to understand the relationship between the chemical structure and potency of binding affinities. The observations were compared with the results obtained for ferrugineic acids, isolated from ***Beilschmiedia ferruginea*** by Apel et al. (2014). From these results, the endiandric acids can be separated into three groups according to their tetracyclic carbon skeletons.

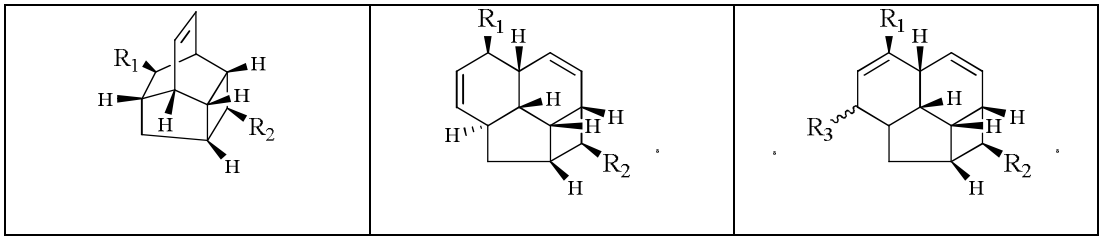

Group 1 **Group 2** **Group 3**

Figure 4.4: Endiandric acid tetracyclic carbon skeletons

In the first group characterized by a tetracyclic ring system formed with 11 carbon atoms (compounds **120, 122, 124**, **93** and **119**), only compounds **122** showed a weak binding affinity for Mcl-1, and no compound showed binding affinity for Bcl-xL. In contrast, in the second group $\Delta^{4,5}$ and $\Delta^{8,9}$ double bonds (compounds **125**, **89** and **109-113**), compounds **110** and **111** exhibited important binding affinities for both anti-apoptotic proteins, and compound **112** showed only a strong binding affinity for Mcl-1. Considering the weak binding affinity for Bcl-xL of compounds **125**, **89**, **109** and **113**, it could be postulated that the length of the saturated carbon side chain at eastern part of skeleton (preferentially five or seven methylene groups) associated with a terminal 4-hydroxyphenyl ring, play a crucial role for Bcl-xL and Mcl-1 binding affinities.

In the third group characterized by the same tetracyclic ring system as the previous one but with $\Delta^{5,6}$ and $\Delta^{8,9}$ double bonds (compound **126**, **114**, **115**, **117** and **118**), only compound **118** showed a important binding affinity for Bcl-xL protein, indicating that the β-oriented C-4 hydroxy group (cf. **118** versus **117**) and the length of the saturated carbon side chain (preferentially five methylene groups, cf. **118** versus **115**) are essential for the activity.

The structural requirement of endiandric acid analogues as dual inhibitors of Bcl-xL/Bak and Mcl-1/Bid interactions are clarified as follows (Figure 4.5):

i. The main tetracyclic skeleton formed with 13 carbon atoms with four ***cis***-form olefinic proton at $\Delta^{4,5}$ and $\Delta^{8,9}$, or at $\Delta^{5,6}$ and $\Delta^{8,9}$) are essential to exhibit good binding affinities for both antiapoptotic proteins (groups 2 and 3).

ii. The length of the saturated carbon side chain at C-11 for compounds in groups 2 and 3 (preferentially five methylene groups) are essential for a strong activity.

iii. The β-orientation of hydroxyl group (-OH) at C-4 for compounds in group 3 is essential for increasing the activity in Bcl-xL/Bak binding affinity.

iv. The presence of the 4-hydroxy phenyl substitution in saturated carbon side chain at C-11 is tolerated (group 2).

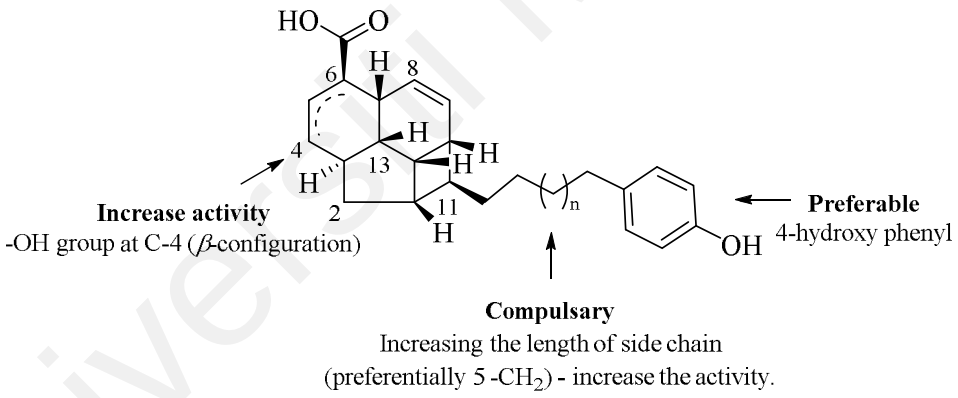

Figure 4.5: The important structural features of endiandric acid analogues for Bcl-xL and Mcl-1 binding affinities

4.2.2 Evaluation of kingianin analogues on Bcl-xL/Bak and Mcl-1/Bid binding affinities

In kingianin series, the binding affinities of the racemic mixtures of compounds **128-130** together with known kingianins A-N were evaluated on Bcl-xL/Bak and Mcl-1/Bid. Results are given by the ***Ki*** value i.e the concentration corresponding to 50% of inhibition of the binding of the labelled reference compound, and corrected for experimental conditions according to Cheng and Prusoff (1973) (Table 4.2). The ***Ki*** value is the inhibitory constant and specifically reflective of the binding affinity. The smaller the ***Ki***, the greater the binding affinity and the smaller amount of medication needed in order to inhibit the activity of that enzyme. The results will be compared with reported values by Litaudon group for structural activity relationship (SAR) (Leverrier et al., 2011).

. Considering the racemic mixtures, it was shown in previous study (Leverrier et al., 2011) that the presence of one, or preferably two acidic chains was essential for a significant binding affinity for the protein Bcl-xL, (±)-kingianin G, and to a lesser extent (±)-kingianins H-J, being the most active compounds (Figure 4.6). Taking into account the stereochemistry of the compounds, the binding affinity was significantly increased for the (-)-enantiomers compared to the (+)-enantiomers, as illustrated by comparing the $\boldsymbol{K}_i$ for (-)- and (+)-kingianins G-L. In contrast with these, the stereochemistry of the molecules does not play such a vital role for a significant binding affinity for Mcl-1. Indeed, it can be noted that (-)-kingianins G, H, J, K and L exhibited similar binding affinities than their respective (+)-counterparts. It should be noted that (-)- and (+)-kingianins G, H, and J exhibited the most potent binding affinities for the protein Mcl-1 with $\boldsymbol{K}_i$ comprised between 2 and 4 $\boldsymbol{\mu}$M, while (-)- and (+)-kingianins K and L were less active ($13 < \boldsymbol{K}_i < 17$ µM) , suggesting that two acidic chains located at either positions 1 and 8' or 1' and 8 on the pentacyclic core are essential for a significant

binding affinity. Based on these results, it could be deduced that (-)-kingianins G, H, and J proved to be the most potent dual inhibitors of Bcl-xL/Bak and Mcl-1/Bid interactions. For new kingianins, only kingianin P (**129**) showed potent binding for Bcl-xL (13 ± 2 µM) and moderate binding affinity for Mcl-1 (30 ± 1 µM) (Table 4.2).

Table 4.2: Bcl-xL and Mcl-1 binding affinities of kingianin analogues

Compounds	**Bcl-xL/Bak binding affinity (Ki, µM)[b]**			**Mcl-1/Bid binding affinity (Ki, µM)[b]**		
	Racemic mixture	**Enantiomer (-)**	**Enantiomer (+)**	**Racemic mixture**	**Enantiomer (-)**	**Enantiomer (+)**
Kingianin O (**1**)	> 23	n.d	n.d	> 33	n.d	n.d
Kingianin P (**2**)	13 ± 2	n.d	n.d	30 ± 1	n.d	n.d
Kingianin Q (**3**)	> 23	n.d	n.d	> 33	n.d	n.d
Kingianin A (**4**) [a]	213 ± 53	60 ± 2	> 300	n.d	> 33	> 33
Kingianin B [a]	> 300	n.d	n.d	> 33	n.d	n.d
Kingianin C [a]	> 300	n.d	n.d	> 33	n.d	n.d
Kingianin D [a]	> 300	n.d	n.d	> 33	n.d	n.d
Kingianin E [a]	> 300	n.d	n.d	> 33	n.d	n.d
Kingianin F (**5**) [a]	231 ± 47	n.d	n.d	> 33	n.d	n.d
Kingianin G [a]	2 ± 0	1 ± 1	5 ± 1	n.d	2 ± 2	3 ± 1
Kingianin H [a]	18 ± 7	4 ± 1	27 ± 1	n.d	4 ± 2	4 ± 3
Kingianin I [a]	18 ± 3	12 ± 1	16 ± 2	n.d	n.d	n.d
Kingianin J [a]	29 ± 6	9 ± 1	25 ± 3	n.d	2 ± 1	2 ± 1
Kingianin K (**6**) [a]	80 ± 36	6 ± 1	112 ± 15	n.d	17 ± 7	13 ± 4
Kingianin L (**7**) [a]	36 ± 11	4 ± 1	71 ± 10	n.d	15 ± 4	16 ± 2
Kingianin M (**8**) [a]	236 ± 34	n.d	n.d	> 33	n.d	n.d
Kingianin N (**9**) [a]	177 ± 9	n.d	n.d	19 ± 7	n.d	n.d
Meiogynin A (control)	4 ± 1			5 ± 1		

n.d: not determined

[a] Data for comparison and SAR study. Data from Leverrier et al., 2011.

[b] The ***Ki*** values are the means +/- standard deviation from three replicates

Figure 4.6: Binding affinity increase with the number of acid substituents

From these results, it could be postulated that the kingianins bind to the proteins through probable H-bonding. So, the presence of two acidic, or one acidic and one ***N***-ethylacetamide side chains, and their spatial position are essential for a significant binding affinities for Bcl-xL and Mcl-1. This is explained in Figure 4.7.

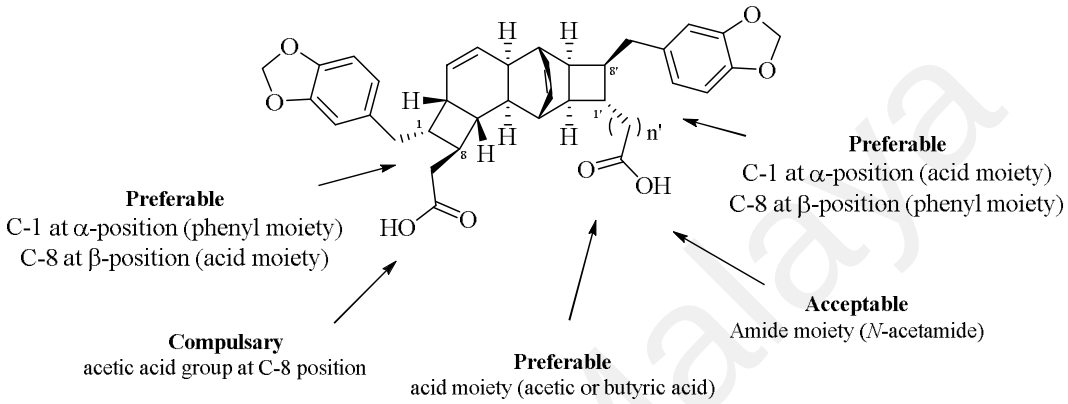

Figure 4.7: The important structural features of kingianins for binding affinities

4.3 Evaluation of Cytotoxic Activities of Endiandric Acid Derivatives

Cytotoxic therapy is a cancer treatment that uses chemical substance, especially one or more anti-cancer drugs that are given as part of the standardized chemotherapy regimen. Chemotherapy may be given a curative intent, or it may be aimed to prolong life or to reduce symptoms. This treatment is often used in conjunction with other cancer treatments, such as radiation therapy, surgery and/or hyperthermia therapy. Treatments such as radiation and surgery are considered as local treatments (Masui et al., 2013). They act only in one area of the body such as the breast, lung, or prostate, and usually target the cancer directly. Chemotherapy differs from surgery or radiation in that it is used as a systemic treatment, in which the drugs travel throughout the body to target the cancer cells. Traditional chemotherapeutic agents are cytotoxic; they act by killing cells that divide rapidly, one of the main properties of most cancer cells. This

means chemotherapy also harm cells that divide rapidly under normal circumstances (Masui et al., 2013).

Most chemotherapeutic drugs work by impairing mitosis, effectively targeting fast-dividing cells. These drugs cause damage to cells and prevent mitosis by various mechanisms including damaging DNA and inhibition of the cellular machinery involved in cell division (Chabner & Roberts, 2005). One theory as to why these drugs kill cancer is that they induce a programmed form of cell death known as apoptosis (Nuňeza et al., 1998).

Nowadays, targeted therapies have significantly changed the treatment of cancer over the past 15 years (Masui et al., 2013). These drugs are now a component of therapy for many common malignancies including breast, colorectal, lung, pancreatic cancers, lymphoma, leukemia and multiple myeloma. The mechanisms of action and toxicities of targeted therapies differ from those of traditional cytotoxic chemotherapy. Targeted therapies are generally better tolerated than traditional chemotherapy, and would rather target proteins that are abnormally expressed in cancer cells and that are essential for their growth (Masui et al., 2013; Kang & Reynolds, 2009). These treatments are often used alongside traditional chemotherapeutic agents in antineoplastic treatment regimens (Masui et al., 2013).

Keating et al., (2012) published the finding on combination therapy as a novel treatment strategy for patients with medullosblastoma. The studies on targeting inhibitors of apoptosis proteins (IAPs), in combination with cisplatin (**134**) (cytotoxic therapy) resulted in significantly increased antitumor activity with similar effects observed in combination with radiotherapy. Meanwhile, Desrat et al., (2014) synthesized the meiogynin A analogues (**135-139**) that target Bcl-xL and Mcl-1. Among them, analogue 6 (**139**) was found to be active on these proteins, cytotoxic at the

micromolar range on three lymphoid cell lines and was shown to induce apoptotic cell death through a classical pathway involving caspase protease (Nuňeza et al., 1998).

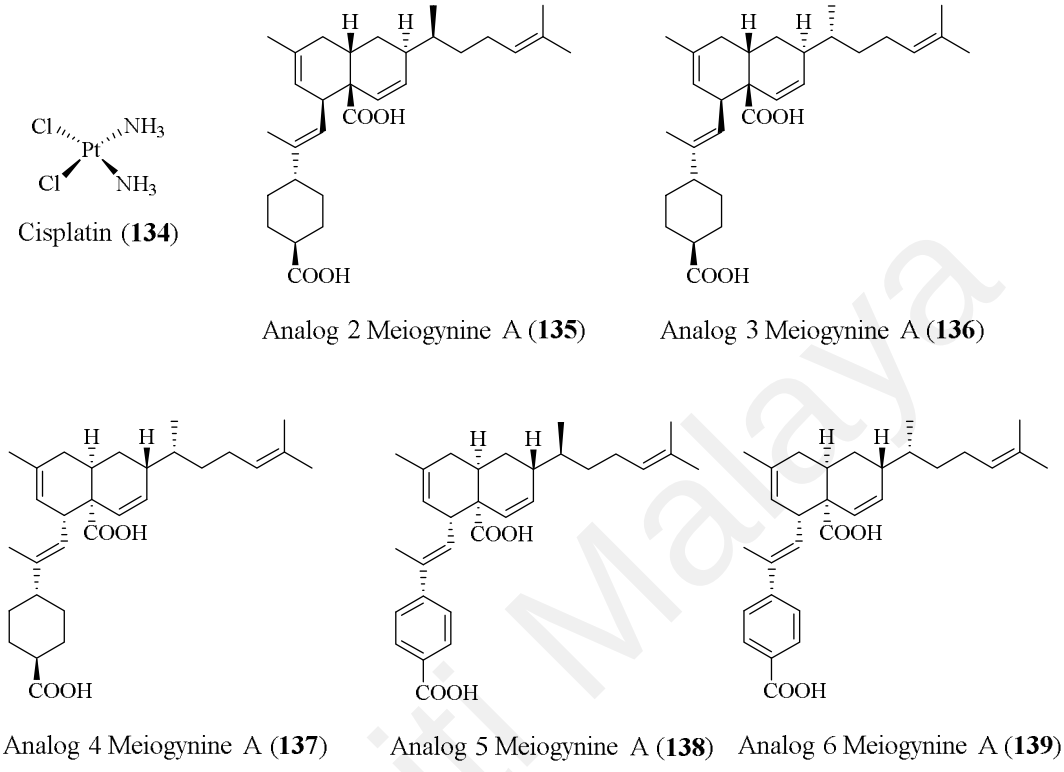

Cisplatin (**134**)

Analog 2 Meiogynine A (**135**)

Analog 3 Meiogynine A (**136**)

Analog 4 Meiogynine A (**137**)

Analog 5 Meiogynine A (**138**)

Analog 6 Meiogynine A (**139**)

Figure 4.8: Cisplatin and meiogynine A analogues

In this study, the goal was to investigate the cytotoxic activity of endiandric acid analogues in various tumor cells. From this study, we hope that these types of compounds can be further developed as drug candidates in targeted and cytotoxic therapies. The cytotoxic activities on compounds **120**, **122**, **124**, **93** and **89** were evaluated against A549 (lung adenocarcinoma epithelial), HT-29 (colorectal adenocarcinoma) and PC3 (prostate adenocarcinoma) cell lines using MTS-based assay (3-(4,5-dimethylthiazol-2-yl)-5-(3-carboxymethoxyphenyl)-2-(4-sulfophenyl)-2***H***-tetrazolium, inner salt).

As shown in Table 4.3, the results indicated that cells treated with kingianic acid E (**124**) induced cytotoxicity. Highest levels of cytotoxicity were observed in lung

adenocarcinoma epithelial (A549) and colorectal adenocarcinoma cell lines (HT-29) with IC_{50s} of 15 ± 1 µM and 17 ± 1 µM, respectively at 72 hrs post-treatment times. Meanwhile, kingianic acid A (**120**) was successful in inhibiting the HT-29 cell lines with IC_{50} 35 ± 1 µM, two times better than treatment with control (cisplatin). Cytotoxicity induced by tsangibeilin B (**89**) was observed in human lung cancer cells (A549) with IC_{50} value of 38 ± 1 µM, similar to cisplatin. The other compounds showed very weak cytotoxic activity against the cancer cell lines tested.

Solvent controls showed that the viability of cells were insignificantly affected (< 1.0 %; data not shown), indicating that cytotoxicity was not induced by the presence of DMSO, which has been shown to be cytotoxic at high concentration (Volante et al., 2002). The results are in agreement with a previous study by Williams et al. (2012) in which some synthetic tetracyclic endiandric acids were not active on prostate adenocarcinoma cancer cells (PC3) but significantly active on lung carcinoma cells.

Table 4.3: Cytotoxic Activity of Selected Endiandric Acids

Compound	**Cytotoxicity (IC_{50}, in µM, mean ± s.d., n = 3)**		
	HT-29	**A549**	**PC3**
Kingianic acid A (**120**)	35 ± 1	85 ± 1	>100
Tsangibeilin B (**89**)	>100	38 ± 1	>100
Kingianic acid C (**122**)	>100	85 ± 1	>100
Endiandric acid M (**93**)	>100	>100	>100
Kingianic acid E (**124**)	17 ± 1	15 ± 1	77 ± 1
Cisplatin	70 ± 1	36 ± 1	45 ± 8

4.4 Conclusion

The interests in this research are based on cancer treatments and prevention. So, some of these compounds were subjected to Bcl-xL and Mcl-1 binding affinities, and cytotoxic activity on various cancer cell lines. In the Bcl-xL and Mcl-1 binding affinity study, the assays on endiandric acid and kingianin series were performed. For endiandric acid series, no binding was detected for Bcl-xL, however moderate binding affinity for Mcl-1 (25-30% inhibition at 20 μM and ≥ 75% at 100 μM) were obtained with compounds **89**, **122** and **125.** For new kingianins, only kingianin P (**129**) showed potent binding for Bcl-xL (13 ± 2 μM) and moderate binding affinity for Mcl-1 (30 ± 1 μM). The other compounds showed very weak (>23 μM and >33 μM for Bcl-xL and Mcl-1 binding affinities, respectively). In cytotoxic assays, only kingianic acid E (**124**) showed moderate cytotoxic activity against lung adenocarcinoma epithelial (A549) and colorectal adenocarcinoma cell lines (HT-29) at the micromolar range between 15 – 18 μM, respectively.

Chemotherapy and molecularly targeted approaches represent two different modes of cancer treatment and each is associated with unique benefits and limitation. Both type of therapy share the overarching limitation of the emergence of drug resistance, which prevents these drugs from eliciting lasting clinical benefits. The rational combinations of cytotoxic and targeted therapies are based on understanding the mechanisms underlying sensitivity and resistance to each. It also represents an improved approach for cancer treatment by simultaneous inhibition of complementing general proliferation mechanism together with blockade of driver mutations or pathways conferring survival.

From these results, the compounds, which possess a good binding affinity for antiapoptotic proteins are not cytotoxic. These compounds can be used as adjuvant in chemotherapy and they are less toxic than the traditional chemotherapy drugs because cancer cells are more dependent on the targets than are normal cells. These types of

compounds are often cytostatic and they block tumor cell proliferation. Further studies such as flow cytometry and western blots are needed in order to confirm that cell death occurred via apoptosis, and not necrosis. Meanwhile, in order to identify the nature of the interactions between compounds and Bcl-xL at the molecular levels, docking calculation can be done using a conformer of Bcl-xL generated previously using ligand-driven conformer selection from molecular dynamics simulation.

CHAPTER 5

APPROACHES TO THE SYNTHESIS OF KINGIANINS

5.1 Introduction

In 2010, the new pentacyclic compound named kingianin A (**45**), isolated from ***Endiandra kingiana*** was published (Leverrier et al., 2010) (Figure 5.1). The pentacyclic skeleton was formed by Diels-Alder reaction between two monomers having a bicyclo[4.2.0]octadiene backbone formed by a stereospecific electrocyclization of compound of polyketide origin.

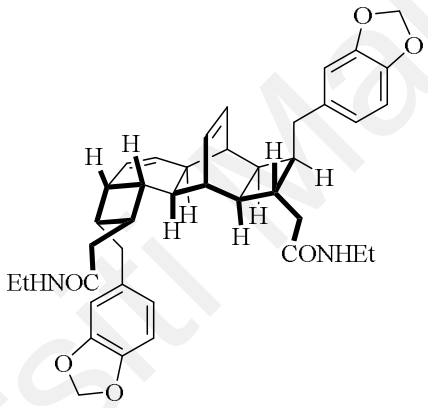

Figure 5.1: Kingianin A (**45**)

In addition, thirteen kingianin analogues; kingianins B-N (**46-58**) were published in the following year (Leverrier et al., 2011). These compounds were isolated as optically inactive white powders and their respective spectroscopic data were very similar with differences in the nature and the position of substitutions. An ***in vitro*** biological screening of these compounds showed good binding affinity for the protein Bcl-xL. Among them, kingianin G (**51**) has the most potent binding affinity for the protein Bcl-xL with ***Ki*** ≈ 2.0 μM (Leverrier et al., 2011) (Figure 5.2). This compound has a promising approach in the development of anticancer agents.

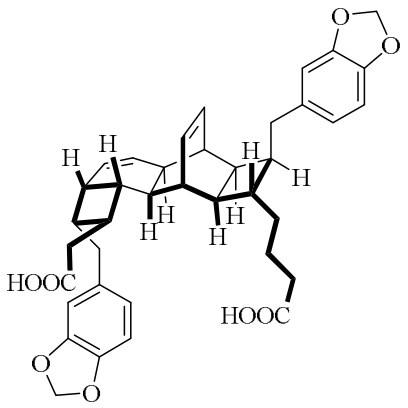

Figure 5.2: Kingianin G (**51**)

As mentioned in Chapters 3 and 4, several kingianins have successfully been isolated in milligram scale. However, a study on their biological properties including the mechanism could not be performed. Therefore, an approach to the synthesis of kingianins which involved the construction of bicyclo[4.2.0]octadiene backbone will be described.

5.2 Previous work: biomimetic syntheses of kingianin A

Generally, the idea for total synthesis of kingianin A was based on Black's hypothesis (Bandaranayake et al., 1980) and Nicolaou's work (Nicolaou et al., 1982, 1984) in construction of endiandric acids. Central to this hypothesis was the formation of a bicyclo[4.2.0]octadiene core through a non-enzyme mediated domino 8π-6π electrocyclization sequence of either an ***E***,***Z***,***Z***,***E***-tetraene or ***Z***,***Z***,***Z***,***Z***-tetraene. Finally, an intermolecular Diels-Alder (4π***s*** + 2π***s***) cycloaddition would provide kingianin A (**45**) as shown in Scheme 5.1.

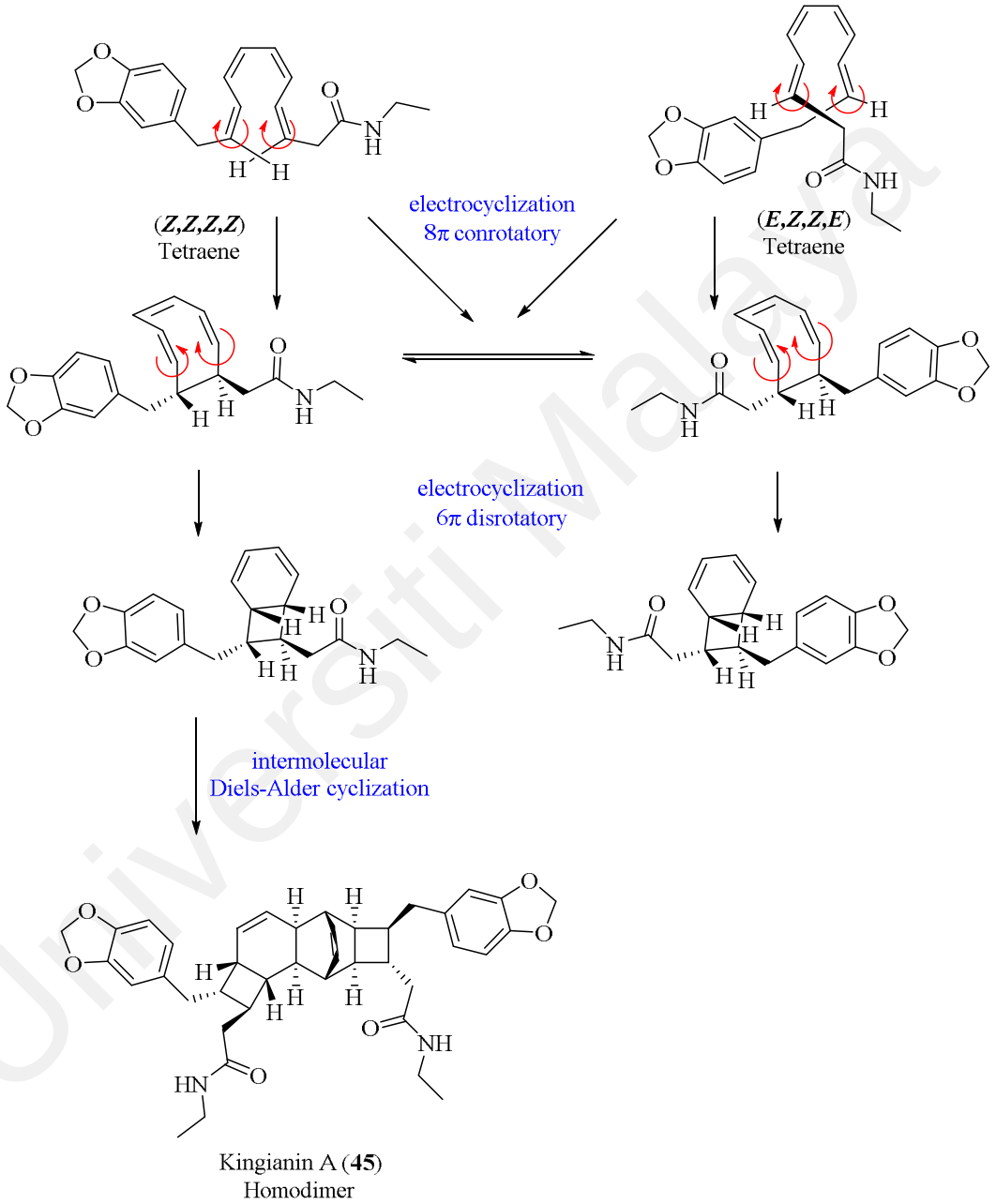

Scheme 5.1: Biosynthesis of kingianin A

5.2.1 The first attempt in synthesis of kingianin A

The first attempt by Sharma et al., (2011) was reported in 2011. The strategy involved a cascade of complexity generating reactions. The retrosynthetic disconnection of kingianin A revealed the vinyl bromide **140** and the stannane **141** as key precursors (Scheme 5.2) (Sharma et al., 2011).

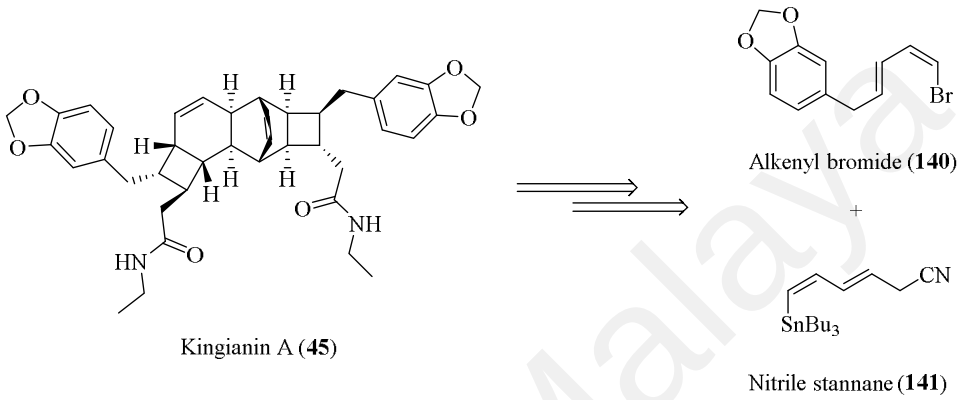

Scheme 5.2: Retrosynthesis of kingianin A by Sharma et al., (2011)

The synthesis of vinyl bromide **140** began from conjugated ester **142** (Capuano et al., 2003; Jubert & Knochel, 1992)**.** DIBAL-H reduction of **142** gave the allylic alcohol **143**, which underwent oxidation with Dess-Martin periodinane to the corresponding aldehyde **144**. Finally, elaboration of **144** to the corresponding 1,1-dibromo diene (Desai et al., 1962), followed by selective reduction using tributyltin hydride and palladium (0) catalyst gave the vinyl bromide **140** (Scheme 5.3) (Uenishi et al., 1998). The bromide **140** was stable at room temperature with no sign of isomerisation. Meanwhile, the synthesis of stannane **141** began from the known diene ester **145** (Webb et al., 2008; Corey & Eckrich, 1984; Jung & Light, 1982). The reduction of **145** with DIBAL-H afforded alcohol **146** in 65% yields. Finally, the conversion of alcohol **146** to nitrile stannane **141** was done using acetone cyanohydrin (Scheme 5.3) (Wilk, 1993; Lerner et al., 2003).

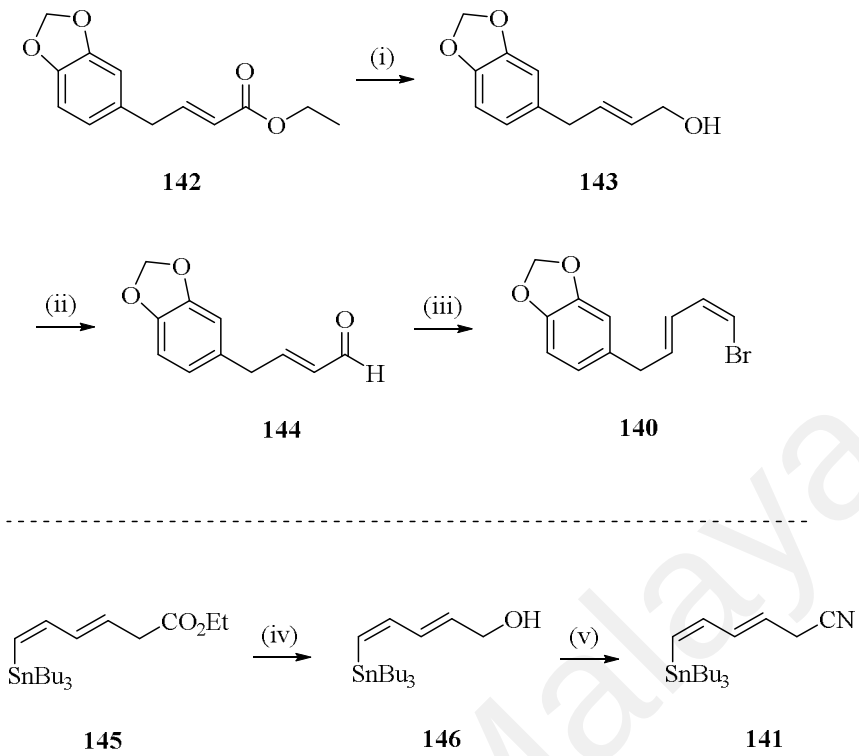

Scheme 5.3: Synthesis of fragment **140** and **141** (i) DIBAL-H, DCM, -78°C to rt, 40 min, 71%; (ii) DMP, DCM, 0°C, 30 min, 96%; (iii) (a) CBr_4, PPh_3, Et_3N, DCM, rt, 15 min (b) $HSnBu_3$, $Pd(PPh_3)_4$, toluene, rt, 1 h, 67% (2 steps); (iv) DIBAL-H, DCM, -78°C to rt, 16 h, 65%; (v) Acetone cyanohydrin, THF, 0°C, 15 min, 55%.

The tetraene **147** was achieved using a Stille cross-coupling reaction between alkenyl **140** and stannane **141** at 100°C (Andersen & Keay, 2001). Under these conditions, tetraene **147** could not be isolated and a mixture of bicyclo[4.2.0]octa-2,4-diene diastereomers **149** and **150** was obtained in 60% yield. The formation of compounds **149** and **150** can be explained by rapid 8π-6π electrocyclizations of **147**. The hydrolysis of nitrile functionality gave the corresponding amide which underwent reductive ***N***-alkylation to give isomer bicyclooctadienes **151** and **152** in 62% yield (Scheme 5.4) (Katagiri et al., 2000; Dubé & Scholte, 1999). The precursor **151** was found to be stable at ambient temperature over several weeks with no sign of dimerization to kingianin A (**45**). Heating the solution of bicyclooctadiene **151** to 195°C provided no evidence for

the formation of **45,** only interconversion to **152** was observed. It is clear that the process of dimerization is not spontaneous and consistent with the known chemistry of cyclohexadienes, which do not undergo Diels-Alder cyclization readily (Scheme 5.5).

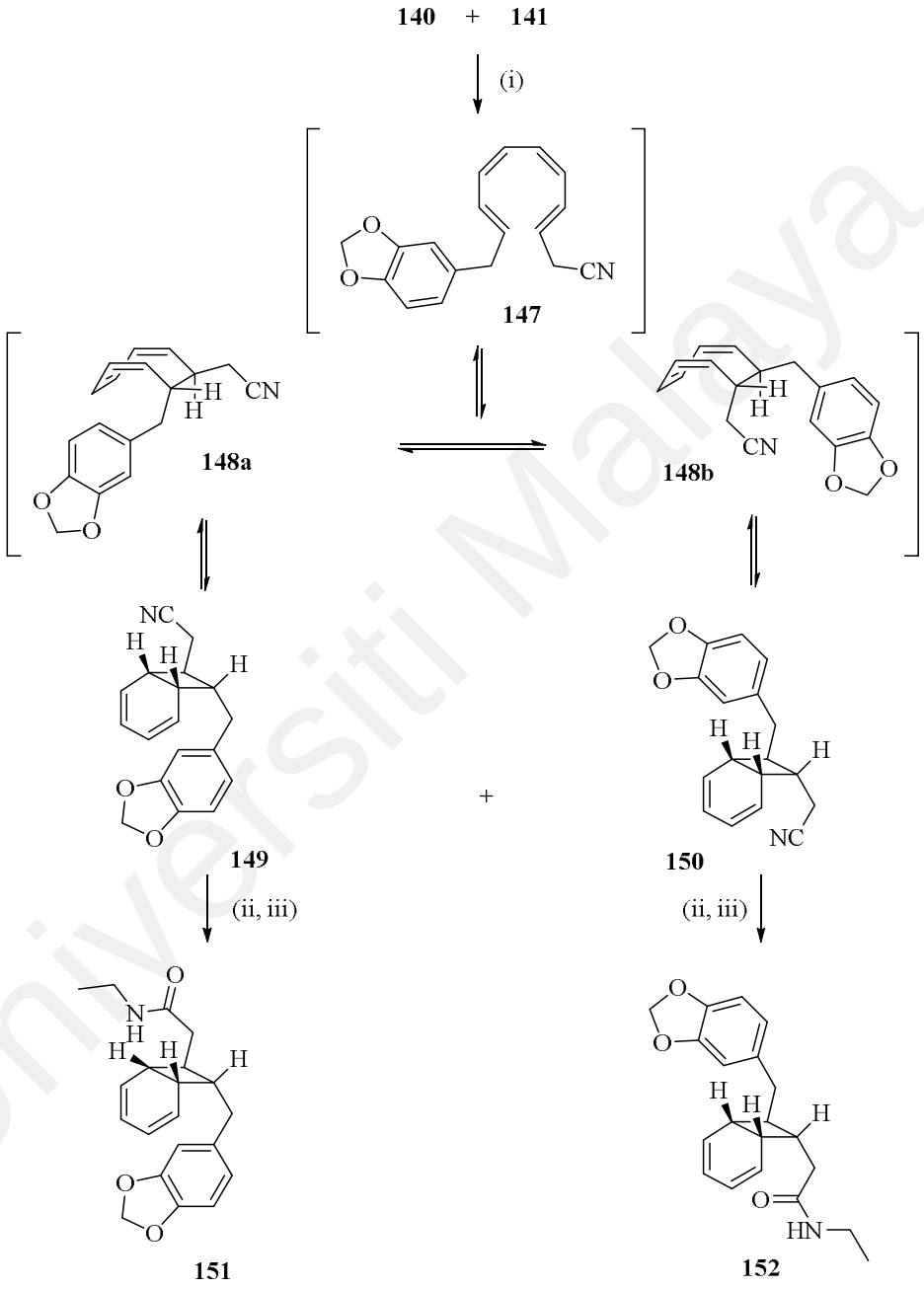

Scheme 5.4: Tandem coupling electrocyclization reaction sequence to kingianin monomers **151** and **152** (i) $Pd_2(dba)_3$, TFP, toluene, 100°C, 10 h, 60%; (ii) KOH, EtOH, 5 h; (ii) CH_3CHO, toluene, EtSiH, TFA, 120°C, 1 h, 62% (2 steps).

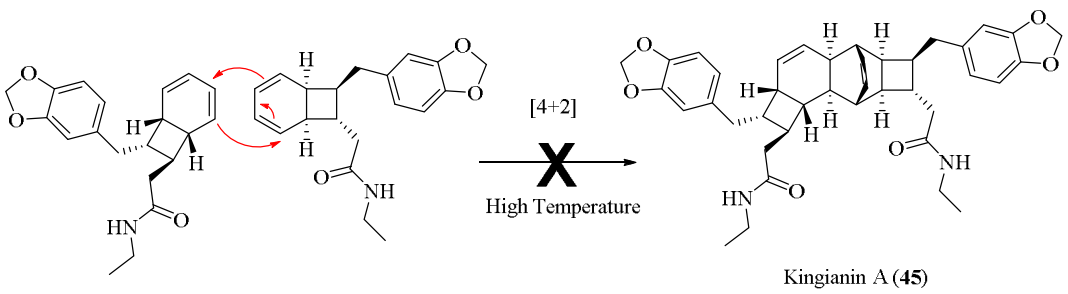

Scheme 5.5: Unsuccessful Diels-Alder cyclization of monomer kingianin A

5.2.2 Kingianin monomer cyclization: radical cation Diels-Alder (RCDA)

The second attempt was found in 2013, where Lim et al., (2013) reported the success of total synthesis of kingianin A (**45**) using intermolecular radical cation (RCDA) reaction of bicyclooctadienes. This reaction has been known for 30 years, but it had not been previously applied in the synthesis of complex natural product structures (Harirchian & Bauld, 1989; Lin et al., 2011). The application of radical cation catalysis overcomes the resistance of cyclohexadiene to undergo the Diels-Alder dimerization reaction (Lin et al., 2011, 2012; Ischay & Yoon, 2012; Gieseler et al., 1991). Ledwith-Weitz salt in catalytic amount is used to perform the intermolecular radical cation (RCDA) reaction of bicyclooctadienes.

The synthesis began with cross-metathesis of safrole **153** with acrolein to give known aldehyde **154**. Stork-Zhao olefination with **155** provided the (***E***,***Z***)-iododiene **156**. Meanwhile, vinyl boronic ester **157** was prepared in two steps and coupled with iododoene **156** under Suzuki condition (Robles & McDonald, 2009). The mixture of bicyclooctadiene **159** and **160** was isolated from this reaction. Deprotection of TBDPS ethers gave a mixture of alcohol **161** and **162**.

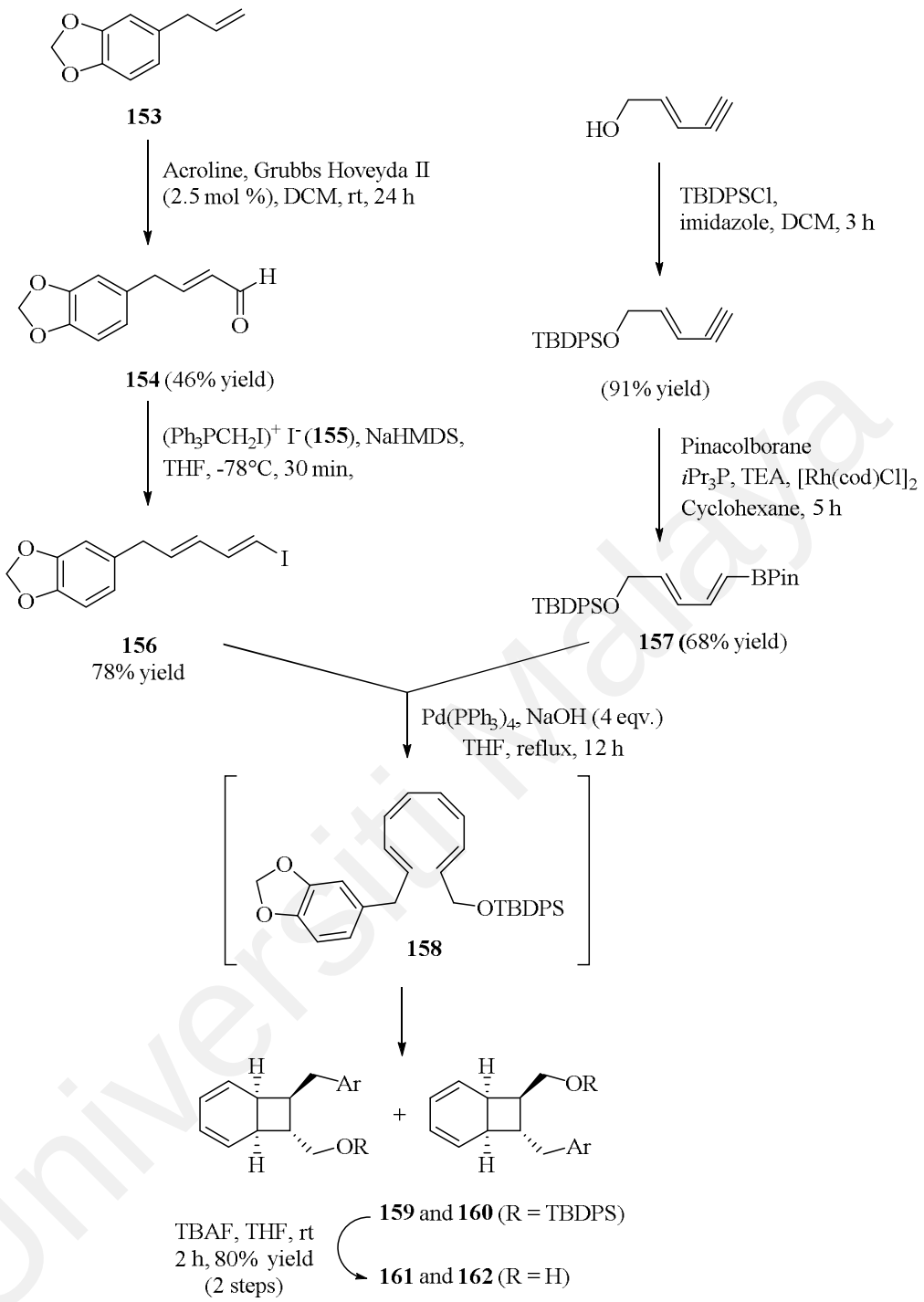

Scheme 5.6: Tandem Suzuki coupling and 8π-6π electrocyclization cascade

The dimeric diester were prepared from alcohol **161** and subjected to RCDA condition (5 mol% of the Ledwith-Weitz salt catalyst for 1 h). The use of a tether in the

key RCDA steps was intended to control the regiochemistry of the cycloaddition, leading to the desired core structure.

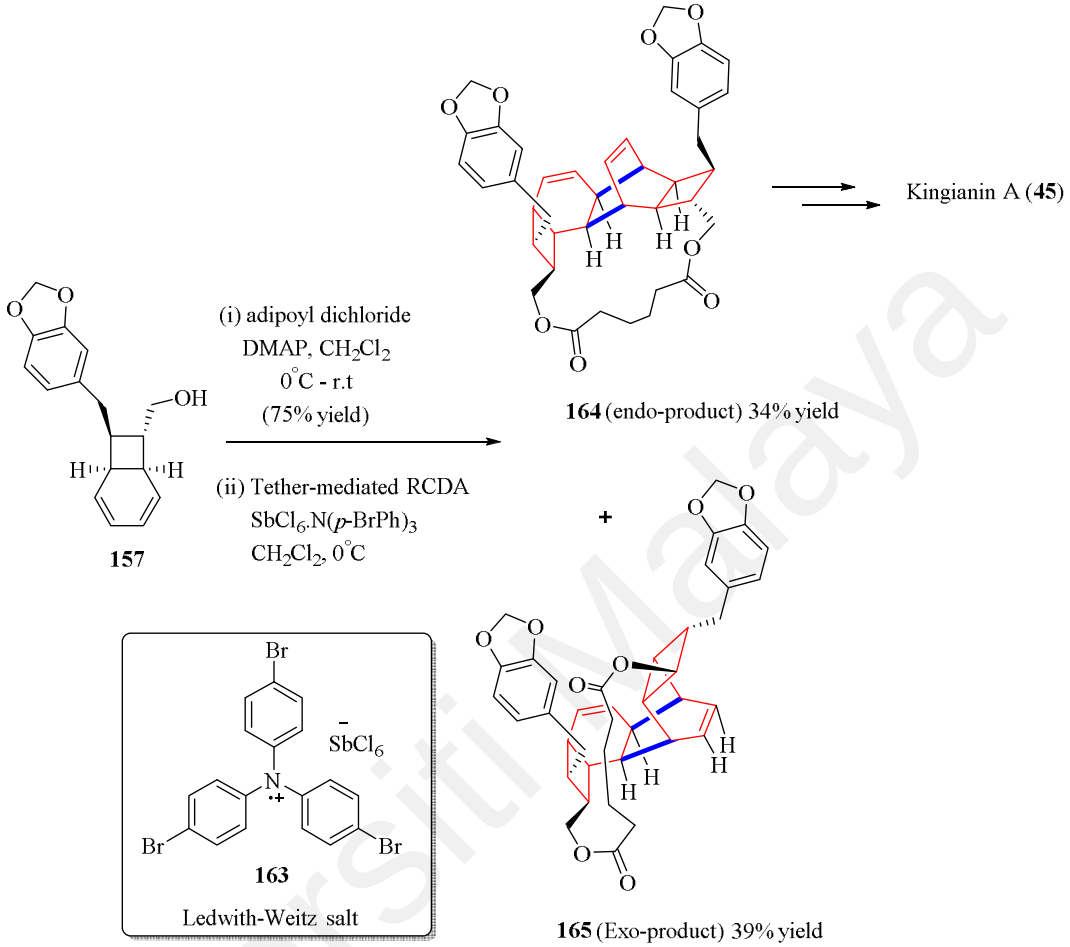

Scheme 5.7: Formation of kingianin A using radical cation Diels-Alder reaction

The reaction of dimeric diester with Ledwith-Weitz salt **163** gave two products ***i.e*** **164** and **165**. Separation and characterization of these compounds confirmed that **164** was an ***endo*** product suitable for the synthesis of kingianin A (**45**) while compound **165** was an ***exo*** Diels-Alder product. Compound **164** was engaged in the next step, where the tether was released using $LiAlH_4$. Then, mesylation and displacement by cyanide were followed by peroxide-promoted hydrolysis (Brinchi et al., 2009) and reductive ***N***-alkylation (Dubé & Scholte, 1999) to give kingianin A (**45**) in 26% yield.

In summary, the total synthesis of kingianin A (**45**) required 12 steps (from **164**). The intramolecular experiment established the radical cation Diels-Alder (RCDA) strategy as an entry to the kingianins and provided an element of regiocontrol to this key reaction. However, the yield of isolated kingianin A from this reaction is low (26% yield from ***endo***-product **164**).

5.2.3 Other total synthesis of kingianin A and its analogues

In 2013, Sherburn and co-workers published the total synthesis of kingianins A, D and F (Drew et al., 2013). Inspired by Bauld's work, the radical cation Diels-Alder dimerization could explain the formation of kingianins in nature (Lim & Parker, 2013; Harirchian & Bauld, 1989; Lin et al., 2011). This publication demonstrated the feasibility of preparing monomer kingianins by using reduction of (***Z,Z,Z,Z***)-tetraene precursors and subsequent 8π-6π electrocyclization (Drew et al., 2013).

The synthesis began with preparation of unsymmetrical tetrayne **166** by using Mori-Hiyama protocol (Nishihara et al., 2000; Fiandanese et al., 2008). Two requisite diynes **167** and **168** were successfully prepared in three and two steps, respectively (Scheme 5.8). To synthesize diyne **168**, the Cadiot–Chodkiewicz (Alami & Ferri, 1996) coupling of bromobutynol **169** (Montierth et al., 1998) with ethynyltrimethylsilane **170** afforded TMS-diyne **171**, which was converted into TBS-ether **168** under standard conditions (Corey & Venkateswarlu, 1972). Meanwhile, known benzyl bromide **172** was employed in a Negishi reaction (Qian & Negishi, 2005) with organozinc reagent **173** (Hoheisel & Frauenrath, 2008), which was derived from 1,4-bis(trimethylsilyl)-buta-1,3-diyne (Holmes & Jones, 1980). Finally, these two diynes (**167** and **168**) were subjected to cross Mori–Hiyama coupling reaction (Nishihara et al., 2000; Fiandanese et al., 2008) to form unsymmetrical tetrayne **166** (Gung & Kumi, 2003; Vail et al., 2005; Sabitha et al., 2006).

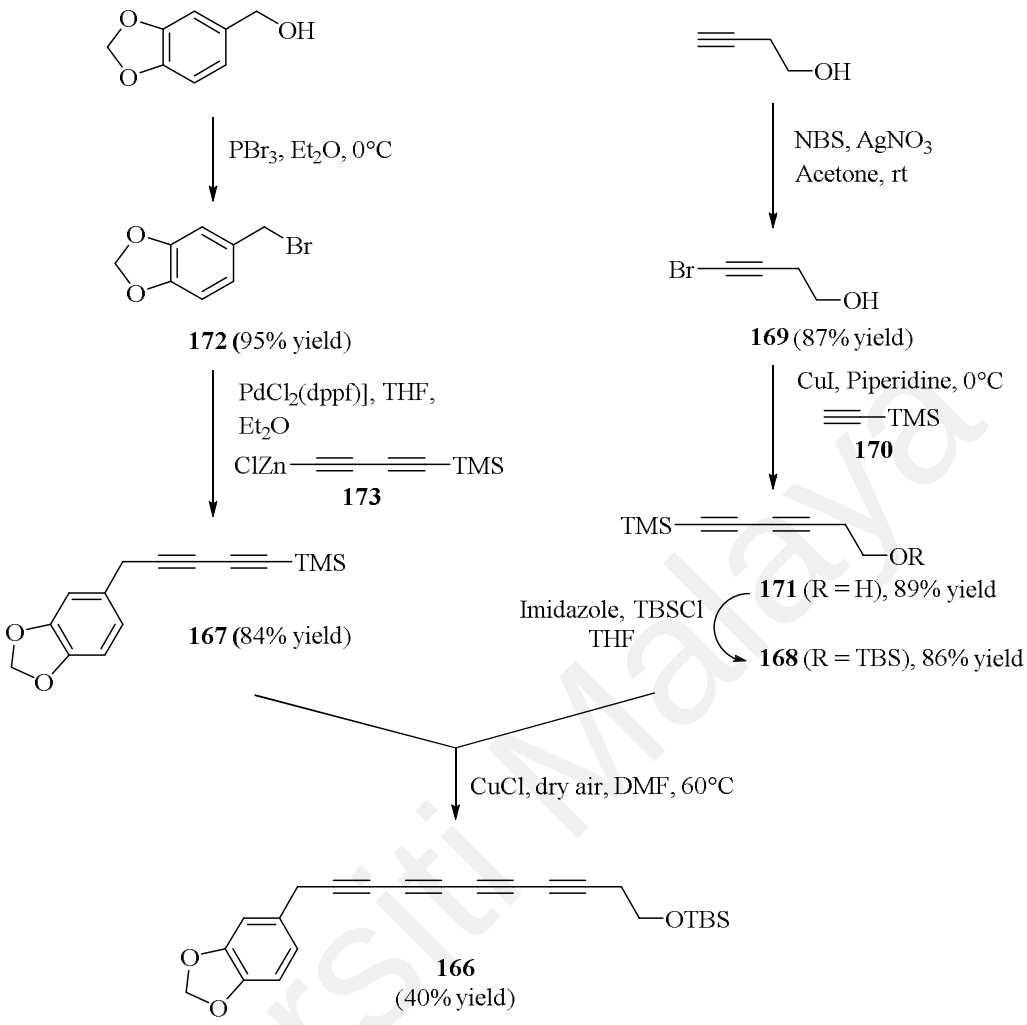

Scheme 5.8: Synthesis of unsymmetrical tetrayne **166**

The key bicyclo[4.2.0]octadiene precursors were prepared by a stereoselective semireduction of unsymmetrical conjugated tetra alkyne to give (***Z,Z,Z,Z***)-tetraene **174** (Marvell & Toshiro, 1965; Paquette et al., 2004; Wang et al., 2011; Matovic et al., 2011).

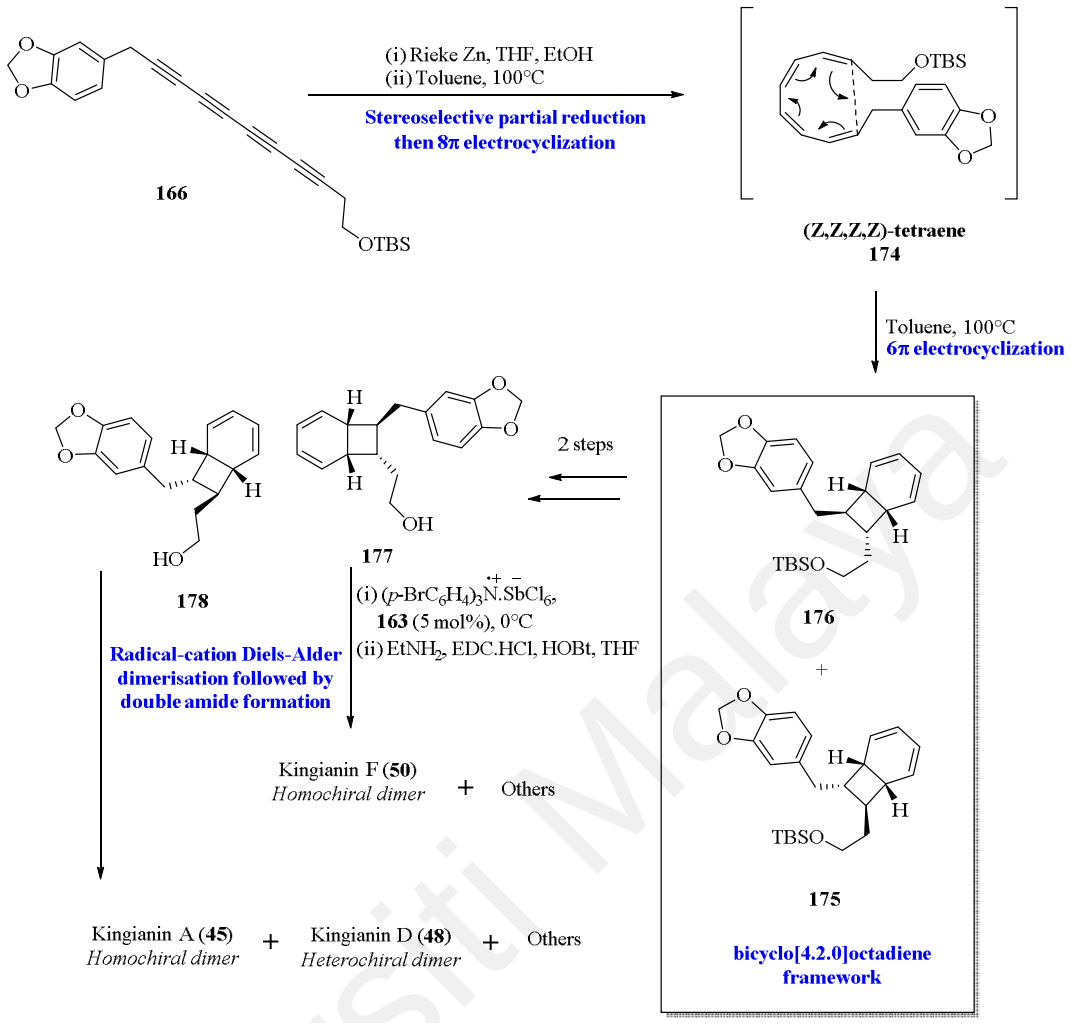

Scheme 5.9: Completion of the total synthesis of kingianin A, D and F

It was found that Rieke zinc in ethanol afforded (***Z,Z,Z,Z***)-tetraene **174** in a completely chemoselective and highly diastereoselective manner (Matovic et al., 2011; Chou et al., 1991). A solution of tetraene in toluene was immediately heated to 100°C, which triggered the domino 8π–6π electrocyclization sequence (Huisgen et al., 1967) to give bicyclo[4.2.0]octadiene precursors **175** and **176**. Following deprotection, the two diastereomeric alcohols **177** and **178** were isolated in a combined yield of 21% from tetrayne **166.** Both alcohols **177** and **178** underwent fast radical cation Diels–Alder dimerizations using catalytic quantities of the Ledwith–Weitz amminium salt **163**, (***p***-$BrC_6H_4)_3N{\cdot}SbCl_6$ (Scheme 5.9) (Bell et al., 1969).

Even though the cyclization process succeeded, the yield of final product was low (17% yield, mixture of three dimeric diamide; kingianins A, D and F) after column chromatography. Meanwhile, TBS-diyne **168** was used in excess to increase the yield of the cross-coupled product (<40% yield). A 1:1 ratio of diynes **167** and **168** typically afforded unsymmetrical tetrayne **166** in 25-30% yield. The electrocyclization of the all-(***Z***) isomer **174** required high temperature (≈ 100°C) to go to completion.

In August 2014, Moses team reported the formal synthesis of the complex and dimeric kingianin A, which employed an electrochemically-mediated radical cation Diels-Alder cycloaddition as the key step (Moore et al., 2014; Rosen et al., 2014; Park & Little, 2008; Gregory et al., 1990; Frontana-Uribe et al., 2010; Nigenda et al., 1987). The electrolysis was performed on a mixture of bicyclo[4.2.0]octadienyl monomers **179** and **180** in 0.4 M nBu_4NBF_4 in CH_2Cl_2 and it was electrolysed at 1.5 V using a reticulated vitreous carbon electrode (Nigenda et al., 1987; Bard & Faulkner, 2001). During this process the polycyclic **181** and **182** were isolated as the major compounds in 13% and 16% yields respectively (Scheme 5.10). In summary, this reaction offers an alternative to reagent-controlled Diels-Alder dimerization, but unsurprisingly, the yield of intermediate **181** is still low (<13% yield).

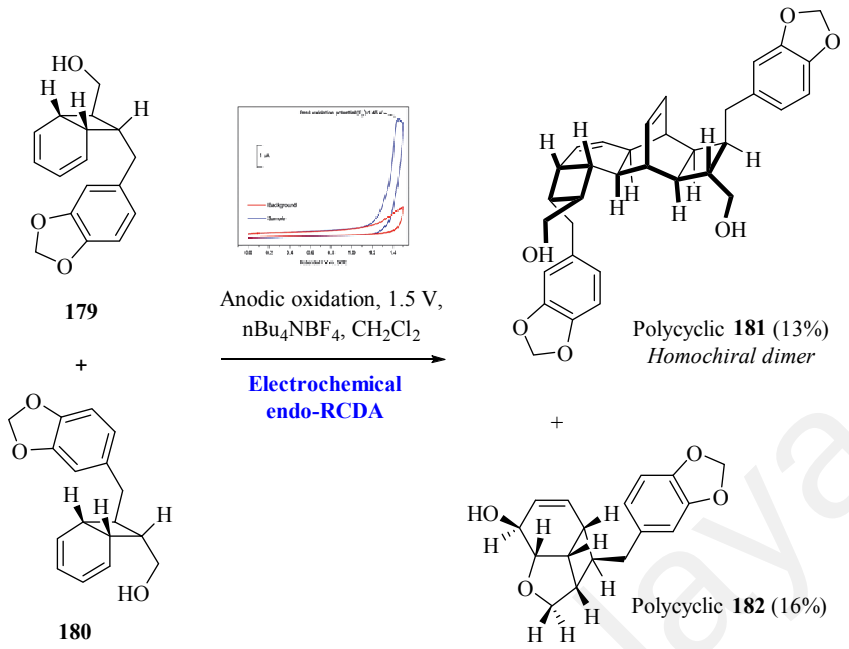

Scheme 5.10: Electrochemical ***endo***-RCDA of monomer **179** and **180**

5.3 Previous work in the ICSN, CNRS laboratory

The first research on the total synthesis of kingianin A by ICSN, CNRS group was undertaken in 2011 (Leverrier, 2011). Fourteen kingianins have been isolated including kingianin A and a plausible biosynthesis was proposed, which involved a key ***endo***-Diels-Alder dimerization reaction of the homochiral bicyclo[4.2.0]octadiene (Leverrier, 2011). This proposal had been developed on the basis of Black's hypothesis (Bandaranayake et al., 1980) and biomimetic syntheses of endiandric acids by Nicolaou et al. (1982).

The retrosynthetic analysis is illustrated in Scheme 5.11 (Leverrier, 2011). The retro-intermolecular Diels-Alder, as indicated lead, to bicyclo[4.2.0]octadiene **183**. The bicyclooctadiene **183** could be prepared from ***cis***-selective semi-hydrogenation of octa-1,7-diene-3,5-diyne **186**. Thermal conrotatory 8π electrocyclisation in the tetraene **185** is predicted to lead to the corresponding cyclooctatriene **184** which would then undergo a diastereoselective disrotatory 6π electrocyclisation reaction. This step is suitable in the final stage of synthetic strategy. It was thought that the diyne **186** could

be obtained by double dehydration of hexa-2,4-diyne-1.6-diol **187**. The diol **187** can be prepared by nucleophilic addition between bis(trimethylsilyl)butadiyne **189** and aldehyde **190**. Presumably, this strategy would efficiently generate a tetraene substrate with unsymmetrical substitution, unlike Nicolaou's sequence using Glaser coupling.

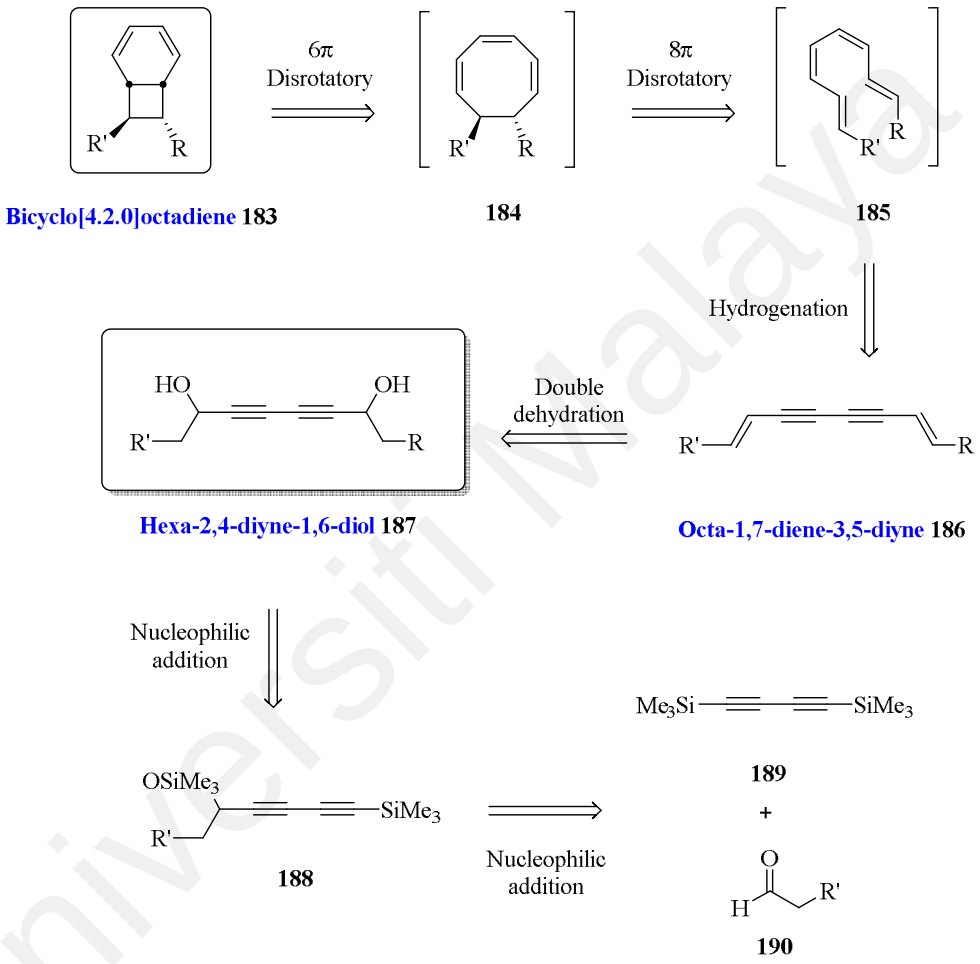

Scheme 5.11: Retrosynthesis of monomer kingianins by Leverrier (2011)

As described in the literature, Kuwajima et al. (1983) have showed that TBAF (tetrabutylammonium fluoride) can be used to catalyze the reaction between bis(trimethylsilyl)butadiyne **189** and carbonyl compound **191**, leading to propargylic silyl ethers **192** and **193**. These were then deprotected with acetic acid to afford

compounds **194** and **195** were obtained in 61% and 29% yield, respectively (Scheme 5.12).

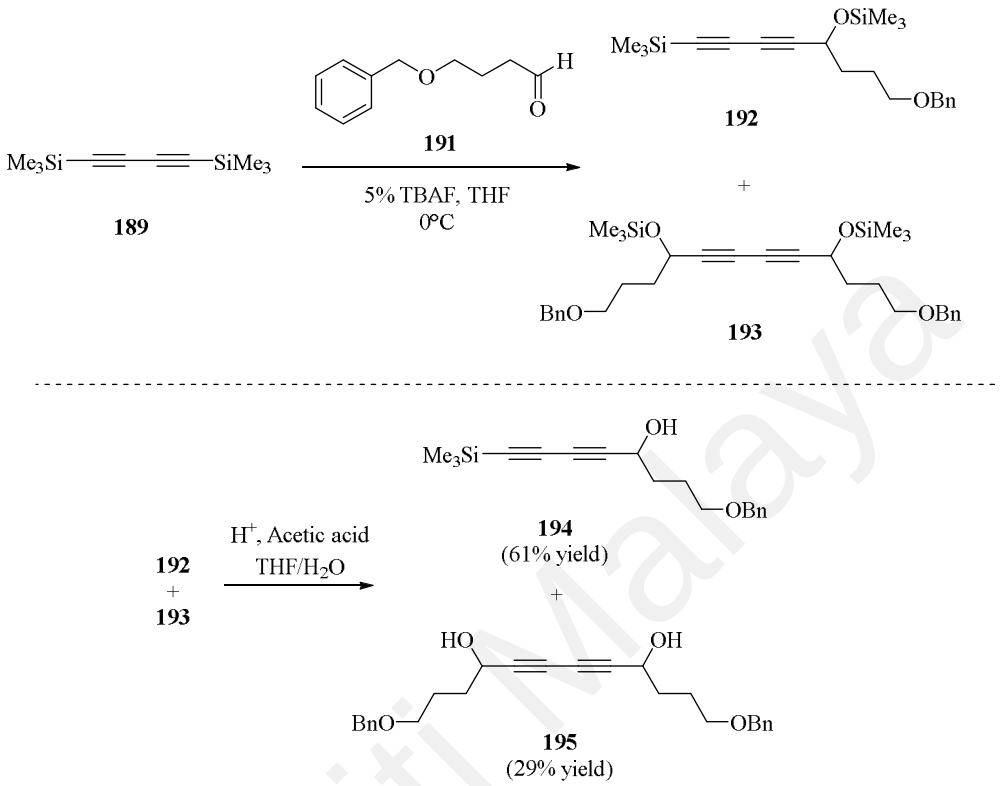

Scheme 5.12: Synthesis of **195** using nucleophilic addition

Saksena's work indicated that P_2O_5 (2.5 eqv.) is capable of dehydrating propargyl alcohols in dichloromethane at 0-5°C, leading to the formation of enynes (Saksena et al., 1985). The diyne **193** was therefore dissolved in CH_2Cl_2 in the presence of P_2O_5 (6 eqv.) at 0°C. The desired dehydration product could not be obtained. But, under these conditions double cyclization took place, leading to compound **197** (21% yield) (Scheme 5.13).

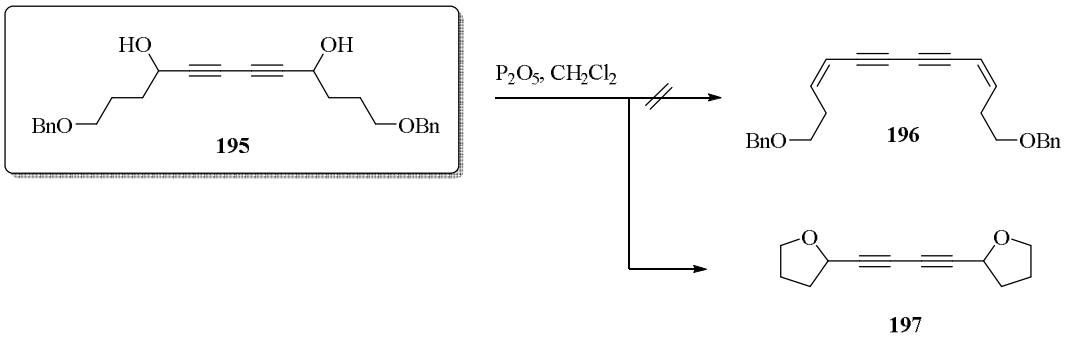

Scheme 5.13: Double dehydration of enyne **195** using P_2O_5

A second attempt of dehydration of the compound **195** was carried out in the presence of a strong acid, i.e. ***p***-toluenesulfonic acid in toluene at reflux. Under these conditions, compound **195** decomposed. Meanwhile, Shibuya et al. (1995) had reported the synthesis of enediynes from propargylic alcohols via mesylates in the presence of triethylamine (3 eqv.). The propargyl diol was engaged under the same conditions (with 6 eqv. of triethylamine and 2.3 eqv. of mesyl chloride). The bismesylate is immediately formed. However, no dehydration product could be observed. A stronger base, DBU was then used, leading to compound **198**, and not the desired product **199** (Scheme 5.14).

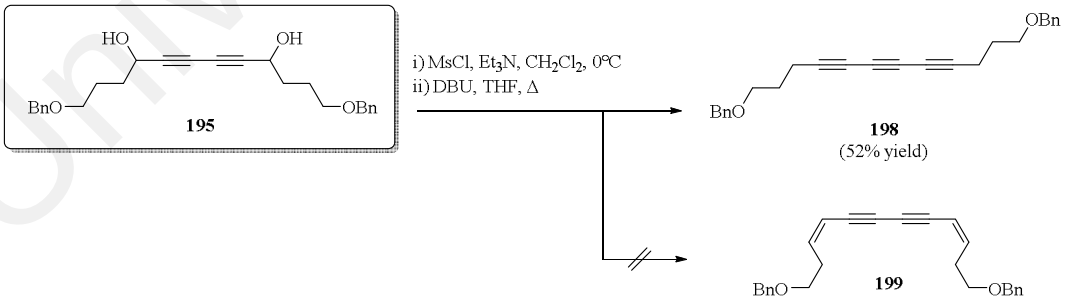

Scheme 5.14: Double dehydration of enyne **195** using mesylate

After these preliminary results, a new strategy with a more original and diversity-oriented approach was designed.

5.4 Approaches to the total synthesis of kingianins

5.4.1 Retrosynthesis of kingianins

A new and more direct synthetic approach to the bicyclo[4.2.0]octadiene sub-units of kingianins are designed and explored. This strategy is displayed in Scheme 5.15. It involves a [2+2] cycloaddition of cyclohexadiene substrates to functionalized ketenes which, by simultaneous C-C bond formation, could lead to bicyclo[4.2.0]octadienes as potential precursors for the synthesis of kingianins. One of the main advantages of such a strategy is the rapid assembly of the carbon skeleton of kingianins, thus maximizing the chances for good overall yields of the final products.

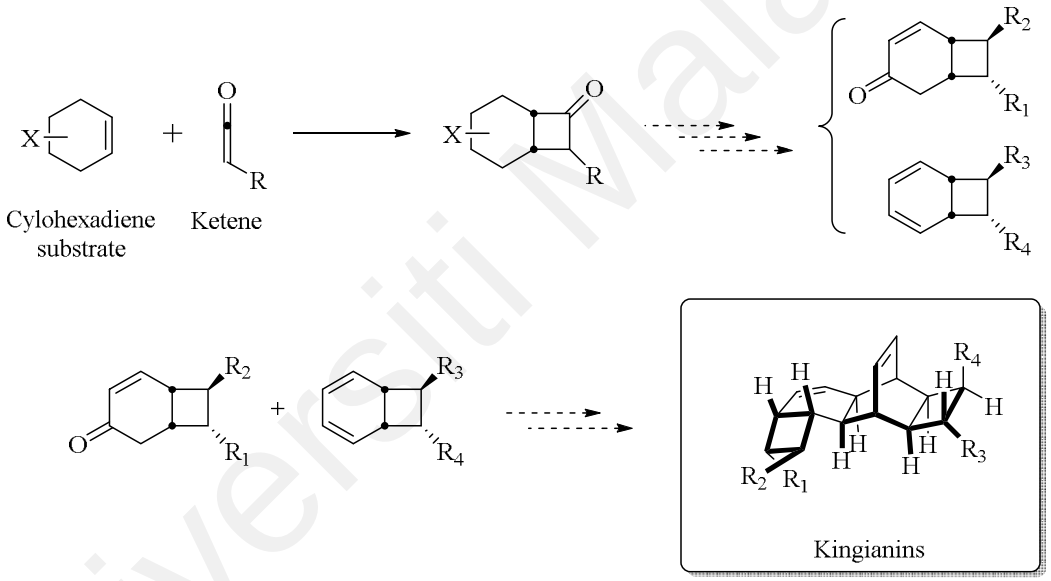

Scheme 5.15: Strategy for the synthesis of kingianins

Also, in this part the functionalization of this skeleton to build dienes and dienophiles are studied. This approach allows the selective preparation of both homodimers and heterodimers, in contrast to what is permitted by application of the strategies already described. In addition, simplified analogues should be accessible, whose biological activity can be evaluated (Scheme 5.16).

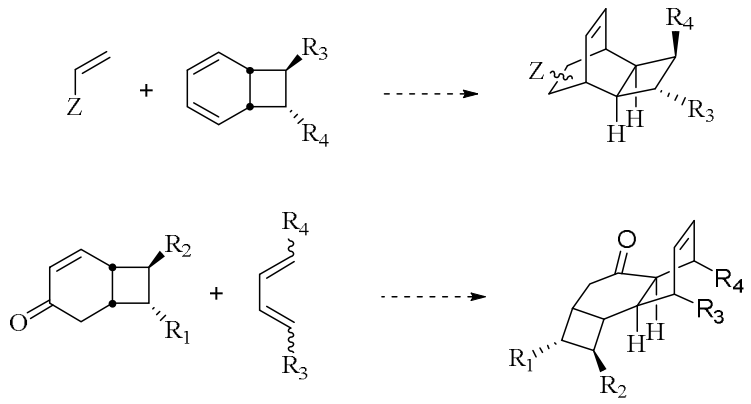

Scheme 5.16: Strategy for synthesis of simplified kingianin analogues

5.4.2 [2+2] Ketene-alkene cycloaddition: overview

As shown in Scheme 5.15, the strategy for the synthesis of the bicyclo[4.2.0]octadiene framework rests on a [2+2] ketene-alkene cycloaddition reaction. Ketenes have been extensively exploited in mechanistic studies and in the synthesis of complex molecules, as versatile organic reactive intermediates (Tidwell, 2005, 2006). The first ketene, diphenylketene (**200**), was discovered by Hermann Staudinger in 1905, by the reaction of α-chlorodiphenylacetyl chloride (**201**) with zinc (Staudinger, 1905). The simplest ketene (**202**) was prepared from the pyrolysis of acetic anhydride using a hot platinum wire (Wilsmore, 1907).

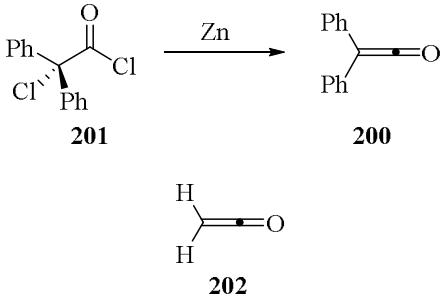

Scheme 5.17: Ketenes **200** and **202**

Early in the study of ketene chemistry, Smith and Hoehn (1939) had obtained cyclobutenone **203** from [2+2] cycloaddition of diphenylketene (**200**) with phenyl acetylene (**204**). This cyclobutene undergoes thermal ring opening to the alkenylketene **205**, which undergoes electrocyclisation to form **206** (Smith-Hoehn reaction) (Scheme 5.18).

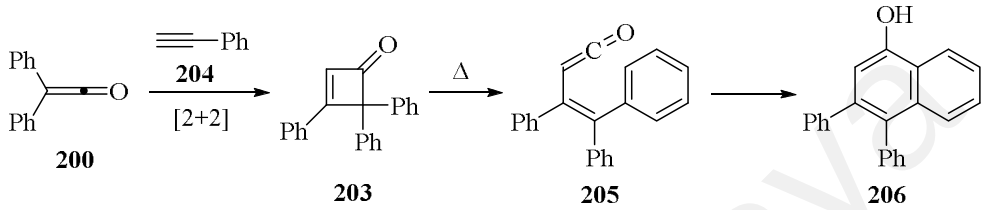

Scheme 5.18: Smith-Hoehn reaction of diphenylketene **200**

One of the first examples of the [2+2] cycloaddition of a ketene with a carbon–carbon double bond was the reaction of diphenylketene (**200**) with cyclopentadiene (**207**) (Staudinger, 1907). Surprisingly, it was found by Machiguchi et al. (1999) that the net [2+2] cycloaddition observed in this canonical process was not the initial reaction in the sequence, but that instead (as observed at low temperature) a [4+2] cycloaddition with the carbonyl group formed **208**, which upon warming underwent a formal Claisen rearrangement to **209** (Scheme 5.19).

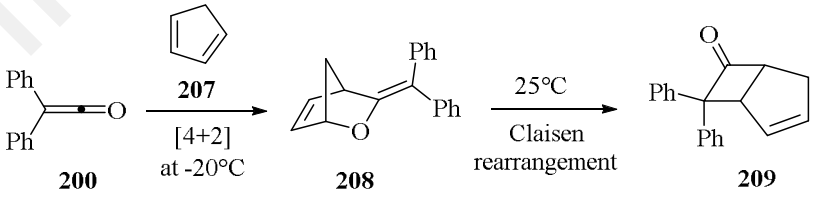

Scheme 5.19: Cycloaddition of ketene **200** and cyclopentadiene **207**

Ketenes are powerful electrophiles, where the π* C=O orbital is quite low in energy and very susceptible to nucleophilic attack (Woodward & Hoffmann, 1969). Because of these reasons, the ketenes have the tendency to undergo concerted [2+2] cycloadditions. In ketene-alkene [2+2] cycloaddition, Woodward and Hoffmann proposed the mechanism which occurred with an orthogonal approach of the ketene **210** to alkene double bond **211** from the least hindered direction to form **212** (Wagner & Gompper, 1970; Gompper, 1969). In the transition state for cyclization, the **212** was proposed from initial bond formation from more nucleophilic carbon of the alkene **211**, to the carbonyl carbon **210** with an interaction between the cationic carbon and the enolate system of the dipolar intermediate (antarafacial-suprafacial) (Zimmerman, 1971; Baldwin & Kapeckki, 1970). The smaller substituent on the ketene **210** moved away from the nearest alkene **211** substituent. The bond rotation happen at C2 and the second bond formed (Scheme 5.20).

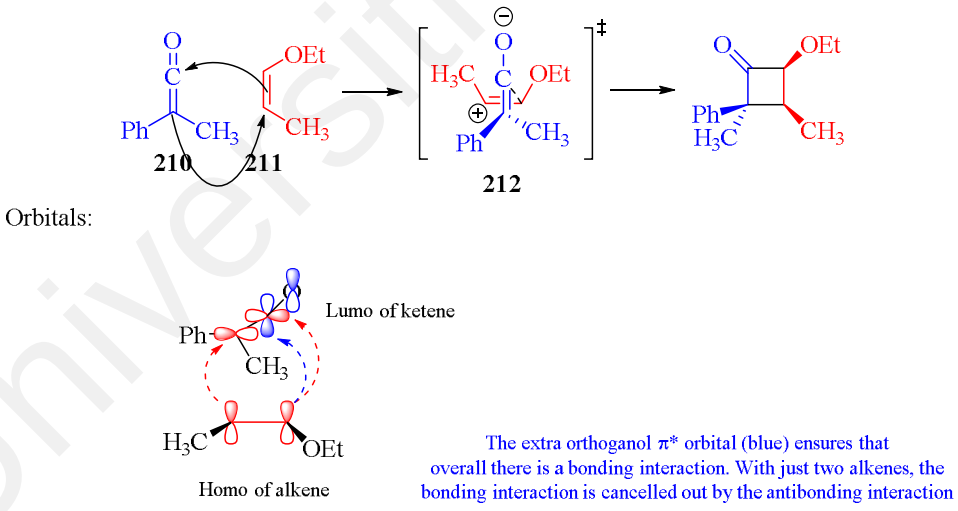

Scheme 5.20: [2+2] cycloaddition mechanism

Ketene-alkene [2+2] cycloadditions are an important class of transformations for chemical synthesis. This is largely due to the synthetic utility of the resultant cyclobutanone products as evidenced by the numerous reports regarding their use in total synthesis. For example, dichloroketene (**213**) was prepared by the

dehydrochlorination of dichloroacetyl chloride (**214**), and trapped with cyclopentadiene (**207**) by [2+2] cycloaddition to form bicyclo[3.2.0]pent-2-ene-6-one (**215**). Hydrolysis of **215** is a simple and efficient method for the preparation of tropolone (**216**) (Stevens et al., 1965; Minns, 1977, 1988).

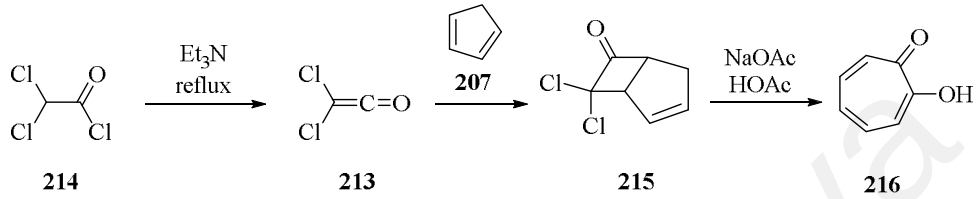

Scheme 5.21: Preparation of tropolone (**216**)

This reaction was utilized as a key reaction in the synthesis of bakkane natural products. Dichloroketene (**213**) was generated ***in situ*** from trichloroacetyl chloride (**217**) by zinc-copper couple in the presence of phosphorus oxychloride (Brocksom et al., 2002). The [2+2] cycloaddition between dichloroketene (**213**) and 1,6-dimethylcyclohexene (**218**) gave the product in high yield and excellent regio- and diastereoselectivity. The cycloadduct **219** was successfully converted to (±) – bakkenolide A (Brocksom et al., 2002).

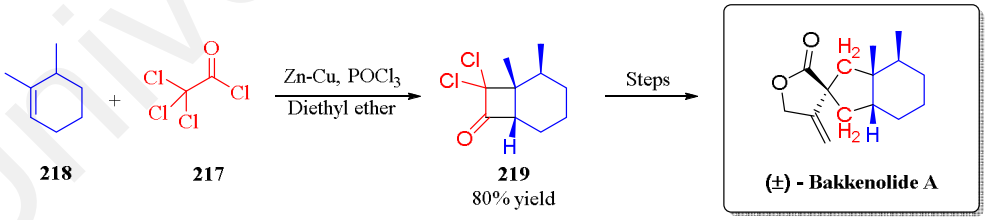

Scheme 5.22: Synthesis of (±) – bakkenolide A

Faria and co-workers devised an efficient synthesis of indolizidine systems and the total synthesis of the necine base (±) – platynecine (De Faria et al., 2002). This approach, utilized a [2+2] ketene cycloaddition between five-membered endocyclic enecarbamate (**220**) and alkylketene, generated ***in situ*** from 5-chlorovaleryl chloride

(**221**) by treatment with triethylamine in cyclohexane was used (De Faria et al., 2002). The cycloaddition reaction occurred in good and high yield with high stereoselectivity (90% yield, ratio **222**:**223**; 7:1). Baeyer-Villiger ring expansion of the cycloadduct **222** provided the corresponding *γ*-lactone **224** in high yield with remarkable regioselectivity.

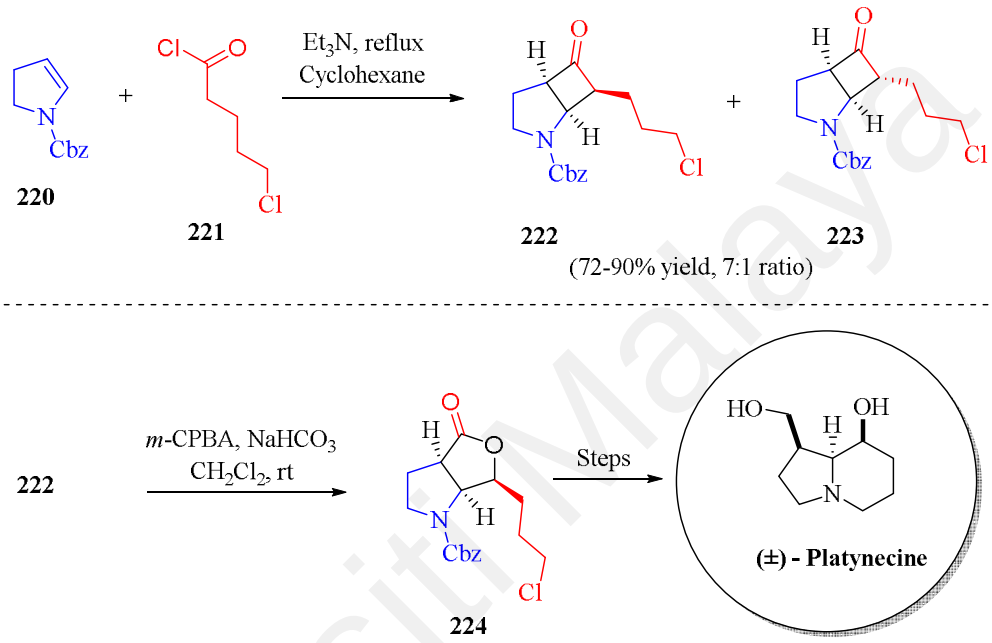

Scheme 5.23: Synthesis of (±) – platynecine

(±) – Welwitindolinone A isonitrile is a natural product isolated from blue-green algae and exhibits potent antifungal activity. Wood team developed a synthesis for this compound that incorporates [2+2] ketene cycloaddition as the key step (Reisman et al., 2006; Ready et al., 2004). The reaction between the cyclohexadiene acetonide (**225**) and dimethylketene that was generated ***in situ*** from **226**, was carried out in the presence of triethylamine in refluxing THF. This transformation led to the formation of tricycle ketone **227** in 85% yield as a single regio- and diastereo isomer.

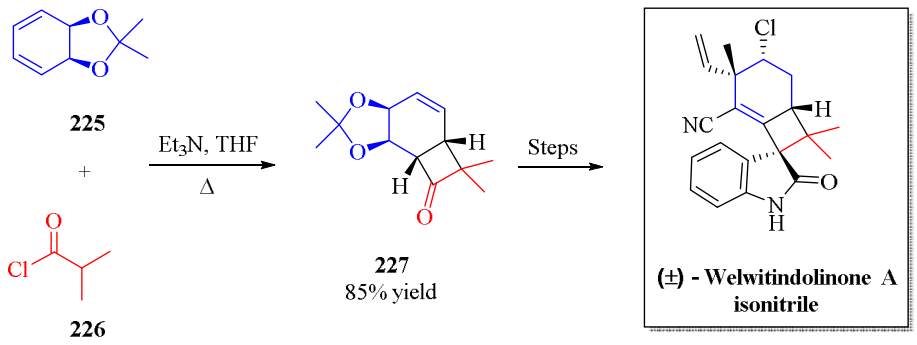

Scheme 5.24: Synthesis of (±) – welwitindolinone A isonitrile

5.4.3 Approach A: [2+2] intermolecular ketene cycloaddition

5.4.3.1 1,3-Cyclohexadiene[1]

To validate this strategy, Lonca G. started this project to prepare the bicyclo [4.2.0] octadiene **228** as monomer of kingianins. As shown in Scheme 5.25, the bicyclo precursor could be obtained by using the same ketene-alkene [2+2] cycloaddition. The major questions are the formation of cyclohexadiene at carbon C-2 and C-4, and functionalization of substituent at C-7 and C-8 position with the correct relative configuration.

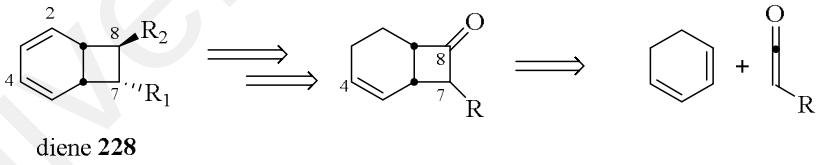

Scheme 5.25: Strategy for synthesis of diene **228**

The sequence began with the synthesis of bicyclo[4.2.0]octadiene **229** and **230**. The diene **231** was reacted with chloropropionyl chloride **232** and Et_3N in ether to give a separable mixture of 7-methylchloro ketones **229** and **230** in a ratio of 4:1 (Scheme 5.26) (Wu et al., 1994). From the ^1H NMR analysis, cyclobutanones **229** and **230** shows characteristic signals corresponding to the olefinic protons at δ_H 5.76 (H-5) and 5.96

[1] Disclaimer: this subsection describes unpublished experimental work carried out by Geoffroy Lonca

(H-4). Comparison of ^{1}H NMR spectra between compounds **229** and **230**, indicated the proton signals for the ring junction H-1 (δ_H 4.07) and H-6 (δ_H 3.08) of compound **229** is more deshielded than compound **230** [H-1 (δ_H 3.67) and H-6 (δ_H 2.89)]. In addition, formation of **229** and **230** was confirmed by analysis of the high resolution mass spectrum, showing ***m/z*** = 170.0489 ($\mathbf{M}^{+\bullet}$).

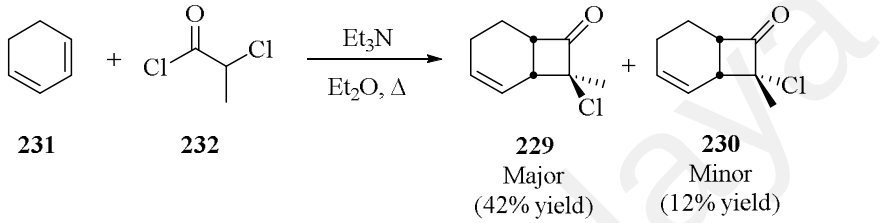

Scheme 5.26: Synthesis of cyclobutanones **229** and **230**

Reduction with zinc/copper couple of **229** gave the product **233** (Wu et al., 1994). Carbonyl homologation of **233** to obtain the aldehyde **234** was achieved by reaction at low temperature of the bicyclic ketone **233** with ylide **235** to form enol ether **236** (***E/Z*** mixture) (Kozikowski et al., 1995; Rosini et al., 1998). The enol ether **236** was directly converted into a diastereoisomeric mixture of bicyclic aldehyde **234** by hydrolysis with formic acid (Scheme 5.27) (Rosini et al., 1998).

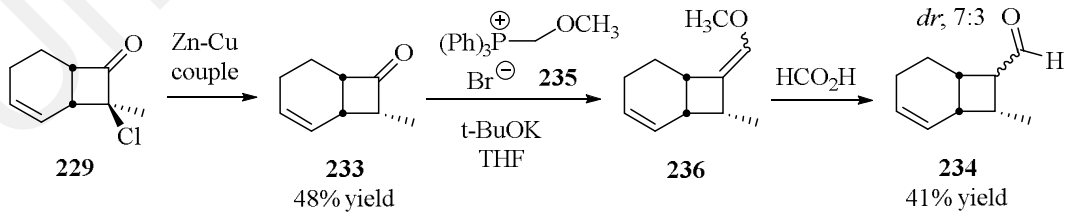

Scheme 5.27: Carbonyl homologation of **234**

The diastereoisomeric mixture of bicyclic aldehyde **234** was observed on the ^{1}H NMR spectrum, where a doublet signal appeared at 9.75 and 9.76 ppm for **234a** and **234b**, respectively. Epimerization of **234** was done in small scale by using DBU in $CDCl_3$ for 24 h to afford a single isomer aldehyde **256a** (Scheme 5.28).

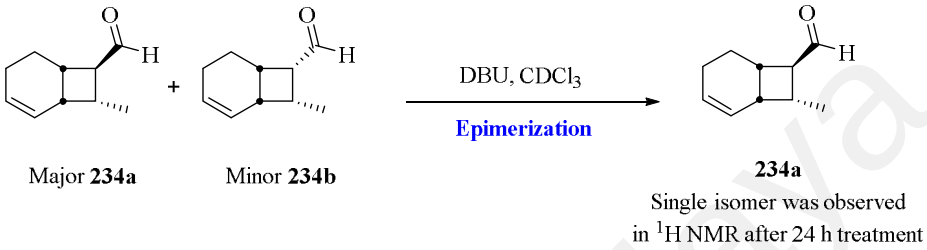

Scheme 5.28: Epimerization of bicyclic aldehyde **234**

Based on this observation, combination olefination reaction with epimerization was envisaged. A Horner-Wadsworth-Emmons reaction (HWE) was chosen to perform the olefination of the aldehyde **234** (Rosini et al., 1998; Blanchette et al., 1984). The mixture of the aldehydes **234** was treated with ylide **237** in tetrahydrofuran in the presence of LiCl and DBU to obtain **238** (50% yield, ***dr***; 7:3) (Scheme 5.29). Unfortunately, no epimerization occurred, indicating that the HWE reaction was a faster process.

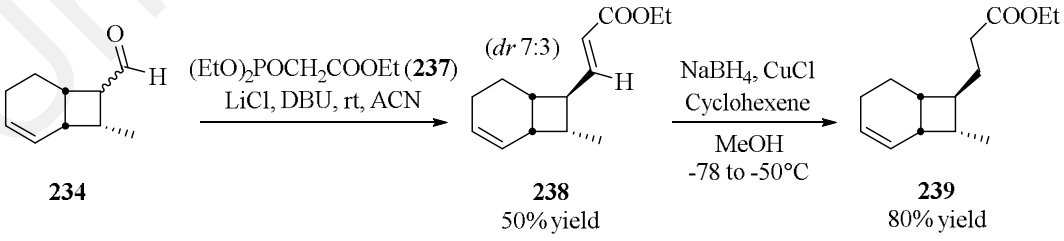

Scheme 5.29: Synthesis of compound **239**

Treatment of ester **238** with $NaBH_4$ catalyzed by CuCl gave ester **239** in 80% yield (Shi & Aldrich, 2012). The use of cyclohexene in large excess is essential to minimise reduction of the alkene function. Finally, Wohl-Ziegler radical bromination of ester **239** gave allylic bromide **240** among a complex mixture of products (Koltun & Kass, 2000). After column chromatography, two products were isolated, namely bicyclo[4.2.0]octadiene **241** and 3,6-dibromo-bicyclo[4.2.0]octene **242** (Scheme 5.30). Compound **241**, which had not been observed in the crude product, is similar to the target model compound but it was isolated in small quantity (9% yield). Bicyclo [4.2.0]octane **242** was found to be an over bromination product, showing the reaction was difficult to control in this case. Therefore, another model study was planned using a different substrate (starting material).

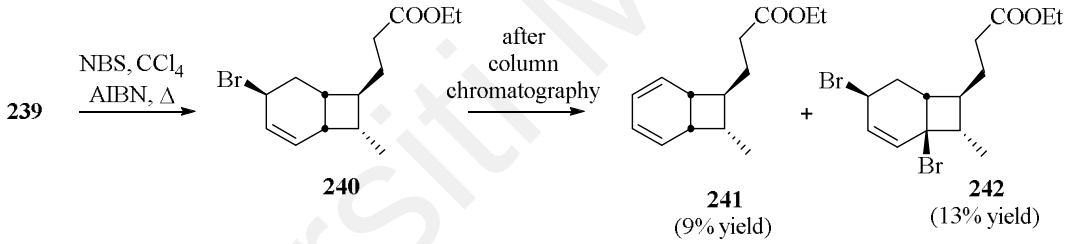

Scheme 5.30: Synthesis of cyclohexadiene **261**

5.4.3.2 4-Methoxy-1,4-cyclohexadiene

Based on preliminary work above, the research of constructing the bicyclo[4.2.0]octane was continued by using similar approach with different substrates; 4-methoxy-1,4-cyclohexadiene. The aim of this synthesis is to prepare the dienophile **243**, as monomer of kingianins. It involves a ketene-alkene [2+2] cycloaddition between cyclohexadiene **245** and ketene **246** (Scheme 5.31).

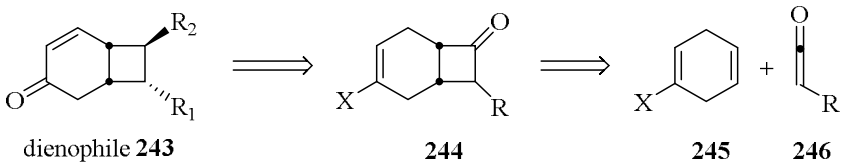

dienophile **243** **244** **245** **246**

Scheme 5.31: Strategy for synthesis of dienophiles **243**

The synthesis was initiated with the preparation of cyclobutanone in gram quantities, as an adaptation of the sequence reported by Wu et al. (1994). The reaction of 4-methoxy-1,4-cyclohexadiene **(247**) with 2-cholopropionyl chloride (**232**) and Et_3N in ether gave a separable mixture of 7-methylchloroketones **248** and **249** in a ratio of 3:1 (Scheme 5.32). The displacement of the double bond from C-3-C-4 to C-4-C-5 was observed during the reaction to give chloroketones **248** and **249**. From the ^{1}H NMR analysis, cyclobutanones **248** and **249** showed characteristic signals corresponding to the olefinic protons between δ_H 4.69-4.73 (H-5). Comparison of ^{1}H NMR spectra, indicated the proton signals for the ring junction H-6 (δ_H 3.05) and H-1 (δ_H 3.67) of compound **249** is more shielded than those of compound **248** [H-6 (δ_H 3.26) and H-1 (δ_H 4.12)]. In addition, formation of **248** and **249** was confirmed by analysis of the high resolution mass spectrum, showing ***m/z*** = 170.0606 ($\mathbf{M^{+\bullet}}$). Furthermore, the position of methyl group for compound **249** was in ***endo*** position, this was confirmed by NOE experiments. The cross peak between H-1/H-6 indicated that the junctions C1-C6 was ***cis*** and H-1 and H-6 were arbitrarily assigned as *β*–oriented. Other NOE correlation between H-6/H-9 and H-5/H-10 indicated that H-5, H-10, H6 and H-9 were a *β*-oriented and no correlation was observed between H-5/H9. This implied the ***exo*** position of methyl group for compound **248**.

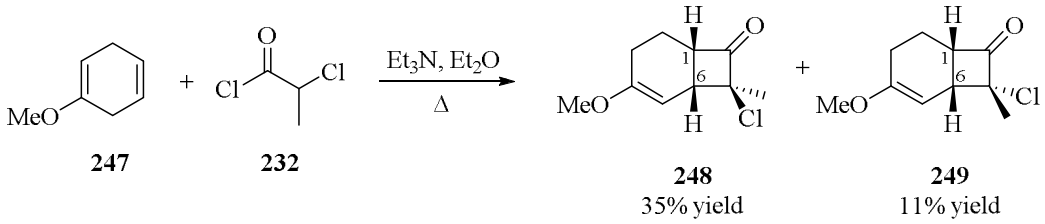

247 **232** **248** 35% yield **249** 11% yield

Scheme 5.32: Synthesis of cyclobutanones **248** and **249**

Hydrolysis of **248** in acidic media afforded cyclohexanone **250** in 91% yield (Scheme 5.33) (Blair et al., 1981).

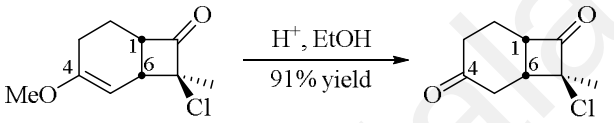

248 **250**

Scheme 5.33: Hydrolysis of methoxyl group at C-4

5.4.3.2.1 Formation of *α,β*-unsaturated ketone

Having obtained cyclohexanone **250**, next is to synthesize the *α,β*-unsaturated ketone **251** (Scheme 5.34). The dehydrogenation of cyclohexanone **250** was attempted using IBX with 4-methoxypyridine-N-oxide (MPO) as decribed in Baran's works (Nicolaou et al., 2002). IBX dissolved in DMSO acts as a single electron transfer (SET) agent and as such can affect oxidation adjacent to a carbonyl functionality to produce *α,β*-unsaturated counterpart (Scheme 5.34). By using this protocol, the compound **250** decomposed.

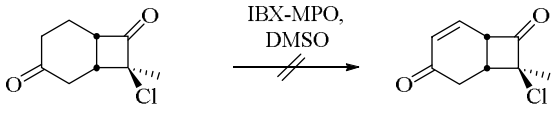

250 **251**

Scheme 5.34: Dehydrogenation of cyclohexanone **250**

Inspired by Chen's work, Saegusa-Ito oxidation [$Me_3SiOTf.NEt_3$; then $Pd(OAc)_2/O_2$] was attempted to make enone **251** (Richard & Chen, 2012). The reaction started by silyl enol ether formation of the bicyclic ketone **250** to afford chloroketone **252** as a mixture with its regioisomer **253** (**252** is more stable than **253**). Evidence for the formation of silyl enol ethers **252** and **253** were confirmed by the ^1H NMR spectrum with the signals and coupling patent at δ_H 3.0-5.0 corresponding to H-1, H-3, H-5 and H-6. The silyl enol ethers **252** and **253** are inseparable mixture in a 2:1 ratio as determined by ^1H NMR.

Oxidation of bicyclic silyl enol ethers **252** and **253** was done by using $Pd(OAc)_2$ as oxidant together with oxygen (co-oxidant) in DMSO at 80°C (Scheme 5.35). However, under these conditions, both compounds **252** and **253** decomposed.

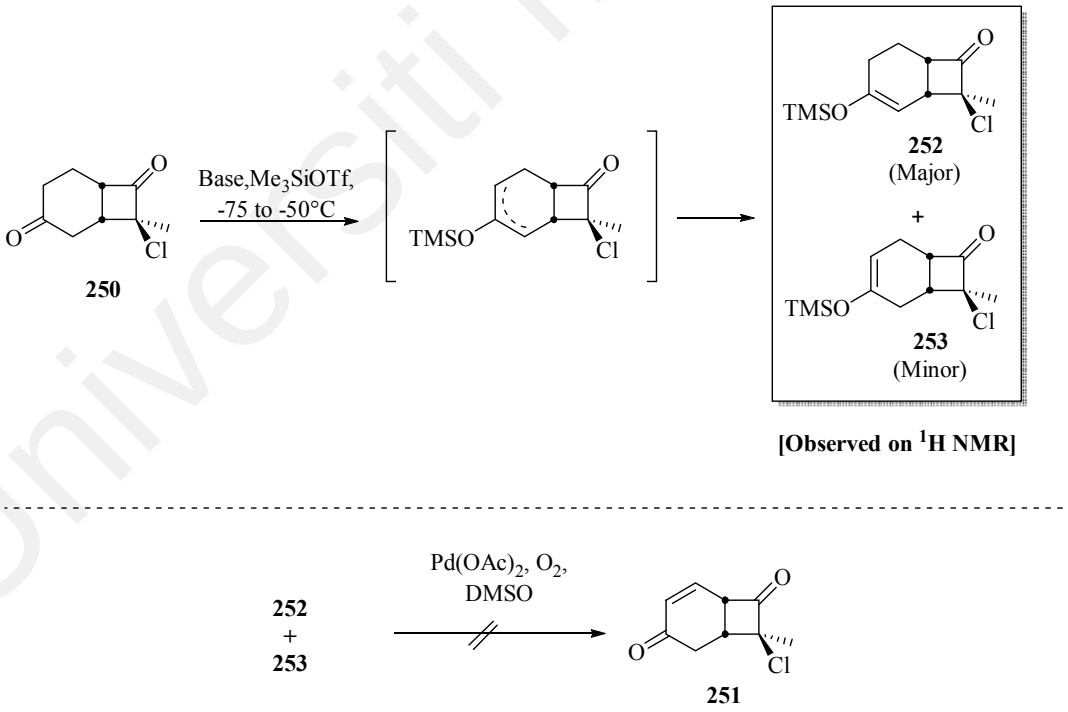

Scheme 5.35: Saegusa-Ito oxidation of **250**

5.4.3.2.2 Allylic bromination at C-3 position

Disappointed with the decomposition of compounds **252** and **253** in the oxidation, allylic bromination of **248** was attempted to afford the *α,β*-unsaturated ketone **251** (Scheme 5.36). Wohl-Ziegler radical bromination (Koltun & Kass, 2000) of **248** by means of ***N***-bromosuccinimide in CCl_4 gave an allylic bromide **254** in 20% yield. The formation of allylic bromine **254** was observed in ^{1}H NMR spectra, where the signal at δ_H 4.49 (H-3) appeared as a triplet (***J*** = 7.2 Hz). After 3 weeks of storage in the freezer, the enol ether **254** had suffered hydrolysis into ketone **255**. Dehydrobromination (Ando et al., 1987) of the allylic bromination product **255** with lithium carbonate (Li_2CO_3) and lithium bromide (LiBr) in DMF at 120°C gave a complex mixture of products, containing the desired cyclohexenone **251** (Scheme 5.36).

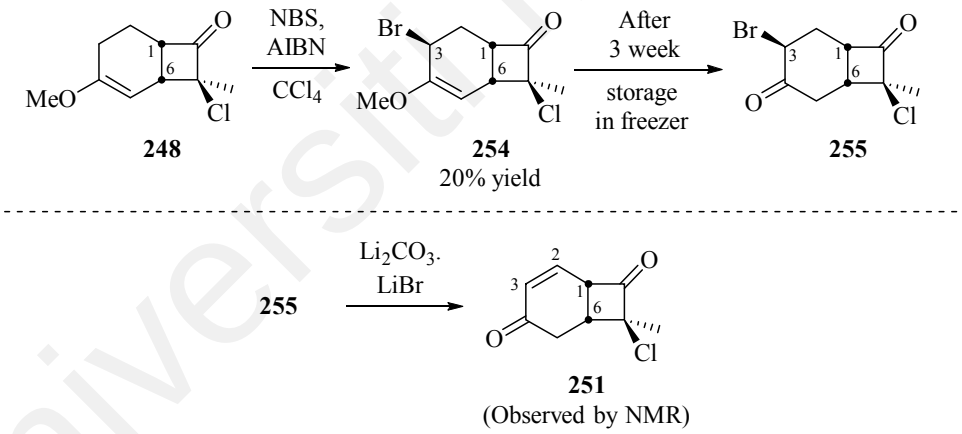

Scheme 5.36: Radical bromination of **248**

The formation of *α,β*-unsaturated ketone was evidenced by ^{1}H NMR ($CDCl_3$) spectroscopy, with signals appearing in the ^{1}H NMR spectra at 7.0 and 6.5 ppm, corresponding to H-3 and H-2 of the double bond **251**, respectively.

5.4.3.2.3 Substitution at C-8 position

Introduction of benzyl groups at C-8 position of **248** was attempted by using Wittig, Barbier and Grignard protocols, without success due to the chlorine substituent at C-7 position which causes steric hindrance (Scheme 5.37) (Li et al., 2011; Fournier & Poirier, 2011). The problem is expected to be solved, in principle, by dechlorination of the ketone **248**.

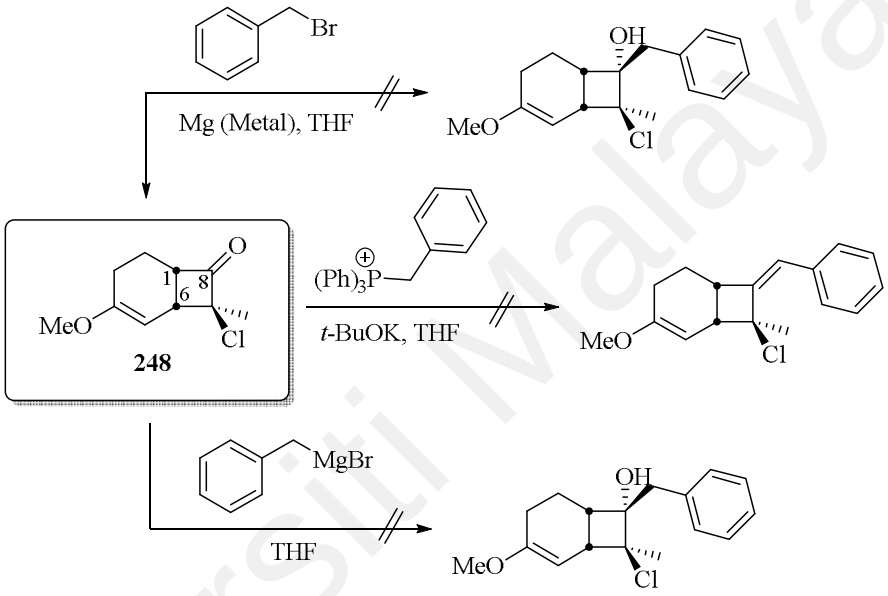

Scheme 5.37: Nucleophilic substitution at C-8 position of compound **248**

Thus, bicyclic[4.2.0]octanene **248** was subjected to dechlorination at C-7 using activated Zn, TMEDA and acetic acid to afford cyclobutanone **256** in 45% yield (Koltun & Kass, 2000). The formation of cyclobutanone **256** was confirmed by ^{1}H NMR spectrum with the signal at δ_H 0.91 (d, ***J*** = 8.4, H_3-9) corresponding to methyl group attached to C-7. This compound was found to be relatively unstable and had to be used rapidly. Wittig reaction of 7-methyl ketone **256** with ylide **257** gave the expected 7-methyl products **258** and its geometrical isomer (***Z/E***:1:1) in 51% yield (Scheme 5.38) (Wu et al., 1994).

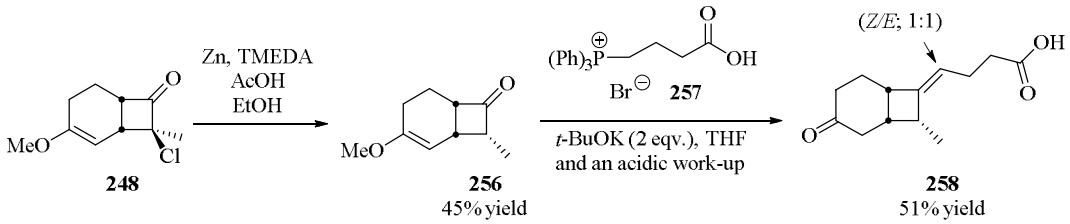

Scheme 5.38: Homolongation of cyclobutanone **248**

The sequence was continued by palladium-catalyzed hydrogenation of **258** in methanol to afford compound **259a** and **259b** (80% yield)[2] (Scheme 5.39) (Ranu & Sarkar, 1994; Avlonitis et al., 2003). On the basis of Robinson's work, selective bromination of both **259a** and **259b** using phenyl trimethyl ammonium perbromide (THF, -78 to 0°C) would give the bromoketone **260** as the major product (Robinson et al., 2009; Pettit et al., 2012). But ^{1}H NMR ($CDCl_3$) examination of the crude product showed the typical signals for bromoketone **261** and not bromoketone **260**. The doublet signal at 4.86 ppm showed the correlation between protons at C-5 and C-6. The synthesis was stopped at this stage and another approach using 1,4-cyclohexadiene.

[2] Isolated two diastereoisomers, the major compound is **259a**

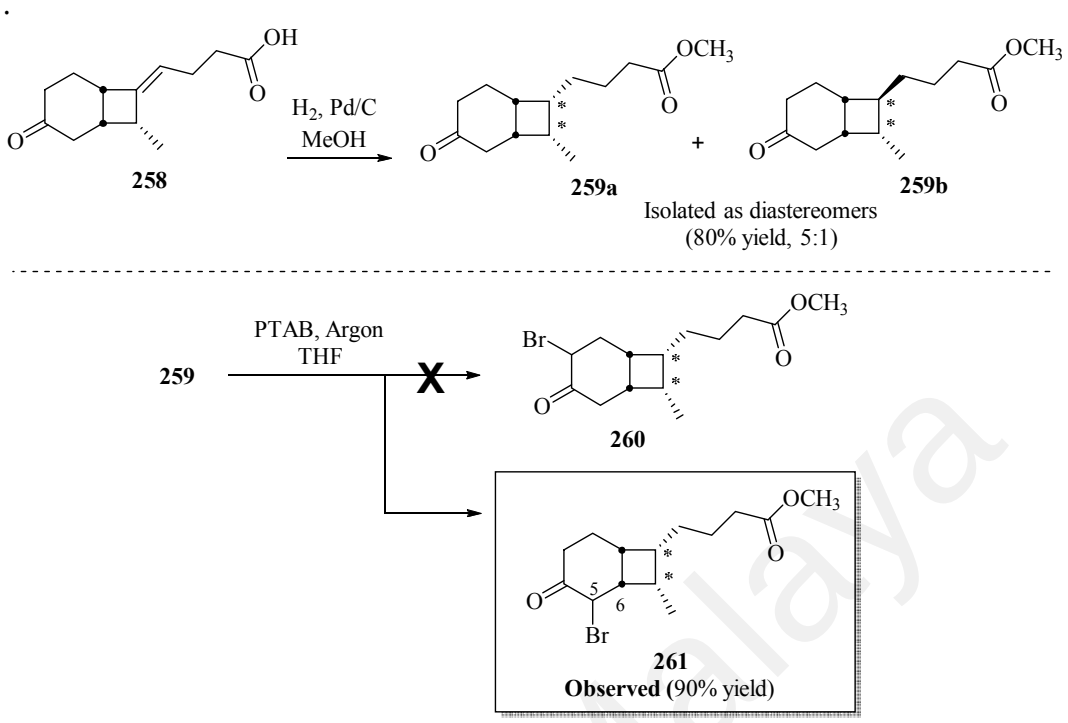

Scheme 5.39: Synthesis of compound **261**

5.4.3.3 1,4-Cyclohexadiene

Encouraged by subchapters 5.4.3.1 and 5.4.3.2 results, a model to synthesize the allylic alcohol **262** from bicyclo **263** was designed (Scheme 5.40). The allylic alcohol **262** could provide a diversity-oriented access to make dienophile **263** and/or diene **264**. The synthesis started with the preparation of the bicyclo[4.2.0]octane system followed by epoxidation. To generate an allylic alcohol moiety, an elimination reaction was envisaged from epoxide **263**.

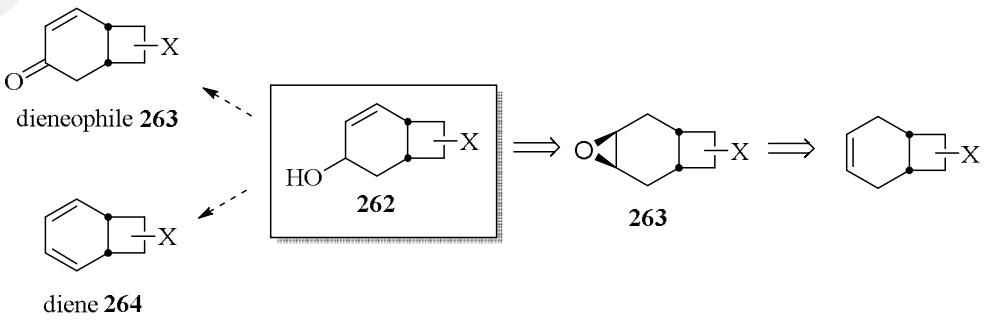

Scheme 5.40: Strategy for synthesis of allylic alcohol **262**

Summarized in Scheme 5.40, 1,4-cyclohexadiene (**265**) was used to synthesize bicyclo[4.2.0]oct-3-ene **266**. The building block, 7,7-dichlorobicyclo[4.2.0]oct-3-en-7-one (**266**) was prepared by the addition of dichloroketene, generated ***in situ*** from **217**, to 1,4-cyclohexadiene (**265**) in 69% yield (Mori et al., 1997; Horasan et al., 2011; Davis & Carpenter, 1996). The reaction was done under ultrasonic irradiation (Scheme 5.41).

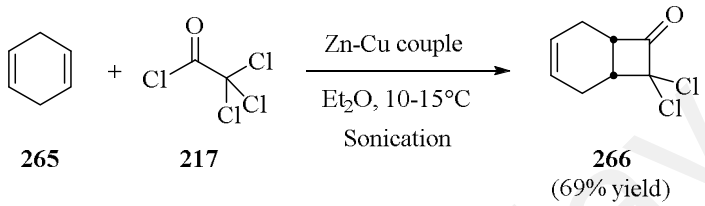

Scheme 5.41: Synthesis of dichlorocyclobutanone **266**

5.4.3.3.1 Oxidation of alkene

The epoxidation of alkene group of **266** at C-3 was done using ***m***-CPBA in dichloromethane (Wu et al., 1994). During this transformation, Baeyer-Villiger oxidation (Davis & Carpenter, 1996) also took place to give the unwanted lactone **267** in 30% yield together with the desired epoxide **268** (10% yield) (Scheme 5.42).

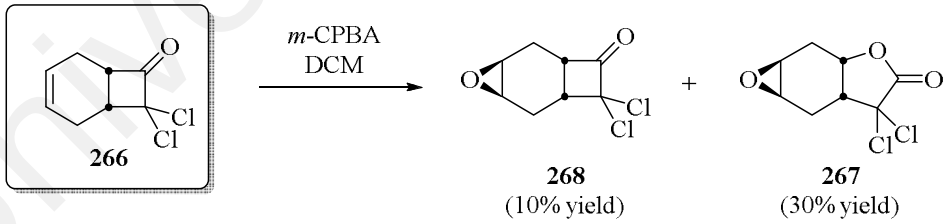

Scheme 5.42: Oxidation of dichlorocyclobutanone **266**

To circumvent this difficulty, singlet oxygen ($^1O_2$) ene-reaction was used to synthesize cyclohexenol **269**. Singlet oxygen can be produced chemically by reacting hydrogen peroxide (H_2O_2) with sodium hypochlorite (Foote et al., 1968).

$$H_2O_2 + NaOCl \rightarrow {}^1O_2 + NaCl + H_2O$$

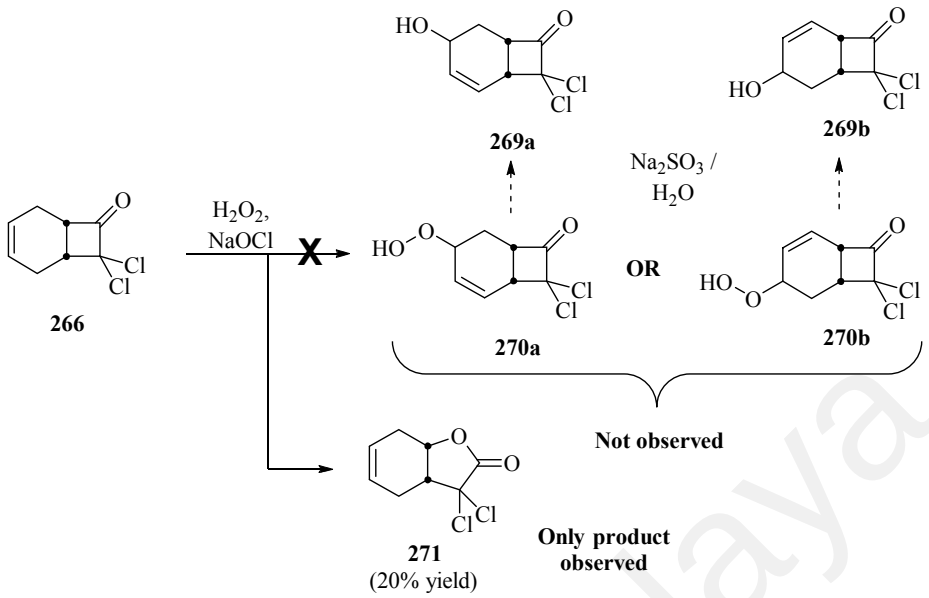

Scheme 5.43: Singlet oxygen ($^1O_2$) ene-reaction of **266**

The methanolic solution containing excess hydrogen peroxide was oxidized by adding dilute aqueous sodium hypochlorite (Scheme 5.43). However, no sign of formation of hydroperoxide **270** was observed and only the unwanted lactone **271** was obtained as a result of Baeyer-Villiger oxidation reaction (Horasan et al., 2011; Davis & Carpenter, 1996). To avoid this problem, a photochemical method would have to be used for the generation of $^1O_2$ involving the irradiation of normal oxygen gas in the presence of an organic dye as a sensitizer, such as tetraphenylporphyrin (Horasan et al., 2011; Davis & Carpenter, 1996).

5.4.3.3.2 "Protection" of the carbonyl group

In order to prevent the formation of the unwanted lactones **267** and **271**, next step was to modify the substrate **266** by reducing the carbonyl group. Reduction of compound **266** with $NaBH_4$ offered alcohol **272** in 68% yield (Powers et al., 2007). Epoxidation of double bond in **272** using ***m***-CPBA produced the epoxide **273** in 79%

yield (Wu et al., 1994). To remove excess acid from ***m***-CPBA, treatment work-up with 1 M NaOH was performed. Unexpectedly, a new compound was produced, with very simple ^{1}H and ^{13}C NMR spectra corresponding to the symmetrical dialdehyde structure **274** (Scheme 5.44). The mechanism of formation of dialdehyde **274** is explained in Scheme 5.44. The experiment to synthesize the epoxide **273** was repeated without basic washing.

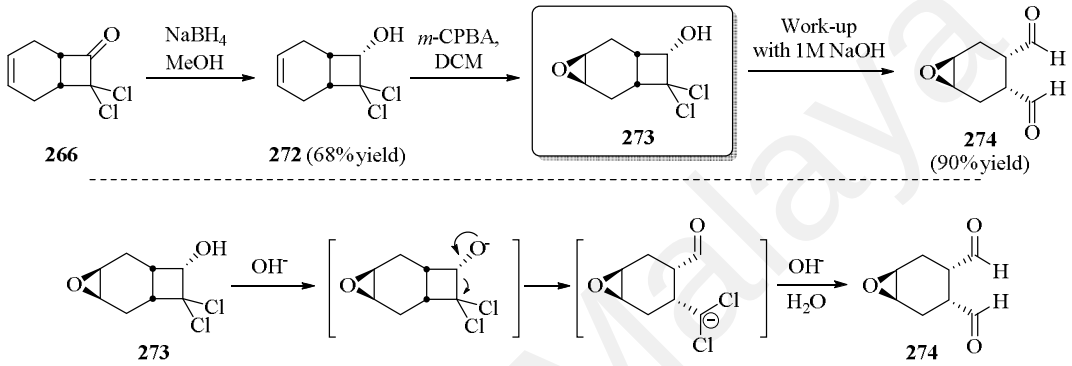

Scheme 5.44: Formation of dialdehyde **274**

To generate the allylic alcohol moiety (**276a** and **276b**), E1 elimination was attempted from epoxide **273**. Reactions of epoxide **273** with PTSA and/or concentrated H_2SO_4 were carried out to give the tricyclic compound **275**, instead, with no formation of the allylic alcohols **276a** and **276b** (Scheme 5.45).

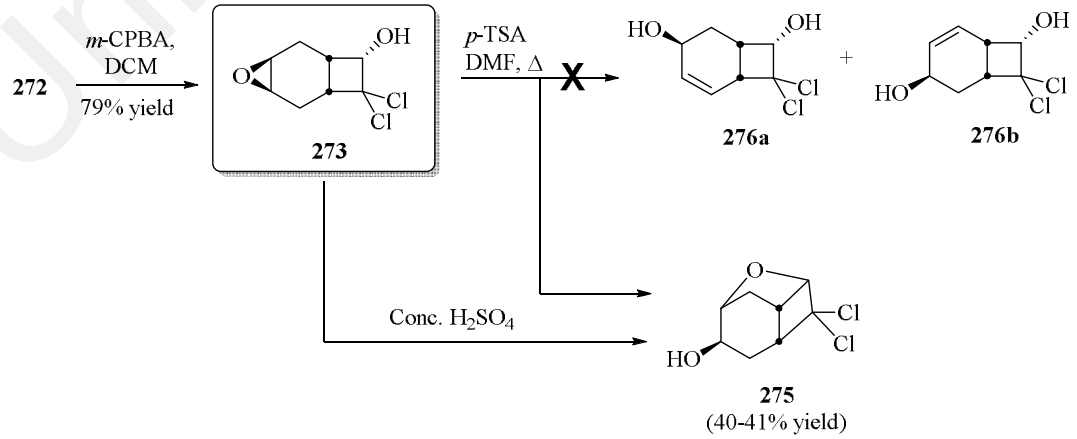

Scheme 5.45: Attempted E1 elimination of **273** under acidic condition

Another possibility to generate an allylic alcohol moiety was to open the epoxide by a selenide ion, oxidise the selenium atom and then perform an elimination reaction. For this study, the model substrate **277** was used (Scheme 5.46). It was synthesized by reducing the dichloro compound **266** with activated zinc and acetic acid to give **278** (Koltun & Kass, 2000). The carbonyl group was protected using 1,2-bis[(trimethylsilyl)oxy]ethane to give the ketal **279** in order to prevent the formation of lactone analogues of **271** and increase the yield of epoxide **277** (Wu et al., 1994). Oxidation of ketal **279** with ***m***-CPBA yielded the epoxide **277** in 65% yield.

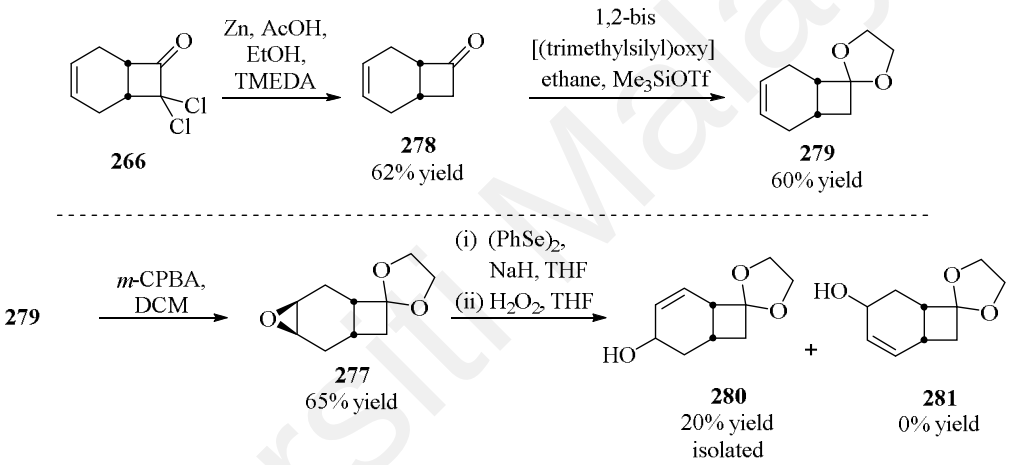

Scheme 5.46: Synthesis of cyclohexenol **280**

The epoxide **277** was transformed into allylic alcohol **280** using mild conditions developed by Sharpless and Lauer (1973). The selenium anion is an excellent nucleophile and easily opens the epoxide ring of **277** via S_N2 reaction to give the hydroxy selenide **282**. Treatment of **282** with excess hydrogen peroxide gave the unstable selenoxide **283** as the intermediate then, which decomposed to the allylic alcohol **280** in 20% yield (Scheme 5.47).

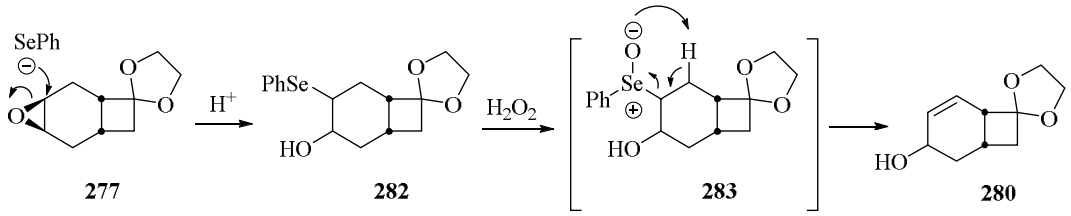

Scheme 5.47: Mechanism reaction of allylic alcohol **280**

5.4.4 Approach B: [2+2] intramolecular ketene cycloaddition

In the previous approaches, [2+2] intermolecular ketene cycloaddition were attempted. In this model study, intramolecular [2+2] ketene cycloaddition, instead of intermolecular reaction (the previous attempts), was explored. Retrosynthetic analysis of cyclobutanone **284** is shown in Scheme 5.48. Compound **285** can be accessed from acetylation of allylic alcohol **286** with acyl chloride **287** followed by ketene-alkene [2+2] cycloaddition. Allylic alcohol **286** could be obtained by a series of conversions of functional groups from 4-methoxy-1,4-cyclohexadiene (**247**).

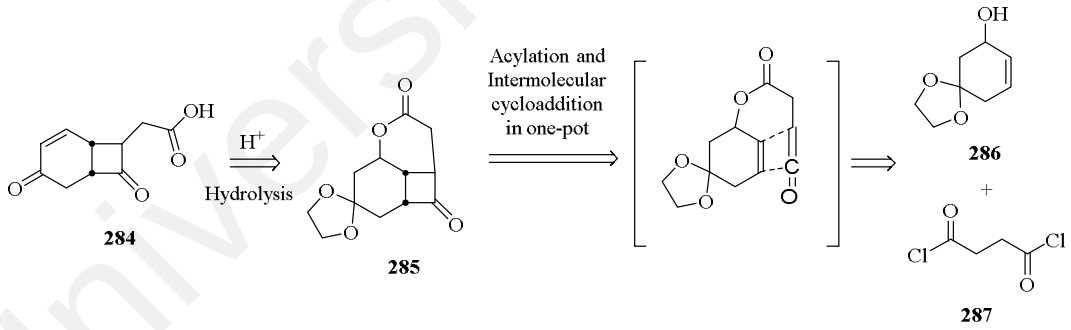

Scheme 5.48: Retrosynthesis of cyclobutanone **284**

5.4.4.1 Intramolecular [2+2] ketene cycloaddition

The synthesis of allylic hydroxyl **286** commenced from the readily available 4-methoxy-1,4-cyclohexadiene (**247**), whose acid catalyzed ketalization led to vinyl ketal **288** (Scheme 5.49) (Zhang & Koreeda, 2002; Allen et al., 1986). Without purification, treatment of **288** with ***m***-CPBA provided epoxide **289** in 55% yield (Cheng

et al., 1992). On the basis of the previous study with organoselenium reagents, the treatment of epoxide **289** with diphenyl diselenide provided the allylic alcohol **286** in 30% yield (Scheme 5.49) (Sharpless & Lauer, 1973; Zhang & Koreeda, 2002; Krief et al., 1992).

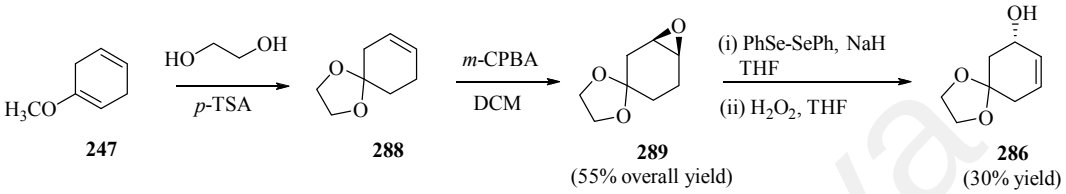

Scheme 5.49: Synthesis of compound **286**

The sequence was continued by doing an acylation reaction and [2+2] ketene-alkene cycloaddition in one-pot between **286** with **287** (Scheme 5.50). Unfortunately, this reaction did not produce the desired product **285** and the synthesis was stopped at this stage.

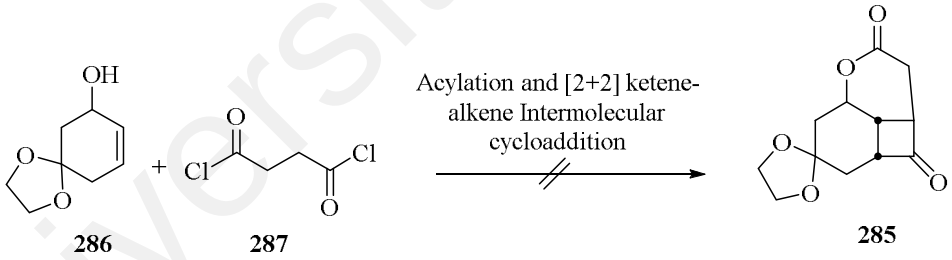

Scheme 5.50: Acylation and intermolecular cycloaddition of **286** and **287**

5.4.5 Approach C: synthesis of bicyclo[4.2.0]octane containing methylenedioxy phenyl moiety at C-7

After several approaches using inter- and intramolecular [2+2] ketene cycloadditions, the intermolecular have shown promising result. Therefore, this approach was taken using the ketene **293**, which is mimics the structure of kingianins. The objective is to

synthesize the compound **290**, which could lead to the formation of dienophile **291** and diene **292**. The key intermediate **290** could be obtained from [2+2] cycloaddition between cyclohexadiene **265** and ketene **293** (Scheme 5.51).

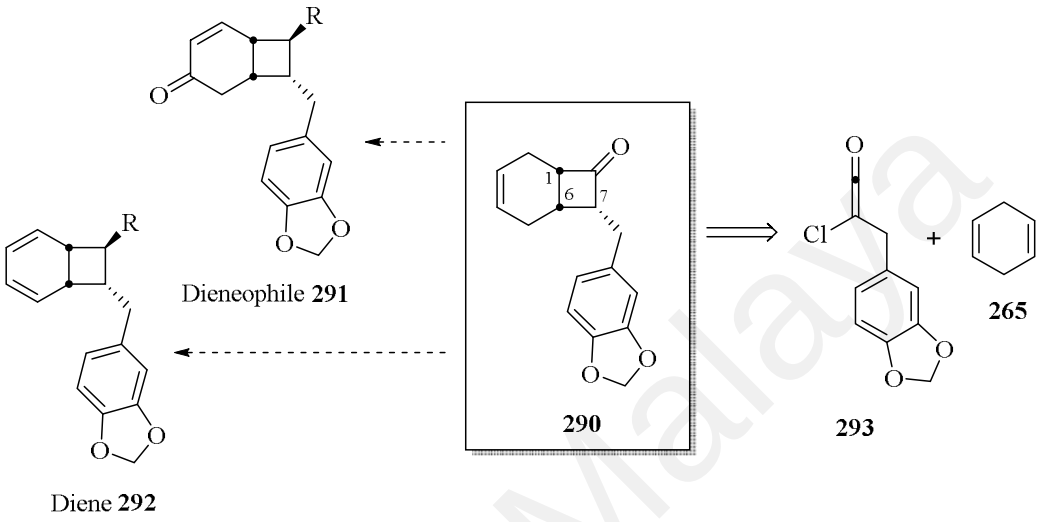

Scheme 5.51: Strategy for synthesis of dienophile **291** and diene **292**

First, the synthesis of the ketene precursor **294** was prepared using Qin's protocol (Qin et al., 2011; Hu et al., 2013). The synthesis of **294** began with the known piperonyl bromide (**295**), which can be prepared from **296** in one step (Qin et al., 2011). Double alkylation of sodium trichloroacetate (**297**) with **295** gave ester **298** and the mechanism of formation of **298** is explained in Scheme 5.52 (Hu et al., 2013; Raths & Dehmlow, 1987). Sodium trichloroacetate (**297**) reacts with phenyl bromide (**295**) to give an ester **299** and concurrently this compound will generate trichloromethyl anion (**300**) (Taschner, 2001; Charette et al., 2001). This anion will extract the chlorine from **299** to provide the active anion **301** (Raths & Dehmlow, 1987). The anion **301** will undergo nucleophilic substitution with phenyl bromide **295** to give the ester **298** (Raths & Dehmlow, 1987), which underwent hydrolysis with NaOH to provide acid **294** in 80% yield.

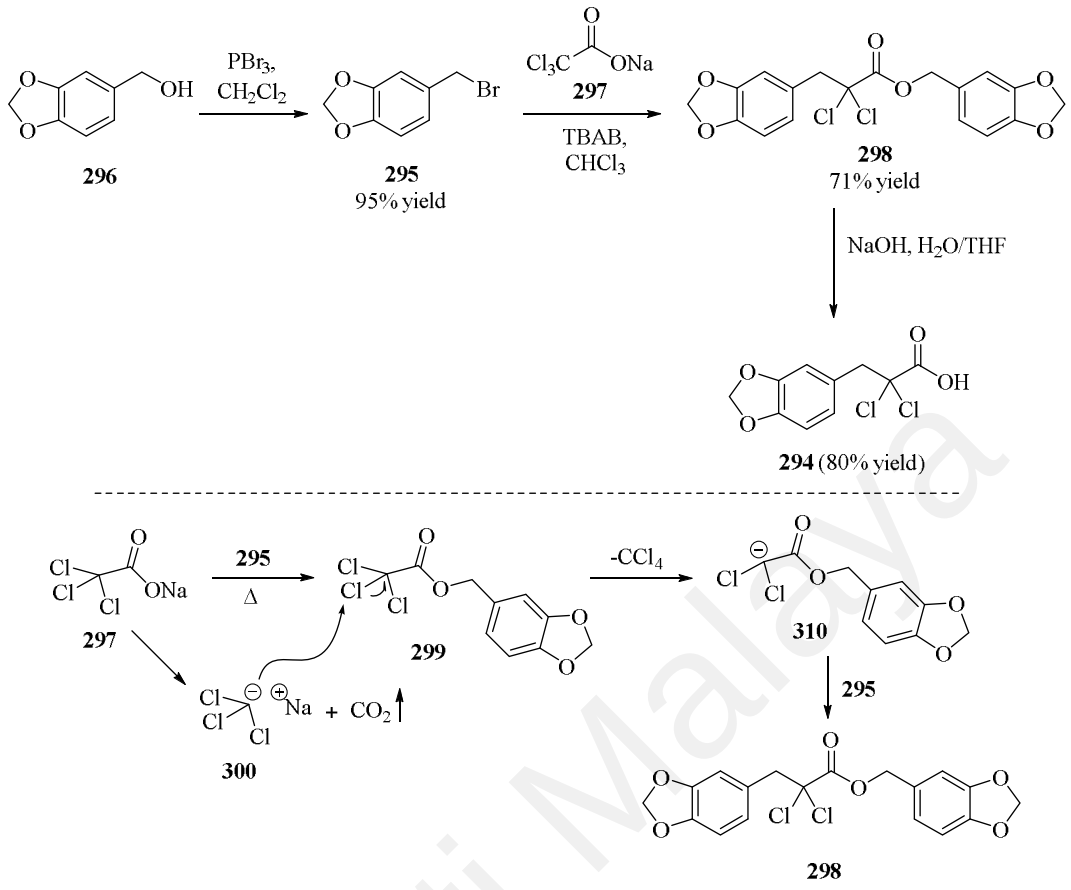

Scheme 5.52: Synthesis of 2,2-dichloro carboxylic acid **294**

The synthesis of dichloroketene from acid **294** was done after acylation with thionyl chloride under reflux conditions (Buurma et al., 2001). Excess thionyl chloride was then removed and without purification, acyl chloride **302** was reacted with 1,4-cyclohexadiene (**265**) in the presence of activated zinc (Zn-Cu couple) under ultrasonic irradiation. After several attempts, the reaction did not give the desired product **303** (Scheme 5.53).

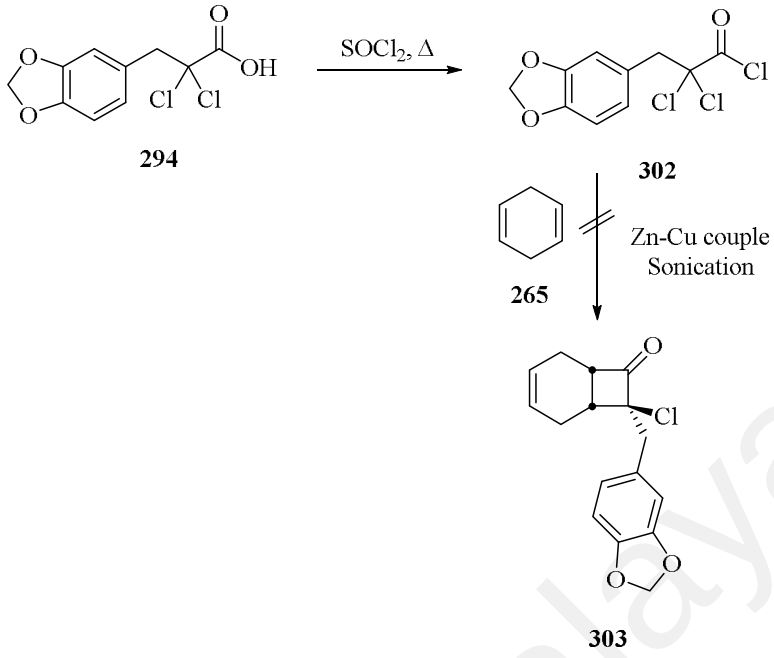

Scheme 5.53: Synthesis of compound **303**

Due to the unsuccessful synthesis of compound **303**, another precursor; 2-chlorocarboxyl chloride **304**, from 2-chlorocarboxylic acid **305** was prepared. The preparation of the corresponding acid **305** was described in the literature (Sohda et al., 1983). The synthesis began with two fragments i.e piperonyl chloride (**306**) and ethyl-2-chloro-3-oxobutanoate (**307**) (Scheme 5.54). The chloride **306** was prepared from piperonyl alcohol (**308**) (Cheon et al., 2005). Meanwhile, compound **307** can be synthesized in one step using sulfuryl chloride from commercially available ethyl-3-oxobutanoate (**309**) (Smith et al., 2008). The nucleophilic substitution of **307** with piperonyl chloride (**306**) gave ethyl-2-acetyl-2-chloro-3-(3,4-methylenedioxyphenyl) propionate (**310**) followed by hydrolysis with NaOH in ethanol to form **305** in 90% yield (Scheme 5.54).

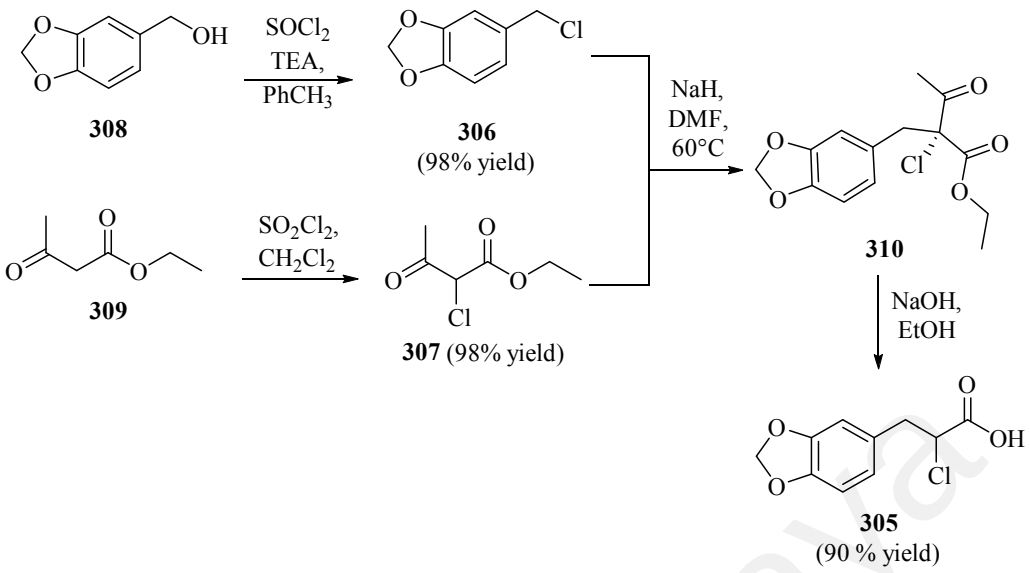

Scheme 5.54: Synthesis of 2-chlorocarboxylic acid **305**

With this 2-chlorocarboxylic acid **305** in hand, the attention was focused on the ketene [2+2] cycloaddition with 1,4-cyclohexadiene (**265**). Acid **305** was transformed into acyl chloride **304** using thionyl chloride to generate benzylketene in the presence of Et_3N. Unfortunately, as shown in Scheme 5.55, the desired product **303** was not obtained.

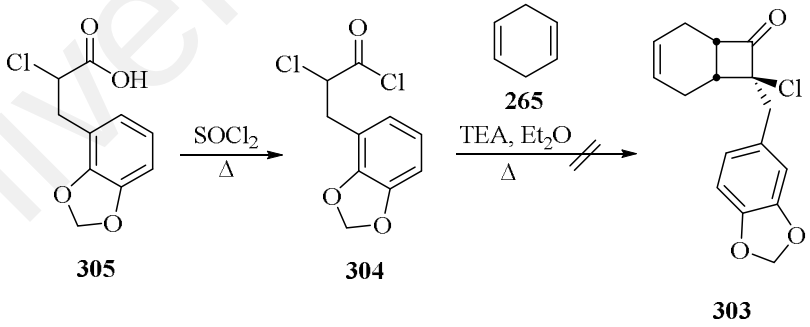

Scheme 5.55: Ketene [2+2] cycloaddition of acyl chloride **304** with diene **265**

The following attempt was carried out by using 1,3-cyclohexadiene (**231**) instead of non-conjugated 1,4-cyclohexadiene (**265**). The [2+2] cycloaddition of 1,3-cyclohexadiene (**231**) to benzylketene (generated ***in situ*** from acyl chloride **304** in the presence of Et_3N) in diethyl ether, at room temperature, provided the corresponding

bicyclic cyclobutanone **311** in small quantity (7% yield). Repeating the same experiment under reflux conditions using several solvents increased the yield to 14% (Table 5.1). Changing the solvent to cyclohexane (bp 81°C) improved the yield of [2+2] cycloaddition provided only cycloadduct **311** in 25% yield. The assignment of compound **311** was based on a NMR experiment.

Table 5.1: Optimization of ketene [2+2] cycloaddition

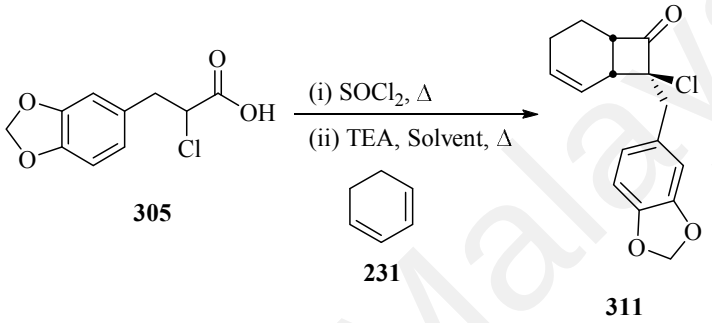

305 **231** **311**

Entry[1]	Condition	Yield (%) [2,3]
1	Et_2O, room temp	7
2	Et_2O, 35°C	14
3	Cyclohexane, 83°C	25
4	CH_2Cl_2, 40°C	6
5	THF, 70°C	7
6	Pet. Ether, 50°C	5
7	Toluene, 100 °C (oil bath)	5

[1] The reaction done in 2.0 mM scale
[2] Only product **311** was isolated
[3] Yield after column chromatography

5.4.5.1 Substitution at C-8 position

The cycloadduct **311** was easily purified by column chromatography and subjected to reduction with activated zinc and acetic acid to give the cycloadduct **312** in 88% yield (Koltun & Kass, 2000). The homologation of bicycle **312** was done with Wittig reactions (Schemes 5.56 and 5.57). The first Wittig reaction was performed using ylide **313** to give enol ether **314 (**Kozikowski et al., 1995; Rosini et al., 1998). Without

purification, the enol ether **314** was subjected to hydrolysis with formic acid to provide aldehyde **315** (Rosini et al., 1998).

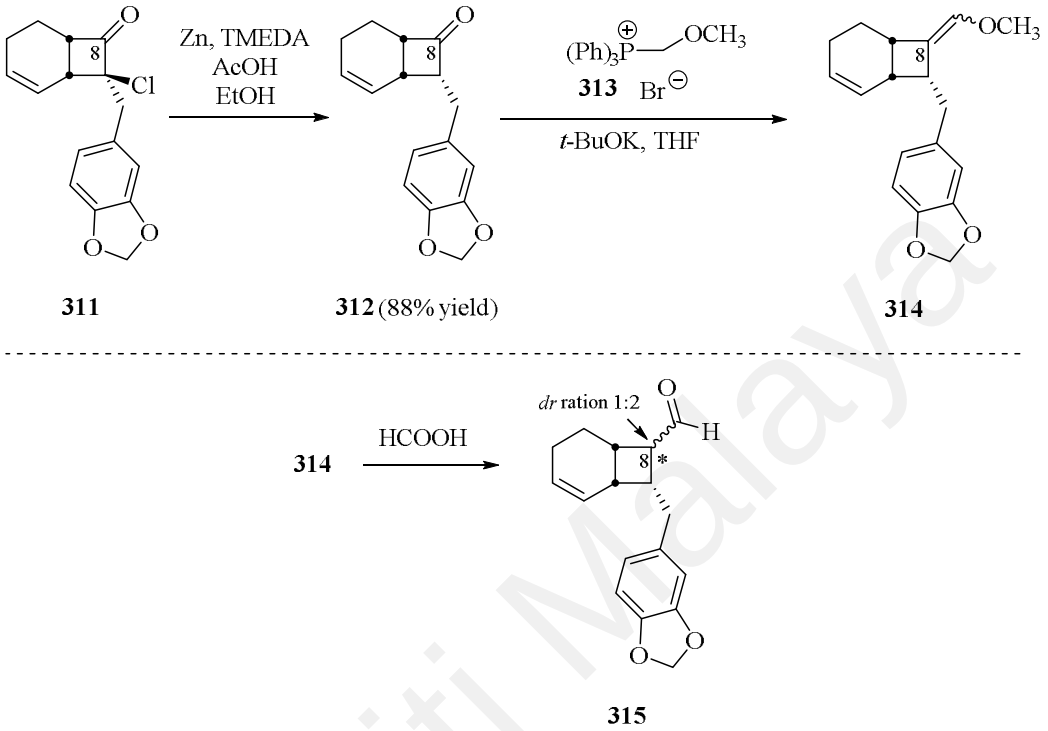

Scheme 5.56: Synthesis of aldehyde **315**

The second attempt at Wittig reaction was carried out with ylide **316** to furnish the desired benzyl **317** with ***E/Z*** isomer in a ratio 1:2 (Wu et al., 1994). The hydrogenation using palladium catalyst and hydrogen gas afforded ester **318** in 80% yield (Ranu & Sarkar, 1994; Avlonitis et al., 2003).

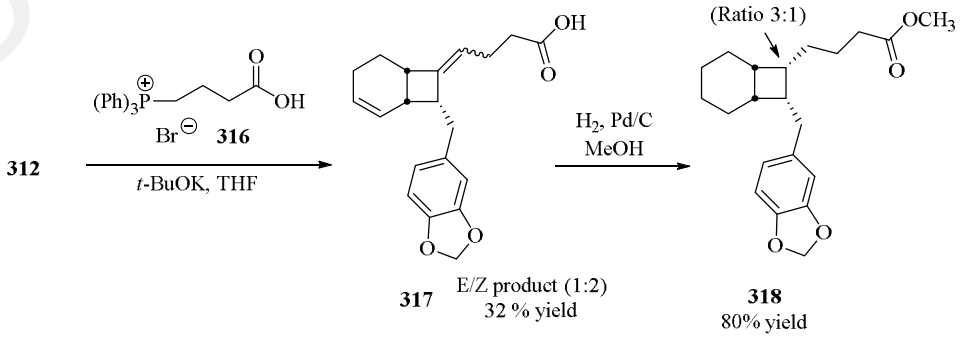

Scheme 5.57: Synthesis of bicyclo **318**

5.5 Conclusion

In summary, the goals of this project were only partially met. The partial structure of kingianins has been successfully achieved, through the completion of several reactions using model compounds. These findings will be the benchmark for the future synthetic work on kingianin series of compounds. The preparation of bicyclo[4.2.0]octane core (for example compound **311**) can lead to a greater range of analogues, which could be further developed (Scheme 5.58). Ideally, this approach was a rapid assembly of the kingianins carbon skeleton, thus maximizing the chance for good overall yields of the final products. The proposed total synthesis of kingianins is currently in progress.

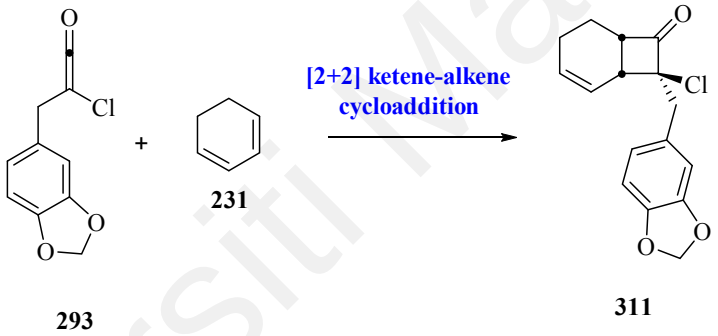

Scheme 5.58: Synthesis of bicyclo[4.2.0]octane **311**

In the future, with this molecule in hand, functionalization at the C-8 position can be prepared (i.e compounds **319** and **320**). Next, compounds **319** and **320** can be converted to diene **321** and/or dienophile **322**. The final step in the total synthesis of kingianins is envisioned to be a [4+2] Diels-Alder cyclization forming the pentacyclic structure of kingianins. The plan for this work is outlined in Scheme 5.59.

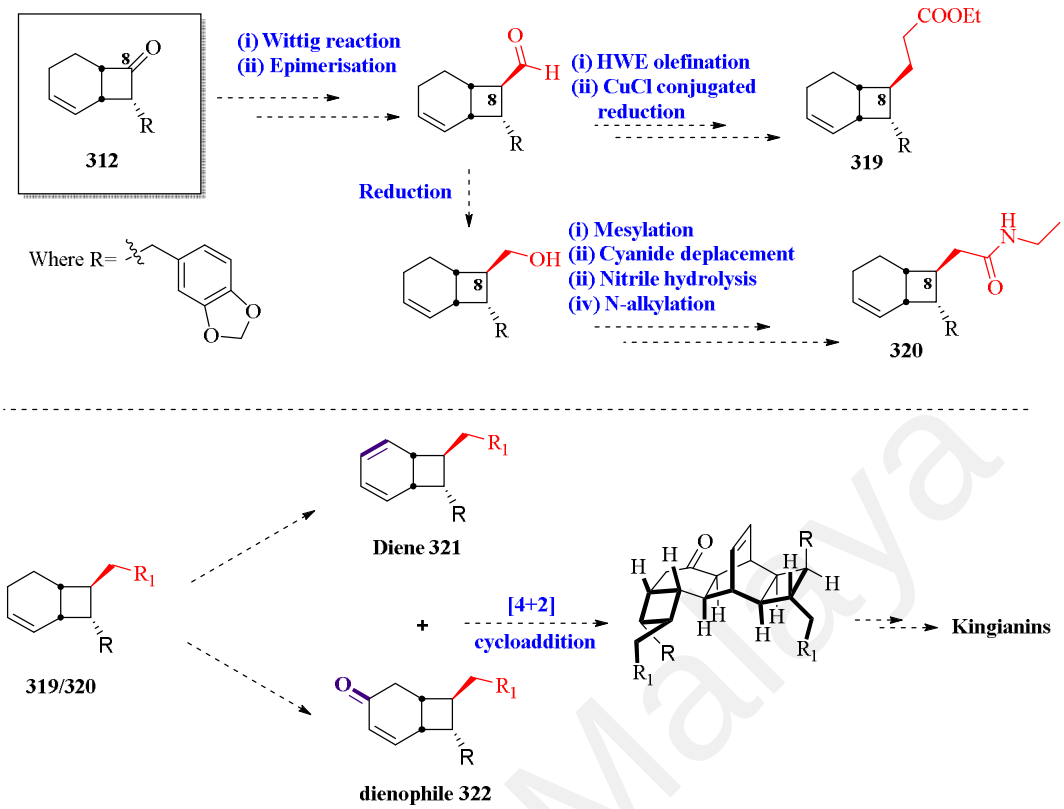

Scheme 5.59: Proposed synthesis of diene **321** and dienophiles **322**

The second approach was inspired from the result in Chapter 5.4.3.3, which involved the synthesis of allylic alcohol **323**. The allylic alcohol **323** is a suitable precursor to make dienophile **324** and/or diene **325**. The next strategy involves the synthesis of the pentacyclic skeleton **326**, followed by derivatization of the substituents. This constitutes an alternative way to the synthesis of kingianins and a flexible route to analogues. The plan for this work is outlined below (Scheme 5.60).

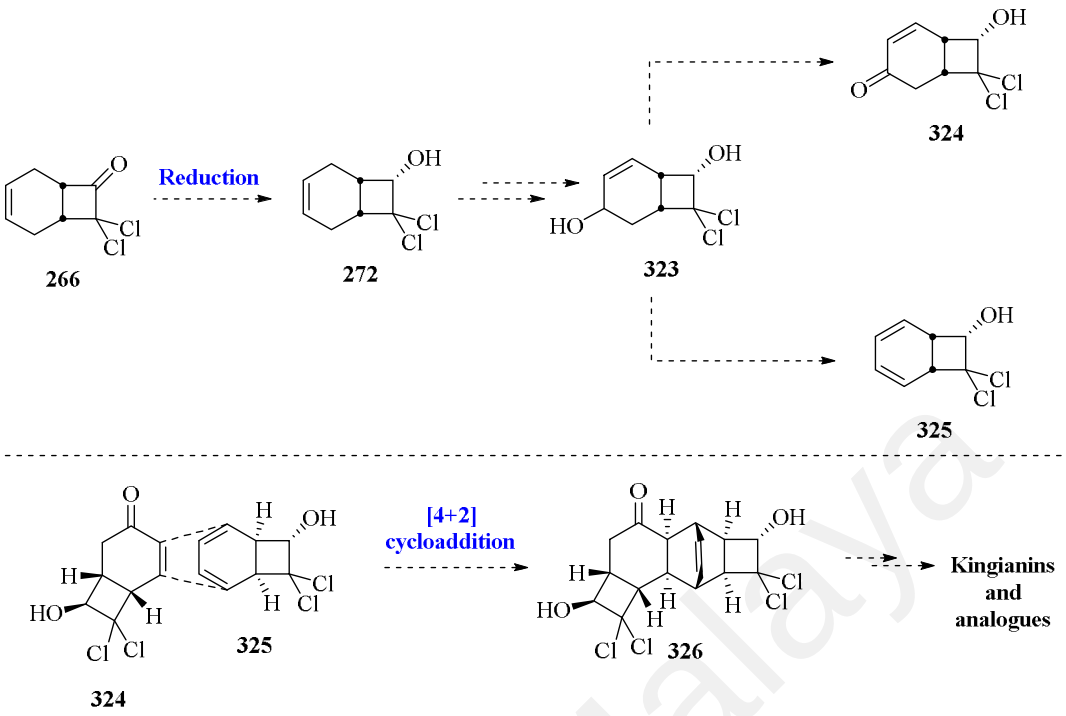

Scheme 5.60: Synthesis of pentacyclic **326**

Further investigation for this total synthesis is still in progress and there are plenty of platforms available for further investigation. In the future, the intermediates will be evaluated for Bcl-xL and Mcl-1 binding affinities.

CHAPTER 6

CONCLUSION

The chemistry of the genus ***Endiandra*** and ***Beilschmiedia*** has attracted great interest since the isolation of the first endiandric acid series, endiandric acid A (**35**) from ***Endiandra Introrsa*** (Bandaranayake et al., 1980), and the first kingianin series, kingianin A (**45**) from ***Endiandra kingiana*** (Leverrier et al., 2010). These types of compounds are frequently isolated as racemic mixtures from genus ***Endiandra*** and ***Beilschmiedia***. The abundance of these compounds in different ***Endiandra*** and ***Beilschmiedia*** species is highly variable. It has been hypothesized that these cyclic polyketides are the primary metabolites from these two plant species and may be useful as chemotaxonomic markers within the Lauraceae family. Only three ***Endiandra*** species have been chemically investigated to date. The phytochemical investigation undertaken in this research project has proven that that genus ***Endiandra*** was equally important in producing interesting compounds, both structurally and biologically.

The phytochemical study of methanol extract of ***Endiandria kingiana*** has led to the isolation and characterization of 19 cyclic polyketides. These compounds were divided into two major classes; endiandric acids and kingianins. Ten tetracyclic endiandric acids were isolated; kingianic acids A-H (**120**-**127**), together with known endiandric acid M (**93**) and tsangibeilin B (**89**). Among them, three were new (kingianin O-Q [**128**-**130**]) while the remaining have been reported by Leverrier et al. (2011). The detailed spectroscopic discussions on these compounds were presented in Chapter 3.

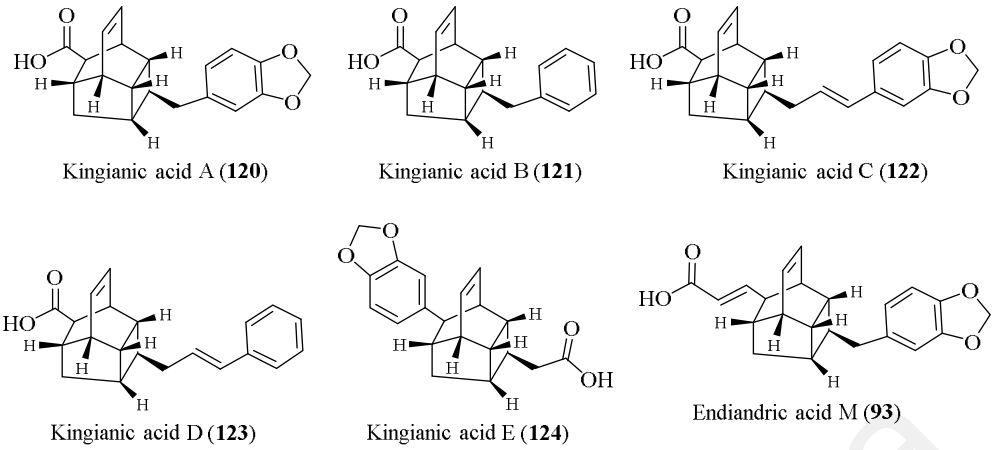

Figure 6.1: Endiandric acid Series (Type A)

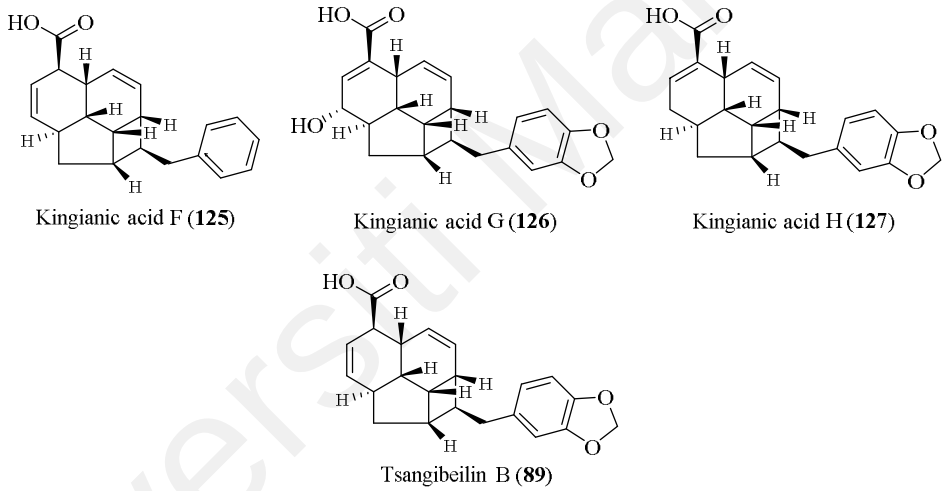

Figure 6.2: Endiandric acid Series (Types B and B')

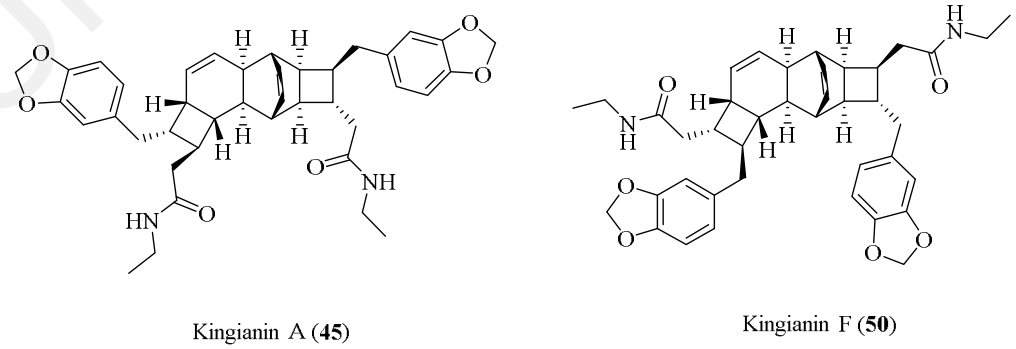

Figure 6.3: Kingianin Series

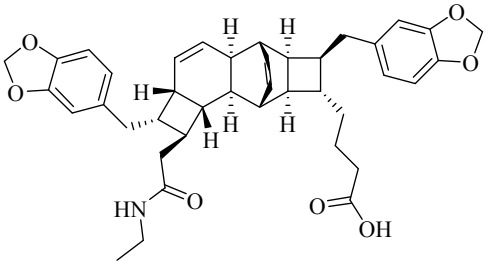

Kingianin K (**55**)

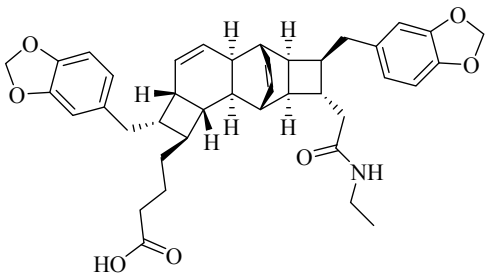

Kingianin L (**56**)

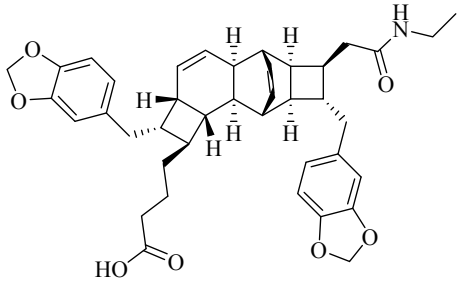

Kingianin M (**57**)

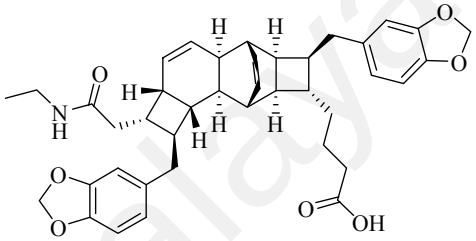

Kingianin N (**58**)

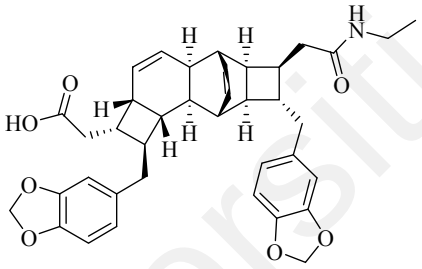

Kingianin O (**128**)

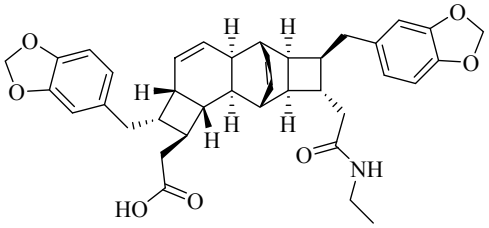

Kingianin P (**129**)

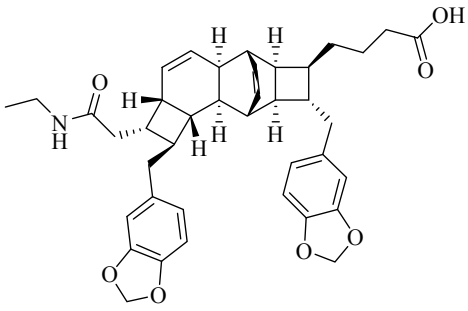

Kingianin Q (**130**)

Figure 6.3: Continue

The interest of this research were based on cancer treatments and prevention, therefore these isolates were evaluated for two bioassays; binding affinities towards Bcl-xL/Bak and Mcl-1/Bid (on antiapoptotic proteins) and cytotoxic effects against various human tumour cells (Chapter 4). For endiandric acid series, no binding was detected for Bcl-xL, however moderate binding affinity for Mcl-1 (25-30% inhibition at 20 µM and ≥ 75% at 100 µM) were obtained with compounds **89**, **122** and **125.** Meanwhile, for new kingianins, only kingianin P (**129**) showed potent binding for Bcl-xL (13 ± 2 µM) and moderate binding affinity for Mcl-1 (30 ± 1 µM). The other compounds showed very weak (>23 µM and >33 µM for Bcl-xL and Mcl-1 binding affinities, respectively). Meanwhile, in cytotoxic assays, only kingianic acid E (**124**) showed moderate cytotoxic activity against lung adenocarcinoma epithelial (A549) and colorectal adenocarcinoma cell lines (HT-29) at the micromolar range between 15 – 18 µM, respectively.

The progression towards the total synthesis of kingianin analogues are currently in progress (Chapter 5). The research began with the synthetic efforts toward kingianins with the aim of showcasing the construction of bicyclo[4.2.0]octane by [2+2] ketene-alkene cycloaddition followed by functionalization of substituent at C-7 and C-8 position with the correct relative configuration, with compounds spiro[bicyclo[4.2.0]octane-8,2'-[1,3]dioxolan]-2-en-4-ol (**280**) and 7-chloro-7-(3,4-methylenedioxyphenyl)bicyclo [4.2.0]oct-4-en-8-one (**311**) were identified as the key intermediates. This key step of the synthesis provided an access to the kingianin skeleton. The preparation of bicyclo[4.2.0]octane core can lead to a greater range of analogues, which could be further developed. The advantage of this strategy is the rapid assembly of the kingianin carbon skeleton, thus maximizing the chance for good overall yields of the final products.

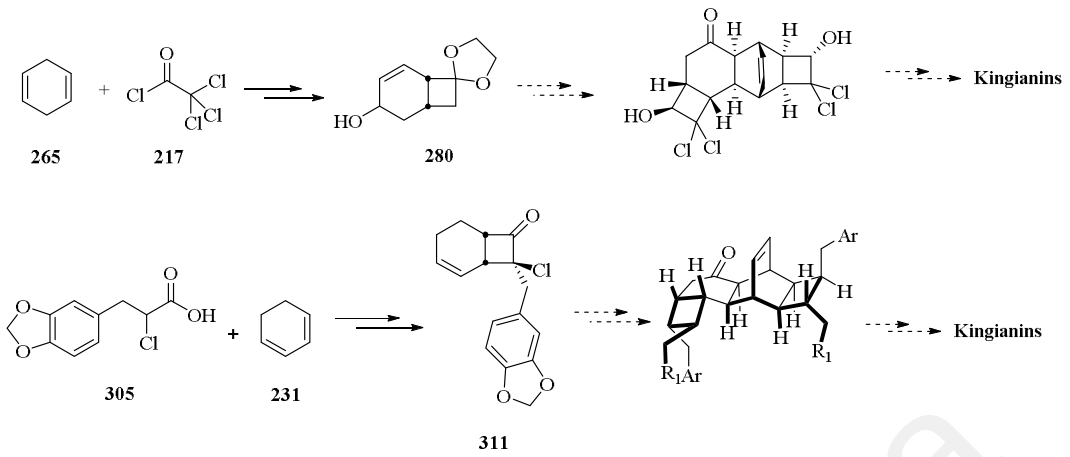

Scheme 6.1: Approaches to synthesis of kingianins

Further studies such as design and synthesis of analogues can be done in order to better understand the relationship between chemical structures and potency of activity. Meanwhile, the quantitative structure-activity relationship (QSAR), ***in vivo*** pharmacological and pharmacokinetic studies need to be carried out in order to clarify the mode of action mechanism.

CHAPTER 7

METHODOLOGY AND EXPERIMENTAL

7.1 Plant material

The bark of ***Endiandra kingiana*** Gamble was collected in 2006 at Kuala Lipis Reserved Forest, East-coast of Peninsular Malaysia and the series number was given KL5243. These species was identified by T. Leong Eng and voucher specimens were identified and deposited in the herbarium of the Department of Chemistry, University of Malaya, Kuala Lumpur.

Endiandra kingiana is an evergreen tree belonging to the Laurel family, Lauraceae and also known locally as '***Medang'.*** It is a large sub-canopy tree up to 33 m tall, 210 cm girth, and bole with buttresses. Bark is ochre grey and smooth. Inner bark is reddish and sapwood is pale yellow. Leaves stalk up to 2 cm long, stout, hairy to glabrous, blade thickly leathery and elliptic to oblong. Inflorescences in 5 cm long pubescent panicles. The flowers are perianth waxy yellow, 3 mm diameter and placed in panicles. Fruits are oblong shape (3 x 1.5 cm), shiny green to drying brown. The species distributed in Asia, from India and Indochina, China, Malaysia, Australia, and Pacific islands, with 10 species endemic to Malaysia (Ng, 1989; Burkill, 1966; Maberley, 2008).

7.2 Spectroscopic and physical analysis (instrumentation)

7.2.1 NMR spectra were obtained using Bruker Avance 600 (600 MHz for ^{1}H NMR, 150 MHz for ^{13}C NMR) spectrometer and Bruker Avance 400 (400 MHz for ^{1}H NMR, 100 MHz for ^{13}C NMR) spectrometer systems. Data were analysed via TopSpin software package. Chemical shifts were internally referenced to the solvent signals in $CDCl_3$ (^{1}H δ 7.26 ; ^{13}C δ 77.0) and pyridine-D_5 (^{1}H δ 7.22, 7.58, 8.74 ; ^{13}C δ 123.9, 135.9, 150.4).

7.2.2 High-resolution ESIMS and LCMS-IT-TOF spectra were obtained from Agilent Technologies 6530 Accurate-Mass Q-TOF LC/MS, or a Thermoquest TLM LCQ Deca ion-trap mass spectrometer.

7.2.3 The infrared (IR) spectra were obtained through Perkin Elmer FT-IR spectrometer RX1.

7.2.4 UV spectra were recorded on Shimadzu UV-160A UV-Visible Recording Spectrophotometer.

7.2.5 Optical rotations were measured on a JASCO P-1020 polarimeter.

7.2.6 A PL-ELS 1000 ELSD Polymer Laboratory detector. X-ray data collection was obtained from a Bruker APEX2; cell refinement: SMART; data reduction: SAINT; program(s) used to solve the structure: SHELXTL; program(s) used to refine structure: SHELXTL.

7.3 Separation and Purification (Chromatography)

7.3.1 Thin layer chromatography (TLC)

Aluminium supported silica gel 60 F_{254} plates (Merck) was used to see the spots of the isolated compounds. UV light model Spectroline model ENF-260C/PE (230 Volt / 50Hz / 0.17 Amp) was used to examine spots on the TLC after spraying with the required reagent.

7.3.2 Column chromatography (CC)

All solvents used in this experiment were analytical grade (AR grade). Silica gel 60 (63-200 µm – 70-230 mesh ASTM) and silica gel 60 (40-63 µm – 70-230 mesh ASTM) were used for column chromatography. A slurry of silica gel 60 (approximately 30:1, silica gel to sample ratio) in ***n***-hexane solvent system was poured into a glass column of appropriate size with gentle tapping to remove trapped air bubbles. The crude extract

was initially dissolved in a minimum amount of solvent and loaded on top of the packed column. The extract was eluted with an appropriate solvent system at a certain flow rate. The fractions of each test tube were collected and evaporated for the next step. The fractions with similar profile in TLC were pooled together to obtain the sub-fractions which were then subjected to further chromatographic analysis.

7.3.3 High performance Liquid chromatography (HPLC)

High-performance Liquid Chromatography (HPLC) was used during purification of fractions and sub-fractions. In this stage, reverse phase analytical and semi-preparative were performed on four devices:-

a) Semi-preparative HPLC separations using a Waters auto purification system equipped with a sample manager (Waters 2767).
b) A column fluidics organizer (Waters SFO)
c) A binary pump (Waters 2525)
d) A UV–Vis diode array detector (190–600 nm, Waters 2996)

The products were eluted with a mixture of solvents between ACN/H_2O or MeOH/H_2O in the presence of 0.1% formic acid as a buffer. The separations were done using several types of columns:

a) Agilent® Eclipse Zorbax C18 column (250 × 9.4 mm, 3.5 μm)
b) Waters® X-Bridge C18 column (250 × 10.0 mm, 5.0 μm)
c) Thermo® Hypersil-Keystone KR100-5 C18 (250 x 10.0 mm, 5.0 μm)

7.3.4 Detector reagents

7.3.4.1 Vanillin

Vanillin (0.5 g) in 2.0 mL concentrated H_2SO_4 was added with cooling to 8.0 mL ethanol (8.0 mL) before sprayed to the TLC plate. Dried chromatography TLC plates were sprayed with vanillin reagent. The plate was heated at 100˚C–110˚C until full development of colour had occurred.

7.3.4.2 Anisaldehyde

p-Anisaldehyde (26 mL) is mixed with acetic acid glacial (10.5 mL), followed by ethanol (950 mL) and concentrated H_2SO_4 (35 mL), in that order before sprayed to the TLC plate. Dried chromatography TLC plates were sprayed with vanillin reagent. The plate was heated at 100˚C–110˚C until full development of colour had occurred.

7.4 Extraction and purification of plant materials

The air-dried bark of ***E. kingiana*** (1.5 kg) were sliced, ground and extracted with EtOAc (3 × 1.5 L) followed by MeOH (3 × 1.5 L) at 40°C and 100 bar using a static high-pressure, high-temperature extractor, Zippertex, developed at the ICSN pilot unit. The methanol (MeOH) extract was investigated for its chemical constituents. The extract was partitioned with EtOAc/H_2O (1:1, v/v) to afford an EtOAc-soluble fraction and H_2O-soluble fraction. The EtOAc-soluble fraction was subjected to CC (SiO_2, 230 – 400 mesh; hexane/dichloromethne/methanol step gradient) to give several fractions. The fraction and sub-fraction were subjected to semi-preparative C_{18} HPLC, isocratically with MeCN-H_2O + 0.1% formic acid to give the desired product. The isolated compounds were analyzed and elucidated by using spectroscopic methods such as NMR, IR and HRMS. This extract was prepared two times to find these types of

compounds. The pure compounds were carried out for biological assays (Bcl-xL and Mcl-1 binding affinities and cytotoxic activity on various cancer cell lines).

7.4.1 First extraction (AM1)

The first extraction process was done in small scale to investigate the major component in methanol extract (Scheme 7.1). The methanol (40.5 g) extract was partitioned with EtOAc/H_2O (1:1, v/v) to afford an EtOAc-soluble fraction (10.5 g) and H_2O-soluble fraction (28.7 g). The EtOAc-soluble fraction (10.0 g) was subjected to flash column chromatography Companion® (SiO_2, hexane/dichloromethne/methanol step gradient) to give 9 fractions: AM1.Fr.1 – AM1.Fr.9. Fraction AM1.Fr.6 was subjected to CC (SiO_2, 230 – 400 mesh; hexane/AcOEt step gradient) to obtain 8 subfractions base on TLC profile: AM1.Fr.6.1 – AM1.Fr.6.8. Fraction AM1.Fr.6.3 was separated using Preparative C_{18} HPLC to afford kingianic acid A (**120**) and tsangibeilin B (**89**). Fractions AM1.Fr.6.6 and AM1.Fr6.7 were subjected to a Preparative C_{18} HPLC to give kingianin A (**45**) and kingianin F (**50**), respectively (Table 7.1). The detail of the first extraction process is summarized in Table 7.1 and Scheme 7.1.

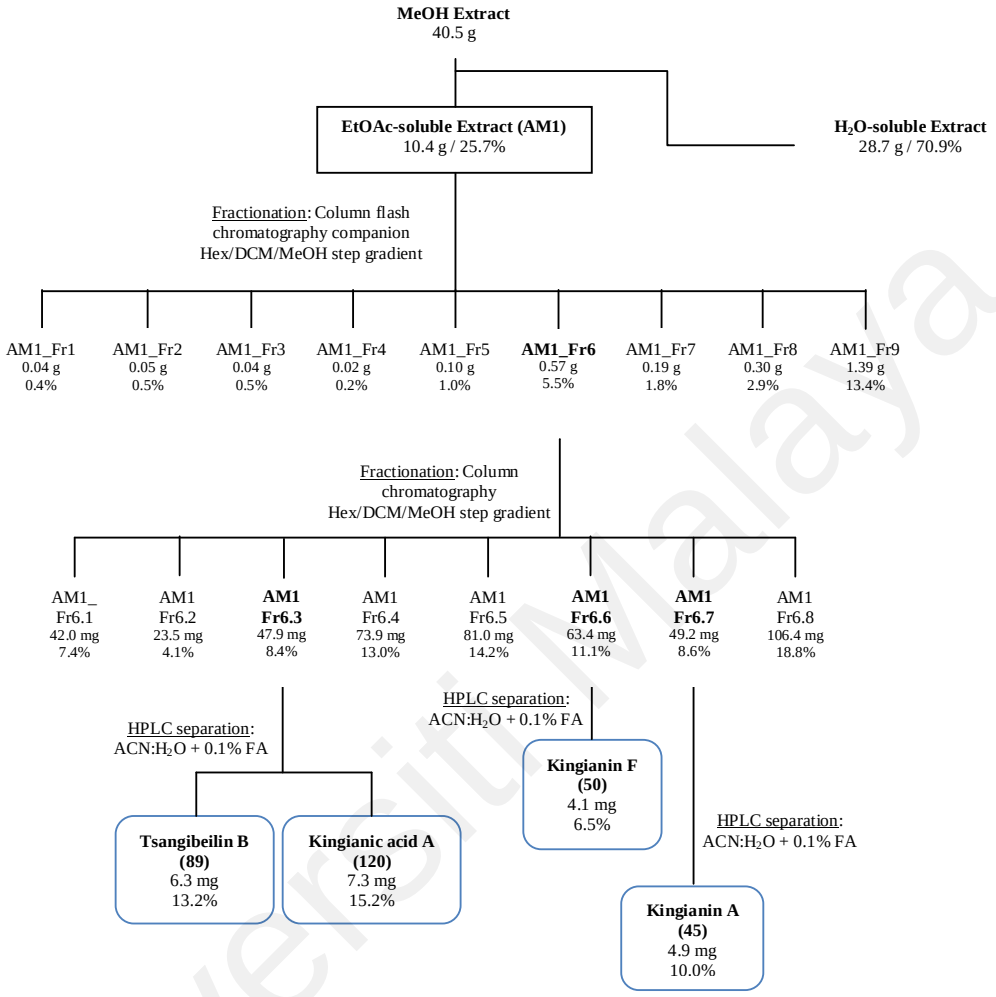

Scheme 7.1: Separation and fractionation scheme of first extraction (AM1) process

Table 7.1: Compounds isolated from first extraction process

Name of Compound	Weight (mg)	Yield (%)
Tsangibeilin B (**89**)	6.3	4.2×10^{-4}
Kingianic acid A (**120**)	7.3	4.9×10^{-4}
Kingianin A (**45**)	4.9	3.3×10^{-4}
Kingianin F (**50**)	4.1	2.7×10^{-4}

7.4.2 Second extraction (AM2)

The second extraction process was carried out in large scale to isolate more endiandric acid and kingianin analogues (Schemes 7.2-7.4). In this stage, the methanol extract (118.0 g - same extract as subchapter 7.4.1) was partitioned with EtOAc/H_2O (1:1, v/v) to afford an EtOAc-soluble fraction (22.5 g) and H_2O-soluble fraction (91.7 g). The EtOAc-soluble fraction (22.0 g) was subjected to CC (SiO_2, 230 – 400 mesh; hexane/dichloromethne/methanol step gradient) to give 8 fractions: AM2.Fr.1 – AM2.Fr.8.

Fraction AM2.Fr.4 was subjected to CC (SiO_2, 230 – 400 mesh; hexane/EtOAc step gradient) to obtain 20 sub-fractions base on TLC profile: AM2.Fr.4.1 – AM2.Fr.4.20. Fractions AM2.Fr.4.3 to AM2.Fr.4.17 were separated using semi-preparative C_{18} HPLC to afford endiandric acid series named; kingianic acids A-H (**120**-**127**), together with endiandric acid M (**93**) and tsangibeilin B (**89**). While separation of fraction AM2.Fr.4.20 afforded kingianin A (**45**) and kingianin F (**50**). Further compounds were isolated from fractions AM2.Fr.5 – AM2.Fr.7 where the fraction was subjected to CC (SiO_2, 230 – 400 mesh; hexane/ EtOAc step gradient) followed by purification using a semi-preparative C_{18} HPLC to give kingianic acid G (**126**), kingianin A (**45**), F (**50**), K (**55**), L (**56**), M (**57**), N (**58**), O (**128**), P (**129**) and Q (**130**). The detail of the second extraction process is summarized in Table 7.2 and Schemes 7.2-7.4.

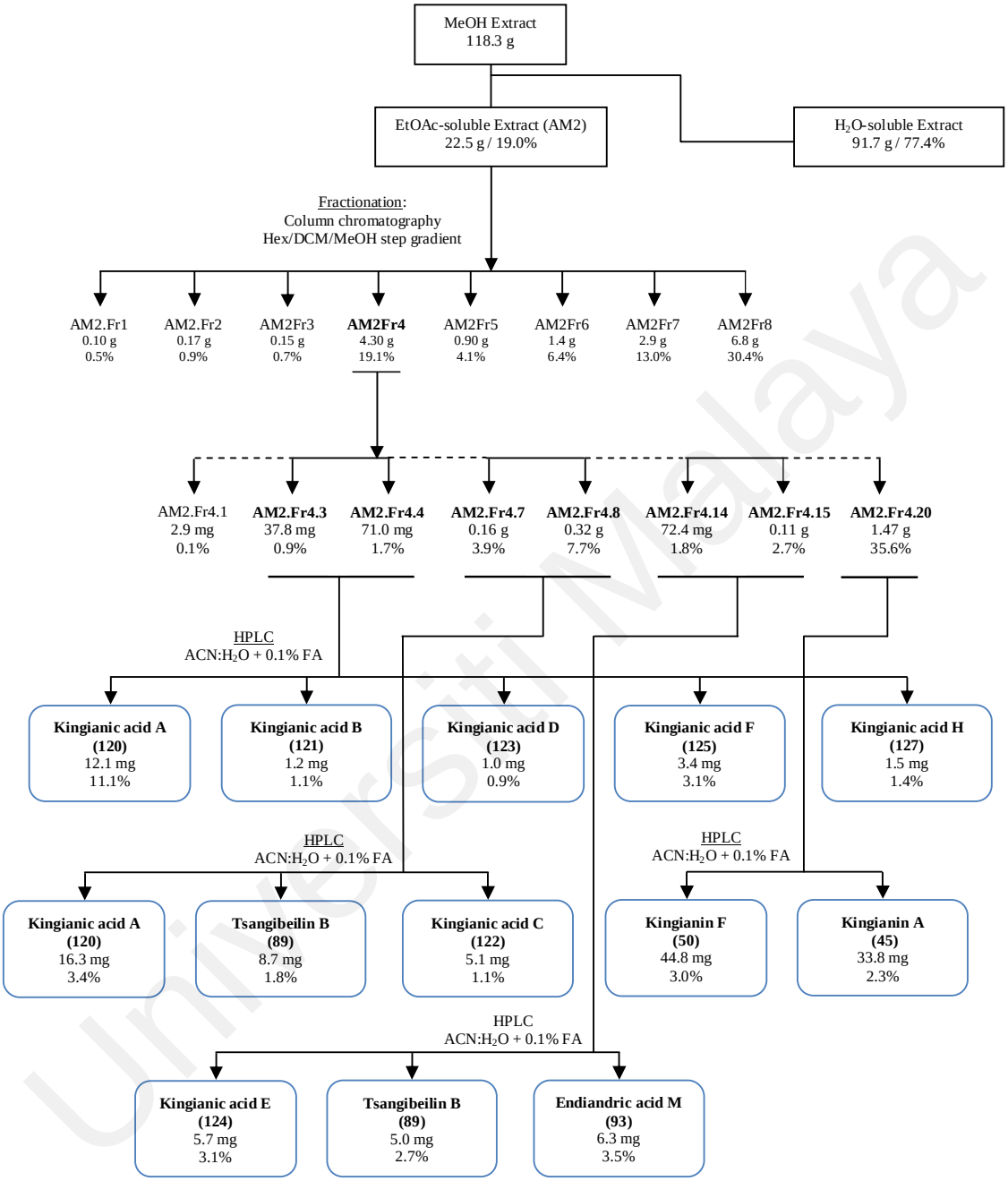

Scheme 7.2: Separation and fractionation scheme of AM2.Fr.4 (2nd Extraction)

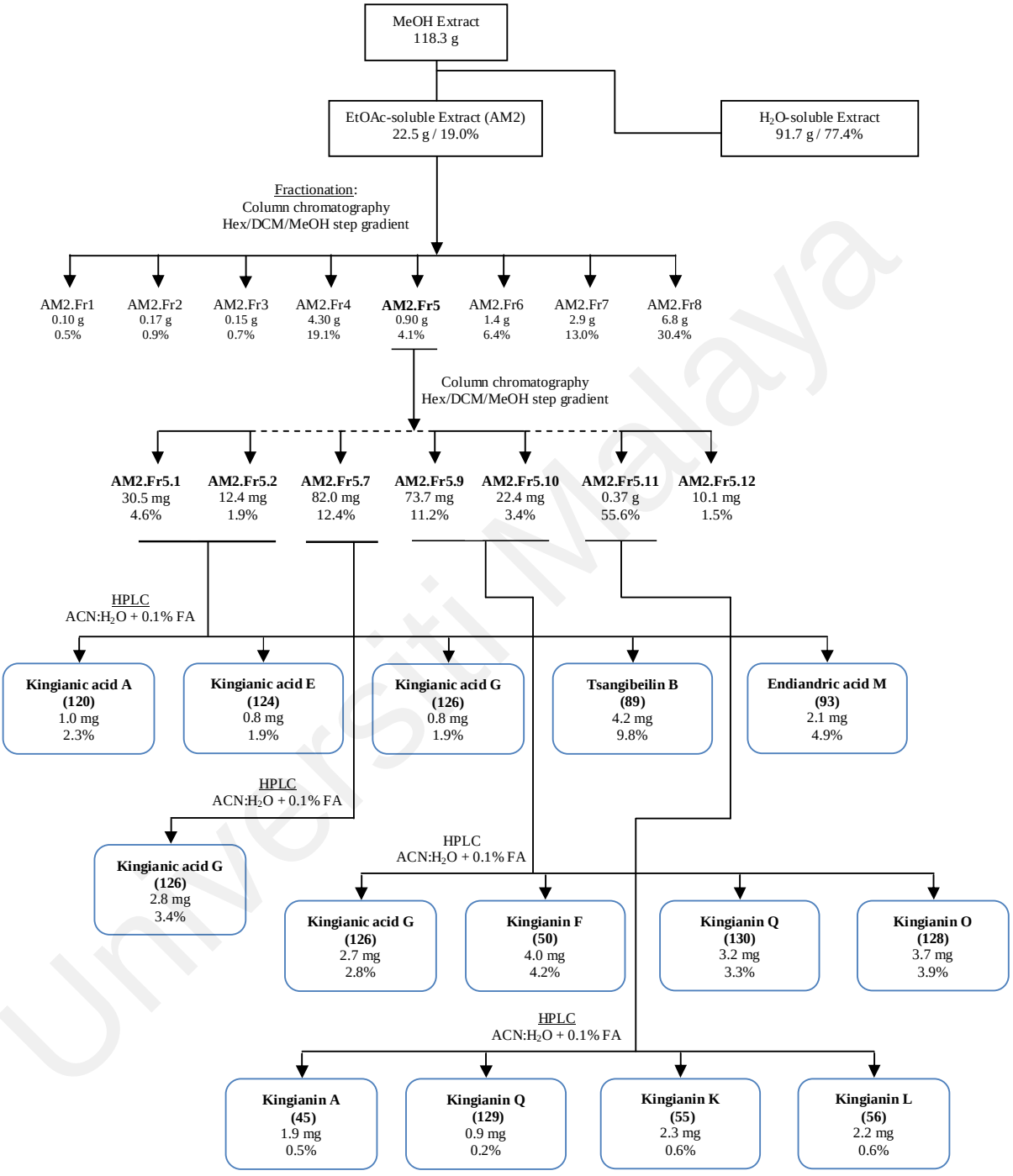

Scheme 7.3: Separation and fractionation scheme of AM2.Fr.5 (2nd Extraction)

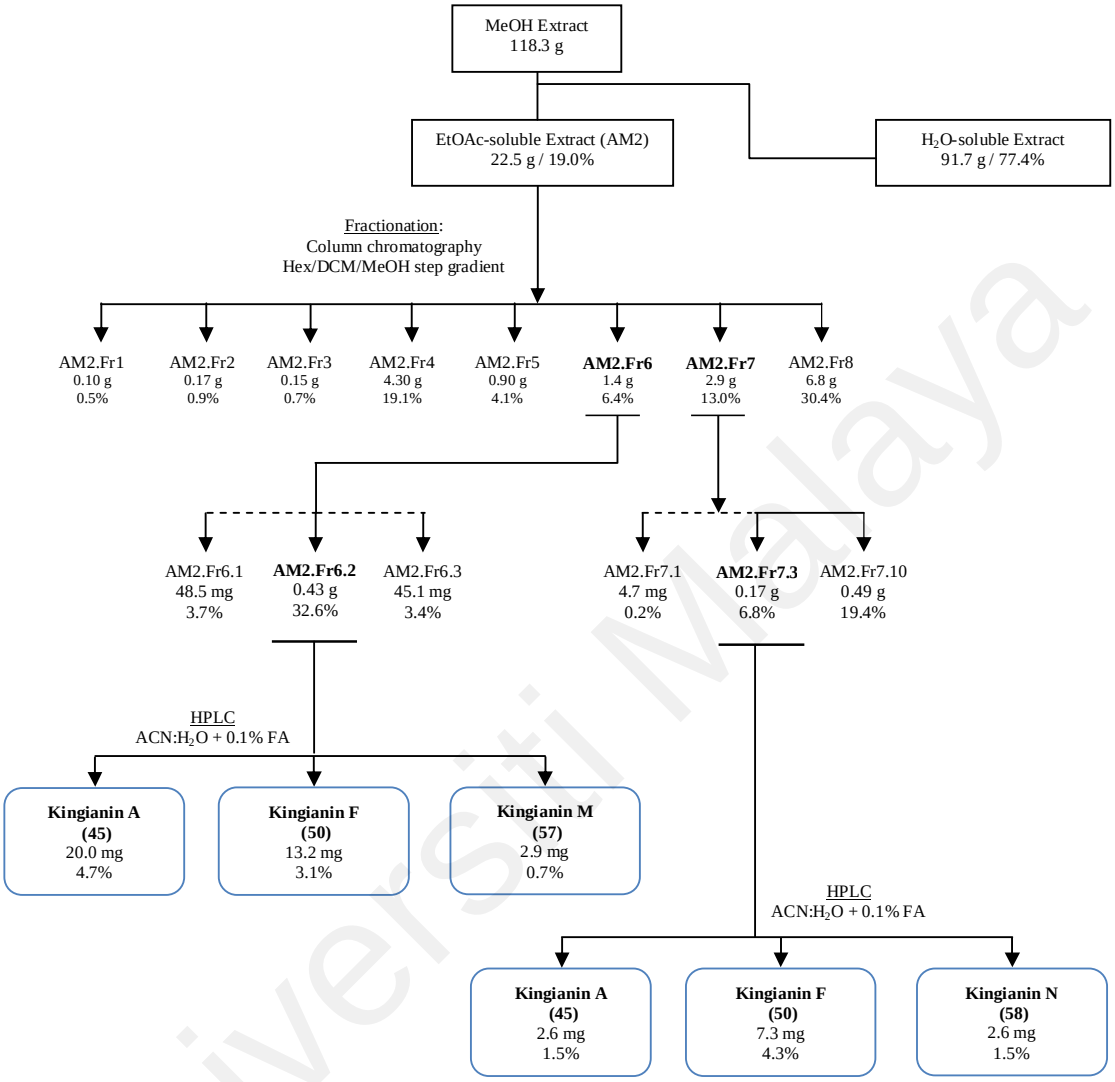

Scheme 7.4: Separation and fractionation scheme of AM2.Fr.6 and AM2.Fr.7 (2^{nd} Extraction)

Table 7.2: Compounds isolated from second extraction process

Name of Compound	Weight (mg)	Yield (%)
Kingianic acid A (**120**)	71.4	4.8×10^{-3}
Kingianic acid B (**121**)	1.2	8.0×10^{-5}
Kingianic acid C (**122**)	7.0	4.7×10^{-4}
Kingianic acid D (**123**)	1.0	6.7×10^{-5}
Kingianic acid E (**124**)	6.5	4.3×10^{-4}
Kingianic acid F (**125**)	3.4	2.3×10^{-4}
Kingianic acid G (**126**)	6.3	4.2×10^{-4}
Kingianic acid H (**127**)	1.5	1.0×10^{-4}
Endiandric acid M (**93**)	8.4	5.6×10^{-4}
Tsangibeilin B (**89**)	67.0	4.5×10^{-3}
Kingianin A (**45**)	63.2	4.2×10^{-3}
Kingianin F (**50**)	73.4	4.9×10^{-3}
Kingianin K (**55**)	2.3	1.5×10^{-4}
Kingianin L (**56**)	2.2	1.5×10^{-4}
Kingianin M (**57**)	2.9	1.9×10^{-4}
Kingianin N (**58**)	2.6	1.7×10^{-4}
Kingianin O (**128**)	3.7	2.5×10^{-4}
Kingianin P (**129**)	0.9	6.0×10^{-5}
Kingianin Q (**130**)	3.2	2.1×10^{-4}

7.5 Selected HPLC chromatograms

HPLC was used during purification of fractions and sub-fractions. In this stage, reverse phase analytical and semi-preparative were performed and the products were eluted with a mixture of solvents between ACN/H_2O or MeOH/H_2O in the presence of 0.1% formic acid as a buffer. The chromatograms of selected fractions during purification are showed in Figures 7.1-7.9.

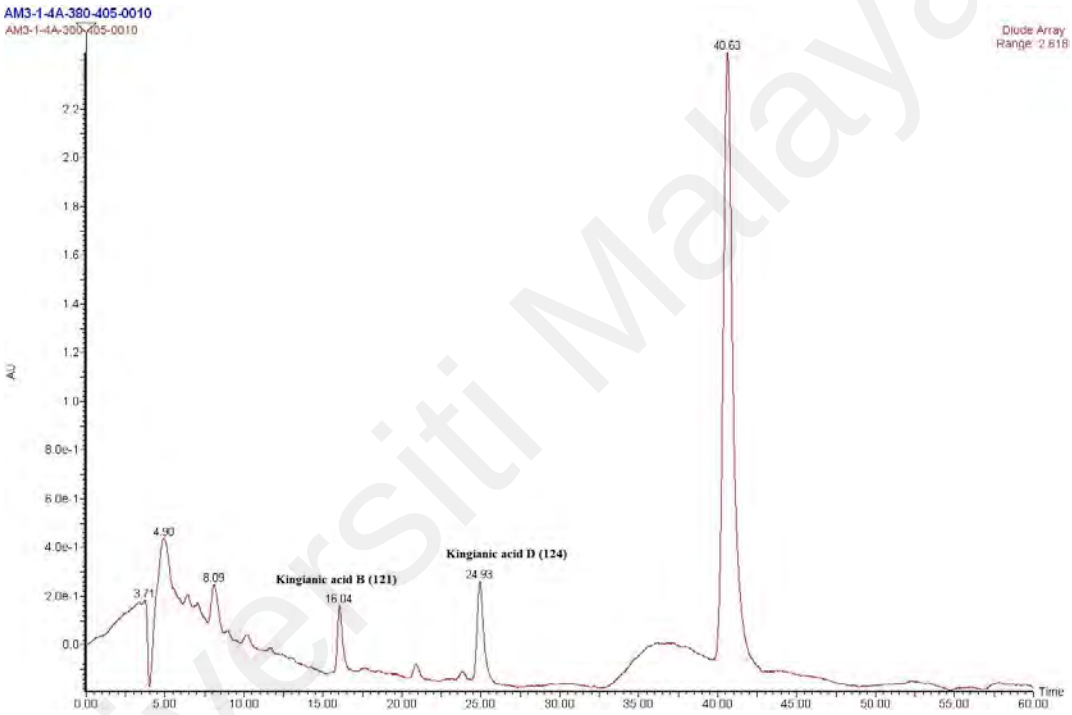

HPLC Unit : Waters® Semi-Preparative HPLC; AM2.Fr.4.3

Column : Agilent® Eclipse Zorbax C18 column (250 × 9.4 mm, 3.5 μm)

Solvent system : 3.5 mL/min isocratically (MeCN-H_2O 65:35 + 0.1% FA)

Serial collections : Kingianic acid B (**121**) (t_R 16.0 min, 1.2 mg)

Kingianic acid D (**124**) (t_R 24.8 min, 1.0 mg).

Figure 7.1: Chromatogram of fraction AM2.Fr.4.3

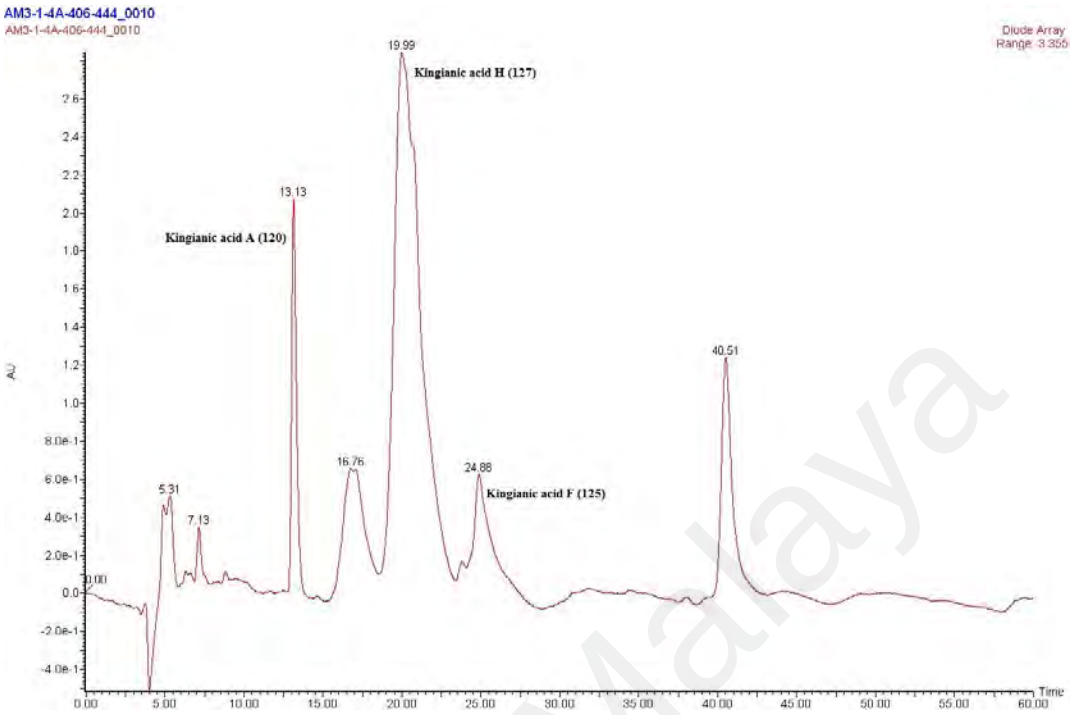

HPLC Unit : Waters® Semi-Preparative HPLC; AM2.Fr.4.4

Column : Agilent® Eclipse Zorbax C18 column (250 × 9.4 mm, 3.5 μm)

Solvent system : 3.5 mL/min isocratically (MeCN-H_2O 65:35 + 0.1% FA)

Serial collections : Kingianic acid A (**120**) (t_R 13.1 min, 12.1 mg)

Kingianic acid F (**125**) (t_R 19.9 min, 1.2 mg).

Kingianic acid H (**127**) (t_R 24.8 min, 3.4 mg)

Figure 7.2: Chromatogram of fraction AM2.Fr.4.4

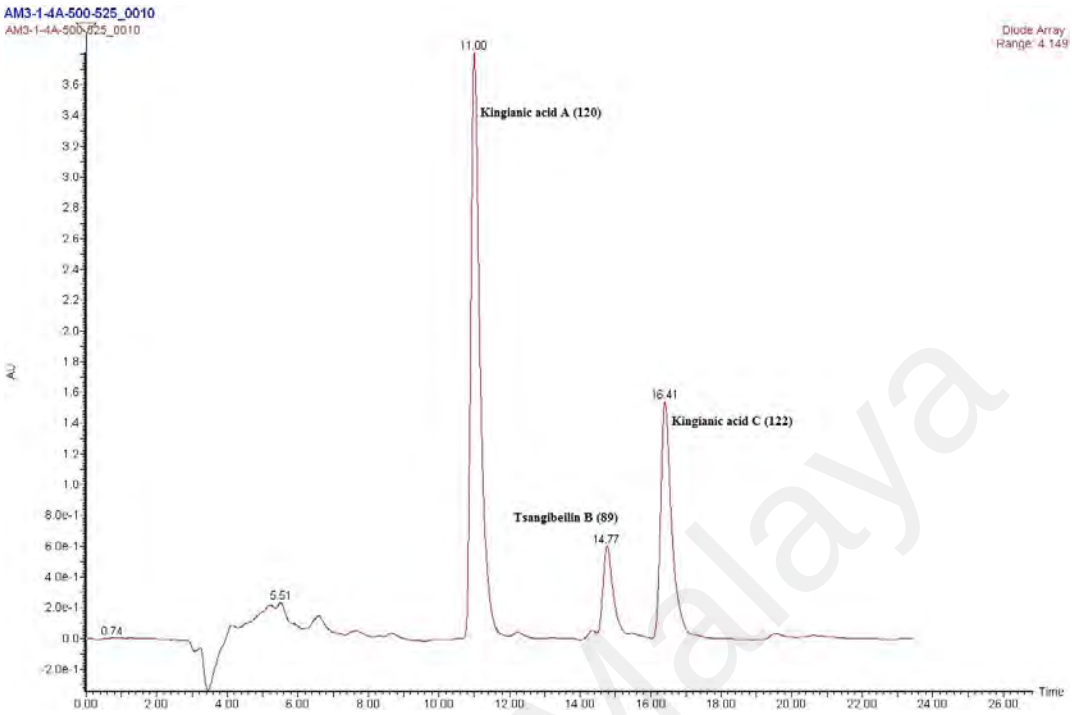

HPLC Unit : Waters® Semi-Preparative HPLC;
AM2.Fr.4.7 and AM2.Fr.4.8

Column : Agilent® Eclipse Zorbax C18 column (250 × 9.4 mm, 3.5 µm)

Solvent system : 3.5 mL/min isocratically (MeCN-H_2O 65:35 + 0.1% FA)

Serial collections : Kingianic acid A (**120**) (t_R 11.0 min, 16.3 mg)
Tsangibeilin B (**89**) (t_R 14.7 min, 8.7 mg).
Kingianic acid C (**122**) (t_R 16.4 min, 5.1 mg)

Figure 7.3: Chromatogram of fractions AM2.Fr.4.7 and AM2.Fr.4.8

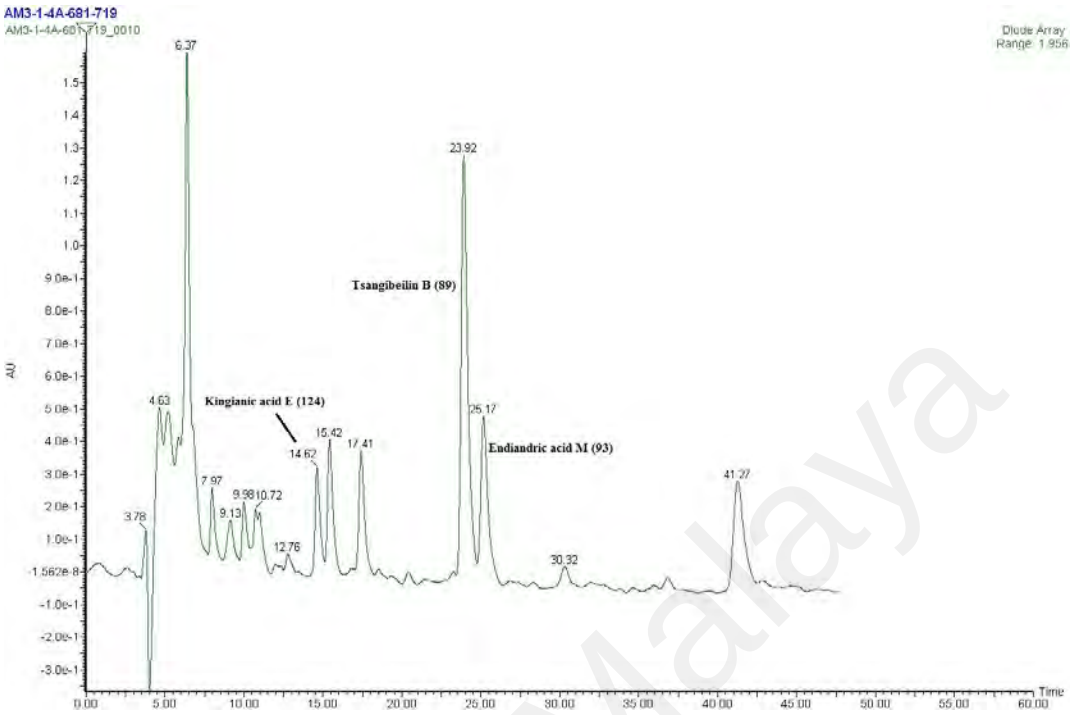

HPLC Unit : Waters® Semi-Preparative HPLC;
AM2.Fr.4.14 and AM2.Fr.4.15

Column : Agilent® Eclipse Zorbax C18 column (250 × 9.4 mm, 3.5 μm)

Solvent system : 3.5 mL/min isocratically (MeCN-H_2O 65:35 + 0.1% FA)

Serial collections : Kingianic acid E (**124**) (t_R 14.6 min, 5.7 mg)
Tsangibeilin B (**89**) (t_R 23.9 min, 5.0 mg).
Endiandric acid M (**93**) (t_R 25.1 min, 6.3 mg)

Figure 7.4: Chromatogram of fractions AM2.Fr.4.14 and AM2.Fr.4.15

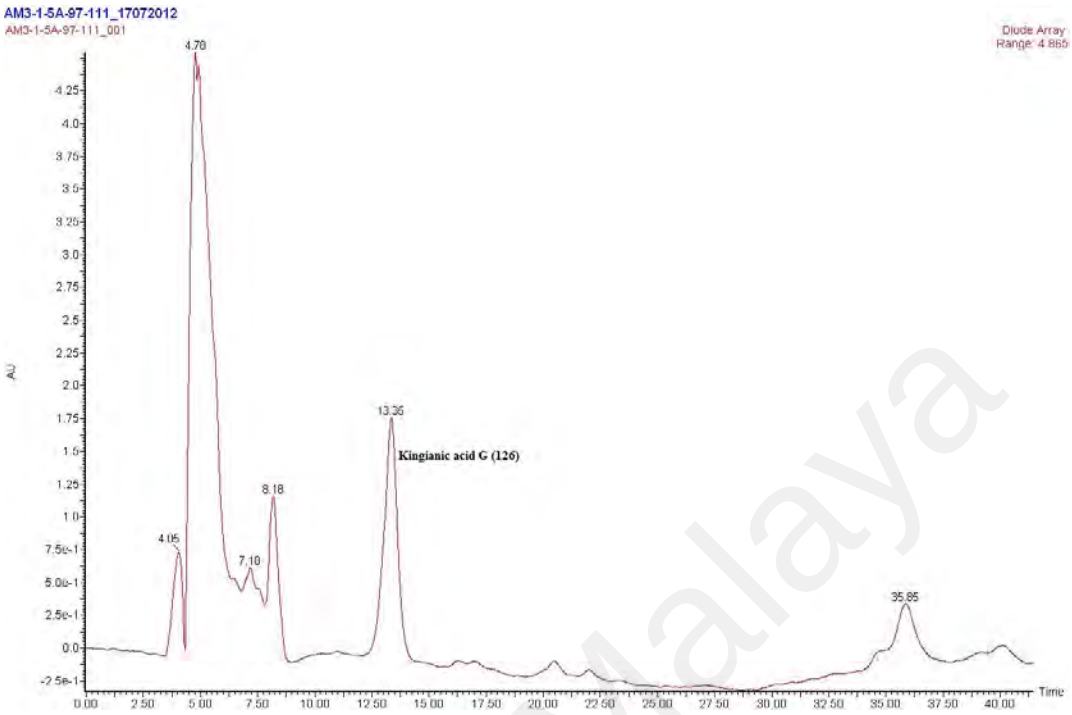

HPLC Unit : Waters® Semi-Preparative HPLC; AM2.Fr.5.7

Column : Waters® X-Bridge C18 column (250 × 10.0 mm, 5.0 µm)

Solvent system : 3.0 mL/min isocratically (MeCN-H_2O 50:50 + 0.1% FA)

Serial collections : Kingianic acid G (**126**) (t_R 13.4 min, 1.5 mg)

Figure 7.5: Chromatogram of fraction AM2.Fr.5.7

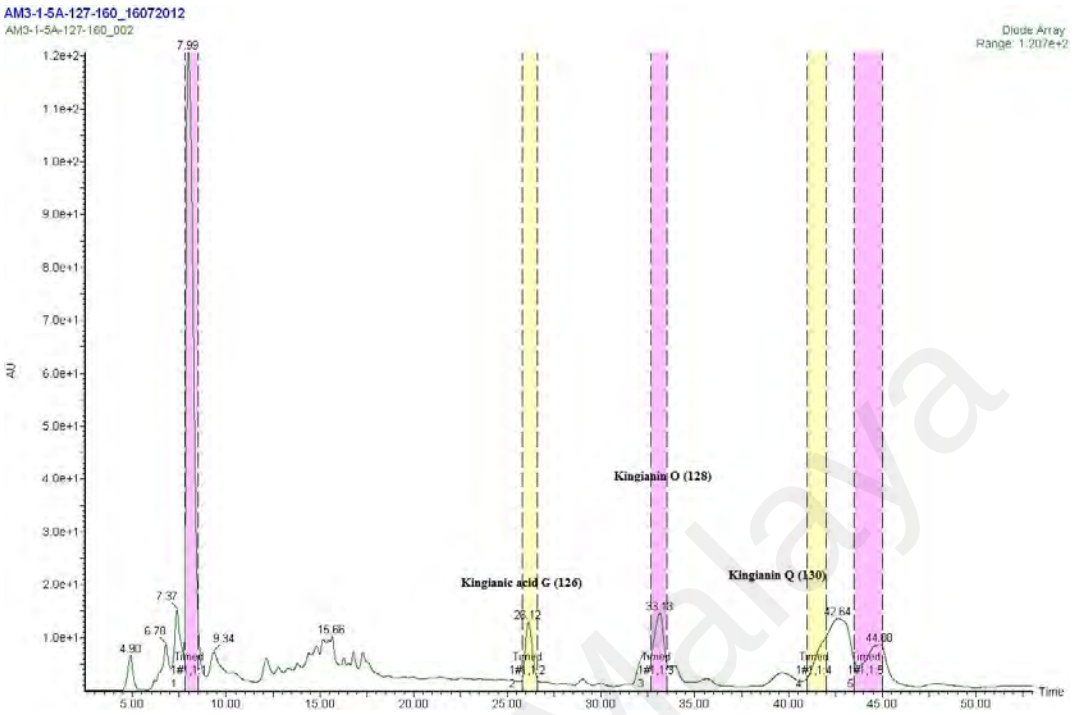

HPLC Unit : Waters® Semi-Preparative HPLC; AM2.Fr.5.9

Column : Waters® X-Bridge C18 column (250 × 10.0 mm, 5.0 μm)

Solvent system : 3.0 mL/min isocratically (MeCN-H_2O 60:40 + 0.1% FA)

Serial collections : Kingianic acid G (**126**) (t_R 26.1 min, 2.7 mg)

Kingianin O (**128**) (t_R 33.1 min, 3.7 mg)

Kingianin Q (**130**) (t_R 42.1 min, 3.2 mg)

Figure 7.6: Chromatogram of fraction AM2.Fr.5.9

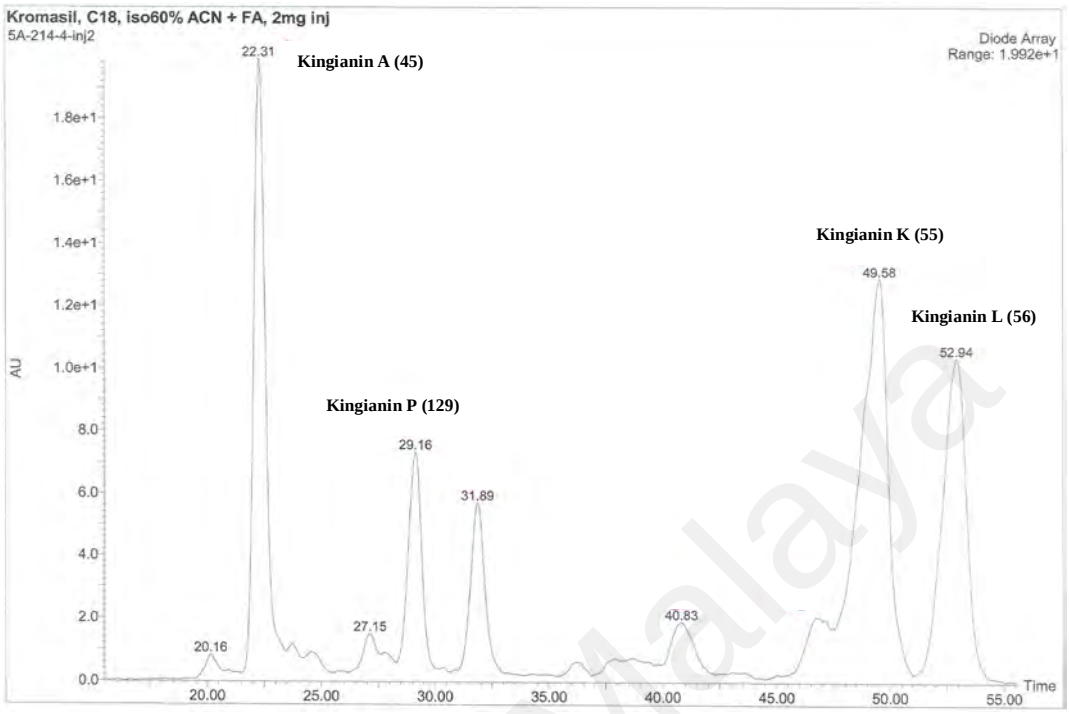

HPLC Unit : Waters® Preparative HPLC; AM2.Fr.5.11.4

Column : Thermo® Hypersil-Keystone KR100-5 C18 (250 x 10.0 mm, 5.0 μm)

Solvent system : 4.7 mL/min isocratically (MeCN-H_2O 60:40 + 0.1% FA)

Serial collections : Kingianin A (**45**) (t_R 22.3 min, 1.9 mg)

Kingianin P (**129**) (t_R 29.1 min, 0.9 mg)

Kingianin K (**55**) (t_R 49.5 min, 2.3 mg)

Kingianin L (**56**) (t_R 52.9 min, 2.2 mg)

Figure 7.7: Chromatogram of fraction AM2.Fr.5.11.4

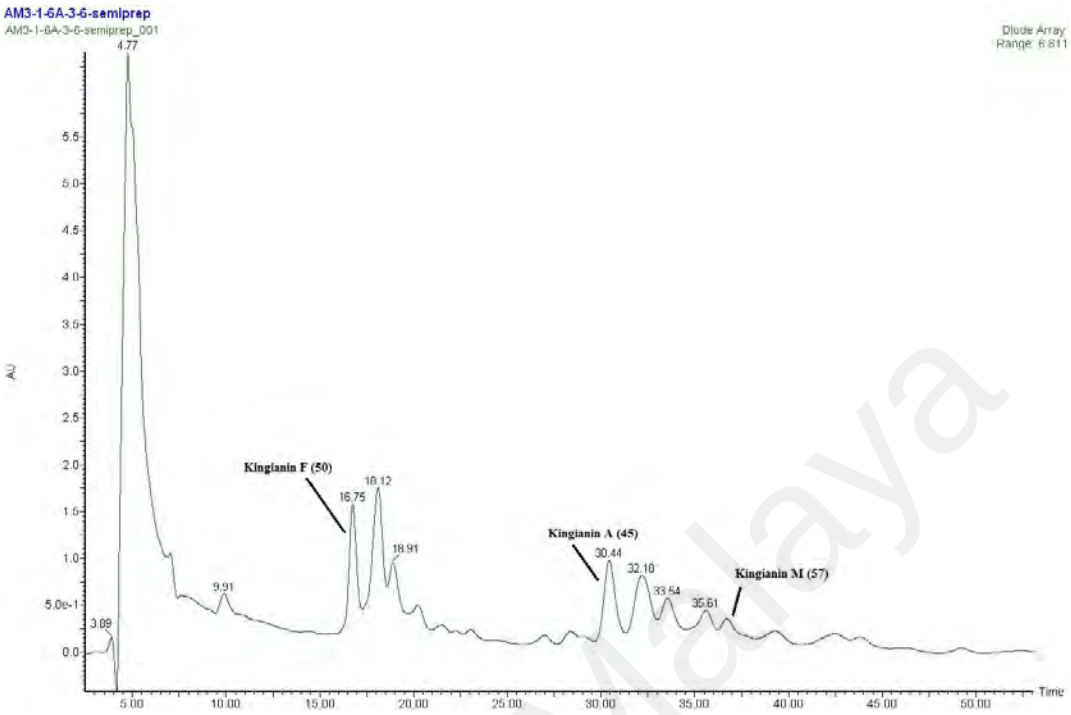

HPLC Unit : Waters® Semi-Preparative HPLC; AM2.Fr.6.2

Column : Waters® X-Bridge C_{18} column, (250 × 10.0 mm, 5.0 μm)

Solvent system : 3.5 mL/min isocratically (MeCN-H_2O 55:45 + 0.1% FA)

Serial collections : Kingianin F (**50**) (t_R 16.5 min, 10.6 mg)

Kingianin A (**45**) (t_R 30.1 min, 17.5 mg)

Kingianin M (**57**) (t_R 36.7 min, 2.9 mg)

Figure 7.8: Chromatogram of fraction AM2.Fr.6.2

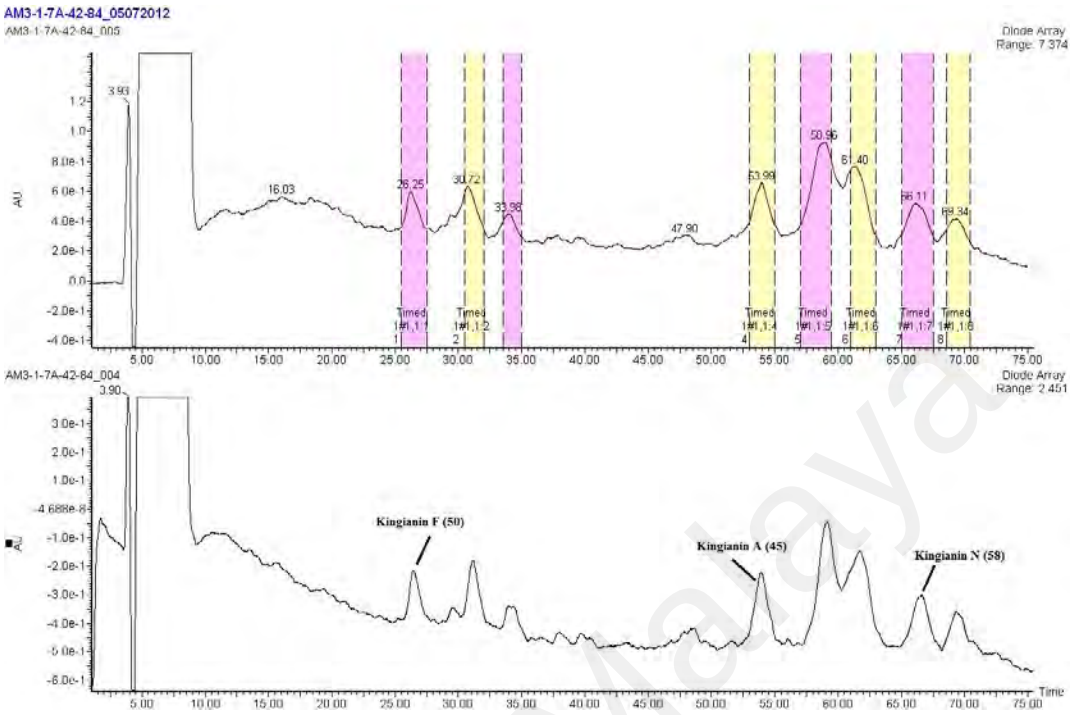

HPLC Unit : Waters® Semi-Preparative HPLC; AM2.Fr.7.3

Column : Waters® X-Bridge C_{18} column, (250 × 10.0 mm, 5.0 µm)

Solvent system : 3.5 mL/min isocratically (MeCN-H_2O 50:50 + 0.1% FA)

Serial collections : Kingianin F (**50**) (t_R 26.2 min, 5.1 mg)

Kingianin A (**45**) (t_R 153.9 min, 2.6 mg)

Kingianin N (**58**) (t_R 66.1 min, 2.6 mg)

Figure 7.9: Chromatogram of fraction AM2.Fr.7.3

7.6 Biological Activity Studies

The main focus here is to investigate the biological activities of the pure compounds isolated from ***Endiandra kingiana***. In this investigation, the isolated compounds were tested for Bcl-xL and Mcl-1 binding affinities and cytotoxic activity on various cancer cell lines.

7.6.1 Bcl-xL and Mcl-1 binding affinities

The binding affinities of compounds for Bcl-xL and Mcl-1 were evaluated by competition against fluorescently labelled reference compounds, Bak and Bid, respectively, as described by Qian et al. (2004). Human 45-84/C37 Bcl-xL and mouse DN150/DC25 Mcl-1 proteins were recombinantly produced by N. Birlirakis at ICSN. Bak, 5-Carboxyfluorescein-Bak, Bid and 5-carboxyfluorescein-Bid peptides were synthetized by PolyPeptide Laboratories (Strasbourg, France). Unlabelled peptides were dissolved in DMSO (Carlo Erba, Val de Reuil, France) and labelled peptides were diluted in assay buffer, which contained 20 mM Na_2HPO_4 (pH 7.4), 50 mM NaCl, 2 μM EDTA, 0.05% Pluronic F-68, without pluronic acid for storage at −20°C. Liquid handling instrument, Biomek®NX and Biomeck®3000 (Beckman Coulter, Villepinte, France), were used to add protein and fluorescein-labelled peptides. Labelled BH3 peptide (15 nM), 100 nM protein, and 100 μM of unlabelled BH3 peptide or compound (first diluted in 10 mM DMSO and then buffer for final concentration from 10^{-9} to 10^{-4} M) into a final volume of 40 μL were distributed in a 96 well black polystyrene flat-bottomed microplate (VWR 734-1622).

The microplate was then incubated at room temperature for 1 h and shaken before measuring the fluorescent polarization. Fluorescence polarization was measured in millipolarization units with a Beckman Coulter Paradigm® using FP cartridge (λ_{ex} 485 nm, λ_{em} 535 nm). The exposure time was 300 ms per channel. All experimental data

were collected using the Biomek Software® (Beckman Coulter, Inc, Brea, CA, USA) and analysed using Microsoft Excel 2010 (Microsoft, Redmond, WA, USA). Results are expressed as binding affinity, ***i.e.***, percentage of inhibition (%) of the binding of labelled reference compound, or as ***Ki***, [the concentration corresponding to 50% of such inhibition, and corrected for experimental conditions according to Kenakin rearranged equation (Nikolovska-Coleska et al., 2004), which is adapted from Cheng and Prusoff equation (1973)]. In general, The Ki value is the inhibitory constant and specifically reflective of the binding affinity. The smaller the Ki, the greater the binding affinity and the smaller amount of medication needed in order to inhibit the activity of that enzyme. ABT-737, which was kindly provided by O. Nosjean (Institut de Recherche Servier, Croissy, France), and unlabeled peptides Bak and Bid were used as positives control. The performance of the assays was monitored by use of Z' factors as described by Zhang et al. (1999). The Z' factors for these assays are 0.8 (Bcl-xL/Bak) and 0.7 (Mcl-1/Bid) indicating that they should be robust assays. Both protein targets include an ***N***-terminal His-tag followed by the thrombin cleavage site, to facilitate purification. Our Bcl-xL construct includes the four homology domains of the human protein, whereas our Mcl-1 construct includes the three homology domains of the mouse protein. ***Trans***-membrane domains have been deleted in both sequences.

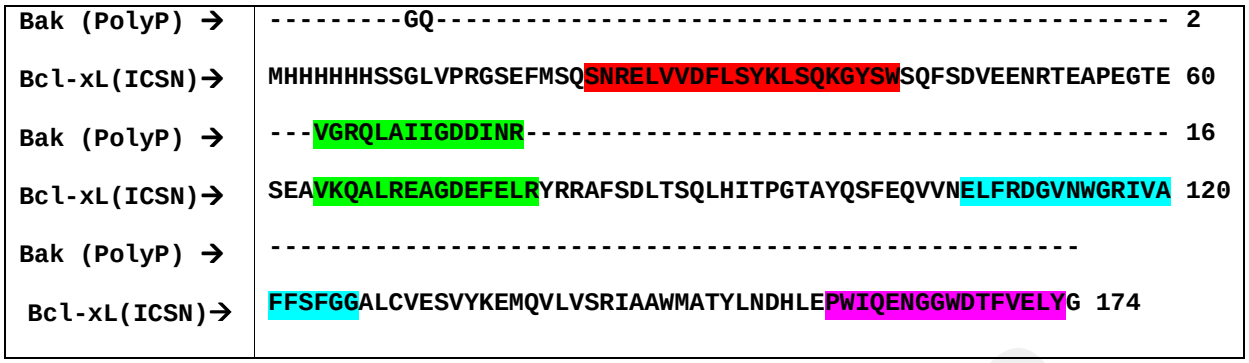

→ BH4 domain

→ BH3 domain

→ BH1 domain

→ BH2 domain

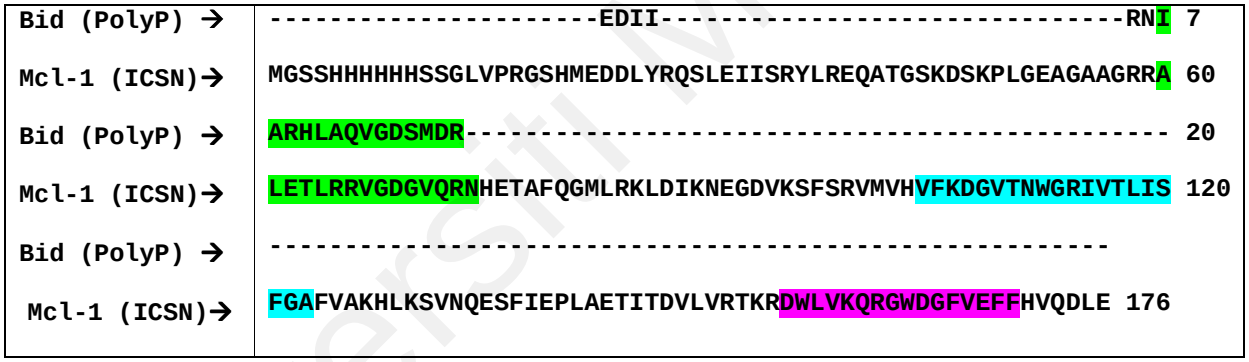

→ BH3 domain

→ BH1 domain

→ BH2 domain

Scheme 7.5: Sequence alignment of Bcl-xL and Mcl-1 with Bak-BH3 and Bid-BH3 peptides, respectively

7.6.2 Cytotoxic activity

The selected endiandric acid analogues isolated from ***Endiandra kingiana*** were individually tested for anticancer activity. A total of three tumour cell lines were used in this study. Human cancer cell lines A549 (Lung adenocarcinoma epithelial), HT-29 (Colorectal adenocarcinoma) and PC3 (Prostate adenocarcinoma) cells were obtained from the ATCC (Manassas, VA, USA). Cells were grown in RPMI-1640 or DMEM medium with 10% FBS supplemented with 4 mM L-glutamine and 1% penicillin-streptomycin. For experimental purposes, the cells were grown exponentially and maintained at 70% – 80% confluency were used. Cells were seeded into 96-well plates at 104 cells/well and allowed to adhere overnight; the medium was then removed. A stock solution of test compound in DMSO was diluted in medium to generate a series of working solutions. Aliquots (100 μL) of the working solutions were added to the appropriate test wells to expose cells to the final concentrations of compound in a total volume of 100 μL. Nine different concentrations (100 μL–0.4 μL) were tested, in triplicates. Cisplatin was used as a positive control and wells containing vehicle without compound were used as negative controls. Plates were kept for 48 h in a 37°C, 5% CO_2 incubator. After incubation, viable cells were detected with the CellTiter 96 AQueous cell proliferation assay (Promega Corp., Madison, WI, USA). Plates were read in a microplate reader (Tecan Infinite® 200 PRO series, Mannedorf, Switzerland) at 490nm. Then, dose-response curves were generated and the IC_{50} values were determined using GraphPad Prism 5.04 software (La Jolla, CA, USA) (Riss & Moravec, 1992).

Results were expressed as mean values with ± standard error of the mean (SEM). All data were performed in triplicates and analyzed using one-way ANOVA, where differences were considered significant at $\boldsymbol{p} \leq 0.05$.

7.7 Synthesis protocol and spectroscopic data analysis

7.7.1 Generals

All reactions were carried out in heat-dried glassware under an atmosphere of nitrogen unless otherwise stated. All liquid transfers were conducted using standard syringe or cannula techniques. THF, Et_2O, DCM, toluene and MeOH were purified by MBraun® Solvent Purification system. DMF and cyclohexane were dried under molecular sieves 4Å. All other reagents were obtained from Merck, Across, Alfa-Aesar or Aldrich and used as received. Column chromatography was performed on silica gel (Merck, 60 Å C. C. 40-63 mm) as the stationary phase. Thin Layer Chromatography (TLC) was performed on alumina plates pre-coated with silica gel (Merck silica gel, 60 F254), which were visualized by the quenching of UV fluorescence when applicable (λ_{max} = 254 nm and/or 366 nm) and/or by spraying with vanillin or anisaldehyde in acidic ethanol followed by heating with a heat gun. HRMS was run on a JEOL JMS-GCmate II mass spectrometer. NMR spectra were recorded on a Bruker Avance (400 MHz for ^{1}H NMR, 100 MHz for ^{13}C NMR) spectrometer system. Data were analysed via TopSpin software package. Spectra were referenced to TMS or residual solvent ($CDCl_3$ = 7.26 ppm in ^{1}H spectroscopy and 77.0 ppm in ^{13}C spectroscopy).

7.7.2 Approach A: [2+2] intermolecular ketene cycloaddition

7.7.2.1 1,3-Cyclohexadiene

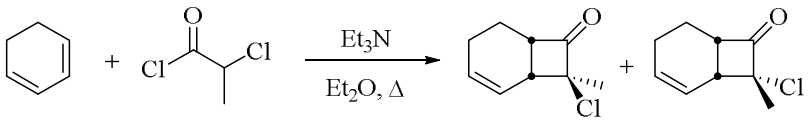

231 **232** **229** Major (42% yield) **230** Minor (12% yield)

7-Chloro-7-methyl-bicyclo[4.2.0]oct-4-en-8-ones (229 and 230) (Wu et al., 1994). A refluxing mixture of 1,3-cyclohexadiene (**231**) (2.52 g, 31.5 mmol) and 2-chloropropanoyl chloride (**232**) (5.12 g, 40.9 mmol) in diethyl ether (100 mL) under nitrogen was treated with triethylamine (5.76 mL, 40.9 mmol) within 10 min. The reaction mixture was stirred at room temperature for 3 h and then filtered and the solid was washed with diethyl ether. The filtrate was washed with 1 M HCl (12 mL) and 1 M NaOH (12 mL). The organic layer was washed further with brine (20 mL). After drying (Na_2SO_4), the organic layer was concentrated and the crude product was purified using normal column chromatography. Chromatography on silica gel, eluting with petroleum ether/ethyl acetate (98:2) gave **229** (2.26 g, 42%) and **230** (0.65 g, 12%).

(1***R****,6***S****,7***R****)-7-Chloro-7-methyl-bicyclo[4.2.0]oct-4-en-8-one	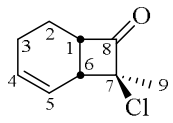

Yellowish oil. $\boldsymbol{R}_f \approx 0.45$ [UV-active, EtOAc/Pet. ether 5%, anisaldehyde (violet spot)]**. IR (neat)**: ν_{max} 3049 (m), 2984 (s), 2685 (w), 2306 (m), 1791 (s, C=O), 1444 (m), 1423 (m), 1263 (s), 895 (m) cm^{-1}. **^{1}H NMR ($CDCl_3$)** 1.43 (3H, s, H9), 1.50 (1H, m, H2a), 1.83–2.00 (3H, m, H2b, H3), 3.08 (1H, dd, ***J*** = 9.0, 3.0 Hz, H6), 4.07 (1H, ddd, ***J*** = 9.0, 6.9, 3.0, 4.4 Hz, H1), 5.79 (1H, ddd, ***J*** = 10.3, 3.0, 3.0 Hz, H5), 5.96 (1H, ddd, ***J*** = 10.3, 3.0, 3.0 Hz, H4). **^{13}C NMR ($CDCl_3$)** 18.7 (C2), 19.4 (C9), 21.3 (C3), 40.3 (C6), 54.7 (C1), 77.2 (C7), 120.0 (C5), 131.8 (C4), 205.8 (C8). **MS *m/z* (positive CI, NH_3)** 107, 135, 146, 171 (MH^+ with ^{35}Cl), 173 (MH^+ with ^{37}Cl), 188 ($MH^+..NH_3$ with ^{35}Cl), 190 ($MH^+..NH_3$ with ^{37}Cl), 192, 225, 227, 242, 244, 255, 278, 325, 418. **MS *m/z* (EI)** 107, 115, 117, 121, 126, 135, 142, 151, 162, 170 ($M^{+\bullet}$ with ^{35}Cl), 172. **HRMS *m/z* (EI)**: 170.0436 ($M^{+\bullet}$ $C_9H_{11}{}^{35}ClO^{+\bullet}$ requires 170.0498)**.**

All spectral characteristics are identical to those previously reported (Wu et al., 1994).

(1***R****,6***S****,7***S****)-7-Chloro-7-methyl-bicyclo[4.2.0]oct-4-en-8-one	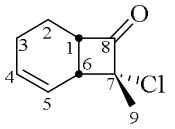

Yellowish oil. $\boldsymbol{R}_f \approx 0.25$ [UV-active, EtOAc/Pet. ether 5%, anisaldehyde (violet spot)]**. IR (neat)**: ν_{max} 3155 (m), 2984 (m), 2930 (m), 2854 (w), 2254 (s), 1793 (s, C=O), 1468 (w), 1384 (m), 1166 (w) 1137 (w), 1097 (m), 991 (w) cm^{-1}. **^{1}H NMR ($CDCl_3$)** 1.53 (1H, m, H2a), 1.75 (3H, s, H9), 1.97 (2H, m, H3), 2.04 (1H, m, H2b), 2.89 (1H, m, H6), 3.67 (1H, ddd, ***J*** = 9.3, 6.7, 3.1 Hz, H1), 5.76 (1H, m, H5), 5.94 (1H, m, H5). **^{13}C NMR ($CDCl_3$)** 18.9 (C2), 20.9 (C3), 26.4 (C9), 37.9 (C6), 52.3 (C1), 76.0 (C7), 124.6 (C5), 130.3 (C4), 206.8 (C8). **MS *m/z* (positive CI, NH_3)** 107, 135, 146, 152, 170, 171 (MH^+ with ^{35}Cl), 173 (MH^+ with ^{37}Cl), 188 ($MH^+..NH_3$ with ^{35}Cl), 190 ($MH^+..NH_3$ with ^{37}Cl), 192, 225, 271, 306, 308, 310. **MS *m/z* (EI)** 107, 115, 117. 121, 134, 135, 170 ($M^{+\bullet}$ with ^{35}Cl). **HRMS *m/z* (EI)**: 170.0489 ($M^{+\bullet}$ $C_9H_{11}{}^{35}ClO^{+\bullet}$ requires 170.0498)**.**

All spectral characteristics are identical to those previously reported (Wu et al., 1994).

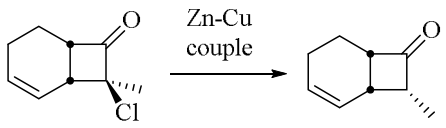

229 **233**
48% yield

7-Methyl-bicyclo[4.2.0]oct-4-en-8-one (233). To mixture of cyclobutanone **229** (815 mg, 4.06 mmol) and NH_4Cl (1.04 g, 19.5 mmol) in ethanol 20 mL at room temperature was added zinc/copper couple (800 mg) in portions. The mixture was stirred at room temperature for 3 h, diluted with ether, and filtered. The filtrate was washed with brine

and dried (Na_2SO_4), and the solvent was removed under reduced pressure. The residue was purified by chromatography on silica gel, eluting with petroleum ether/ethyl acetate (98:2) to give a desired product **233** (265 mg, 48%).

(1***R****,6***S****,7***R****)-7-Methyl-bicyclo[4.2.0]oct-4-en-8-one	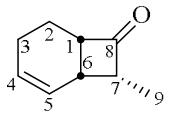

Yellowish oil. $R_f \approx 0.45$ [non-UV-active, EtOAc/Pet. ether 10%, anisaldehyde (violet spot)]**. ^{1}H NMR ($CDCl_3$)** 0.93 (3H, d, ***J*** = 7.3, H9), 1.43 (1H, m, H2a), 1.88–1.99 (3H, m, H2b, H3), 2.93 (1H, td, ***J*** = 9.5, H6), 3.34 (1H, ddq, ***J*** = 2.1, 7.4, 9.5, H7), 3,52 (1H, m, H1), 5,67 (1H, br d, ***J*** = 9.5, H5), 5.87 (1H, m, H4). **^{13}C NMR ($CDCl_3$)** 8.9 (C9), 18.6 (C2), 21.4 (C3), 27.7 (C6), 55.3 (C7), 55.5 (C1), 125.6 (C5), 130.2 (C4), 214.3 (C8). **MS *m/z* (EI)** 97, 101, 105, 109, 111, 117, 121, 123, 126, 133, 136 ($M^{+\bullet}$). **HRMS *m/z* (EI)**: 136. 0890 ($M^{+\bullet}$ $C_9H_{12}O^{+\bullet}$ requires 136.0888)**.**

All spectral characteristics are identical to those previously reported (Wu et al., 1994).

7.7.2.2 4-Methoxy-1,4-cyclohexadiene

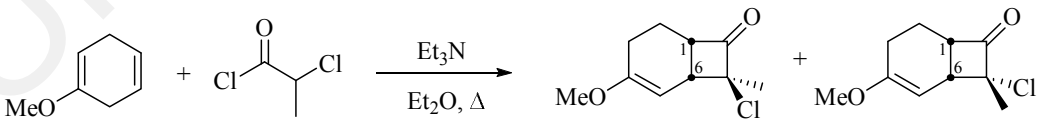

247 **232** **248** 35% yield **249** 11% yield

7-Chloro-4-methoxy-7-methyl-bicyclo[4.2.0]oct-4-en-8-ones (248 and 249). A refluxing mixture of 4-methoxy-1,4-cyclohexadiene (**247**) (5.59 g, 50.8 mmol) and 2-chloropropanoyl chloride (**232**) (3.81 g, 30.0 mmol) in diethyl ether (25 mL) under

nitrogen was treated with triethylamine (1.18 mL, 30.0 mmol). The reaction mixture was stirred at room temperature for 1.5 h and then filtered and the solid was washed with diethyl ether. The filtrate was washed with 1 M HCl and 1 M NaOH. The organic layer was washed further with brine. After drying (Na_2SO_4), the organic layer was concentrated and the crude product was distilled with a Kugelrohr apparatus at 150°C (0.62 mBar) for 1 h to give a mixture of **248** and **249** isomers. Chromatography on silica gel, eluting with petroleum ether/ethyl acetate (98:2) gave **248** (2.11 g, 35%) and **249** (0.66 g, 11%).

(1***R****,6***S****,7***R****)-7-Chloro-4-methoxy-7-methyl-bicyclo[4.2.0]oct-4-en-8-one	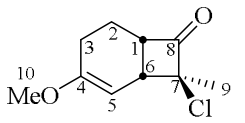

Pale yellow oil. $R_f \approx 0.30$ [UV-active, EtOAc/Pet. ether 5%, anisaldehyde (yellow spot)]**. IR (neat):** $_{max}$ 2939 (m), 2855 (w), 2836 (w), 1786 (s, C=O), 1656 (m), 1443 (m), 1380 (m), 1285 (w), 1219 (m), 1197 (m), 1174 (m), 1139 (m), 1066 (m), 1031 (m), 952 (m), 826 (m) cm^{-1}. **^{1}H NMR ($CDCl_3$)** 1.48 (3H, s, H9), 1.67 (1H, m, H2a), 1.95–2.15 (3H, m, H2b, H3), 3.26 (1H, ddt, ***J*** = 10.0, 5.0, 1.0 Hz, H6), 3.55 (3H, s, H10), 4.12 (1H, dddd, ***J*** = 10.0, 6.0, 3.5, 1.5 Hz, H1), 4.73 (1H, dd, ***J*** = 5.0, 1.5 Hz, H5). **^{13}C NMR ($CDCl_3$)** 19.2 (C9), 19.4 (C3), 24.7 (C2), 40.7 (C6), 53.9 (C1), 54.1 (C10), 77.3 (C7), 90.3 (C5), 158.7 (C4), 206.1 (C8). **MS *m/z* (positive CI, NH_3)** 110, 129, 137, 165, 167, 183, 201 (MH^+ with ^{35}Cl), 202, 203 (MH^+ with ^{37}Cl), 204, 222, 257. **MS *m/z* (EI)** 105, 109, 110, 111, 112, 113, 125, 132, 135, 137, 147, 150, 151, 162, 170, 182, 200 ($M^{+\bullet}$ with ^{35}Cl). **HRMS *m/z* (EI)**: 200.0599 ($M^{+\bullet}$ $C_{10}H_{13}{}^{35}ClO_2{}^{+\bullet}$ requires 200.0604).

NOESY ($CDCl_3$) observed correlations: H5 – H9, H5 – H10. Correlations not observed: H1 – H9, H6 – H9.

(1***R****,6***S****,7***S****)-7-Chloro-4-methoxy-7-methyl-bicyclo[4.2.0]oct-4-en-8-one	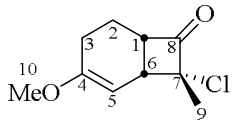

Pale yellow oil. $R_f \approx 0.20$ [UV-active, EtOAc/Pet. ether 5%, anisaldehyde (dark orange spot)]**. IR (neat)**: $_{max}$ 3049 (m), 2984 (m), 2306 (m), 2685 (w), 1796 (m, C=O), 1723 (m) 1688 (w), 1443 (m), 1422 (m), 1263 (s), 1155 (w) 1070 (w) 1024 (w), 895 (m) cm^{-1}. **^{1}H NMR ($CDCl_3$)** 1.68 (1H, m, H2a), 1.77 (3H, s, H9), 1.94 (1H, m, H3a), 2.05–2.17 (2H, m, H2b, H3b), 3.05 (1H, ddt, ***J*** = 10.0, 5.0, 1.0 Hz, H6), 3.54 (3H, s, H10), 3.67 (1H, distorted dddd, ***J*** = 10.0, 6.0, 3.0, 1.0 Hz, H1), 4.69 (1H, dd, ***J*** = 5.0, 1.5 Hz, H5). **^{13}C NMR ($CDCl_3$)** 19.8 (C3), 24.3 (C2), 26.2 (C9), 38.5 (C6), 51.6 (C1), 54.2 (C10), 77.4 (C7), 91.4 (C5), 157.6 (C4), 206.7 (C8). **MS *m/z* (positive CI, NH_3)** 110, 137, 158, 165, 167, 183, 201 (MH^+ with ^{35}Cl), 202, 203 (MH^+ with ^{37}Cl), 204, 206, 218 ($MH^+..NH_3$ with ^{35}Cl). **MS *m/z* (EI)** 109, 110, 111, 112, 113, 125, 132, 135, 137, 150, 151, 158, 162, 182, 200 ($M^{+\bullet}$ with ^{35}Cl). **HRMS *m/z* (EI)**: 200.0606 ($M^{+\bullet}$ $C_{10}H_{13}{}^{35}ClO_2{}^{+\bullet}$ requires 200.0604).

NOESY ($CDCl_3$) observed correlations: H5 – H10 (very intense), H6 – H9 (moderate). Correlation not observed: H5 – H9.

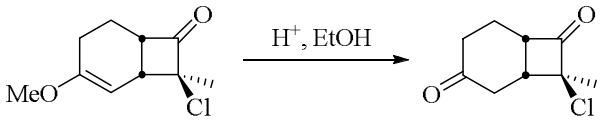

248 **250**
91% yield

7-Chloro-7-methyl-bicyclo[4.2.0]octane-4,8-dione (250). A solution of enol ether **248** (0.48 g, 2.4 mmol) in ethanol (12 mL) was treated with 2 M HCl (0.3 mL) under an

atmosphere of nitrogen. After stirring for 40 min, the excess ethanol was removed and the residue was poured into water (20 mL). The mixture was extracted with diethyl ether (3 x 20 mL), dried and evaporate under vacuum to give the cyclohexanone **250** as a yellowish oil (0.41 g, 91%) which was of sufficient purity for subsequent transformation.

(1***R****,6***S****,7***R****)-7-Chloro-7-methyl-bicyclo[4.2.0]octane-4,8-dione	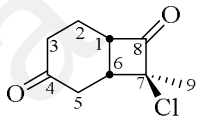

Pale yellow oil. $R_f \approx 0.20$ [UV-active, EtOAc/Pet. ether 15%, anisaldehyde (dark brown spot)]**. IR** $_{max}$ 2948 (m), 1789 (s, cyclobutanone C=O), 1716 (s, cyclohexanone C=O), 1447 (w), 1411 (w), 1376 (w), 1342 (w), 1321 (w), 1294 (w), 1235 (w), 1218 (w), 1193 (w), 1167 (w), 1092 (w), 1071 (w), 984 (w), 923 (w), 795 (w) cm^{-1}. **^{1}H NMR ($CDCl_3$)** 1.80 (3H, s, H9), 2.07 (1H, dddd, ***J*** = 14.5, 9.0, 7.0, 5.5 Hz, H2a), 2.19 (1H, dddd, ***J*** = 14.5, 7.5, 5.5, 5.0 Hz, H2b), 2.34 (2H, AB part of an ABXY system, $_A$ 2.32, $_B$ 2.37, J_{AB} = 18.5, J_{AX} = 7.0, J_{AY} = 5.0, J_{BX} = 9.0, J_{BY} = 5.5, H3), 2.67 (2H, AB part of an ABX system, $_A$ 2.62, $_B$ 2.72, J_{AB} = 17.0, J_{AX} = 7.0, J_{BX} = 6.5, H5), 2.94 (1H, ddd, ***J*** = 10.5, 7.0, 6.5 Hz, H6), 3.80 (1H, ddd, ***J*** = 10.5, 7.5, 5.0 Hz, H1). **^{13}C NMR ($CDCl_3$)** 19.8 (C2), 25.7 (C9), 36.9 (C3), 37.4 (C6), 38.6 (C5), 52.5 (C1), 77.4 (C7), 206.3 (C8), 208.9 (C4). **MS *m/z* (positive CI, NH_3)** 158, 201, 202, 203, 204, 205 (MH^+..NH_3 with ^{35}Cl), 206, 205, 207 (MH^+..NH_3 with ^{37}Cl). **MS *m/z* (EI)** 116, 118, 123, 135, 150, 151, 158, 159, 160, 162, 186 ($M^{+\bullet}$ with ^{35}Cl). **HRMS *m/z* (EI)**: 186.0451 ($M^{+\bullet}$ $C_9H_{11}{}^{35}ClO_2{}^{+\bullet}$ requires 186.0448)**.**

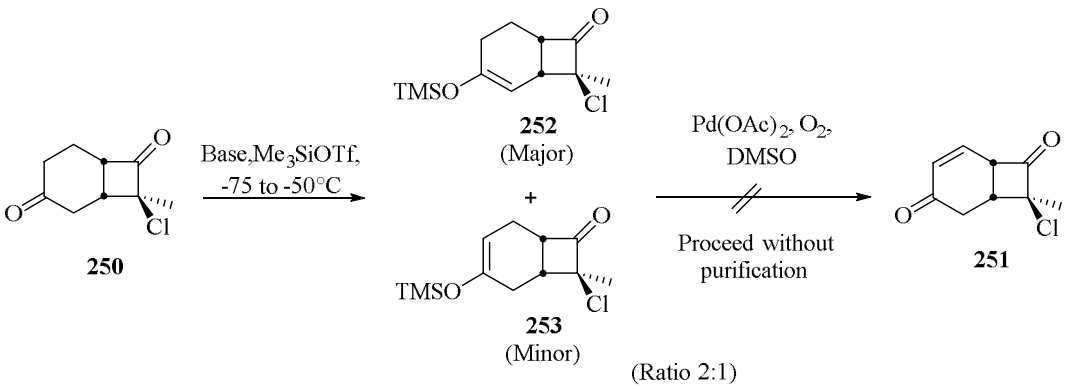

Bicyclo[4.2.0]oct-4-en-8-ones (252 and 253). To a stirred solution of ketone **250** (110.9 mg, 0.594 mmol) in CH_2Cl_2 (10 mL) at 0°C were added Et_3N (241 mg, 2.38 mmol) and Me_3SiOTf (198 mg, 0.891 mmol). The resulting mixture was stirred for 45 min before it was quenched with $NaHCO_3$ (sat. aq. 10 mL). The layers were separated and the aqueous layer was extracted with CH_2Cl_2 (2 × 10 mL). The combined organic layers were dried (Na_2SO_4) and concentrated in ***vacuo*** afforded the corresponding silyl enol ethers **252** and **253** as a light yellow oil, which was directly used in the next step without further purification.

To a stirred solution of the above silyl enol ethers **252** and **253** (111 mg, 0.429 mmol) in DMSO (40 mL) at room temperature was added $Pd(OAc)_2$ (9.63 mg, 0.043 mmol). The resulting solution was heated at 80°C for 16 h under an oxygen atmosphere before Et_2O (30 mL) and H_2O (10 mL) were added. The layers were separated and the aqueous layer was extracted with Et_2O (2 × 20 mL). The combined organic layers were dried (Na_2SO_4) and concentrated in ***vacuo***. Based on ^1H NMR observation the desired product **251** was not produced and decomposition happened.

(1***R****,6***S****,7***R****)-7-Chloro-7-methyl-4-((trimethylsilyl)oxy)bicyclo [4.2.0]oct-4- en-8-one	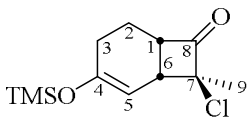

Pale yellow oil. **^{1}H NMR ($CDCl_3$)** 1.84 (3H, s, H9), 1.92 - 2.56* (4H, m, H2, H3), 3.09 (1H, dd, ***J*** = 9.7, 5.2 Hz, H6), 3.70 (1H, ddd, ***J*** = 9.7, 5.2, 2.2 Hz, H1), 5.04 (1H, dd, ***J*** = 5.2, 2.1 Hz, H5) (*obscured by other resonances).

(1***R****,6***S****,7***R****)-7-Chloro-7-methyl-4-((trimethylsilyl)oxy)bicyclo [4.2.0]oct-4- en-8-one	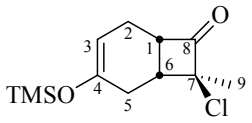

Pale yellow oil. **^{1}H NMR ($CDCl_3$)** 1.78 (3H, s, H9), 1.92 - 2.56* (4H, m, H2, H5), 2.96 (1H, dt, ***J*** = 9.7, 5.4 Hz, H6), 3.62 (1H, ddd, ***J*** = 9.7, 5.4, 2.2 Hz, H1), 4.88 (1H, dt, ***J*** = 5.4, 2.5 Hz, H3) (*obscured by other resonances).

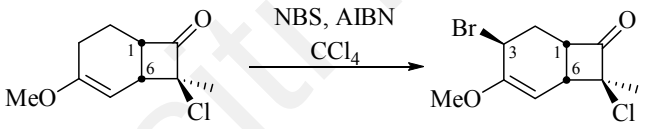

248 **254**
20% yield

3-Bromo-7-chloro-4-methoxy-7-methyl-bicyclo[4.2.0]oct-4-en-8-one (254). A solution of of NBS (204 mg, 1.14 mmol) of enol ether **248** (300 mg, 1.14 mmol) and a catalytic amount of AIBN (9 mg, 0.006 mmol) in 15 ml of CCl_4 was refluxed for 1 h. The reaction mixture was left in refrigerator overnight so that all of the succinimide would crystallize out of the solution. The cold CCl_4 solution was filtered, and the precipitate was washed with additional cold CCl_4. The filtrate was concentrated under reduced pressure to give a crude product. Chromatography on silica gel, eluting with petroleum ether/ethyl acetate (95:5) to gave a desired product **254** as yellowish oil (64 mg, 20%).

(1***R****,6***S****,7***R****)-3-Bromo-7-chloro-4-methoxy-7-methyl-bicyclo[4.2.0]oct-4- en-8-one	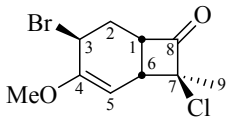

Pale yellow oil. $R_f \approx 0.40$ [UV-active, EtOAc/Pet. ether 10%, anisaldehyde (yellow spot)]**. IR** $_{max}$ 2253 (m), 1811 (s, cyclobutanone C=O), 1692 (w), 1659 (w), 1467 (w), 1384 (m), 1175 (m), 1143 (m), 1098 (m), 1014 (w), 910 (s) cm^{-1}. **^{1}H NMR ($CDCl_3$)** 1.60 (3H, s, H9), 2.30 (1H, m, H2a), 2.44 (1H, m, H2b), 3.45 (1H, m, H6), 3.65 (3H, s, H10), 4.00 (1H, td, ***J*** = 11.0, 7.2 Hz, H1), 4.49 (1H, t, ***J*** = 7.2 Hz, H3), 4.88 (1H, d, ***J*** = 7.2 Hz, H5). **^{13}C NMR ($CDCl_3$)** 21.6 (C9), 30.7 (C2), 40.3 (C6), 42.1 (C3), 49.8 (C1), 55.1 (C10), 76.6 (C7), 91.7 (C5), 157.9 (C4), 205.3 (C8). **MS *m/z* (EI)** 105, 123, 125, 132, 158, 160, 188, 204, 240, 266, 268, 278 ($M^{+\bullet}$ with ^{35}Cl). **HRMS *m/z* (EI)**: 277.9704 ($M^{+\bullet}$ $C_{10}H_{13}{}^{35}Cl^{79}BrO_2{}^{+\bullet}$ requires 277.9709)**.**

248 **256**
45% yield

4-Methoxy-7-methyl-bicyclo[4.2.0]oct-4-en-8-one (256). To mixture of 2 g of Zn dust and 4.5 mL of TMEDA (29.0 mmol) in 10 mL of absolute EtOH at 0°C was added 2.0 mL (33.0 mmol) of AcOH. The reaction mixture was maintained at 0°C while a solution of enol ether **248** (1.10 g, 5.0 mmol) in 2 mL of EtOH was added over 10 min period. After an additional 15 min at 0°C the reaction mixture was allowed to warm to room temperature and stirred for 15 min. The resulting grey mixture was filtered, and the solid was washed with diethyl ether. The filtrated was extracted with ice cold 1 M HCl (10 mL), H_2O (10 mL), sat. $NaHCO_3$ (10 mL) and sat NaCl (10 mL). The resulting

material was dried over $MgSO_4$ and concentrated under reduced pressure to afford 374 mg (45%) of desired enol ether **256** which was of sufficient purity for subsequent transformation.

(1***R****,6***S****,7***R****)-4-Methoxy-7-methyl-bicyclo[4.2.0]oct-4- en-8-one	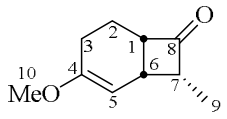

Colourless oil. $R_f \approx 0.30$ [UV-active, EtOAc/Pet. ether 5%, anisaldehyde (yellow spot)]**.** **IR (neat)**: $_{max}$ 3020 (s), 2985 (m), 2410 (w), 1771 (s, C=O), 1713 (s), 1553 (m), 1422 (m), 1264 (s), 1216 (s), 1017 (m), 890 (s) cm^{-1}. **^{1}H NMR ($CDCl_3$)** 0.91 (3H, d, ***J*** = 8.4 Hz, H9), 1.65 (1H, m, H2a), 1.87 (1H, m, H3a), 1.98–2.12 (2H, m, H2b, H3b), 3.07 (1H, qd, ***J*** = 8.4, 4.6 Hz, H7), 3.31 (1H, td, ***J*** = 9.1, 4.6 Hz, H6), 3.47 (3H, s, H10), 3.52 (1H, m, H1), 4.55 (1H, dd, ***J*** = 4.6, 2.0 Hz, H5). **^{13}C NMR ($CDCl_3$)** 8.77 (C9), 19.2 (C2), 24.6 (C3), 27.6 (C7), 53.9 (C10), 54.5 (C1), 56.0 (C6), 91.0 (C5), 157.4 (C4), 213.9 (C8). **MS *m/z* (positive CI, NH_3)** 165, 167 (MH^+), 171, 172, 183, 200. **MS *m/z* (EI)** 109, 114, 121, 124, 135, 137, 151, 152, 161, 166 ($M^{+\bullet}$). **HRMS *m/z* (EI)**: 166. 0993 ($M^{+\bullet}$ $C_{10}H_{14}O_2^{+\bullet}$ requires 166.0994)**.**

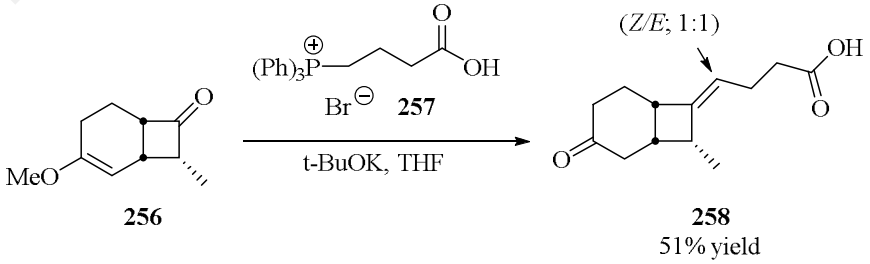

256 **258**
51% yield

7-Methyl-4-oxobicyclo[4.2.0]octan-8-ylidene)butanoic acid (258). To a stirred slurry of (3-carboxypropyl)-triphenylphosphonium bromide (**257**) (2.11 g, 4.91 mmol) in dry

THF (10 mL) under nitrogen at -75°C was added potassium ***tert***-butoxide (1.38 g, 12.3 mmol). After 15 min at -75°C, a solution of enol ether **256** (680 mg, 4.09 mmol) in 5 mL dry THF was added to a mixture and stirred at -75°C for 10 min. The mixture was continued stirred at room temperature for overnight. The mixture was pouring into 5% Na_2CO_3 solution (30 mL), washed with ethyl acetate (30 mL), and then acidified with conc. HCl. The aqueous layer was extracted with ether (3 x 50 mL) and the combined extracts were concentrated to 20 mL and kept at -20°C for 2 h. The resulting precipitate was filtered off and discarded. Evaporation of the filtrate gave a yellowish oil (788 mg) which was purified by column chromatography on silica gel, eluted with petroleum ether/ethyl acetate (7:3) to give the desired product **258** in racemic mixture (1:1) as a yellowish oil (464 mg, 51%).

(1***R****,6***S****,7***R****)-7-Methyl-4-oxobicyclo[4.2.0]octan-8-ylidene)butanoic acid	(*Z*/*E*; 1:1) 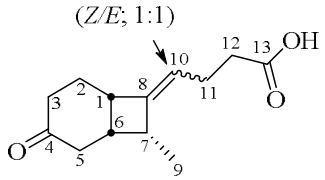

Yellowish oil. $R_f \approx 0.20$ [UV-active, EtOAc/Pet. ether 50%, anisaldehyde (violet spot)]**.** **IR (neat)**: $_{max}$ 2950 (m), 2362 (w), 1736 (s, C=O), 1708 (m, C=O), 1438 (w), 1170 (m), 923 (w), 634 (w) cm^{-1}. **$^1H_{Z\text{-}isomer}$ NMR ($CDCl_3$)** 1.13 (3H, d, ***J*** = 7.7 Hz, H-9), 1.90* (1H, m, H2a), 2.02* (1H, m, H2b), 2.24* (1H, m, H3b), 2.31 – 2.47* (5H, m, H5, H11, H12a), 2.51* (1H, m, H3b), 2.55* (1H, m, H12b), 2.61* (1H, m, H6), 3.22* (1H, m, H-1), 3.34* (1H, m, H-7), 5.22 (1H, t, ***J*** = 7.7 Hz, H10) (*obscured by other resonances). **$^{13}C_{Z\text{-}isomer}$ NMR ($CDCl_3$)** 13.5 (C9), 23.2 (C2), 23.5 (C11), 31.7 (C6), 34.5 (C12), 36.8 (C3), 37.8 (C1), 38.2 (C5), 38.5 (C7), 121.5 (C10), 148.4 (C8), 178.5 (C13), 214.5 (C4). **$^1H_{E\text{-}isomer}$ NMR ($CDCl_3$)** 0.98 (3H, d, ***J*** = 7.7 Hz, H-9), 1.90* (1H, m, H2a), 2.02* (1H, m, H2b), 2.24* (1H, m, H3b), 2.31 – 2.47* (5H, m, H5, H11, H12a), 2.51*

(1H, m, H3b), 2.55* (1H, m, H12b), 2.61* (1H, m, H6), 3.22* (1H, m, H-1), 3.34* (1H, m, H-7), 5.24 (1H, t, ***J*** = 7.7 Hz, H10) (*obscured by other resonances). **^{13}C *E-isomer* NMR ($CDCl_3$)** 13.5 (C9), 23.2 (C2), 23.5 (C11), 31.7 (C6), 34.5 (C12), 36.8 (C3), 37.8 (C1), 38.2 (C5), 38.5 (C7), 121.5 (C10), 148.4 (C8), 178.5 (C13), 214.5 (C4). **MS *m/z* (positive CI, NH_3)** 167, 205, 207, 223 (MH^+), 225, 240 ($MH^+..NH_3$), 241. **MS *m/z* (EI)** 105, 107, 120, 123, 135, 149, 162, 163, 176, 182, 204, 222 ($M^{+\bullet}$). **HRMS *m/z* (EI)**: 222.1252 ($M^{+\bullet}$ $C_{13}H_{18}O_3^{+\bullet}$ requires 222.1256)**.**

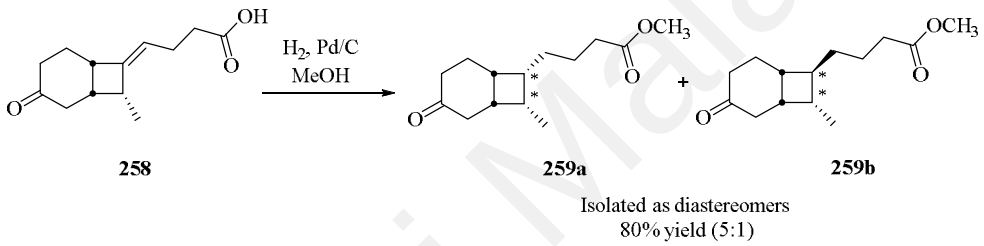

Methyl-({7-methyl-4-oxobicyclo[4.2.0]octan-8-yl})butanoate (259). To a solution of the bicycloalkene **258** (244 mg, 1.10 mmol) in MeOH (5 mL) was added 10% Pd/C (10% w/w, 24.4 mg), and the resulting mixture was hydrogenated at 1 atm for 12 h. Filtration through Celite and evaporation of the filtrate in vacuo afforded the pure **259** as yellowish oil (210 mg, 80.0%).

Methyl-({(1***R****,6***S****,7***R****)-7-methyl-4-oxobicyclo[4.2.0] octan-8-yl})butanoate	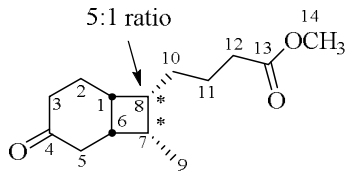

Yellowish oil. $R_f \approx 0.40$ [non UV-active, EtOAc/Pet. ether 50%, anisaldehyde (red-violet spot)]**. IR (neat)**: $_{max}$ 2933 (m), 1738 (s, C=O), 1714 (s, C=O), 1455 (w), 1436 (w), 1377 (w), 1197 (m), 1170 (m), 1112 (w), 1015 (w), 883 (w) cm^{-1}. **$^1H_{8\alpha}$ NMR**

($CDCl_3$) 1.05 (3H, d, ***J*** = 7.4 Hz, H9), 1.46* (2H, m, H10), 1.56* (2H, m, H11), 1.87* (1H, m, H2a), 1.97 – 2.06* (2H, m, H2b, H3a), 2.19* (1H, m, H5a), 2.34 (2H, t, ***J*** = 7.2 Hz, H12), 2.40 – 2.62* (4H, m, H1, H3b, H5b, H8), 2.72* (1H, qd, ***J*** = 8.1, 2.0 Hz, H7), 2.79* (1H, q, ***J*** = 8.1 Hz, H6), 3.69 (3H, s, H14) (*obscured by other resonances). **^{13}C NMR ($CDCl_3$)** 12.3 (C9), 22.1 (C2), 23.9 (C11), 26.0 (C10), 31.3 (C6), 34.2 (C12), 32.7 (C7), 34.4 (C1), 37.2 (C8), 37.4 (C5), 38.4 (C3), 51.5 (C14), 173.8 (C13), 214.4 (C4). **$^1H_{8\beta}$ NMR ($CDCl_3$)** 0.97 (3H, d, ***J*** = 7.4 Hz, H9), 1.46* (2H, m, H10), 1.56* (2H, m, H11), 1.87* (1H, m, H2a), 1.97 – 2.06* (2H, m, H2b, H3a), 2.19* (1H, m, H5a), 2.33 (2H, t, ***J*** = 7.2 Hz, H12), 2.40 – 2.62* (4H, m, H1, H3b, H5b, H8), 2.72* (1H, qd, ***J*** = 8.1, 2.0 Hz, H7), 2.79* (1H, q, ***J*** = 8.1 Hz, H6), 3.69 (3H, s, H14) (*obscured by other resonances). **^{13}C NMR ($CDCl_3$)** 12.2 (C9), 22.2 (C2), 23.7 (C11), 25.5 (C10), 31.5 (C6), 34.0 (C12), 32.7 (C7), 34.4 (C1), 37.2 (C8), 37.3 (C5), 38.4 (C3), 51.5 (C14), 174.2 (C13), 215.2 (C4). MS ***m/z* (EI)** 110, 123, 135, 151, 162, 182, 195, 206, 224, 236, 238 ($M^{+\bullet}$). **HRMS *m/z* (EI)**: 238.1562 ($M^{+\bullet}$ $C_{14}H_{22}O_3^{+\bullet}$ requires 238.1569)**.**

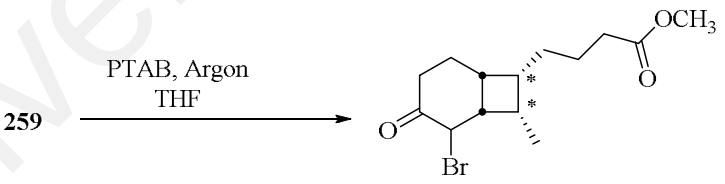

261
90% yield

Methyl-{5-bromo-7-methyl-4-oxobicyclo[4.2.0]octan-8-yl})butanoate (261). To a stirred solution of the bicycloalkene **259** (189 mg, 0.794 mmol) in dry THF (10 mL) at -75°C under argon was added phenyltrimethylammonium tribromide (298 mg, 0.794 mmol). The mixture was allowed to stirred at -75°C for 20 min and then allowed to slowly warm to room temperature over 30 min. Brine (10 mL) was added, and then the resulting mixture was extracted with ether (2 x 20 mL). The combined extracts were

dried ($MgSO_4$) and concentrated to give an orange oil **261** (227 mg, 90.0%) which was of sufficient purity for subsequent transformation.

Methyl-{(1***R****,6***S****,7***R****)-5-bromo-7-methyl-4-oxobicyclo [4.2.0]octan-8-yl})butanoate	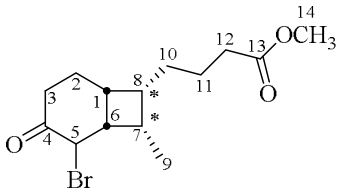

Orange oil. $R_f \approx 0.15$ [non UV-active, EtOAc/Pet. ether 30%, anisaldehyde (red-violet spot)]**. IR (neat)**: $_{max}$ 2937 (m), 1738 (s, C=O), 1731 (s, C=O), 1455 (w), 1436 (w), 1379 (w), 1246 (w), 1170 (w), 1066 (w), 1030 (w), 884 (w), 755 (w) cm^{-1}. **^{1}H NMR ($CDCl_3$)** 1.24 (3H, d, ***J*** = 8.2 Hz, H9), 1.49 (2H, m, H10), 1.58 (2H, m, H11), 1.97 (1H, m, H2a), 2.15 (1H, dd, ***J*** = 8.2, 5.4 Hz, H2b), 2.37 (2H, m, H12), 2.49 (1H, dd, ***J*** = 8.2, 5.4 Hz, H3a), 2.62 – 2.68 (4H, m, H1, H3b, H8), 2.89 (1H, qd, ***J*** = 8.2, 2.9 Hz, H7), 3.04 (1H, q, ***J*** = 8.2 Hz, H6), 3.71 (3H, s, H14), 4.86 (1H, d, J = 8.2 Hz, H5). **^{13}C NMR ($CDCl_3$)** 11.5 (C9), 22.4 (C2), 23.7 (C11), 25.3 (C10), 33.1 (C7), 34.1 (C12), 36.2 (C8), 37.0 (C1), 37.6 (C3), 41.9 (C6), 51.6 (C-14), 53.5 (C5), 174.0 (C13), 203.6 (C4). **MS *m/z* (positive CI, NH_3)** 223, 237, 239, 255, 271, 287, 317 (MH^+), 333, 334 ($MH^+..NH_3$), 335, 336. **MS *m/z* (EI)** 110, 123, 142, 151, 177, 187, 205, 237, 259, 287, 299, 316 ($M^{+\bullet}$), 317. **HRMS *m/z* (EI)**: 316.0670 ($M^{+\bullet}$ $C_{14}H_{21}{}^{79}BrO_3{}^{+\bullet}$ requires 316.0674)**.**

7.7.2.3 1,4-Cyclohexadiene

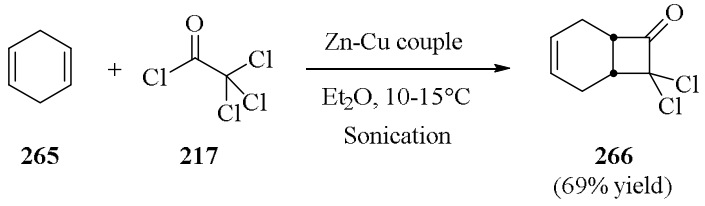

265 **217** **266** (69% yield)

7-Dichloro-bicyclo[4.2.0]oct-3-en-8-one (266) (Mori et al., 1997; Horasan et al., 2011; Davis & Carpenter, 1996). A 250 mL two-neck round bottom flask was equipped with a nitrogen inlet and pressure-regulated dropping funnel. A solution of 1,4-cylohexadiene (**265**) (1.69 g, 21.1 mmol) and Zn-Cu couple powder (5.45 g, 42.3 mmol) in dry ether (120 mL) of was immersed in an ultrasound bath where sonication was greatest to acquire maximum agitation. The water bath was cooled to 15°C by adding pieces of ice periodically. A solution of trichloroacetyl chloride (**217**) (7.67 g, 42.3 mmol) in dry ether (50 mL) was added dropwise within 2 h under sonication. Stirring of the reaction continued for an additional hour while the water bath temperature was maintained at 15°C. When the reaction was complete, the solids were removed by simple filtration. The filtrate was extracted first with H_2O (2 x 70 mL) and then with saturated $NaHCO_3$ (2 x 70 mL). The organic solution over Na_2SO_4 and the solvent was evaporated. The resulting mixture was purified with a Kugelrohr apparatus at 150°C (17.0 mBar). The fraction was identified as the desired addition product **266** (2.78 g, 69%).

(1***R****,6***S****)-7,7-Dichloro-bicyclo[4.2.0]oct-3-en-8-one	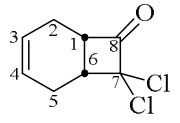

Pale yellow oil. $\boldsymbol{R}_f \approx 0.40$ [UV-active, EtOAc/Pet. ether 10%, anisaldehyde (violet spot)]**. IR (neat):** ν_{max} 3039 (w), 2925 (w), 2841 (w), 1783 (s, C=O), 1436 (w), 1388 (w), 1183 (w), 1106 (w), 1010 (w) cm^{-1}. **^{1}H NMR ($CDCl_3$)** 2.11 (1H, m, H5a), 2.33 (1H, m, H2a), 2.47 (1H, dd, ***J*** = 16.7, 3.5 Hz, H5b), 2.55 (1H, dd, ***J*** = 16.7, 3.5 Hz, H2b), 3.31 (1H, td, ***J*** = 9.1, 3.5 Hz, H6), 4.02 (1H, td, ***J*** = 9.1, 3.5 Hz, H1), 5.81 (2H, br t, ***J*** = 3.5 Hz, H3, H4). **^{13}C NMR ($CDCl_3$)** 21.4 (C5), 23.1 (C2), 44.9 (C6), 53.6 (C1), 88.1 (C7), 126.1 (C4), 127.1 (C3), 198.4 (C8). **MS *m/z* (EI)** 109, 113, 120, 132, 136,

150, 155, 162, 169, 175, 186, 190 ($M^{+\bullet}$). **HRMS *m/z* (EI)**: 189.9944 ($M^{+\bullet}$ $C_8H_8{}^{35}Cl_2O^{+\bullet}$ requires 189.9952).

All spectral characteristics are identical to those previously reported (Mori et al., 1997; Horasan et al., 2011; Davis & Carpenter, 1996).

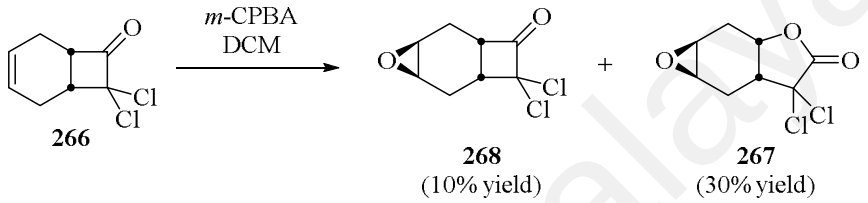

266 **268** (10% yield) **267** (30% yield)

Oxidation of 7-dichloro-bicyclo[4.2.0]oct-3-en-8-one (**266)**. ***m***-CPBA (763 mg, 4.42 mmol) was added to a solution of dichloroketene **266** (360 mg, 2.95 mmol) in 10 mL CH_2Cl_2 at room temperature and the mixture was stirred overnight. The organic phase was washed with saturated $NaHCO_3$ (2 x 50 mL) and H_2O (2 x 50 mL). After drying ($MgSO_4$), the organic layer was concentrated and the crude product was purified using column chromatography on silica gel, eluting with petroleum ether/ethyl acetate (8:2) gave two products **267** (193 mg, 30%) and **268** (61 mg, 10%).

(1a***S****,2a***S****,5a***R****,6a***R****)-5,5-Dichlorohexahydrooxireno[2,3-f] benzofuran-4(1aH)-one	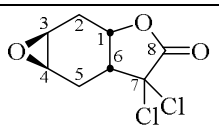

Yellowish oil. $\boldsymbol{R}_f \approx 0.45$ [non UV-active, EtOAc/Pet. ether 30%, anisaldehyde (green-blue spot)]**. IR (neat):** ν_{max} 2896 (w), 1813 (s), 1775 (w), 1742 (s, C=O), 1702 (w), 1372 (w), 1239 (s), 1166 (m), 1047 (m), 985 (w), 958 (w) cm^{-1}. **^{1}H NMR ($CDCl_3$)** 1.90 (1H, dd, ***J*** = 15.4, 2.7 Hz, H5a), 2.34 (1H, dt, ***J*** = 16.4, 2.7 Hz, H2a), 2.52 (1H, ddt,

J = 15.4, 5.6, 2.7 Hz, H5b), 2.65 (1H, dd, ***J*** = 16.4, 7.6 Hz, H2b), 3.05 (1H, m, H6), 3.22 (1H, q, ***J*** = 2.7 Hz, H3), 3.32 (1H, q, ***J*** = 2.7 Hz, H4), 4.85 (1H, dt, ***J*** = 7.6, 2.7 Hz, H1). **^{13}C NMR ($CDCl_3$)** 22.9 (C5), 26.0 (C2), 46.4 (C6), 49.6 (C3), 50.8 (C4), 73.8 (C1), 82.6 (C7), 166.9 (C8). **MS *m/z* (EI)** 50, 63, 77, 95, 107, 125, 127, 142, 160, 169, 187, 205, 222 ($M^{+\bullet}$).

(1***R****,3R*, 5S*,6***S****)-8,8-Dichloro-4-oxatricyclo[5.2.0.0^{3,5}]nonan-9-one	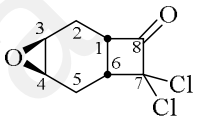

Yellowish oil. $R_f \approx 0.30$ [non UV-active, EtOAc/Pet. ether 30%, anisaldehyde (blue-violet spot)]**. IR (neat):** ν_{max} 2985 (w), 1813 (s), 1775 (w), 1742 (s, C=O), 1702 (w), 1438 (w), 1372 (w), 1240 (s), 1166 (m), 1047 (m), 1023 (w), 985 (w), 958 (w) cm^{-1}. **^{1}H NMR ($CDCl_3$)** 2.20 (1H, dd, ***J*** = 16.6, 8.0 Hz, H5a), 2.32 (1H, dd, ***J*** = 17.5, 8.0 Hz, H2a), 2.63 (1H, d, ***J*** = 16.6 Hz, H5b), 2.71 (1H, d, ***J*** = 17.5 Hz, H2b), 2.97 (1H, t, ***J*** = 8.0 Hz, H6), 3.15 (2H, br s, H3, H4), 3.60 (1H, dd, ***J*** = 10.7, 8.0 Hz, H1). **^{13}C NMR ($CDCl_3$)** 23.1 (C2), 23.8 (C5), 42.4 (C6), 48.0 (C1), 49.6 (C3), 50.3 (C4), 90.4 (C7), 198.4 (C8). **MS *m/z* (EI)** 50, 68, 79, 88, 107, 115, 135, 143, 162, 178, 191, 206 ($M^{+\bullet}$).

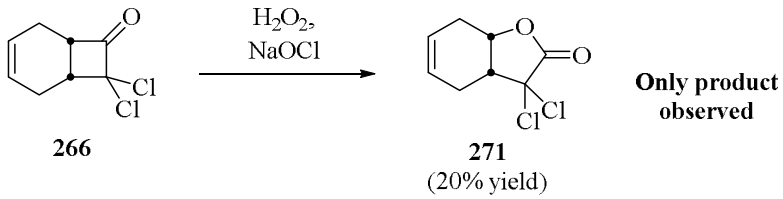

266 **271** (20% yield)

Singlet oxygen ($^1O_2$) ene-reaction of 7-dichloro-bicyclo[4.2.0]oct-3-en-8-one (266). A solution of bicyclo[4.2.0]oct-3-en-8-one **266** (0.57 g, 3.0 mmol) in MeOH (10 mL) was chilled to -5°C and treated with 1.8 mL (16 mmol) of 30% H_2O_2. To this solution

10.1 mL (9 mmol) of 0.89M NaOCl solution was added dropwise with stirring. The reaction mixture was diluted with water and extracted with ether. The organic phase was dried over $MgSO_4$ and evaporated under reduced pressure to give the yellowish oil. Based on ^{1}H NMR of crude product, compound **266** was transformed to lactone **271** together with complex mixture.

(3a***R****,7a***S****)-3,3-Dichloro-3a,4,7,7a-tetrahydrobenzofuran-2(3H)-one	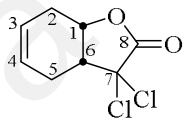

Yellowish oil. **^{1}H NMR ($CDCl_3$)** 2.20 – 3.10 (4H, m, H2, H5), 3.05 (1H, q, ***J*** = 7.5 Hz, H6), 5.06 (1H, q, ***J*** = 7.5 Hz, H1), 5.72 (1H, d, ***J*** = 7.5 Hz, H3), 5.82 (1H, d, ***J*** = 7.5 Hz, H4). **^{13}C NMR ($CDCl_3$)** 23.0 (C5), 26.6 (C2), 47.9 (C6), 50.8 (C4), 75.5 (C1), 83.0 (C7), 122.7 (C3), 123.8 (C4), 165.7 (C8).

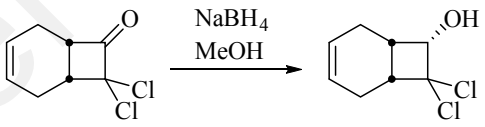

266 **272**
68% yield

7,7-Dichloro-bicyclo[4.2.0]oct-3-en-8-ol (272). To a solution of 191 mg of dichlorobutanone **266** (1.00 mmol) and 4 mL of MeOH at 0°C was added 40.5 mg of $NaBH_4$ (1.10 mmol) over 1 h. The solvent was concentrated and the crude product was extracted with dichloromethane (3 x 25 mL), washed sequentially with H_2O and then dried with MgSO4. The organic layer was concentrated and the crude product was purified using column chromatography on silica gel, eluting with petroleum ether/ethyl acetate (95:5) gave a desired product **272** (132 mg, 68%).

(1***R****,6***S****,8S*)-7,7-Dichloro-bicyclo[4.2.0]oct-3-en-8-ol	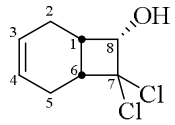

Colourless oil. $R_f \approx 0.20$ [nonUV-active, EtOAc/Pet. ether 10%, anisaldehyde (dark blue spot)]**. IR (neat):** *v* 3569 (m, -OH), 3034 (m), 2957 (m), 2838 (w), 2253 (w), 1792 (w), 1431 (w), 1406 (m), 1254 (w), 1163 (s), 1113 (m), 999 (w), 883 (w) cm^{-1}. **^{1}H NMR ($CDCl_3$)** 2.05 (1H, m, H2a), 2.21–2.40 (3H, m, H2b, H5), 2.89 (1H, m, H1), 3.07 (1H, m, H6), 4.67 (1H, d, ***J*** = 8.2 Hz, H8), 5.81 (2H, s, H3, H4). **^{13}C NMR ($CDCl_3$)** 17.8 (C2), 20.9 (C5), 32.4 (C1), 43.8 (C6), 78.0 (C8), 94.4 (C7), 124.9 (C3), 125.4 (C4). **MS *m/z* (positive CI, NH_3)** 92, 97, 113, 120, 139, 148, 149, 156, 169, 174, 176, 185, 190, 193 (MH^+ with ^{35}Cl), 204, 205, 210 ($MH^+..NH_3$ with ^{35}Cl), 215, 222. **MS *m/z* (EI)** 113, 115, 121, 127, 139, 148, 150, 157, 162, 170, 182, 191, 192 ($M^{+\bullet}$ with ^{35}Cl). **HRMS *m/z* (EI)**: **192.0107** ($M^{+\bullet}$ $C_8H_{10}{}^{35}Cl_2O^{+\bullet}$ requires 192.0109)**.**

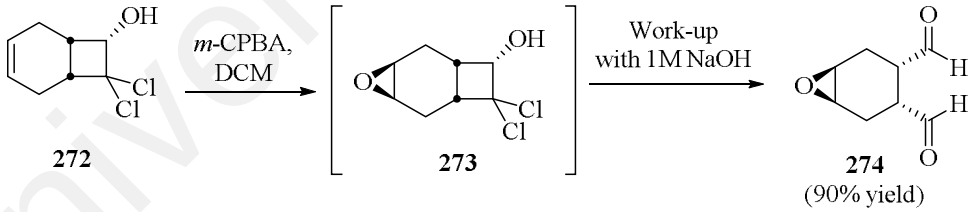

7-Oxabicyclo[4.1.0]heptanes-3,4-dicarbaldehyde (274). ***m***-CPBA (763mg, 4.42 mmol) was added to a solution of dichlorocyclobutanol **272** (70.0 mg, 0.363 mmol) in 4 mL CH_2Cl_2 at 0°C mixture was stirred for 2 h. The organic phase was diluted with dichloromethane (20 mL), washed with NaOH aq. (1.0 M, 10 mL) and H_2O (10 mL) and then dried with $MgSO_4$. The organic layer was concentrated and gives the dialdehyde **274** product (53.4 mg, 90%) as a yellowish oil which was sufficient purity.

(1***R****,3R*,4S*,6***S****)-7-Oxabicyclo[4.1.0]heptanes-3,4-dicarbaldehyde	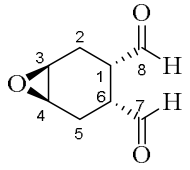

Yellowish oil. $R_f \approx 0.40$ [nonUV-active, EtOAc/Pet. ether 30%, anisaldehyde (brown spot)]**.** **^{1}H NMR ($CDCl_3$)** 1.87 (2H, d, ***J*** = 6.5, H1, H6), 1.95 (2H, d, ***J*** = 16.5, H2a, H5a), 2.48 (2H, dd, ***J*** = 16.5, 6.5, H2b, H5b), 3.13 (2H, s, H3, H4), 9.42 (2H, s, H7, H8). **^{13}C NMR ($CDCl_3$)** 18.2 (C2, C5), 21.7 (C1, C6), 50.0 (C3. C4),197.5 (C7, C8). **MS *m/z* (positive CI, NH_3)** 128, 137, 139, 155 (MH^+), 157, 172 (MH^+..NH_3), 173, 175, 190, 192, 201, 209, 211, 220. **MS *m/z* (EI)** 109, 111, 113, 115, 117, 120, 125, 128, 139, 141, 143, 149, 151, 154 ($M^{+\bullet}$). **HRMS *m/z* (EI)**: 154. 0631 ($M^{+\bullet}$ $C_8H_{10}O_3^{+\bullet}$ requires 154.0630)**.**

272 **273**
79% yield

8,8-Dichloro-4-oxatricyclo[5.2.0.0^{3,5}]nonan-9-ol (273). ***m*-**CPBA (700 mg, 3.62 mmol) was added to a solution of dichlorocyclobutanol **272** (894 mg, 3.62 mmol) in 5 mL CH_2Cl_2 at 0°C mixture was stirred for 2 h. The organic phase was diluted with dichloromethane (20 mL), washed with $NaHCO_3$ sat. (3 x 10 mL) and H_2O (10 mL) and then dried with $MgSO_4$. The organic layer was concentrated and give the epoxy-dichlorocyclobutanol product **273** (597 mg, 79%) as a yellowish oil which was sufficient purity.

(1***R****,3***R****,5***S****,7***S****,8***S****)-8,8-Dichloro-4-oxatricyclo[5.2.0.0^{3,5}]nonan-9-ol	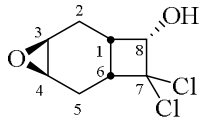

Yellowish oil. $R_f \approx 0.25$ [nonUV-active, EtOAc/Pet. ether 30%, anisaldehyde (brown spot)]**. IR (neat):** *v* 3622 (w), 2953 (m), 1804 (m), 1702 (s, C=O), 1436 (m), 1287 (m), 1259 (m), 1189 (w), 1091 (m), 1055 (m), 1026 (w) cm^{-1}. **^{1}H NMR ($CDCl_3$)** 1.95 – 2.23 (4H, m, H2, H5), 2.70 (2H, m, H1, H6), 3.17 (2H, m, H3, H4), 4.54 (1H, d, ***J*** = 8.6, H8). **^{13}C NMR ($CDCl_3$)** 17.6 (C2), 19.5 (C5), 31.5 (C1), 40.1 (C6), 50.2 (C4), 51.2 (C3), 77.4 (C8), 93.4 (C7). **MS *m/z* (positive CI, NH_3)** 139, 183, 184, 203, 219, 222, 226 ($MH^{+\cdot}..NH_3$), 236, 238, 241. **MS *m/z* (EI)** 111, 113, 121, 123, 127, 139, 141, 156, 158, 162, 170, 182, 191, 201, 207, 208 ($M^{+\bullet}$). **HRMS *m/z* (EI)**: 208.0047 ($M^{+\bullet}$ $C_8H_{10}{}^{35}ClO_2{}^{+\bullet}$ requires 208.0058)**.**

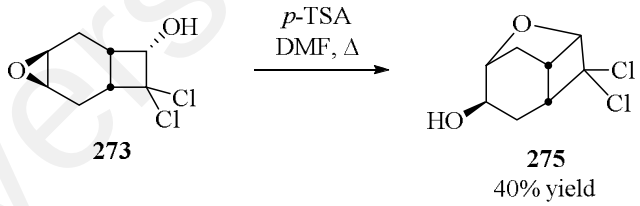

273 **275**
40% yield

2,2-Dichloro-9-oxatricyclo[4.2.1.0^{3,8}]nonan-5-ol (275). To dichloroalcohol **273** (327 mg, 1.56 mmol) in 5 mL of dry DMF at room temperature was added 298 mg (1.56 mmol) of ***p***-toluenesulfonic acid (***p***-TSA). The reaction was stirred at room temperature. After 4 hr, the resulting mixture was diluted with ethyl acetate (15 mL), washed with saturated $CuSO_4$ solution (2 x 5 mL) and H_2O (2 x 5 mL) and then dried over $MgSO_4$. The organic layer was concentrated under reduced pressure. The residue was purified by chromatography on silica gel, eluting with petroleum ether/ethyl acetate (7:3) to give a desired product **275** as yellowish oil (130 mg, 40.0 %).

(3***R****,5***R****,8***S****)-2,2-Dichloro-9-oxatricyclo[4.2.1.$0^{3,8}$]nonan-5-ol	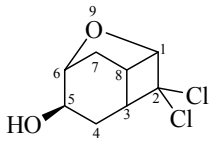

Pale yellow oil. $R_f \approx 0.35$ [UV-active, EtOAc/Pet. ether 50%, anisaldehyde (brown spot)]**. IR (neat):** $_{max}$ 2951 (m), 1804 (w), 1736 (m), 1435 (w), 1374 (w), 1264 (m), 1241 (w), 1190 (m), 1178 (m), 1091 (s), 1055 (s) cm^{-1}. **^{1}H NMR ($CDCl_3$)** 1.48 (1H, dt, ***J*** = 14.3, 5.7 Hz, H7a), 1.70 (1H, dt, ***J*** = 12.6, 5.7 Hz, H4a), 2.14 (1H, d, ***J*** = 12.6 Hz, H4b), 2.35 (1H, ddd, ***J*** = 14.3, 5.7, 2.4 Hz, H7b), 3.09 (1H, m, H8), 3.43 (1H, m, H3), 4.26 (1H, td, ***J*** = 5.7, 1.2 Hz, H6), 4.38 (1H, d, ***J*** = 5.7 Hz, H5), 4.60 (1H, t, ***J*** = 5.7 Hz, H1). **^{13}C NMR ($CDCl_3$)** 25.7 (C4), 28.4 (C7), 37.7 (C8), 50.1 (C3), 68.6 (C5), 83.4 (C6), 86.7 (C2), 88.6 (C1). **MS *m/z* (EI)** 111, 123, 129, 138, 155, 173, 179, 191, 206, 208 ($M^{+\bullet}$). **HRMS *m/z* (EI)**: 208.0059 ($M^{+\bullet}$ $C_8H_{10}{}^{35}Cl_2O_2{}^{+\bullet}$ requires 208.0058).

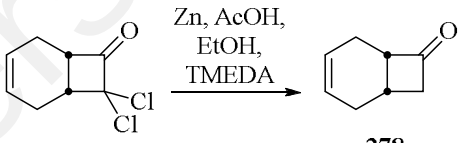

266 **278** 62% yield

Bicyclo[4.2.0]oct-3-en-8-one (278) (Mori et al., 1997; Horasan et al., 2011; Davis & Carpenter, 1996). To mixture of 3.2 g of Zn dust and 7.0 mL of TMEDA (46.6 mmol) in 10mL of absolute EtOH at 0°C was added 3.0 mL (52.3 mmol) of AcOH. The reaction mixture was maintained at 0°C while a solution of ketone **266** (1.62 g, 8.48 mmol) in 5 mL of EtOH was added over 10 min period. After an additional 15 min at 0°C the reaction mixture was allowed to warm to room temperature and stirred for 1 hr.

The resulting grey mixture was filtered, and the solid was washed with diethyl ether. The filtrate was extracted with ice cold 1 M HCl (5 mL), H_2O (5 mL), sat. $NaHCO_3$ (5 mL), sat NaCl (5 mL) and H_2O (10 mL). The resulting material was dried over $MgSO_4$ and concentrated under reduced pressure to afford 642 mg (62%) of desired ketone **278** which was of sufficient purity for subsequent transformation.

(1***R****,6***S****)-Bicyclo[4.2.0]oct-3-en-8-one	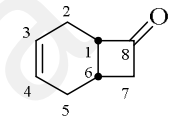

Yellowish oil. $R_f \approx 0.40$ [nonUV-active, EtOAc/Pet. ether 10%, anisaldehyde (brown spot)]**. IR (neat):** *v* 3038 (m), 2925 (m), 2890 (m), 2841 (m), 1781 (s, C=O), 1550 (m), 1436 (w), 1388 (w), 1371 (w), 1245 (m), 1140 (w), 1106 (m), 1086 (w), 1053 (w), 1008 (m), 981 (w) cm^{-1}. **^{1}H NMR ($CDCl_3$)** 2.08 – 2.24 (2H, m, H2a, H5a), 2.33 -2.45 (2H, m, H2b, H5b), 2.58 (1H, ddd, ***J*** = 17.2, 4.8, 2.6, H7a), 2.84 (1H, m, H6), 3.26 (1H, ddd, ***J*** = 17.2, 8.4, 3.2, H1), 3.49 (1H, m, H7b), 5.91 (2H, m, H3, H4). **^{13}C NMR ($CDCl_3$)** 21.8 (C6), 22.1 (C2), 26.5 (C5), 52.1 (C7), 56.6 (C1), 126.5 (C3), 127.5 (C4), 213.6 (C8). **MS *m/z* (positive CI, NH_3)** 121, 139, 140 ($MH^{+\cdot}..NH_3$), 141, 156, 181, 198, 199, 216. **MS *m/z* (EI)** 102, 103, 104, 105, 107, 109, 112, 114, 117, 118, 121, 122 ($M^{+\bullet}$). **HRMS *m/z* (EI)**: 122.0730 ($M^{+\bullet}$ $C_8H_{10}O^{+\bullet}$ requires 122.0732)**.**

All spectral characteristics are identical to those previously reported (Mori et al., 1997; Horasan et al., 2011; Davis & Carpenter, 1996).

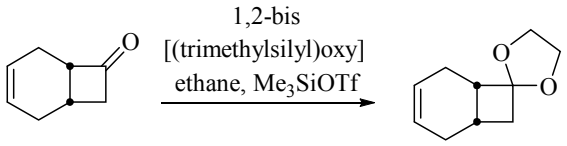

278 **279**
60% yield

Spiro[bicyclo[4.2.0]oct-3-ene-6,2'-(1',3'-dioxolane)] (279). A mixture of bicycloketone **278** (530 mg, 4.34 mmol) and 1,2-bis[(trimethylsilyl)oxy]ethane (2.46 mg, 9.11 mmol) was cooled to -78°C under N_2, and Me_3SiOTf (34.0 µL, 0.18 mmol) was added in portion (3 x 12.0 µL). The reaction mixture was stirred for a total 16 h at room temperature and the quenched by addition of excess pyridine (5.0 mL). The mixture was then poured into saturated $NaHCO_3$ (5 mL) and extracted with ether (2 x 10 mL). Evaporation of the solvent under reduced pressure and chromatography of the residue on silica gel, eluting with petroleum ether/ethyl acetate (9.5:5) to give bicyclo[4.2.0]oct-3-ene **279** (433 mg, 60%).

(1***R****,6***S****)-Spiro[bicyclo[4.2.0]oct-3-ene-6,2'-(1',3'-dioxolane)]	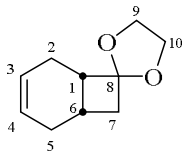

Yellowish oil. $R_f \approx 0.35$ [nonUV-active, EtOAc/Pet. ether 10%, anisaldehyde (brown spot)]**. ^{1}H NMR ($CDCl_3$)** 1.79 – 2.09 (5H, m, H2, H5, H6), 2.27 (2H, m, H7), 2.62 (1H, m, H1), 3.68 – 3.78 (4H, m, H8, H9), 5.71 (1H, m, H3), 5.80 (1H, m, H4). **^{13}C NMR ($CDCl_3$)** 20.7 (C2), 22.0 (C6), 26.2 (C5), 39.7 (C7), 43.3 (C1), 63.1 (C9), 64.3 (C10), 107.5 (C8), 125.6 (C3), 127.3 (C4). **MS *m/z* (positive CI, NH_3)** 87, 105, 123, 139, 156, 167 (MH^+ with ^{35}Cl), 169 (MH^+ with ^{37}Cl), 181, 191, 198. **MS *m/z* (EI)** 105, 112, 116, 121, 125, 133, 138, 147, 151, 155, 162, 166 ($M^{+\bullet}$ with ^{35}Cl). **HRMS *m/z* (EI)**: 166.1003 ($M^{+\bullet}$ $C_{10}H_{14}O_2^{+\bullet}$ requires 166.0994)**.**

279 **277** (65% yield)

4'-Oxaspiro[(1,3)dioxolane-2,8'-tricyclo[5.2.0.0^{3,5}]nonane] (277). ***m***-CPBA (621 mg, 2.52 mmol) was added to a solution of bicycloalkene **279** (419 mg, 2.52 mmol) in 4 mL CH_2Cl_2 at 0°C mixture was stirred for 2 h. The organic phase was extracted with dichloromethane (15 mL), washed with $NaHCO_3$ sat. (3 x 10 mL) and H_2O (10 mL) and then dried with $MgSO_4$. The organic layers were concentrated and give the epoxy-bicyclo product **277** (298 mg, 65%) as a yellowish oil.

(1'***S****,3'***R****,5'***S****,7'***S****)-4'-Oxaspiro[(1,3)dioxolane-2,8'-tricyclo[5.2.0.0^{3,5}]nonane]	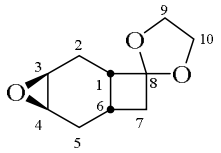

Yellowish oil. $\boldsymbol{R}_f \approx 0.30$ [nonUV-active, EtOAc/Pet. ether 30%, anisaldehyde (dark spot)]**. IR (neat):** *ν* 2984 (s), 2939 (s), 2884 (s), 1783 (w), 1725 (s), 1702 (s), 1474 (w), 1438 (m), 1332 (w), 1271 (s), 1254 (s), 1172 (m), 1141 (m), 1070 (s) cm^{-1}. **^{1}H NMR ($CDCl_3$)** 1.82 (1H, dd, ***J*** = 15.3, 9.0 Hz, H5a), 1.91 (1H, dd, ***J*** = 12.4, 4.0 Hz, H7a), 2.02 (2H, m, H2), 2.13 (1H, m, H7b), 2.29 (1H, m, H5b), 2.41 (1H, ddd, ***J*** = 12.4, 9.0, 1.6 Hz, H6), 2.67 (1H, q, ***J*** = 9.0 Hz, H1), 3.13 – 3.18 (2H, m, H3, H4), 3.79-3.88 (4H, m, H9, H10). **^{13}C NMR ($CDCl_3$)** 18.5 (C2, C5), 19.3 (C6), 26.1 (C5), 39.7 (C1), 41.0 (C7), 50.6 (C4), 51.2 (C3), 63.8 (C9), 64.6 (C10), 109.8 (C8). **MS *m/z* (positive CI, NH_3)** 88, 100, 125, 139, 155, 165, 183 (MH^+), 185, 200 ($MH^+...NH_3$), 207, 217. **MS *m/z* (EI)** 109, 112, 118, 129, 139, 141, 148, 156, 158, 160, 167, 177, 182 ($M^{+\bullet}$). **HRMS *m/z* (EI)**: 182.1016 ($M^{+\bullet}$ $C_{10}H_{14}O_3^{+\bullet}$ requires 182.0943)**.**

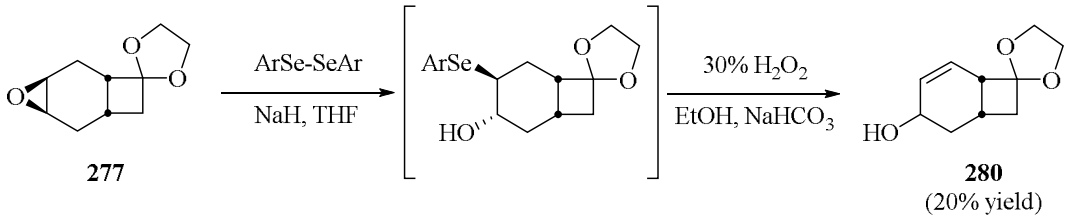

Spiro[bicyclo[4.2.0]octane-8,2'-[1,3]dioxolan]-2-en-4-ol (280). To a round-bottom flask containing THF (5 mL) were added diphenyl diselenide (202 mg, 0.648 mmol) and NaH (108 mg, 2.70 mmol). The reaction mixture was then heated at reflux (80°C) for 90 min during which time a white suspension was generated. Upon cooling to room temperature, epoxide **277** (197 mg, 1.08 mmol) in THF (2 mL) was added. The reaction was stirred at reflux at 80°C for 14 h. The reaction mixture was quenched carefully with saturated aqueous NH_4Cl (5 mL) and then diluted with H_2O (20 mL). The resulting mixture was extracted with diethyl ether (3 x 10 mL) and the combined organic layers were washed with brine (10 mL) and dried ($MgSO_4$). The residue obtained upon removal of the solvent by rotary evaporation was continued for next transformation.

To a solution of crude in ethanol (5 mL) was added dropwise 30% H_2O_2 (612 mg, 5.40 mmol). After stirring for 30 min at room temperature, the reaction mixture was diluted with a large amount of ethanol (50 mL), to which $NaHCO_3$ (594 mg, 10.8 mmol) was added. The resulting mixture was then heated at reflux for 12 h. The solid was removed by filtration and the ethanol solution was concentrated by rotary evaporation. The oily residue thus obtained was purified by column chromatography eluting with petroleum ether/ethyl acetate (7:3) to give allylic alcohol **280** as yellowish oil (40 mg, 20%).

(1***R****,6***S****)-Spiro[bicyclo[4.2.0]octane-8,2'-[1,3]dioxolan]-2-en-4-ol	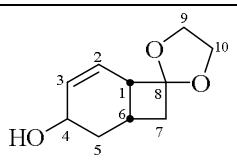

Yellowish oil. $R_f \approx 0.10$ [nonUV-active, EtOAc/Pet. ether 30%, anisaldehyde (green-blue spot)]**. IR (neat):** ν_{max} 3622 (m), 3504 (m, -OH) 3024 (m), 2984 (s), 2940 (s), 2886 (s), 1741 (S, C=O), 1474 (w), 1423 (w), 1397 (w), 1372 (w), 1287 (s), 1264 (m), 1240 (s), 1047 (s), 1020 (s) cm^{-1}. **^{1}H NMR ($CDCl_3$)** 1.53 (1H, dt, ***J*** = 13.8, 6.7 Hz, H5a), 2.01 (1H, m, H7a), 2.13 (1H, dt, ***J*** = 13.8, 5.2 Hz, H5b), 2.58 (1H, m, H1, H7b), 2.97 (1H, m, H6), 3.90 (4H, m, H9, H10), 4.53 (1H, t, ***J*** = 6.7 Hz, H4), 5.91 (2H, br s, H2, H3). **^{13}C NMR ($CDCl_3$)** 22.8 (C6), 29.7 (C5), 40.8 (C7), 41.8 (C1), 63.3 (C4), 63.6 (C9), 64.7 (C10), 108.4 (C8), 131.1 (C3), 131.2 (C2). **MS *m/z* (positive CI, NH_3)** 88, 104, 122, 165, 166, 183 (MH^+), 184, 199, 200 ($MH^+...NH_3$), 211, 216. **MS *m/z* (EI)** 112, 120, 122, 141, 150, 164, 182 ($M^{+\bullet}$). **HRMS *m/z* (EI)**: 182.0567 ($M^{+\bullet}$ $C_{10}H_{14}O_3^{+\bullet}$ requires 182.0943)

7.7.3 Approach B: [2+2] intramolecular ketene cycloaddition

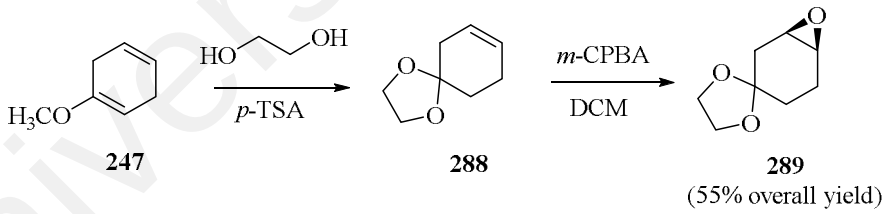

247 **288** **289** (55% overall yield)

7-Oxaspiro[bicyclo[4.1.0]heptane-3,2'-[1,3]dioxolane] (289) (Cheng et al., 1992). 4-Methoxy-1,4-cyclohexadiene (**247**) (3.00 g, 27.2 mmol) was dissolved in 50 mL of anhydrous toluene and placed in a 100 mL round-bottomed flask fitted with a Dean-Stark trap. Ethylene glycol (1.68 g, 27.2 mmol) was then added along with ***p***-toluenesulfonic acid (62.1 mg, 0.325 mmol). The solution was heated to 110°C, and H_2O was taken off via the trap for 2 h. The organic solution was washed with saturated

$NaHCO_3$ (2 x 20 mL), H_2O (20 mL), dried ($MgSO_4$) and concentrated to give the ketal **288** as a colourless liquid. This material was subsequently used in the following step.

To a stirred solution of ketal **288** in CH_2Cl_2 (30 mL) at 0°C was added ***m***-chloroperbenzoic acid (7.04 g, 40.8 mmol). The mixture was stirred for overnight and washed with saturated $NaHCO_3$ (20 mL) and H_2O (20 mL). After drying ($MgSO_4$), the organic layer was concentrated to give the epoxy ketal **289** as colourless oil (4.24 g, 55%) which was sufficient purity for subsequent transformation.

(1***S****,6***R****)-7-Oxaspiro[bicyclo[4.1.0]heptane-3,2'-[1,3]dioxolane]	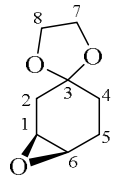

Light yellow oil. $R_f \approx 0.15$ [nonUV-active, EtOAc/Pet. ether 20%, anisaldehyde (red-violet spot)]**. IR (neat):** $_{max}$ 2986 (m), 2947 (m), 2927 (m), 2881 (m), 1702 (w), 1430 (w), 1417 (w), 1372 (m), 1356 (m), 1260 (m), 1163 (m), 1149 (m), 1110 (s), 1054 (m), 1024 (m), 996 (m), 945 (m), 931 (m) cm^{-1}. **^{1}H NMR ($CDCl_3$)** 1.45 – 2.25 (6H, m, H2, H4, H5), 3.17 (2H, m, H1, H6), 3.85 – 3.96 (4H, m, H7, H8). **^{13}C NMR ($CDCl_3$)** 22.6 (C5), 27.3 (C4), 34.7 (C2), 51.4 (C1), 52.1 (C6), 64.1 (C7), 64.5 (C8). **MS *m/z* (positive CI, NH_3)** 100, 102, 113, 114, 127, 139, 157 (MH^+), 158, 174 (MH^+...NH_3).

All spectral characteristics are identical to those previously reported **(**Cheng et al., 1992).

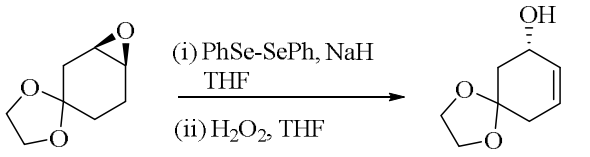

289 **286** (30% yield)

1,4-Dioxaspiro[4.5]dec-8-en-7-ol (286) (Zhang & Koreeda, 2002). To a round-bottom flask containing THF (6 mL) were added diphenyl diselenide (468 mg, 1.5 mmol) and NaH (263 mg, 6.2 mmol). The reaction mixture was then heated at reflux (80°C) for 90 min during which time a white suspension was generated. Upon cooling to room temperature, epoxide **289** (393 mg, 2.5 mmol) in THF (2 mL) was added. After stirring at room temperature for 5 h, the reaction mixture was quenched carefully with saturated aqueous NH_4Cl (10 mL) and then diluted with H_2O (10 mL). The resulting mixture was extracted with diethyl ether (3 x 10 mL) and the combined organic layers were washed with brine (10 mL) and dried ($MgSO_4$). The residue obtained upon removal of the solvent by rotary evaporation was gave desired product as yellowish oil, which was sufficient purity for subsequent transformation.

To a solution of alcohol in ethanol (5 mL) was added dropwise 30% H_2O_2 (765 µL, 7.5 mmol). After stirring for 30 min at room temperature, the reaction mixture was diluted with a large amount of ethanol (50 mL), to which $NaHCO_3$ (869 mg, 15.8 mmol) was added. The resulting mixture was then heated at reflux for 12 h. The solid was removed by filtration and the ethanol solution was concentrated by rotary evaporation. The oily residue thus obtained was purified by column chromatography eluting with petroleum ether/ethyl acetate (75:25) to give allylic alcohol as light orange oil **286** (71 mg, 30%)

1,4-Dioxaspiro[4.5]dec-8-en-7-ol	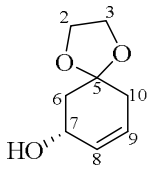

Light orange oil. $R_f \approx 0.20$ [nonUV-active, EtOAc/Pet. ether 30%, anisaldehyde (violet spot)]**. IR (neat):** ν_{max} 3036 (w), 2960 (m), 2932 (m), 2885 (m), 1437 (w), 1407 (m), 1363 (m), 1339 (w), 1140 (s), 1051 (s), 1022 (s), 947 (w) cm^{-1}. **^{1}H NMR ($CDCl_3$)** 1.86 – 2.02 (2H, m, H6), 2.23 (2H, br s, H10), 3.10 (-OH, br s), 3.93 (4H, m, H2, H3), 4.27 (1H, br s, H7), 5.68 (1H, dt, ***J*** = 9.9, 3.6 Hz, H9), 5.80 (1H, dt, ***J*** = 9.9, 1.7 Hz, H8). **^{13}C NMR ($CDCl_3$)** 35.3 (C10), 39.3 (C6), 64.1 (C2, C3), 66.5 (C7), 108.3 (C5), 126.0 (C9), 129.5 (C8). **MS *m/z* (positive CI, NH_3)** 87, 100, 114, 126, 140, 157 (MH^+), 158, 175, 204. **HRMS *m/z* (EI)**: 156.0786 ($M^{+\bullet}$ $C_8H_{12}O_3^{+\bullet}$ requires 156.0786)**.**

All spectral spectral characteristics are identical to those previously reported (Zhang & Koreeda, 2002).

7.7.4 Approach C: synthesis of bicyclo[4.2.0]octane containing methylenedioxyphenyl moiety at C-7

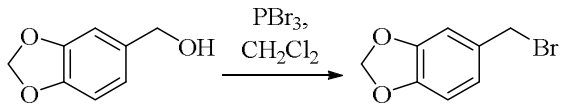

296 **295**
95% yield

Piperonyl bromide (295). To a solution of piperonyl alcohol **296** (1.61 g, 10.6 mmol) in CH_2Cl_2 (100 mL) was added PBr_3 (13.5 g, 50.0 mmol) slowly at 0°C. The reaction mixture was stirred for 3 h at room temperature and then poured into ice water. The aqueous layer was extracted with CH_2Cl_2 (2 x 25 mL) and the combined organic layers

were washed with a saturated $NaHCO_3$ solution (20 mL), dried ($MgSO_4$) and concentrated to afford a desired product **295** (2.57 g, 95%).

Piperonyl bromide	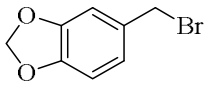

Yellowish oil. $R_f \approx 0.30$ [UV-active, EtOAc/Pet. ether 5%, anisaldehyde (dark blue spot)]**. IR (neat)**: $_{max}$ 3013 (w) 2971 (w), 2887 (m, C-H aromatic), 2776 (w), 1504 (s), 1448 (s), 1446 (s), 1361 (m), 1276 (s), 1252 (s), 1213 (m), 1192 (m), 1096 (m), 1043 (s, O-CH_2-O) cm^{-1}. **^{1}H NMR ($CDCl_3$)** 4.46 (2H, s, H1), 5.97 (2H, s, H8), 6.75 (1H, d, ***J*** = 7.8 Hz, H7), 6.86 (1H, d, ***J*** = 7.8 Hz, H6), 6.88 (1H, br s, H3). **^{13}C NMR ($CDCl_3$)** 34.2 (C1), 101.3 (C8), 108.2 (C6), 109.4 (C3), 122.7 (C7), 131.4 (C2), 147.7 (C4), 147.8 (C5). **MS *m/z* (EI)** 105, 119, 135, 137, 146, 156, 158, 165, 192, 207, 213 ($M^{+\bullet}$), 215, 222. **HRMS *m/z* (EI)**: 213.9628 ($M^{+\bullet}$ $C_8H_7{}^{79}BrO_2{}^{+\bullet}$ requires 213.9629)**.**

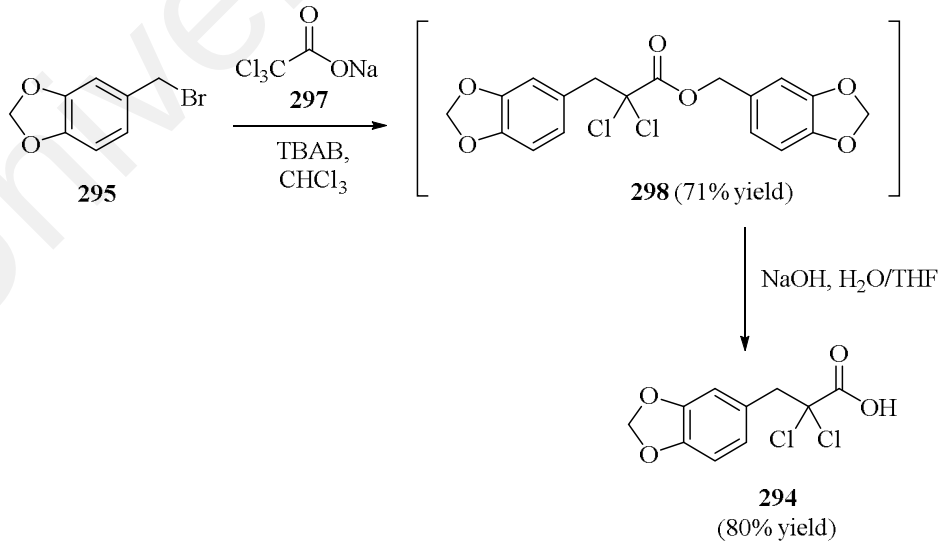

2,2-Dichloro-3-(3,4-methylenedioxyphenyl)propanoic acid (294) (Qin et al., 2011; Hu et al., 2013). To a solution of piperonyl bromide **295** (9.24 g, 43.0 mmol) in $CHCl_3$

(9 mL) was added trichloroacetic acid, sodium salt **297** (11.9 g, 64.5 mmol) and tetrabutyl ammonium bromide (1.39 g, 4.3 mmol). The resultant reaction mixture was stirred at 80°C for 40 h. The reaction mixture was poured in to H_2O and extracted with ether. The combined organic layers were washed with brine, dried ($MgSO_4$) and concentrated at reduced pressure to give brown oil, which was of sufficient purity for subsequent transformation.

The crude was dissolved in THF/H_2O (3/1, 60 mL); NaOH was added (4.08 g, 98.6 mmol) and the mixture was stirred for 3 h. The solvent was removed under reduced pressure, and the residue was taken up with CH_2Cl_2 (20 mL) and H_2O (50 mL). The aqueous phase was washed with CH_2Cl_2 (10 mL) and the aqueous phase was acidified with 150 mL HCl solution (1 M) and extracted with ether (3 x 30 mL). The combine organic layers were washed with brine (20 mL), dried ($MgSO_4$) and concentrated at reduced pressure to give a desired product **294** (9.05 g, 80%).

3,4-Methylenedioxyphenyl-[2,2-dichloro-2-(3,4-methylenedioxyphenyl)]propanoate	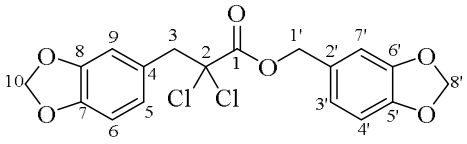

Brown oil. **IR (neat)**: $_{max}$ 3013 (w) 2963 (w), 2887 (m, C-H aromatic), 2776 (w), 1763 (m), 1744 (m, C=O), 1505 (s), 1490 (s), 1446 (s), 1364 (w), 1250 (s), 1200 (m), 1225 (w), 1101 (w), 1044 (s, O-CH_2-O) cm^{-1}. **^{1}H NMR ($CDCl_3$)** 3.88 (2H, s, H3), 4.58 (2H, s, H1'), 6.02 (2H, s, H10), 6.04 (2H, s, H8'), 6.81 – 6.94 (6H, m, H6, H7, H9, H3', H4', H7'). **^{13}C NMR ($CDCl_3$)** 46.7 (C3), 59.2 (C1'), 84.2 (C2), 101.3 (C10), 101.4 (C8'),

108.1 (C6), 108.3 (C4'), 109.2 (C9), 111.8 (C7'), 122.4 (C3'), 125.5 (C5), 126.9 (C2'), 131.3 (C4), 147.4 (C7), 147.8 (C8), 147.9 (C5'), 148.0 (C6'), 165.5 (C1).

All spectral spectral characteristics are identical to those previously reported ((Qin et al., 2011; Hu et al., 2013).

2,2-Dichloro-3-(3,4-methylenedioxyphenyl)propanoic acid	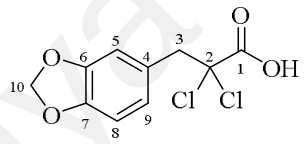

Brown oil. $R_f \approx 0.30$ [UV-active, EtOAc/Pet. ether 5%, anisaldehyde (white spot)]**.** **^{1}H NMR ($CDCl_3$)** 3.65 (2H, s, H3), 5.96 (2H, s, H10), 6.75 – 6.88 (3H, m, H5, H8, H9). **^{13}C NMR ($CDCl_3$)** 49.9 (C3), 83.8 (C2), 101.2 (C10), 108.1 (C8), 111.5 (C5), 124.9 (C9), 126.6 (C4), 147.5 (C6, C7), 169.7 (C1). **MS *m/z* (EI)** 105, 122, 135, 137, 147, 152, 182, 217, 226, 262 ($M^{+\bullet}$), 264, 266. **HRMS *m/z* (EI)**: 261.9803 ($M^{+\bullet}$ $C_{10}H_8{}^{35}Cl_2O_4{}^{+\bullet}$ requires 261.9800)**.**

All spectral spectral characteristics are identical to those previously reported (Qin et al., 2011; Hu et al., 2013).

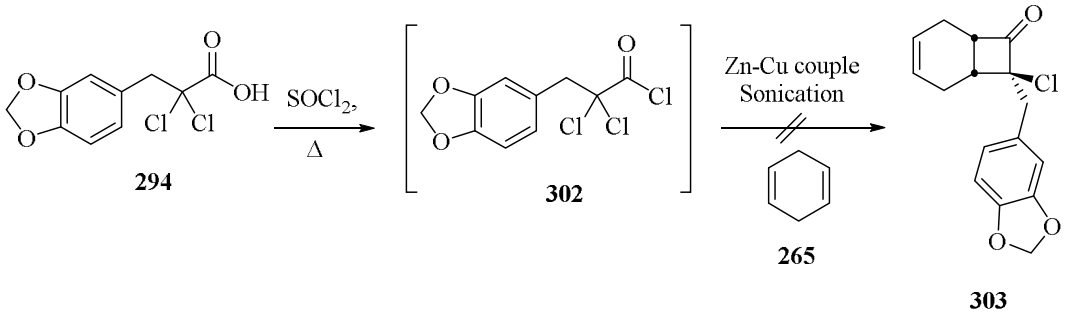

294 **302** **265** **303**

2,2-Dichloro-3-(3,4-methylenedioxyphenyl)propanoyl chloride (302). The 2,2-dichlorocarboxylic acid **294** (1.23 g, 4.68 mmol) was dissolved in thionyl chloride (1.67 g, 14.0 mmol). The mixture was stirred at 80°C. After 3 h, excess thionyl chloride was removed under reduced pressure to give brown oil **302** (1.29 g, 98.0%), which was of sufficient purity for subsequent transformation.

2,2-Dichloro-3-(3,4-methylenedioxyphenyl)propanoyl chloride	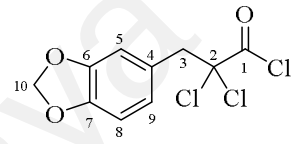

Brown oil. **^{1}H NMR ($CDCl_3$)** 3.68 (2H, s, H3), 5.98 (2H, H10), 6.76 – 6.88 (3H, H5, H8, H9). **^{13}C NMR ($CDCl_3$)** 49.6, (C3), 89.2 (C2), 101.3 (C10), 108.2 (C8), 111.5 (C5), 125.0 (C9), 125.5 (C4), 147.6 (C6), 147.8 (C7), 168.2 (C1).

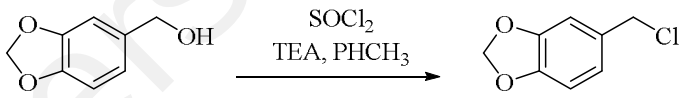

308 **306** (98% yield)

Piperonyl chloride (306). Piperonyl alcohol (**308**) (10.0 g, 65.7 mmol) was dissolved in dry toluene (100 mL). Triethylamine (7.98 g, 78.9 mmol) and thionyl chloride (15.6 g, 131.4 mmol) were added dropwise thereto and was stirred for 24 h at 0°C. The reaction mixture was extracted with saturated $NaHCO_3$ (2 x 100 mL) and ethyl acetate. The organic layer was separated, and dried ($MgSO_4$) and concentrated under vacuum to give the desired product as a brown oil **306** (10.9 g, 98%) which was of sufficient purity for subsequent transformation.

Piperonyl chloride	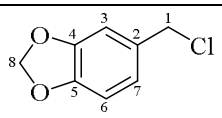

Pale yellow oil**.** R_f ≈ 0.30 [UV-active, EtOAc/Pet. ether 5%, anisaldehyde (dark blue spot)]**. IR (neat)**: $_{max}$ 2962 (w), 2886 (m, C-H aromatic), 2777 (w), 1504 (s), 1491 (s), 1447 (s), 1363 (s), 1251 (s), 1194 (m), 1100 (m), 1043 (s, O-CH_2-O), 947 (m), 932 (s, O-CH_2-O) cm^{-1}. **^{1}H NMR ($CDCl_3$)** 4.41 (2H, s, H1), 5.84 (2H, s, H8), 6.64-6.77 (3H, m, H3, H6, H7). **^{13}C NMR ($CDCl_3$)** 46.5 (C1), 101.2 (C8), 108.1 (C6), 109.0 (C3), 122.2 (C7), 131.2 (C2), 147.7 (C4), 147.8 (C5). **MS *m/z* (positive CI, NH_3)** 118, 136, 148, 152, 161, 171 (MH^+), 172, 180, 208, 225. **MS *m/z* (EI)** 105, 117, 121, 135, 136, 170 ($M^{+\bullet}$ with ^{35}Cl), 171, 172. **HRMS *m/z* (EI)**: 170.0137 ($M^{+\bullet}$ $C_8H_7{}^{35}ClO_2{}^{+\bullet}$ requires 170.0135).

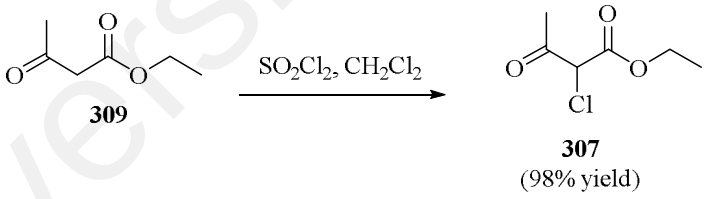

Ethyl-2-chloro-3-oxobutanoate (307). Sulfuryl chloride (11.4 g, 84.5 mmol) was added dropwise by dropping funnel to ethyl acetoacetate **309** (10.0 g, 76.8 mmol) maintained at 0°C. The mixture was stirred overnight at room temperature. The mixture was washed with H_2O (2 x 100 mL), dried ($MgSO_4$) and evaporate under vacuum to give the desired product as a yellowish oil **307** (12.3 g, 98%) which was of sufficient purity for subsequent transformation.

Ethyl-2-chloro-3-oxobutanoate	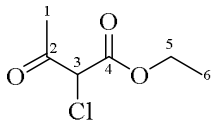

Pale yellow oil. **IR (neat):** $_{max}$ 2985 (m), 2941 (w), 1735 (s, C=O), 1645 (w), 1616 (w), 1445 (w), 1369 (m), 1255 (s), 1163 (s), 1096 (w), 1070 (w), 1034 (m) cm^{-1}. **^{1}H NMR ($CDCl_3$)** 1.23-1.31 (3H, m, H6), 2.32 (3H, s, H1), 4.20-4.34 (2H, m, H5), 4.71 (1H, s, H3). **^{13}C NMR ($CDCl_3$)** 13.5 (C6), 25.9 (C1), 61.0 (C3), 62.7 (C5), 164.6 (C4), 196.1 (C2). **MS *m/z* (positive CI, NH_3)** 103, 135, 137, 148, 152, 162, 165 (MH^+), 170, 182, 184. **MS *m/z* (EI)** 118, 120, 121, 122, 124, 136, 164 ($M^{+\bullet}$ with ^{35}Cl), 166. **HRMS *m/z* (EI)**: 164.0245 ($M^{+\bullet}$ $C_6H_9{}^{35}ClO_3{}^{+\bullet}$ requires 164.0240).

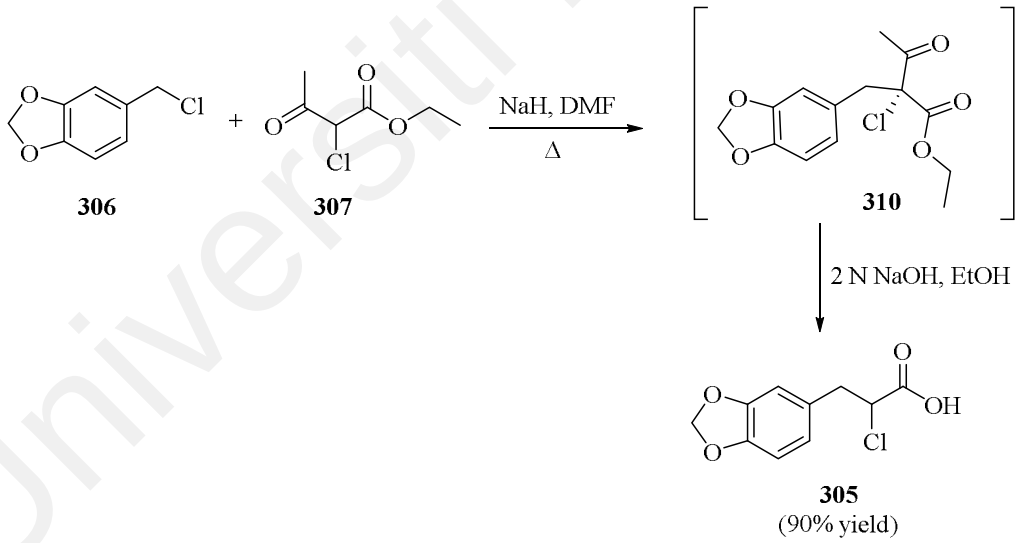

306 **307** **310**

305
(90% yield)

2-Chloro-3-(3,4-methylenedioxyphenyl)propanoic acid (305) (Sohda et al., 1983). A solution of ethyl 2-chloroacetoacetate (**307**) (2.47 g, 15.0 mmol) in DMF (25 mL) was treated with 60% NaH in oil (600 mg) at room temperature for 20 min. A solution of 3,4-methylenedioxybenzyl chloride (**306**) (2.56 g, 15.0 mmol) in DMF (5 mL) was added thereto, and the mixture was stirred at 80°C for 2 h, poured into ice-H_2O and

extracted with EtOAc (100 mL). The extract was washed with H_2O (2 x 50 mL), dried ($MgSO_4$) and evaporate under vacuum to give the desired product as a brown oil **310**, which was of sufficient purity for subsequent transformation.

A stirred solution of crude **310** in EtOH (50 mL) was treated with 2 N NaOH (20 mL) at room temperature for 1 h. The solvent was removed at reduced pressure, and the residue was taken up with EtOAc (25 mL) and H_2O (50 mL). The aqueous phase was acidified with 5 mL conc. HCl and extracted with EtOAc (3 x 50 mL). The combine organic layers were dried ($MgSO_4$) and concentrated at reduced pressure to give solids **305** (3.08 g, 90%).

Ethyl 2-acetyl-2-chloro-3-(3,4-methylenedioxyphenyl) propionate	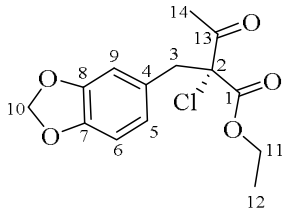

Brown liquid. **^{1}H NMR ($CDCl_3$)** 1.20 (3H, t, J = 7.0 Hz, H12), 2.22 (3H, s, H14), 3.33 (2H, an AB system, δ_A 3.38, δ_B 3.26, $\boldsymbol{J}_{AB}$ = 16.1 Hz, H3), 4.17 (2H, q, J = 7.0 Hz, H11), 5.89 (2H, s, H10), 6.57 – 6.66 (3H, m, H5, H6, H9). **^{13}C NMR ($CDCl_3$)** 13.8 (C12), 26.3 (C14), 41.8 (C3), 63.0 (C11), 75.4 (C2), 101.0 (C10), 107.9 (C6), 110.1 (C9), 123.8 (C5), 127.4 (C4), 147.0 (C7), 147.4 (C8), 166.8 (C1), 198.4 (C13).

All spectral spectral characteristics are identical to those previously reported (Sohda et al., 1983).

2-chloro-3-(3,4-methylenedioxyphenyl)propanoic acid	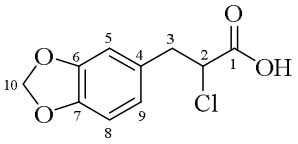

Amorphous white solid. $R_f \approx 0.15$ [non UV-active, EtOAc/Pet. ether 50%, anisaldehyde (red-violet spot)]**. IR (neat):** $_{max}$ 3155 (w), 2895 (w), 2902 (w), 2253 (s, C=O), 1795 (w), 1728 (w), 1490 (w), 1469 (m), 1447 (w), 1384 (m), 1166 (w), 1097 (m), 1044 (w, O-CH_2-O) cm^{-1}. **^{1}H NMR ($CDCl_3$)** 3.21 (2H, AB part of an ABX system, δ_A 3.31, δ_B 3.12, J_{AB} = 14.1, J_{AX} = 7.7, J_{BX} = 7.7 Hz, H3), 4.44 (1H, t, J = 7.5 Hz, H2), 5.95 (2H, s, H10), 6.70 (1H, dd, J = 7.3, 1.6 Hz, H9), 6.73 (1H. d, J = 1.6 Hz, H-5), 6.76 (1H, d, J = 7.3 Hz, H-8). **^{13}C NMR ($CDCl_3$)** 40.6 (C3), 57.2 (C2), 101.1 (C10), 108.5 (C8), 109.7 (C5), 122.7 (C9), 129.1 (C4), 147.0 (C7), 147.9 (C6), 173.3 (C1). **MS *m/z* (positive CI, NH_3)** 135, 137, 152, 175, 192, 195, 210, 229 ($MH^{+\bullet}$), 230, 246, 248. **MS *m/z* (EI)** 117, 120, 122, 135, 136, 152, 170, 175, 192, 220, 118, 228 ($M^{+\bullet}$ with ^{35}Cl), 230. **HRMS *m/z* (EI)**: 228.0186 ($M^{+\bullet}$ $C_{10}H_9{}^{35}ClO_4{}^{+\bullet}$ requires 228.0189).

All spectral spectral characteristics are identical to those previously reported (Sohda et al., 1983).

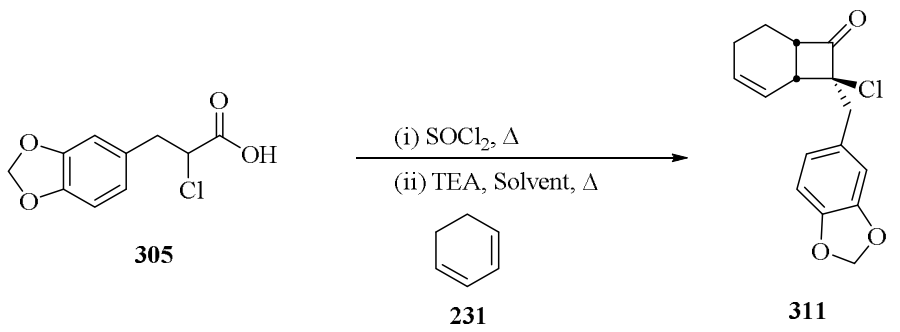

305 **231** **311**

7-Chloro-7-(3,4-methylenedioxyphenyl)bicyclo[4.2.0]oct-4-en-8-one (311). The 2-chlorocarboxylic acid **305** (456 mg, 2.00 mmol) was added to 2 mL of $SOCl_2$, and the reaction solution was heated at 90°C for 3 h. The reaction solution was cooled, and the solvent was removed in vacuo. Then, the residue was dissolve in 5 mL of cyclohexane.

The residue and cyclohexadiene **231** (504 mg, 6.30 mmol) was dissolve in cyclohexane (5 mL) and the mixture was treated with triethylamine (436 mg, 4.31 mmol) within 10 min under nitrogen. The reaction mixture was reflux for 3 h and then filtered and the solid was washed with cyclohexane (5 mL). The filtrate was washed with 1 M HCl (10 mL) and 1 M $NaHCO_3$ (10 mL). The organic layer was washed further with brine (20 mL). After drying ($MgSO_4$), the organic layer was concentrated and the crude product was purified using column chromatography on silica gel, eluting with petroleum ether/ethyl acetate (95:5) gave **311** (145 mg, 25%).

(1***R****,6***S****,7***S****)-7-Chloro-7-(3,4-methylenedioxyphenyl)bicyclo [4.2.0]oct-4-en-8-one	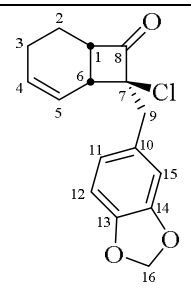

Yellowish oil. $\boldsymbol{R}_f \approx 0.40$ [UV-active, EtOAc/Pet. ether 15%, anisaldehyde (violet spot)]**.** **IR (neat):** ν_{max} 3031 (w), 2931 (m), 2775 (w), 1788 (s, C=O), 1746 (m), 1687 (w), 1542 (m), 1505 (s), 1490 (s), 1481 (s), 1445 (s), 1365 (w), 1293 (w), 1250 (s), 1191 (w), 1121 (w), 1043 (s) cm^{-1}. **^{1}H NMR ($CDCl_3$)** 1.47 (1H, m, H2a), 1.91–2.01 (3H, m, H2b, H3), 2.96 (2H, q, ***J*** = 15.7, H9), 3.11 (1H, m, H6), 4.01 (1H, m, H1), 5.81 (2H, s, H16), 5.84 (1H, m, H5), 5.96 (1H, m, H4), 6.64 (2H, d, ***J*** = 0.9, H11, H12), 6.74 (1H, s, H15). **^{13}C NMR ($CDCl_3$)** 18.5 (C2), 21.1(C3), 37.0 (C9), 40.6 (C6), 54.4 (C1), 80.2 (C7),

100.7 (C16), 107.7 (C12), 110.4 (C15), 123.1 (C5), 124.1 (C4), 128.7 (C10), 132.1 (C11), 146.2 (C13), 147.2 (C14), 204.6 (C8). **MS *m/z* (positive CI, NH_3)** 108, 136, 170, 255, 274, 291 (MH^+ with ^{35}Cl), 293 (MH^+ with ^{37}Cl), 308 ($MH^+..NH_3$ with ^{35}Cl), 310 ($MH^+..NH_3$ with ^{37}Cl), 342. **MS *m/z* (EI)** 105, 135, 136, 149, 170, 179, 210, 235, 255. 267, 290 ($M^{+\bullet}$ with ^{35}Cl). **HRMS *m/z* (EI)**: 290.0696 ($M^{+\bullet}$ $C_{16}H_{15}{}^{35}ClO_3{}^{+\bullet}$ requires 290.0710).

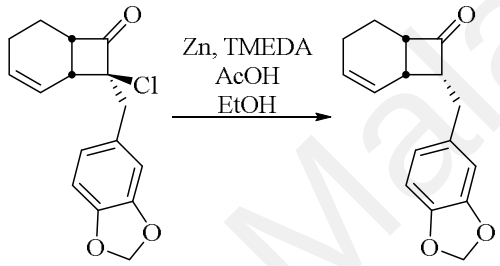

311 **312**
88% yield

7-(3,4-Methylenedioxyphenyl)bicyclo[4.2.0]oct-4-en-8-one (312). To a mixture of 1.30 g of Zn dust and 3 mL of TMEDA (20.1 mmol) in 7 mL of absolute EtOH at 0°C was added 1.5 mL (30.9 mmol) of AcOH. The reaction mixture was maintained at 0°C while a solution of cyclobutanone **311** (1.00 mg, 3.45 mmol) in 3 mL of EtOH was added over 10 min period. After an additional 15 min at 0°C the reaction mixture was allowed to warm to room temperature and stirred for 2 h. The resulting grey mixture was filtered, and the solid was washed with diethyl ether. The filtrated was extracted with 1 M HCl (10 mL), H_2O (10 mL), sat. $NaHCO_3$ (10 mL) and sat NaCl (10 mL). The resulting material was dried over $MgSO_4$ and concentrated under reduced pressure to afford 778 mg (88%) of desired cyclobutanone **312** which was of sufficient purity for subsequent transformation.

(1***R****,6***S****,7***S****)-7-(3,4-Methylenedioxyphenyl)bicyclo[4.2.0]oct-4-en-8-one	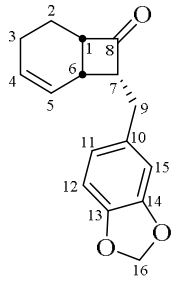

Yellowish oil. $\boldsymbol{R}_f \approx 0.35$ [UV-active, EtOAc/Pet. ether 15%, anisaldehyde (violet spot)]**. IR (neat):** ν_{max} 3025 (m), 2931 (s), 2653 (m), 2774 (m), 1773 (s, C=O), 1645 (w), 1610 (w), 1505 (s), 1489 (s), 1445 (s), 1413 (w), 1366 (w), 1293 (w), 1247 (s), 1189 (m), 1099 (m), 1043 (s), 942 (m) cm^{-1}. **^{1}H NMR ($CDCl_3$)** 1.43 (1H, m, H2a), 1.87-2.02 (3H, m, H2b, H3), 2.60 (2H, AB part of an ABX system, δ_A 2.73, δ_B 2.49, $\boldsymbol{J}_{AB}$ = 15.0, $\boldsymbol{J}_{AX}$ = 5.7, $\boldsymbol{J}_{BX}$ = 9.7 Hz, H9), 3.00 (1H, m, H6), 3.50-3.55 (2H, m, H1, H7), 5.70 (1H, m, H5), 5.84 (2H, s, H16), 5.91 (1H, m, H4), 6.55-6.66 (3H, m, H11, H12, H15). **^{13}C NMR ($CDCl_3$)** 18.5 (C2), 21.3 (C3), 27.7 (C6), 30.3 (C9), 55.0 (C7), 61.9 (C1), 100.8 (C16), 108.1 (C12), 108.7 (C15), 121.0 (C11), 125.8 (C4), 130.4 (C5), 133.5 (C10), 145.7 (C13), 147.5 (C14), 212.3 (C8). **MS *m/z* (positive CI, NH_3)** 136, 149, 157, 177, 183, 202, 211, 228, 240, 257 (MH^+), 274 ($MH^+..NH_3$), 275. **MS *m/z* (EI)** 105, 122, 135, 148, 175, 176, 186, 210, 220, 236, 256 ($M^{+\bullet}$), 258. **HRMS *m/z* (EI)**: **256.1097** ($M^{+\bullet}$ $C_{16}H_{16}O_3^{+\bullet}$ requires 256.1099)**.**

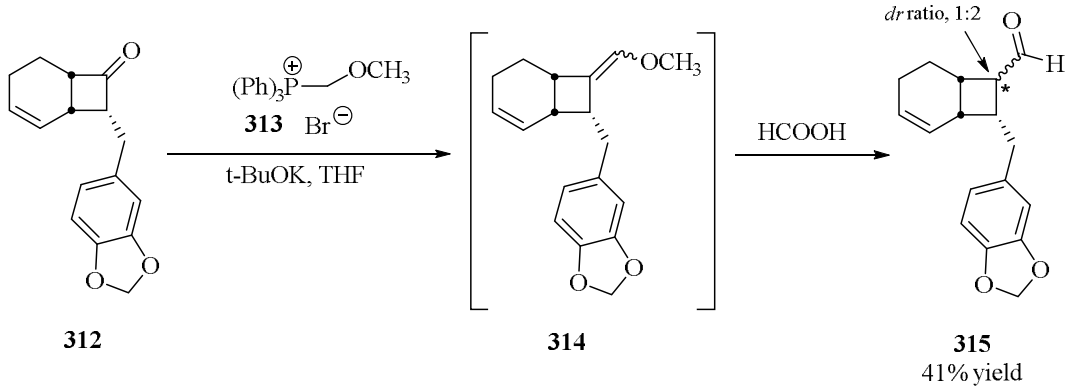

7-(3,4-Methylenedioxyphenyl)bicyclo[4.2.0]oct-4-ene-8-carbaldehyde (315). To a stirred slurry of (methoxymethyl)-triphenylphosphonium chloride (**313**) (583 mg, 1.70 mmol) in dry THF (7 mL) under nitrogen at -75°C was added potassium ***tert***-butoxide (143 mg, 1.27 mmol). After 15 min at -75°C, a solution of bicyclo[4.2.0] oct-4-en-8-one **312** (217 mg, 0.850 mmol) in 3 mL of dry THF was added to the mixture and stirred at -75°C for 10 min. The mixture was stirred at room temperature overnight. The mixture was diluted with water (20 mL) and extracted with ether (30 mL). The organic extracts were washed with brine (2 x 20 mL), dried ($MgSO_4$) and evaporated under reduced pressure to give a yellowish oil **314,** which was used for the next transformation.

The mixture of bicyclo[4.2.0]oct-4-ene **314** was stirred with 90% formic acid (10 mL) at room temperature for 1 h. The mixture was poured into a saturated aqueous sodium bicarbonate solution and extracted with ethyl acetate (3 x 10 mL), dried (Na_2SO_4), and filtered. Evaporation of the filtrate gave a yellowish oil which was purified by column chromatography on silica gel, eluting with petroleum ether/ethyl acetate (95:5) to give the desired product **315** as a yellowish oil (94.1 mg, 41%, ***dr*** ratio; 1:2).

(1***R****,6***S****,7***S****)-8-(Methoxymethylene)-7-(3,4-methylenedioxy phenyl)bicyclo[4.2.0]oct-4-ene	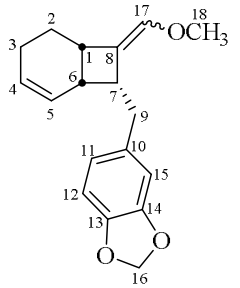

Yellowish oil. $R_f \approx 0.50$ [UV-active, EtOAc/Pet. ether 10%, anisaldehyde (violet spot)]**.** **^{1}H NMR ($CDCl_3$)** 1.90 – 1.45 (3H, m, H2, H3), 2.39 – 2.78 (3H, m, H6, H9), 3.32 – 3.60 (2H, m, H1, H7), 4.07 (3H, s, H18), 5.10 (1H, s, H17), 5.52 – 5.85 (4H, m, H4, H5, H16), 6.49 – 6.68 (3H, m, H11, H12, H15). **^{13}C NMR ($CDCl_3$)** 20.7 (C3), 21.9 (C2), 34.2 (C6), 35.2 (C9), 37.4 (C7), 44.8 (C1), 59.7 (C18), 100.6 (C16), 108.0 (C12), 108.9 (C15), 121.2 (C11), 126.8 (C4), 128.8 (C8), 131.4 (C5), 133.7 (C10), 139.6 (C17), 145.4 (C13), 147.6 (C14). **MS *m/z* (EI)** 108, 121, 135, 149, 170, 183, 201, 216, 252, 262, 277, 284 ($M^{+\bullet}$). **HRMS *m/z* (EI)**: 284.1412 ($M^{+\bullet}$ $C_{18}H_{20}O_3^{+\bullet}$ requires 284.1412)**.**

(1***R****,6***S****,7***S****)-7-(3,4-Methylenedioxyphenyl)bicyclo[4.2.0]oct-4-ene-8-carbaldehyde	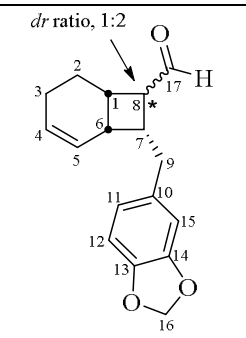

Yellowish oil. **IR (neat):** ν_{max} 2928 (m), 1717 (s, C=O), 1504 (m), 1484 (s), 1444 (w), 1372 (w), 1226 (m), 1179 (m), 1039 (m, O-CH_2-O), 1096 (w), 939 (m, m, O-CH_2-O), 8669 (w) cm^{-1}. **^{1}H$_{Exo}$ NMR ($CDCl_3$)** 0.75 – 2.45* (10H, m, H1, H2, H3, H6, H7, H8, H9), 5.68* (1H, m, H5), 5.82 (2H, s, H16), 5.95* (1H, m, H5), 6.47 – 6.74* (3H, m, H11, H12, H15), 9.33 (1H, s, H17) (*obscured by other resonances). **^{13}C$_{Exo}$ NMR**

($CDCl_3$) 21.2 (C3), 29.8 (C2), 31.2 (C9), 34.4 (C6), 36.7 (C1), 41.1 (C7), 51.8 (C8), 100.7 (C16), 108.3 (C12), 109.7 (C15), 121.2 (C11), 126.4 (C5), 129.5 (C4), 130.6 (C10), 145.8 (C13), 146.7 (C14), 202.6 (C17). **$^1H_{Endo}$ NMR ($CDCl_3$)** 0.75 – 2.45* (10H, m, H1, H2, H3, H6, H7, H8, H9), 5.68* (1H, m, H5), 5.85 (2H, s, H16), 5.95* (1H, m, H5), 6.47 – 6.74* (3H, m, H11, H12, H15), 9.94 (1H, s, H17) (*obscured by other resonances). **$^{13}C_{Endo}$ NMR ($CDCl_3$)** 21.5 (C3), 31.0 (C2), 33.1 (C9), 34.7 (C6), 38.7 (C1), 42.6 (C7), 52.0 (C8), 101.6 (C16), 108.9 (C12), 110.0 (C15), 121.2 (C11), 126.6 (C5), 129.7 (C4), 130.8 (C10), 145.8 (C13), 146.7 (C14), 205.6 (C17). **MS *m/z* (EI)** 115, 135, 173, 190, 224, 252, 270 ($M^{+\bullet}$), 298, 304. **HRMS *m/z* (EI)**: **270.1262** ($M^{+\bullet}$ $C_{17}H_{18}O_3^{+\bullet}$ requires 270.1250)**.**

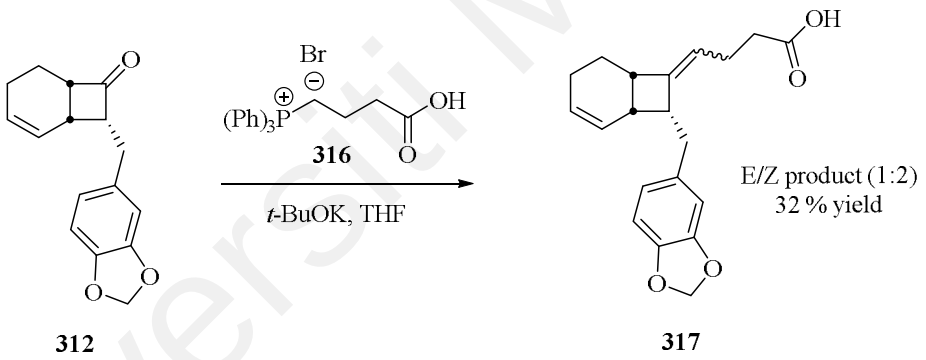

312 **317**

4-[7-(3,4-Methylenedioxyphenyl)bicyclo[4.2.0]oct-4-en-8-ylidene]butanoic acid (317). To a stirred slurry of (3-carboxypropyl)-triphenylphosphonium bromide (**316**) (770 mg, 1.79 mmol) in dry THF (7 mL) under nitrogen at -75°C was added potassium ***tert***-butoxide (350 mg, 3.13 mmol). After 15 min at -75°C, a solution of cyclobutanone **312** (210 mg, 0.820 mmol) in 3 mL dry THF was added to a mixture and stirred at -75°C for 10 min. The mixture was stirred at room temperature for overnight. The mixture was poured into 5% Na_2CO_3 solution (20 mL), washed with ethyl acetate (20 mL), and then acidified with conc. HCl. The aqueous layer was extracted with ether (3 x 20 mL) and the combined extract was concentrated to 20 mL and keep at -20°C for 2 h.

The resulting precipitate was filtered off and discarded. Evaporation the filtrate gave a yellowish oil (660 mg) which was purified by column chromatography on silica gel, eluting with petroleum ether/ethyl acetate (7:3) to give a desired product in ***Z/E*** isomer (2:1) as a yellowish oil **317** (261 mg, 32%).

4-[(1***R****,6***S****,7***S****)-7-(3,4-Methylenedioxyphenyl)bicyclo[4.2.0]oct-4-en-8-ylidene]butanoic acid	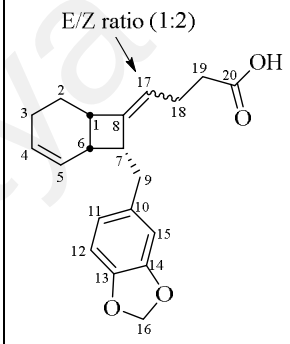

Yellowish oil. $R_f \approx 0.30$ [UV-active, EtOAc/Pet. ether 60%, anisaldehyde (blue spot)]**. IR (neat):** ν_{max} 2928 (s), 2863 (m), 1738 (s, C=O), 1504 (m), 1490 (m), 1441 (m), 1246 (s), 1188 (m), 1040 (m, O-CH_2-O), 927 (m, O-CH_2-O), 859 (w), 810 (w) cm^{-1}. **$^1H_{Z\text{-}isomer}$ NMR ($CDCl_3$)** 1.44* (1H, m, H2a), 1.86 – 1.97* (3H, m, H2b, H3), 2.20 – 2.36* (4H, m, H18, H19), 2.53 (2H, dd, ***J*** = 6.0, 4.4 Hz, H9), 2.79 (1H, m, H6), 3.22* (2H, m, H1, H7), 4.97 (1H, t, ***J*** = 7.2 Hz, H17), 5.57 (1H, m, H5), 5.84 (2H, s, H16), 5.92* (1H, m, H4), 6.54* (1H, dd, ***J*** = 8.1, 2.0 Hz, H11), 6.60 (1H, d, ***J*** = 2.0 Hz, H15), 6.63* (1H, d, ***J*** = 8.1 Hz, H12) (*obscured by other resonances). **$^{13}C_{Z\text{-}isomer}$ NMR ($CDCl_3$)** 21.9 (C3), 23.1 (C2), 23.7 (C18), 33.6 (C6), 34.2 (C19), 34.9 (C9), 39.2 (C7), 46.6 (C1), 100.7 (16), 108.0 (C12), 109 (C15), 118.0 (C17), 121.2 (C11), 126.8 (C5), 129.9 (C4), 135.0 (C10), 145.4 (C13), 146.6 (C8), 147.4 (C14), 179.0 (C20). **$^1H_{E\text{-}isomer}$ NMR ($CDCl_3$)** 1.44* (1H, m, H2a), 1.86 – 1.97* (3H, m, H2b, H3), 2.20 – 2.36* (4H, m, H18, H19), 2.56 (2H, m, H9), 2.80 (1H, m, H6), 3.22* (2H, m, H1, H7), 5.07 (1H, t, ***J*** = 7.2 Hz, H17), 5.51 (1H, m, H5), 5.89 (2H, s, H16), 5.92* (1H, m, H4), 6.54* (1H,

dd, ***J*** = 8.1, 2.0 Hz, H11), 6.59 (1H, d, ***J*** = 2.0 Hz, H15), 6.63* (1H, d, ***J*** = 8.1 Hz, H12) (*obscured by other resonances). **$^{13}C_{E\text{-}isomer}$ NMR ($CDCl_3$)** 22.0 (C3), 23.1 (C2), 23.7 (C18), 33.7 (C6), 34.4 (C19), 34.9 (C9), 38.7 (C7), 46.6 (C1), 100.7 (16), 108.0 (C12), 109 (C15), 118.0 (C17), 121.2 (C11), 127.0 (C5), 129.9 (C4), 135.0 (C10), 145.4 (C13), 146.7 (C8), 147.5 (C14), 179.6 (C20). **MS *m/z* (EI)** 106, 132, 135, 136, 137, 148, 149, 174, 185, 239, 272, 274, 298, 326 ($M^{+\bullet}$). **HRMS *m/z* (EI)**: 326.1515 ($M^{+\bullet}$ $C_{20}H_{22}O_4^{+\bullet}$ requires 326.1518)**.**

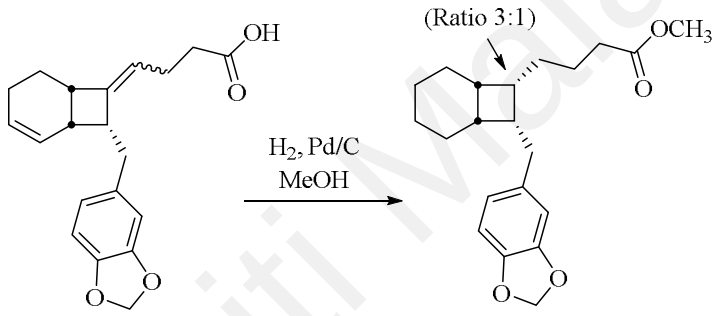

317 **318**
80% yield

Methyl 4-[7-(3,4-methylenedioxyphenyl)bicyclo[4.2.0]octan-8-yl]butanoate (318). To a solution of the bicycloalkene **317** (55 mg, 0.169 mmol) in MeOH (2 mL) was added 10% Pd/C (10% w/w, 5.5 mg), and the resulting mixture was hydrogenated at 1 atm for 12 h. Filtration through Celite and evaporation of the filtrate in vacuo afforded the pure **318** (3:1) as yellowish oil (46.5 mg, 80.0%).

Methyl 4-[(1***R****,6***S****,7***S****)-7-(3,4-methylenedioxyphenyl)bicyclo [4.2.0]octan-8-yl]butanoate	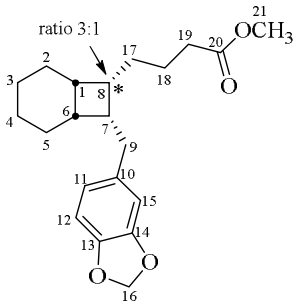

Yellowish oil. $R_f \approx 0.35$ [UV-active, EtOAc/Pet. ether 60%, anisaldehyde (blue spot)]**.** **IR (neat):** $_{max}$ 2929 (s), 2863 (m), 1739 (s, C=O), 1504 (s), 1490 (s), 1442 (m), 1246 (s), 1188 (m), 1122 9w), 1096 (w), 1040 (m, O-CH2-O), 927 (m, O-CH2-O), 861 (w), 811 (w) cm^{-1}. **$^1H_{8\alpha}$ NMR ($CDCl_3$)** 1.14 – 1.23* (4H, m, H3, H4), 1.39 – 1.59* (H8, m, H2, H5, H17, H18), 2.15 – 2.24* (3H, m, H8, H19), 2.30 – 2.40* (2H, H1, H6), 2.62 – 2.74* (3H, m, H7, H9), 3.58 (3H, s, H21), 5.82* (2H, s, H16), 6.55* (1H, dd, ***J*** = 8.1, 1.7 Hz, H11), 6.60* (1H, d, ***J*** = 1.7 Hz, H15), 6.62* (1H, d, ***J*** = 8.1 Hz, H12) (*obscured by other resonances) **^{13}C NMR ($CDCl_3$)** 22.6 (C3), 22.7 (C4), 23.1 (C2), 23.2 (C5), 24.8 (C18), 27.6 (C17), 32.9 (C9), 33.8 (C6), 34.1 (C8), 34.4 (C19), 40.2 (C1), 40.3 (C7), 51.6 (C21), 100.6 (C16), 108.1 (C12), 108.9 (C15), 121.2 (C11), 136.2 (C10), 145.2 (C13), 147.4 (C14), 174.3 (C20). **$^1H_{8\beta}$ NMR ($CDCl_3$)** 1.14 – 1.23* (4H, m, H3, H4), 1.39 – 1.59* (H8, m, H2, H5, H17, H18), 2.15 – 2.24* (3H, m, H8, H19), 2.30 – 2.40* (2H, H1, H6), 2.62 – 2.74* (3H, m, H7, H9), 3.40 (3H, s, H21), 5.82* (2H, s, H16), 6.55* (1H, dd, ***J*** = 8.1, 1.7 Hz, H11), 6.60* (1H, d, ***J*** = 1.7 Hz, H15), 6.62* (1H, d, ***J*** = 8.1 Hz, H12) (*obscured by other resonances). **^{13}C NMR ($CDCl_3$)** 22.6 (C3), 22.7 (C4), 23.1 (C2), 23.2 (C5), 24.8 (C18), 27.6 (C17), 32.9 (C9), 33.8 (C6), 34.1 (C8), 34.4 (C19), 40.2 (C1), 40.3 (C7), 50.3 (C21), 100.8 (C16), 108.2 (C12), 109.1 (C15), 121.4 (C11), 136.42 (C10), 145.2 (C13), 147.4 (C14), 174.3 (C20). **MS *m/z* (EI)**

102, 145, 158, 167, 194, 214, 239, 279, 295, 313, 325, 331, 344 ($M^{+\bullet}$), 362, 380. **HRMS *m/z* (EI)**: **344.1992** ($M^{+\bullet}$ $C_{21}H_{28}O_4^{+\bullet}$ requires 344.1988)**.**

REFERENCES

Ackler, S., Xiao, Y., Mitten, M. J., Foster, K., Oleksijew, A., Refici, M., Schlessinger, S., Wang, B., Chemburkar, S. R., Bauch, J., Tse, C., Frost, D. J., Fesik, S. W., Rosenberg, S. H., Elmore, S. W., & Shoemaker, A.R. (2008). ABT-263 and rapamycin act cooperatively to kill lymphoma cells in vitro and in vivo. *Mol. Cancer Ther., 7*, 3265-3274

Alami, M., & Ferri, F. (1996). A convenient route to unsymmetrical conjugated diynes. *Tetrahedron Lett., 37*, 2763-2766

Alberts, A. W. (1988). Discovery, biochemistry and biology of lovastatin. *Am. J. Cardiol., 62*, J10-J15

Allen, T. L., Scheiner, A. C., Yamaguchi, Y., & Schaefer, H. F. (1986). Theoretical studies of diphosphene and diphosphinylidene in their closed-shell states, low-lying open-shell singlet and triplet states, and transition states. Search for a stable bridged structure. *J. Am. Chem. Soc., 108*, 7579-7588

Altmann, K., & Gertsch, J. (2007). Anticancer drugs from nature-natural products as a unique source of new microtubule-stabilizing agents. *Nat. Prod. Rep., 24*, 327-357

Andersen, N. G., & Keay, B. A. (2001). 2-Furyl phosphines as ligands for transition-metal-mediated organic synthesis. *Chem. Rev., 101*, 997-1030

Anderson, M. A., Huang, D., & Roberts, A. (2014). Targeting BCL2 for the treatment of lymphoid malignancies. *Seminars in Hematology, 51*(3), 219-227

Ando, M., Wada, T., Kusaka, H., Takase, K., Hirata, N., & Yanagi, Y. (1987). Studies on the syntheses of sesquiterpene lactones. 10. Improved syntheses of (+)-tuberiferin and the related .alpha.-methylene-.gamma.-lactones and their biological activities. *J. Org. Chem., 52*, 4792-4796

Apel, C., Gény, C., Dumontet, V., Birlirakis, N., Roussi, F., Pham, V. C., Doan T. H., Nguyen, V. H., Chau, V. M., & Litaudon, M. (2014). Endiandric acid analogues from *Beilschmiedia ferruginea* as dual inhibitors of Bcl-xL/Bak and Mcl-1/Bid interactions. *J. Nat. Prod., 77*, 1430-1437

Appendino, G., Fontana, G., & Pollastro, F. (2010). Natural products drug discovery. In Liu, H.-W. & Mander, L. (Eds.), *Comprehensive Natural Products II* (pp. 205-236). Oxford: Elsevier

Aristoff, P. A., Garcia, G. A., Kirchhoff, P. D., & Hollis, S. H. D. (2010). Rifamycins – obstacles and opportunities. *Tuberculosis, 90,* 94-118

Avlonitis, N., Lekka, E., Detsi, A., Koufaki, M., Calogeropoulou, T., Scoulica, E., Siapi, E., Kyrikou, I., Mavromoustakos, T., Tsotinis, A., Grdadolnik, S. G., & Makriyannis, A. (2003). Antileishmanial ring-substituted ether phospholipids. *J. Med. Chem., 46*, 755-767

Azmi, A. S., & Mohammad, R. M. (2009). Non-peptidic small molecule inhibitors against Bcl-2 for cancer therapy. *J. Cell Physiol., 218*, 13-21

Baldwin, J. E., & Kapecki, J. A. (1970). Stereochemistry and secondary deuterium kinetic isotope effects in the cycloadditions of diphenylketene with styrene and deuteriostyrenes. *J. Am. Chem. Soc., 92*, 4874-4879

Bandaranayake, W. M., Banfield, J. E., & Black, D. S. C. (1980). Postulated electrocyclic reactions leading to endiandric acid and related natural products. *J. Chem. Soc. Chem. Commun.*, 902-903

Bandaranayake, W. M., Banfield, J. E., & Black, D. S. C. (1982). Constituents of *Endiandra* species. (*E*)-4-(6'-phenyltetracyclo[5.4.2.03,13.010,12]trideca-4',8'-dien-11'yl)but-2-enoic acid from *Endiandra introrsa* (Lauraceae) and a derived lactone. *Aust. J. Chem., 35*, 557-565

Bandaranayake, W. M., Banfield, J. E., Black, D. S. C., Fallon, G. D., & Gatehouse, B. M. (1980). Endiandric acid, a novel carboxylic acid from *Endiandra introrsa* (Lauraceae): X-ray structure determination. *J. Chem. Soc. Chem. Commun.*, 162-163

Bandaranayake, W. M., Banfield, J. E., Black, D. S. C., Fallon, G. D., & Gatehouse, B. M. (1981). Constituents of *Endiandra* species. Endiandric acid, a novel carboxylic acid from *Endiandra introrsa* (Lauraceae) and a derived lactone. *Aust. J. Chem., 34*, 1655-1667

Bandaranayake, W. M., Banfield, J. E., Black, D. S. C., Fallon, G. D., & Gatehouse, B. M. (1982). Constituents of *Endiandra* species. 4-[(*E*,*E*)-5'-Phenylpenta-2',4'-dien-1'-yl]tetracyclo[5,4,0,02,5,03,9]undec-10-ene-8-carboxylic acid from *Endiandra introrsa* (Lauraceae). *Aust. J. Chem., 35*, 567-579

Banfield, J.E., Black, D.C., Collins, D.J., Hyland, B.P.M., Lee, J.J., & Pranowo, R. S. (1994). Constituents of some species of *Beilschmiedia* and *Endiandra* (Lauraceae): new endiandric acid and benzopyran derivatives isolated from *B. oligandra*. *Aust. J. Chem., 47*, 587-607

Banfield, J. E., Black, D. S. C., Fallon, G. D., & Gatehouse, B. M. (1983). Constituents of *Endiandra* species. 2-[3',5'-Dioxo-4'-phenyl-10'-{(*E*,*E*)-5"-phenyl-penta-2",4"-dien-1"-yl}-2',4',6'-triazatetracyclo [5,4,2,02,6,08,11] tridec12'-en-9'-yl]-acetic acid derived from *Endiandra introrsa* (Lauraceae). *Aust. J. Chem., 36*, 627-632

Banfield, J. E., Black, D. S. C., Johns, S. R., & Willing, R. I. (1982). Constituents of *Endiandra* species. 2-(8'-[(*E*,*E*)-5"-phenylpenta-2",4"-dien-1"-yl]bicyclo[4.2.0] octa-2',4'-dien-7'-yl)acetic acid, a biogenetically predicted metabolite of *Endiandra introrsa* (Lauraceae) and its structure determination by means of 1D and 2D NMR spectroscopy. *Aust. J. Chem., 35*, 2247-2256

Bard, A. J., & Faulkner, R. (2001). *Electrochemical Methods: Fundamentals and Applications* (2nd ed.): John Wiley & Sons

Barnett, C. J., Cullinan, G. J., Gerzon, K., Hoying, R. C., Jones, W. E., Newlon, W. M., et al. (1978). Structure-activity relationships of dimeric *Catharanthus* alkaloids. Deacetyl vinblastine amide (vindesine) sulfate. *J. Med. Chem., 21*, 88-96

Bedin, M., Gaben, A.-M., Saucier, C., & Mester, J. (2004). Geldanamycin, an inhibitor of the chaperone activity of HSP90, induces MAPK-independent cell cycle arrest. *Int. J. Cancer, 109*, 643-652

Bell, F. A., Ledwith, A., & Sherrington, D. C. (1969). Cation-radicals: *tris*-(*p*-bromophenyl)amminium perchlorate and hexachloroantimonate. *J. Chem. Soc. C: Organic*, 2719-2720

Ben, S., Yi-Qiang, C., Steven, D. C., Hui, J., Jianhua, J., Hyung-Jin, K., Si-Kyu, L., Wen, L., Koichi, N., Jeong-Woo, S., Wyatt, C. S., Scott, S., Gong-Li, T., Steven, V. L., & Jian, Z. (2007). Polyketide biosynthesis beyond the type I, II, and III polyketide synthase paradigms: a progress report. *Polyketides* (Vol. 955, pp. 154-166): American Chemical Society.

Beroukhim, R., Mermel, C. H., Porter, D., Wei, G., Raychaudhuri, S., Donovan, J., Barretina, J., Boehm, J. S., Dobson, J., Urashima, M., Mc Henry, K. T., Pinchback, R. M., Ligon, A. H., Cho, Y.-J., Haery, L., Greulich, H., Reich, M., Winckler, W., Lawrence, M. S., Weir, B. A., Tanaka, K. E., Chiang, D. Y., Bass, A. J., Loo, A., Hoffman, C., Prensner, J., Liefeld, T., Gao, Q., Yecies, D., Signoretti, S., Maher, E., Kaye, F. J., Sasaki, H., Tepper, J. E., Fletcher, J. A., Tabernero, J., Baselga, J., Tsao, M.-S., Demichelis, F., Rubin, M. A., Janne, P. A.,

Daly, M. J., Nucera, C., Levine, R. L., Ebert, B. L., Gabriel, S., Rustgi, A. K., Antonescu, C. R., Ladanyi, M., Letai, A., Garraway, L. A., Loda, M., Beer, D. G., True, L. D., Okamoto, A., Pomeroy, S. L., Singer, Samuel Golub, T. R. Lander, E. S., Getz, G., Sellers, W. R., & Meyerson, M. (2010). The landscape of somatic copy-number alteration across human cancers. *Nature, 463*, 899-905

Blair, I., Mander, L., Mundill, P., & Pyne, S. (1981). Studies on the total synthesis of gibberellins. A new strategy for A-ring construction. *Aust. J. Chem., 34*, 1887-1898

Blanchette, M. A., Choy, W., Davis, J. T., Essenfeld, A. P., Masamune, S., Roush, W. R., & Sakai, T. (1984). Horner-wadsworth-emmons reaction: Use of lithium chloride and an amine for base-sensitive compounds. *Tetrahedron Lett., 25*, 2183-2186

Bohen, S. P. (1998). Genetic and biochemical analysis of p23 and ansamycin antibiotics in the function of Hsp90-dependent signalling proteins. *Mol. Cell. Biol., 18*, 3330-3339

Boonen, J., Malysheva, S. V., Taevernier, L., Diana Di Mavungu, J., De Saeger, S., & De Spiegeleer, B. (2012). Human skin penetration of selected model mycotoxins. *Toxicol., 301*, 21-32

Bourgaud, F., Gravot, A., Milesi, S., & Gontier, E. (2001). Production of plant secondary metabolites: a historical perspective. *Plant Sci., 161*, 839-851

Brian, P., Riggle, P. J., Santos, R. A., & Champness, W. C. (1996). Global negative regulation of *Streptomyces coelicolor* antibiotic synthesis mediated by an absA-encoded putative signal transduction system. *J. Bacteriol., 178*, 3221-3231

Brinchi, L., Chiavini, L., Goracci, L., Profio, P., D, & Germani, R. (2009). Efficient hydrolysis of nitriles to amides with hydroperoxide anion in aqueous surfactant solutions as reaction medium. *Lett. Org. Chem., 6*, 175-179

Brocksom, T. J., Coelho, F., Deprés, J.-P., Greene, A. E., Freire de Lima, M. E., Hamelin, O., Hartmann, B., Kanazawa, A. M., & Wang, Y. (2002). First comprehensive bakkane approach: stereoselective and efficient dichloroketene-based total syntheses of (±)- and (−)-9-acetoxyfukinanolide, (±)- and (+)-bakkenolide A, (−)-bakkenolides III, B, C, H, L, V, and X, (±)- and (−)-homogynolide A, (±)-homogynolide B, and (±)-palmosalide C. *J. Am. Chem. Soc., 124*, 15313-15325

Brossi, A. (1984). *The Alkaloids - Chapter 23*.: Academic Press: New York

Bundscherer, A., Hafner, C., Maisch, T., Becker, B., Landthaler, M., & Vogt, T. (2008). Antiproliferative and proapoptotic effects of rapamycin and celecoxib in malignant melanoma cell lines. *Oncol. Rep., 19*, 547-553

Burkill, I. H. (1966). *A Dictionary of the Economic Products of the Malay Peninsular* (2nd ed.): Government of Malaya and Singapore: Kuala Lumpur, Malaysia

Burnley, J., Ralph, M., Sharma, P., & Moses, J. E. (2011). Biomimetic electrocyclization reactions toward polyketide-derived natural products. *Biomimetic organic synthesis* (pp. 591-635): Wiley-VCH Verlag GmbH & Co. KGaA

Butler, M. S. (2004). The role of natural product chemistry in drug discovery. *J. Nat. Prod., 67*, 2141-2153

Buurma, N. J., Pastorello, L., Blandamer, M. J., & Engberts, J. B. F. N. (2001). Kinetic evidence for hydrophobically stabilized encounter complexes formed by hydrophobic esters in aqueous solutions containing monohydric alcohols. *J. Am. Chem. Soc., 123*, 11848-11853

Capuano, B., Crosby, I. T., Lloyd, E. J., Podloucka, A., & Taylor, D. A. (2003). Synthesis and preliminary pharmacological evaluation of arylalkyl analogues of clozapine. II. Effect of the nature and length of the linker. *Aust. J. Chem., 56*, 875-886

Chabner, B. A., & Roberts, T. G. (2005). Chemotherapy and the war on cancer. *Nat. Rev. Cancer, 5*, 65-7

Chan, S.-L., Lee, M. C., Tan, K. O., Yang, L.-K., Lee, A. S. Y., Flotow, H., Fu, N. Y., Butler, M. S., Soejarto, D. D., Buss, A. D., & Yu, V. C. (2003). Identification of chelerythrine as an Inhibitor of Bcl-xl function. *J. Biol. Chem., 278*, 20453-20456

Charette, A. B., Chinchilla, R., & Nájera, C. (2001). Tetrabutylammonium bromide *Encyclopedia of Reagents for Organic Synthesis*: John Wiley & Sons, Ltd

Chen, J.-J., Chou, E.-T., Duh, C.-Y., Yang, S.-Z., & Chen, I.-S. (2006). New cytotoxic tetrahydrofuran- and dihydrofuran-type lignans from the stem of *Beilschmiedia tsangii*. *Planta Med., 72*, 351-357

Chen, J.-J., Chou, E.-T., Peng, C.-F., Chen, I.-S., Yang, S.-Z., & Huang, H.-Y. (2007). Novel epoxyfuranoid lignans and antitubercular constituents from the leaves of *Beilschmiedia tsangii*. *Planta Med., 73*, 567-571

Cheng, C. Y., Wu, S. C., Hsin, L. W., & Tam, S. W. (1992). Selective reversible and irreversible ligands for the .kappa. opioid receptor. *J. Med. Chem., 35*, 2243-2247

Cheng, Y., & Prusoff, W. H. (1973). Relationship between the inhibition constant (*Ki*) and the concentration of inhibitor which causes 50 per cent inhibition (IC_{50}) of an enzymatic reaction. *Biochem. Pharmacol., 22*, 3099-3108

Cheon, H. G., Yoo, S.-E., Kim, S. S., Yang, S.-D., Kim, K.-R., Rhee, S. D., Ahn, J. H., Kang, S., K., Jung, W. H., Park, S. D., Kim, N. G., Lee, J. H.,Huh, S., C., Lee, J. M., Song, S. B., Kwon, S. J., Kim, J. H., Lee, J.-H., & Kim, S. J. (2005). South Korea Patent No.: I. A. P. U. T. P. C. T. (PCT) World Intellectual Property Organization WO2005/100303 A1

Chih, H.-W., Chiu, H.-F., Tang, K.-S., Chang, F.-R., & Wu, Y.-C. (2001). Bullatacin, a potent antitumor annonaceous acetogenin, inhibits proliferation of human hepatocarcinoma cell line by apoptosis induction. *Life Sci., 69*, 1321-1331

Chon, H. S., Hu. W., & Kavanagh. J. (2006). Targeted therapies in gynecologic cancers. *Curr. Cancer Drug Targets, 6*, 333-363

Chou, W.-N., Clark, D. L., & White, J. B. (1991). The use of rieke zinc metal in the selective reduction of alkynes. *Tetrahedron Lett., 32*, 299-302

Chouna, J. R., Alango Nkeng-Efouet, P., Ndjakou Lenta, B., Duplex Wansi, J., Neumann, B., Stammler, H.-G., Fon Kimbu, S., & Sewald, N. (2011). Beilschmiedic acids F and G, further endiandric acid derivatives from *Beilschmiedia anacardioides*. *Helv. Chim. Acta, 94*, 1071-1076

Chouna, J. R., Nkeng-Efouet, P. A., Lenta, B. N., Devkota, K. P., Neumann, B., Stammler, H.-G., Kimbu, S. F., & Sewald, N. (2009). Antibacterial endiandric acid derivatives from *Beilschmiedia anacardioides. Phytochemistry, 70*, 684-688

Chouna, J. R., Nkeng-Efouet, P. A., Lenta, B. N., Wansi, J. D., Kimbu, S. F., & Sewald, N. (2010). Endiandric acid derivatives from the stem bark of *Beilschmiedia anacardioides. Phytochem. Lett., 3*, 13-16

Clezy, P. S., Gellert, E., Lau, D. Y. K., & Nichol, A. W. (1966). The alkaloids of *Beilschmiedia elliptica*. *Aust. J. Chem., 19*, 135-142

Corey, E. J., & Eckrich, T. M. (1984). A method for the stereospecific synthesis of chiral *cis*-2-alkylcyclopropyllithium reagents. *Tetrahedron Lett., 25*, 2415-2418

Corey, E. J., & Venkateswarlu, A. (1972). Protection of hydroxyl groups as *tert*-butyldimethylsilyl derivatives. *J. Am. Chem. Soc., 94*, 6190-6191

Corner E. J. (1988). *Wayside trees of Malaya* (3 ed.): Malaysian Nature Society

Cotter, T. G. (2009). Apoptosis and cancer: the genesis of a research field. *Nat. Rev. Cancer, 9*, 501-507

Cragg, G., & Suffness, M. (1988). Metabolism of plant-derived anticancer agents. *Pharmacol. Ther., 37*, 425-461

Cragg, G. M., & Newman, D. J. (2005). Biodiversity: A continuing source of novel drug leads. *Pure Appl. Chem., 77*, 7-24

Crews, P., Rodríguez J., & Jaspars M. (1998). *Organic structure analysis* (1st ed.): Oxford University Press

Crozier, A., Clifford M. N., & Ashihara H. (2006). *Plant secondary metabolites: occurrence, structure and role in the human diet*: Blackwell Publishing Ltd

Cummings, M., Breitling R., & Takano E. (2014). Steps towards the synthetic biology of polyketide biosynthesis. *FEMS Microbiol. Lett., 351*, 116-125

Czabotar, P. E., Westphal, D., Dewson, G., Ma, S., Hockings, C., Fairlie, W. D., Lee, Erinna F., Yao, S., Robin, A. Y., Smith, B. J., Huang, D. C. S., Kluck, R. M., Adams, J. M., & Colman, P. M. (2013). Bax crystal structures reveal how BH3 domains activate Bax and nucleate its oligomerization to induce apoptosis. *Cell, 152*, 519-531

Dardenne, J., Desrat, S., Guéritte, F., & Roussi, F. (2013). Asymmetric synthesis of two analogues of meiogynin A. *Eur. J. Org. Chem.*, 2116-2122

Davids, M. S., & Letai, A. (2012). Targeting the B-cell lymphoma/leukemia 2 family in cancer. *J. Clin. Oncol., 30*, 3127-3135

Davids, M. S., & Letai, A. (2013). ABT-199: Taking dead aim at BCL-2. *Cancer Cell, 23*, 139-141

Davis, K. M., & Carpenter, B. K. (1996). Unusual facial selectivity in the cycloaddition of singlet oxygen to a simple cyclic diene. *J. Org. Chem., 61*, 4617-4622

De Faria, A. R., Salvador, E. L., & Correia, C. R. D. (2002). Synthesis of indolizidines and pyrrolizidines through the [2 + 2] cycloaddition of five-membered endocyclic enecarbamates to alkyl ketenes. Unusual regioselectivity of Baeyer−Villiger ring expansions of alkyl aza-bicyclic cyclobutanones. *J. Org. Chem., 67*, 3651-3661

Degli, E. M., Ghelli, A., Ratta, M., Cortes, D., & Estornell, E. (1994). Natural substances (acetogenins) from the family *Annonaceae* are powerful inhibitors of mitochondrial NADH dehydrogenase (Complex I). *Biochem. J., 301*, 161-167

Desai, N. B., McKelvie, N., & Ramirez, F. (1962). A new synthesis of 1,1-dibromoölefins via phosphine-dibromomethylenes. The reaction of triphenylphosphine with carbon tetrabromide. *J. Am. Chem. Soc., 84*, 1745-1747

Desch H. E. (1957). *Malayan forest records no.15: Manual of Malayan timbers* (Vol. 1): Tien Wah and Co. Singapore

Desrat, S., Pujals, A., Colas, C., Dardenne, J., Gény, C., Favre, L., Dumontet, V., Iorga, B. I., Litaudon, M., Raphaël, M., Wiels, J., & Roussi, F. (2014). Pro-apoptotic meiogynin A derivatives that target Bcl-xL and Mcl-1. *Bioorg. Med. Chem. Lett., 24*, 5086-5088

Desrat, S., Remeur, C., Geny, C., Riviere, G., Colas, C., Dumontet, V., Birlirakis, N., Iorga, B. I., & Roussi, F. (2014). From meiogynin A to the synthesis of dual inhibitors of Bcl-xL and Mcl-1 anti-apoptotic proteins. *Chem. Comm., 50*, 8593-8596

Dharap, S. S., P. Chandna, P., Wang, Y., Khandare, J. J., Qiu, B., Stein, S., & Minko, T. (2006). Molecular targeting of Bcl2 and Bcl-xL proteins by synthetic BH3 peptide enhances the efficacy of chemotherapy. *J. Pharmacol. Exp. Ther. , 316*, 992-998

Dias, D. A., Urban, S., & Roessner, U. (2012). A historical overview of natural products in drug discovery. *Metabolites, 2*, 303-336

Dickschat J. S. (2011). Biosynthesis and function of secondary metabolites. *Beilstein J. Org. Chem., 7*, 1620-1621

Dodou, K., Anderson, R. J., Small, D. A., & Groundwater, P. W. (2005). Investigations on gossypol: past and present developments. *Expert Opin. Investig. Drugs, 14*, 1419-1434

Drew, S. L., Lawrence, A. L., & Sherburn, M. S. (2013). Total synthesis of kingianins A, D, and F. *Angew. Chem. Int. Ed., 52*, 4221-4224

Dubé, D., & Scholte, A. A. (1999). Reductive *N*-alkylation of amides, carbamates and ureas. *Tetrahedron Lett., 40*, 2295-2298

Eder, C.; Kogler, H.; Haag-Richter S. **2004**. German Patent 10235624

Eder, C.; Kogler, H.; Haag-Richter S. **2004**. United State Patent US2004/0138313A1

Eder, C., Kogler, H., & Haag-Richter S. (2006). United State Patent No. United State Paten US7019028B2: Avantis Pharma Deutschland GmbH. & A. P. Ins.

Elmore S. (2007). Apoptosis: a review of programmed cell death. *Toxicol. Pathol., 35*, 495-516

Enyedy, I. J., Ling, Y., Nacro, K., Tomita, Y., Wu, X., Cao, Y., Guo, R., Li, B., Zhu, X., Huang, Y., Long, Y.-Q., Roller, P. P., Yang, D., & Wang, S. (2001). Discovery of small-molecule inhibitors of Bcl-2 through structure-based computer screening. *J. Med. Chem., 44*, 4313-4324

Fesik, S. W. (2005). Promoting apoptosis as a strategy for cancer drug discovery. *Nat. Rev. Cancer, 5*, 876-885

Fiandanese, V., Bottalico, D., Marchese, G., & Punzi, A. (2008). A straightforward synthesis of indole and benzofuran derivatives. *Tetrahedron, 64*, 53-60

Foote, C. S., Wexler, S., Ando, W., & Higgins, R. (1968). Chemistry of singlet oxygen. IV. Oxygenations with hypochlorite-hydrogen peroxide. *J. Am. Chem. Soc., 90*, 975-981

Fotsop, D. F., Roussi, F., Leverrier, A., Bretéché, A., & Guéritte, F. (2010). Biomimetic total synthesis of meiogynin A, an inhibitor of Bcl-xL and Bak interaction. *J. Org. Chem., 75*, 7412-7415

Fournier, D., & Poirier, D. (2011). Chemical synthesis and evaluation of 17α-alkylated derivatives of estradiol as inhibitors of steroid sulfatase. *Eur. J. Med. Chem., 46*, 4227-4237

Foxworthy, F. W. (1927). *Malayan forest records no. 3: commercial timber trees of the Malay Peninsular*: Fraser and Neave, LTD Singapore

Frontana-Uribe, B. A., Little, R. D., Ibanez, J. G., Palma, A., & Vasquez-Medrano, R. (2010). Organic electrosynthesis: a promising green methodology in organic chemistry. *Green Chem., 12*, 2099-2119

Futamura, Y., Sawa, R., Umezawa, Y., Igarashi, M., Nakamura, H., Hasegawa, K., Yamasaki, M., Tashiro, E., Takahashi, Y., Akamatsu, Y., & Imoto, M. (2008). Discovery of incednine as a potent modulator of the anti-apoptotic function of Bcl-xL from microbial origin. *J. Am. Chem. Soc., 130*, 1822-1823

Gieseler, A., Steckhan, E., Wiest, O., & Knoch, F. (1991). Photochemically induced radical-cation Diels-Alder reaction of indole and electron-rich dienes. *J. Org. Chem., 56*, 1405-1411

Glaser, S. P., Lee, E. F., Trounson, E., Bouillet, P., Wei, A., Fairlie, W. D., Izon, D. J., Zuber, J., Rappaport, A. R., Herold, M. J., Alexander, W. S., Lowe, S. W., Robb, L., & Strasser, A. (2012). Anti-apoptotic Mcl-1 is essential for the development and sustained growth of acute myeloid leukemia. *Genes Dev., 26*, 120-125

Gompper, R. (1969). Cycloadditions with polar intermediates. *Angew. Chem. Int. Edit., 8*, 312-327

Gravel, E., & Poupon, E. (2008). Biogenesis and biomimetic chemistry: can complex natural products be assembled spontaneously?. *Eur. J. Org. Chem.*, 6-6

Gravel, E., & Poupon, E. (2008). Biogenesis and biomimetic chemistry: can complex natural products be assembled spontaneously?. *Eur. J. Org. Chem.*, 27-42

Gregory Sowell, C., Wolin, R. L., & Daniel Little, R. (1990). Electroreductive cyclization reactions. Stereoselection, creation of quaternary centers in bicyclic frameworks, and a formal total synthesis of quadrone. *Tetrahedron Lett., 31*, 485-488

Gung, B. W., & Kumi, G. (2003). Remarkable reactivity difference in oxygen-substituted versus non-oxygen-substituted bromoalkynes in Cu (I)-catalyzed cross-coupling reactions: total synthesis of (−)-*S*-18-hydroxyminquartynoic acid. *J. Org. Chem., 68*, 5956-5960

Hall, S. W., Knight, J., Broughton, A., Benjamin, R. S., & McKelvey, E. (1983). Clinical pharmacology of the anticancer polypeptide neocarzinostatin. *Cancer Chemother. Pharmacol., 10*, 200-204

Hann, C. L., Daniel, V. C., Sugar, E. A., Dobromilskaya, I., Murphy, S. C., Cope, L., Lin, X., Hierman, J. S., Wilburn, D. L., Watkins, D. N., & Rudin, C. M. (2008). Therapeutic efficacy of ABT-737, a selective inhibitor of BCL2, in small cell lung cancer. *Cancer Res., 68*, 2321-2328

Hanson J. R. (2003). *Natural products: the secondary metabolites*: The Royal Society of Chemistry

Harborne, J. B., & Méndez, J. (1969). Flavonoids of *Beilschmiedia miersii*. *Phytochem., 8*, 763-764

Harirchian, B., & Bauld, N. L. (1989). Cation radical Diels-Alder cycloadditions in organic synthesis. A formal total synthesis of (-)-beta-selinene. *J. Am. Chem. Soc., 111*, 1826-1828

Harvey, A. L. (2008). Natural products in drug discovery. *Drug Discov. Today, 13*, 894-901

Hertweck, C. (2009). The biosynthetic logic of polyketide diversity. *Angew. Chem. Int. Edit., 48*, 4688-4716

Hoheisel, T. N., & Frauenrath, H. (2008). A convenient Negishi protocol for the synthesis of glycosylated oligo(ethynylene)s. *Org. Lett., 10*, 4525-4528

Holmes, A. B., & Jones, G. E. (1980). Synthesis of 4-alkyl-1-trimethylsilylbuta-1,3-diynes. *Tetrahedron Lett., 21*, 3111-3112

Horasan K. N., Doğan, D., Şahin, E., Gunel, A., Kara, Y., & Balci, M. (2011). Stereoselective synthesis of deoxycarbaheptopyranose derivatives: 5a-carba-6-deoxy-α-dl-galacto-heptopyranose and 5a-carba-6-deoxy-α-dl-gulo-hepto pyranose. *Tetrahedron, 67*, 1193-1200

Hu, W., Qin, H., Cui, Y., & Jia, Y. (2013). Total synthesis of (+)- and (−)-decursivine and (±)-serotobenine through a cascade Witkop photocyclization/elimination /addition sequence: scope and mechanistic insights. *Chem. Eur. J., 19*, 3139-3147

Huang Y. T., Chang H. S., Wang G. J., Lin C. H., & Chen I. S. (2012). Secondary metabolites from the roots of *Beilschmiedia tsangii* and their anti-Inflammatory activities. *Int. J. Mol. Sci., 13*, 16430-16443

Huang, Y.-T., Chang, H.-S., Wang, G.-J., Cheng, M.-J., Chen, C.-H., Yang, Y.-J., & Chen, I.-S. (2011). Anti-inflammatory endiandric acid analogues from the roots of *Beilschmiedia tsangii. J. Nat. Prod., 74*, 1875-1880

Huczyński, A., Stefańska, J., Przybylski, P., Brzezinski, B., & Bartl, F. (2008). Synthesis and antimicrobial properties of monensin A esters. *Bioorg. Med. Chem. Lett., 18*, 2585-2589

Hui, Y. H., Rupprecht, J. K., Liu, Y. M., Anderson, J. E., Smith, D. L., Chang, C. J., & McLaughlin, J. L. (1989). Bullatacin and bullatacinone: two highly potent bioactive acetogenins from *Annona bullata*. *J. Nat. Prod., 52*, 463-477

Huisgen, R., Dahmen, A., & Huber, H. (1967). Stereospecific conrotatory valence isomerization of octatetraenes to cycloocta-1,3,5-trienes. *J. Am. Chem. Soc., 89*, 7130-7131

Ian Chopra, I., & Roberts, M. (2001). Tetracycline antibiotics: mode of action, applications, molecular biology, and epidemiology of bacterial resistance. *Microbiol. Mol. Biol. Rev., 65*, 232-260

Ischay, M. A., & Yoon, T. P. (2012). Accessing the synthetic chemistry of radical ions. *Eur. J. Org. Chem., 2012*, 3359-3372

Jeng, P. S., & Cheng, E. H. (2013). Pulling the plug on Bcl-xL. *Nat. Chem. Biol. 9*, 351-352

Jubert, C., & Knochel, P. (1992). Preparation of new classes of aliphatic, allylic, and benzylic zinc and copper reagents by the insertion of zinc dust into organic halides, phosphates, and sulfonates. *J. Org. Chem., 57*, 5425-5431

Jung, M. E., & Light, L. A. (1982). Preparation of iodoallylic alcohols via hydrostannylation: spectroscopic proof of structures. *Tetrahedron Lett., 23*, 3851-3854

Kamei, H., Nishiyama, Y., Takahashi, A., Obi, Y., & Oki, T. (1991). Dynemicins, new antibiotics with the 1,5-diyn-3-ene and anthraquinone subunit. II. Antitumor activity of dynemicin A and its triacetyl derivative. *J. Antibiot., 44*, 1306-1311

Kang, M. H., & Reynolds, C. P. (2009). Bcl-2 Inhibitors: targeting mitochondrial apoptotic pathways in cancer therapy. *Clin. Cancer Res., 15*, 1126-1132

Katagiri, T., Irie, M., & Uneyama, K. (2000). Syntheses of optically active trifluoronorcoronamic acids. *Org. Lett., 2*, 2423-2425

Keating, J., Tsoli, M., Hallahan, A. R., Ingram, W. J., Haber, M., & Ziegler, D. S. (2012). Targeting the inhibitor of apoptosis proteins as a novel therapeutic strategy in medulloblastoma. *Mol. Cancer Ther., 11*, 2654-2663

Keng H. (1978). *Orders and families of Malayan seed plants* (2nd ed.): Singapore University Press

Kerrigan, R. A., & Dixon D. J. (2011). *Lauraceae. In short, P.S. & Cowie, I.D. (eds), Flora of the Darwin Region*. (Vol. 1): Northern Territory Herbarium, Department of Natural Resources, Environment, the Arts and Sport

Kim, H., Tu, H.-C., Ren, D., Takeuchi, O., Jeffers, J. R., Zambetti, G. P., Hsieh, J. J. D., & Cheng, E. H. Y. (2009). Stepwise activation of BAX and BAK by tBID, BIM, and PUMA initiates mitochondrial apoptosis. *Mol. Cell, 36*, 487-499

Kingston, D. G. I. (1991). The chemistry of taxol. *Pharmacol. Ther., 52* 1-34

Kirkin, V., Joos, S., & Zörnig, M. (2004). The role of Bcl-2 family members in tumorigenesis. *Biochim. Biophys. Acta, 1644*, 229-249

Kitagawa, I., Minagawa, K., Zhang, R.-s., Hori, K., Doi, M., Inoue, M., Ishida, T., Kimura, M., Uji, T., & Shibuya, H. (1993). Dehatrine, an antimalarial bisbenzylisoquinoline alkaloid from the Indonesian medicinal plant *Beilschmiedia Madang*, isolated as a mixture of two rotational isomers. *Chem. Pharm. Bull., 41*, 997-999

Kobayashi, S., Hori, M., Wang, G. X., & Hirama, M. (2006). Formal total synthesis of neocarzinostatin chromophore. *J. Org. Chem., 71*, 636-644

Koltun, E. S., & Kass, S. R. (2000). Synthesis and reactivity of *trans*-Tricyclo[4.2.0.01,3]oct-4-ene. *J. Org. Chem., 65*, 3530-3537

Konishi, M., Ohkuma, H., Tsuno, T., Oki, T., VanDuyne, G. D., & Clardy, J. (1990). Crystal and molecular structure of dynemicin A: a novel 1,5-diyn-3-ene antitumor antibiotic. *J. Am. Chem. Soc., 112*, 3715-3716

Kozikowski, A. P., Campiani, G., Saxena, A., & Doctor, B. P. (1995). Synthesis and acetylcholinesterase inhibitory activity of several pyrimidone analogues of huperzine A. *J. Chem. Soc., Chem. Commun.*, 283-285

Krief, A., Trabelsi, M., & Dumont, W. (1992). Syntheses of alkali selenolates from diorganic diselenides and alkali metal hydrides: scope and limitations. *Synthesis*, 933-935

Kuwajima, I., Nakamura, E., & Hashimoto, K. (1983). Fluoride catalyzed reaction of silylacetylenes with carbonyl compounds. *Tetrahedron, 39*, 975-982

Kwan. D. H., & Schulz F. (2011). The stereochemistry of complex polyketide biosynthesis by modular polyketide synthases. *Molecules, 16*, 6092-6115

Law, B. K. (2005). Rapamycin: an anti-cancer immunosuppressant?. *Crit. Rev. Oncol. Hematol., 56*, 47-60

Lee, F. Y. F., Covello, K. L., Castaneda, S., Hawken, D. R., Kan, D., Lewin, A., Wen, M.-L., Ryseck, R.-P., Fairchild, C. R., Fargnoli, J., & Kramer, R. (2008). Synergistic antitumor activity of ixabepilone (BMS-247550) plus bevacizumab in multiple in vivo tumor models. *Clin. Cancer Res., 14*, 8123-8131

Lenta, B., Chouna, J., Nkeng-Efouet, P., & Sewald, N. (2015). Endiandric Acid Derivatives and Other Constituents of Plants from the Genera Beilschmiedia and Endiandra (Lauraceae). *Biomolecules, 5*, 910

Lenta, B. N., Chouna, J. R., Nkeng-Efouet, P. A., Fon, K. S., Tsamo, E., & Sewald, N. (2011). Obscurine, a new cyclostachine acid derivative from *Beilscmiedia obscura*. *Nat. Prod. Comm., 6*, 1591-1592

Lenta, B. N., Tantangmo, F., Devkota, K. P., Wansi, J. D., Chouna, J. R., Soh, R. C. F., Neumann, B., Stammler, H.-G., Tsamo, E., & Sewald, N. (2009). Bioactive constituents of the stem bark of *Beilschmiedia zenkeri*. *J. Nat. Prod., 72*, 2130-2134

Lerner, C., Masjost, B., Ruf, A., Gramlich, V., Jakob-Roetne, R., Zurcher, G., Borroni, E., & Diederich, F. (2003). Bisubstrate inhibitors for the enzyme catechol-O-methyltransferase (COMT): influence of inhibitor preorganisation and linker length between the two substrate moieties on binding affinity. *Org. Biomol. Chem., 1*, 42-49

Lessene, G'., Czabotar, P. E., & Colman, P. M. (2008). BCL2 family antagonists for cancer therapy. *Nat. Rev. Drug Discov., 7*, 989-1000

Lessene, G'., Peter, E. C., Brad, E. S., Kerry, Z., Kym, N. L., Jerry, M. A., Jonathan, B. B., Peter, M. C., Kurt, D., Wayne, J. F., John, A. F., Paul, G., Wilhelmus, J. A. K., Sanji, K., Rebecca, M. M., John, P. P., Brian, J. S., Ian P. Street., Hong, Yang., David, C. S. H., & Keith, G. W. (2013). Structure-guided design of a selective Bcl-xL inhibitor. *Nat. Chem. Biol., 9*, 390-400

Leverrier, A. (2010). Nouveaux ligands naturels de la protéine anti-apoptotique Bcl-xL, isolés de deux plantes de Malaisie : *Xylopia caudata* et *Endiandra kingiana*. *Faculty of Pharmacy Chatenay-Malabry, Doctor of Philosophy (PhD)*

Leverrier, A., Awang, K., Guéritte, F., & Litaudon, M. (2011). Pentacyclic polyketides from *Endiandra kingiana* as inhibitors of the Bcl-xL/Bak interaction. *Phytochem. Lett., 72*, 1443-1452

Leverrier, A., Tran huu Dau, M. E., Retailleau, P., Awang, K., Guéritte, F., & Litaudon, M. (2010). Kingianin A: a new natural pentacyclic compound from *Endiandra kingiana*. *Org. Lett, 12*, 3638-3641

Li, N., Shi, Z., Tang, Y., Chen, J., & Li, X. (2008). Recent progress on the total synthesis of acetogenins from *Annonaceae*. *Beilstein J. Org. Chem., 4*, 48

Li, S., Wang, J.-X., Wen, X., & Ma, X. (2011). Mild and efficient barbier allylation reaction mediated by magnesium powder under solvent-free conditions. *Tetrahedron, 67*, 849-855

Li, Z. M., Jiang W. Q., Zhu Z. Y., Zhu X. F., Zhou J. M., Liu Z. C., Yang, D. J., & Guan, Z. Z. (2008). Synergistic cytotoxicity of Bcl-xL inhibitor, gossypol and chemotherapeutic agents in non-Hodgkin's lymphoma cells. *Cancer Biol. Ther., 7*, 51-60

Lim, H. N., & Parker, K. A. (2013). Total synthesis of kingianin A. *Org. Lett., 15*, 398-401

Lim, H. N., & Parker, K. A. (2014). Intermolecular radical cation Diels–Alder (RCDA) reaction of bicyclooctadienes: biomimetic formal total synthesis of kingianin A and total syntheses of kingianins D, F, H, and J. *J. Org. Chem., 79*, 919-926

Lin, S., Ischay, M. A., Fry, C. G., & Yoon, T. P. (2011). Radical cation Diels–Alder cycloadditions by visible light photocatalysis. *J. Am. Chem. Soc., 133*, 19350-19353

Lin, S., Padilla, C. E., Ischay, M. A., & Yoon, T. P. (2012). Visible light photocatalysis of intramolecular radical cation Diels–Alder cycloadditions. *Tetrahedron Lett., 53*, 3073-3076

Litaudon, M., Bousserouel, H., Awang, K., Nosjean, O., Martin, M.-T., Hadi, H. A., Boutin, J. A., Sévenet, T., & Guéritte, F. (2009). A dimeric sesquiterpenoid from a Malaysian *Meiogyne* as a new inhibitor of Bcl-xL/BakBH3 domain peptide interaction. *J. Nat. Prod., 72*, 480-483

Lund, E. (1953). Erythromycin. *Acta Pathologica Microbiologica Scandinavica, 33*, 393-400

Maberley, D. J. (2008). *Mabberley's Plant-Book: A Portable Dictionary of Plants, Their Classification and Uses* (3rd ed.): Cambridge University Press: Cambridge, UK

Machiguchi, T., Hasegawa, T., Ishiwata, A., Terashima, S., Yamabe, S., & Minato, T. (1999). Ketene recognizes 1,3-dienes in their *S-Cis* forms through [4 + 2] (Diels−Alder) and [2 + 2] (Staudinger) reactions. An innovation of ketene chemistry. *J. Am. Chem. Soc., 121*, 4771-4786

Magnolo, S. K., Leenutaphong, D. L., DeModena, J. A., Curtis, J. E., Bailey, J. E., Galazzo, J. L., & Hughes, D. E. (1991). Actinorhodin production by *Streptomyces coelicolor* and growth of *Streptomyces lividans* are improved by the expression of a Bacterial Hemoglobin. *Nat. Biotech., 9*, 473-476

Manfredi, J. J., & Horwitz, S. B. (1984). Taxol: an antimitotic agent with a new mechanism of action. *Pharmacol. Ther., 25*, 83-125

Marvell, E. N., & Tashiro, J. (1965). Catalyst selectivity in semihydrogenation of some conjugated acetylenes. *J. Org. Chem., 30*, 3991-3993

Masui, K., Gini, B., Wykosky, J., Zanca, C., Mischel, P. S., Furnari, F. B., & Cavenee, W. K. (2013). A tale of two approaches: complementary mechanisms of cytotoxic and targeted therapy resistance may inform next-generation cancer treatments. *Carcinogenesis, 34*, 725-738

Matovic, N. J., Hayes, P. Y., Penman, K., Lehmann, R. P., & De Voss, J. J. (2011). Polyunsaturated alkyl amides from *Echinacea*: synthesis of diynes, Enynes, and dienes. *J. Org. Chem., 76*, 4467-4481

Mcguire, J. M, Bunch R. L, Anderson R. C, Boaz H. E, Flynn E. H, Powell H. M, & Smith, J. W. (1952). Ilotycin, a new antibiotic. *Schweiz Med. Wochenschr., 82* 1064-1065

Minns, R., A. (1977). Tropolone. *Org. Synth., 57*, 117

Minns, R., A. (1988). Tropolone. *Org. Synth., Coll., 6*, 1037-1041

Mishra, B. B., & Tiwari, V. K. (2011). Natural products: An evolving role in future drug discovery. *Eur. J. Med. Chem., 46*, 4769-4807

Miyata, Y. (2005). Hsp90 inhibitor geldanamycin and its derivatives as novel cancer chemotherapeutic agents. *Curr. Pharm. Des., 11*, 1131-1138

Mollataghi, A., Coudiere, E., Hadi, A. H. A., Mukhtar, M. R., Awang, K., Litaudon, M., & Ata, A. (2012). Anti-acetylcholinesterase, anti-α-glucosidase, anti-leishmanial and anti-fungal activities of chemical constituents of *Beilschmiedia* species. *Fitoterapia, 83*, 298-302

Mollataghi, A., Hadi, A. H. A., Awang, K., Mohamad, J., Litaudon, M., & Mukhtar, M. R. (2011). (+)-Kunstlerone, a new antioxidant neolignan from the leaves of *Beilschmiedia kunstleri* Gamble. *Molecules, 16*, 6582-6590

Mollataghi, A., Hadi, A. H. A., & Cheah, S.-C. (2012). (−)-Kunstleramide, a new antioxidant and cytotoxic dienamide from the bark of *Beilschmiedia kunstleri* Gamble. *Molecules, 17*, 4197-4208

Mollenhauer, H. H., James Morré, D., & Rowe, L. D. (1990). Alteration of intracellular traffic by monensin; mechanism, specificity and relationship to toxicity. *Biochim. Biophy. Acta (BBA) - Reviews on Biomembranes, 1031*, 225-246

Montierth, J. M., DeMario, D. R., Kurth, M. J., & Schore, N. E. (1998). The polymer-supported Cadiot-Chodkiewicz coupling of acetylenes to produce unsymmetrical diynes. *Tetrahedron, 54*, 11741-11748

Moore, J. C., Davies, E. S., Walsh, D. A., Sharma, P., & Moses, J. E. (2014). Formal synthesis of kingianin A based upon a novel electrochemically-induced radical cation Diels-Alder reaction. *Chem. Commun., 50*, 12523-12525

Mori, K., Audran, G., Nakahara, Y., Bando, M., & Kido, M. (1997). Synthesis and absolute configuration of phyllanthurinolactone, the leaf-closing factor of a nyctinastic plant, *Phyllanthus urinaria* L. *Tetrahedron Lett., 38*, 575-578

Mullard, A. (2012). Protein–protein interaction inhibitors get into the groove. *Nat. Rev. Drug Discov., 11*, 173-175

Myers, A. G., Fraley, M. E., Tom, N. J., Cohen, S. B., & Madar, D. J. (1995). Synthesis of (+)-dynemicin A and analogs of wide structural variability: establishment of the absolute configuration of natural dynemicin A. *Chem. Biol., 2*, 33-43

Naito, H., Kawahara, E., Maruta, K., Maeda, M., & Sasaki, S. (1995). The first total synthesis of (+)-bullatacin, a potent antitumor annonaceous acetogenin, and (+)-(15,24)-bis-epi-bullatacin. *J. Org. Chem., 60*, 4419-4427

Newman, D. J., Cragg, G. M., & Snader, K. M. (2003). Natural products as sources of new drugs over the period 1981−2002. *J. Nat. Prod., 66*, 1022-1037

Ng, F. S. P. (1989). *Tree Flora of Malaya, a Manual for the Forester*. In T. C. Whitmore (Ed.) (Vol. 4): Longman: Kuala Lumpur, Malaysia,

Nicolaou, K. C., & Dai, W. M. (1991). Chemistry and biology of the enediyne anticancer antibiotics. *Angew. Chem. Int. Ed., 30*, 1387-1416

Nicolaou, K. C., Montagnon, T., & Baran, P. S. (2002). Modulation of the reactivity profile of IBX by ligand complexation: ambient temperature dehydrogenation of aldehydes and ketones to α,β-unsaturated carbonyl compounds. *Angew. Chem. Int. Ed., 41*, 993-996

Nicolaou, K. C., & Petasis, N. A. (1984). *Strategies and tactics in organic synthesis* (Vol. 1): Academic Press: San Diego, CA, USA.

Nicolaou, K. C., Petasis, N. A., & Zipkin, R. E. (1982). The endiandric acid cascade. Electrocyclizations in organic synthesis. Biomimetic approach to endiandric acids A-G. Total synthesis and thermal studies. *J. Am. Chem. Soc., 104*, 5560-5562

Nicolaou, K. C., Yang, Z., Shi, G.-q., Gunzner, J. L., Agrios, K. A., & Gartner, P. (1998). Total synthesis of brevetoxin A. *Nature, 392*, 264-269

Nicolaou, K. C., Zipkin, R. E., & Petasis, N. A. (1982). The endiandric acid cascade. Electrocyclizations in organic synthesis. "Biomimetic" approach to endiandric acids A-G. Synthesis of precursors. *J. Am. Chem. Soc., 104*, 5558-5560

Nigenda, S. E., Schleich, D. M., Narang, S. C., & Keumi, T. (1987). Electrochemical oxidation of 1,3-cyclohexadiene. *J. Electrochem. Soc., 134*, 2465-2470

Nikolovska-Coleska, Z., Wang, R., Fang, X., Pan, H., Tomita, Y., Li, P., Roller, P. P., Krajewski, K., Saito, N. G., & Stuckey, J. A. (2004). Development and optimization of a binding assay for the XIAP BIR3 domain using fluorescence polarization. *Anal. Biochem., 332*, 261-273

Nishihara, Y., Ikegashira, K., Hirabayashi, K., Ando, J.-i., Mori, A., & Hiyama, T. (2000). Coupling reactions of alkynylsilanes mediated by a Cu (I) salt: novel syntheses of conjugate diynes and disubstituted ethynes. *J. Org. Chem., 65*, 1780-1787

Nuñeza, G., Benedict, M., A, Hu, Y., & Inohara, N. (1998). Caspases: the proteases of the apoptotic pathway. *Oncogene, 14*, 3237-3245

Olszewska, M. (2006). Oxytetracycline-mechanism of action and application in skin diseases. *Wiad Lek., 59*, 829-833

Ōmura, S., & Shiomi, K. (2007). Discovery, chemistry, and chemical biology of microbial products. *Pure Appl. Chem., 79*, 581-591

Paquette, L. A., Chang, J., & Liu, Z. (2004). Synthetic studies aimed at (−)-cochleamycin A. Evaluation of late-stage macrocyclization alternatives. *J. Org. Chem., 69*, 6441-6448

Park, C.-M., Bruncko, M., Adickes, J., Bauch, J., Ding, H., Kunzer, A., Marsh, K. C., Nimmer, P., Shoemaker, A. R., Song, X., Tahir, S. K., Tse, C., Wang, X., Wendt, M. D., Yang, X., Zhang, H., Fesik, S. W., Rosenberg, S. H. & Elmore, S. W. (2008). Discovery of an orally bioavailable small molecule inhibitor of prosurvival B-cell lymphoma 2 proteins. *J. Med. Chem., 51*, 6902-6915

Park, Y. S., & Little, R. D. (2008). Redox electron-transfer reactions: electrochemically mediated rearrangement, mechanism, and a total synthesis of daucene. *J. Org. Chem., 73*, 6807-6815

Parker, K. A., & Lim, H. N. (2014). Chapter 3 - the mysterious case of the kingianins. In H. Michael (Ed.), *Strategies and tactics in organic synthesis* (Vol. 10, pp. 51-78): Academic Press

Pavia, D. L., Lampman, G. M., & Kriz, G. S. (2009). *Introduction to spectroscopy: a guide for students of organic chemistry* (4th ed.): Brooks/Cole-Thomson Learning

Petros, A. M., Dinges, J., Augeri, D. J., Baumeister, S. A., Betebenner, D. A., Bures, M. G., Elmore, S. W., Hajduk, P. J., Joseph, M. K., Landis, S. K., Nettesheim, D. G., Rosenberg, S. H., Shen, W., Thomas, S., Wang, X., Zanze, I., Zhang, H., & Fesik, S. W. (2005). Discovery of a potent inhibitor of the antiapoptotic protein Bcl-xL from NMR and parallel synthesis. *J. Med. Chem., 49*, 656-663

Pettit, G. R., Moser, B. R., Mendonça, R. F., Knight, J. C., & Hogan, F. (2012). The cephalostatins. Synthesis of bis-steroidal pyrazine pyrones. *J. Nat. Prod., 75*, 1063-1069

Pitterna, T., Cassayre, J., Hüter, O. F., Jung, P. M. J., Maienfisch, P., Kessabi, F. M., Quaranta, L., & Tobler, H. (2009). New ventures in the chemistry of avermectins. *Bioorg. Med. Chem., 17*, 4085-4095

Placzek, W. J., Wei, J., Kitada, S., Zhai, D., Reed, J., C., & Pellecchia, M. (2010). A survey of the anti-apoptotic Bcl-2 subfamily expression in cancer types provides a platform to predict the efficacy of Bcl-2 antagonists in cancer therapy. *Cell Death Dis., 1*, e40

Powers, D. C., Leber, P. A., Gallagher, S. S., Higgs, A. T., McCullough, L. A., & Baldwin, J. E. (2007). Thermal chemistry of bicyclo[4.2.0]oct-2-enes. *J. Org. Chem., 72*, 187-194

Pradhan, L., Sharma, S., Nalamada, S., Sahu, S. K., Das, S., & Garg, P. (2011). Natamycin in the treatment of keratomycosis: Correlation of treatment outcome and in vitro susceptibility of fungal isolates. *Ind. J. Ophthalmol., 59*, 512-514

Pretsch, E., Buhlmann, P., & Badertscher, M. (2009). *Structure determination of organic compounds* (4th ed.): Springer-Verlag Berlin Heidelberg

Pudjiastuti, P., Mukhtar, M. R., Hadi, A. H. A., Saidi, N., Morita, H., Litaudon, M., & Awang, K. (2010). (6,7-Dimethoxy-4-methylisoquinolinyl)-(4'-methoxyphenyl)-methanone, a new benzylisoquinoline alkaloid from *Beilschmiedia brevipes*. *Molecules, 15*, 2339-2346

Qian, J., Voorbach, M. J., Huth, J. R., Coen, M. L., Zhang, H., Ng, S. C., Comess, K. M., Petros, A. M., Rosenberg, S. H., Warrior, U., & Burns, D. J. (2004). Discovery of novel inhibitors of Bcl-xL using multiple high-throughput screening platforms. *Anal. Biochem., 328*, 131-138

Qian, M., & Negishi, E.-I. (2005). Palladium-catalyzed cross-coupling reaction of alkynylzincs with benzylic electrophiles. *Tetrahedron Lett., 46*, 2927-2930

Qin, H., Xu, Z., Cui, Y., & Jia, Y. (2011). Total synthesis of (±)-decursivine and (±)-serotobenine: A Witkop photocyclization/elimination/O-Michael addition cascade approach. *Angew. Chem. Int. Ed., 50*, 4447-4449

Ranu, B. C., & Sarkar, A. (1994). Regio- and stereoselective hydrogenation of conjugated carbonyl compounds via palladium assisted hydrogen transfer by ammonium formate. *Tetrahedron Lett., 35*, 8649-8650

Raths, H.-C., & Dehmlow, E. V. (1987). Anwendungen der phasentransfer-katalyse, eine neuartige reaktion des trichloracetats. *Chemische Berichte, 120*, 647-648

Rautureau, G. J. P., Day, C. L., & Hinds, M. G. (2010). Intrinsically Disordered Proteins in Bcl-2 Regulated Apoptosis. *Int. J. Mol. Sci., 11*, 1808-1824

Ready, J. M., Reisman, S. E., Hirata, M., Weiss, M. M., Tamaki, K., Ovaska, T. V., & Wood, J. L. (2004). A mild and efficient synthesis of oxindoles: progress towards the synthesis of welwitindolinone A isonitrile. *Angew. Chem. Int. Edit., 43*, 1270-1272

Redin, G. S. (1966). Antibacterial activity in mice of minocycline, a new tetracycline. *Antimicrob. Agents Chemother., 6*, 371-376

Reisman, S. E., Ready, J. M., Hasuoka, A., Smith, C. J., & Wood, J. L. (2006). Total synthesis of (±)-welwitindolinone A isonitrile. *J. Am. Chem. Soc., 128*, 1448-1449

Ren, D., Tu, H. C., Kim, H., Wang, G. X, Bean, G. R., Takeuchi, O., Jeffers, J. R., Zambetti, G. P., Hsieh, J. J. D., & Cheng, E. H. Y. (2010). BID, BIM, and PUMA are essential for activation of the BAX- and BAK-dependent cell death program. *Science, 330*, 1390-1393

Richard, J.-A., & Chen, D. Y. K. (2012). A chiral-pool based approach to the core structure of (+)-hyperforin. *Eur. J. Org. Chem.*, 484-487

Riss, T. L., & Moravec, R. A. (1992). Comparison of MTT, XTT, and a novel tetrazolium compound MTS for in vitro proliferation and chemosensitivity assays. *Mol. Biol. Cell, 3*, 184a-188a

Roberts, A. W., Seymour, J. F., Brown, J. R., Wierda, W. G., Kipps, T. J., Khaw, S. L., Carney, D. A., He, S. Z., Huang, D. C. S., Xiong, H., Cui, Y., Busman, T. A., McKeegan, E. M., Krivoshik, A. P., Enschede, S. H., & Humerickhouse, R. (2012). Substantial susceptibility of chronic lymphocytic leukemia to BCL2 inhibition: results of a phase I study of Navitoclax in patients with relapsed or refractory disease. *J. Clin. Oncol., 30*, 488-496

Robinson, R. P., Buckbinder, L., Haugeto, A. I., McNiff, P. A., Millham, M. L., Reese, M. R., Schaefer, J. F., Abramov, Y. A., Bordner, J., Chantigny, Y. A., Kleinman, E. F., Laird, E. R., Morgan, B. P., Murray, J. C., Salter, E. D., Wessel, M. D., & Yocum, S. A. (2009). Octahydrophenanthrene-2,7-diol analogues as dissociated glucocorticoid receptor agonists: discovery and lead exploration. *J. Med. Chem., 52*, 1731-1743

Robles, O., & McDonald, F. E. (2009). Convergent synthesis of fostriecin via selective alkene couplings and regioselective asymmetric dihydroxylation. *Org. Lett. 11*, 5498-5501

Rohan, A. D., Anthony, R. C., Sandra, D., Vicky, M. A., Gordon, P. G., Paul, I. F., & Ronald, J. Q. (2007). Endiandrin A, a potent glucocorticoid receptor binder isolated from the Australian plant *Endiandra anthropophagorum*. *J. Nat. Prod., 70*, 1118-1121

Rohan, A. D., Emma, C. B., James, L., Vicky, M. A., & Peter, C. H. (2009). Isolation, structure elucidation and cytotoxic evaluation of endiandrin B from the Australian rainforest plant *Endiandra anthropophagorum*. *Bioorg. Med. Chem., 17*, 1387-1392

Rohwer, J. G. (1993). Lauraceae. In K. Kubitzki, J. Rohwer & V. Bittrich (Eds.), *Flowering plants · Dicotyledons* (Vol. 2, pp. 366-391): Springer Berlin Heidelberg

Rooswinkel, R. W., Van de Kooij, B., Verheij, M., & Borst, J. (2012). Bcl-2 is a better ABT-737 target than Bcl-xL or Bcl-w and only Noxa overcomes resistance mediated by Mcl-1, Bfl-1, or Bcl-B. *Cell Death Dis., 3*, e366

Rosen, B. R., Werner, E. W., O'Brien, A. G., & Baran, P. S. (2014). Total synthesis of dixiamycin B by electrochemical oxidation. *J. Am. Chem. Soc., 136*, 5571-5574

Rosini, G., Laffi, F., Marotta, E., Pagani, I., & Righi, P. (1998). Total synthesis of the marine sesquiterpenoid raikovenal through a novel utilization of the bicyclo[3.2.0]heptenone approach. *J. Org. Chem., 63*, 2389-2391

Rouhi, A. M. (2003). Rediscovering natural products. *Chem. Eng. News Archive, 81*, 77-91

Rupprecht, J. K., Hui, Y.-H., & McLaughlin, J. L. (1990). Annonaceous acetogenins: a review. *J. Nat. Prod., 53*, 237-278

Sabitha, G., Reddy, C. S., & Yadav, J. S. (2006). Total syntheses of the highly potent anti-cancer polyacetylenes, (*S*)-18-hydroxyminquartynoic acid, (*S*)-minquartynoic acid and (*E*)-15,16-dihydrominquartynoic acid. *Tetrahedron Lett., 47*, 4513-4516

Saksena, A. K., Green, M. J., Mangiaracina, P., Wong, J. K., Kreutner, W., & Gulbenkian, A. R. (1985). Synthesis of 7,8-acetylenic analogs of hexahydro leukotriene-*E*4 with agonist and antagonist activities: convenient stereoselective routes to *E*- and *Z*-enynes. *Tetrahedron Lett., 26*, 6423-6426

Sanchez, S., & Demain, A. L. (2011). 1.12 - Secondary metabolites. In M. Moo-Young (Ed.), *Comprehensive biotechnology (2nd ed.)* (pp. 155-167). Burlington: Academic Press

Scott, R. B., & Agnes, M. R. (2007). A plethora of polyketides: structures, biological activities, and enzymes. *Polyketides* (Vol. 955, pp. 2-14): American Chemical Society

Selva, E., & Lancini, G. (2010). Rifamycins, antibacterial antibiotics and their new applications. *Analogue-based drug discovery II* (pp. 173-187): Wiley-VCH Verlag GmbH & Co. KGaA

Sharma, P., Ritson, D. J., Burnley, J., & Moses, J. E. (2011). A synthetic approach to kingianin A based on biosynthetic speculation. *Chem. Commun., 47*, 10605-10607

Sharpless, K. B., & Lauer, R. F. (1973). Mild procedure for the conversion of epoxides to allylic alcohols. First organoselenium reagent. *J. Am. Chem. Soc., 95*, 2697-2699

Shen, B. (2003). Polyketide biosynthesis beyond the type I, II and III polyketide synthase paradigms. *Curr. Opin. Chem. Biol., 7*, 285-295

Shi, C., & Aldrich, C. C. (2012). Design and synthesis of potential mechanism-based inhibitors of the aminotransferase bioA involved in biotin biosynthesis. *J. Org. Chem., 77*, 6051-6058

Shibuya, M., Sakai, Y., & Naoe, Y. (1995). A convenient synthesis of acyclic conjugated enediynes. *Tetrahedron Lett., 36*, 897-898

Silverstein, R. M., Bassler, G. C., & Morril T. C. (1997). *Spectroscopic indentification of organic compounds* (6th ed.): John Wiley and Sons Inc

Silverstein, R. M., Bassler, G. C., & Morril, T. C. (1991). *Spectroscopic identification of organic compounds* (5th ed.): John Wiley & Sons Inc

Smith, L. I., & Hoehn, H. H. (1939). The reaction between diphenylketene and phenylacetylene. *J. Am. Chem. Soc., 61*, 2619-2624

Smith, N. D., Roppe, J. R., Bonnefous, C., Payne, J. E., Zhuang, H., Chen, X., Lindstrom, A. K., Duron, S. G., Hassig, C. A., & Noble, S. A. (2008). United State (US) Patent No. 20080139558 GLOBAL PATENT GROUP - KAL: I. KALYPSYS

Sohda, T., Mizuno, K., Hirata, T., Maki, Y., & Kawamatsu, Y. (1983). Antiulcer activity of 5-benzylthiazolidine-2,4-dione derivatives. *Chem. Pharm. Bull., 31*, 560-569

Souers, A. J., Leverson, J. D., Boghaert, E. R., Ackler, S. L., Catron, N. D., Chen, J., Dayton, B. D., Ding, H., Enschede, S. H., Fairbrother, W. J., Huang, D. C. S., Hymowitz, S. G., Jin, S., Khaw, S. L., Kovar, P. J., Lam, L. T., Lee, J., Maecker, H. L., Marsh, K. C., Mason, K. D., Mitten, M. J., Nimmer, P. M., Oleksijew, A., Park, C. H., Park, C.-M., Phillips, D. C., Roberts, A. W., Sampath, D., Seymour, J. F., Smith, M. L., Sullivan, G. M., Tahir, S. K., Tse, C., Wendt, M. D., Xiao, Y., Xue, J. C., Zhang, H., Humerickhouse, R. A., Rosenberg, S. H., & Elmore, S. W. (2013). ABT-199, a potent and selective BCL-2 inhibitor, achieves antitumor activity while sparing platelets. *Nat. Med., 19*, 202-208

Stanforth S. P. (2006). *Natural product chemistry at a glance*: Blackwell Publishing Ltd

Staudinger, H. (1905). Ketene, eine neue körperklasse. *Berichte der deutschen chemischen Gesellschaft, 38*, 1735-1739

Staudinger, H. (1907). Zur kenntniss der ketene. Diphenylketen. *Justus Liebigs Annalen der Chemie, 356*, 51-123

Staunton, J., & Weissman, K. J. (2001). Polyketide biosynthesis: a millennium review. *Nat. Prod. Rep., 18*, 380-416

Stevens, H. C., Reich, D. A., Brandt, D. R., Fountain, K. R., & Gaughan, E. J. (1965). A new tropolone synthesis via dichloroketene. *J. Am. Chem. Soc., 87*, 5257-5259

Strasser, A., Cory, S., & Adams, J. M. (2011). Deciphering the rules of programmed cell death to improve therapy of cancer and other diseases. *EMBO J., 30*, 3667-3683

Strauss, J. S., Krowchuk, D. P., Leyden, J. J., Lucky, A. W., Shalita, A. R., Siegfried, E. C., Thiboutot, D. M., Van Voorhees, A. S., Beutner, K. A., Sieck, C. K., & Bhushan, R. (2007). Guidelines of care for acne vulgaris management. *J. Am. Acad. Dermatol., 56*, 651-663

Tahir, S. K., Yang, X., Anderson, M. G., Morgan-Lappe, S. E., Sarthy, A. V., Chen, J., Warner, R. B., Ng, S.-C., Fesik, S. W., Elmore, S. W., Rosenberg, S. H., & Tse, C. (2007). Influence of Bcl-2 family members on the cellular response of small-cell lung cancer cell lines to ABT-737. *Cancer Res., 67*, 1176-1183

Talontsi, F. M., Lamshöft, M., Bauer, J. O., Razakarivony, A. A., Andriamihaja, B., Strohmann, C., & Spiteller, M. (2013). Antibacterial and antiplasmodial constituents of *Beilschmiedia cryptocaryoides*. *J. Nat. Prod. , 76*, 97-102

Tang, G., Nikolovska-Coleska, Z., Qiu, S., Yang, C.-Y., Guo, J., & Wang, S. (2008). Acylpyrogallols as inhibitors of antiapoptotic Bcl-2 proteins. *J. Med. Chem., 51*, 717-720

Taschner, M. J. (2001). Sodium trichloroacetate. *Encyclopedia of Reagents for Organic Synthesis*: John Wiley & Sons, Ltd

Tempesta, M. S., Kriek, G. R., & Bates, R. B. (1982). Uvaricin, a new antitumor agent from *Uvaria accuminata* (Annonaceae). *J. Org. Chem., 47*, 3151-3153

The Plant List **(**2013). Version 1.1. Retrieved from http://www.theplantlist.org/

Thomas, P. A. (2003). Fungal infections of the cornea. *Eye, 17*, 852-862

Tidwell, T., T. (2005). *Ketenes* (2nd ed.): Wiley-Interscience

Tidwell, T. T. (2005). The first century of ketenes (1905–2005): the birth of a versatile family of reactive intermediates. *Angew. Chem. Int. Ed., 44*, 5778-5785

Tidwell, T. T. (2006). Ketene chemistry after 100 years: ready for a new century. *Eur. J. Org. Chem., 2006*, 563-576

Touzeau, C., Dousset, C., Le Gouill, S., Sampath, D., Leverson, J. D., Souers, A. J., Maiga, S., Bene, M. C., Moreau, P., Pellat-Deceunynck, C., & Amiot, M. (2014). The Bcl-2 specific BH3 mimetic ABT-199: a promising targeted therapy for t(11;14) multiple myeloma. *Leukemia, 28*, 210-212

Tse, C., Shoemaker, A. R., Adickes, J., Anderson, M. G., Chen, J., Jin, S., Johnson, E. F., Marsh, K. C., Mitten, M. J., Nimmer, P., Roberts, L., Tahir, S. K., Xiao, Y., Yang, X., Zhang, H., Fesik, S., Rosenberg, S. H., & Elmore, S. W. (2008). ABT-263: a potent and orally bioavailable Bcl-2 family inhibitor. *Cancer Res., 68*, 3421-3428

Uenishi, J. I., Kawahama, R., Yonemitsu, O., & Tsuji, J. (1998). Stereoselective hydrogenolysis of 1,1-dibromo-1-alkenes and stereospecific synthesis of conjugated (*Z*)-alkenyl compounds. *J. Org. Chem., 63*, 8965-8975

Vail, S. A., Krawczuk, P. J., Guldi, D. M., Palkar, A., Echegoyen, L., Tomé, J. P. C., Fazio, M. A., & Schuster, D. I. (2005). Energy and electron transfer in polyacetylene-linked zinc–porphyrin–[60]fullerene molecular wires. *Chem. Eur. J., 11*, 3375-3388

Vézina, C., Kudelski, A., & Sehgal, S. N. (1975). Rapamycin (AY-22,989), a new antifungal antibiotic. I. Taxonomy of the producing streptomycete and isolation of the active principle. *J. Antibiot., 28*, 721-726

Vogler, M., Dinsdale, D., Dyer, M. J. S., & Cohen, G. M. (2008). Bcl-2 inhibitors: small molecules with a big impact on cancer therapy. *Cell Death Differ., 16*, 360-367

Volante, G. D., Zerrouk, N., Richard, I., Provot, G., Chaumil, J. C., & Arnoud, P. (2002). Evaluation of the cytotoxicity effect of dimethyl sulfoxide (DMSO) on Caco21TC7 colon tumor cell cultures. *Biol. Pharm. Bull., 25*, 1600-1603

Wagner, H. U., & Gompper, R. (1970). Ein modell zur beschreibung der cycloaddition von keten an olefine. *Tetrahedron Lett., 11*, 2819-2822

Walensky, L. D. (2012). From mitochondrial biology to magic bullet: Navitoclax disarms BCL-2 in chronic lymphocytic leukemia. *J. Clin. Oncol., 30*, 554-557

Wan, K. F., Chan, S. L, Sukumaran, S. K., Lee, M. C., & Yu, V. C. (2008). Chelerythrine induces apoptosis through a Bax/Bak-independent mitochondrial mechanism. *J. Biol. Chem., 283*, 8423-8433

Wang, G., Mohan, S., & Negishi, E.-I. (2011). Highly selective synthesis of conjugated dienoic and trienoic esters via alkyne elementometalation–Pd-catalyzed cross-coupling. *Proc. Natl. Acad. Sci. U.S.A., 108*, 11344-11349

Wang, S., Xu, Y., Maine, E. A., Wijeratne, E. M. K., Espinosa-Artiles, P., Gunatilaka, A. A. L., & Molnár, I. (2008). Functional characterization of the biosynthesis of radicicol, an Hsp90 inhibitor resorcylic acid lactone from *Chaetomium chiversii*. *Chem. Biol., 15*, 1328-1338

Wang, S. (2008). Targeting Bcl-xL enhances the cytotoxicity of chemotherapeutics. *Cancer Biol. Ther., 7*, 61-62

Wani, M. C., Taylor, H. L., Wall, M. E., Coggon, P., & McPhail, A. T. (1971). Plant antitumor agents. Isolation and structure of taxol, a novel antileukemic and antitumor agent from *Taxus brevifolia*. *J. Am. Chem. Soc., 93*, 2325-2327

Watkins, S. M., Reich, A., Fleming, L. E., & Hammond, R. (2008). Neurotoxic Shellfish Poisoning. *Marine Drugs, 6*, 431-455

Webb, M. R., Addie, M. S., Crawforth, C. M., Dale, J. W., Franci, X., Pizzonero, M., Donald, C., & Taylor, R. J. K. (2008). The syntheses of rac-inthomycin A, (+)-inthomycin B and (+)-inthomycin C using a unified synthetic approach. *Tetrahedron, 64*, 4778-4791

Wehrli, W., & Staehelin, M. (1971). Actions of the rifamycins. *Bacteriol. Rev., 35*, 290-309

Weissman, K. J. (2009). Chapter 1 introduction to polyketide biosynthesis. In A. H. David (Ed.), *Methods in Enzymology* (Vol. 459, pp. 3-16): Academic Press

Wells, J. A., & McClendon, C. L. (2007). Reaching for high-hanging fruit in drug discovery at protein-protein interfaces. [10.1038/nature06526]. *Nature, 450*(7172), 1001-1009

Wilk, B. K. (1993). A convenient preparation of alkyl nitriles by the Mitsunobu procedure. *Synth. Commun., 23*, 2481-2484

Williams, R. B., Martin, S. M., Hu, J.-F., Norman, V. L., Goering, M. G., Loss, S., O'Neil-Johnson, M., Eldridge, G. R., & Starks, C. M. (2012). Cytotoxic and antibacterial beilschmiedic acids from a gabonese species of *Beilschmiedia*. *J. Nat. Prod., 75*, 1319-1325

Wilsmore, N. T. M. (1907). CLXXXVIII.-Keten. *J. Chem. Soc., Trans., 91*, 1938-1941

Wilson, W. H., O'Connor, O. A., Czuczman, M. S., LaCasce, A. S., Gerecitano, J. F., Leonard, J. P., Tulpule, A., Dunleavy, K., Xiong, H., Chiu, Y.-L., Cui, Y., Busman, T., Elmore, S. W., Rosenberg, S. H., Krivoshik, A. P., Enschede, S. H., & Humerickhouse, R. A. (2010). Navitoclax, a targeted high-affinity inhibitor of BCL-2, in lymphoid malignancies: a phase 1 dose-escalation study of safety, pharmacokinetics, pharmacodynamics, and antitumour activity. *Lancet Oncol., 11*, 1149-1159

Wink, M. (2010). Introduction: biochemistry, physiology and ecological functions of secondary metabolites. *Annual Plant Reviews Volume 40: Biochemistry of Plant Secondary Metabolism* (pp. 1-19): Wiley-Blackwell

Winssinger, N., & Barluenga, S. (2007). Chemistry and biology of resorcylic acid lactones. *Chem. Commun.*, 22-36

Woodward, R. B., & Hoffmann, R. (1969). The conservation of orbital symmetry. *Angew. Chem. Int. Ed., 8*, 781-853

Wu, H. Y., Walker, K. A. M., & Nelson, J. T. (1994). Stereochemical consequences of 6- and 8-substitution in reactions of bicyclo[4.2.0]octan-7-ones. *J. Org. Chem., 59*, 1389-1395

Yang, P.-S., Cheng, M.-J., Chen, J.-J., & Chen, I.-S. (2008). Two new endiandric acid analogs, a new benzopyran, and a new benzenoid from the root of *Beilschmiedia erythrophloia*. *Helv. Chim. Acta, 91*, 2130-2138

Yang, P.-S., Cheng, M.-J., Peng, C.-F., Chen, J.-J., & Chen, I.-S. (2009). Endiandric acid analogues from the roots of *Beilschmiedia erythrophloia*. *J. Nat. Prod., 72*, 53-58

Yip, K. W., & Reed, J. W. (2008). Bcl-2 family proteins and cancer. *Oncogene, 27*, 6398-6406

Youle, R. J., & Strasser, A. (2008). The BCL-2 protein family: opposing activities that mediate cell death. *Nat. Rev. Mol. Cell Biol., 9*, 47-59

Zafra-Polo, M. C., González, M. C., Estornell, E., Sahpaz, S., & Cortes, D. (1996). Acetogenins from annonaceae, inhibitors of mitochondrial complex I. *Phytochemistry, 42*, 253-271

Zhang, J. H., Chung, T. D., & Oldenburg, K. R. (1999). A simple statistical parameter for use in evaluation and validation of high throughput screening assays. *J. Biomol. Screen., 4*, 67-73

Zhang, L., & Koreeda, M. (2002). Stereocontrolled synthesis of Kelsoene by the Homo-Favorskii rearrangement. *Org. Lett., 4*, 3755-3758

Zhong, J. J. (2011). 3.27 - Plant secondary metabolites. In M. Moo-Young (Ed.), *Comprehensive Biotechnology (2nd Ed.)* (pp. 299-308). Burlington: Academic Press

Zimmerman, H. E. (1971). Moebius-Hueckel concept in organic chemistry. Application of organic molecules and reactions. *Acc. Chem. Res., 4*, 272-280